PERFORMANCE BASED DESIGN OF R/C TALL BUILDINGS IN TWO DIFFERENT SEISMIC ZONES

A THESIS SUBMITTED TO
THE GRADUATE SCHOOL OF NATURAL AND APPLIED SCIENCES
OF
MIDDLE EAST TECHNICAL UNIVERSITY

BY

MUSTAFA GÜNEŞ ÇİFTÇİOĞLU

IN PARTIAL FULFILLMENT OF THE REQUIREMENTS
FOR
THE DEGREE OF MASTER OF SCIENCE
IN
CIVIL ENGINEERING

JANUARY 2023

Approval of the thesis:

PERFORMANCE BASED DESIGN OF R/C TALL BUILDINGS IN TWO DIFFERENT SEISMIC ZONES

submitted by **MUSTAFA GÜNEŞ ÇİFTÇİOĞLU** in partial fulfillment of the requirements for the degree of **Master of Science** i**n Civil Engineering, Middle East Technical University** by,

Prof. Dr. Halil Kalıpçılar
Dean, Graduate School of **Natural and Applied Sciences** _____

Prof. Dr. Erdem Canbay
Head of the Department, **Civil Engineering** _____

Prof. Dr. Barış Binici
Supervisor, **Civil Engineering Dept., METU** _____

Examining Committee Members:

Prof. Dr. Ahmet Yakut
Civil Engineering Dept., METU _____

Prof. Dr. Barış Binici
Civil Engineering Dept., METU _____

Prof. Dr. Kağan Tuncay
Civil Engineering Dept., METU _____

Prof. Dr. Yalın Arıcı
Civil Engineering Dept., METU _____

Assoc. Prof. Dr. Alper Aldemir
Civil Engineering Dept., Hacettepe University _____

Date: 20.01.2023

I hereby declare that all information in this document has been obtained and presented in accordance with academic rules and ethical conduct. I also declare that, as required by these rules and conduct, I have fully cited and referenced all material and results that are not original to this work.

Name, Last name : Mustafa Güneş Çiftçioğlu

Signature :

ABSTRACT

PERFORMANCE BASED DESIGN OF R/C TALL BUILDINGS IN TWO DIFFERENT SEISMIC ZONES

Çiftçioğlu, Mustafa Güneş
Master of Science, Civil Engineering
Supervisor : Prof. Dr. Barış Binici

January 2023, 326 pages

Performance-based design of R/C tall structures has become mandatory with Turkish Earthquake Code (2018). While some professionals think that linear capacity design is sufficient, others have supported this new approach only in regions where earthquake is more effective. Nonlinear design requires comprehensive and detailed theoretical knowledge. The compatibility of Perform 3D software, widely used in this design, with experiment results is unknown and calibration is not mandatory in the regulation. It is another unknown to what extent calibration will change the design results.

For this purpose, study was carried out on a tall structure with a height of 112 m above basement floor with flat slab, core-wall group and link beams. The design was made according to linear and nonlinear analysis for two different earthquake zones, i.e., Ankara and Istanbul. Necessity of nonlinear analysis in tall structures for both earthquake zones has been confirmed. In order to make the design compatible with experiments, calibration work was carried out for rectangular, T-shaped and U-shaped walls and diagonally and conventionally reinforced link beams. With calibration study, it was seen that cyclic degradation factors were very effective and numerical calibration results were given. The model concrete strain values of walls

were very small from the experimental values. For this, the correction coefficient "a" and formulation for walls concrete strain results are proposed. Ideal wall mesh modeling has been proposed horizontally and vertically.

The results of models with calibrated and 2 alternative uncalibrated cyclic degradation factors were compared, with results that were up to 30% lower in the absence of cyclic degradation factors. Low cyclic energy degradation factors are appropriate and sufficient for the design. As a result of all this study, some suggestions have been made for structural engineers and for some clauses of the Turkish Earthquake Code (2018).

Keywords: Nonlinear performance-based design, linear design, reinforced concrete tall structures, Perform 3D software cyclic degradation factors, wall and link beam calibration study

ÖZ

FARKLI İKİ DEPREM BÖLGESİNDEKİ BETONARME YÜKSEK YAPILARIN PERFORMANSA DAYALI TASARIMI

Çiftçioğlu, Mustafa Güneş
Yüksek Lisans, İnşaat Mühendisliği
Tez Yöneticisi: Prof. Dr. Barış Binici

Ocak 2023, 326 sayfa

Betonarme yüksek yapıların performansa dayalı tasarımı Türkiye Deprem yönetmeliği (2018) ile zorunlu hale gelmiştir. Bazı uzmanlar geleneksel kapasite tasarımının yeterli olduğunu düşünürken, bazılarıysa sadece depremin daha etkin olduğu bölgelerde bu yeni yaklaşımını desteklemiştir. Doğrusal olmayan tasarım kapsamlı ve detaylı teorik bilgi birikimine sahip olmayı gerektirmektedir. Bu tasarımda yaygın olarak kullanılan Perform-3D yazılımının deney sonuçları ile uyumu bilinmemektedir ve yönetmelikte de kalibrasyon zorunlu değildir. Kalibrasyon çalışmasının tasarım sonuçlarını ne ölçüde değiştireceği bir başka bilinmezliktir.

Bu amaçla kirişsiz döşemeli, çekirdek perde grubu ve bağ kirişli bodrum katı üzeri 112 m yüksekliğindeki yüksek bir yapı üzerine çalışma yapılmıştır. Ankara ve İstanbul gibi iki farklı deprem bölgesi için doğrusal ve doğrusal olmayan analize göre tasarım yapılmıştır. Her iki deprem bölgesi için yüksek yapılarda doğrusal olmayan analizin gerekliliği doğrulanmıştır. Deneylerle uyumlu tasarımın yapılması için dörtgen, T şeklinde ve U şeklinde perdeler ile çapraz ve düz donatılı bağ kirişler

için kalibrasyon çalışması yapılmıştır. Bu kalibrasyon çalışması ile çevrimsel enerji sönüm parametrelerinin çok etkin olduğu görülmüştür ve sayısal kalibrasyon sonuçları verilmiştir. Perde yapılarının model beton birim kısalma değerleri deney değerlerinden çok küçük çıkmıştır. Bunun için perde beton birim kısalma değerleri için "a" artırım katsayısı ve formülasyonu önerilmiştir. İdeal perde örgü modelleme aralıkları yatay ve düşeyde önerilmiştir.

Kalibrasyonlu ve seçilen 2 alternatif kalibrasyonuz çevrimsel enerji sönüm parametre değerlerine sahip modellerin sonuçları karşılaştırılmış, enerji sönüm parametreleri kullanılmaması durumunda %30'a varan düşük sonuçlar çıkmıştır. Düşük enerji sönüm parametre değerleri tasarım için uygun ve yeterlidir. Tüm bu çalışma sonucunda yapı mühendisleri ve Türkiye Deprem Yönetmeliği (2018) bazı kaideleri için önerilerde bulunulmuştur.

Anahtar Kelimeler: Doğrusal olmayan performansa dayalı tasarım, doğrusal tasarım, betonarme yüksek yapılar, Perform 3D çevrimsel enerji sönüm parametreleri, perde ve bağ kirişi kalibrasyon çalışması

To My Precious Wife

ACKNOWLEDGMENTS

This thesis has been a work that covers the whole of my twelve years of professional engineering experience in the field of high-rise buildings and my academic knowledge afterwards. I am very grateful to the major people in my life who have been instrumental in my upbringing and sacrifices in the creation of this work.

First of all, it was a very important chance for me that Prof. Dr. Barış Binici, one of the most competent instructors in Türkiye on reinforced concrete structure behavior, which has an important place in the content of the thesis, became my supervisor. In addition to the very important information, I learned from him, I would like to thank him for his guidance, advice, encouragement and very valuable support during the thesis phase.

I would like to thank to Ozkan Hakan, MSc. Civil Engineer, with whom I exchanged information and did not spare his technical support.

Finally, during this thesis phase, I would like to give the greatest thanks to my biggest supporter, the mother of my two daughters, my precious wife, who gave me the opportunity to do these academic studies in my busy business life, who showed great sacrifice and patience. The completion of this work is a fact that I cannot achieve without my precious wife, who supports me, gives me strength and is always by my side.

TABLE OF CONTENTS

LIST OF TABLES

TABLES

LIST OF FIGURES

FIGURES

LIST OF ABBREVIATIONS

ABBREVIATIONS

ACI	American Concrete Institute
ATC	Applied Technology Council
ASCE	American Society of Civil Engineers
BRB	Buckling Restrained Brace
C	Comparison
CB	Coupling Beam
CSI	Computer and Structures, INC.
EQ	Earthquake
EPP	Elastic Perfectly Plastic
FB	Frame Beam
LB	Link Beam
MCE	Maximum Considered Earthquake
MVLEM	Multiple vertical line element model
NIST	National Institute of Standards and Technology
P3D	Perform 3D
PBD	Performance Based Design
PEER	Pacific Earthquake Engineering Research
PGA	Peak ground acceleration
R/C	Reinforced Concrete
RW	Rectangular Wall
SGL	Stain gage length
SLE	Service Level Earthquake
SLIF	Strength Loss Interaction Factor
TBI	Tall Buildings Initiative
TEC	Turkish Earthquake Code
TW	T-Shaped Wall

USF	Unloading Stiffness Factor
W	Wall
WG	Wall Group
YULRX	Perform 3D Cyclic Energy Degradation Limits

LIST OF SYMBOLS

SYMBOLS

a	Proposed concrete strain multiplication factor
A_g	Gross area
A_{ch}	Gross area of walls
A_{sd}	Diagonal reinforcement area
b_w	Width of beam
D	Over-strength factor
E_C	Concrete elastic modulus
$E_d^{(H)}$	Horizontal design earthquake load
f_{ce}	Expected concrete compressive strength
f_{ck}	Characteristic concrete compressive strength
f_{ctd}	Concrete design tensile strength
f_{ye}	Expected reinforcement yield strength
f_{yk}	Characteristic reinforcement yield strength
f_{ywd}	Lateral reinforcement yield strength
G	dead and superimposed dead load
h	Beam height
h_k	Height of beam
H	Building height
H1	Perform 3d X direction coordinate
H2	Perform 3d Y direction coordinate
I	Importance factor
I_g	Gross moment of inertia
I_n	Clear span of beam
L_p	Plastic hinge length
L_s	Shear length
m_t	Total mass of building over basement floor
M_y	Yield moment capacity
M_p	Plastic moment capacity
M_r	Moment capacity
R	Response modification factor

Q	Live load
V	Perform 3d z direction coordinate
V_e	Design shear load
V_{cr}	Cracking shear capacity
V_r	Total shear capacity
V_w	Shear capacity only from reinforcement
V_{tE}	Total equivalent earthquake load
V_{tx}	Total earthquake load according to modal analysis
ε_c	Concrete strain
ε_{cu}	Concrete ultimate strain
ε_{sy}	Reinforcement yield strain
ε_s	Reinforcement strain
ε_{su}	Reinforcement ultimate strain
θ_y	Yield rotation
ζ	Damping ratio
ω_{we}	Confinement effect
γ	Unit weight
μ	Natural period limit factor
β_{tE}	Magnification coefficients
βK	Viscous damping ratio
β_v	Wall dynamic multiplication factor
ρ_{sh}	Lateral reinforcement ratio
Ω	Degree of coupling

CHAPTER 1

INTRODUCTION

1.1 Motivation

The development of computer technology along with developments in structural engineering allows complicated structures to be modeled in extensive detail. This situation has led to new approaches in the design of buildings with an emphasis on analysis under extreme loads such as earthquakes. Design of important structures is now assessed with nonlinear analysis nowadays.

Nonlinear performance-based design approach was included in the Turkish Earthquake Code in 2018. On the other hand, the traditional force-dependent capacity design approach, which is widely used in the design of structures today, is still actively continuing within Turkish Earthquake Code. As with every new approach that is open to development and revisions, "nonlinear performance-based earthquake design" is open to continuous development and improvement as a result of developments in research and practice.

The subject of "nonlinear performance-based design" in the Turkish Earthquake Regulation (2018) is an active area of research that requires continuous evolution of structural engineers. Hence, this new design approach can be seen as a specialized field that should be performed by structural engineers with serious and comprehensive theoretical knowledge. Some of the structural engineers in Türkiye are also keeping up with this new approach in terms of both knowledge and adaptation to the software instruments used and developing themselves in this field. The number of engineers specialized in this field is limited due to the limited number of such projects in Türkiye. With the advent of new earthquake code, the number of engineers who should adapt to this new design approach is increasing. But the

question is; "how uniform is the work done by engineers, who design such complex buildings?" or "to what extent can structural engineers, who are the inspectors in this job, verify the work done?".

Structural engineers model buildings using structural design and analysis computer programs, which usually have some area of specialization. The most widely used software in performance-based design for buildings is "CSI Perform 3D". Some other software can be used for this design approach, but "CSI Perform 3D" is the most popular program designed specifically for this job and preferred by the experts. In a subject where the design has many complications and uncertainties for tall buildings, constructing the right mathematical model, accurate analysis and obtaining “true” appear to be impossible. The capabilities of software, parameter selection, and its sensitivities on the results become key concern. As a result, a competent structural engineer with sufficient theoretical knowledge in performance-based structure design should pass through a complex and precise modeling stage with an analysis software program and evaluate the results correctly. The inaccuracy or inadequacy in any of these stages could raise a question mark in the results of this laborious and competent design approach.

In Turkish Earthquake Code (2018), non-linear performance-based building design is not required for all buildings. Such detailed design is conducted for tall buildings and important structures having the height between 42 m and 70 m that should be used just after earthquakes in severe earthquake zones. In the design of such structures, the force-based traditional capacity design is conducted as the preliminary design, while the performance analysis of the structure is then conducted to assess the sufficiency of design. Hence, important structures are designed in detail in terms of earthquake with a two-stage approach in the Turkish Earthquake Code (2018).

In the light of these explanations, the list of our motivations that led to this thesis study are;

- In the latest earthquake code in Türkiye, this new complex design approach is a matter of debate among both academic members and structural engineers.

- Practical contributions are needed for clauses of Turkish Earthquake Regulation (2018) in terms of verification or revision in the field of nonlinear performance-based design
- To demonstrate practical examples to structural engineers who will design and work on nonlinear performance-based design
- To demonstrate this complex and laborious design approach with the widely used "CSI Perform 3D" software program.

1.2 Research Questions

It has been discussed by many expert engineers and academicians whether nonlinear structural design of tall buildings is necessary or not after the introduction of the design of performance-based design come in New Turkish Earthquake Regulation for buildings in low seismic zones. The necessity of this design should be questioned because there are not many engineers with all the engineering knowledge such as advanced concrete member behavior, structural dynamics, earthquake knowledge, and structural analysis. Furthermore, the accuracy of such a complicated analysis is not known compared to the actual system response. Engineers opposing nonlinear structural design, prefer traditional forced based design approach due to the extensive experience with it. This issue, the need for nonlinear analysis for tall buildings in different seismic zones, is one of the research questions in this thesis.

It is mandatory to perform a nonlinear performance analysis for all high-rise buildings in accordance with the Turkish earthquake code. In the content of this thesis study, a case study high-rise building has been designed with the two-stage approach according to TEC (2018), both in Ankara, which is not a severe earthquake zone, and in Istanbul, which is a severe earthquake zone. The selected example high-rise building is described in detail in Chapter 3. The case study high-rise building has a flat slab system, and there is a core wall group and link beams to carry all earthquake forces. The design of the case study high-rise building is accomplished with traditional linear forced-based design method in stage one, including all

dimensions and reinforcement details. In the second stage, the adequacy of the core wall group and link beams, which are designed as earthquake-resistant system, are checked with performance-based nonlinear analysis. Design results comparison in terms of size and reinforcement for the different earthquake zones in these two stages is aimed to provide us an idea of whether nonlinear performance-based design is required or not.

To compare the nonlinear performance analysis and linear forced-based design, it must be ensured that the nonlinear performance analysis is performed correctly. First stage of the performance analysis is that experimental lateral force-displacement hysterical response results of structural elements, (in the selected case study high-rise building, namely walls and link beams) that meet the earthquake force, should be simulated with used software model. In other words, this model verification and calibration should be performed in such a way that similar cyclic response results are obtained between experimental hysterical results and model results. Such calibration study is not mandatory in accordance with the regulations of the code. Hence, this appears as one of the deficiencies in our current Turkish Earthquake Code (2018). In this study, for case study high-rise building, prior to the building's nonlinear analysis, modeling has been conducted for walls and link beams modeled with "Perform-3D" software to calibrate the modeling approach. With this study, which we call calibration work, it has been determined that how 3D sample high-rise structure performance analysis with "Perform-3D" program is realized. The effect of modeling parameters on the ability of calibration to the test results is also one of the research topics of this thesis.

The summary of the research questions of this thesis are;

- Do we need performance-based design for all tall buildings in different earthquake regions?
- How much is the difference between results of linear and nonlinear design and analysis of tall buildings for different levels of earthquake regions?

- How to correctly model wall and link beam in harmony with experimental cyclic response results with Perform 3D software? Which Perfom-3D software parameters are more effective on calibration work?
- What is the sensitivity of modeling parameters for performance analysis of tall buildings? To what extent does material modeling perfectly consistent with the results of the experiment, have an impact on the results?
- What is the importance of meshing and strain measurement gauge length used in the evaluation of RC walls?

1.3 Outline of Thesis

This thesis consists of 7 main chapters. In each chapter, the following details are given:

In Chapter 2, the concepts and design criteria related to the performance-based design are presented. In this presentation, while design criteria and definitions are mainly clarified according to the Turkish Earthquake Code (2018). Some comparisons with American regulations are given and some recommendations are proposed. Preliminary information is provided for the case study tall building's performance analysis in Chapter 6.

In order to find answers to the research questions of this thesis, linear elastic design results of a high-rise case study building according to TEC-2018 is presented in Chapter 3. Linear elastic design of case study high-rise buildings is fulfilled in two different locations having different seismic characteristics, i.e., in Ankara and Istanbul. In this chapter, first of all, all introduction and necessary information about case study high-rise buildings are given. Core-wall group and link beams located in the center of this high structure typical plan of a flat slab system are our two important types of structural elements that meet all earthquake forces. In the remaining sections of the thesis, all the studies will be focused on structural walls and link beams. At the end of third chapter, dimensions related to core wall group

and link beams of the sample tall building under earthquake load and all reinforcement detail information are presented for two different earthquake regions, i.e., Ankara and Istanbul. This information will be input in, or in other words, a preliminary design, in a nonlinear analysis of our case study tall building in Chapter 6.

Chapter 4 examines CSI Perform 3D software, which is considered to be the most popular software for performance analysis and design of structures today. Commonly used software and trusted by engineers working seriously on performance analysis of structures in Türkiye is CSI Perform 3D, even if it is not a very user-friendly software. So, performance-based design of case study tall structure is realized with this software. Since this program is a very sophisticated and not very user-friendly software, in order to use this software correctly, it is necessary to give detailed information such as details of the software, important points to be considered, working and modeling principles of this software. Perform 3D is ultimately an instrument for structural analysis. It is important that this instrument is used correctly. It is necessary to examine software in proper use. Therefore, Chapter 4 provides the necessary detailed information about software "CSI Perform 3D".

Chapter 5 constitutes an important part of the thesis. In this section, a study is realized on walls and link beams, which are two types of structural elements that meet the earthquake load in case study tall structure. With this study, the results of the experimental study related to nonlinear cyclic behavior of walls and link beams were modeled with Perform 3D software and results were overlapped. This overlapping study is carried out with experimental results of three types of walls, namely rectangular, T and U-shaped walls, while in coupling beams it is made for conventionally reinforced and diagonally reinforced link beams. In addition, for classical frame beams between core wall groups, non-linear results of experiments are matched with Perform 3D software results. With this calibration work, important findings, such as how walls and link beams should be modeled in Perform 3D software and which parameters should be used, are reached. It has been observed to what extent it can be compatible with the results of the experiment. It has been

observed to what extent and which parameters and variables affect the nonlinear behavior of walls and link beams. Within the scope of correct modeling data obtained by this calibration work, an accurate base is created for performance analysis of 3D sample tall structure.

In Chapter 6, the nonlinear design of case study tall building is fulfilled. Dimensions of structural members and reinforcement details obtained according to linear elastic design in Chapter 3 are used as input in this section. Taking into account the correct modeling parameters obtained in Chapter 5 and without taking into consideration, a total of 6 nonlinear analyzes of case study buildings are performed separately for Ankara and Istanbul earthquake regions. It is observed how much it differed from results of performance analysis in the section with results of linear analysis made in Chapter 3. In addition, the effect of calibration work results on 3D structural nonlinear design and total results are observed to what extent.

In Chapter 7, the answers sought to the research questions of the thesis and the important conclusions drawn are indicated. Whether a nonlinear design approach is required or not, the effect of calibration work with the results of PBD is detailed. The calibration parameters of walls and link beams in correct modeling with Perfom-3D software are summarized again. Proposed concrete strain multiplication factor “a” of walls is also explained. New recommendations will be presented for some clauses of TEC-2018.

CHAPTER 2

SOME PRELIMINARIES FOR PERFORMANCE BASED DESIGN CHECK ACCORDING TO TEC (2018)

A summary of the PBD check according to TEC (2018) guidelines is reviewed here to clarify the steps followed in the later chapters of this thesis.

2.1 Buildings Types and Target Building Performance Levels

Structures are designed under four different levels of earthquake force. Definitions of design earthquake force levels are shown in Table 2.1. Intensity of earthquake force is named from DD-1 to DD4 earthquake level. Various levels of damage are expected in structures under different force levels of the earthquake. These damage levels and descriptions of overall damage to the structure are given in Table 2.2. Descriptions of physical damage to each structural member according to structural performance levels are also given in Table 2.3.

Table 2.1 Earthquake Design Load Levels in TEC-2018

EQ Design Level	Probability of Exceedance	Mean Return Period (years)
DD-1	2%/ 50 years	2475
DD-2	10%/ 50 years	475
DD-3	50%/ 50 years	72
DD-4	68%/ 50 years	43

Table 2.2 Structural Performance Levels and Physical Damage Definitions of Overall Structure("Seism. Eval. Retrofit Exist. Build.," 2017)

Structural Performance Level	Overall Damage	Overall Damage of Structure	EQ Level
O- (Operational)	Very Light	No permanent drift. Structure substantially retains original strength and stiffness. Minor cracking of facades, partitions, and ceilings as well as structural elements. All systems important to normal operation are functional. Continued occupancy and use highly likely	DD4
IO- (Immediate Occupancy)	Light	No permanent drift. Structure substantially retains original strength and stiffness. Continued occupancy likely	DD3
LS- (Life Safety)	Moderate	Some residual strength and stiffness left in all stories. Gravity-load-bearing elements function. No out of plane failure of walls. Some permanent drift. Damage to partitions. Continued occupancy might not be likely before repair. Building might not be economical to repair	DD2
CP- (Collapse Prevention)	Severe	Little residual stiffness and strength to resist lateral loads, but gravity load-bearing columns and walls function. Large permanent drifts. Some exits blocked. Building is near collapse in aftershocks and should not continue to be occupied	DD1

Table 2.3 Physical Damage Explanation of Structural Members for Different Damage Levels ("Seism. Eval. Retrofit Exist. Build.," 2017)

Structural Members	IO (Light Damage Level)	LS (Moderate Damage Level)	CP (Severe Damage Level)
Walls	Minor diagonal cracking of walls	Some boundary element cracking and spalling and limited buckling of reinforcement. Some sliding at joints. Damage around openings. Some crushing and flexural cracking	Major flexural or shear cracks and voids. Sliding at joints. Extensive crushing and buckling of reinforcement. Severe boundary element damage
Coupling Beams	Experience diagonal cracking	Extensive shear and flexural cracks; some crushing, but concrete generally remains in place	Shattered and virtually disintegrated
Columns & Beams	Minor spalling in a few places in ductile columns and beams. Flexural cracking in beams and columns. Shear cracking in joints	Major cracking and hinge formation in ductile elements. Limited cracking or splice failure in some nonductile columns. Severe damage in short columns	Extensive spalling in columns and beams. Limited column shortening. Severe joint damage. Some reinforcing buckled

IO: Immediate Occupancy, LS: Life Safety, CP: Collapse Prevention

According to the Turkish Earthquake Code-2018, characteristics of new structures to be built, for which performance analysis is mandatory, are presented in Table 2.4. Accordingly, PBD is mandatory in design of all high-rise buildings in Turkey; meanwhile, height limits to accept as high-rise building vary according to seismicity of region. Building design with nonlinear analysis is also required in important structures (i.e., importance factor is 1.5), that need to be used urgently after an earthquake and are mid-height structures above 42 m in severe earthquake zones.

Structures to be analyzed for performance are also requested to be made according to different earthquake levels and performance target levels. In performance-based building design, design is necessarily started with linear elastic design and this design is accepted as preliminary design. In Table 2.5, intended performance levels under different levels of earthquake loads are indicated for buildings for which performance analysis is mandatory.

Table 2.4 Building Types which must be designed with Performance Analysis according to TEC-2018

Building Type	$S_{DS}<0.33$	$0.33\leq S_{DS}<0.5$	$0.5\leq S_{DS}$
$70>H_N>42$ m & I=1.5			✓
$H_N>70$ m			✓
$H_N>90$ m		✓	
$H_N>105$ m	✓		

S_{DS}: Design Spectral Acceleration Coefficient for DD-2 stage EQ design level; H_N: Building height over podium or foundation; I: Importance Factor

Table 2.5 Performance Target Levels and Analysis Types of Buildings, must be designed according to PBD for different EQ levels according to TEC-2018

Building Type	DD4	DD3	DD2	DD1
$70>H_N>42$ m & I=1.5 ($0.50<S_{DS}$)		IO[1]	LS[2]	LS[1]
$H_N>70$ m ($0.50<S_{DS}$)		IO[1]	LS[2]	LS[1]
$H_N>90$ m ($0.33<S_{DS}<0.50$)	O[2]		LS[2]	CP[1]
$H_N>105$ m ($S_{DS}<0.33$)	O[2]		LS[2]	CP[1]

[1]Perfomance Based Design Target Level; [2]Linear Elastic Capacity Design Target Level; O: Operational, IO: Immediate Occupancy, LS: Life Safety, CP: Collapse Prevention

2.2 Structural Member Actions

Structural members should be grouped for PBD according to how they should behave under EQ loads. They are divided into two main actions, i.e., deformation-controlled

actions and forced controlled actions. With deformation-controlled action, the structural element will exhibit a ductile response with enough strength. Whereas a forced controlled action refers to a brittle response dictated by member strength.

In tall building system behavior, it is expected that flexural deformation under bending and axial load should occur along the critical wall length just above the podium floors or at the base connected to the foundation. On the other hand, flexural deformations are desired at the beam ends. Link beams mainly undergo shear deformations due to their shorter shear span. It must provide enough strength in all remaining regions. In Table 2.6, it is summarized how structural elements are required to behave under EQ load types.

Although forced controlled action is divided into critical and non-critical in both Turkish and American regulations, it is presented in Table 2.6 without separation to include the whole. Difference between critical and non-critical action terms can be defined that while a lack of strength that may occur in critical forced controlled action can cause partial or total structural collapse, there is no situation that can cause any or local collapse in non-critical forced action. In a high-rise building with a podium, force effects on basement wall, foundation and ordinary slabs, except for transfer floors can be thought of as a non-critical forced action class.

Table 2.6 Summary of Deformation and Forced Controlled Actions for Structural Members

	DEFORMATION CONTROLLED ACTION- Inelastic Behavior		
STRUCTURAL MEMBER	Under Moment	Under Shear Load	Under Axial Load
Shearwall	✓[1]	✗	✗
Column	✓[2]	✗	✗
Frame Beam	✓[3]	✗	✗
Coupling Beam	✓	✓[4]	✗
Slab	✓[5]	✗	✗
Basement wall	✗	✗	✗
Foundation	✗	✗	✗
Transfer Girder	✗	✗	--
	FORCED CONTROLLED ACTION- Elastic Behavior		
STRUCTURAL MEMBER	Under Moment	Under Shear Load	Under Axial Load
Shearwall	✗	✓	✓
Column	✗	✓	✓[6]
Frame Beam	✗	✓	✓
Coupling Beam	✗	✓[7]	✓
Slab	✗	✓[8]	✓[9]
Basement wall	✓	✓	✓
Foundation	✓	✓	--
Transfer Girder	✓	✓	--

[1] P-M-M yielding of wall base (on top of foundation or basement podiums), [2] P-M-M yielding of column base (on top of foundation or basement podiums),[3] Flexural yielding of beam ends, [4] Shear yielding of diagonally reinforced coupling beams, [5] Flexural yielding of slab-column connections, [6] Combined moment and axial load in gravity columns, [7] Shear of conventionally reinforced coupling beams, [8] In-plane shear in transfer and other diaphragms,[9] In-plane normal forces in diaphragms

2.3 Design Earthquake Load for PBD

In the design of structures, earthquake forces can be applied to a building model using a number of different approaches such as equivalent lateral forces, response spectrum-modal analysis, push-over analysis and time history analysis. Response spectrum-modal analysis is widely used in the linear elastic design of 3D structures.

In the design, base shear in both directions resulting from modal analysis cannot be lower than base shear found according to the equivalent earthquake load method. Due to the long fundamental period of tall building, base shear is usually the minimum base shear value found according to the equivalent earthquake load method. In linear elastic analysis, structure design using the response spectrum method according to DD2 earthquake level is preliminary design for PBD. In high-rise buildings, time history analysis is mandatory according to Turkish Earthquake Code in PBD used at DD1 or DD3 earthquake level. Push-over analysis is an alternative as long as detail requirements are met in PBD, but push-over analysis is not allowed in nonlinear analysis of high-rise buildings in TEC-2018.

11 horizontal ground motion records are required for the design check of structures for time-history analysis method. The correct selection of horizontal earthquake acceleration-time data sets containing both directions is important. In the selection of horizontal earthquake data sets, ground motion should be selected by taking into account similarities of the following headings:

- Similar spectral shape to target spectrum
- General tectonic regime
- Earthquake source mechanism properties, i.e., magnitude, fault mechanism, fault distance, rupture surface distance (R_{rup}), rising time,
- Propagation path, i.e., distance b/w active fault to site, directivity,
- Site conditions, i.e., soil properties, V_{s30},
- Effective duration of ground motion, $D_{\%5}$-$D_{\%95}$,
- PGV/PGA, arias intensity
- Scale factor closer to unity

Accordingly, 11 horizontal ground motion records are scaled according to the target spectrum. With the scaling, mean of combined spectrums of 11 recordings should be 30% greater than target spectrum components between periods of $0.2T_p$ and $1.5T_p$. Effective duration of selected earthquake recordings should not be shorter than 5 times the first period of structure or 15 sec. Since damping ratio in high-rise buildings

is less than 5% and around 2.5%, damping ratio of 2.5% should be taken into account in acquisition of scaling of earthquake records.

An appropriate damping ratio should be selected for structural models, after obtaining scaled earthquake ground motion records for time history analysis. In Turkish Earthquake Code-2018, it is recommended to choose a 2.5% damping ratio in high-rise buildings analysis under DD4-DD3 and DD1 earthquake level forces. For tall buildings, damping ratio approach is recommended in Figure 2.1. In this figure, MCE_R and SLE represent DD1 and DD4 levels in Turkish Code, respectively.

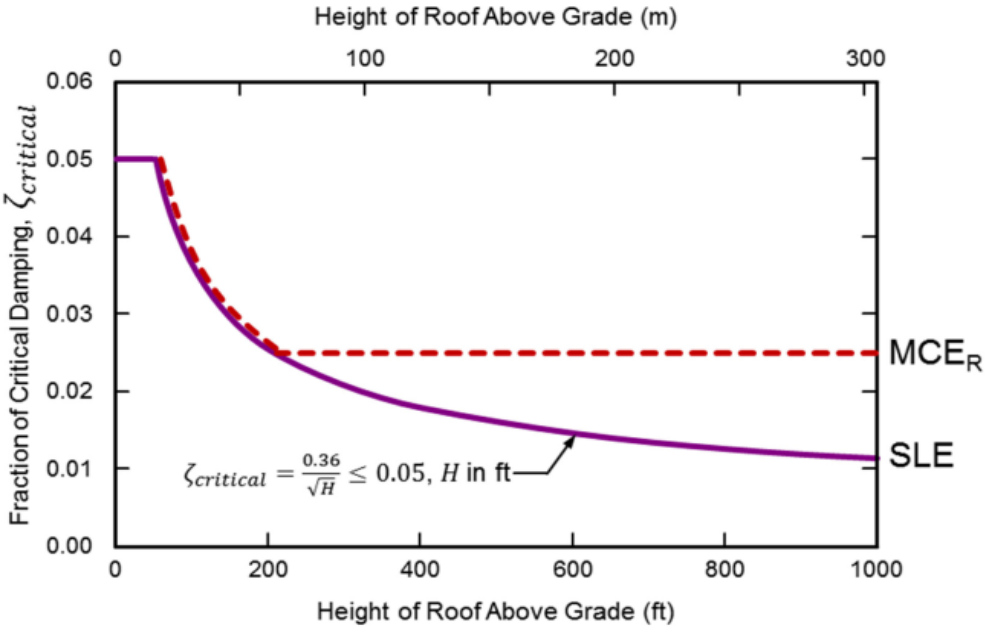

Figure 2.1 Viscous Damping Ratio vs. Building Height (Pacific Earthquake Engineering Center, 2017)

Equation-defining damping as a function of building height is shown in Equation 2.1. According to earthquake level analysis and building height, this damping ratio can be selected by using the following equation (PEER, 2017).

$$\zeta_{\text{critical}} = \frac{0.2}{\sqrt{H}} \leq 0.05 \text{ (H in m)} \qquad \textbf{(2.1)}$$

In nonlinear structural design, order of the load is important in analysis. Analysis is fulfilled under gravity loads followed by earthquake loading with the assumed gravity-loaded initial conditions. It should be mentioned that construction stage approach should also be taken into account in the gravity loads in high-rise buildings. In a nonlinear analysis, expected load and load combination that is closest to reality is generated. Accordingly, expected live load is generally 30% of required live loads in TS498. The load combination to be used generally in performance analysis is shown in Equation 2.2.

$$G + 0.3\ Q + E_d^{(H)} \quad \textbf{(2.2)}$$

Horizontal earthquake load appears in this load combination. The types of structures from which vertical earthquake force is taken are much less. In structures with vertical discontinuities and large spans, vertical earthquake forces can be taken into account. In time history analysis, earthquake recording in both orthogonal directions is defined simultaneously in modeling. After 11 earthquake records are given in directions perpendicular to each other, analysis is repeated after load directions are rotated to 90^o. In other words, a total of 22 different analysis are taken into account in PBD of tall buildings.

2.4 Structural Member Modeling

Nonlinear member behavior from test results and model results must be compatible in order to accurately model nonlinear behavior of the structural elements. This adaptation should ensure that correct modeling approach is obtained by harmonizing the analysis and results of experiment such as expected strength, expected deformation capacity, cyclic response, and strain profiles, energy consumption area, stiffness and strength degradation of each structural element. In nonlinear behavior of walls, it is also important whether uplift, rotation and effect of migration of neutral axis issues are taken into account in the modeling.

Modeling aspects for stiffness, strength and nonlinear mechanical and material aspects are presented next.

2.4.1 Effective Stiffness

The reduction of gross effective stiffness of structural elements compatible with experiments are given in Table 2.7 and Table 2.8 for design of building under different earthquake levels. In the models of building elements in linear or nonlinear design under earthquake force, effective stiffness values will be defined according to this table. In this way, reduction of lateral stiffness after cracking will be considered for building seismic analysis.

Table 2.7 Reinforced Concrete Effective Stiffness Values for Service-Level Models in ACI318-19 and TEC-2018

	Effective Stiffness for Service-Level Models (DD3-DD4 Level)		
Component	Axial	Flexural	Shear
Structural walls (out of-plane)	--	$0.25E_cI_g$ / **$(1.0E_cI_g)$** [1]	--
Basement walls (in-plane)	$1.0E_cA_g$	$1.0E_cI_g$	$0.4E_cA_g$
Basement walls (out of-plane)	--	$0.25E_cI_g$ / **$(1.0E_cI_g)$** [1]	--
Coupling beams	$1.0E_cA_g$	$0.07\ (l/h)\ E_cI_g \leq 0.3E_cI_g$ / **$(0.3E_cI_g)$** [1]	$0.4E_cA_g$
Non-PT transfer diaphragms (in-plane only)	$0.5E_cA_g$	$0.5E_cI_g$	$0.4\ E_cA_g$ / **$(0.32\ E_cA_g)$** [1]
PT transfer diaphragms (in-plane only)	$0.8E_cA_g$ / **(none)**[1]	$0.8E_cI_g$ /**(none)** [1]	$0.4E_cA_g$/ **(none)** [1]
Beams	$1.0E_cA_g$	$0.5E_cI_g$ /**$(0.7E_cI_g)$** [1]	$0.4E_cA_g$
Columns	$1.0E_cA_g$	$0.7E_cI_g$ [2] /**$(0.9E_cI_g)$** [1]	$0.4E_cA_g$

[1] Effective stiffness in TEC-2018 different from ACI318-19; [2] Stiffness in columns dependent in ACI 318-19 on axial load level so that $\geq 0.5A_gf_c$; $0.7E_cI_g$, $\leq 0.1A_gf_c$; $0.3E_cI_g$, $0.1A_gf_c \leq$, $\leq 0.5A_gf_c$; interpolation

Table 2.8 Reinforced Concrete Effective Stiffness Values for MCER-Level Models (DD1-DD2 Level) in ACI318-19 and TEC-2018

	Effective Stiffness for MCER-Level Models (DD1-DD2 Level)		
Component	Axial	Flexural	Shear
Structural walls (out of-plane)	--	$0.25E_cI_g$	--
Basement walls (in-plane)	$1.0E_cA_g$	$0.8E_cI_g$	$0.2E_cA_g$
Basement walls (out of-plane)	--	$0.25E_cI_g$	--
Coupling beams	$1.0E_cA_g$	$0.07\ (l/h)\ E_cI_g \leq 0.3E_cI_g$ / $\mathbf{(0.15E_cI_g)}$ [1]	$0.4E_cA_g$
Non-PT transfer diaphragms (in-plane only)	$0.25E_cA_g$	$0.25E_cI_g$	$0.1E_cA_g$
PT transfer diaphragms (in-plane only)	$0.5E_cA_g$/ **(none)**[1]	$0.5\ E_cI_g$/ **(none)** [1]	$0.2E_cA_g$/ **(none)** [1]
Beams	$1.0E_cA_g$	$0.3E_cI_g$/ $\mathbf{(0.35E_cI_g)}$ [1]	$0.4E_cA_g$
Columns	$1.0E_cA_g$	$0.7\ E_cI_g$ [2]	$0.4E_cA_g$

[1] Effective stiffness in TEC-2018 different from ACI318-19; [2] Stiffness in columns dependent in ACI 318-19 on axial load level so that for $\geq 0.5A_gf_c$; $0.7E_cI_g$, for $\leq 0.1A_gf_c$; $0.3E_cI_g$, for $0.1A_gf_c \leq$, $\leq 0.5A_gf_c$; interpolation

If structural walls or R/C columns are modeled with distributed fiber model, structural element deformation and cracking conditions are automatically defined without the need to use effective stiffness reduction coefficients. So, there is no effective stiffness reduction coefficients for the modeling of these members.

2.4.2 Expected Material Strengths

In nonlinear structure analysis, expected strength is used instead of concrete and reinforcement characteristic strength values. The relationship between expected material strength and characteristic strengths is given in Table 2.9. The expected strength utilization is used in all nonlinear calculations as well as in the modeling context.

Table 2.9 Expected Material Strengths

MATERIAL	EXPECTED STRENGTH
Concrete	f_{ce}= 1.3 f_{ck}
Reinforcing Steel	f_{ye}= 1.2 f_{yk}

2.4.3 Nonlinear Structural Member Model Types

There are different modeling forms of building elements in nonlinear analysis of structures. As the most basic distinction, nonlinear structural elements can be modeled under two main headings as lumped plastic hinge or distributed fiber model. Figure 2.2 shows representative views of modeling patterns suitable for a nonlinear hinge or nonlinear fiber approach.

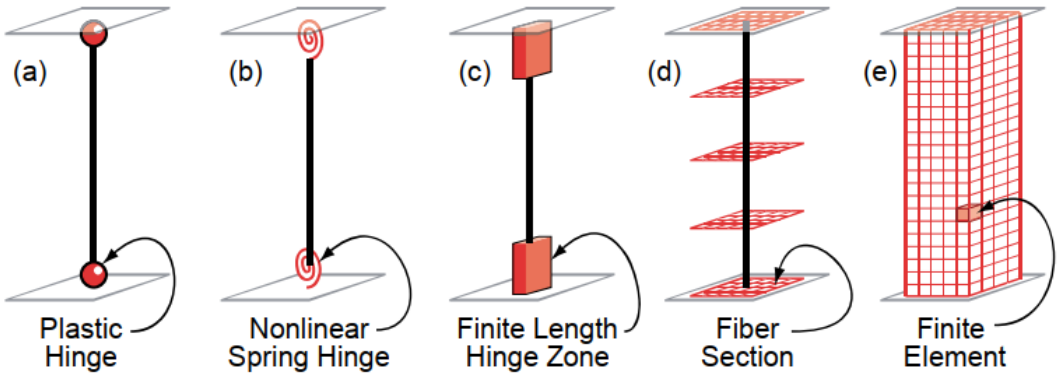

Figure 2.2 Nonlinear Modeling Types of Structural Members (PEER/ATC 72-1, 2010)

In Turkish Earthquake Code, use of lumped plastic hinge model is recommended for columns, and beams, while distributed fiber model approach is the preferred choice for wall elements.

i. Lumped Plasticity Model (Inelastic Hinge Model)

Nonlinear hinge is defined at column or beam ends in lumped plastic models. Force-deformation monotonic curves may be in the form of moment-rotation or force-displacement in the plastic hinge definitions. In addition to defining the yield, ultimate residual strengths and the corresponding rotations, cyclic response behavior compatible with experimental results should be defined in plastic hinge sections. Lumped plastic hinge model subjects are shown in Figure 2.3.

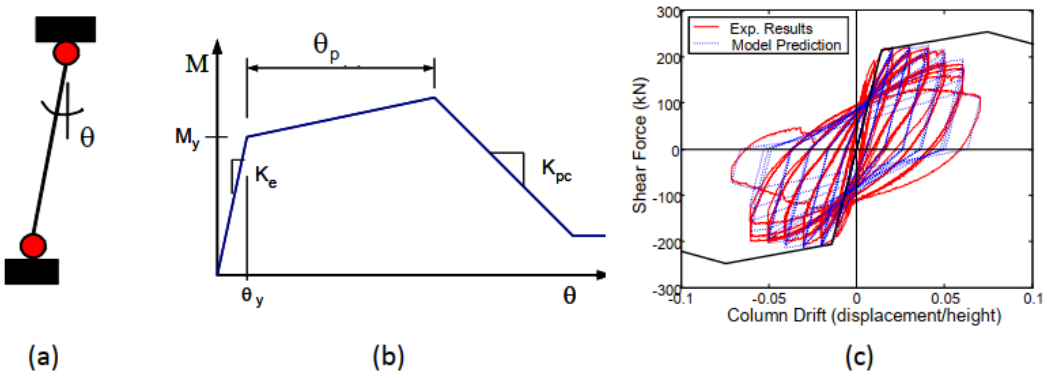

Figure 2.3 Lumped Plastic Hinge Model Subjects a) View of Lumped Plastic Hinge b) Monotonic Moment-Rotation Response of Plastic Hinge c) Cyclic Response of Plastic Hinge (PEER/ATC 72-1, 2010)

Plastic hinge positions of column and beam can be defined at the end of structural elements or in the middle part of plastic hinge length. In TEC (2018), identification at the exact end is allowed. The plastic hinge length (L_p) can be taken as half of the cross-sectional length (h) in which it works (TBDY-2018, 2018)

In ASCE-SI 41, for structural elements modeled with frame elements such as columns and beams, elastic section rigidity between plastic hinge parts allows definition according to cracked section rigidity reduction coefficients specified in Table 2.7 and Table 2.8. According to TEC (2018), effective stiffness should be defined according to a value calculated according to Equation 2.3. The yield rotation value in Equation 2.3 is determined by another empirical complex formula that includes the entire flexural, shear and bond slip effect. Therefore, according to

ACI318, the definition of effective cross-sectional rigidities provides greater convenience. American regulation also includes column effective rigidity reduction, which varies according to the axial load level.

$$(EI)_e = \frac{M_y}{\theta_y}\frac{L_s}{3} \quad \textbf{(2.3)}$$

ii. Distributed Plasticity

Distributed fiber model approach is obtained by both concrete and reinforcement steel filaments in the members according to their exact locations, amount and feature of fibers (Figure 2.4). While material model parameters are defined according to whether concrete is confined or unconfined, both tensile and under compression material parameter definitions are made in reinforcements. The model of behavior of concrete under tensile force can also be optionally included. The advantages of fiber models are direct inclusion of axial-bending interactions, combining section and finite element analysis, and better accuracy due to better section description. The key disadvantage is usually the cost of computations.

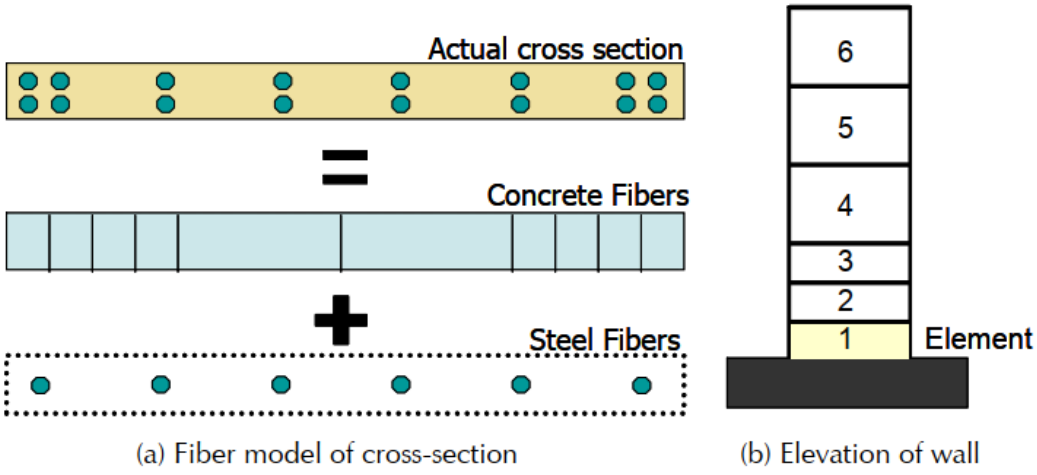

Figure 2.4 Distributed Fiber Model of Wall (PEER/ATC 72-1, 2010)

Wall structural members exhibit bending behavior in sections close to the foundation or just above podium section surrounded by basement walls. Nonlinear behavior is expected in this region, defined as the critical wall height, whereas elastic cracked

behavior occurs in the upper sections. For this reason, frequency of meshing in the section that continues along the critical wall height is important for the accuracy of results. Examples of fiber models along critical wall height are schematically shown in Figure 2.4.

The analytical modeling approaches for distributed fiber modeling approach. One of these analytical approaches is the phenomenological macroscopic or meso-scale model approach named as, multiple vertical line element model (MVLEM) proposed by Vulcano et al. (1988) (Figure 2.5a). The four-node wall panel element solution method, which is also used in the commonly used CSI Perform 3D software solution approach, is another method (Figure2.5b). Finally, according to the 2D microscopic finite element method analytical solution method, nonlinear behavior analysis of walls can be performed (Figure 2.5c).

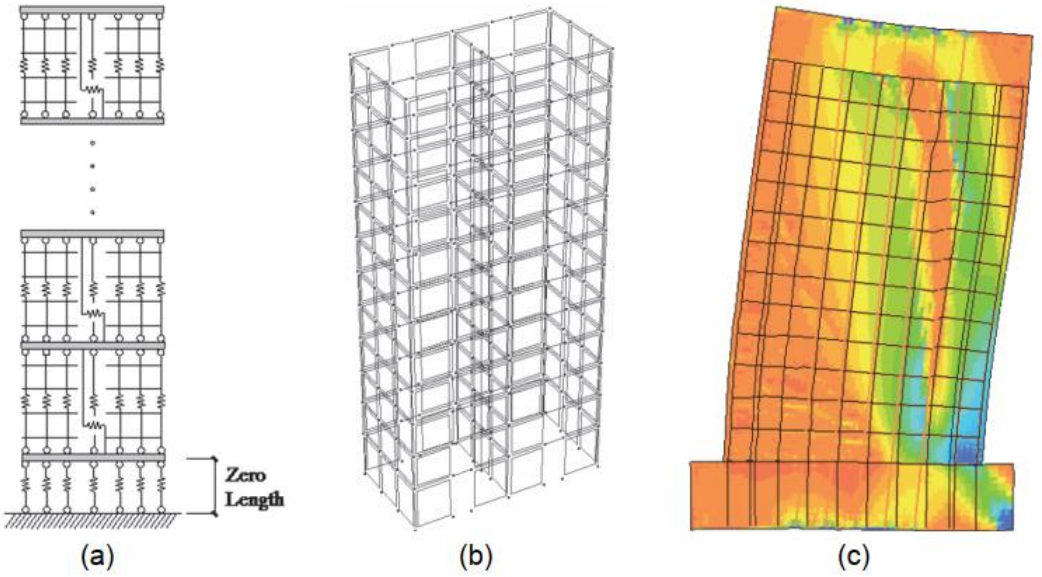

Figure 2.5 Analytical Model Types of Nonlinear Model of Walls(NIST, 2014)

Regardless of the method by which solution is made, the fact that the physical behaviors and subjects such as neutral axis migration, concrete tension stiffening, progressive crack closure, nonlinear shear behavior, effect of fluctuating axial force should be reflected in the nonlinear analysis of wall members in harmony with the results of experiment in modeling shows the success of analytical solution. In content

of this thesis, our solutions have been made according to "four-node wall panel" approach widely used by Perform 3D software.

There is no need to make effective stiffness adjustments within the in-plane behavior of building walls modeled with distributed fibers. Effective stiffness is automatically defined by assigned concrete and reinforcement steel fibers and material modeling is defined for these fibers. Reduction coefficients in Table 2.7 and Table 2.8 can be used for out-of-plane elastic behavior of walls. In addition, as if shear deformations caused by shear force in wall behavior are not more prominent in deformations caused by bending, shear behavior can be modeled as linear elastic.

Material models and material parameters used are an important issue that affects the nonlinear behavior of the wall model. In the Turkish regulation, a concrete material model proposed by Mander et.al is proposed (Figure 2.6a). Also, a recommended model for reinforcement is shown in Figure 2.6b. When different lack of issues such as behavior of reinforcement model under tension, compression and behavior embedded in concrete are considered, it is thought that it can be further elaborated in the regulation in terms of material model of reinforcement.

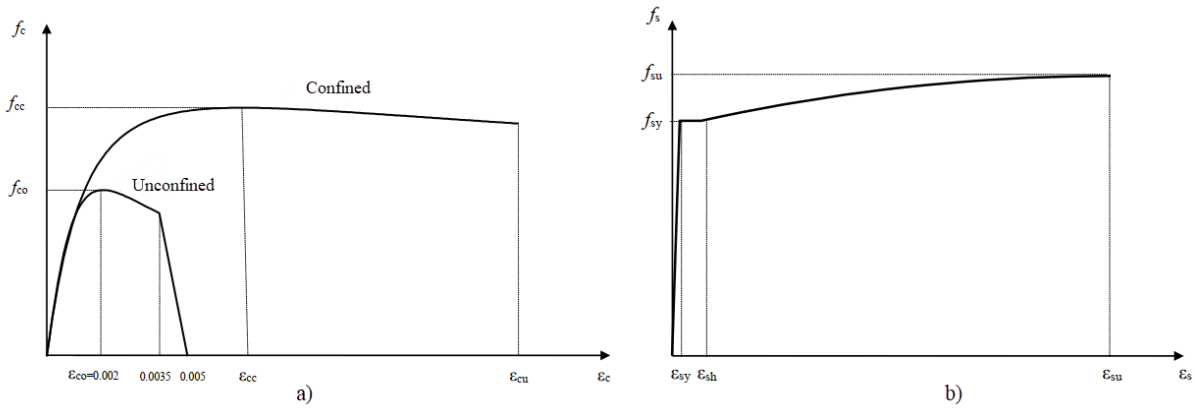

Figure 2.6 Material Models for Fibers a) Confined and unconfined concrete material model b) Reinforcing steel material model

Lastly, other issues to consider for nonlinear analysis of structures are P-delta effect and accidental eccentricity. Accidental eccentricity should be taken into account in the event of torsional irregularity.

2.5 Evaluating the Results of Performance Analysis

i. Drift Ratio

Maximum allowed relative story drift ratio for DD1 earthquake level and all earthquake records (2x11=22 earthquake records) is 0.045, according to Turkish Earthquake Code (2018) for tall buildings. In addition, the mean of absolute values of peak story drift ratios for 22 earthquake records cannot exceed 0.03. No story drift ratio is specified for non-linear structure design except for high-rise structures under DD1-level earthquake force. This deficiency in regulation is an important issue that needs to be eliminated.

For the service stage earthquake level (DD4), no story drift ratio limit is also specified in the Turkish Earthquake Regulation. 0.5% may be recommended for this (PEER (2017) recommendation).

ii. Strain & Rotation Limits

In nonlinear analysis of structures, strain check is performed under bending behavior when wall structural elements are modeled with distributed fiber approach for performance assessment. Design is satisfactory if both concrete and reinforcement strain checks remain within desired limits. On the other hand, under the bending behavior of structural elements such as columns and beams, which are defined as frame elements, it is usually customary to check if plastic rotation amounts remain within limits. Table 2.10 shows concrete and reinforcement strain limits and plastic rotation limits for different performance targets. In Equations 2.4, 2.5, and 2.6, concrete strain, reinforcement strain and plastic rotation limits are defined for the collapse prevention performance target, respectively. The concrete strain definition, ε_c^{CP}, in Equation 2.4 can be applied for rectangular form and confined section. ω_{we} specifies contribution of confined effect to concrete strain. The reinforcement strain, ε_s^{CP}, definition in Equation 2.5 for collapse prevention limit is specified as 40% of ultimate reinforcement strain. So, the reinforcement strain collapse prevention limit is

0.032 for common reinforcement usage, grade B420C, with a ϵ_{su} value of 0.08. This value is 0.05 according to American regulations and study reports (Pacific Earthquake Engineering Center, 2017). In Turkish regulation, the value of 0.032 remains less as a more conservative value.

Table 2.10 Strain and Rotation Limits for Different Performance Levels in TEC-2018 for PBD

	ε_c	ε_s	θ_p
Immediate Occupancy (IO)	0.0025	0.0075	0
Life Safety (LS)	0.75 ε_c^{CP}	0.75 ε_s^{CP}	0.75 θ_p^{CP}
Collapse Prevention (CP)	ε_c^{CP}	ε_s^{CP}	θ_p^{CP}

$$\varepsilon_c^{CP} = 0.0035 + 0.04\sqrt{\omega_{we}} \leq 0.018 \quad \textbf{(2.4)}$$

$$\varepsilon_s^{CP} = 0.4\,\epsilon_{su} \quad \textbf{(2.5)}$$

$$\theta_p^{CP} = \frac{2}{3}\left[(\phi_u - \phi_y)L_p\left(1 - \frac{0.5L_p}{L_s}\right) + 4.5\phi_u d_b\right] \quad \textbf{(2.6)}$$

The plastic rotation limits in the columns and beams are calculated as in Equation 2.6. According to this equation, plastic rotation depends on in addition to ultimate and yield curvature, shear span, plastic hinge length, and longitudinal reinforcement diameter. According to this general definition, plastic rotation limits should be determined at all column and beam nodes according to cross-sectional characteristics and reinforcement configuration. According to ASCE 41-17, instead of such a rotation limit recipe, there is an indication with charts based on equations and numerical limits.

Plastic rotational capacities vary greatly between frame beams and coupling beams. Therefore, rotational capacity defined by Equation 2.6 cannot be valid for link beams. In Turkish Earthquake Regulation, it seems essential to define separate plastic rotation capacity limits for coupling beams.

Strain and plastic rotation evaluations will be made according to the mean of the absolute maximums of the 22 earthquake analysis results. Evaluations for the response being ductile or brittle are completed according to the average values.

iii. Shear Stress Check

Strain and rotation limits are specified before for deformation-controlled inelastic behavior. For forced controlled elastic behavior, shear force capacity checks of wall and link beams that are active in earthquakes, must be made according to Equations 2.7 and Equations 2.8 according to TEC-2018.

$$V_e \leq 0.85 A_{\text{ch}} \sqrt{f_{\text{ck}}} \quad \text{(walls without openings)} \qquad \textbf{(2.7)}$$

$$V_e \leq 0.65 A_{\text{ch}} \sqrt{f_{\text{ck}}} \quad \text{(walls with openings)} \qquad \textbf{(2.8)}$$

In the performance analysis except for tall structures, mean of maximum absolute shear force values of 22 earthquake analyzes are used as demand. In the case of tall structures, shear force demand is determined by the value, $V_{e,mean+sta.dev.}$, in Equation 2.9.

$$1.2\, V_{e,mean} \leq V_{e,mean+sta.dev.} \leq 1.5\, V_{e,mean} \qquad \textbf{(2.9)}$$

CHAPTER 3

LINEAR ANALYSIS AND DESIGN OF THE CASE STUDY BUILDING

The structural design of a high-rise building under earthquake loads consists of two main stages, i.e., linear preliminary elastic design and nonlinear performance-based design according to TEC (2018). In the first stage, the structure is designed and detailed under earthquake loads by using linear elastic analysis. This preliminary stage is an input for the second stage, i.e., nonlinear performance-based design. Thus, all detailed calculations are completed in these two-stage calculations, and so the first preliminary design stage is verified and necessary additions for reinforcement are completed. The first stage design is a minimum and cannot be reduced in the second stage. In this section, we explain the preliminary design results of our case study tall building according to Turkish Earthquake Regulation-2018. After introducing our case study structure with flat slab system, the design results of shear walls and coupling beams that effectively meet earthquake loads, and the results of serviceability limits, i.e., drift ratios, are shown.

3.1 CASE STUDY BUILDING

3.1.1 Building Description and Dimensions

Selected case study tall building has a proper rectangular plan and does not have any horizontal or vertical irregularity. Typical floor plan dimensions of upper and basement floors are 51x42 m (Figure 3.1) and 77.6 m x 68.4 m (Figure 3.2) respectively. Height of the building is 112.4 m from top of the basement and 129.4 m from the foundation level. There are totally 32 floors which include 4 basement floors and 28 upper typical floors (Figure 3.3). Typical floor heights at basement and

upper part of the building are 3.4 m and 3.8 m respectively. Key dimensions describing the structure are given in Table 3.1.

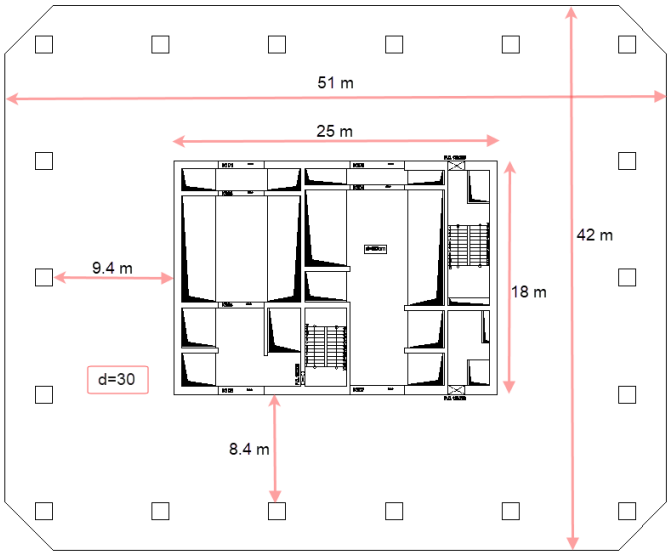

Figure 3.1 Case Study Building Typical Plan View

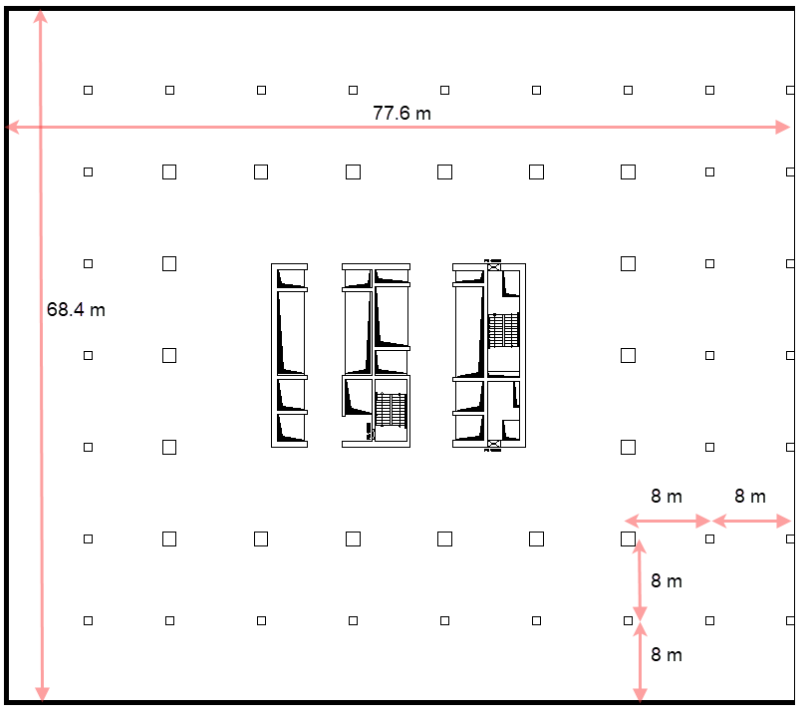

Figure 3.2 Basement Floor Plan

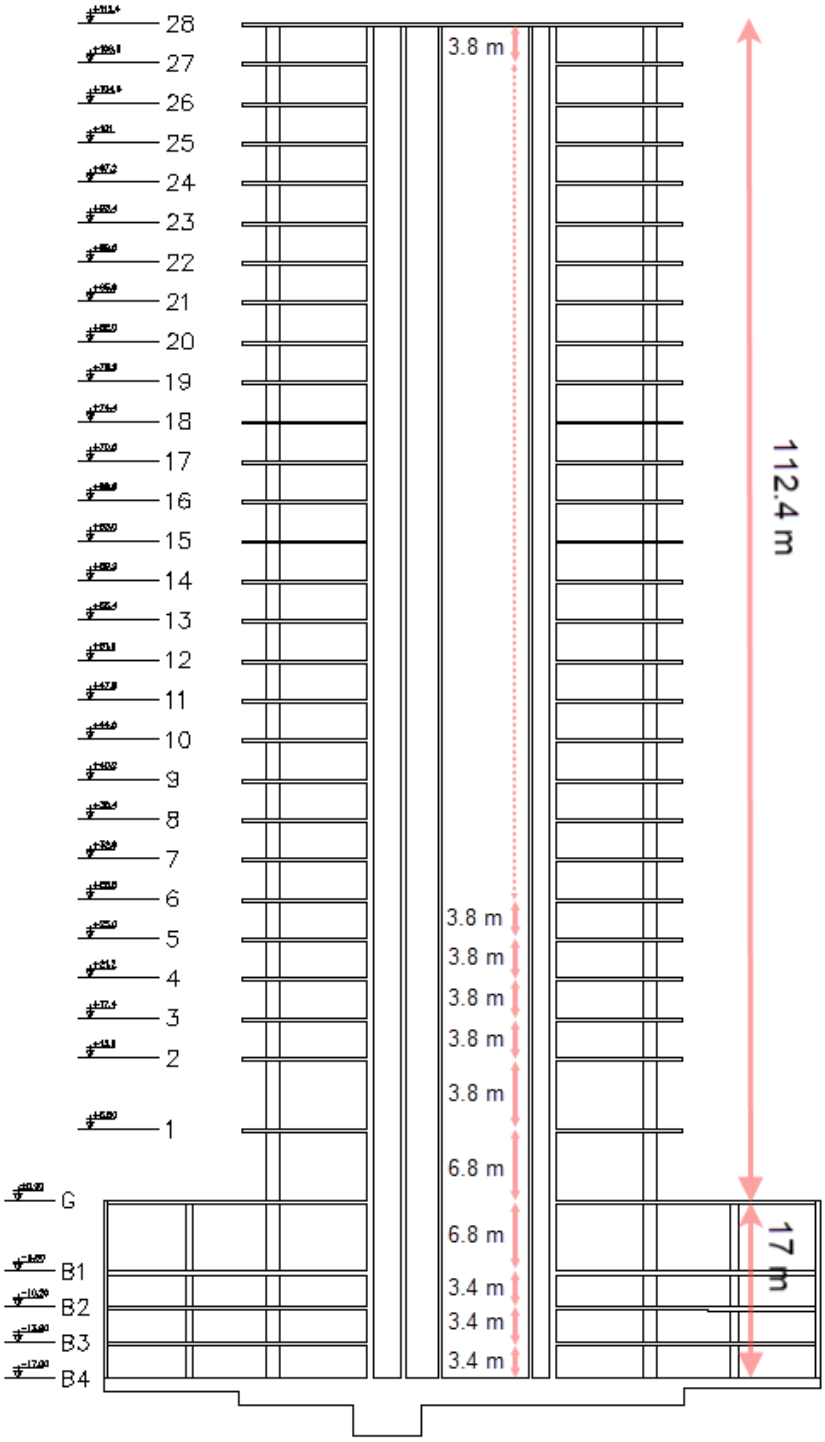

Figure 3.3 Section View of Case Study Building

Table 3.1 Summary Measurements about Case Study Building

Subject	Measurements
Floor plan dimensions for upper floors	51 m x 42 m
Floor plan dimensions for basement floors	77.6 m x 68.4 m
Height of the building above the foundation	129.4 m
Height of the building above the basement	112.4 m
Core wall plan dimensions	18 x 25 m
Max clear span at upper stories	9.4 m
Typical story height for the upper part of building	3.8 m
Typical story height at basement of building	3.4 m

3.1.2 Structural System of the Case Study Building

Case study building has a flat slab system and coupled with a core shear wall. Maximum clear span of the upper typical stories is 9.4 m. Slab thicknesses are 30, 35, and 40 cm at the basement floors respectively and 30 cm at the upper portions. The flat plate system is not considered as a lateral force resisting system, and it only acts as a vertical load bearing part. For this reason, the total earthquake load is assumed to be carried by reinforced concrete shear walls.

There is core wall group in the middle of the upper typical plan to resist earthquake load effectively (Figure 3.4). Core wall plan dimensions are 18x25 m (Figure 3.1). The ratio of the core wall length to the height of the building is a typical indicator for their behavior in high-rise buildings. These ratios are almost 1/ (4.5) for the x-direction and 1/ (6.2) for the y direction. Thickness of the walls inside the core varies from 30 cm to 90 cm according to the two selected seismic spectral acceleration spectrum, as will be described later in the thesis.

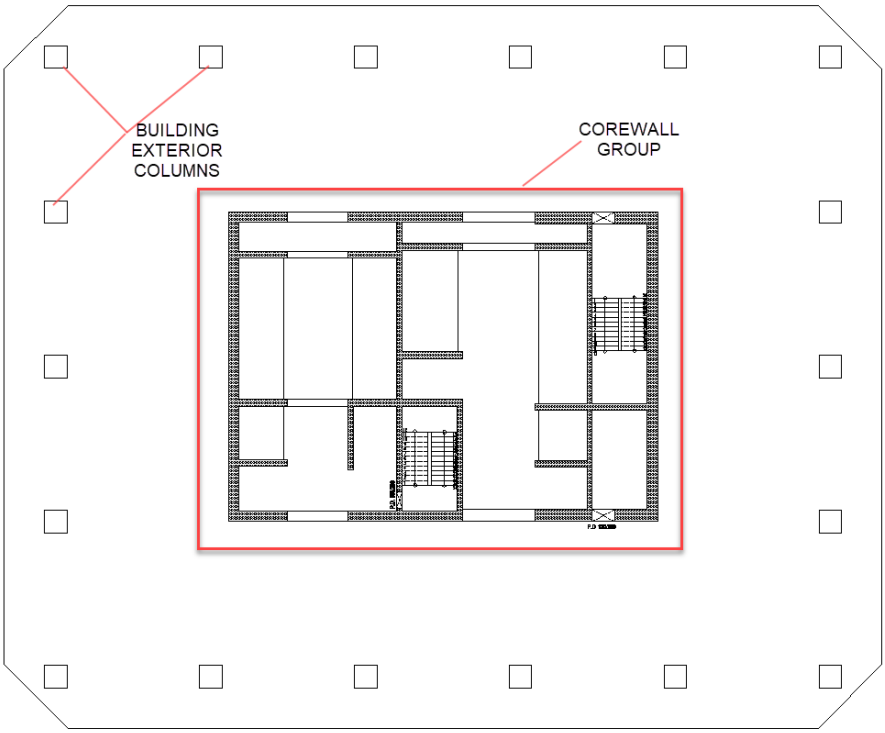

Figure 3.4 Typical High-Rise Building Plan

One additional axis of columns is placed around the core wall (Figure 3.4). Columns are conducted by using gravity loads. Columns dimensions for the outside zone of superstructure projection are 80x80 cm at basement level. The dimensions of the columns near the core wall range from 130x130 cm to 100x100 cm as they rise from the bottom up.

Link beams are important and effective structural members to meet the seismic loads by linking the core wall sub-groups. There are two types of link beams, LB1, LB2 in terms of height and height dimensions are 60 cm and 150 cm (Figure 3.5). Width of beams changes with wall width though height of building. Link beams can be detailed by conventional reinforcement or diagonal reinforcement.

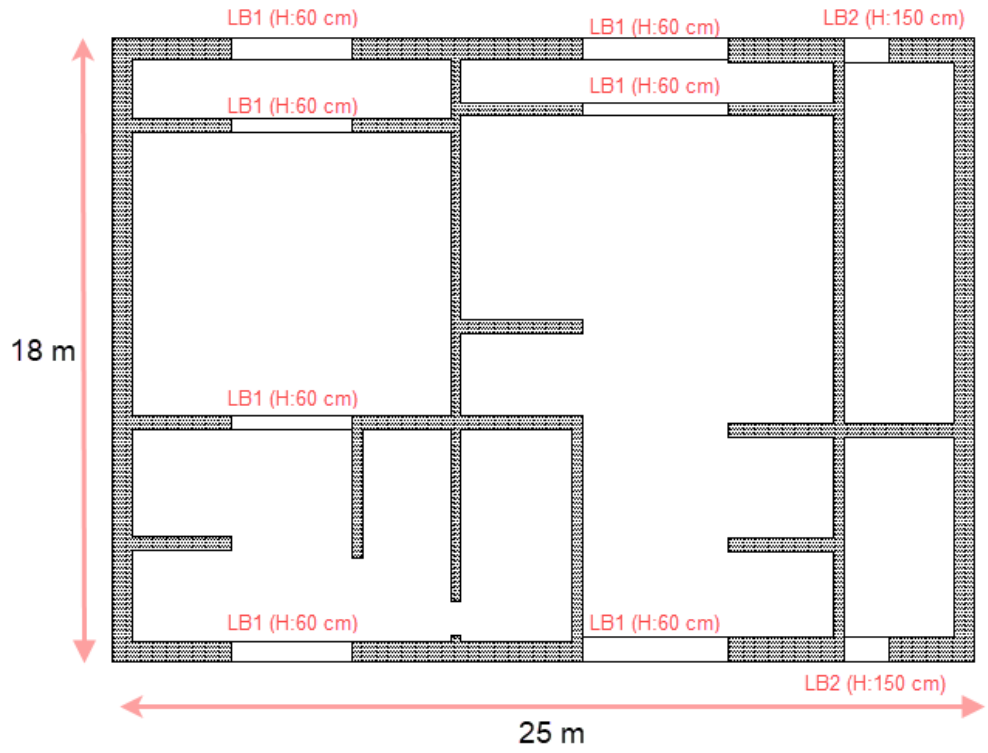

Figure 3.5 Beams Linking Core Wall Sub-groups

In the general architectural formations of high-rise buildings, there are basements and podium floors for usage such as car parking, mechanical area, shopping mall, etc. The most important features of these floors are that they are very rigid compared to the upper floors and are less ductile. In our case study structure, 4 basement floors constitute significant changes in building behavior and ductility. For buildings having very rigid basement floors, the design of building under the earthquake load is specifically described in the regulations. The fact that the basement walls in the case building are located on 3 sides constitutes a situation in which the structure will not behave fully symmetrically in the basement section (Figure 3.2). The fact that the basement walls are 3-sided and asymmetrical also causes asymmetrical behavior on the core walls in the middle of the plan.

3.2 DESIGN CRITERIA

3.2.1 Seismicity

The case study building is assumed to be located in regions with different seismicity. Two metropole cities namely Ankara and Istanbul, are selected for this purpose (Figure 3.6). All analyses and designs are made separately for these two locations. The coordinates of the locations, latitude and longitude, are shown in Table 3.2.

Table 3.2 Location Coordinates of Case Study Buildings

Location	Latitude	Longitude
Ankara	39,946536°	32,874877°
Istanbul	40,978182°	29,100889°

Figure 3.6 Case Building Locations: Ankara & Istanbul

3.2.2 Materials

3.2.2.1 Concrete

The following values are concrete grades for minimum concrete compressive strength values (MPa) of 28 days cylindrical test specimens. According to TEC-2018 7.2.5.1, concrete cannot be selected below C25 concrete class. The selected concrete classes acceptable according to TS EN 206 are given below;

- Foundation: C50
- Slab: C50
- Column and walls: C50

3.2.2.2 Reinforcement Class and Diameters

The selected reinforcement class is suitable according to TS708 and TEC-2018, 7.2.5.3.b. Mechanical properties of all reinforcement classes are shown at Table 2.3.

Table 3.3 Reinforcement Classes and Features (TS 708)

Class	B 420C	B 500B	B 500C	B500A
Yield Strength (min) R_e (N/mm^2)	420	500	500	500
Ultimate Strength (min) R_m (N/mm^2)	-	-	-	550
Ultimate Strength/Yield Strength Ratio R_m/R_e	≥1,15 <1,35	1,08 (min.)	≥1,15 <1,35	-
Experimental Yield Strength/Characteristic Yield Strength ratio $R_{e\ act}/R_{e\ nom}$ (max)	1,30	-	1,30	-
Ultimate Strain (min) A_5 (%)	12	12	12	5
Total strain under max loading (min) A_{gt} (%)	7,5	5	7,5	2,5

- Selected reinforcement class: B420C
- Used reinforcement diameters: 10, 12,14, 16, 18, 20, 22, 25, 26, 30

3.2.3 Design Loads

3.2.3.1 Gravity Loads

Self-weight is automatically calculated in the model by assigning γ=2.5 t/m3 for reinforced concrete.

Cover and live loads are given in Table 3.4. These loads are selected based on TS498, i.e., Turkish standard of design load for buildings. Live load reduction is applied according to the coefficients of office usage in Table 3.5.

Table 3.4 Cover and Live Loads of Case Study Building

	Level	Slab Thickness (cm)	Cover (t/m^2)	Live (t/m^2)	Usage
1-28 Floors	(+6,80/+112, 40)	30	0,25	0,35	Office
Ground Floor (G)	(+0,00)	40	0,60	0,50	Common
1.Basement Floor (B1)	(-6,80)	35	0,50	0,50	Shopping
2.Basement Floor (B2)	(-10,20)	30	0,25	0,50	Car Parking
3.Basement Floor (B3)	(-13,60)	30	0,25	0,50	Car Parking

Table 3.5 Live Load Reduction Factors

a) Houses, offices, etc.													
	# of Floors	1	2	3	4	5	6	7	8	9	10	11	12
1	Reduction (%)	0	0	0	20	40	60	80	80	90	40	40	40
2	Reduction Coeff. (β)	1	1	1	0,95	0,88	0,8	0,71	0,65	0,6	0,6	0,6	0,6
b) Factory, etc.													
3	Reduction (%)	0	0	0	10	20	30	40	40	40	20	20	20
4	Reduction Coeff. (β)	1	1	1	0,98	0,94	0,9	0,86	0,83	0,8	0,8	0,8	0,8

3.2.3.2 Earthquake Load

Earthquake ground motion levels are defined as DD1, DD2, DD3 and DD4 in the TEC-2018. Table 3.6 specifies the definition of earthquake ground motion levels. Linear elastic design, which is the 1st stage for tall buildings under earthquake load, is accomplished by using the DD-2 ground motion level.

Table 3.6 Earthquake Ground Motion Level

DD-1	Peak ground acceleration (PGA) with an exceedance probability of %2 in 50 years and 2475 years return period
DD-2	Peak ground acceleration (PGA) with an exceedance probability of %10 in 50 years and 475 years return period
DD-3	Peak ground acceleration (PGA) with an exceedance probability of %50 in 50 years and 72 years return period
DD-4	Peak ground acceleration (PGA) with an exceedance probability of %68 in 50 years and 43 years return period

Case study building is designed with linear elastic analysis according to the response spectrum curve data in Istanbul and Ankara for DD2 earthquake ground motion level. Important parameters define these response spectrum curves are given in Table 3.7.

Table 3.7 Response Spectrum Parameters

	S_1 (g)	S_{D1} (g)	S_S (g)	S_{DS} (g)	PGA (g)	T_A (s)	T_B (s)
Ankara	0.123	0.178	0.317	0.454	0.152	0.081	0.405
Istanbul	0.259	0.389	0.944	1.133	0.389	0.069	0.343

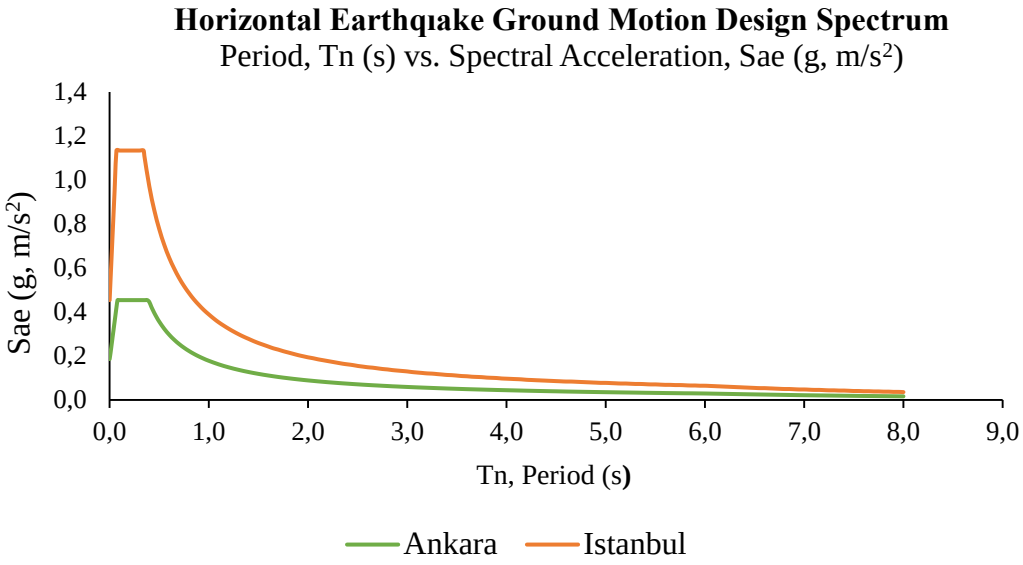

Figure 3.7 Horizontal Earthquake Ground Motion Spectrum

All the parameters for the design of the case building under earthquake load are selected from proper places according to TEC-2018. Seismic force resisting system, response modification factor (R) and overstrength factor (D) are selected from Table 4.1 at TEC-2018. According to Table 4.1, the seismic force resisting system is "A13. All the earthquake loads are resisted by special reinforced shear walls". Response modification factor (R), over-strength factor (D) and all other important selected design parameters are summarized in Table 3.8.

Table 3.8 Seismic Design Parameters

	Ankara	Istanbul
Site Class	ZC	ZC
Importance Factor (I)	1	1
Building Usage Class (BKS)	1	1
Earthquake Design Class (DTS)	3	1
Building Height Class (BYS)	1	1
Response Modification Coefficient (R_{top})	6	6
System Over-strength Factor (D_{top})	2.5	2.5
Response Modification Coefficient (R_{bottom}) at Basement	2.5	2.5
System Over-strength Factor (D_{bottom}) at Basement	1.5	1.5
Damping Ratio (ξ)	0.05	0.05

3.2.4 Load Combinations

According to TEC-2018, used load combinations are given below.

$$G + Q + 0.2S + E_d^{(H)} + 0.3E_d^{(Z)} \quad \textbf{(3.1)}$$

$$0.9G + H + E_d^{(H)} - \ 0.3E_d^{(Z)} \quad \textbf{(3.2)}$$

3.3 MODELING of CASE STUDY BUILDING

Case study building is modelled with a three-dimensional (3D) model by using ETABS 18.1.1 (Figure 3.8).

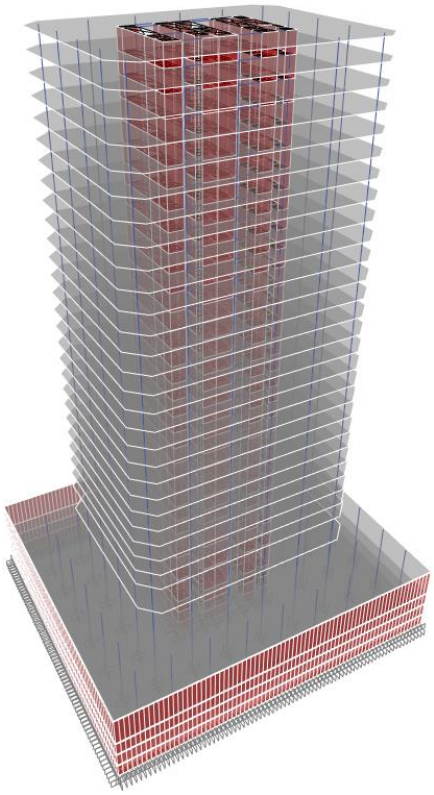

Figure 3.8 3D Model of Case Study Building at ETABS 18.1.1

The modeling approach considered herein is fully compliant with TEC-2018, and with the following assumptions;

- Finite element method (FEM) is used in the analysis of the model.
- While columns and beams are modelled as frame elements, slab and shear walls are defined by using shell elements.
- Shell and frame elements have all 6 degrees of freedom (u_x, u_y, u_z, r_x,r_y,r_z) at the node.
- In-plane forces and deformations are taken into account in the modeling of slab in order to accurately consider back-stay effects. (+/-) 0.05 % of the central mass to central rigidity difference as the accidental eccentricity is assigned automatically.
- Mass modelling is succeeded by ETABS automatically by assigning the load participation coefficient. Mass participation ratio for live load is taken as 0.3.
- Second order geometric nonlinear analysis, i.e., P-Delta effect, is taken into account in models by using moment magnification factor.
- Analysis type is the linear elastic analysis. The structural members' rigidities are reduced according to coefficients in Table 3.9 (TBDY-2018, 2018) when structure is designed only under load combinations, includes earthquake loads. For statical combinations excluding earthquake loads, the model should not contain rigidity reduction factors for structural elements.

Table 3.9 Rigidity Reduction Factors

Reinforce Concrete Structural Elements	Rigidity Reduction Factors	
Wall-Slab (In-Plane)	***Axial***	***Shear***
Wall	0.50	0.50
Basement wall	0.80	0.50
Slab	0.25	0.25
Wall – Slab (Out of Plane)	***Flexural***	***Shear***
Wall	0.25	1.00
Basement wall	0.50	1.00
Slab	0.25	1.00
Frame Element	***Flexural***	***Shear***
Link Beam	0.15	1.00
Frame Beam	0.35	1.00
Columns	0.70	1.00
Wall (equivalent frame)	0.50	0.50

3.4 DESIGN FLOW CHART

1-Determine Design Material Strengths

- Concrete Strengths
- Concrete Elastic Modulus
- Reinforcement Class

2-Determine Design Loadings

- Gravity Loads: Self-weight, live load, cover, partition walls, fillings, soil loads for recreation areas, parapets, facades
- Lateral Loads: Wind loads, earthquake loads, soil loads,

3-Determine Flat Slab Thickness under Design Loadings

- Design for deflection limits

- Design for enough slab strength
- Design for punching

4-Generating Building Models-1. MODEL (Design for DD2-EQ)

- Rigidity reduction factors of DD2 design EQ level is used for structural elements
- Determine EQ Base Shear: Period is very long for tall buildings so earthquake load is determined according to minimum code base shear for tall buildings.
- Design columns under load combinations includes EQ load
- Column axial stress should not exceed 0.35 f_{ck} under EO load combinations to determine preliminary column dimensions
- Check drift limit (use R=1) and other irregularities
- Check slabs for punching design under load combinations includes EQ load

5-Generating Building Models-2. MODEL (Design for DD2-EQ)

- Rigidity reduction factors of DD2 design EQ level remains the same with 1. MODEL
- For shear wall design, columns ends are assigned with moment releases where columns show more flexural behavior like just above podium or foundation.
- Column end moment release assignment causes period change and so if model base-shear scale factor is determined according to model period, rearrange the model base-shear scale factor to get minimum base shear. In other words, be sure that minimum code base shear should be valid in the 2. Model without any change.
- Shear wall axial stress should not exceed 0.4 f_{ck} under EO load combinations to determine preliminary shear wall dimensions
- Design shear walls under shear load with different wall leg parts inside core wall group.

- Determine shear wall boundaries and web regions and design shear walls under moment with different core wall group parts

6-Generating Building Models-3. MODEL (Design for Wind and Statical Gravity Load Combinations)

- No Rigidity reduction factors is used for structural elements or "0.5" factor can be used for lateral structural elements (beams, slabs) flexural rigidity.
- All structural members should be designed under wind and statical gravity load combinations

3.5 LINEAR ELASTIC ANALYSIS STAGE

3.5.1 Base Shear Calculation

Modal analysis method is mandatory in high-rise buildings (TBDY-2018, 2018). In order to obtain the correct earthquake force, some basic rules and equations requested by the regulation are specified in the details below.

Firstly, both x and y directions of earthquakes will be separately determined by the rule that the sum of effective modal masses should not be less than 95% of the total mass of the building (Equation 3.3).

$$\sum_{n=1}^{YM} m_{txn}^{(X)} \geq 0.95\, m_t \quad ; \quad \sum_{n=1}^{YM} m_{tyn}^{(Y)} \geq 0.95\, m_t \qquad \textbf{(3.3)}$$

Table 3.10 Mass Participation Ratio Results for Case Study Buildings

Mass Participation Ratio (%)	X	Y
Ankara	95.31	96.47
Istanbul	96.08	95.60

Base shear $V_{tx}^{(X)}$ obtained from modal analysis method for any (X) earthquake direction cannot be less than base shear $V_{tE}^{(X)}$ gotten from equivalent lateral load

method for tall buildings. In the event that it is for any (X) earthquake direction, $V_{tx}^{(X)} < V_{tE}^{(X)}$, all reduced internal forces and displacements obtained by modal analysis method are multiplied by the $\beta_{tE}^{(X)}$ *magnification coefficient.* This magnification factor is only applied for the upper part of the building over basement level.

$$\beta_{tE}^{(X)} = \frac{V_{tE}^{(X)}}{V_{tx}^{(X)}} \geq 1 \qquad \textbf{(3.4)}$$

Base shear from equivalent lateral load is calculated according to Equation 3.5 to compare base shear gotten from modal analysis method.

$$V_{tE}^{(X)} = m_t S_{aR}(T_p^{(X)}) \;\geq\; 0.04\, \alpha_H\, m_t I S_{DS}\, g \qquad \textbf{(3.5)}$$

$\boldsymbol{m_t}$: Total mass of the upper part of building calculated with Equation 3.6. Total mass of case building for the upper part is 81,636 tons.

$$m_t = \sum_{i=1}^{N} m_i \qquad \textbf{(3.6)}$$

$\boldsymbol{\alpha_H}$: This coefficient is correction factor to calculate minimum base shear for tall buildings and gotten from Equation 3.7. This coefficient is 0.93 for the case building having 112.4 m height.

$$\begin{aligned} \alpha_H &= 1.0 && H_N \leq 105 \text{ m} \\ \alpha_H &= 2.05 - 0.01 H_N && 105 \text{ m} < H_N \leq 155 \text{ m} \\ \alpha_H &= 0.5 && 155 \text{ m} < H_N \end{aligned} \qquad \textbf{(3.7)}$$

$\boldsymbol{T_p^{(X,Y)}}$: First natural period of building for any direction that is calculated with modal analysis by ETABS software (Figure 3.9). However, this period is restricted to Equation 3.8. This equation is advised by Prof. Ahmet Yakut to revise current regulation at TEC-2018. Periods are different for buildings in Ankara and in Istanbul because of different rigidity and dimensions of core walls.

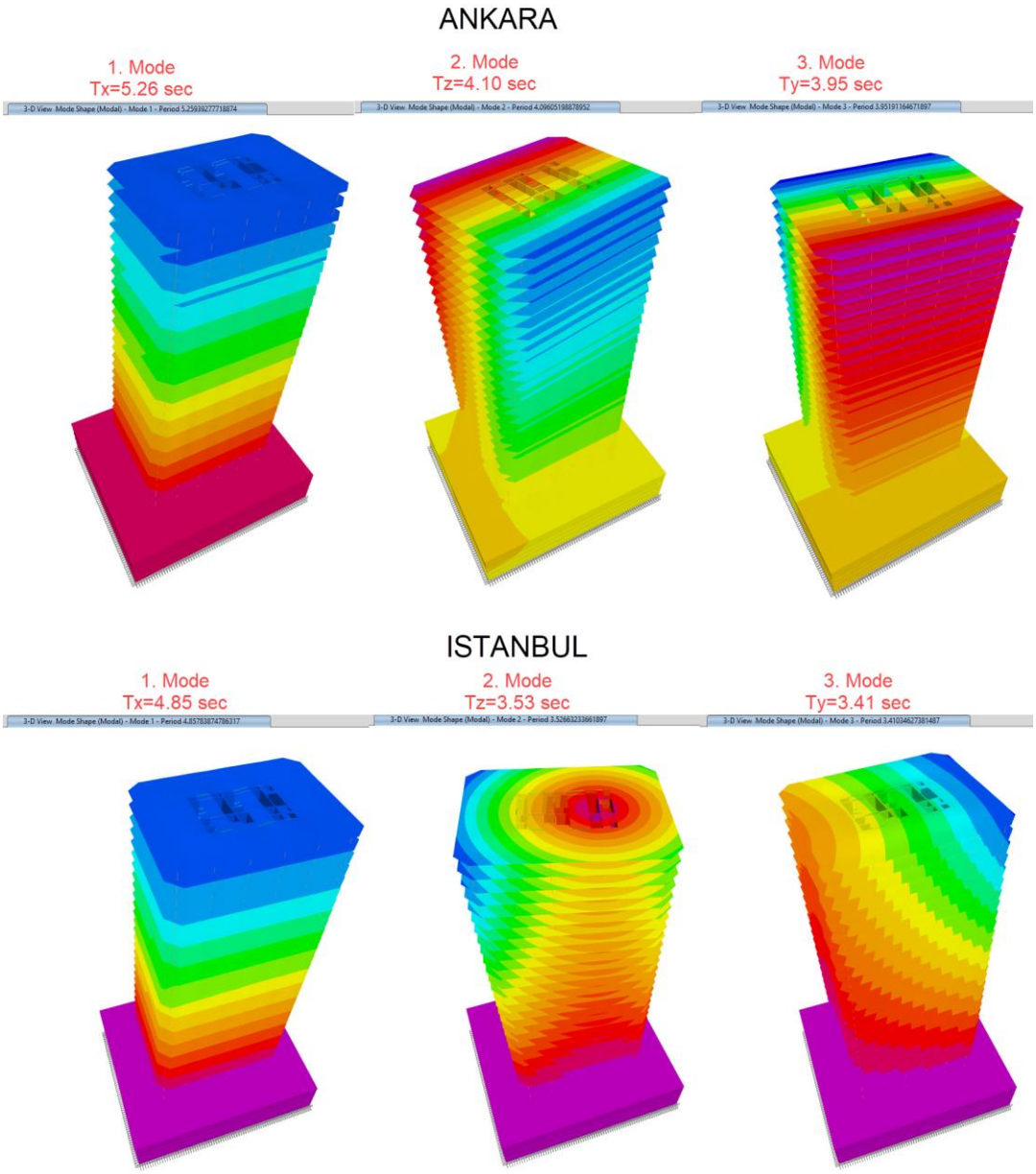

Figure 3.9 Natural periods of Case Study Buildings in Ankara and in Istanbul calculated with modal analysis by ETABS software

$$T_p^{(X)} < \mu\, T_{\mathrm{pA}} \qquad \textbf{(3.8)}$$

μ: This value is given Table 3.10.

Table 3.11 Natural Period Limit Factor (μ)

DTS	1	1a	2	2a	3	3a	4	4a
μ	1.4	1.4	1.4	1.4	1.5	1.5	1.6	1.6

It is advised by Dr. Yakut that T_{pA} is calculated by Equation 3.9, 3.10 and 3.11 for flat plate systems or buildings that having shear walls to respond all earthquake design load.

$$T_{pA} = C_t H_N^x \quad \textbf{(3.9)}$$

$$C_t = \frac{0.1}{\sqrt{A_t}} \leq 0.07 \quad \textbf{(3.10)}$$

$$A_t = \sum_j A_{wj}\left[0.2 + \left(\frac{\ell_{wj}}{H_N}\right)^2\right] \leq \sum_j A_{wj} \quad \textbf{(3.11)}$$

Design period is calculated for the buildings with these procedures and more detail information is shown in Table 3.12.

Table 3.12 Parameters for Design Period Calculation

	ANKARA		ISTANBUL	
	X	Y	X	Y
$T_{P,Etabs}^{x,y}$ (s)	5,26	3,95	4,85	3,41
C_t	0,07	0,07	0,07	0,07
x	0,75	0,75	0,75	0,75
$T_{pA}^{x,y}$ (s)	3,62	3,62	3,38	3,38
DTS	3	3	1	1
μ	1,5	1,5	1,4	1,4
$T_p^{x,y}{}_{max}$ (s)	3,62	3,62	3,38	3,38
$T_p^{x,y}{}_{Design}$ (s)	**3,62**	**3,62**	**3,38**	**3,38**

$S_{aR}\left(T_p^{(X,Y)}\right)$ is the spectral accelerations $S_{ae}(T)$ (Equation 3.12) reduced according to $R_a(T)$ (Equation 3.13, 3.14) depends on response modification factor (R) and importance factor (I) for natural periods of both direction, x and y (Figure 3.10):

$$S_{aR}(T) = \frac{S_{ae}(T)}{R_a(T)} \tag{3.12}$$

$$R_a(T) = \frac{R}{I} \qquad T > T_B \tag{3.13}$$

$$R_a(T) = D + \left(\frac{R}{I} - D\right)\frac{T}{T_B} \qquad T \le T_B \tag{3.14}$$

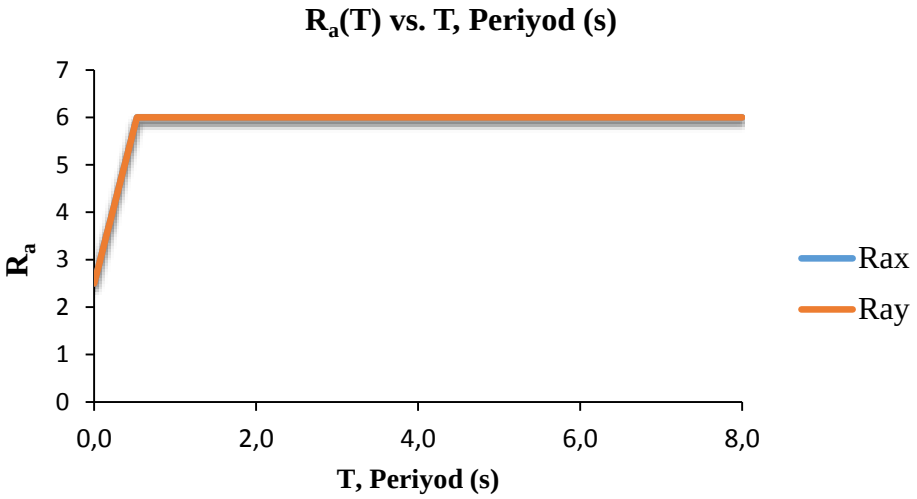

Figure 3.10 Response Modification Factor (R_a) vs. Period (T) Graph

Design base shear forces are calculated for case buildings located in Ankara and in Istanbul with all these regulations and Equations from 3.3 to 3.14. Summary results are given in Table 3.13.

Table 3.13 Base-shear Calculation Parameters and Results

	ANKARA		ISTANBUL	
	X	Y	X	Y
m_t (t)	87589		87589	
S_{DS}	0.454	0.454	1.134	1.134
$T_p{}^{x,y}{}_{modal}$ (s)	5.26	3.95	4.85	3.41
$T_p{}^{x,y}{}_{design}$ (s)	3.62	3.62	3.38	3.38
R_{ax} ($T_p{}^{x,y}$)	6		6	
S_{ae} ($T_p{}^{x,y}$)	0.049	0.049	0.115	0.115
S_{aR} ($T_p{}^{x,y}$)	0.008	0.008	0.019	0.019
$\alpha_{h,x,y}$	0.93		0.93	
$V_{tx,y}$ (ton-f)	461	791	1221	2277
$V_{tE}{}^{x,y}$ (ton-f)	1473	1473	3679	3679
$\beta_{tE}{}^{(x,y)}$	3.20	1.86	3.01	1.62
$V_{t,d\ x,y}$ (ton-f)	**1473**	**1473**	**3679**	**3679**

3.5.2 Modeling Details

Case study buildings are structures with both having flat plate systems and relatively more rigid basement parts. For these two exceptions, special place is reserved for both loading and analysis in the TEC-2018.

For buildings with flat plate systems, it is stated that all earthquake loads should be carried by ductile shear walls. In order to achieve this situation, a two-stage earthquake calculation is applied. In stage one, the upper and lower parts of the columns will be released, while in stage two, these joints are canceled and a model having monolithic joints will be obtained and two types of models are obtained, and these models are shown in Figure 3.11 and Figure 3.12. The most important issue to be considered here is that the behavior and periods of the structure changes if the columns joints are released from the top and bottom parts of them. This causes a change in the base shear of the building for the model with released joints of columns. Arrangement should be made in the Model-B (Figure 3.12) with released joints of columns so that the base shear force is not lower than the first determined base shear force. In our case structures, column joint release is made only for over

basement level. Because the structure behaves in a ductile behavior from this point on. Due to the basement walls, no release is applied in any joints of the columns in the basement part of the building, which has a rigid and low-ductile behavior. While the internal forces in structural elements are selected as the most unfavorable in both models in terms of design, the relative floor displacement should be controlled in the model where the columns joints are monolithic. The values are taken into account as the reactions required for the design of the core walls and link beams create more unfavorable reactions in the model in which the columns joints are released. In the column design, internal forces in the Model-A (Figure 3.11) in which columns joints are not released are taken into account.

Another special issue in case study building is that while there is a very rigid basement part in the lower sections of the buildings, the structure has a more ductile behavior over the basement level. This situation requires the earthquake force to be obtained by applying different system over-strength factor (D) and response modification coefficient (R) to masses above and below the basement level of the structure. Two different models have been created to achieve this, i.e., Model-B (Figure 3.12) and Model-C (Figure 3.13). In Model-C, the masses in the basement part of the structure are only entered into dynamic modal analysis. In the Model-B, only the masses in the upper parts of the structure enter dynamic modal analysis. While response modification coefficient (R) is 2.5 and system over-strength factor (D) is 1.5 for the Model-C, response modification coefficient (R) is 6 and system over-strength factor (D) is 2.5 at the Model-B. In addition, the previously mentioned column joint release principle is valid at the Model-B because of the flat plate system.

ETABS models and usage conditions created according to the regulations are more clearly explained individually with figures below.

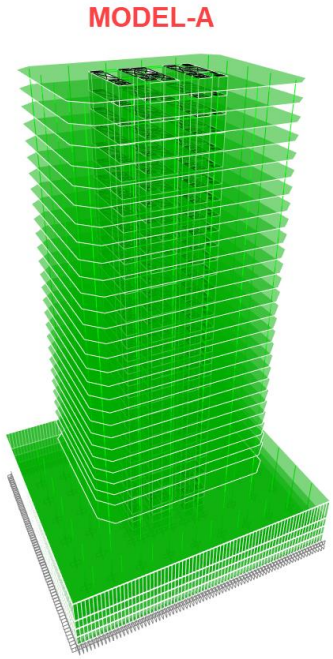

Figure 3.11 Model-A

- Monolithic column joints
- Tx and Ty are firstly determined
- Modal analysis base shear result just over basement is compared with minimum equivalent base shear
- Results of G+Q vertical load combination part is taken from this model for G+Q+$E_{x,y}$ design combination because of column joint releases of other model.
- Story drift checks are carried out with R=1.
- Column design is done with this model and R=6 assignment

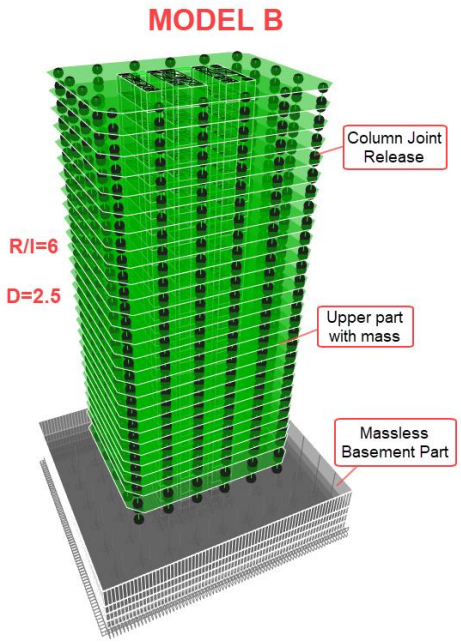

Figure 3.12 Model-B

- Upper part is assigned with mass and basement part is massless.
- Only column joints at the upper part are released
- R/I=6 and D=2.5
- Tx and Ty change. Base shear is revised with new $\beta_{tE}^{(X,Y)}$ *magnification coefficients* according to the first model results.

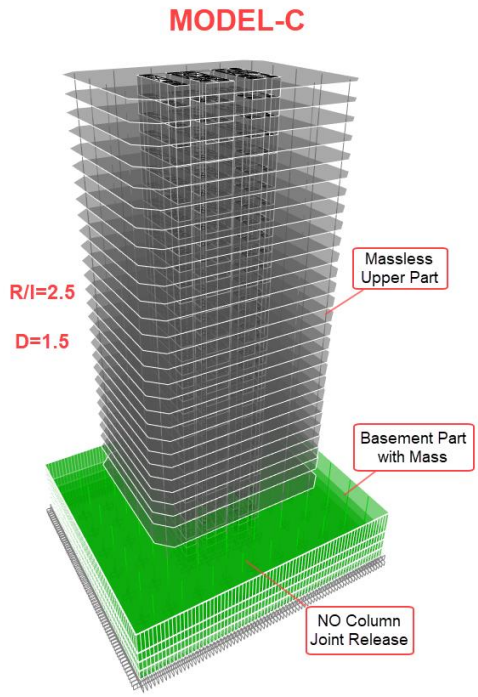

- The upper part is massless and basement part is only assigned with mass.
- All column joints are monolithic.
- R/I=2.5 and D=1.5
- Tx and Ty change. Base shear calculated with modal analysis is valid and no need $\beta_{\mathrm{tE}}^{(X,Y)}$ *magnification coefficients* usage.

Figure 3.13 Model-C

Shear walls and link beams design are carried out with the sum of reactions gotten from Model B and Model C (Figure 3.14).

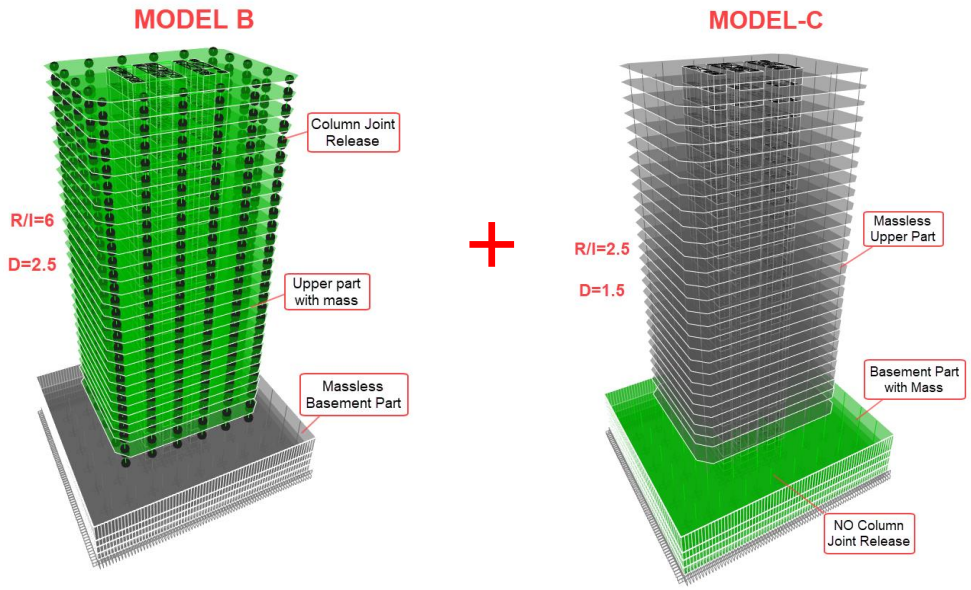

Figure 3.14 Etabs Models Used for Shear wall and Link Beam Design

3.6 DESIGN OF SHEAR WALLS AND LINK BEAMS

As mentioned before, the main structural elements respond to all earthquake loads are shear walls and link beams for buildings having flat slab system. This portion's combination of shear-wall groups and link beams are mainly defined as "core tube" of tall buildings. The tube of case study building is designed according to TEC-2018.

3.6.1 Shear Wall Design of Case Study Building

3.6.1.1 Design Regulations of Ductile Shear Walls in TEC (2018)

Behaviors of structural elements in tall are mainly classified as linear behavior and nonlinear ductile behavior according to capacity design principles. While shear walls and link beams just over basement level are expected to exhibit nonlinear ductile behavior under axial load and moments (A-Mx-My), on the other hand; axial load and shear forces of columns, slabs, basement walls and foundations show linear brittle behaviors. According to the capacity design approach, all brittle and linear designs like punching, shear load transfers between slab and walls under shear and axial loads should be avoided to prevent the collapse of a building.

All vertical load bearing structural elements are designed to be ductile for tall buildings (TBDY-2018, 2018). Key aspects of shear wall design are limiting the axial load, providing sufficient shear capacity and enabling ductile response through detailing.

Shear walls dimensions are mainly determined by the axial load limitation rule and shear design of walls. Axial load, N_{dm} determined by design load combination includes earthquake load (G+Q+E), should supply the condition at Equation 3.15.

$$A_c \geq N_{\mathrm{dm}}/(0.35 f_{\mathrm{ck}}) \quad \textbf{(3.15)}$$

Design shear load, V_e, **s**hould be less than shear capacity**,** $\mathrm{V_r}$ (Equation 3.16).

$$V_e \leq V_r \quad \textbf{(3.16)}$$

Maximum shear capacity is limited by Equations 3.17 and 3.18.

$$V_e \leq 0.85 A_{ch} \sqrt{f_{ck}} \quad \text{(Walls without spacing)} \quad \textbf{(3.17)}$$

$$V_e \leq 0.65 A_{ch} \sqrt{f_{ck}} \quad \text{(Walls with coupling beams)} \quad \textbf{(3.18)}$$

Lateral reinforcement amount is determined according to Equation 3.19.

$$V_r = A_{ch}(0.65 f_{ctd} + \rho_{sh} f_{ywd}) \quad \textbf{(3.19)}$$

Although the wall design under shear load is carried out according to Equation 3.19, frictional shear capacity of the wall should also be checked by using Equation 3.20. In the case of an inadequacy, it is the most practical approach to increase the capacity of frictional shear capacity by increasing the vertical reinforcements of the shear-walls.

$$V_e \leq f_{ctd} A_c + \mu A_s f_{yd}$$
$$V_e \leq \min[0.2 f_{ck} A_c; \quad (3.3 + 0.08 f_{ck}) A_c] \quad \textbf{(3.20)}$$

Shear loads are multiplied by system over-strength factors D_{bottom}=1.5 and D_{top}=2.5 for design shear loads. Term, $\beta_v \frac{(M_p)_t}{(M_d)_t}$, at Equation 3.21 can be taken by 1.0 for structural system having shear walls met all earthquake loads. However, over-strength factor D is used in our design.

$$V_e = \beta_v \frac{(M_p)_t}{(M_d)_t} V_d \quad \textbf{(3.21)}$$

3.6.1.2 Shear Wall Elastic Design Results of Case Study Building

Dimensions and labels for shear design of core wall of case building in Ankara and in Istanbul are shown in Figure 3.15 and Figure 3.16 respectively. Boundaries of shear walls are arranged according to code regulations. Boundary, web arrangements and longitudinal reinforcement of them are shown in Figure 3.17 and Figure 3.18 for

the case study buildings in Ankara and in Istanbul, respectively. According to minimum vertical reinforcements (ρ_{min}=0.0025) in TEC-2018, practically used longitudinal reinforcement for the web of shear walls is shown in Table 3.14. In addition, lateral design reinforcements of walls of case study building in Ankara and in Istanbul are shown in Table 3.15 and Table 3.16.

Table 3.14 Minimum Vertical Reinforcements of Web of Shear walls

Width of Wall (cm)	30	40	50	60	80	90
Web Vertical Reinforcement	Φ12/20	Φ12/20	Φ14/20	Φ14/20	Φ16/20	Φ18/20

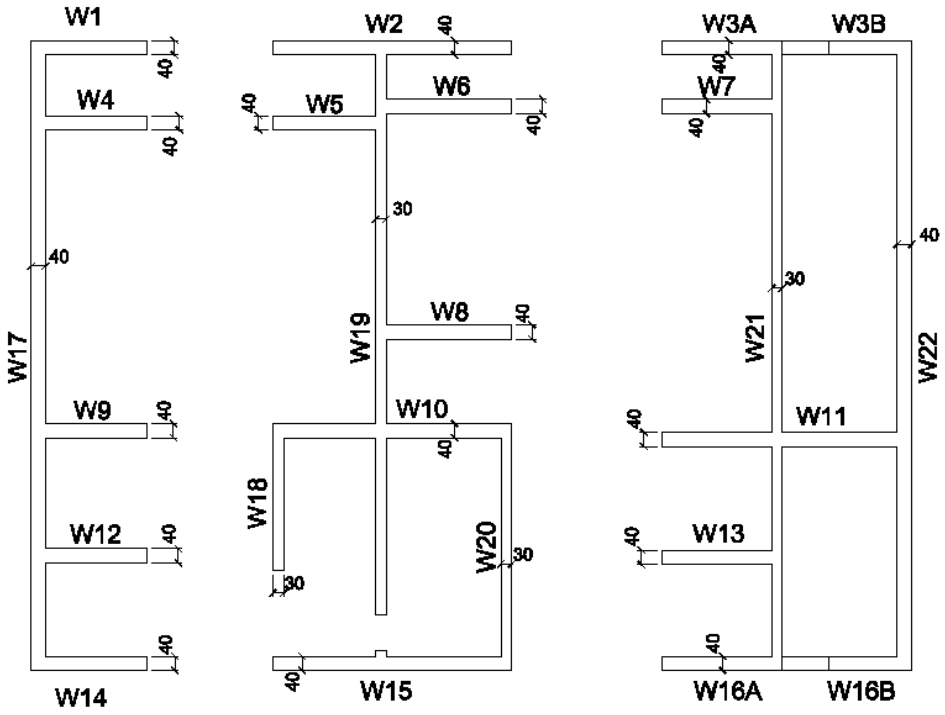

Figure 3.15 Thickness and Labels of Walls of Case Building in Ankara

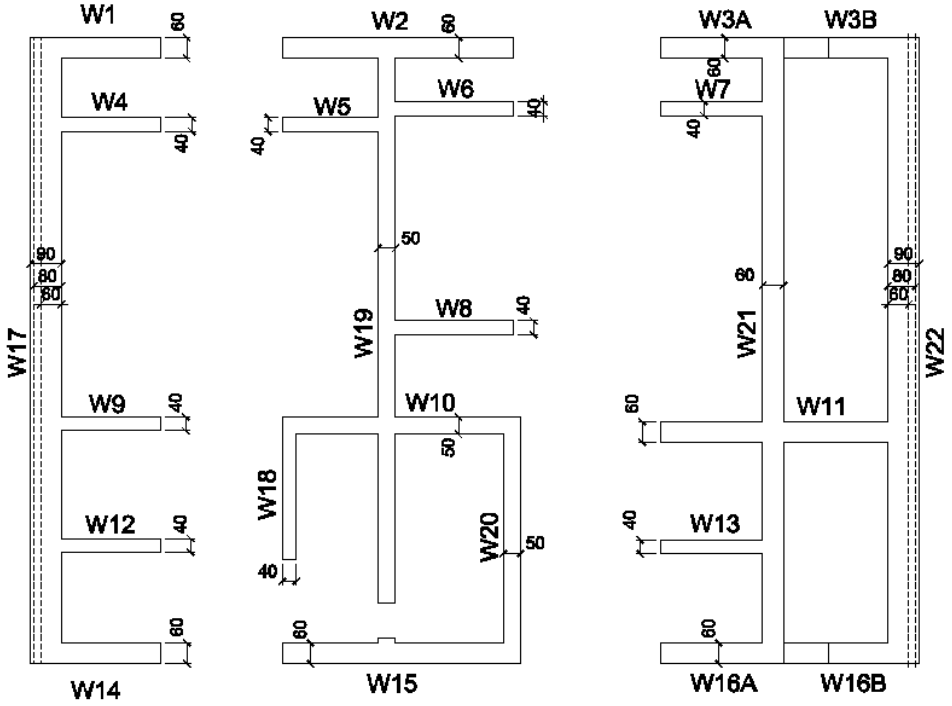

Figure 3.16 Thickness and Labels of Walls of Case Building in Istanbul

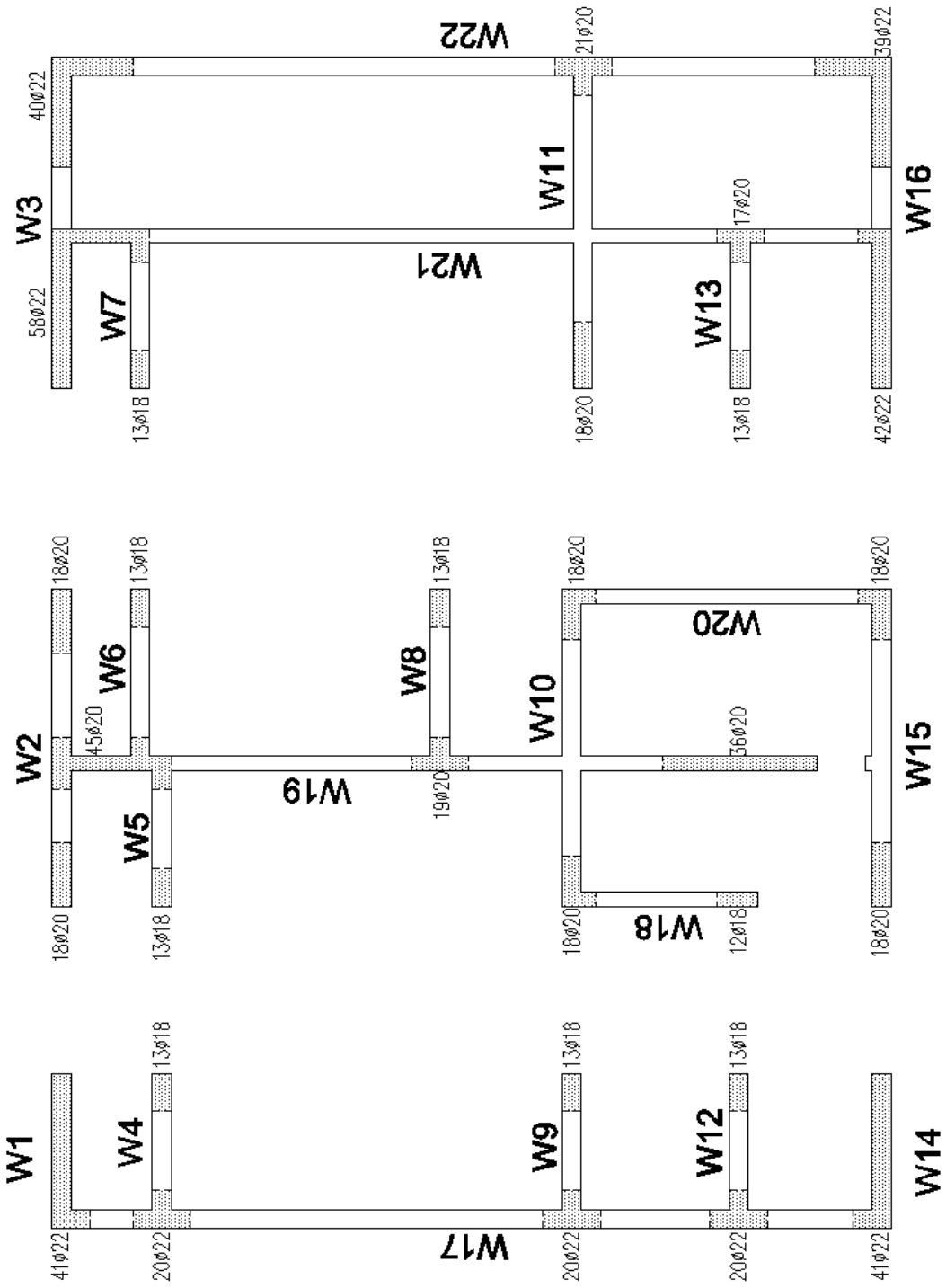

Figure 3.17 Boundary, Web Placement and Boundary Reinforcement of Shear walls of Building in Ankara

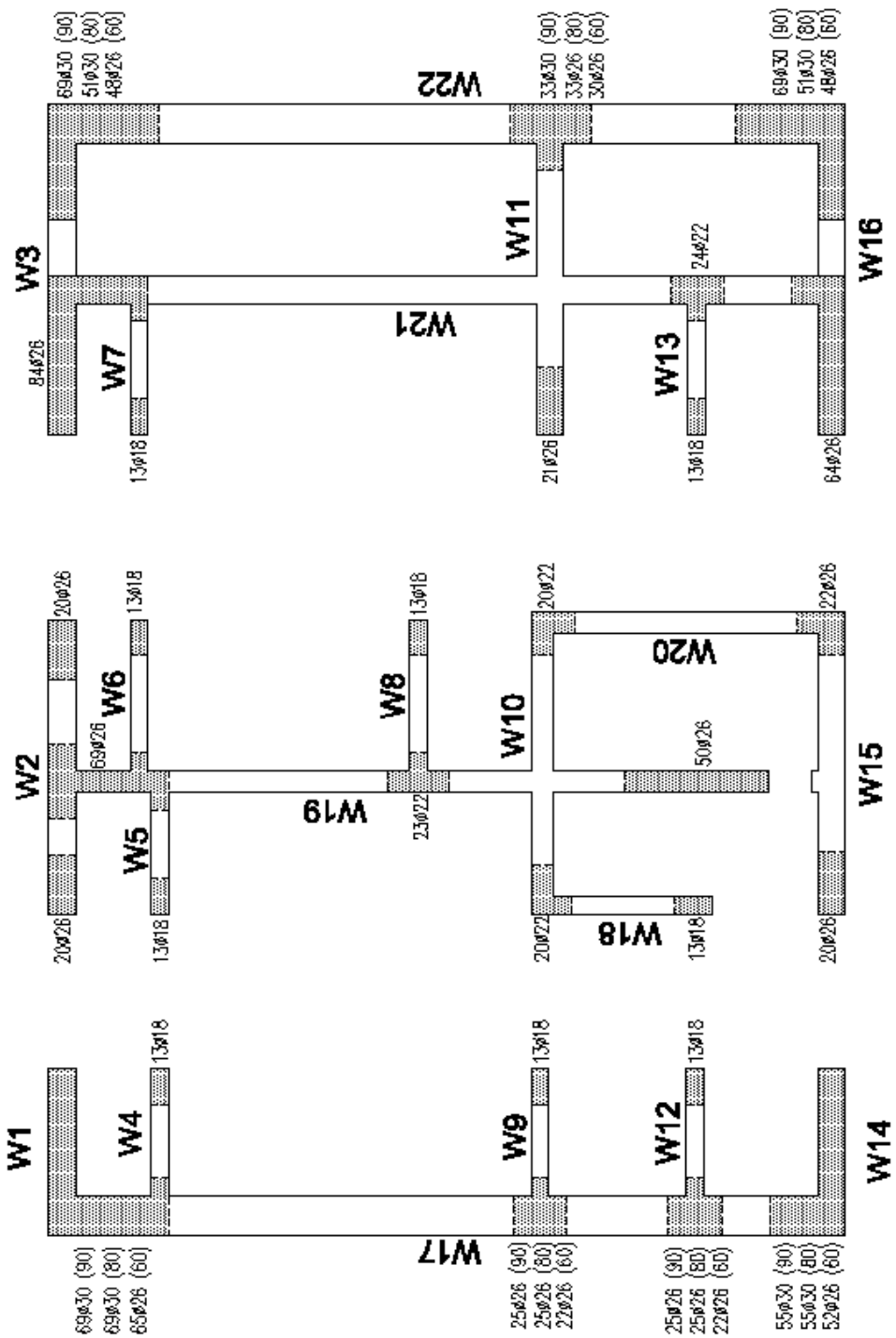

Figure 3.18 Boundary, Web Placement and Boundary Reinforcement of Shear walls of Building in Istanbul

Table 3.15 Lateral Reinforcement of Walls of Case Building in Ankara

			STORIES			
LABEL	Width (cm)	Length (cm)	1--4	5--6	7--9	10--32
W1	40	345	Φ12/20	Φ12/20	Φ12/20	Φ12/20
W2	40	665	Φ12/20	Φ12/20	Φ12/20	Φ12/20
W3	40	585	Φ12/20	Φ12/20	Φ12/20	Φ12/20
W4	40	345	Φ12/20	Φ12/20	Φ12/20	Φ12/20
W5	40	315	Φ12/20	Φ12/20	Φ12/20	Φ12/20
W6	40	380	Φ12/20	Φ12/20	Φ12/20	Φ12/20
W7	40	335	Φ12/20	Φ12/20	Φ12/20	Φ12/20
W8	40	380	Φ12/20	Φ12/20	Φ12/20	Φ12/20
W9	40	345	Φ12/20	Φ12/20	Φ12/20	Φ12/20
W10	40	665	**Φ12/19**	**Φ12/19**	Φ12/20	Φ12/20
W11	40	715	**Φ12/18**	**Φ12/14**	**Φ12/15**	Φ12/20
W12	40	345	Φ12/20	Φ12/20	Φ12/20	Φ12/20
W13	40	335	Φ12/20	Φ12/20	Φ12/20	Φ12/20
W14	40	345	Φ12/20	Φ12/20	Φ12/20	Φ12/20
W15	40	665	Φ12/20	**Φ12/18**	Φ12/20	Φ12/20
W16	40	585	Φ12/20	Φ12/20	Φ12/20	Φ12/20
W17	40	1800	Φ12/20	Φ12/20	Φ12/20	Φ12/20
W18	30	410	Φ10/20	Φ10/20	Φ10/20	Φ10/20
W19	30	1625	**Φ12/20**	Φ10/20	Φ10/20	Φ10/20
W20	30	710	**Φ12/20**	Φ10/20	Φ10/20	Φ10/20
W21	30	1800	**Φ12/14**	Φ10/20	Φ10/20	Φ10/20
W22	40	1800	**Φ12/10**	Φ12/20	Φ12/20	Φ12/20

Table 3.16 Lateral Reinforcement of Walls of Case Building in Istanbul

			STORIES								
Label	Width (cm)	Length (cm)	1--3	4	5	6	7--9	10--12	13--16	17--20	21--32
W1	60	345	Φ14/20	Φ14/20	**Φ16/15**	Φ14/20	Φ14/20	Φ14/20	Φ14/20	Φ14/20	Φ14/20
W2	60	665	**Φ16/15**	Φ14/20	**Φ16/14**	**Φ16/15**	Φ14/20	Φ14/20	Φ14/20	Φ14/20	Φ14/20
W3A	60	335	Φ14/20	Φ14/20	Φ14/20	Φ14/20	Φ14/20	Φ14/20	Φ14/20	Φ14/20	Φ14/20
W3B	60	250	Φ14/20	Φ14/20	Φ14/20	Φ14/20	Φ14/20	Φ14/20	Φ14/20	Φ14/20	Φ14/20
W4	40	345	Φ12/20	Φ12/20	**Φ14/15**	Φ12/20	Φ12/20	Φ12/20	Φ12/20	Φ12/20	Φ12/20
W5	40	315	**Φ12/15**	Φ12/20	**Φ12/14**	**Φ12/15**	Φ12/20	Φ12/20	Φ12/20	Φ12/20	Φ12/20
W6	40	380	**Φ12/13**	Φ12/20	**Φ12/15**	**Φ12/15**	Φ12/20	Φ12/20	Φ12/20	Φ12/20	Φ12/20
W7	40	335	Φ12/20	Φ12/20	**Φ12/15**	Φ12/20	Φ12/20	Φ12/20	Φ12/20	Φ12/20	Φ12/20
W8	40	380	**Φ12/15**	Φ12/20	Φ12/20	Φ12/20	Φ12/20	Φ12/20	Φ12/20	Φ12/20	Φ12/20
W9	40	345	Φ12/20	Φ12/20	**Φ14/15**	Φ12/20	Φ12/20	Φ12/20	Φ12/20	Φ12/20	Φ12/20
W10	50	665	**Φ16/10**	**Φ16/15**	**Φ16/15**	**Φ16/10**	**Φ16/10**	**Φ16/15**	**Φ14/15**	**Φ14/15**	Φ14/20
W11	60	715	**Φ20/10**	**Φ18/10**	**Φ20/10**	**Φ20/10**	**Φ20/10**	**Φ18/10**	**Φ18/15**	**Φ16/15**	**Φ16/20**
W12	40	345	Φ12/20	Φ12/20	Φ12/20	Φ12/20	Φ12/20	Φ12/20	Φ12/20	Φ12/20	Φ12/20
W13	40	335	Φ12/20	Φ12/20	Φ12/20	Φ12/20	Φ12/20	Φ12/20	Φ12/20	Φ12/20	Φ12/20
W14	60	345	Φ14/20	Φ14/20	**Φ14/10**	Φ14/20	Φ14/20	Φ14/20	Φ14/20	Φ14/20	Φ14/20
W15	60	665	**Φ16/10**	**Φ16/15**	**Φ16/10**	**Φ16/14**	**Φ14/15**	Φ14/20	Φ14/20	Φ14/20	Φ14/20
W16A	60	335	Φ14/20	Φ14/20	Φ14/20	Φ14/20	Φ14/20	Φ14/20	Φ14/20	Φ14/20	Φ14/20
W16B	60	250	Φ14/20	Φ14/20	Φ14/20	Φ14/20	Φ14/20	Φ14/20	Φ14/20	Φ14/20	Φ14/20
W17	60-80-90	1800	**Φ18/15**	Φ18/20	**Φ18/15**	Φ16/20	Φ16/20	Φ16/20	Φ16/20	Φ14/20	Φ14/20
W18	40	410	Φ12/20	Φ12/20	Φ12/20	Φ12/20	Φ12/20	Φ12/20	Φ12/20	Φ12/20	Φ12/20
W19	50	1625	**Φ16/10**	**Φ14/10**	**Φ14/15**	**Φ14/15**	Φ14/20	Φ14/20	Φ14/20	Φ14/20	Φ14/20
W20	50	710	**Φ16/13**	**Φ16/15**	Φ14/20	Φ14/20	Φ14/20	Φ14/20	Φ14/20	Φ14/20	Φ14/20
W21	60	1800	**Φ20/10**	**Φ16/10**	**Φ14/15**	Φ14/20	Φ14/20	Φ14/20	Φ14/20	Φ14/20	Φ14/20
W22	60-80-90	1800	**Φ25/11**	**Φ18/10**	**Φ18/20**	Φ16/20	Φ16/20	Φ16/20	Φ16/20	Φ14/20	Φ14/20

Demand and capacity graphs in terms of design under axial load and shear load are given in Figures 3.19 to Figure 3.26 for case study buildings in Ankara and Istanbul separately.

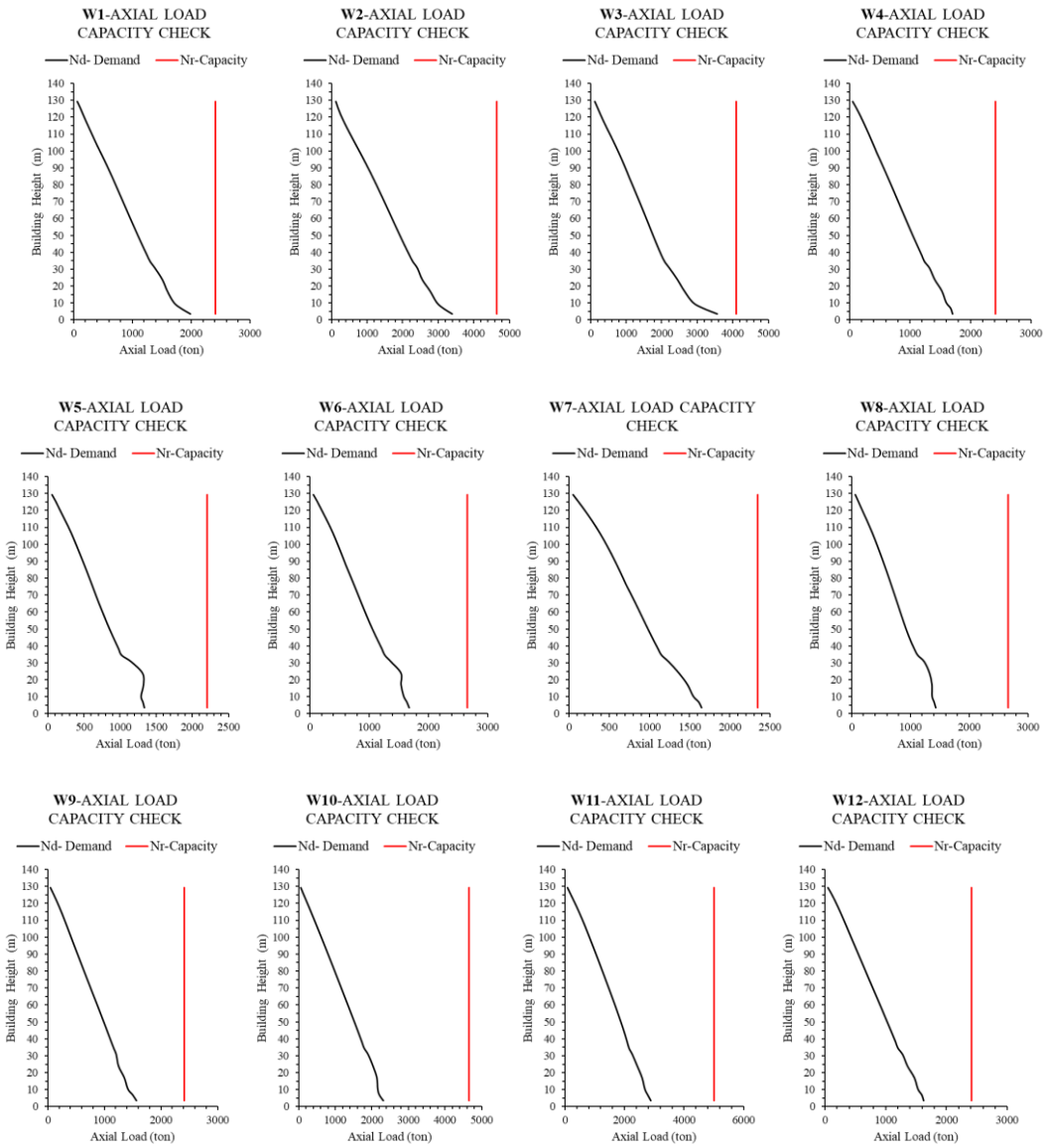

Figure 3.19 Axial Load Capacity Check Diagrams of W1 to W12 Walls (Ankara)

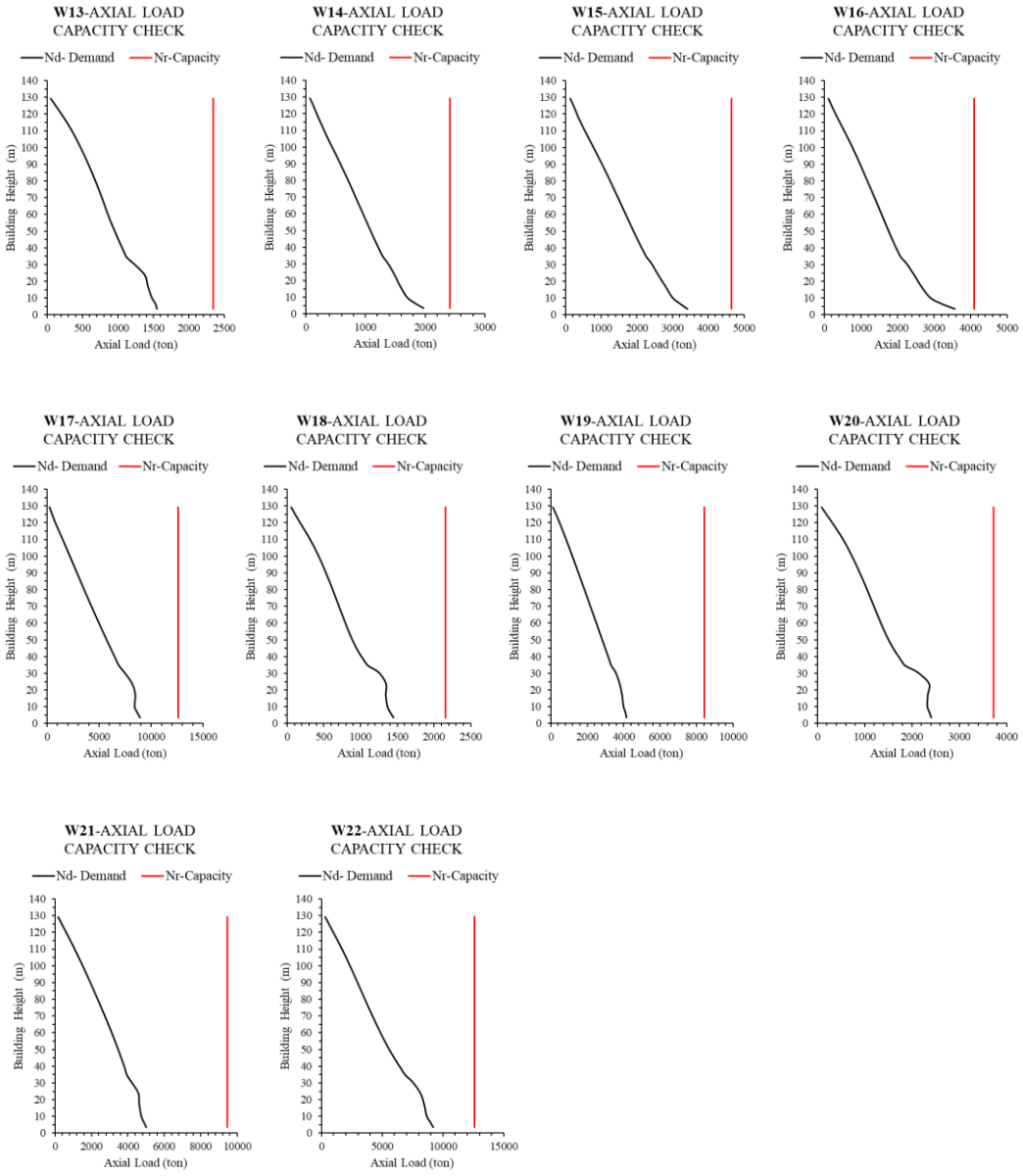

Figure 3.20 Axial Load Capacity Check Diagrams of W13 to W22 Walls (Ankara)

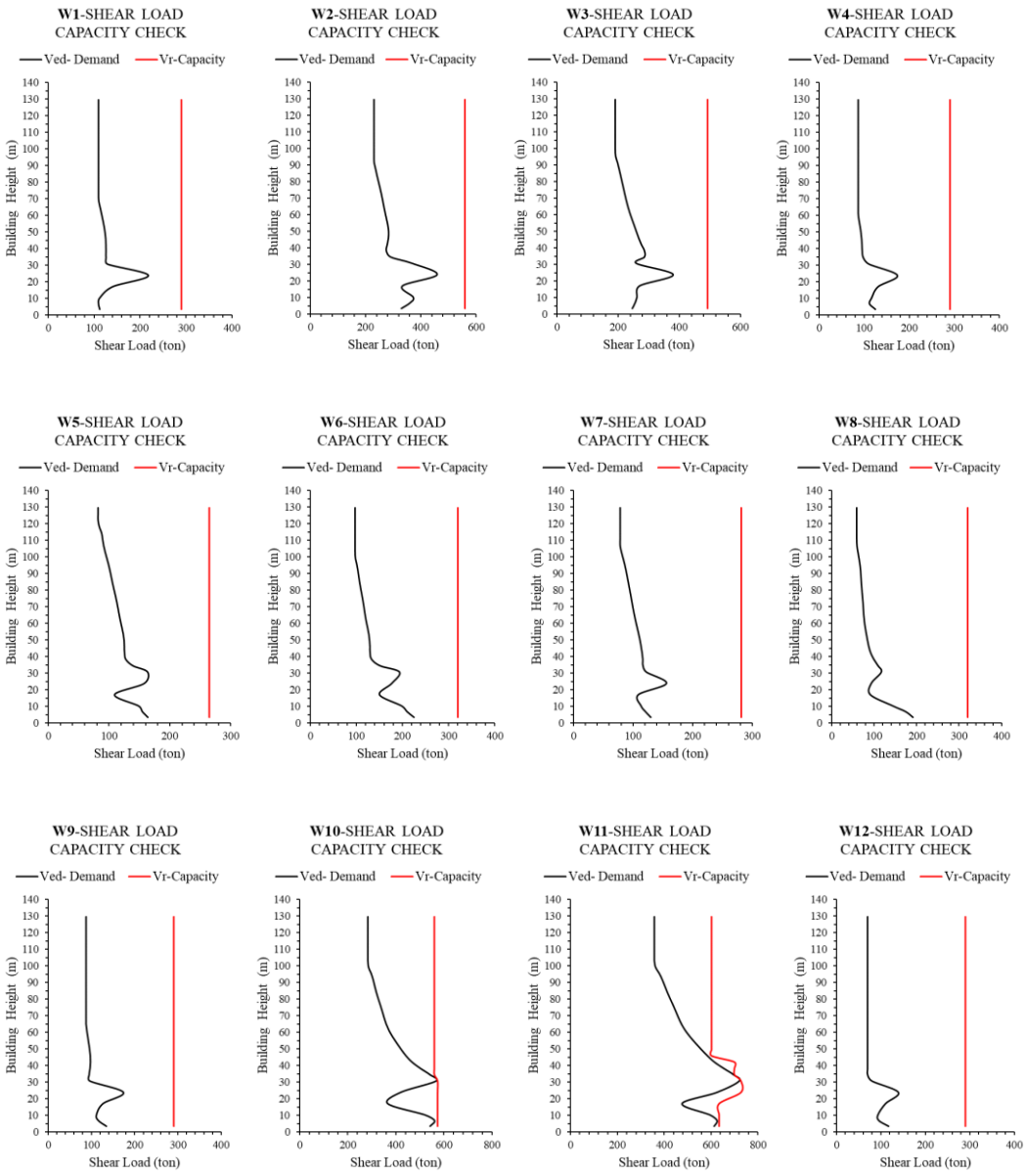

Figure 3.21 Shear Load Capacity Check Diagrams of W1 to W12 (Ankara)

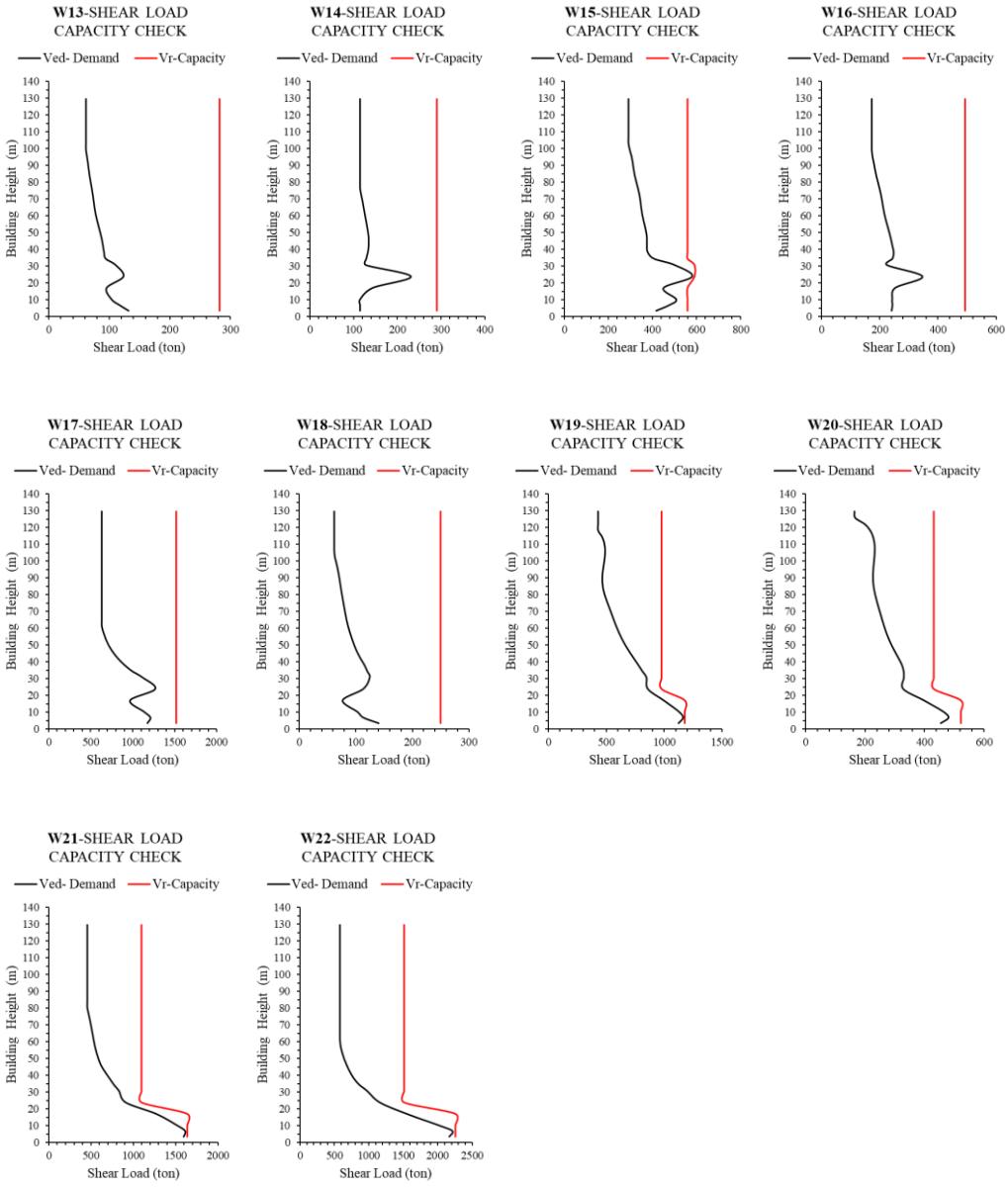

Figure 3.22 Shear Load Capacity Check Diagrams of W13 to W22 Walls (Ankara)

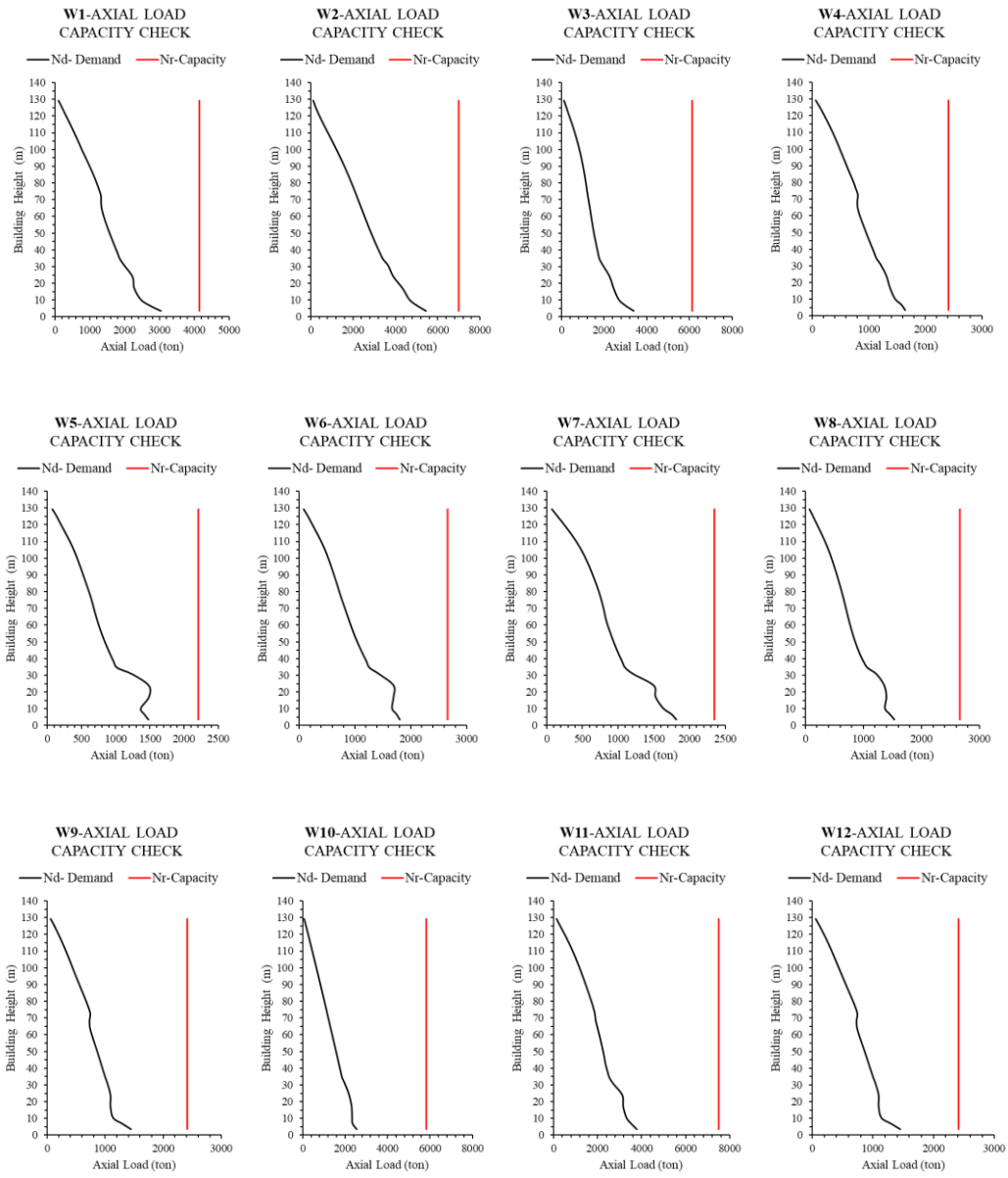

Figure 3.23 Axial Load Capacity Check Diagrams of W1 to W12 (Istanbul)

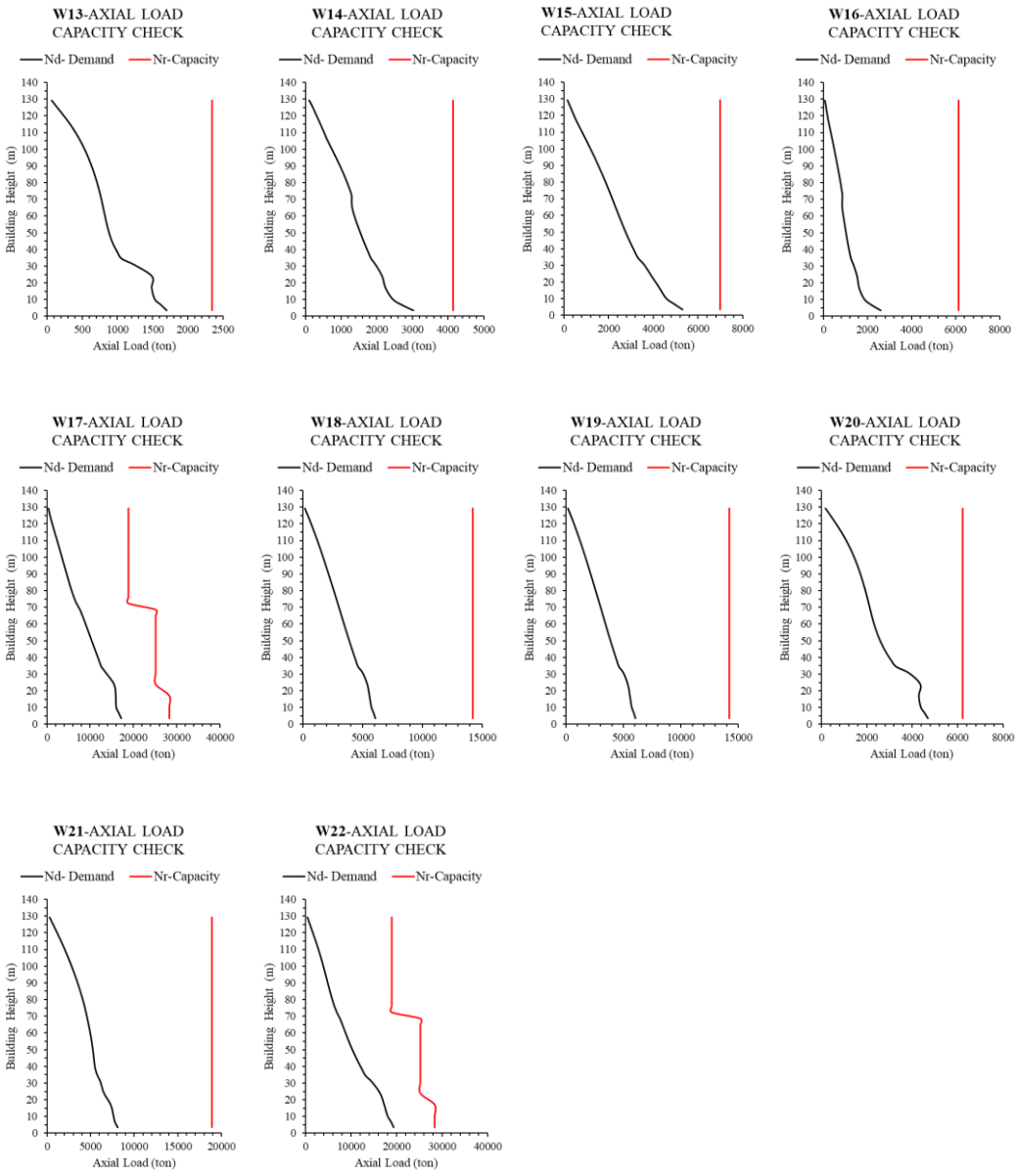

Figure 3.24 Axial Load Capacity Check Diagrams of W13 to W22 (Istanbul)

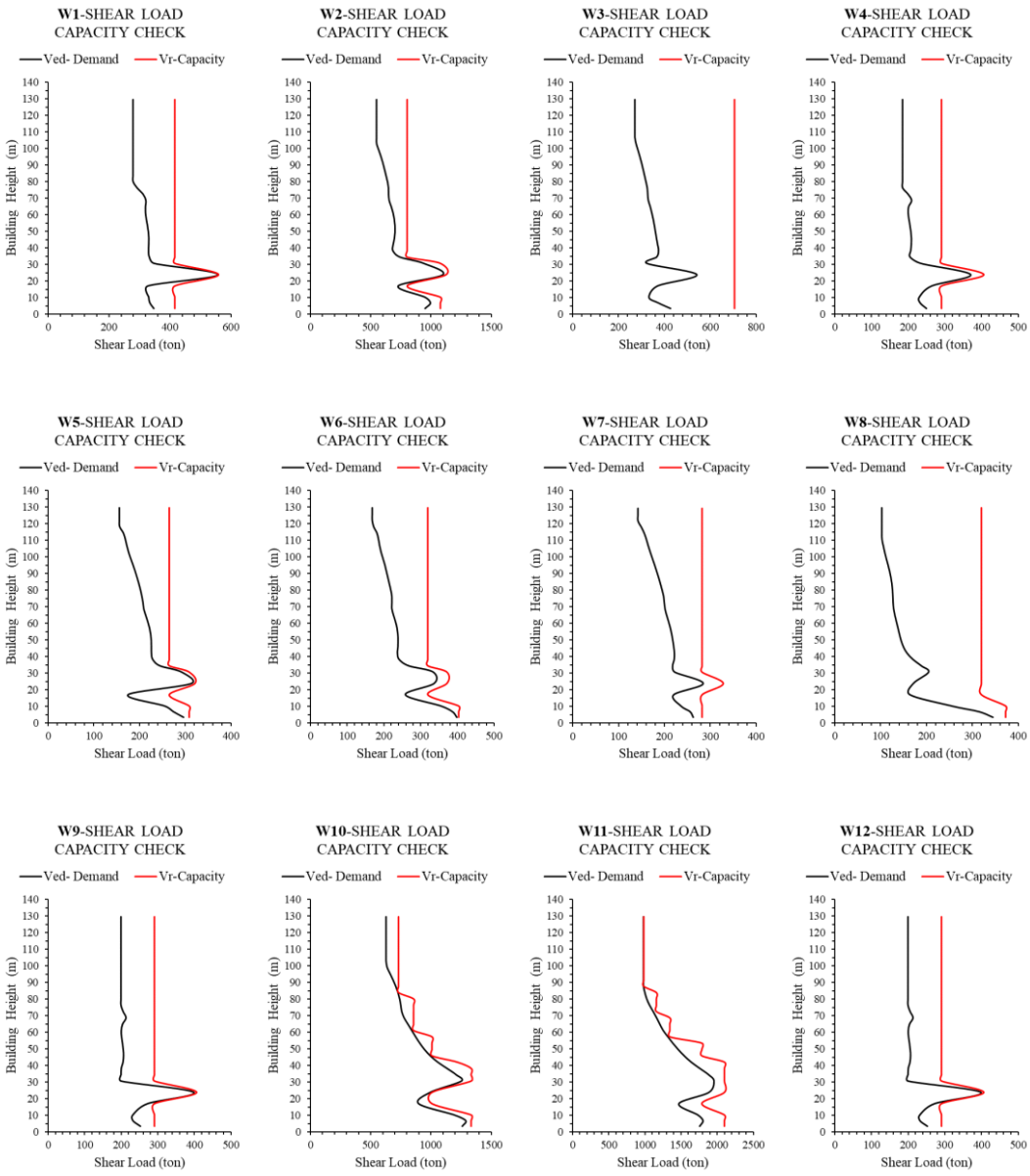

Figure 3.25 Shear Load Capacity Check Diagrams of W1 to W12 Walls (Istanbul)

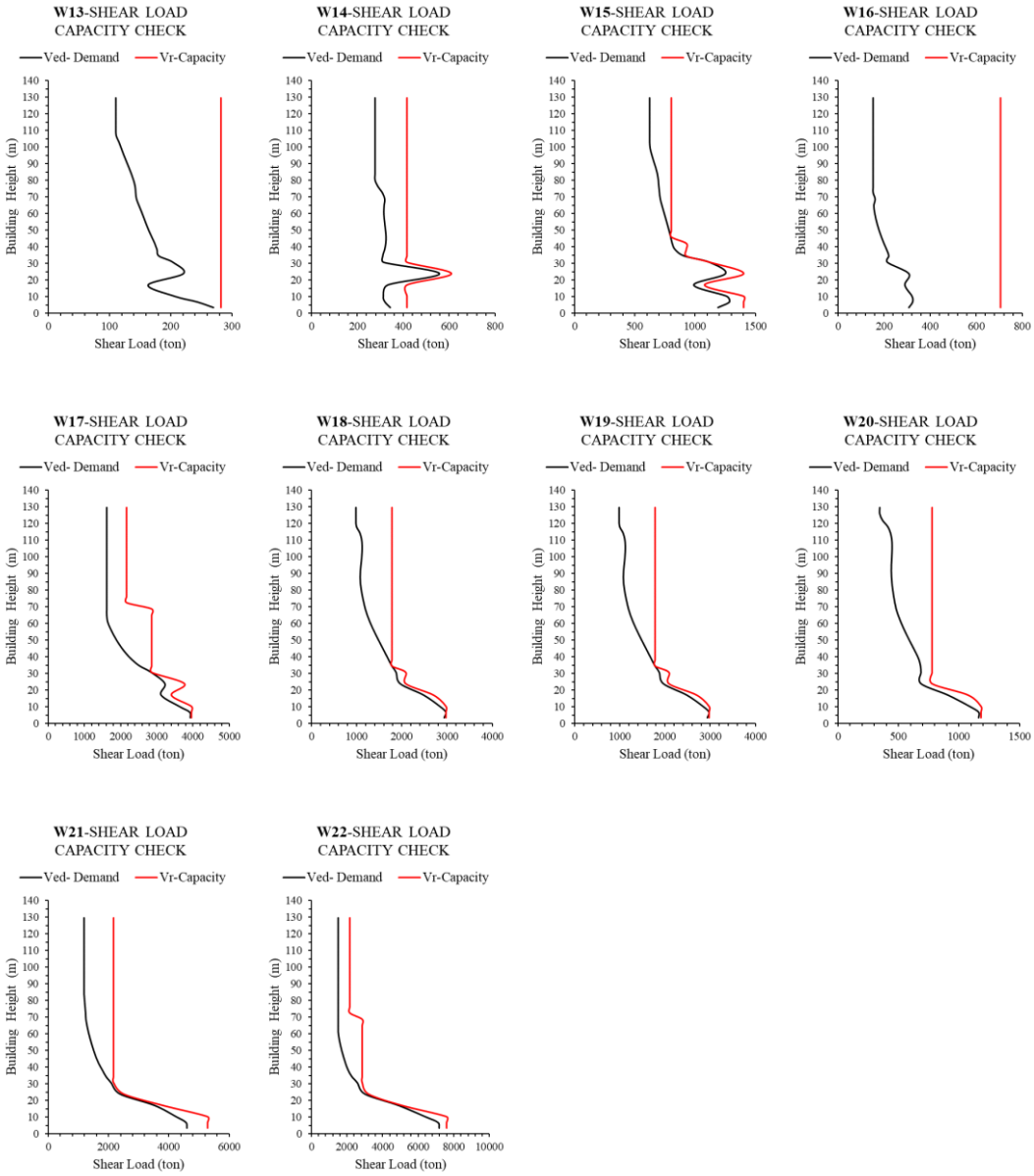

Figure 3.26 Shear Load Capacity Check Diagrams of W13 to W22 (Istanbul)

Shear force distribution according to wall labels just above the basement level is shown in Figure 3.27. W2, W10, W11 and W15 walls for x direction and W17, W19, W21 and W22 walls for y direction are dominant to respond to base shear reaction.

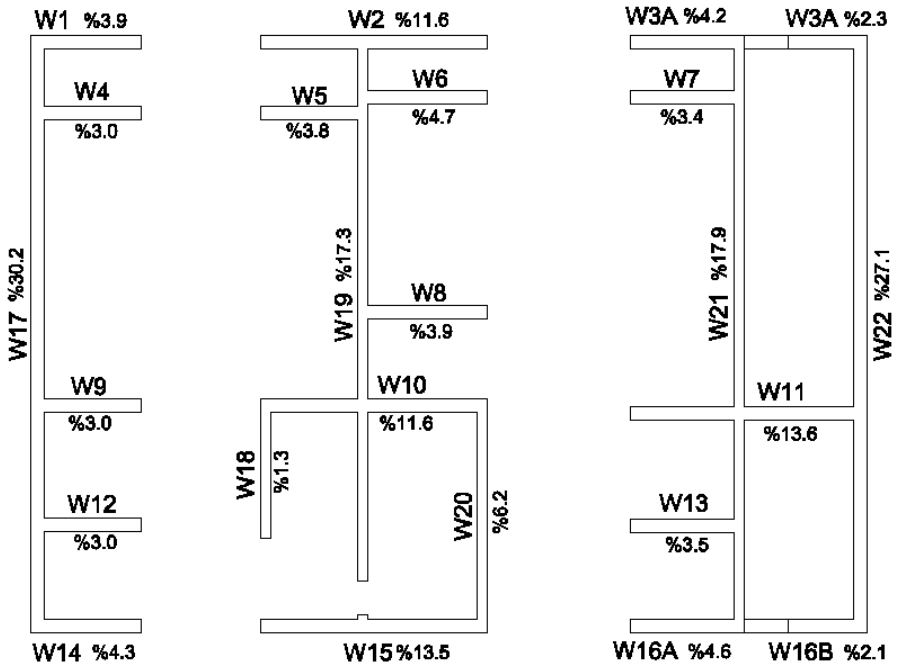

Figure 3.27 Shear Force Distribution Ratio at 5th Story

Labels of flexural design of core wall are different from labels of shear design. Because under flexural behavior in high-rise buildings, it is envisaged that the core-wall works in groups, not separately, as in shear design. Because it is not possible to separate each piece of wall with the common intersection boundaries having dense vertical reinforcements, as in shear design. It is predicted that wall groups work as a single section under flexural behavior in such high structures. For this reason, vertical reinforcement design is carried out as WG1, WG2, WG3 sections (Figure 3.28) and the results are given in Figure 3.29.

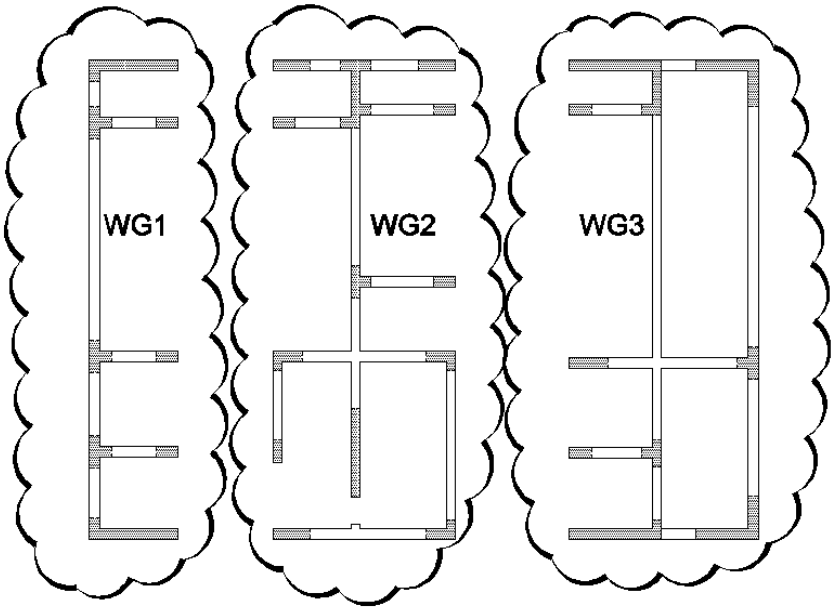

Figure 3.28 Labels and Wall Groups for Flexural Design of Core-wall

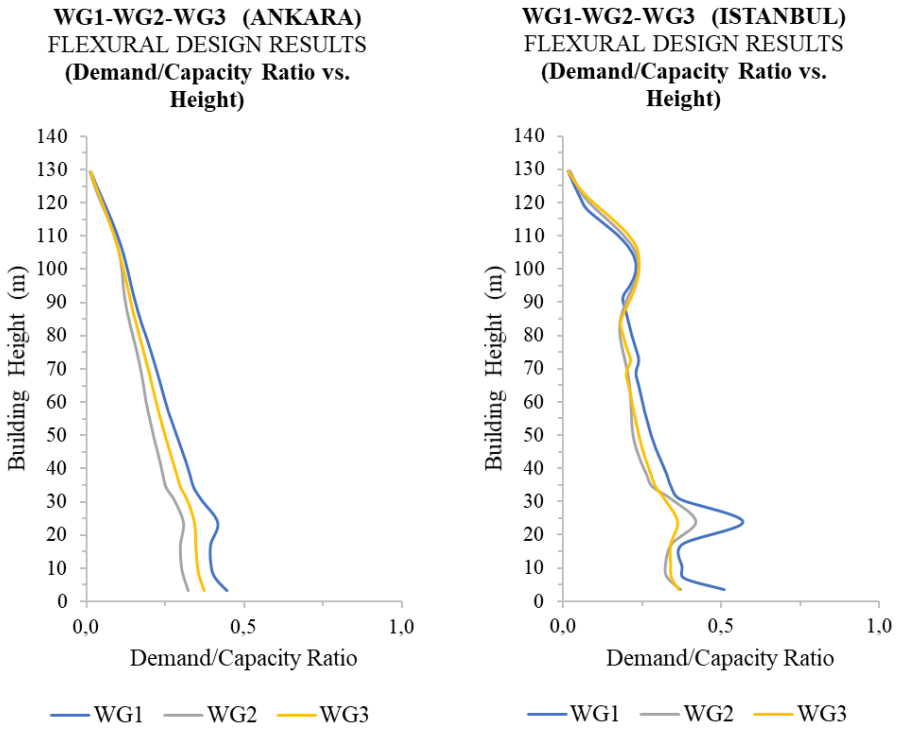

Figure 3.29 Flexural Design Results (Demand/Capacity Ratio vs. Height) of Wall Groups of Building in Ankara and in Istanbul

3.6.2 Coupling Beam Design of Case Study Building

3.6.2.1 Design Regulations of Coupling Beams in TEC (2018)

The coupling beams between wall groups have high shear strength and allow the two different wall groups to work together as a single wall. Whether a single shear wall behavior or two separate shear walls is exhibited depends on whether the beam between the walls serves as a coupling beam, through the coefficient of the degree of coupling, Ω in TEC-2018, provided in Equation 3.24. If this condition is satisfied, the beam is a coupling beam and two separate shear wall pieces are considered to working as a single shear wall. In case Equation 3.24 is not provided, the walls are designed separately. The coefficient of the degree of coupling, Ω, is calculated by Equation 3.22 and Equation 3.23. M_1 and M_2 are moments of shear walls under only earthquake load at the base level, where walls show maximum flexural behavior. Nv and c are the sum of all coupling beams shear forces at the same beam joint and the distance of center of gravity of wall sections, respectively.

$$M_{\mathrm{DEV}} = M_1 + M_2 + c\,N_{\mathrm{V}} \tag{3.22}$$

$$\Omega = \frac{c\,N_{\mathrm{V}}}{M_{\mathrm{DEV}}} = \frac{c\,N_{\mathrm{V}}}{M_1 + M_2 + c\,N_{\mathrm{V}}} \tag{3.23}$$

$$\Omega \geq \frac{1}{3} \tag{3.24}$$

The shear design of the coupling beams is very important. For this reason, the reinforcement detail varies in the coupling beams according to the magnitude of the shear force. If both the Equation 3.25 and 3.26 conditions are not met, diagonal reinforcement bars will be placed and the amount of these reinforcements are calculated by Equation 3.27. If the shear force is not excessive and any of Equations 3.25 and 3.26 are satisfied, beam is designed under shear similar to a slender beam according to Equations 3.28, 3.29 and 3.30. If the maximum shear force in the beam

does not meet the condition in Equation 3.30, the beam dimensions should be changed.

$$\ell_n > 2\square_k \quad \textbf{(3.25)}$$

$$V_d \leq 1.5 b_w\, d f_{\text{ctd}} \quad \textbf{(3.26)}$$

$$A_{\text{sd}} = V_{\text{d}} / (2 f_{\text{yd}} \sin\gamma) \quad \textbf{(3.27)}$$

$$V_{\text{e}} = V_{\text{dy}} \pm (M_{\text{pi}} + M_{\text{pj}})/\ell_n \quad \textbf{(3.28)}$$

$$M_{\text{pi}} \approx 1.4 M_{\text{ri}} \quad M_{\text{pj}} \approx 1.4 M_{\text{rj}} \quad \textbf{(3.29)}$$

$$\text{V}_{\text{e}} \leq \text{V}_{\text{r}}$$

$$V_e \leq 0.85 b_w d \sqrt{f_{\text{ck}}} \quad \textbf{(3.30)}$$

3.6.2.2 Coupling Beams Design Results

In our case building, there are both beams and coupling beams between core wall groups. Beam and coupling beam dimensions are 40/60 cm and 40/150 cm respectively in the case structure in Ankara (Figure 3.30). On the other hand, in the case study building in Istanbul, there are beams in dimensions of 40/60 cm and 60/60 cm, and coupling beams in dimensions of 60/150 cm (Figure 3.31).

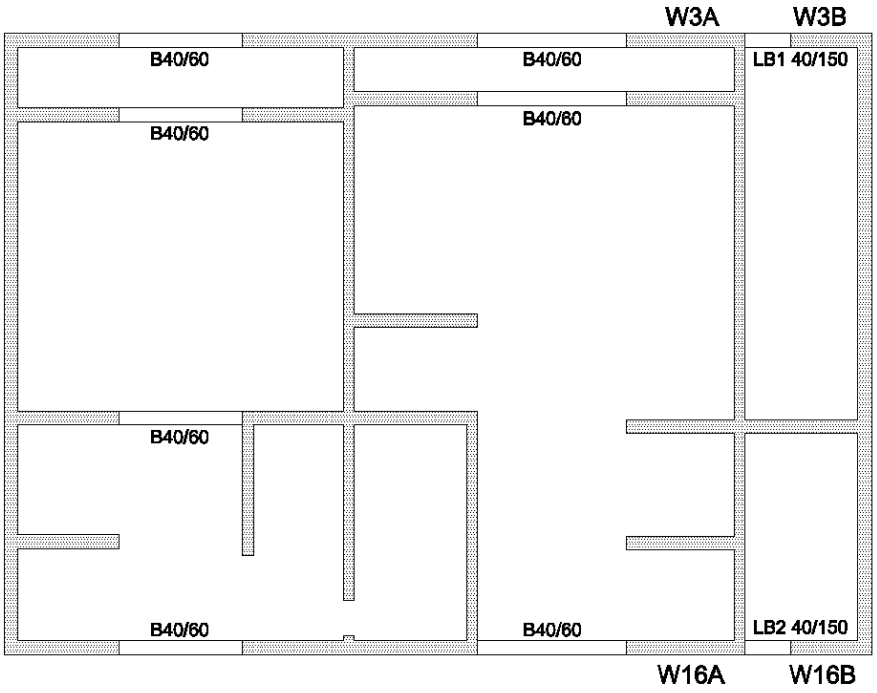

Figure 3.30 Beam and Link Beam Dimensions of Case Study Building in Ankara

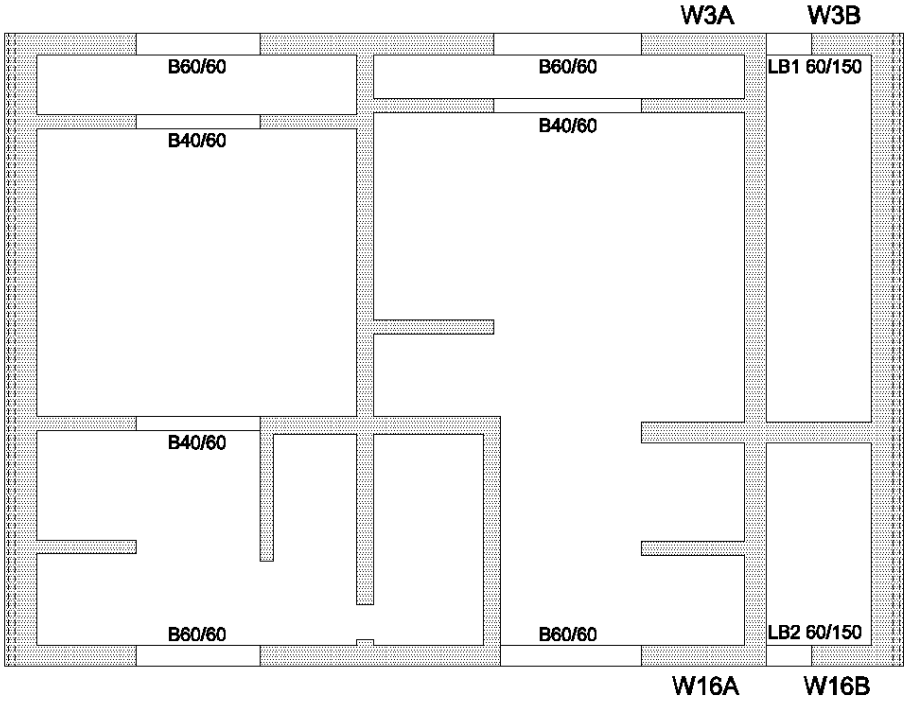

Figure 3.31 Beam and Link Beam Dimensions of Case Study Building in Istanbul

Link beams, LB1 and LB2, are checked as that coefficient of the degree of bond, Ω is greater than 0.33 or not. Results are shown in Table 3.17. Table shows that LB1 and LB2 shows coupling beam behavior.

Table 3.17 The Coefficient of the Degree of Bond, Ω for Coupling Beams

	ANKARA		ISTANBUL	
	LB1 (40/150)	LB2 (40/150)	LB1 (60/150)	LB2 (60/150)
M_1 (t.m)	372	350	940	829
M_2 (t.m)	152	137	366	318
N_V (t)	220	250	630	650
c (m)	4.1	4.1	4.1	4.1
Ω	**0.63**	**0.68**	**0.67**	**0.70**

Design results of coupling and frame beams are shown for case study buildings in Ankara and In Istanbul in Table 3.18 and Table 3.19, respectively.

Table 3.18 Coupling Beam Design Results of Case Study Building in Ankara

	ANKARA		
	LB1 (40/150)	LB2 (40/150)	Beam (40/60)
V_{cr} (t)	0,0	0,0	0,0
V_c (t)	0,0	0,0	0,0
V_w (t)	163,0	163,0	62,0
V_{max} (t)	349,0	349,3	133,0
V_e (t)	150,0	118,7	50,6
V_r (t)	0,0	0,0	0,0
M_d (t.m)	53,7	45,2	32,3
Stirrup	Φ14/10	Φ14/10	Φ14/10
Rein. $_{top, bot.}$	5Φ25	5Φ25	5Φ22
	Conventionally Reinforced	Conventionally Reinforced	Conventionally Reinforced

Table 3.19 Coupling Beam Design Results of Case Study Building in Istanbul

	ISTANBUL			
	LB1 (60/150)	LB2 (60/150)	Beam (40/60)	Beam (60/60)
V_{cr} (t)	0	0	0	0
V_c (t)	0	0	0	0
V_w (t)	425.1	425.1	123.8	161.1
V_{max} (t)	523.3	523.3	132. 5	198.0
V_e (t)	211	159	97.5	127.4
V_r (t)	0	0	0	0
M_d (t.m)	187	139	56.2	81.3
Stirrup	2 x Φ16/10	2 x Φ16/10	2 x Φ14/10	2 x Φ16/10
Rein. top, bot.	6Φ30	6Φ30	5Φ30	7Φ30
Diagonal Bars	8Φ30	8Φ30	--	--
	Diagonally Reinforced	Diagonally Reinforced	Conventionally Reinforced	Conventionally Reinforced

All design beam drawings are shown in Figure 3.32 and Figure 3.33 below.

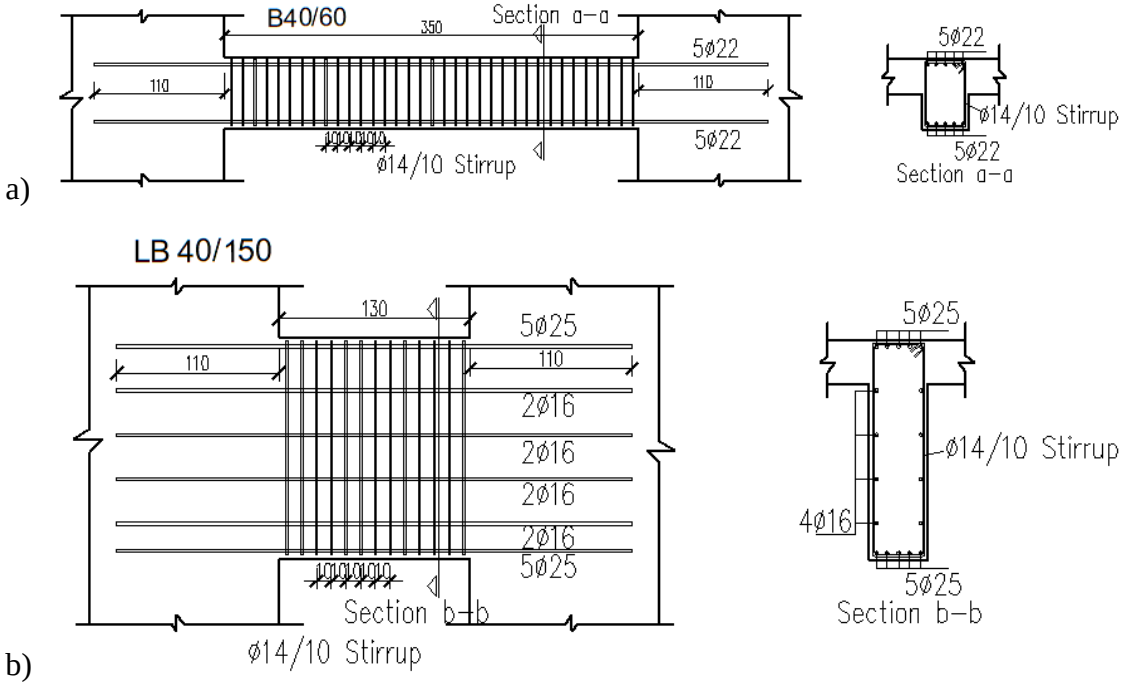

Figure 3.32 a) Beam (40/60) and b) Link Beam (40/150) Reinforcement Details fo Case Study Building in Ankara

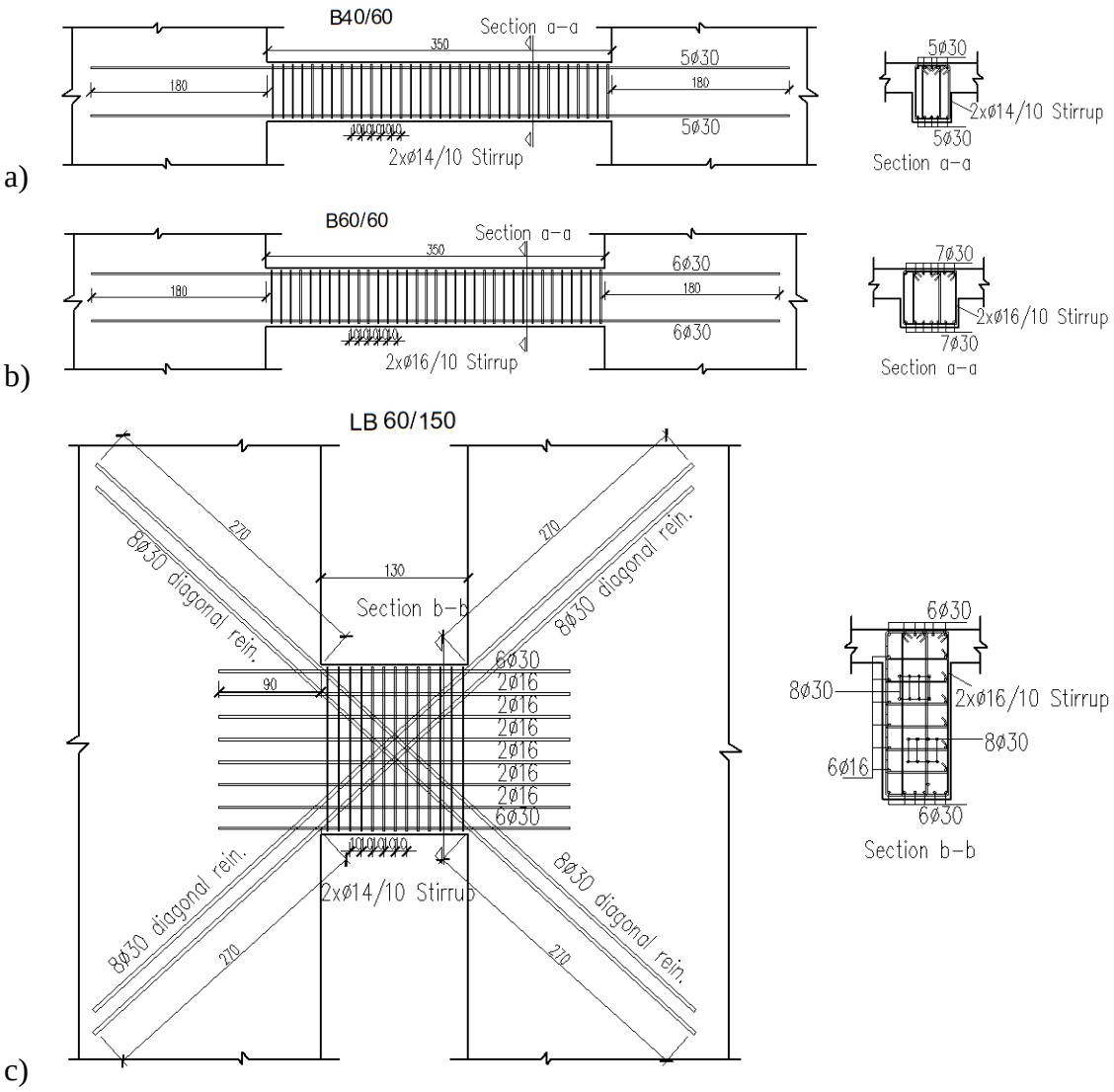

Figure 3.33 a) Beam (40/60), b) Beam (60/60) and b) Link Beam (60/150) Reinforcement Details of Case Study Building in Istanbul

3.7 DRIFT RATIO RESULTS OF CASE STUDY BUILDING FOR LINEAR ELASTIC DESIGN

In TEC-2018, the story drift ratio is controlled according to the Equation 3.31. According to this formula, κ is 0.5 for concrete buildings and λ is 0.398 and 0.526 for buildings in Ankara and in Istanbul, respectively. According to these values, the simplified version of Equation 3.31 is shown in Equation 3.32 and 3.33 for building

in Ankara and Istanbul, respectively. The story drift ratio check is shown in Figure 3.34.

$$\lambda \frac{\delta_{i,max}^{(X)}}{h_i} \leq 0.008\ \kappa \quad \textbf{(3.31)}$$

$$\frac{\delta_{i,max}^{(X)}}{h_i} \leq 0.01 \quad \textbf{(3.32)}$$

$$\frac{\delta_{i,max}^{(X)}}{h_i} \leq 0.0076 \quad \textbf{(3.33)}$$

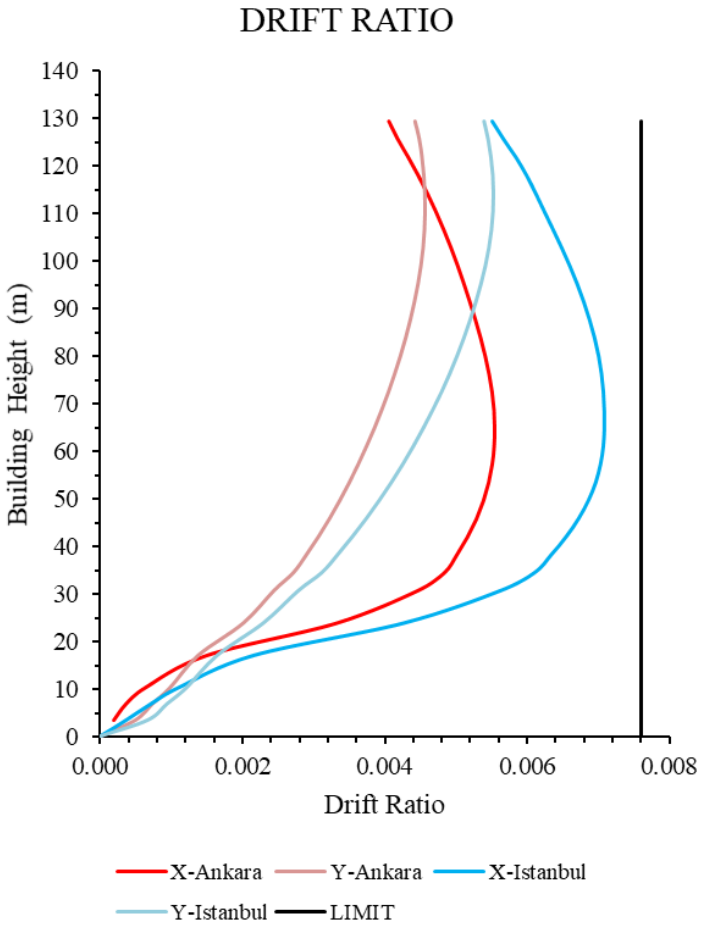

Figure 3.34 Drift Ratio Results of Case Study Building in Ankara and in Istanbul

CHAPTER 4

PERFORM 3D V7.0.0 SOFTWARE

Perform 3D program is the most widely used program for nonlinear inelastic modeling and design check of tall buildings. It is important to know the working principles of this program in order to conduct modeling correctly. The displacement-based design is a very different approach from the strength-based design. The nonlinear inelastic behavior of each structural element should be well understood by the engineer who will use the program and accurately reflect the behavior accordingly. In this complex modeling, it is important to simplify the model to minimize the time of analysis and the accuracy of models. The correct modeling of walls and link beams with Perform 3D is explained in detail in this chapter.

Perform 3D has basically 2 phases, i.e., the modelling phase and the analysis phase. In the modelling phase; nodes, component properties, elements, loads, drifts, structure sections, and limit states are defined. At the analysis phase; load cases, analysis series, modal analysis results, energy balance results, deflected shapes, time histories, hysteresis loops, moment-shear diagrams, push-over plots, usage ratio graphs, combinations and envelopes parts are visualized.

4.1 MODELING PHASE

4.1.1 Nodes

The first step in the modeling phase is the definition of nodal points. Nodes can be created in the nodes section with the desired number and position to connect the building elements together to create the geometry of the structure. Coordinates are defined in 3D with x, y and z coordinates as H1, H2 and V. The minimum distance between the nodes can be determined by the user. In addition, restraints or supports

can be assigned to the desired nodes. Masses can only be assigned to nodes. Mass assignment on an element basis is not possible. Mass assignment to 3 displacement directions and 3 rotation directions can be made separately. With the slaving section; horizontal rigid floor, eccentric connection in a rigid floor, full rigid link and simple equal displacement options can be modeled. In the use of the horizontal rigid floor option, all axial loads in beam models will be zero. However, when fiber sections or concrete type P-M-M hinges models are used in the beam model, rigid floor constraint, which prevents the beams extension, will cause compression forces.

4.1.2 Components Properties

The component properties section is one of the most time-consuming parts of modeling in the P3D program. This section describes materials, cross sections, basic structural components, strength sections, and compound components (Figure 4.1). While material definitions help define element sections, basic structural components are defined through both material and cross sections. Also, the strength check of the building elements that will exhibit elastic behavior is possible, while all the characteristics of the building elements are combined according to their behavior in the compound component task.

Figure 4.1 Perform 3D Component Properties Task

4.1.2.1 Material Properties

The materials of the structural elements to be used can be defined first. In the materials section, which is mainly elastically and inelastically distinguished, force-displacement behavior curves of steel and concrete materials are obtained. In the inelastic materials section, steel material is defined in 3 forms, i.e., inelastic steel materials non-buckling, tension only and buckling. The remaining inelastic material definitions are 1D concrete material, shear material and compression for a wall. On the other hand, elastic material definitions are divided as elastic material for a fiber section, elastic shear material for a wall and elastic material for a slab or shell. Slabs are only defined as elastic material.

In our model, "inelastic steel material, non-buckling" (Figure 4.2) is used to define the reinforcement of the walls, on the other hand, "inelastic 1D concrete material" (Figure 4.3) is selected for the reinforced concrete fiber sections model. The option of "elastic shear material for a wall" (Figure 4.4) is considered for the design of a wall under shear force because it is assumed that the behavior of a wall under shear force would be elastic in the walls of high-rise buildings where bending behavior is governed.

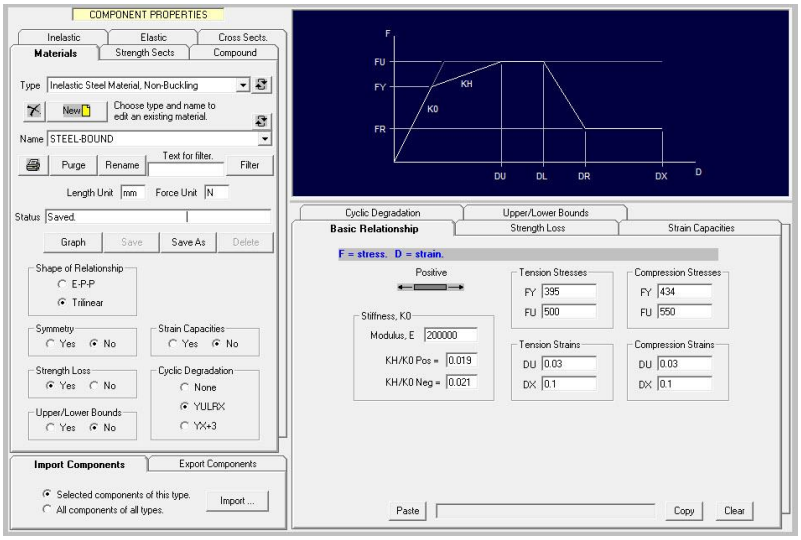

Figure 4.2 "Inelastic Steel Material" Input Panel

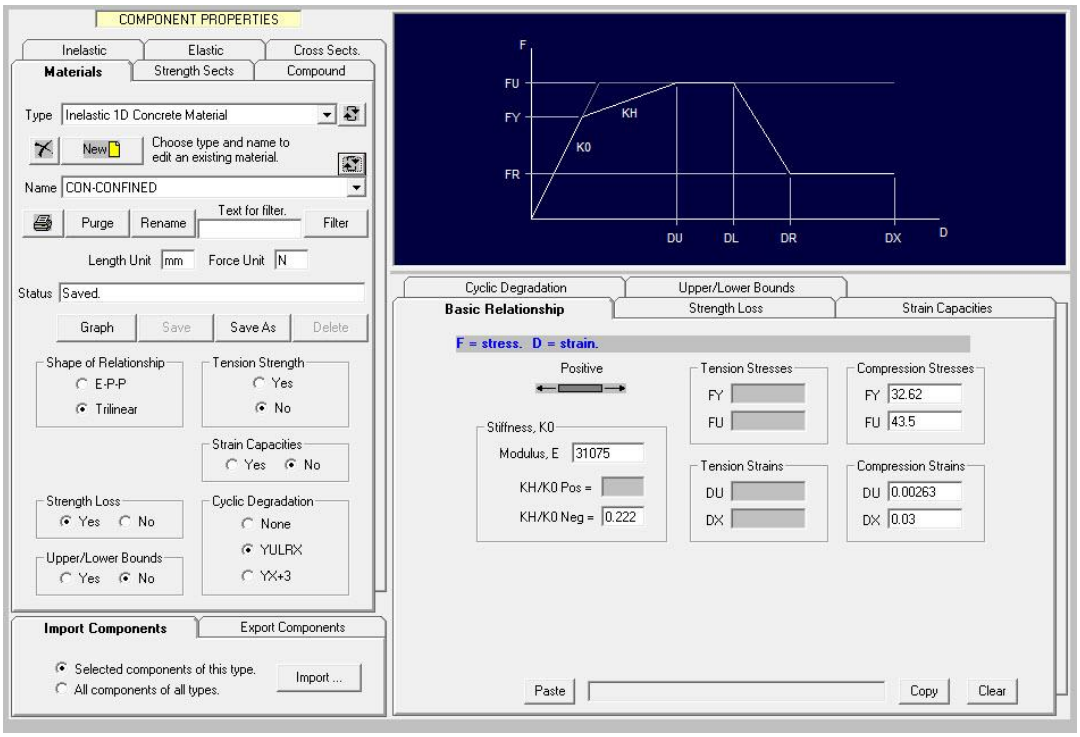

Figure 4.3 ”Inelastic 1D Concrete Material” Input Panel

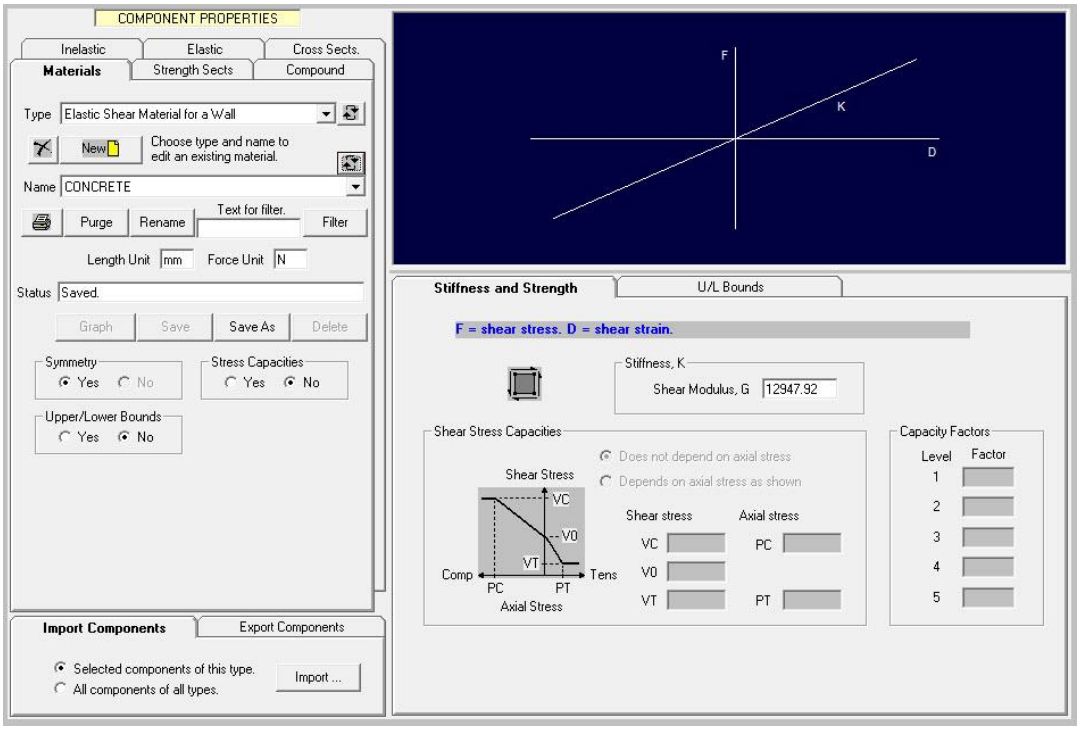

Figure 4.4 ”Elastic Shear Material for a Wall” Input Panel

Inelastic behavior can be created with various parameters and options to define hysteric loop at P3D in the form of force-displacement, stress-strain, force-rotation, and force-curvature curves, both on the material inelastic behavior level or the basis of section inelastic behavior. With these definitions, the hysteric loop model "YULRX" is created. Highlights of the backbone curve, which defines the outlines of the hysteric loop, can be defined as yielding point (Y), ultimate strength point (U), ductile limit point (L), residual strength point (R), and analysis stop point (X) (Figure 4.5 and Figure 4.6).

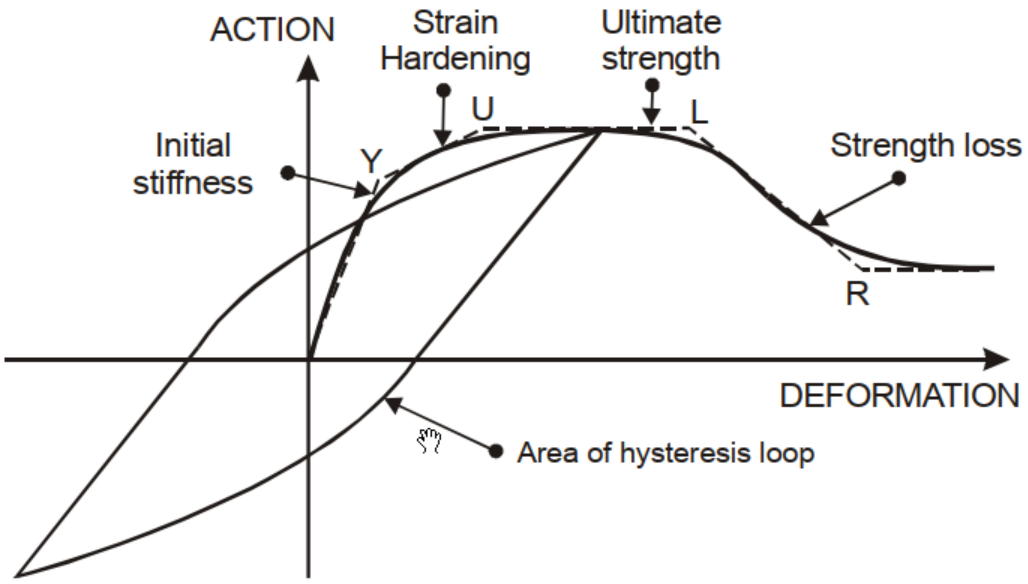

Figure 4.5 Perform 3D "YULRX" Backbone Curve(Computers and Structures, Inc., 2006)

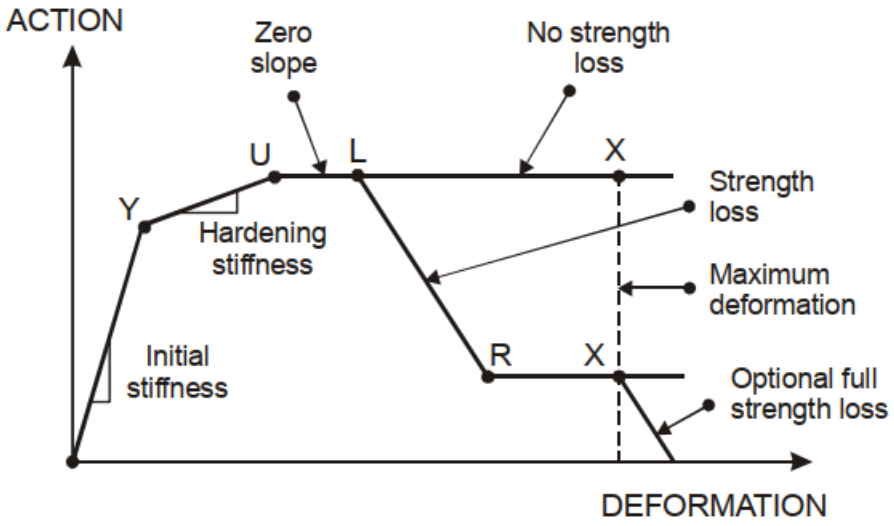

Figure 4.6 Perform 3D Hysteretic Loop Model(Computers and Structures, 2006)

"YULRX" hysteric loop is defined by the parameters under the basic headings, that define the shape of the force deformation relationship, cyclic degradation and strength loss. In terms of "shape of relationship", one of two options can be selected as in the form of elastic perfectly plastic (EPP) or trilinear relationship. Dissipated energy (the area of the loop) in the hysteric loop can be determined by cyclic degradation energy factors in the "YULRX" model. This energy degradation also affects reloading and unloading stiffness values. In addition, the change of stiffness in the case of unloading behavior for the shape of the trilinear backbone curve can be controlled by the unloading stiffness factor. Although the ductile limit point (L) cannot be exceeded even by the collapse prevention limit in the regulations, the strength loss situation in the hysteric loop can be considered in the modeling at P3D. There is a strength loss interaction factor (SLIF) determining strength loss only in the positive direction (SLIF=0) or both positive and negative direction symmetrically (SLIF=1) of the cyclic loop (Figure 4.7). A value between 0 and 1 will give a strength loss midway behavior in terms of loss direction at a hysteric loop. So, hysteric loop behavior can be created in symmetrical order or asymmetrically with different SLIF values while all other relationships are maintained.

This principled approach is the same both in the definition of inelastic behavior within the material itself and in the definition of inelastic behavior of the section.

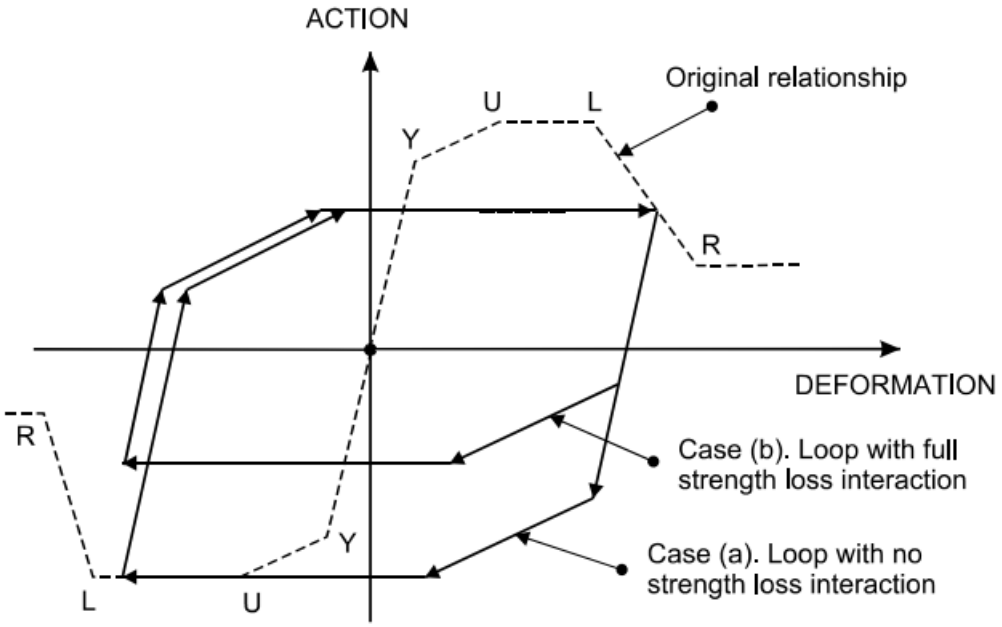

Figure 4.7 Strength Loss Interaction Factor (SLIF=0 (a), 1 (b)) (Computers and Structures, Inc., 2006)

There can be a decrease in stiffness, strength and dissipated energy under cyclic loading of structural elements. The reduction in stiffness and strength affects energy dissipation. In the P3D program, a cyclic hysteric loop can be adjusted by using the energy degradation factor and unloading stiffness factors (Figure 4.8). Energy degradation factor is the ratio of reduced area of degraded hysterical loop to initial area of undegraded hysterical loop (Figure 4.9 (a)). In Figure 4.9 (b), the energy degradation factor for loops A, B, and C is the same in three and is 0.55 (1.0=no degradation). But the difference in these three is adjusted by the unloading stiffness factor. The unloading stiffness factor is +1, -1, and 0 for loop A, B, and C, respectively. Elastic range is reduced in loop A, while stiffness decreases in loop B. In loop C, however, there is a decrease in both elastic range and stiffness. Energy degradation factor and unloading stiffness factor are two important parameters for determining the hysteric loop. For this reason, the correct selection of these two

factors is important to reflect the correct structural element inelastic behavior confirmed by experiments on the model. As in many high-rise buildings, experimental behaviors of walls and link beams, that also exhibit inelastic behavior in our sample structure, were reflected in the model by calibration of these two parameters. In this study, the recommended values for these coefficients for different types of walls and link beams were identified by conducting detailed parametric studies.

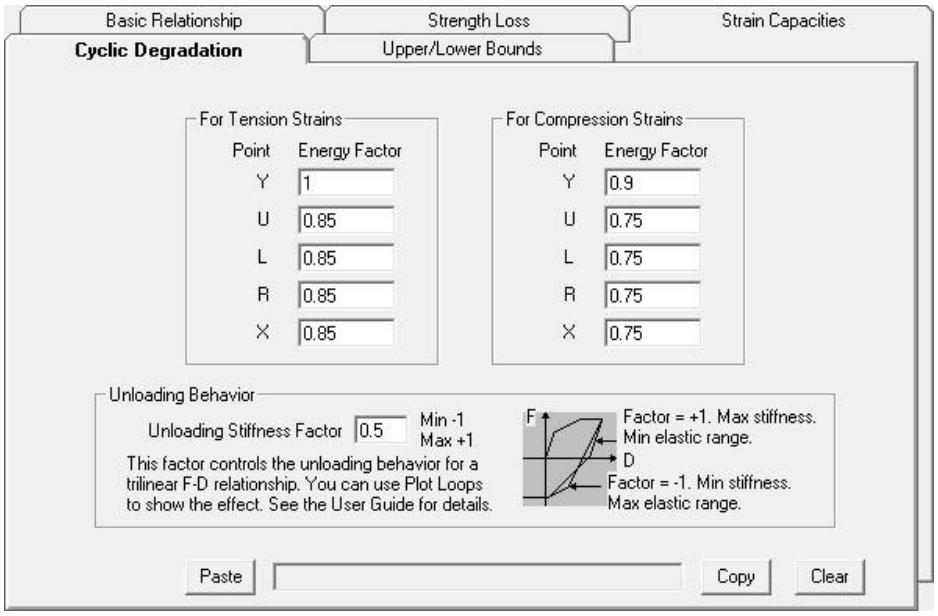

Figure 4.8 Perform 3D Input Panel for Cyclic Degradation Factor and Unloading Stiffness Factor

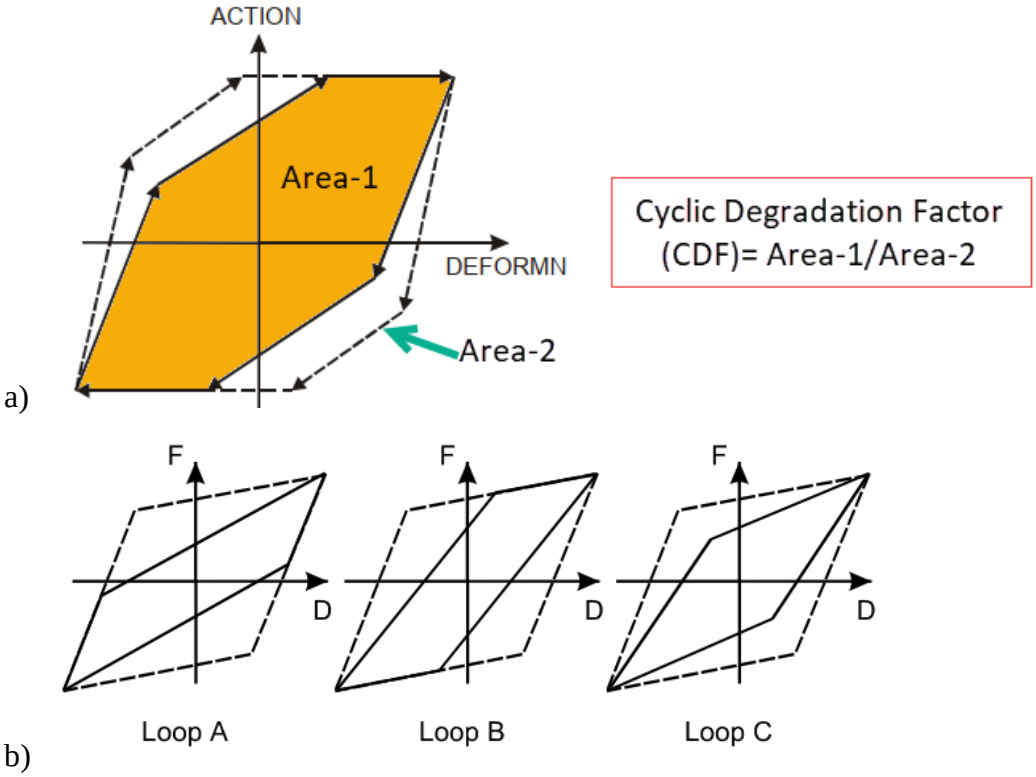

Figure 4.9 a) Cyclic Degradation Factor b) Hysteric Loop with The Same Cyclic Degradation Factor and Different Unloading Stiffness Factors (USF=+1 (A), -1 (B), 0 (C)) (Computers and Structures, 2006)

4.1.2.2 Cross Section Definition at Perform 3D

Cross-section definitions are made for walls and link beams. The wall structural element cross sections can be modeled by fibers as both the reinforcement and the concrete fibers are separately defined horizontally and vertically at P3D (Figure 4.10). The cracking or crushing behavior of the concrete regions and the yielding or buckling of the reinforcement parts of the wall section under bending and axial load can be modeled with the uniaxial material behavior define the fibers. The number of fibers, area of concrete and reinforcement parts can be defined in the P3D program either as “fixed size” or “auto-size” (Figure 4.11). While areas, amount and coordinates of fibers are specified numerically in a computational inefficient way for the fixed size option, the auto size option more easily specifies the number of

reinforcement and concrete fibers divided into equal areas within the same wall width length. As a result, “auto-size” gives you a faster modeling option, while “fixed size” gives you a more flexible modeling option.

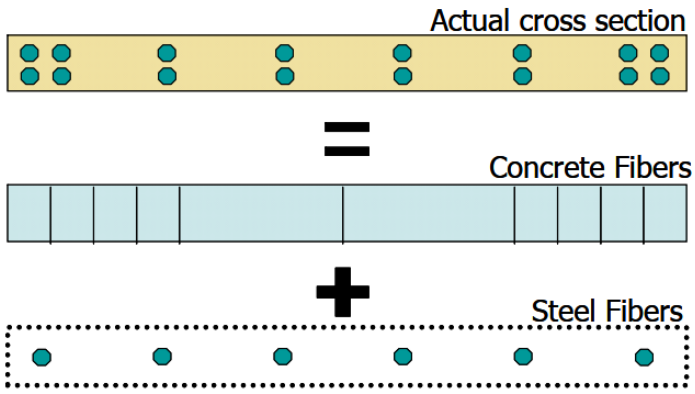

Figure 4.10 Fiber Model of Walls at Perform 3D (PEER/ATC 72-1, 2010)

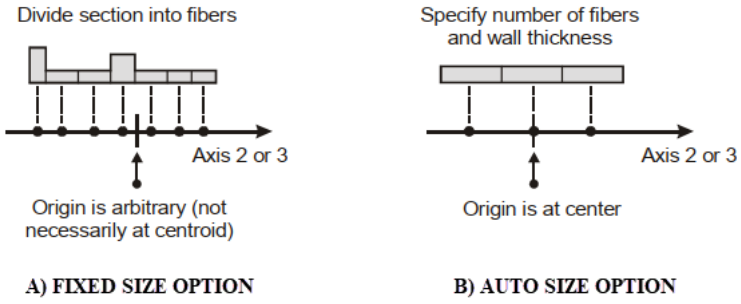

Figure 4.11 Wall Fiber Modeling Options at Perform 3D (Computers and Structures, Inc., 2006)

“Beam, Reinforced Concrete Section” can generally be used for the link beams as well. Various properties of the link beam sections can be defined in this selection. (Figure 4.12). These are the dimensions of the beam, section stiffness properties, axial and shear areas, inertias, and material stiffness properties like young’s modulus, shear modulus and poison’s ratio. In addition to these properties, inelastic bending strength, inelastic shear strength, elastic nominal bending or shear strengths of that

section can be defined. Maximum allowable axial force or axial stress can also be defined in terms of elastic capacity.

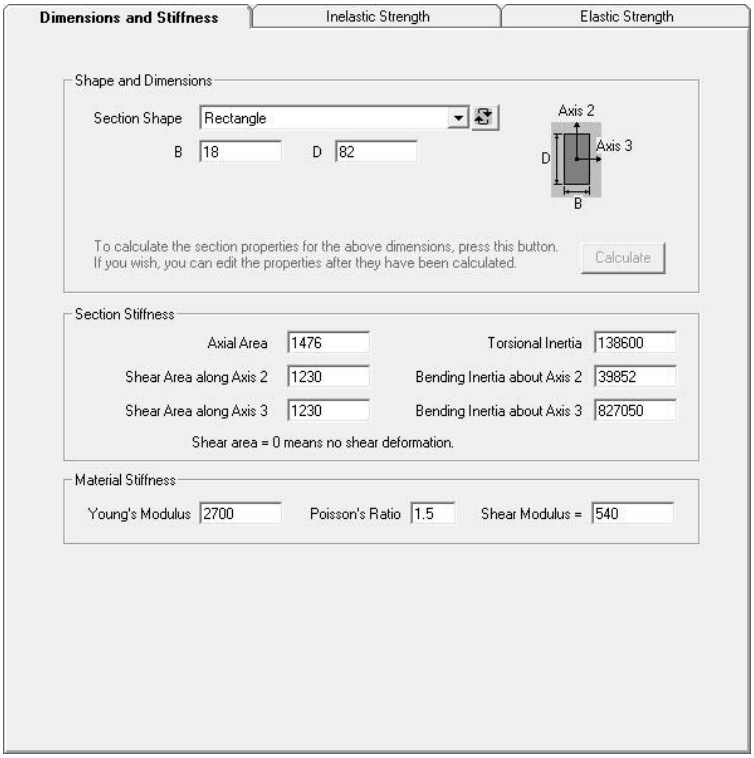

Figure 4.12 Beam, Reinforced Cross Section Input Panel at P3D

There is a modeling sequence while using P3D. Defining materials of concrete and reinforcement are the first stage of modeling for fiber wall elements. Cross-section definitions are first conducted for frame elements like beams and columns at P3D. After material definitions and section properties are determined, inelastic or elastic basic components should be defined. Then, all the detailed components are created with these definitions to exhibit structural behavior, and these components can be properly combined with the compound component task at the last step of modeling.

4.1.2.3 Basic Components and Strength Section

Basic components can be defined in two separate sections: inelastic and elastic components. A response curve for inelastic behavior, i.e., force vs. displacement

curves or derivatives such as moment-rotation, moment-curvature, axial force-strain, shear force-displacement, can be defined. Such material models can be defined for beams, columns, bars, connection panel regions, seismic isolator, fluid damper and BRB (Buckling Restrained Brace) at P3D. End zones of column and beam connections, linear hinge and release parts, elastic bars and springs, elastic connection panel zones, strain and rotation gages are components that can be defined elastically. Inelastic or elastic section definitions can be made with basic component tabs, while section checks in terms of force-based behavior can be made with definitions on the strength sections tab. All critical sections of structural elements that do not have ductile behavior can be checked in terms of strength with moment, shear and axial load capacity definitions.

In the modeling of the high-rise case study building in this study, “Moment Hinge, Rotation Type” and “Shear Hinge, Displacement Type” components of the inelastic section of link beams can be used in the model (Figure 4.13). In addition, the components “Axial Strain Gage (2-node)”, “Rotation Gage, Beam Type (2-node)” and “Rotation Gage, Wall Type (4-node)” from the elastic section can also be used (Figure 4.14).

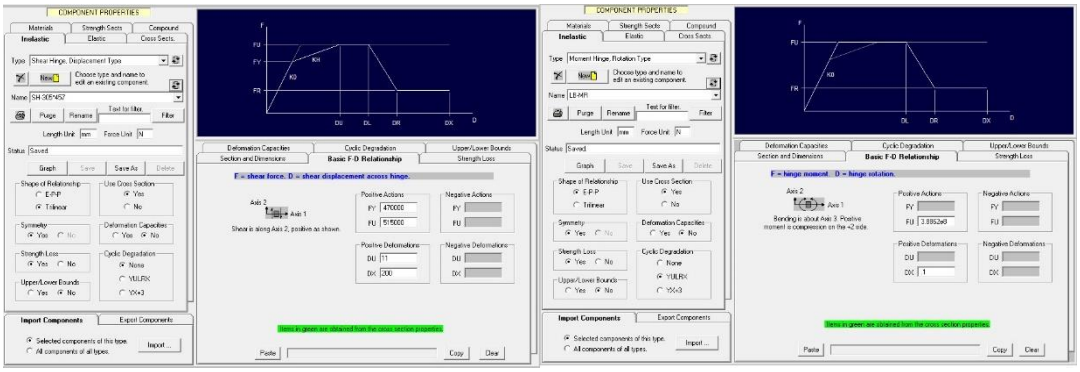

Figure 4.13 Inelastic Components Input Panel of Link Beam at P3D

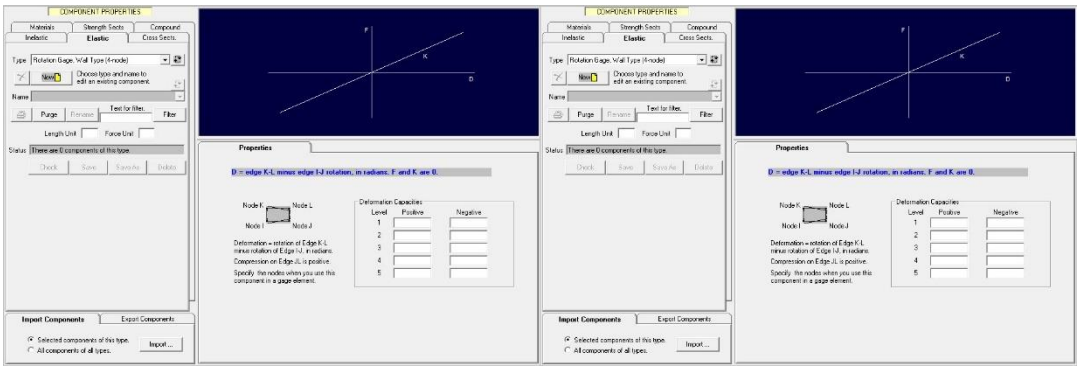

Figure 4.14 Elastic Gage Component Input Panel at P3D

4.1.3 Compound Components

The definitions of structural elements to be used in modeling are completed step by step in P3D. In these definitions, many sub-parameters and model definitions are made according to the behavior of the structural element. Many minor components such as material models, cross-section properties, elastic and inelastic behavior models, and strength definitions are defined. The formation of elements at P3D is done by the proper combination of these components. The behavior of structural materials is complemented by the proper join of the components according to the structural elements that are columns, beams and walls.

Elastic parts of the beam elements are defined by “cross-section” components including stiffness and strength properties. In addition, the shear strength definition is defined separately. If the beam is not a link beam, the beam exhibits inelastic behavior under bending and while elastic behavior is assumed for the shear response. Plastic hinge behavior is expected at the ends of the beam. Plastic hinge definition can be done in terms of rotation or curvature by defining a plastic hinge length (Figure 4.15). After all the components required for beam element definitions are completed, they are combined in the compound component task at P3D (Figure 4.16).

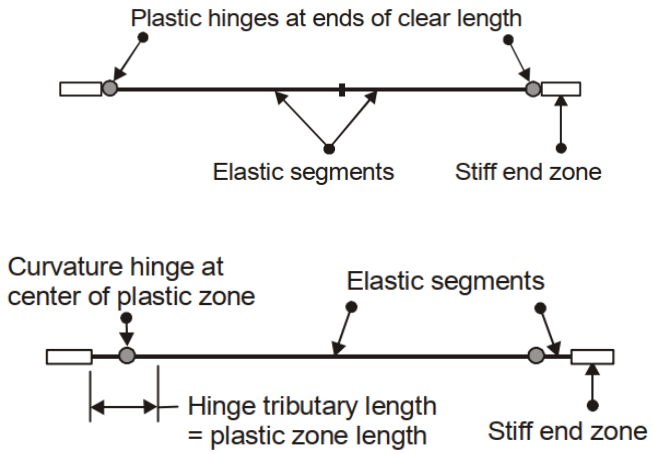

Figure 4.15 Beam Models with Plastic Hinge and Curvature Hinge Components (Computers and Structures, Inc., 2006)

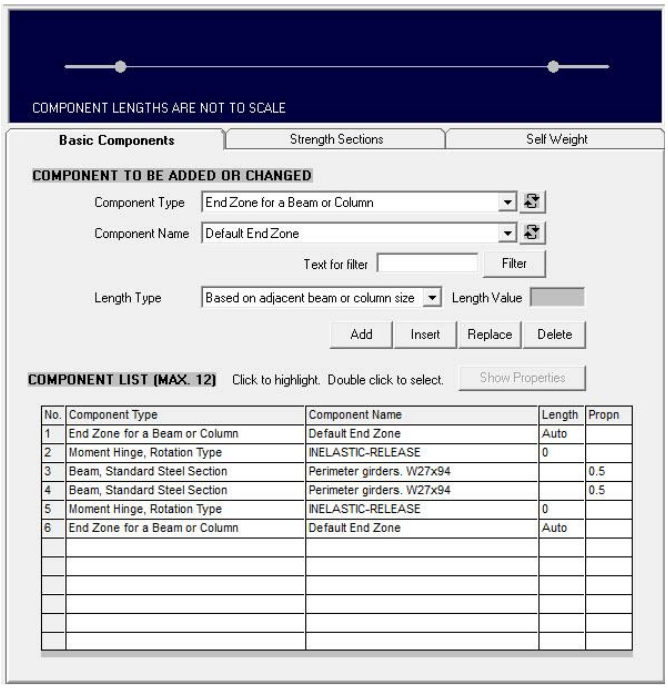

Figure 4.16 Compound Components of Beam with Moment Hinges at P3D

While many beam behaviors are inelastic under bending and elastic under shear demands, the opposite is true for link beams. Inelastic shear behavior is active in link beams because of the dominance of shear force. The link beam model basically consists of the plastic shear-hinge in the middle of the elastic segment of the beam

and ends where moment strength sections are shown in Figure 4.17. Also, shear hinge can be modeled on the basis of strain or displacement in P3D. Typical link beam element model is shown in Figure 4.18.

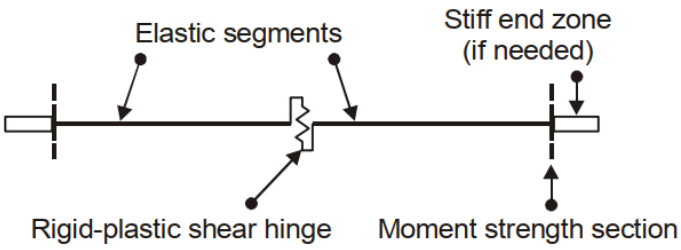

Figure 4.17 General Approach for Compound Components of Link Beam (Computers and Structures, Inc., 2006)

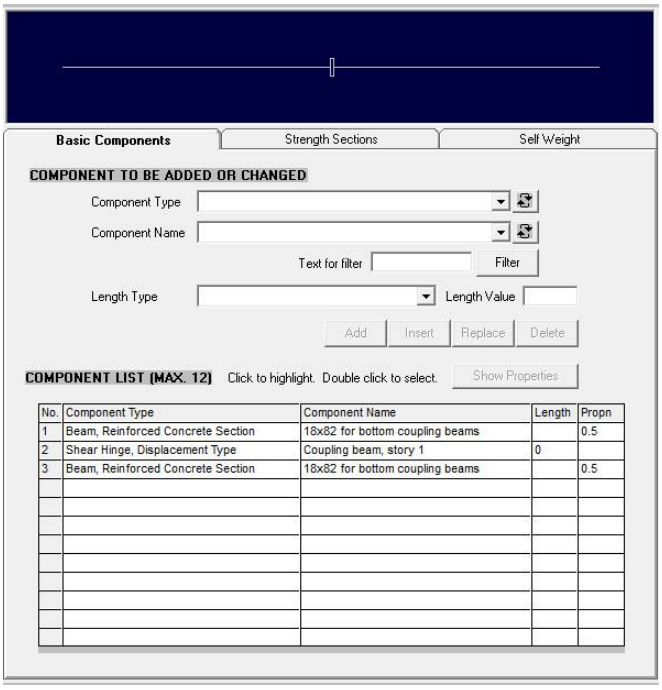

Figure 4.18 Compound Components Sample of Link Beam at P3D

The compound components formation of walls includes combination of fiber-cross section definitions for axial-bending properties and "Elastic/Inelastic Shear Material for a Wall" component for shear properties. In the fiber-cross section, definition can be made as shear wall or general shear wall components. Only vertical inelastic fiber

formation is allowed for the shear wall module, on the other hand both vertical and horizontal inelastic fibers can be defined with the general shear wall module. If the wall type is a squat wall, or if a wall has irregular openings, it is appropriate to use a general shear wall module. But shear wall component is generally used for slender common walls.

4.1.4 Wall and Link Beam Elements

The components of wall and link beam elements are initially created and combined, then assignments of them are made to the elements in the model. All structural elements in the model can be generally grouped to control the results of analysis conveniently according to their types, sizes, positions and reinforcement ratios. In addition, local axis directions should be defined individually at P3D. Geometric nonlinearity identification can be considered for all elements. The "βK" viscous damping ratio for each element can be increased and reduced individually.

The working principles and true modeling of wall and link beam elements in P3D should be known for correct modeling of 3D total structure. For this reason, some important subjects related to wall element are stated in the following items below:

- Each wall element consists of 4 nodes (K-L-I-J) and each node has six degrees of freedom.
- Common definition of three local axes is axis 1, 2 and 3 for normal, vertical and horizontal directions respectively.
- Positive sign convention of wall element for axial force, shear force and bending moment is shown in Figure 4.19.

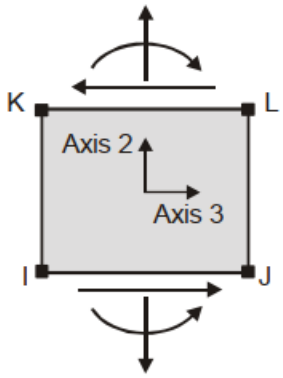

Figure 4.19 Positive Sign Convention of Wall Element(Computers and Structures, Inc., 2006)

- Using the minimum number of elements and fibers by providing real structural behavior in the model will reduce analysis time and margin of error. Therefore, walls should be modeled with an optimum number of fibers.
- Neutral axis shifts towards the compression zone after cracking and yielding of reinforcement in the tension section of the walls. It is important to take into account the shift of the neural axis in the wall under axial loads and bending loads in order to accurately reflect inelastic wall structural behavior. P3D takes this important behavior into account.
- The amount of mesh of the walls vertically and horizontally should be kept at the optimum level, so that both accurately reflecting the structure behavior and shortening the analysis time. In high-rise buildings, it may be enough to model one wall element on each floor in a vertical direction. Curvature, axial and shear strains are constant throughout each wall mesh element. For this reason, the number of elements can be increased or selected at a reasonable height in the hinge section, which has plastic behavior for the walls.
- Appropriate inelastic hinge section height is very important in the modeling of walls because it affects the calculated strain and bending moment capacities. The correct height selection of elements representing hinge length is a very sensitive parameter that affects the accuracy of the calculated strain.

According to ASCE 41, the hinge length of walls is minimum of one-half of cross-section depth and story height.

- In high-rise structures, core wall groups exhibit elastic behavior as they continue upward while inelastic behavior exists in the hinge section of the wall where they are connected with the foundation. As an alternative modeling, inelastic modeling can be used in the lower hinge sections, while the elastic wall component can be used in the upper sections. So, this will both shorten the analysis time and minimize the error. The point to note here is that a sufficient number of inelastic elements should be defined to represent the hinge section.

- There is no definition of in-plane rotational stiffness in the nodes of a wall element. Therefore, the connection between the beam and the wall is pin connection. For this reason, imbedded beam modeling is required in order to have moment-resisting connection between wall and beam. As in our sample structure, it is necessary to pay close attention to the use of imbedded beam for the correct model of link beams and core wall groups. The wall element can also be used in the modeling of link beams, but the use of frame elements together with the imbedded beam allows for better control. The use of imbedded beam for deep link beams ($1.0 < \ln / h < 2.0$) is throughout vertically linking with walls at beams own height (Figure 4.20). For conventionally reinforced link beams ($3.0 < l_n/h < 4.0$), imbedded beams are connected horizontally to walls (Figure 4.21). The bending inertia of imbedded beams modeled for slender link beams is taken as 20 times more than the stiffness of the connected link beams inertia, while the axial area and torsional stiffness are close to zero. The bending rigidities of the imbedded beams required for deep beams in the weak direction should also be close to zero. The reason for reducing the rigidities too much is to prevent increased local stiffness in a way that affects the behavior of the wall.

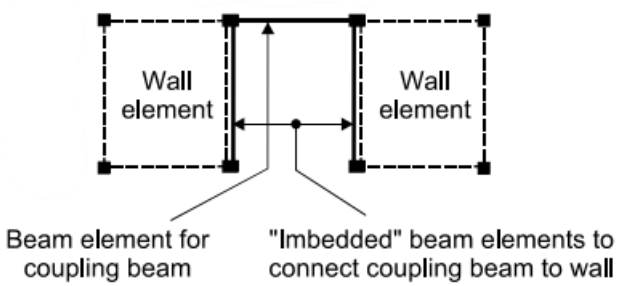

Figure 4.20 Deep Link Beam ($1.0 < l_n/h < 2.0$) Connected to Wall with Imbedded Beam (Computers and Structures, Inc., 2006)

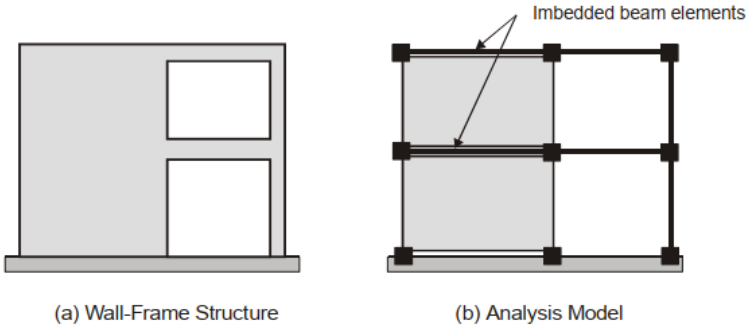

Figure 4.21 Link Beam ($3.0 < l_n/h < 4.0$) Connected to Wall with Imbedded Beam (Computers and Structures, Inc., 2006)

- "Monitored" fiber sections can be used to observe concrete and steel strain demands while identifying shear wall fiber cross-section. However, it is more appropriate to define strain gages describing the gage length for the curvature calculation and detect curvatures at the boundary of the walls. Because average measurements, which are more accurate and suitable, can be obtained with average strain measurements, while local stress concentrations can be detected with the "monitored" fiber method. The important thing here is to make the determination of the gage length correctly.
- It is appropriate to make shear strength demand/capacity check with the "structure section" for each wall arm. Because “structure section” help to see the average shear strength of walls.

- In-plane behavior of shear wall element is more effective and dominant than out-of-plane behavior. For this reason, out of plane bending is defined as elastic behavior, while in-plane behavior is defined as fiber inelastic cross-section. The out-of-plane elastic bending rigidities of walls should be reduced by one-quarter.

Walls and link beams can effectively transfer earthquake forces to the foundation. Acceptances and necessary information in the modeling of wall elements in P3D are listed in the items above. In addition, having the necessary information about link beam will be important for accurate modeling and result evaluations. The important subject related to the modeling of beams in P3D are presented in the following items:

- Sign convention of beams is shown in Figure 4.22. Tension axial load, shear force along axis 2 and bending about axis 3 are positive signs.

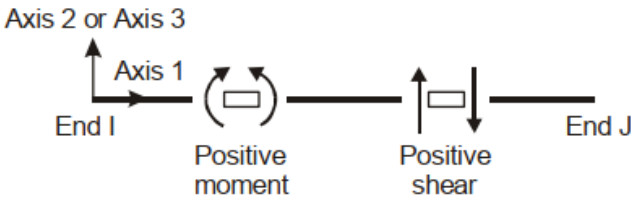

Figure 4.22 Sign Convention of Beam at P3D (Computers and Structures, Inc., 2006)

- There are lots of component alternatives when creating compound components for beam elements. These can be auto stiff end zone, P/V/M release or linear hinge, elastic cross-section segment, inelastic fiber cross section, rotation or curvature moment hinges, semi-rigid moment connections and strain/displacement shear hinge components.
- The auto end zone component is actually automatically defined in column and beam connections at P3D. This zone has rigidity of 10 times more than the body of components according to the size of the column and beam.

- Rotation measurements of the beams having the stiff end zones are made according to the clear span of the beams (Figure 4.23). This desired approach is also considered in P3D.

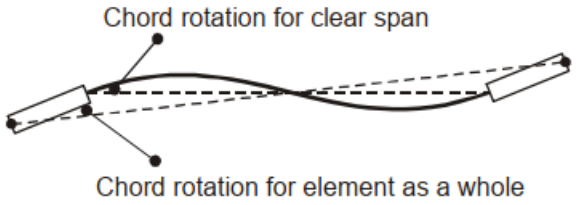

Figure 4.23 Chord Rotation of Beam with Stiff End Zone (Computers and Structures, Inc., 2006)

4.1.5 Other Modeling Phase Subjects

Some of the remaining important notes on the modeling phase in P3D are as follows:

- Slabs can be only modeled elastically by "Elastic Slab/Shell Element" component with in-plane and out-plane bending stiffness for deformable floor diaphragms. The sign convention of slabs can be seen in Figure 4.24. Slab/shell elements have not any dissipated energy function in terms of βK damping.

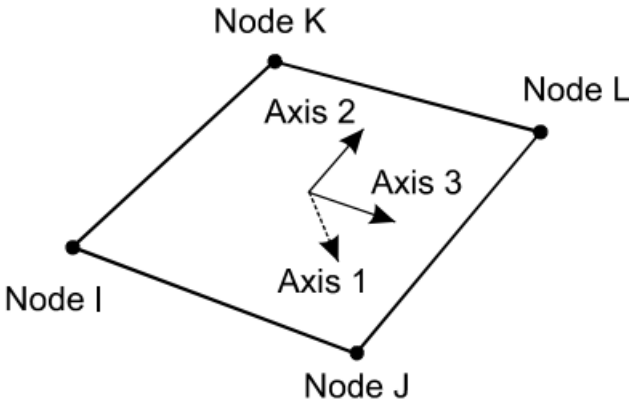

Figure 4.24 Elastic Slab/Shell Component Sign Convention (Computers and Structures, Inc., 2006)

- Loads can be given on nodes and elements. Self-weight is automatically calculated according to gravity nodal loads, and geometric properties of elements by P3D.
- "Structure Section" module can be used to determine the total sum of average forces of a number of elements. It is common to check the shear strength of a wall with this function. This can be accomplished by checking the ratios of walls strength with average internal force.
- Limit states of deformation (rotations, curvature, and displacements), strength, drifts, deflection and shear strength of structure sections can easily be defined at P3D, and the demand-capacity ratio of these states is generally 1.0. If you want to easily increase the capacity of a component with %20, demand-capacity ratio can easily be selected as 1.2. It is possible to assign several limit states for different element groups and performance levels, i.e., immediate occupancy, life safety and collapse prevention.

4.2 ANALYSIS PHASE

4.2.1 Load Cases

There are a number of analysis options namely, gravity, dynamic earthquake (time history analysis), push-over and response spectrum analysis at P3D. Linear and nonlinear options can be assigned with gravity load cases. Most of the structures can be accepted as elastic under gravity loads. So, there is no need to use nonlinear analysis under gravity loads.

Event to event solution strategy is used for the nonlinear analysis. P3D conducts nonlinear analysis in a number of predetermined load steps. These load steps are also divided into events. These numbers should be enough to have a stable solution for nonlinear analysis. There can be unstable situation and analysis will stop at the end of maximum number of load steps.

Dynamic earthquake analysis, i.e., time history analysis, is conducted with a step-by-step integration method, i.e., Newmark-constant average acceleration method with acceleration records of H1 and H2 directions. Any earthquake records can be defined and assigned with placing acceleration-time pair data to records folder.

4.2.2 Analysis Sub-Options and Damping

Analysis time is very important for seismic performance nonlinear analysis. In particular, it is even more important in the solutions of high-rise structures with high analysis time. The amount of overshoot tolerances for a yielding element can be adjusted to decrease run time. So, event overshoot default factor "1 (%1)" can be increased to "5 (%5)" or "10 (%10)" for large structures. However, one should make sure that there is not a significant difference between external and internal work energy after analyzes. These should be almost the same.

Structure dissipates some of the total input energy with viscous damping. Correct damping assignments affect the remaining part of energy release and analysis results. Viscous damping can be modeled as modal damping or Rayleigh damping.

P3D calculates up to 50 mode shapes. However lower modes after 50 modes are also important for high-rise buildings or great structures for correct total behavior in terms of including damping. While all mode shapes are damped up to 50 modes, but lower modes are not damped if program user only use "Modal Damping" module. Damping in short period modes should also be included for high-rise buildings. So, it is strictly advised that small amount of βK Rayleigh damping should be added to modal damping to damp higher mode displacements for high-rise buildings.

Rayleigh damping is used also for nonlinear analysis. This damping model is given by Equation 4.1. $\underline{M}$ is structure mass matrix, $\underline{K}$ is the initial elastic stiffness matrix, and α and β are multiplying factors.

$$\underline{C} = \alpha \underline{M} + \beta \underline{K} \qquad \textbf{(4.1)}$$

Velocity dependent viscous dampers are arranged as Figure 4.25. While βK viscous dampers are internally connected between masses, αM viscous dampers are connected to external masses (Figure 4.25). βK and αM viscous dampers complete each other for different periods. αK viscous dampers results less damping in lower modes and more damping in higher modes, on the other hand, βK viscous dampers results more damping in lower modes and less damping in higher modes (Figure 4.26). Rayleigh damping solutions are uncoupled between mode shapes. There is no effect of a damping force related to a mode with another mode.

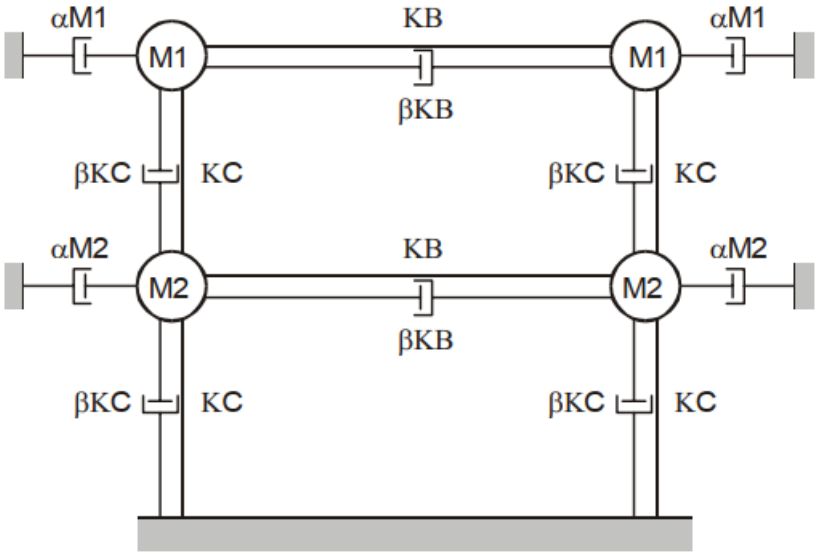

Figure 4.25 α and β Viscous Damper Arrangement in Model (Computers and Structures, Inc., 2006)

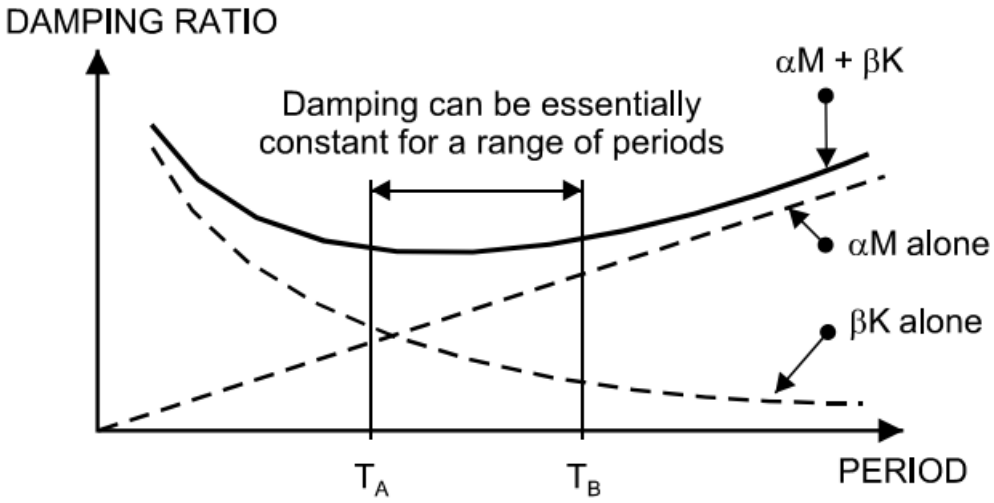

Figure 4.26 Variation of αM and βK Damping Ratios with Periods (Computers and Structures, Inc., 2006)

βK damping uses initial stiffness of the structure in a nonlinear calculation. However, stiffness continuously changes after cracking of concrete at nonlinear analysis. Inelastic concrete fibers cracks, neutral axis changes and initial high stiffness decreases. The same situation is valid for a coupling panel, modeled with wall module, between coupled shear walls. P3D automatically decreases initial total stiffness to %15 of initial stiffness for damping calculation purposes. For other elements which use inelastic fibers, user should have an awareness that P3D does not decrease initial stiffness of that element like wall if Rayleigh damping option is used. This causes the estimation of βk type energy dissipation. βk values should be revised for some element groups like coupling panels and include concrete fiber with "Scale Factor for Beta-K Damping".

Both damping methods are suitable, but to decrease run time and to get enough mode shapes, it is advised that both Rayleigh and modal damping method can be run within an order for preliminary analyzes then after checking that both methods give similar results, modal damping method can be used with enough number of mode shape and optimum run time.

4.2.3 Energy Balance

External earthquake energy is converted on structure to internal energy as stored elastic energy and dissipated inelastic energy. Stored elastic energy can be divided as kinetic energy on masses and recoverable strain energy in the elements while non-recoverable (damaged) inelastic energy dissipated in the elements and viscous damping energy can be generally thought as dissipated inelastic energy (Figure 4.27). Earthquake energy can be consumed on structure with movement, elastic deformations, yielding, cracking, damage and friction etc. P3D shows us the amount of consumed energy at different forms mentioned above separately. Energy balance plots are drawn only for dynamic analyzes (time history analyzes) at P3D.

Energy balance task helps the P3D users to assess the performance of the structure. It can be determined that which element or element group contributes to the inelastic dissipated energy with how much amount. In addition, it can be observed that relative amount of dissipated energy is contributed by different structural element groups. This shows us that which structural elements or portions are more effective under the earthquake load. Also, the correctness of the model can be checked by comparing external and internal energies shown in the ECHO file. Energy differences should not be greater than %5. If Rayleigh damping model is used at the model, contribution of βK dissipated viscous energy can be determined for all elements groups separately.

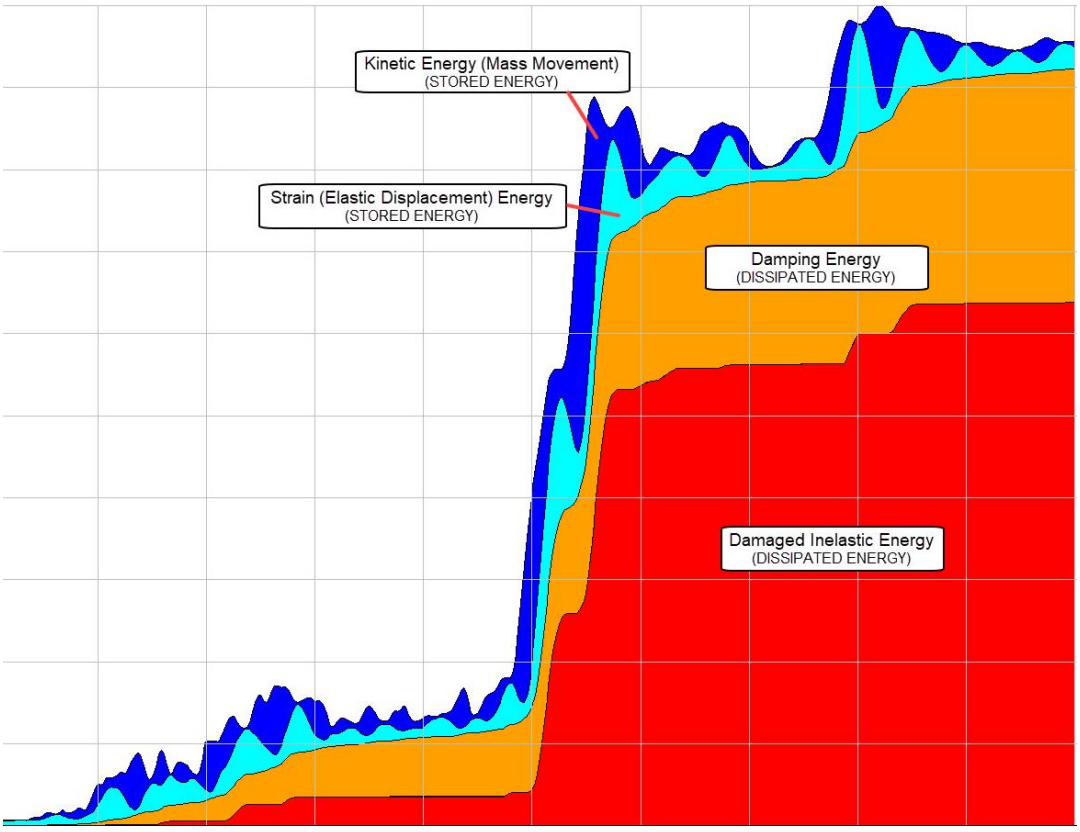

Figure 4.27 View of Dissipated Energy Diagram at P3D

There is a small calculation error at P3D, when a model consists of components with stiffness degradation. P3D does not consider stiffness degradation during energy calculation. This causes that the elastic displacement part of strain energy is underestimated and inelastic damage energy is overestimated. This error gets smaller for dynamic earthquake analysis. To sum up, that small error is not very important for the right evaluation of the model analysis results.

CHAPTER 5

STRUCTURAL WALL AND LINK BEAM CALIBRATON WORK

The key structural elements in resisting lateral forces are structural wall connected with link beams. In the performance analysis of high-rise buildings equipped with walls, it is very important that walls and link beams are modelled correctly in harmony with the horizontal load-displacement cyclic response results from the experiments. There is no such requirement in Turkish Earthquake Code-2018 about such a calibration and engineers are free to select any constitutive model, whose sensitivity requires detailed investigations.

The first issue that needs to be done or verified in the performance analysis of the structures, is the calibration of the horizontal load-displacement cyclic response with experimental behavior, called herein “Model Calibration”. The working principle and the modeling provided in an existing software used in modeling to performance based nonlinear structural analyses should be verified. This confirmation is carried out by comparing with results of the experiment and simulations at the simple structural element level. Cyclic hysterical response curves of structural elements are complex behavioral patterns that depend on many physical parameters. For this reason, there are many input values affects these curves according to the working principle of the programs used in modeling. This is closely related to one of our key research questions: "How much error occurs in the 3D high-rise building PBD for various different selection of material parameters?”

The comparisons of experimental and model results in terms of hysterical response are conducted for a rectangular wall, a T-shaped wall, a U-shaped wall, a diagonally detailed link beam and conventionally detailed link beam. After providing detailed information on the experimental studies, modelling, calibration and input recommendation results are presented in this chapter.

5.1 CALIBRATION WORK FOR STRUCTURAL WALLS

Structural walls are widely used in the form of rectangular form or U-shaped for fire escapes or elevator perimeter walls. In addition, T-shaped wall layouts are common in buildings depending on architecture. In high-rise buildings, as in our sample building, there are wall groups, i.e., core wall, where architectural requirements such as fire escape, elevator, mechanical shaft. Experimental studies have been carried out for rectangular, T-shaped and U-shaped walls so far. The modelling results of these three examinations are reflected in core wall in high-rise buildings. In high-rise buildings, it is common practice to assume walls to work as a group under moment on core wall, while each wall leg of a group is evaluated separately under shear force. Since there is still no experiment to examine hysterical behavior of a full core wall with realistic dimensions, core wall in our high building sample case is modelled through calibration work results obtained from the wall shapes that have been experimented with.

5.1.1 Experimental Data for Sample Rectangular and T-Shape Walls

Rectangular and T-shape specimens, RW2 and TW2, which were tested by Thomsen and Wallace, are used for simulations. Test samples with plan dimensions of 102 x1219 mm and height of 3660 mm are presented in Figure 5.1.

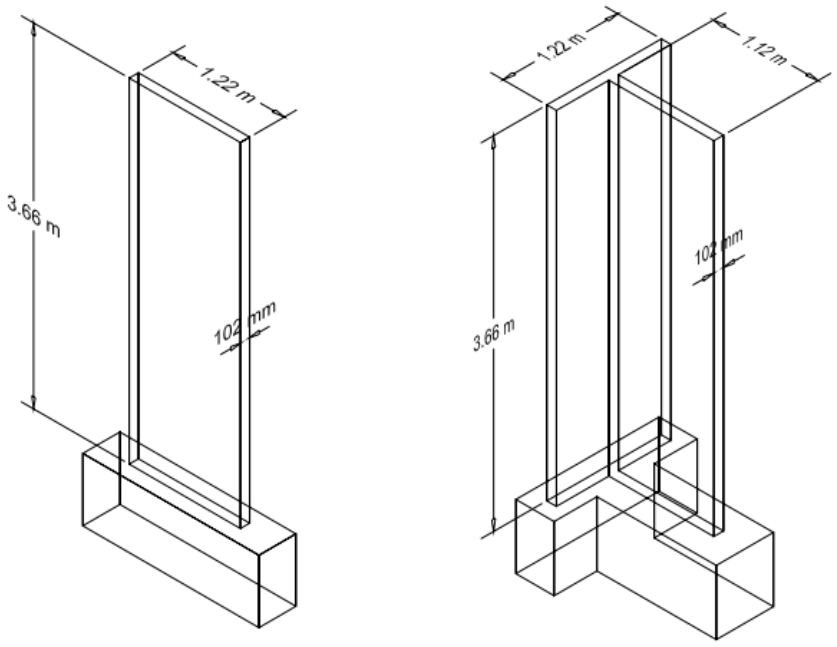

Figure 5.1 Rectangular and T-Shape, i.e. RW2 and TW2, Wall Test Samples (Orakcal et al., 2004)

Compressive strength of concrete at the test day was 42.7 MPa. There were longitudinal steel bars, i.e., 8-#3 bars (db=9.53 mm) and #2 (db=6.35 mm) @191 mm, at boundary and web part of wall respectively. While stirrups of the boundary are placed with db=4.76 mm @ 76 mm, lateral reinforcement of the web of wall were placed with #2 (db=6.35 mm) @191 mm (Figure 5.2, Figure 5.3). Although #3 bars were typical Grade 60 (414 MPa), yield stress of #2 and 4.76 mm smooth wires was approximately 448 MPa. Measured stress-strain profiles of reinforcements are shown in Figure 5.4.

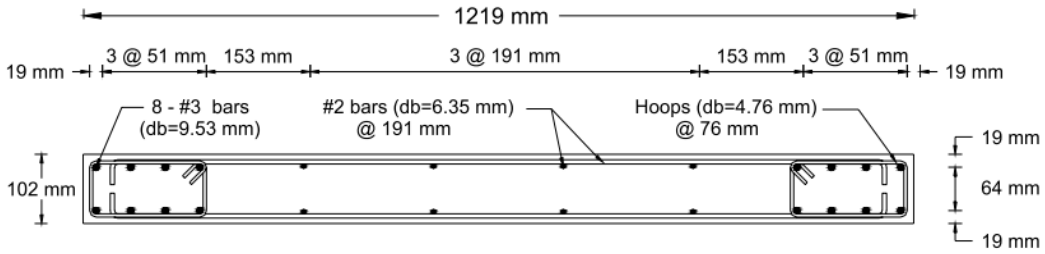

Figure 5.2 Specimen RW2 (Orakcal et al., 2004)

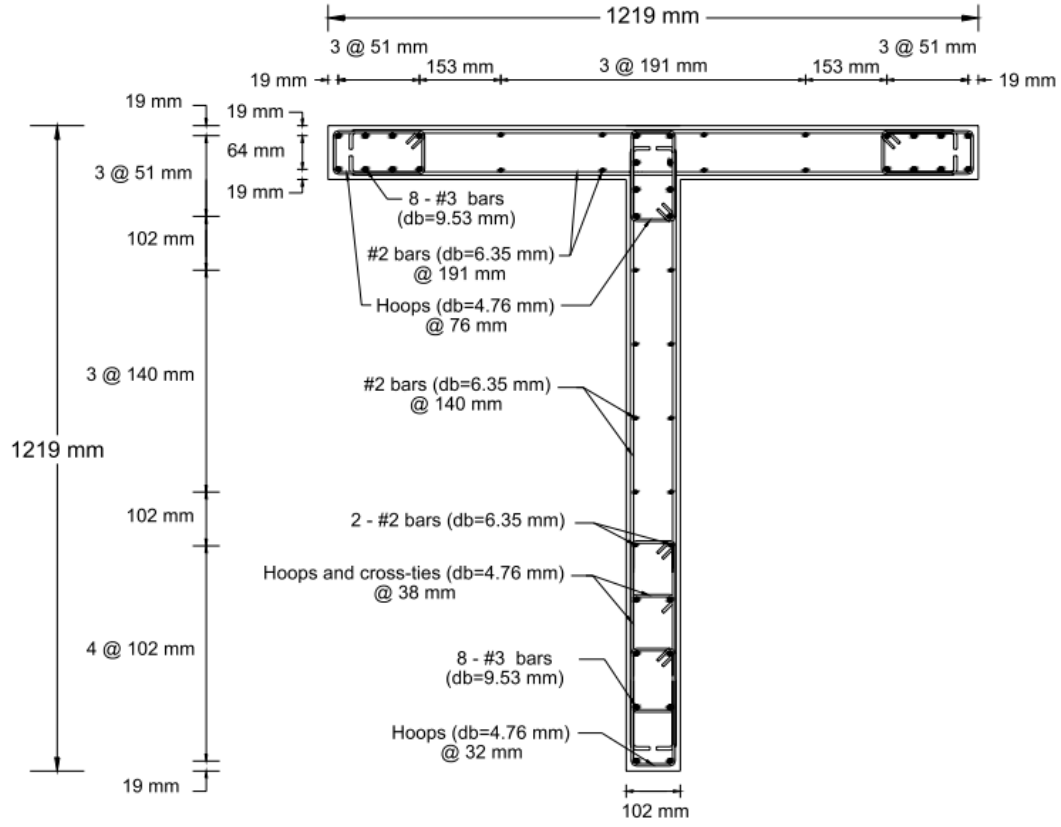

Figure 5.3 Specimen TW2 (Orakcal et al., 2004)

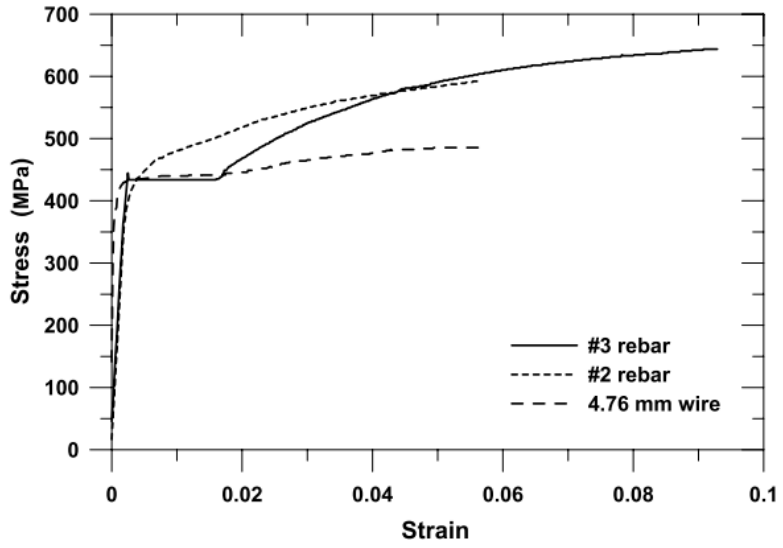

Figure 5.4 Measured Stress-Strain Relation of Reinforcements of RW2 (Orakcal et al., 2004)

Schematic test setup is shown in Figure 5.5. Firstly, an axial load of 0.07-0.075 *A_g f_c' was applied continuously by using hydraulic jacks and high-strength post-tensioning cables. After axial load was applied, displacement controlled reversed lateral cyclic loads were applied by hydraulic actuator from the top of the specimen.

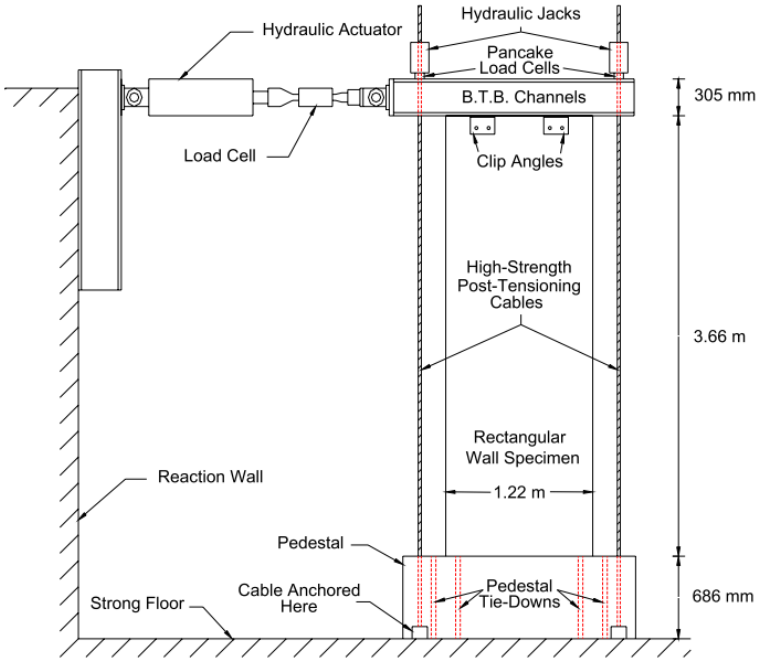

Figure 5.5 RW2 Test Setup (Thomsen and Wallace, 1995)

A total of 20-22.5 lateral load cycles were applied with a sequence of 0.1%, 0.25%, 0.50%, 0.75%, 1.00%, 1.50%, 1.00%, 1.50%, 2.00%, 2.50% drift levels under displacement-controlled approach.

Different instruments were placed at critical regions of specimens to measure forces, displacements, and strains (Figure 5.6). Wire potentiometers were used to measure horizontal, vertical displacements and shear deformations. Vertical linear variable differential transducers (LVDTs) were placed at the bottom portion of specimens to measure axial strains and to calculate section curvatures. Concrete strain gages were placed to both end of specimen to measure the strains of concrete. Hollow pancake load cells and hydraulic actuator were used to measure axial load and lateral cyclic loads respectively.

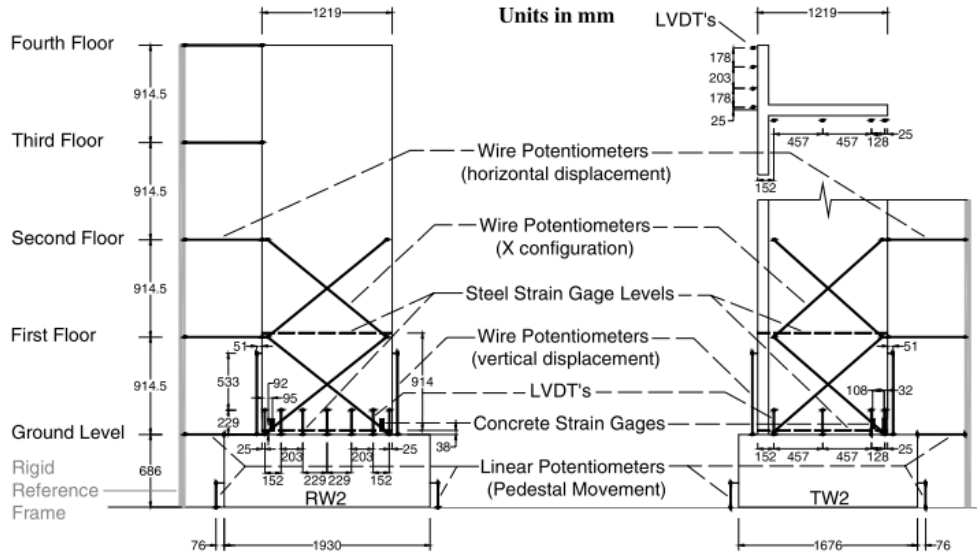

Figure 5.6 Different Instruments Placed on Specimens (Thomsen and Wallace, 1995)

According to the test results, RW2 and TW2-Lateral Load vs. Top Flexural Displacement Cyclic Responses are given below in Figure 5.7 and Figure 5.8.

RW2-Cyclic Response Test Result

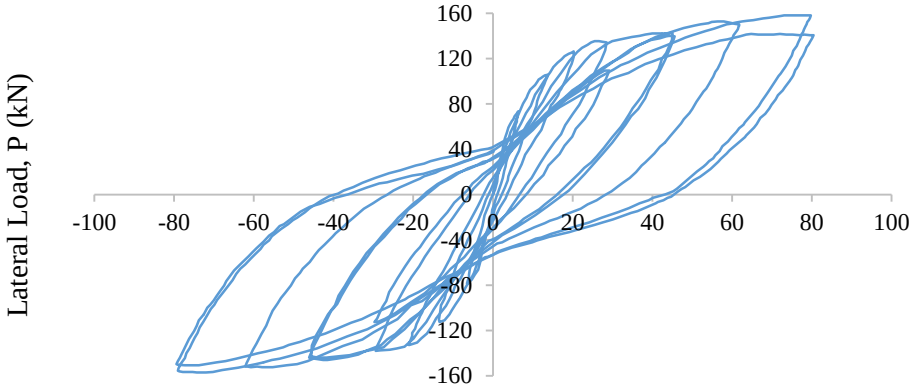

Figure 5.7 RW2-Lateral Load vs. Top Flexural Displacement Cyclic Response Test Result

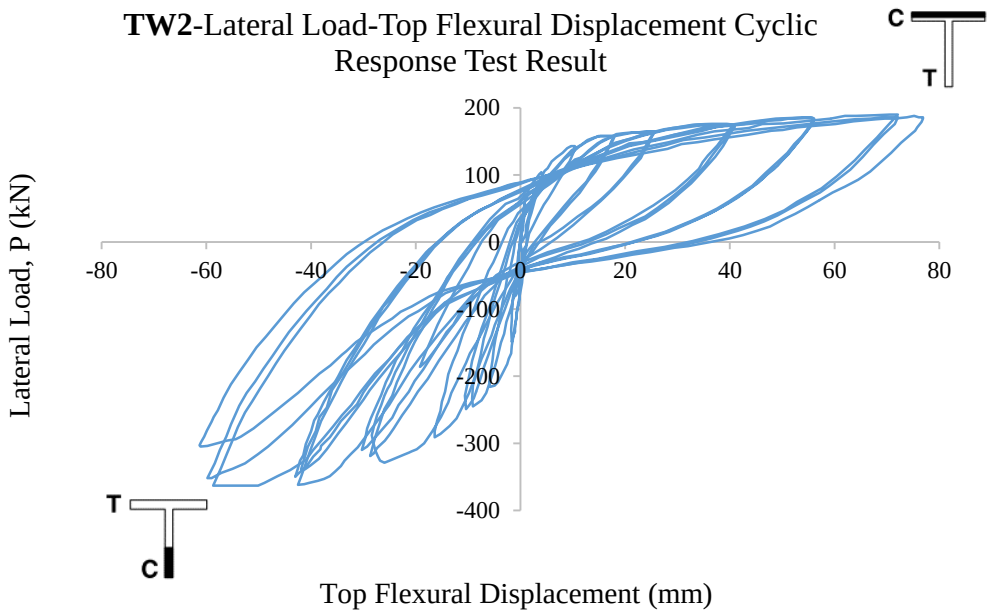

Figure 5.8 TW2-Lateral Load vs. Top Flexural Displacement Cyclic Response Test Result

5.1.2 Experimental Data for Sample U Shape Wall

U-shaped form for shear-walls is widely used in structures such as fire escape, elevator perimeter walls etc. For this reason, the cyclic behavior of this shear-wall form under earthquake load is important and was tested by Pegeon et al. at Elsa Laboratory. This test was conducted within the framework of the "Shear Wall Structures" of the European Research Programs for the development of Eurocode 8.

Three U-shape wall specimens were used at this cyclic test. These specimens were separately used for uniaxial cyclic test for X and Y direction, and biaxial cyclic test in XY direction. Only uniaxial cyclic test results (X and Y direction) were used for the simulation of U-shape walls. Wall 1 and Wall 2 specimens were used for X and Y direction cyclic test respectively.

The lengths of U-shape walls' two leg and section depth were 125 cm and 150 cm respectively. Thickness of the wall was 25 cm. Dimensions of boundaries were 25 cm x 37.5 cm. Longitudinal reinforcements of boundaries were 9ϕ12 (at corners) and 10ϕ12 (others). Web portion longitudinal reinforcements were ϕ10/25. Horizontal reinforcements were ϕ8/12.5 and ϕ8/7.5 at flanges and web of U-shape wall respectively. Boundary stirrups were ϕ8/9. All these details are shown in Figure 5.9.

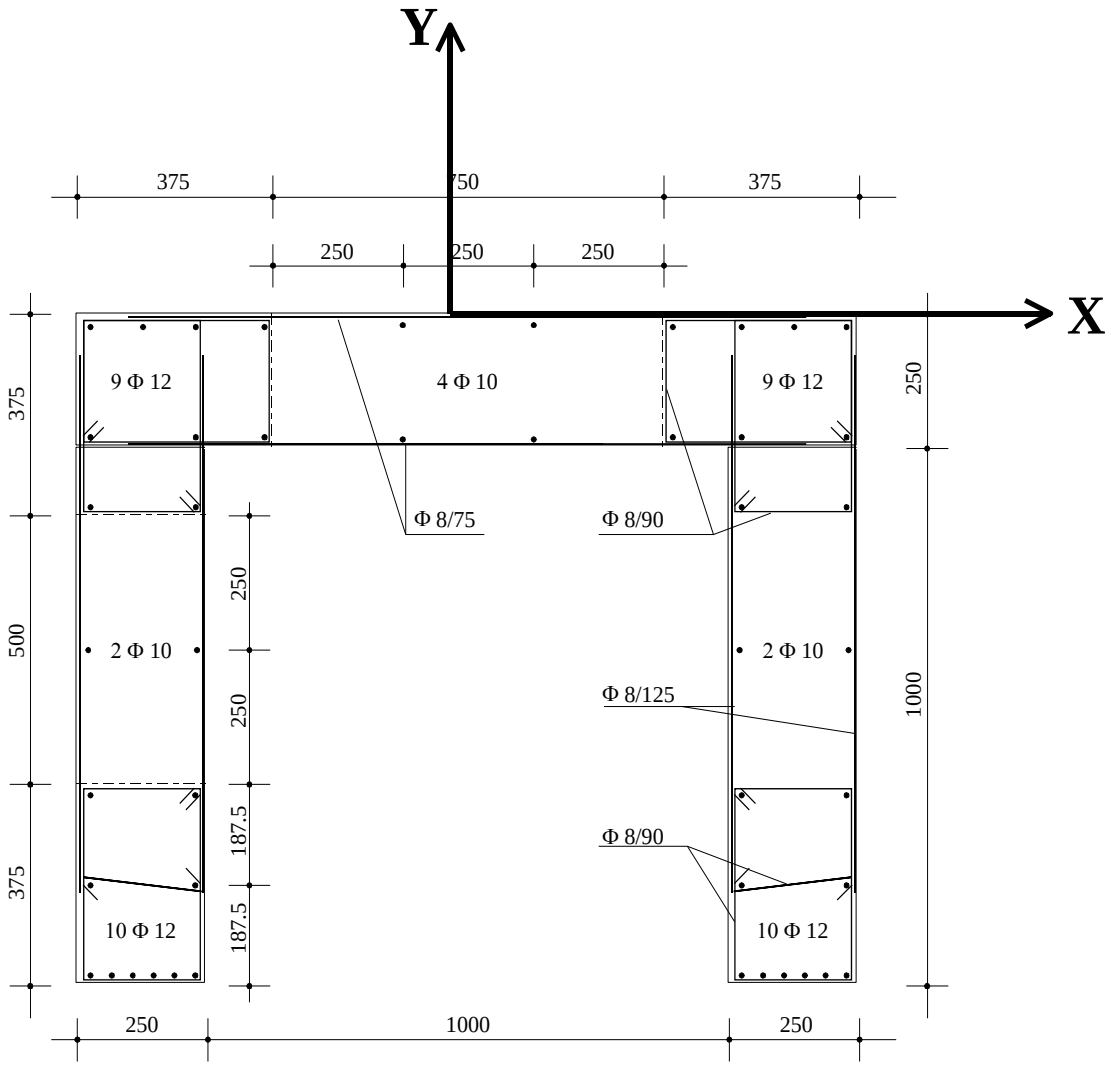

Figure 5.9 U-Shape Wall Specimen Dimension and Reinforcement Detail (Ile & Reynouard, 2005)

Height of the wall was 3.6 m (Figure 5.10). Foundation was clamped down to laboratory strong floor with 22 anchorages. There was 2 MN continuous vertical force on wall, which was applied at gravity center of wall with help of six distributed post-tensioning bars goes through top slab. Uniaxial lateral loads were separately applied through X and Y direction from on the top of the slab with two pistons with a displacement-controlled approach.

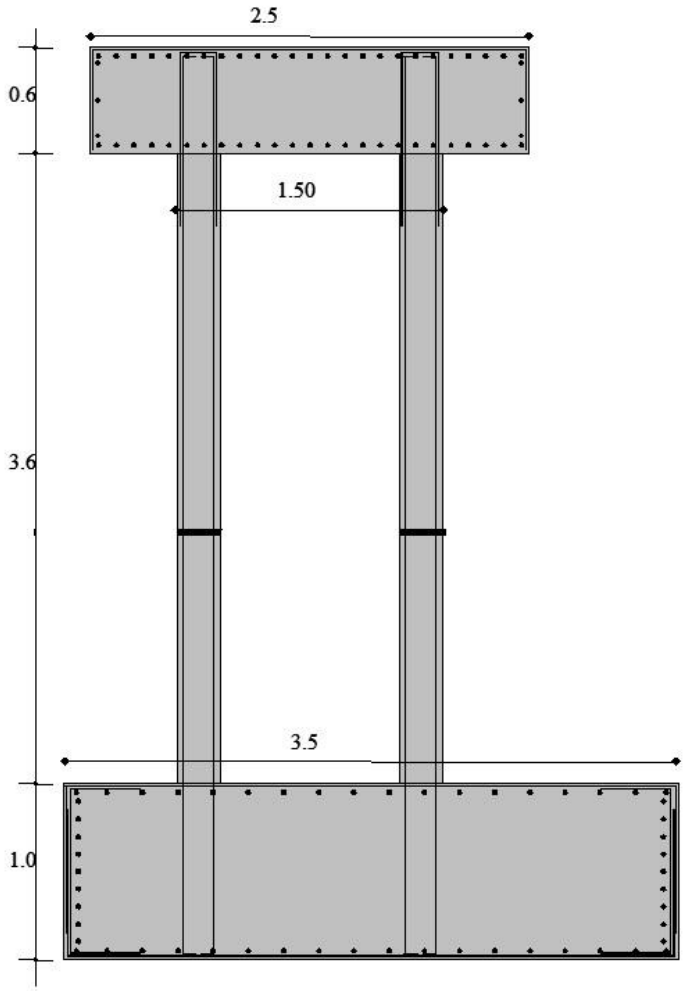

Figure 5.10 U-Shape Wall Specimen Section View (Ile & Reynouard, 2005)

Average cylindrical strength of the concrete used at Wall-1 and Wall-2 specimens was 23.73 MPa. Mechanical properties of reinforcements used at Walls are shown at Table 5.1.

Table 5.1 Mechanical Properties of Reinforcement used at Wall Specimens

Bar diameter	Yield strength f_{sy} (MPa)	Ultimate strength f_{su} (MPa)	Ultimate strain ε_{su} (%)
8 mm	557	642	25.0
10 mm	525	617	24.2
12 mm	516	615	24.8

X and Y direction uniaxial cyclic loading test were realized at very slow rate, i.e. quasi-static. Loading protocol were applied to failure stage for both direction test (Figure 5.11).

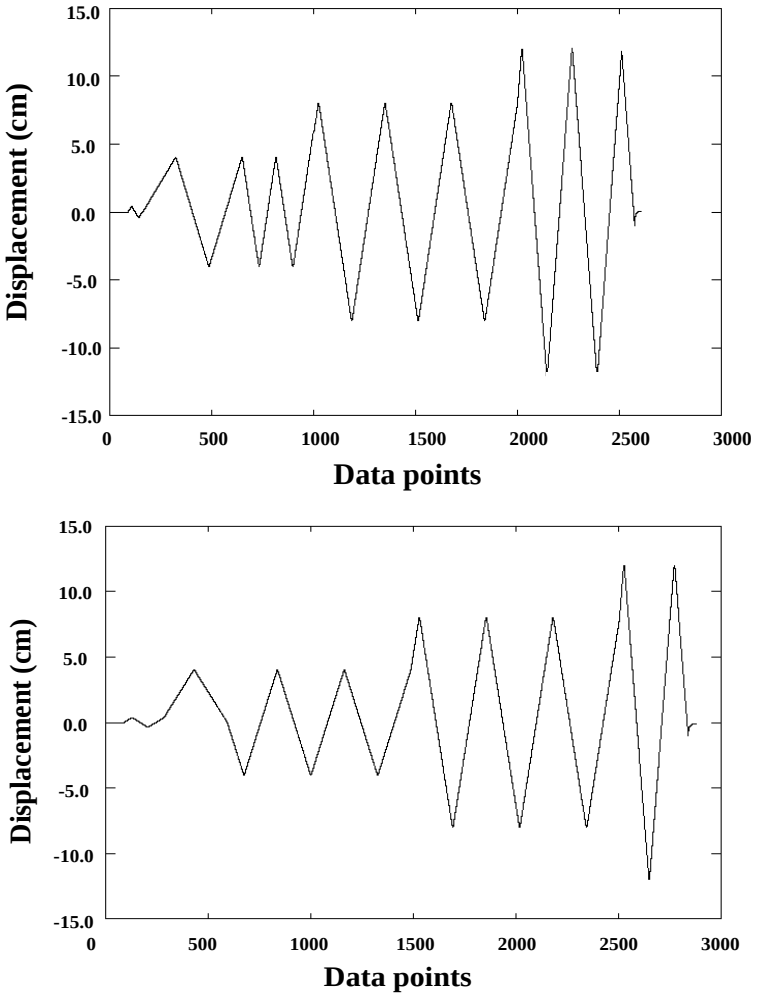

Figure 5.11 Loading Protocol (Average Displacement vs Data Point) for Wall-1 (X Direction-Left) and Wall-2 (Y Direction-Right) (Ile & Reynouard, 2005)

First cracking of wall base, cracks through the whole wall height, concrete crushing, buckling of longitudinal reinforcement, rupture of stirrups and longitudinal reinforcement situations are observed at increasing drift ratios. These observations are tabulated in Table 5.2 and Table 5.3 for X and Y direction loading below. Displacement ductility factor of cyclic test for each direction was about 6.

Table 5.2 Wall-1 (X direction loading) Physical Observations through Cyclic Test

Displacement (cm)	Drift (%)	OBSERVATIONS
1	0,3%	First inclined cracking at the base
2	0,5%	Flange cracks through whole wall height
4	1,0%	Web cracks through whole wall height
8	2,1%	Bucking of some of flange longitudinal reinforcements
12	3,1%	Severe buckling, rupture of some stirrups and longitudinal bars at flanges and web ends

Table 5.3 Wall-2 (Y direction loading) Physical Observations through Cyclic Test

Displacement (cm)	Drift (%)	OBSERVATIONS
2	0,5%	First inclined cracking at the base
4	1,0%	Web cracks through whole wall height
8	2,1%	Strong damage at the base of flange ends but wall still performed very well
12	3,1%	Bar buckling, rupture of some stirrups and longitudinal bars at flanges and web ends

Experimental results of cyclic responses of Wall-1 and Wall-2 are given in Figure 5.12 and Figure 5.13 respectively below.

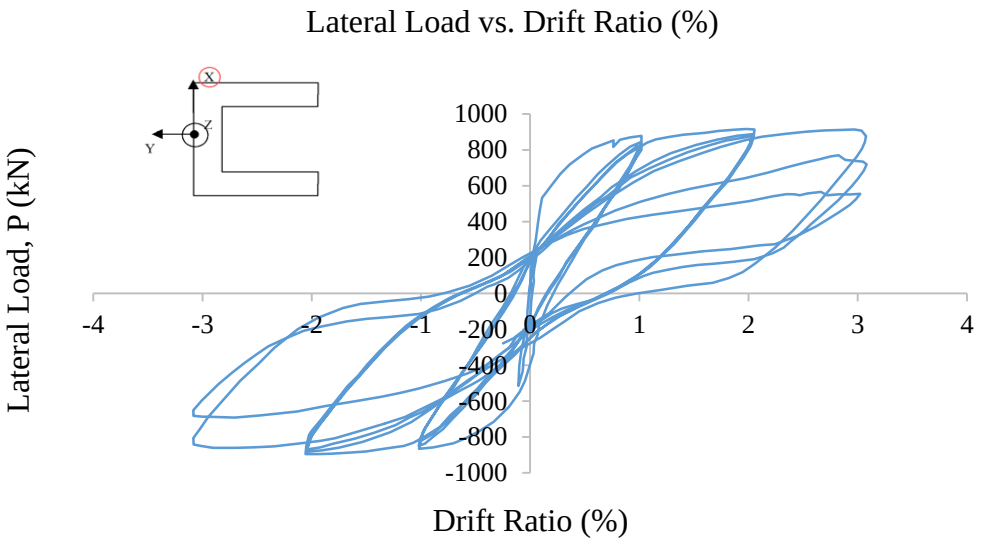

Figure 5.12 Cyclic Experimental Response of **U-Shape Wall-1** (**X** Direction Loading)

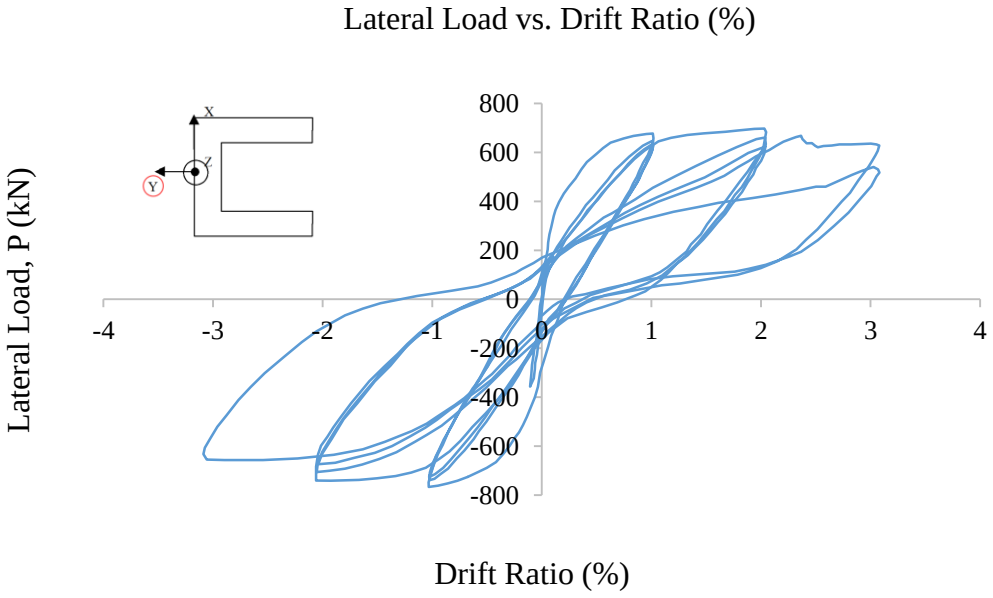

Figure 5.13 Cyclic Experimental Response of **U-Shape Wall-2** (**Y** Direction Loading)

5.1.3 Simulation of Walls Test Samples at Perform 3D V7.0

5.1.3.1 General Modeling Approach for Rectangular, T and U Shape Sample Walls at P3D

Rectangular, T and U-shaped walls in the test wall samples was modelled according to their geometry and reinforcement details in Perform 3D (Figure 5.14). Foundation connection of walls was defined as fixed connection. Equal displacement through laterally was assigned to top nodes of walls (Figure 5.15). Continuous axial load on top of walls were also assigned (Figure 5.16). Drift directions and drift reference nodes were separately defined for each sample walls (Figure 5.17). Because of displacement controlled test approach, all wall samples were defined with horizontal displacement from the top of walls according to the load protocol in the appropriate experiment. Horizontal and vertical mesh of wall were made taking into account through web and boundaries of walls. The mesh sensitivity was also examined later.

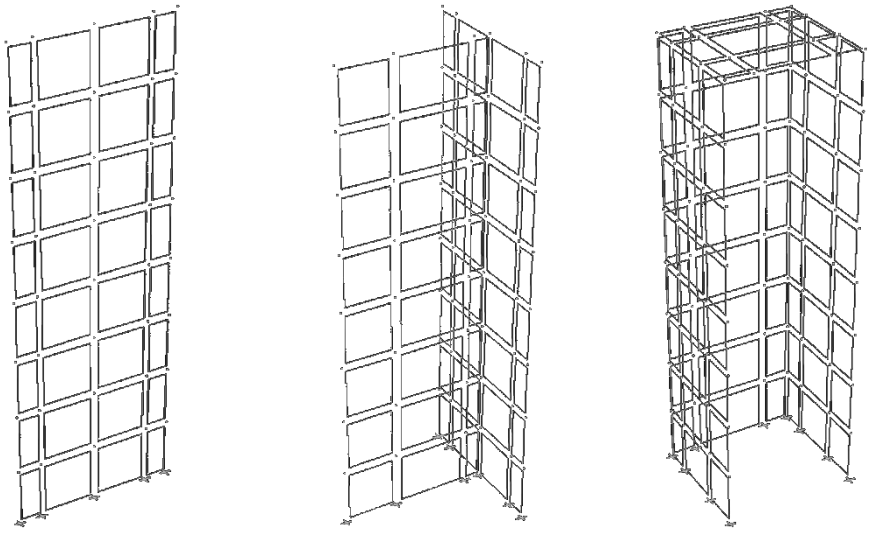

Figure 5.14 Rectangular, T and U Shape Test Wall Model Views at P3D

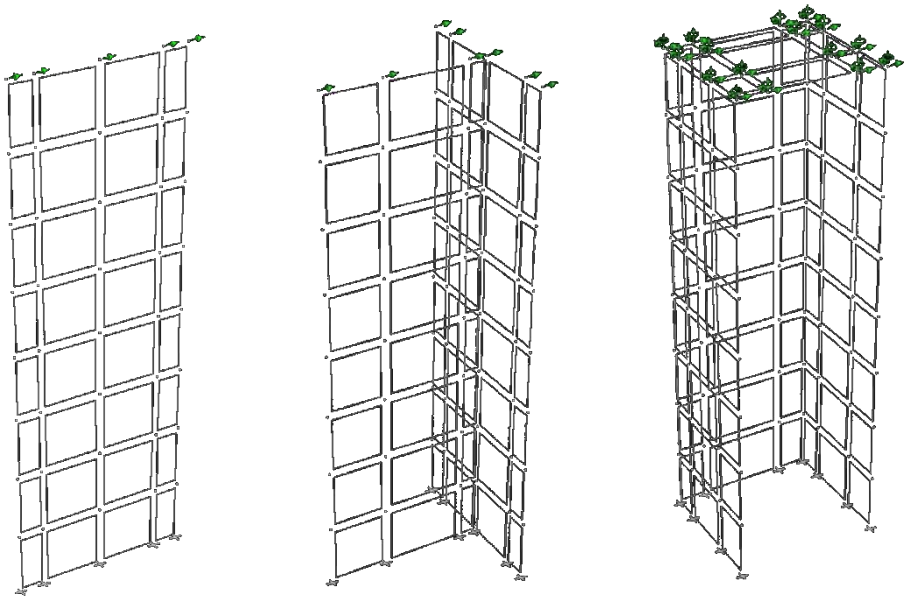

Figure 5.15 Views of Top Slaving Assignments of Walls

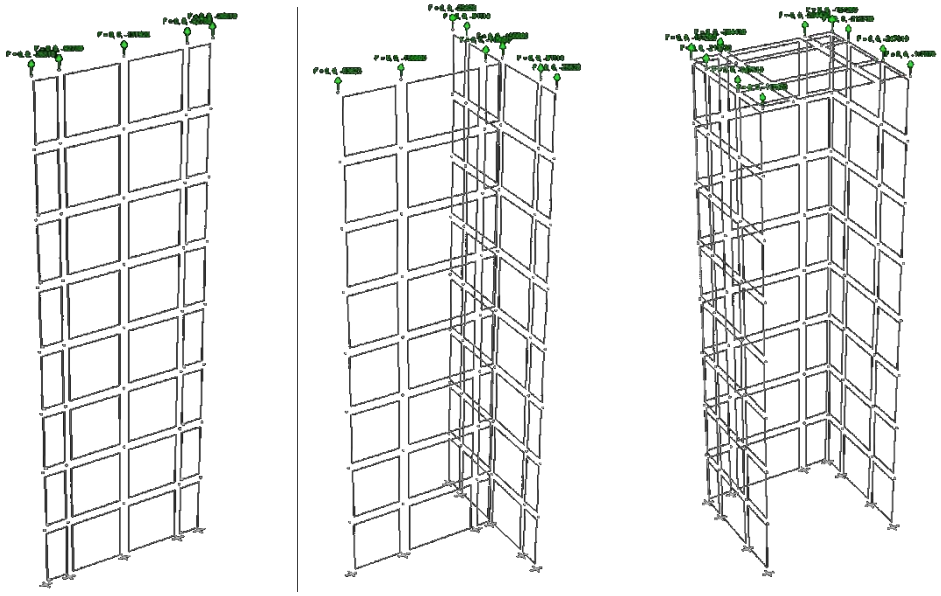

Figure 5.16 Axial Load Assignment Views of Test Walls

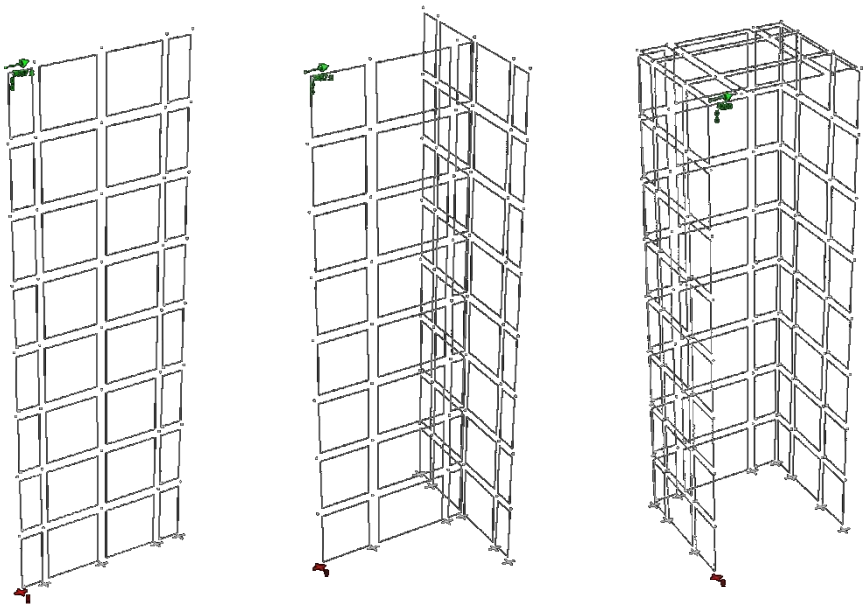

Figure 5.17 Views of Drift Reference Node and Direction Assignments of Walls

Wall material models defined with the components of "Inelastic Steel Material, Non-Buckling", "Inelastic 1D Concrete Material" and "Elastic Shear Material for a Wall". With "Shear Wall, Inelastic Section" cross section component and the "Fixed Size" fiber modeling module, concrete and reinforcement fiber definitions are made according to predefined material properties (Figure 5.18 and Figure 5.19). Details of the modal parameters are discussed in the next section. After these basic definitions, wall components are ready for assignment of element identification with the "Shear Wall Compound Component" section. Also, the displacement loading protocol is finally provided, then cyclic response model results are obtained to compare with experimental cyclic response of walls.

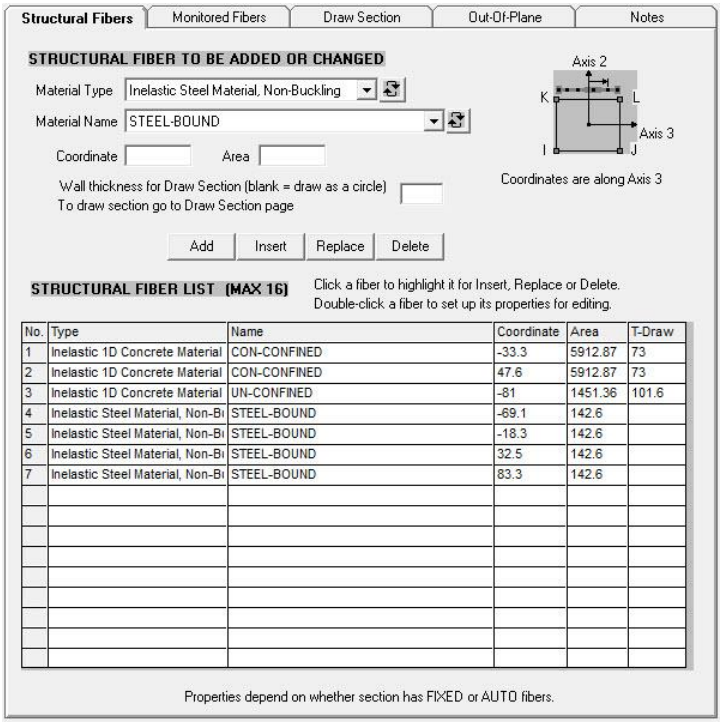

Figure 5.18 View of Fixed Size Wall Fiber Module for Boundary of RW2 Wall

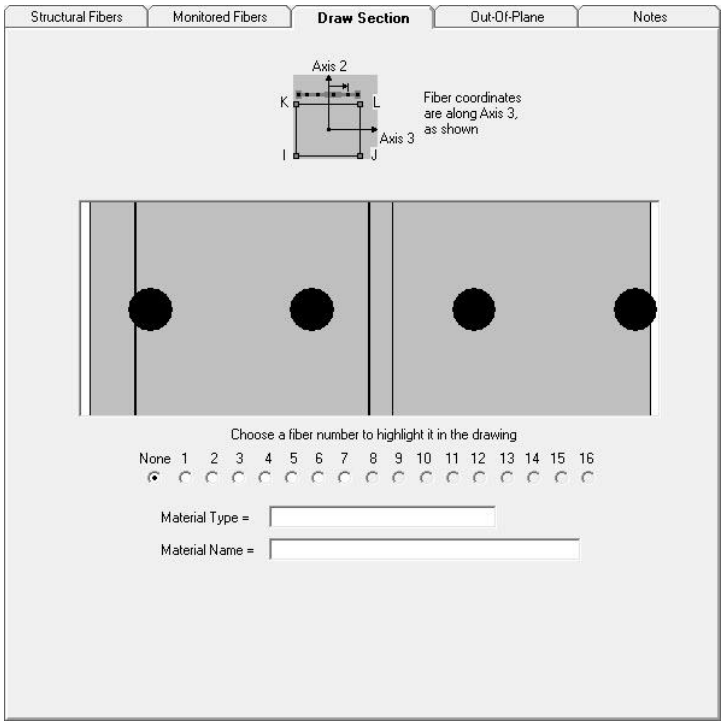

Figure 5.19 View of Fibers for Boundary of RW2 Wall

5.1.3.2 P3D Material Parameters and Their Effects on RW2 and TW2 Sample Walls Cyclic Response Results

Concrete and reinforcement material models and the parameters of these models are of great importance in wall modeling in Perform 3D. The cyclic response results are mainly influenced by 3 main headings: material modeling parameters, cross-section fiber definitions and wall meshing. Achieving the ideal modeling method under these 3 main headings is main goal for correct 3D main building wall solutions and design.

Using the cyclic response results of experiments as reference helps us to gel ideal modeling results. The first P3D wall model with default values for all wall shapes is accepted as a reference model without thinking the correctness of parameter values. To understand how much and to what extent change of each main title, i.e., material model parameters, cross-section fiber modeling and model mesh, and sub parameters influences the cyclic response results, only one parameters value is changed and compared with first reference model results regardless of the accuracy or inaccuracy of the model result. Wall model mesh is also remained as the same with reference models. New models are obtained with only single feature or parameter value changes. The cyclic response results of these new models are compared with the first reference model each time to observe what changes from cyclic response behavior. According to these observations, the ideal coefficient and modeling method are finally obtained to achieve the closest result of the cyclic response result of experiment.

a) P3D Material Parameters and Their Effects on RW2 Sample Walls' Cyclic Response Results

RW2 Wall is modeled with all default material parameter values in Table 5.4 and reference model result (1. Model) is obtained. Figure 5.20 demonstrates cyclic response result of the experiment and 1. Model (P3D Reference Model). As shown Figure 5.20, according to the initial material parameter definitions, there is a reasonable agreement of the experimental and simulation cyclic response results.

The first predicted values of both reinforcement and concrete material parameters for force displacement curves and for the cyclic degradation factors values that will affect these curves have been assigned, as shown in Table 5.4. Separate reinforcement and concrete basic materials definitions are made for the boundary and web sections of walls according to the experimental information. In cyclic degradation factor definitions, the first predicted values are separately entered for the tensile and compression behavior of the reinforcement, while for the concrete compression cyclic degradation YULRX factor values, 1; 0.4 ; 0.4 ; 0.1 ; 0.1, recommended by Lowes et al. are used in the initial assignment of the first reference P3D model of RW2 (Lowes et al., 2016).

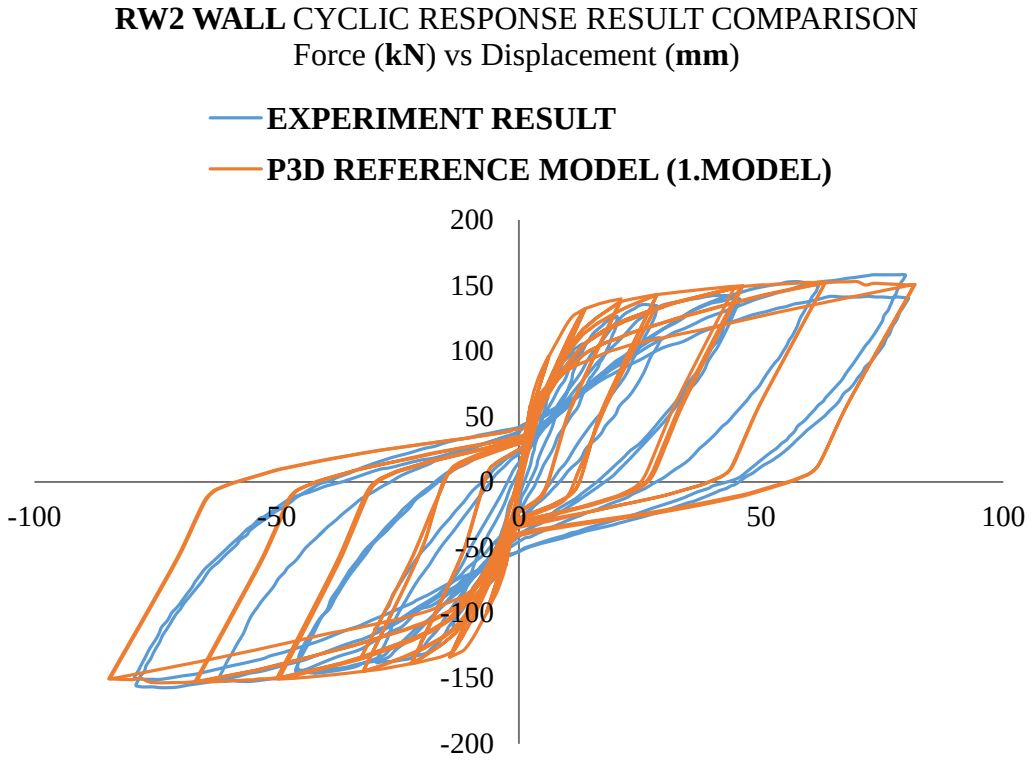

Figure 5.20 RW2 Wall Cyclic Response Comparison Results of Experiment and P3D Reference Model (1. Model)

Table 5.4 RW2 Wall P3D Reference Model (1. Model) Material Parameters

					MATERIALS			
					STEEL		CONCRETE	
					Web	Boundary	Confined	Unconfined
Basic Relationship	All		1	E (MPa)	2E+05	2E+05	31075	31075
	Stresses	Tens.	2	FY (MPa)	336	395	1.9	1.9
			3	FU (MPa)	550	500	2	2
		Compr	4	FY (MPa)	448	434	32.62	39.15
			5	FU (MPa)	550	550	43.8	43.5
	Strains	Tens.	6	DU	0.03	0.03	0.0001	0.0001
			7	DX	0.1	0.1	0.0015	0.0015
		Compr	8	DU	0.03	0.03	0.00263	0.002
			9	DX	0.1	0.1	0.003	0.02
Strength Loss	Strains	Tension	10	DL	0.07	0.07	0.00012	0.00012
			11	DR	0.08	0.08	0.001	0.001
			12	FR/FU	0.1	0.1	0.001	0.001
		Compr.	13	DL	0.07	0.07	0.0027	0.00202
			14	DR	0.08	0.08	0.0268	0.01
			15	FR/FU	0.1	0.1	0.185	0.001
	All		16	TSLX	No	No	---	---
			17	SLI	0	0	---	---
Cyclic Degradation	Tension Strains Energy Factors		18	Y	1	1	---	---
			19	U	0.85	0.85	---	---
			20	L	0.85	0.85	---	---
			21	R	0.85	0.85	---	---
			22	X	0.85	0.85	---	---
	Compr. Strains Energy Factors		23	Y	0.9	0.9	1	1
			24	U	0.75	0.75	0.4	0.4
			25	L	0.75	0.75	0.4	0.4
			26	R	0.75	0.75	0.1	0.1
			27	X	0.75	0.75	0.1	0.1
	All		28	USF	0.5	0.5	---	---

TSLX: Total Strength Loss at Point X; **SLI:** Strength Loss Interaction; **USF:** Unloading Stiffness Factor; **Y:**Yielding; **U:**Ultimate; **L:**Ductile Limit; **R:**Residual Limit; **X:**Analysis Stop Limit

RW2 Wall hysterical response solution trials have been conducted with 34 different P3D models. In the solution of many of the models, only one parameter is changed from the 1st reference model, and it is tried to observe the extent to which this parameter affects the cyclic response result and how much sensitivity it affects. While investigating the effect of parameter values on cyclic response result, it is tried to reach the correct result by comparing with the 1st model as well as by comparing with other model results. Table 5.6 and Table 5.7 describe subject that is the difference for each model from the first model and the degree of sensitivity that this change creates on the cyclic response. All representations between Figure 5.21 and Figure 5.24 provide cyclic response comparisons between models.

Various observations are made between Model-2 and Model-34 with different material parameters, properties and modeling type changes (Table 5.6, Table 5.7, and Table 5.8). Models 31, 32, 33 and 34 are some ideal optional modeling results with material parameters that is as a result of the first 30 model comparison studies. In the first 30 models, material parameters are varied to observe model sensitivity, so different sensitivity levels of high, moderate, low and none are selected based on the ratio of area under the cyclic response curve to area under the cyclic response curve of the reference model. Sensitivity level definitions are shown in Table 5.5. It is observed that energy factors of tension strains of reinforcement and unloading stiffness factors of reinforcement have very high effects on results. Another effective material parameters are yielding and ultimate strength values of reinforcement under tension loading behavior with moderate sensitivity level. All remaining parameters, in other words, material parameter changes that belong to concrete in general, have low effects on the cyclic response results. Summary results of sensitivity of material parameters on cyclic response is shown in Table 5.9. In addition, the last ideal suggestion coefficient values appear in Table 5.10 according to the comparison of simulation that fit the best with the test results.

Table 5.5 Sensitivity Level Rates (Change Rate in Area or Boundary Value of Cyclic Response)

Change Rate Top Boundary	Sensitivity Level	Change Rate Bottom Boundary
%100>	High	>15%
%15 >	Moderate	>5%
%5 >	Low	>2%
%2 >	None	>0%

Table 5.6 P3D Models Differences from Reference RW2 Wall Model (Model-1)

Model #	CHANGE FROM REFERENCE MODEL-1	SENSITIVITY
Model-1	Reference P3D Model	--
Model-2	Tension strength model of confined concrete material is omitted	None
Model-3	Tension strength model of both confined and unconfined concrete material is omitted	Low
Model-4	Unconfined part of boundary cross-section is not modelled (this situation is valid from Model 5 to19)	Low
Model-5	Both criteria of Model-3 and Model-4 is considered	Low
Model-6	Unloading stiffness factor "USF" is taken as "+1", instead of "+0.5"	Moderate
Model-7	Unloading stiffness factor "USF" is taken as "-1", instead of "+0.5"	Moderate
Model-8	Unloading stiffness factor "USF" is taken as "0", instead of "+0.5"	Low
Model-9	YX+3 model is used with different energy factors values for steel material. Energy factors of tension steel strains are 1, 0.95, 0.9, 0.85, 0.8 for Y, 0.01, 0.02, 0.03, X strain stages respectively, and energy factors of compression steel strains are 0.9, 0.85, 0.8, 0.75, 0.7 for Y, 0.01, 0.02, 0.03, X strain stages respectively	Low
Model-10	ULRX energy factors of tension & compression strains of steel material model are 0.5 decreased from 0.85.	High
Model-11	ULRX energy factors for compression strains of steel material model are decreased from 0.75 to 0.5	Low
Model-12	ULRX energy factors of tension strains of steel material model are decreased from 0.85 to 0.5	High
Model-13	ULRX energy factors of tension strains of steel material model are decreased from 0.85 to 0.5 and unloading stiffness factor "USF" is changed from "0.5" to "-1"	High
Model-14	YULRX energy factors of tension strains of steel material model are changed as Y:1 U:0.85 L:0.85 R:0.5 X:0.5	None

Table 5.7 P3D Models Differences from Reference RW2 Wall Model (Model-1)

Model #	DIFFERENCE FROM REFERENCE MODEL-1	SENSITIVITY
Model-15	YULRX energy factors of tension strains of steel material model are changed as Y:1 U:0.85 L:0.5 R:0.5 X:0.5	Low
Model-16	YULRX energy factors of tension strains of steel material model are changed as Y:0.5 U:0.5 L:0.5 R:0.5 X:0.5	High
Model-17	Tension yielding stress of steel material of boundary is decreased as an amount of 45 MPa	Low
Model-18	Tension yielding stress of steel material of web and boundary is decreased as an amount of 45 MPa	Low
Model-19	Tension ultimate stress of steel material of web is decreased from 550 MPa to 400 MPa and tension ultimate stress of steel material of boundary is decreased from 500 MPa to 400 MPa	Moderate
Model-20	YULRX energy factors of tension strains of steel material model are changed as Y:1 U:0.5 L:0.5 R:0.5 X:0.5	High
Model-21	Compression yielding stress of steel material of web is decreased from 434 MPa to 334 MPa and compression yielding stress of steel material of boundary is decreased from 438 MPa to 338 MPa	Moderate
Model-22	Tension yielding stress of steel material of web is decreased from 336 MPa to 250 MPa and tension yielding stress of steel material of boundary is decreased from 395 MPa to 300 MPa	Moderate
Model-23	Confined concrete compression strength is increased 43 MPa to 50 MPa and confined concrete compression strain is increased 0.00263 to 0.003	None
Model-24	Confined and unconfined concrete compression strength is increased to 50 MPa and also confined concrete compression strain is increased 0.00263 to 0.003	None
Model-25	Energy factors of compression strains of confined and unconfined concrete are changed as Y:1, U:0.8, L:0.8, R:0.8, X:0.1	None

Table 5.8 P3D Models Differences from Reference RW2 Wall Model (Model-1)

Model #	DIFFERENCE from REFERENCE MODEL-1	SENSITIVITY
Model-26	Energy factors of compression strains of confined and unconfined concrete are changed as Y:1, U:0.1, L:0.1, R:0.1, X:0.1	None
Model-27	Energy factors of compression strains of confined and unconfined concrete are changed as Y:0.1, U:0.1, L:0.1, R:0.1, X:0.1	None
Model-28	Energy factors of compression strains of confined and unconfined concrete are changed as Y:0.8, U:0.8, L:0.8, R:0.8, X:0.0.8	None
Model-29	Cyclic degradation option of concrete is taken as "none".	None
Model-30	Ultimate compression strain of confined concrete is decreased to unconfined ultimate compression strain value	Low
Model-31	Tension yielding stress of steel material of web and boundary is decreased as an amount of 45 MPa (0.85 f_y), and YULRX energy factors of tension strains of steel material model are changed as Y:0.65 U:0.65 L:0.65 R:0.65 X:0.65 and unloading stiffness factor "USF" is changed from "0.5" to "-0.5"	Ideal-(The best fitted to Test)
Model-32	Tension yielding stress of steel material of web and boundary is decreased as an amount of 45 MPa (0.85 f_y), and YULRX energy factors of tension strains of steel material model are changed as Y:0.65 U:0.65 L:0.65 R:0.65 X:0.65 and unloading stiffness factor "USF" is changed from "0.5" to "-0.5" and unconfined part of boundary cross-section is not modelled	Ideal-(The best fitted to Test)
Model-33	Tension yielding stress of steel material of web and boundary is decreased as an amount of 45 MPa (0.85 f_y), and YULRX energy factors of tension strains of steel material model are changed as Y:0.65 U:0.65 L:0.65 R:0.65 X:0.65 and Unloading Stiffness Factor "USF" is changed from "0.5" to "-0.5" and unconfined part of boundary cross-section is not modelled, symmetry model is used for steel compression and tension stress models, tension strength of concrete is selected as "No", cyclic degradation of concrete is selected as "none",	Ideal-(The best fitted to Test)
Model-34	All materials properties are similar with Model-31. Cross-section definitions of web and boundaries are used as "auto size module" instead of "fixed size module".	Ideal-(The best fitted to Test)

Table 5.9 RW2 Wall P3D Model Material Parameters Sensitivity Summary Results

					MATERIALS			
					STEEL		CONCRETE	
					Web	**Boundary**	**Confined**	**Unconfined**
Basic Relationship	All		1	E (MPa)	--	--	--	--
	Stresses	**Tens.**	2	FY (MPa)	Low	Low	None	None
			3	FU (MPa)	**Moderate**	**Moderate**	None	None
		Comp	4	FY (MPa)	Low	Low	None	None
			5	FU (MPa)	Low	Low	None	None
	Strains	**Tens.**	6	DU	--	--	None	None
			7	DX	--	--	None	None
		Comp	8	DU	--	--	**Moderate**	None
			9	DX	--	--	None	None
Strength Loss	**Strains**	**Tension**	10	DL	--	--	None	None
			11	DR	--	--	None	None
			12	FR/FU	--	--	---	---
		Compr.	13	DL	--	--	None	None
			14	DR	--	--	None	None
			15	FR/FU	--	--	---	---
	All		16	TSLX	--	--	---	---
			17	SLI	--	--	---	---
Cyclic Degradation	Tension Strains **Energy Factors**		18	Y	**Moderate**	**Moderate**	---	---
			19	U	**High**	**High**	---	---
			20	L	Low	Low	---	---
			21	R	None	None	---	---
			22	X	None	None	---	---
	Compr. Strains **Energy Factors**		23	Y	Low	Low	None	None
			24	U	Low	Low	None	None
			25	L	Low	Low	None	None
			26	R	Low	Low	None	None
			27	X	Low	Low	None	None
	All		28	USF	**Moderate**	**Moderate**	---	---

TSLX: Total Strength Loss at Point X; **SLI:** Strength Loss Interaction; **USF:** Unloading Stiffness Factor; **Y:**Yielding; **U:**Ultimate; **L:**Ductile Limit; **R:**Residual Limit; **X:**Analysis Stop Limit

Table 5.10 RW2 Wall P3D Ideal Model Material Parameters (Model-31)

					MATERIALS			
					STEEL		CONCRETE	
					Web	**Boundary**	**Confined**	**Unconfined**
Basic Relationship	All		1	E (MPa)	2E+05	2E+05	31075	31075
	Stresses	**Tens.**	2	FY (MPa)	**280**	**350**	1.9	1.9
			3	FU (MPa)	550	500	2	2
		Compr	4	FY (MPa)	448	434	32.62	39.15
			5	FU (MPa)	550	550	43.8	43.5
	Strains	**Tens.**	6	DU	0.03	0.03	0.0001	0.0001
			7	DX	0.1	0.1	0.0015	0.0015
		Compr	8	DU	0.03	0.03	0.00263	0.002
			9	DX	0.1	0.1	0.003	0.02
Strength Loss	**Strains**	**Tension**	10	DL	0.07	0.07	0.00012	0.00012
			11	DR	0.08	0.08	0.001	0.001
			12	FR/FU	0.1	0.1	0.001	0.001
		Compr.	13	DL	0.07	0.07	0.0027	0.00202
			14	DR	0.08	0.08	0.0268	0.01
			15	FR/FU	0.1	0.1	0.185	0.001
	All		16	TSLX	No	No	---	---
			17	SLI	0	0	---	---
Cyclic Degradation	Tension Strains **Energy Factors**		18	Y	**0.65**	**0.65**	---	---
			19	U	**0.65**	**0.65**	---	---
			20	L	**0.65**	**0.65**	---	---
			21	R	**0.65**	**0.65**	---	---
			22	X	**0.65**	**0.65**	---	---
	Compr. Strains **Energy Factors**		23	Y	0.9	0.9	1	1
			24	U	0.75	0.75	0.4	0.4
			25	L	0.75	0.75	0.4	0.4
			26	R	0.75	0.75	0.1	0.1
			27	X	0.75	0.75	0.1	0.1
	All		28	USF	**-0.5**	**-0.5**	---	---

TSLX: Total Strength Loss at Point X; **SLI:** Strength Loss Interaction; **USF:** Unloading Stiffness Factor; **Y:**Yielding; **U:**Ultimate; **L:**Ductile Limit; **R:**Residual Limit; **X:**Analysis Stop Limit

It is observed that there is no need to model the tensile strength of confined and unconfined concrete material for wall elements. In addition, the modeling of unconfined concrete cross sections in the wall boundary part does not change the result much. This can be observed among comparisons b/w comparison 1 (C1) and 4 (C4) in the Figure 5.21. However, unloading stiffness factor, “USF” for reinforcement material has a high effect on stiffness in general cyclic response behavior. This can also be observed among comparisons b/w C5 and C7 in the Figure 5.21. Unloading stiffness factor value, “USF” ranging from "-1" to "+1" is recommended as "-0.5" (Table 5.10). In addition, for reinforcement, the energy factor, “EF” is one of the parameters that most influences cyclic response behavior that can be seen b/w C9 and C15 at Figure 5.22, but concrete material energy factor parameters have little effect on the results. This can be observed between comparisons. Among energy factors levels, ultimate level value, “U”, changes the result with a very dominant effect. After the ultimate limit energy factor "U", yielding "Y" and ductile limit "L" have a more partial effect on the result. Energy factor values "R" and "X" levels have almost no effect. "0.65" is recommended for YULRX energy factor inputs (Table 5.10). According to Pacific Engineering Research Center, YULRX energy factors are recommended as a value of 0.6-0.7 (Moehle et al., 2011). Also, it is observed in comparison C16, C17 and C21 that reducing reinforcement tension yielding strength by 50-100 MPa decreases the yielding force result in cyclic response by almost 10%, while reducing reinforcement ultimate strength value under tension by 100-150 MPa causes decrease at ultimate force limit by almost 10%-15% (Figure 5.23). As can be seen in the comparison 20, (C20), reducing compression yielding strength by around 100 MPa increases the pinching behavior of cyclic response behavior (Figure 5.23). There is a little effect on cyclic response with change at parameters related to concrete material. As it appears between 22. and 29. comparisons (C22 and C29) reducing or increasing the compression strain and strength of concrete has little effect on the cyclic response result. In addition, in these comparisons, it is seen that the value of energy factors defined for concrete has little effect on the results.

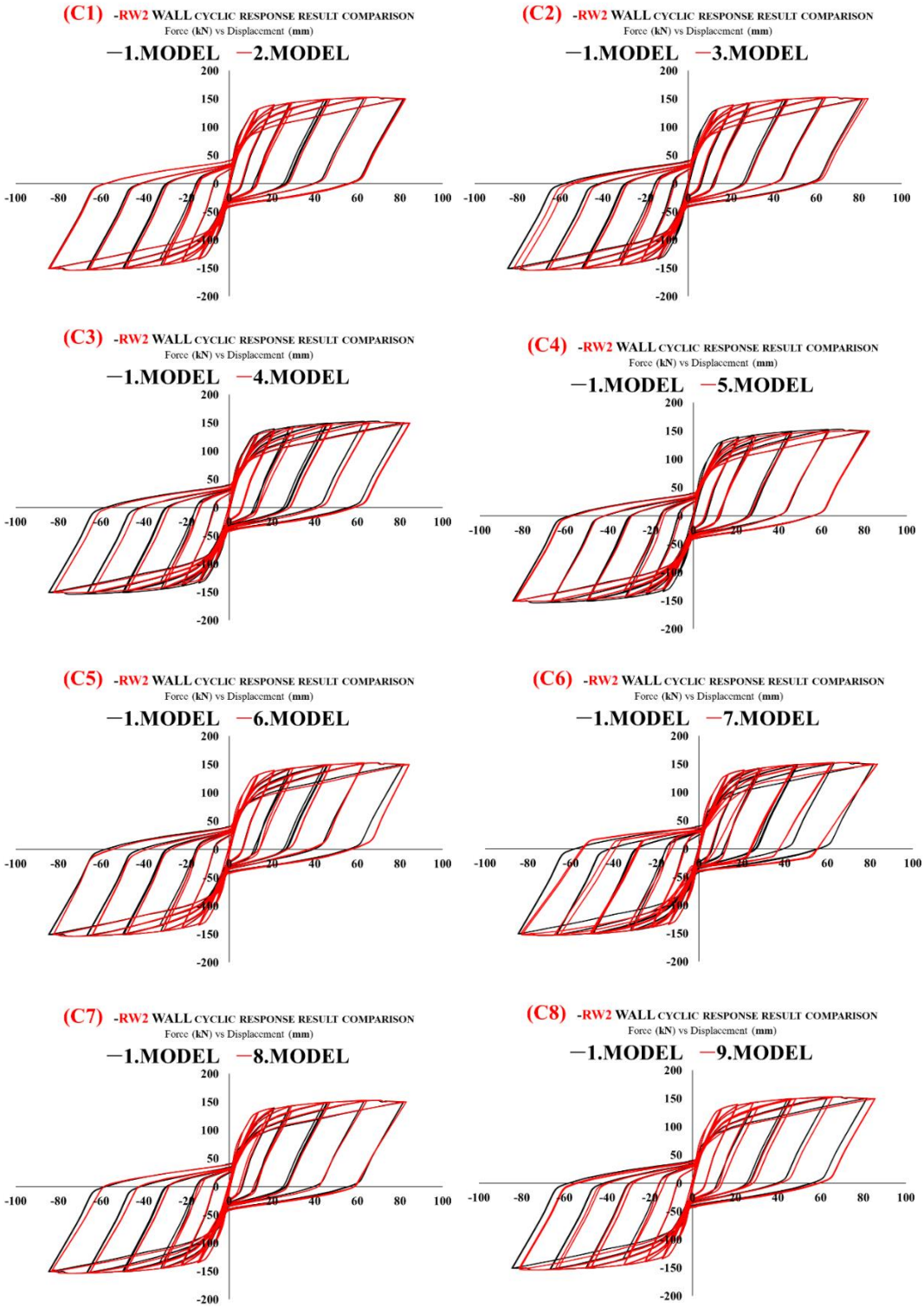

Figure 5.21 Cyclic Response Comparisons b/w C1-C8 for RW2 P3D Models

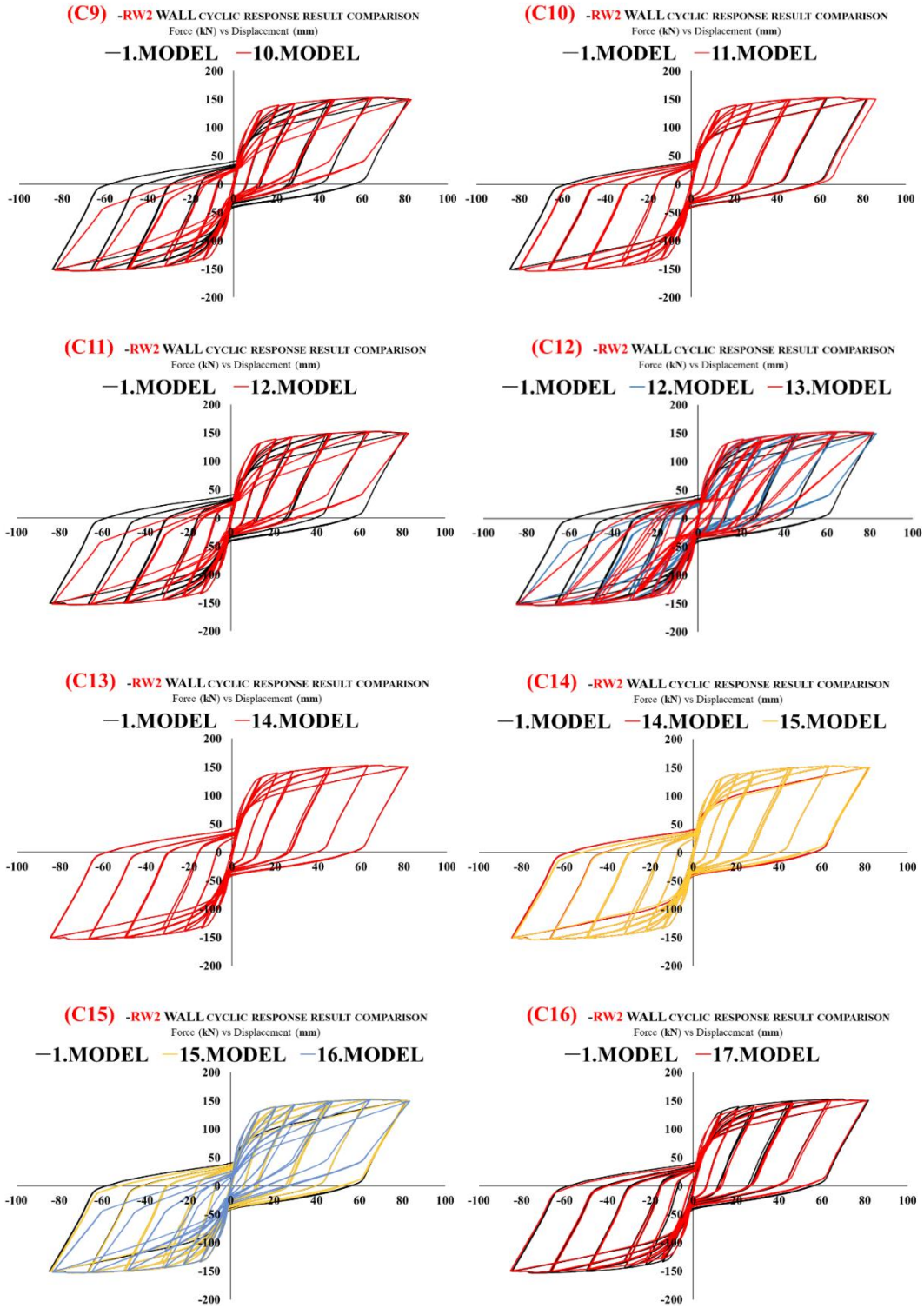

Figure 5.22 Cyclic Response Comparisons b/w C9-C16 for RW2 P3D Models

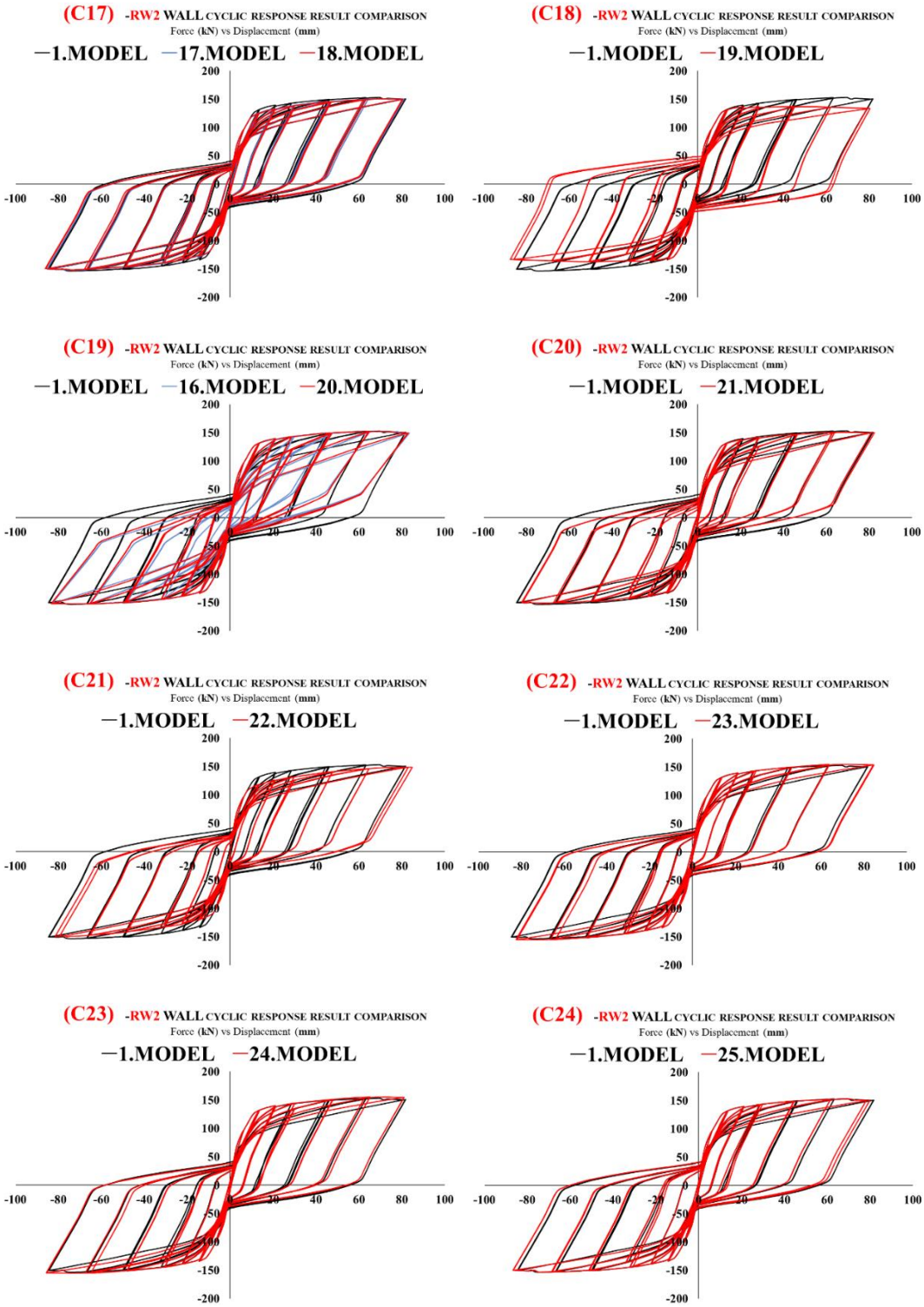

Figure 5.23 Cyclic Response Comparisons b/w C17-C24 for RW2 P3D Models

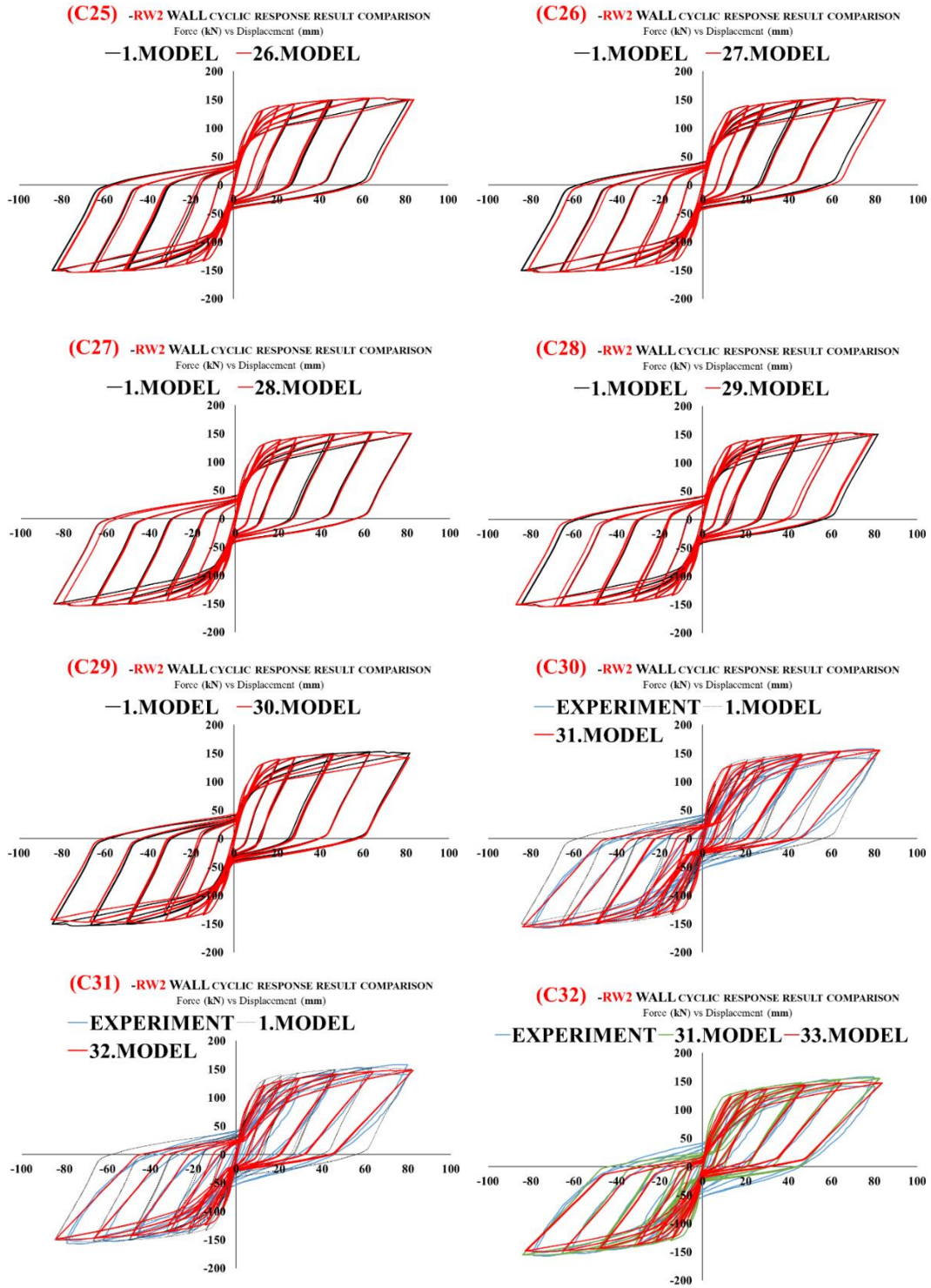

Figure 5.24 Cyclic Response Comparisons b/w C25-C32 for RW2 P3D Models

The results of the first 30 models and 29 comparisons are observed and applied at 31. 32. 33. and 34.ideal models. There is a simplification in terms of modeling and

parameters through ideal Model-31 to ideal Model-33. The ideal model material proposal parameter values are presented in Table 5.10 for Model-31. The important another issue worth mentioned about that it has been observed that the yielding force limit in P3D cyclic response results is above from that of experiment results. For this reason, it is proposed that Belarbi and Hsu (1994) recommendation should be taken into account in reinforcement model. If the average stress -strain relationship for reinforcing bars embedded in concrete recommended by Belarbi and Hsu (1994) is used in the reinforcement model, the reinforcement yielding strength is decreased by about %10-%15 and P3D model results will be closer to the result of the experiment. For this reason, the reinforcement yielding strength shown in Table 5.4 in our first reference model is higher than the reinforcement yielding strength offered in Table 5.10 for Model-31. According to the reinforcement model proposed by Belarbi and Hsu (1994), yielding stress of embedded bars in concrete is lower than bare steel bars yielding stress. In other words, tension stiffening on reinforcement causes lowering of yielding stress.

b) P3D Material Parameters and Their Effects on TW2 Sample Walls' Cyclic Response Results

Hysteric response study is performed for the T-shaped wall according to the recommended material parameters obtained from rectangular wall work. The reference model cyclic response results for T-shaped wall fit relatively well with experiment results (Figure 5.26). Trials on similar subjects in the RW2 model are carried out in a T-shaped walls in terms of cyclic response. For this purpose, 11 different trial models have been created. All comparison results are presented in Figure 5.27 and Figure 5.28. Description details and sensitivity results for these trial models are presented in Table 5.11. The sensitivity of the material parameters does not differ from that of the work carried out for the rectangular walls, and similar results are obtained in general. Firstly, removal of the tensile strength of the concrete from the model has little effect on hysteric results (C1 and C2 in Figure 5.27). The unloading stiffness factor, USF, is again dominant effect on results for T-shaped wall-TW2 like rectangular wall-RW2 (C3, C4 in Figure 5.27). The reduction of 100

MPa in yielding and ultimate strength of reinforcement does not make a huge difference to the behavior of the first reference model. In this regard, the 10-15% capacity change, moderate effect, in rectangular walls is not be observed for T-shaped wall works. This can be observed in comparisons, C5, C6 and C7 in Figure 5.27. However, the energy factor change for reinforcement under tension significantly affects cyclic response behavior for T-shape walls like rectangular walls (C8, C9, C10, C11 in Figure 5.27 and Figure 5.28).

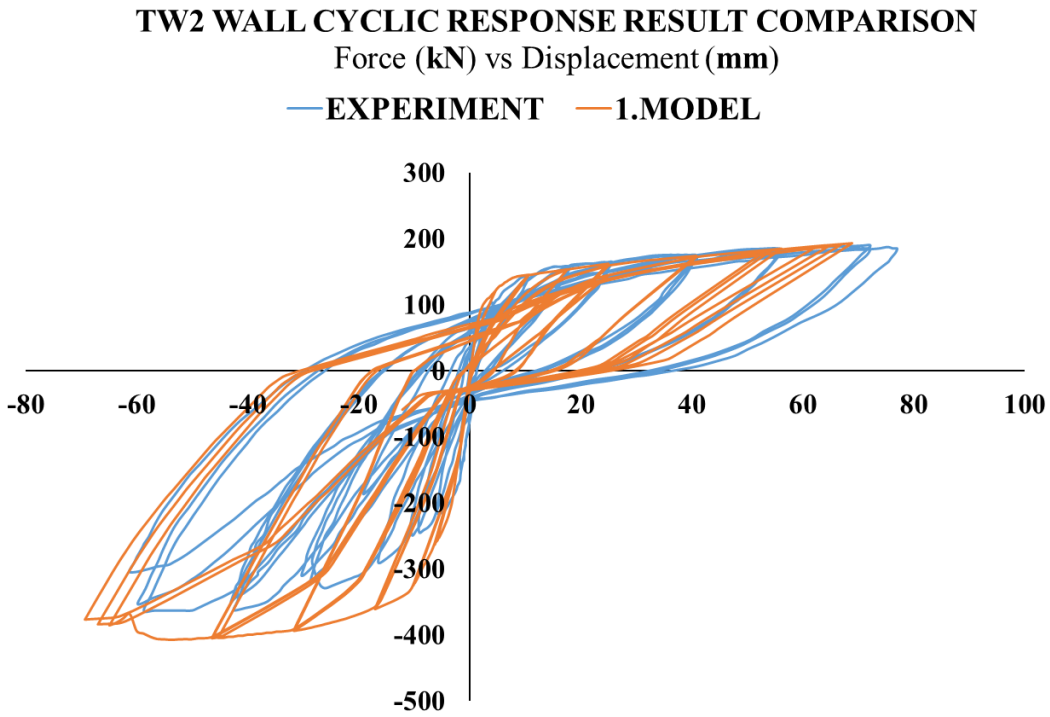

Figure 5.25 TW2 Wall Cyclic Response Comparison Results of Experiment and P3D TW2 Reference Model (1. Model)

Table 5.11 P3D Models Differences from Reference TW2 Wall Model (1. Model) for Sensitivity

Model #	CHANGE FROM REFERENCE 1. MODEL	SENSIVITY
TModel-1	Reference P3D Model	Ideal-(The best fitted to Test)
TModel-2	Tension strength model of both confined and unconfined concrete material is omitted	None
TModel-3	Tension strength model of both confined and unconfined concrete material is omitted and unconfined part of boundary cross-section is not modelled	Moderate
TModel-4	Unloading stiffness factor "USF" is taken as "0", instead of "-0.5"	Low
TModel-5	Unloading stiffness factor "USF" is taken as "+0.5", instead of "-0.5"	Moderate
TModel-6	Confined concrete compression strain is decreased from 0.00263 to 0.002	None
TModel-7	Tension yielding stress of steel material of web is taken as original value as 336 MPa instead of decreased value,250 MPa and tension yielding stress of steel material of boundary is taken as original value as 395 MPa instead of decreased value,300 MPa	Low
TModel-8	Tension ultimate stress of steel material of web is decreased from 550 MPa to 500 MPa and tension ultimate stress of steel material of boundary is decreased from 500 MPa to 450 MPa	Low
TModel-9	YULRX energy factors of tension strains of steel material model are changed as Y:1 U:0.1 L:0.65 R:0.65 X:0.65	High
TModel-10	YULRX energy factors of tension strains of steel material model are changed as Y:0.65 U:0.5 L:0.5 R:0.5 X:0.5	High
TModel-11	YULRX energy factors of tension strains of steel material model are changed as Y:1 U:0.8 L:0.65 R:0.65 X:0.65	High
TModel-12	YULRX energy factors of tension strains of steel material model are changed as Y:0.8 U:0.8 L:0.65 R:0.65 X:0.66	High
TModel-13	Tension yielding stress of steel material of web and boundary is decreased as an amount of 45 MPa (0.85 f_y), and YULRX energy factors of tension strains of steel material model are changed as Y:0.65 U:0.65 L:0.65 R:0.65 X:0.65 and unloading stiffness factor "USF" is changed from "0.5" to "-0.5" and unconfined part of boundary cross-section is not modelled, symmetry model is used for steel compression and tension stress models, tension strength of concrete is selected as "No", cyclic degradation of concrete is selected as "none", unconfined concrete model parts are cancelled.	Ideal-(The best fitted to Test)
TModel-14	All materials properties are similar with TModel-1. Cross-section definitions of web and boundaries are used as "auto size module" instead of "fixed size module".	Ideal-(The best fitted to Test)

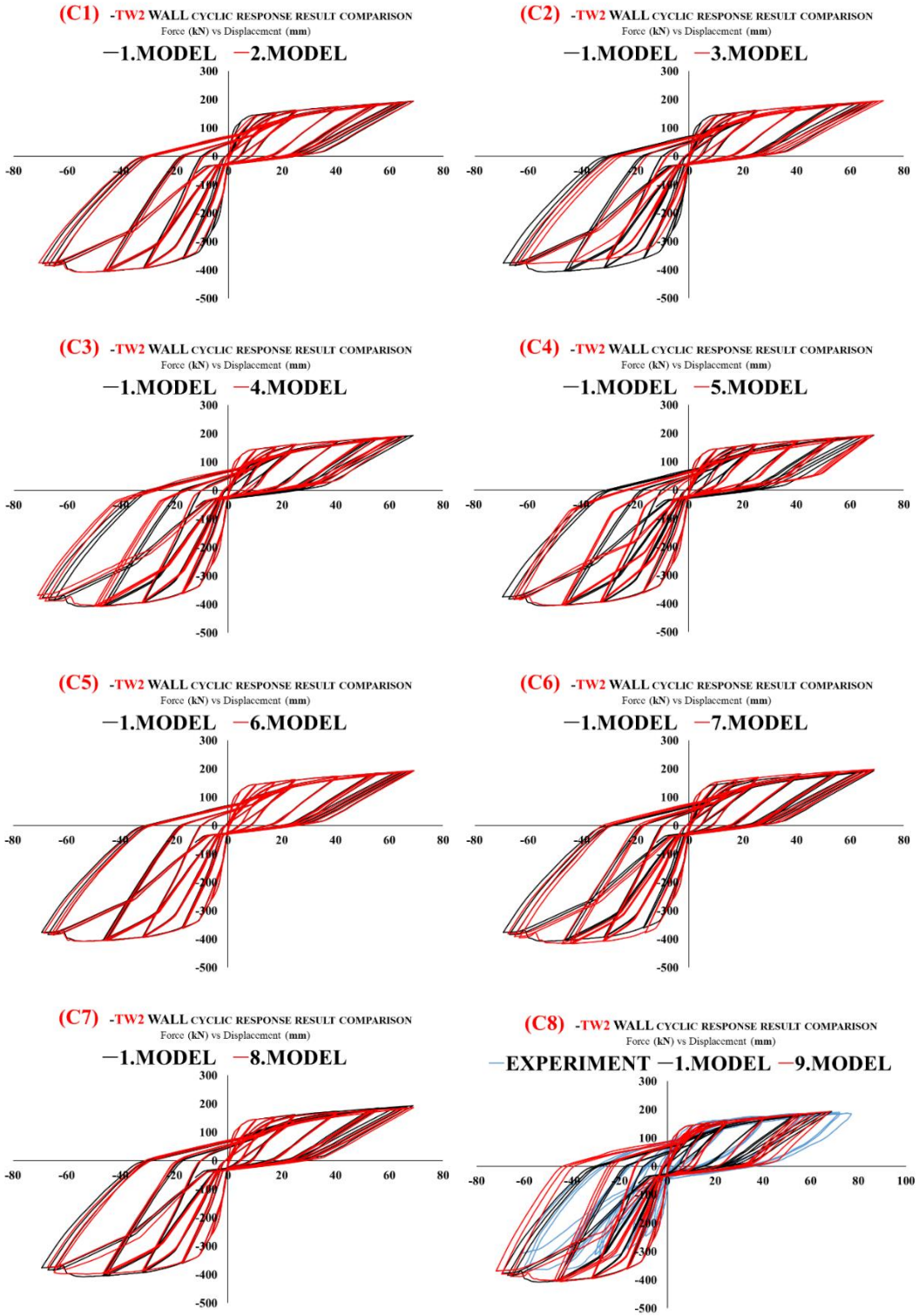

Figure 5.26 Cyclic Response Comparisons b/w C1-C8 for TW2 P3D Models

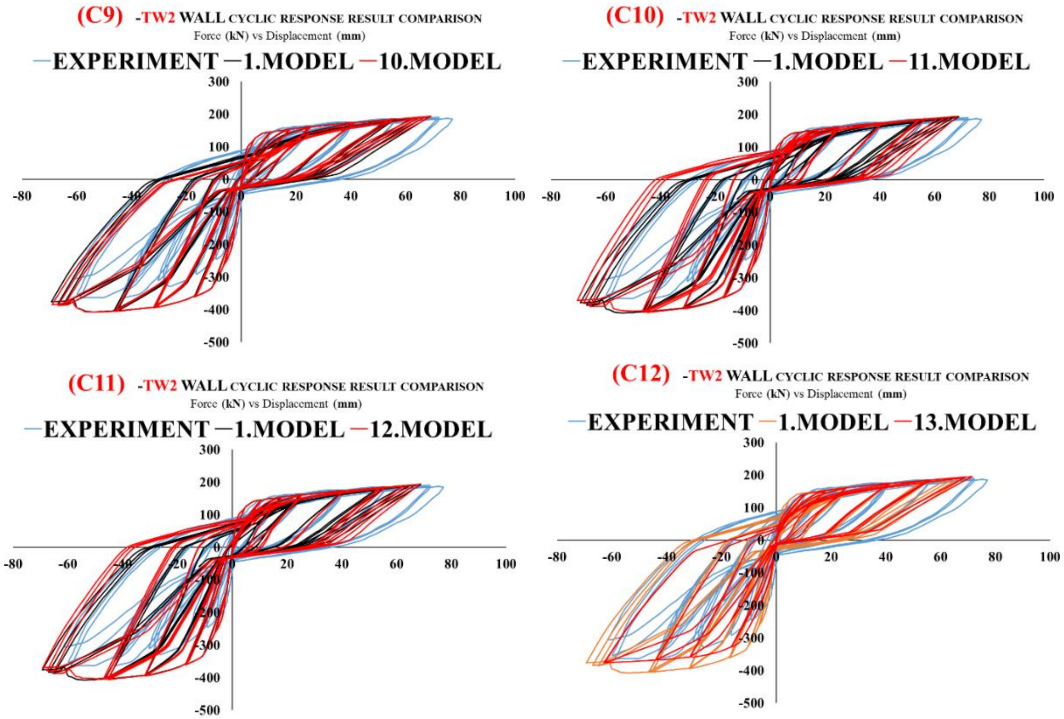

Figure 5.27 Cyclic Response Comparisons b/w C9-C12 for TW2 P3D Models

5.1.3.3 Cyclic Response Results with Ideal Model Material Parameters for Walls

a) RW2

Model-31 is found to be the most compatible with the test result for RW2 wall as a result of modeling according to the ideal material model parameters obtained (Figure 5.28). According to the calibration work of RW2, P3D model results showed good compatibility with experiment results in terms of hysteretic shape and at first glance, energy absorption capacities are almost similar. In addition, there is a very good agreement in terms of lateral load capacity, lateral displacement capacity, stiffness degradation properties. Although agreement is not perfect in terms of pinching behavior, lateral yielding capacity and plastic displacement, it is reasonable in general. The fact of the lateral yielding force capacity being higher than the test result may be explained by the insufficient simulation of yielding behavior of the reinforcement embedded in the concrete.

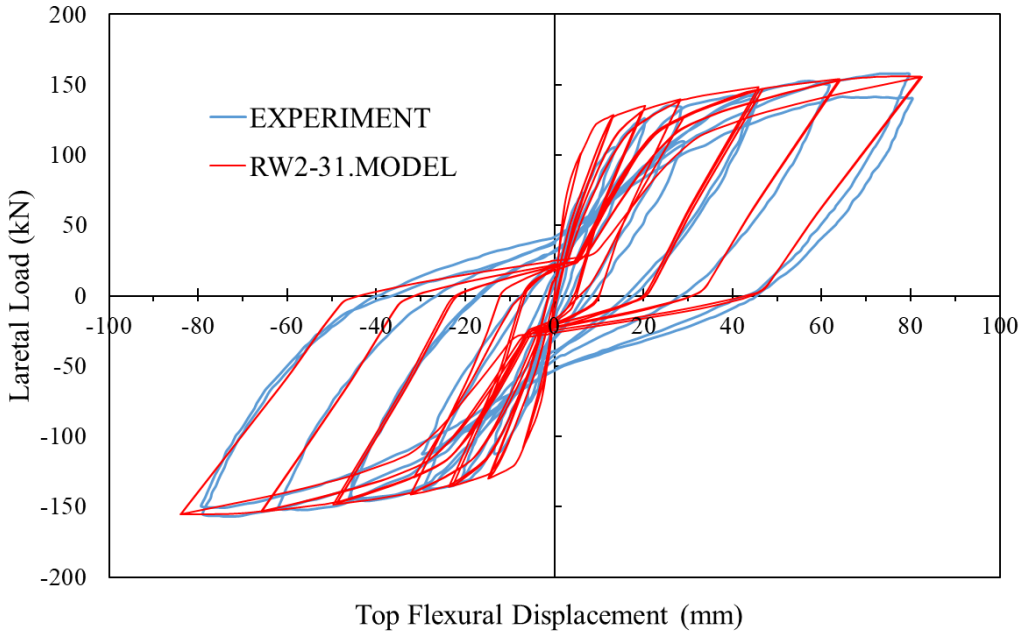

Figure 5.28 RW2, Most Ideal P3D Cyclic Response Result

After obtaining the ideal results with Model-31, in order to increase computer analysis speed and facilitate modeling (especially for use in computationally demanding tall building analysis), new ideal model works have been conducted i.e., Model-32 and Model-33, by disabling material parameters with a low sensitivity effect. Firstly, unconfined part has been omitted in the modeling of Model-32. Almost 5% decrease in the lateral load capacity of the wall was observed as a result of this cancellation (Figure 5.29). In addition to the change in Model-32, the reinforcement material is modelled as symmetrically for both tension and compression, concrete tensile strength and energy factors of concrete are not taken into account for Model-33 (Table 5.8). With Model-33, pinching behavior of the cyclic response has increased compared to the experiment result and energy absorption area is even reduced. Also, lateral ultimate load capacity, shown in Model-33, reduced, as in the Model-32. Material modeling approach at Model-33 can be considered as fast and acceptable in complex modeling of core wall in 3D dimensional structure analysis of high-rise buildings.

The lateral flexural displacement profile prepared on each floor and for different drift ratios for Model-31 can be observed at Figure 5.30. Both the experiment and P3D model lateral flexural displacement profile results seem to be very compatible on each floor, along the wall height and for different drift ratios.

In addition to hysteric shape and lateral flexural displacement profile comparisons to confirm the accuracy of modeling, the experimental and simulation of strain profiles of wall at basement level is also conducted. Although the stain gage lengths of experiment (229 mm) and PBD Model (457 mm) are different (it should be the same), strain comparisons results are again given in Figure 5.31 and Figure 5.32. In terms of different model strain gage length comparison investigation, more detailed investigation is presented later. But for these strain gage lengths, i.e., 229 mm and 457 mm, experiment and P3D Model strain comparison also results in very good compatibility (Figure 5.31 and Figure 5.32). These average strain profiles for both concrete and steel are compatible with the test results. In addition, location of neutral axis is also successful in this compatibility. For both concrete and reinforcement, the tensile strains remain on the safe side according to the test results, however compression strains for all drift ratios are below the measured compression strain results. In terms of crushing strain values of concrete, it cannot be said that successful modeling results are achieved due to the fact that lower strain values are obtained with P3D Model from experiment values. The cause of the larger compressive strain may be stress concentration and additional nonlinear shear behavior due to geometric reasons. On the other hand, it is observed that the results of tension strain of reinforcement in P3D Model are very compatible with the experiment.

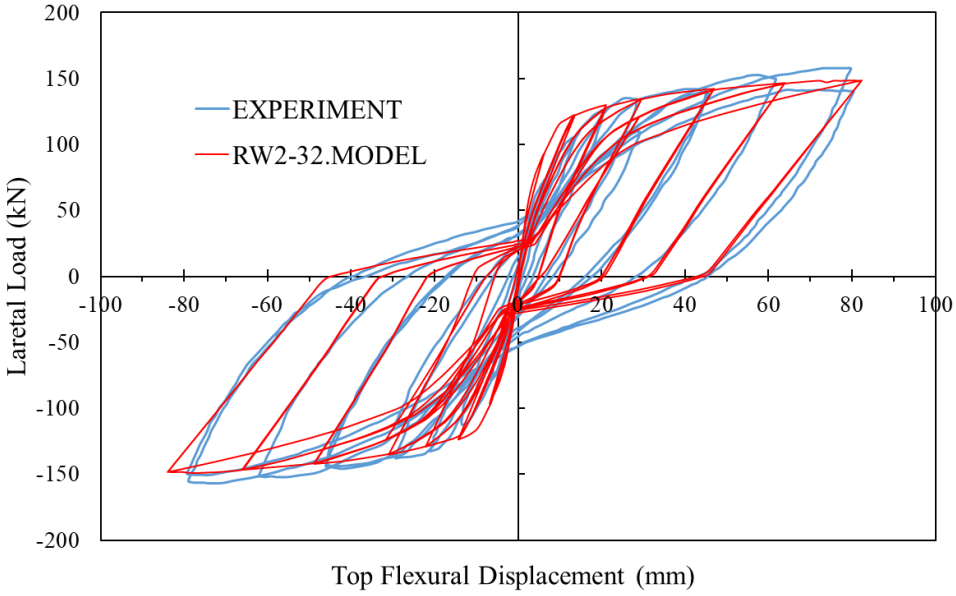

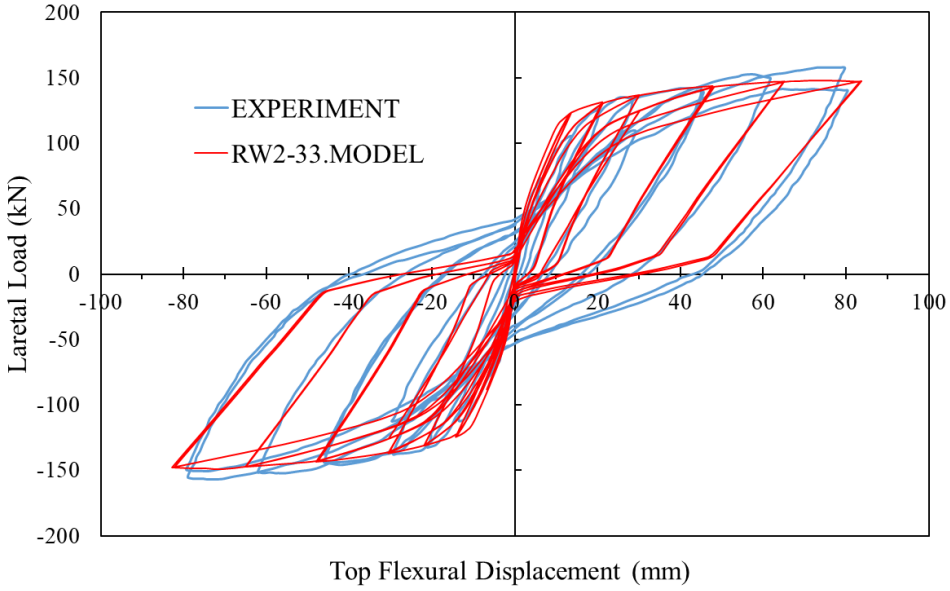

Figure 5.29 RW2, Close to Ideal P3D Cyclic Response Results for Rapid Analysis

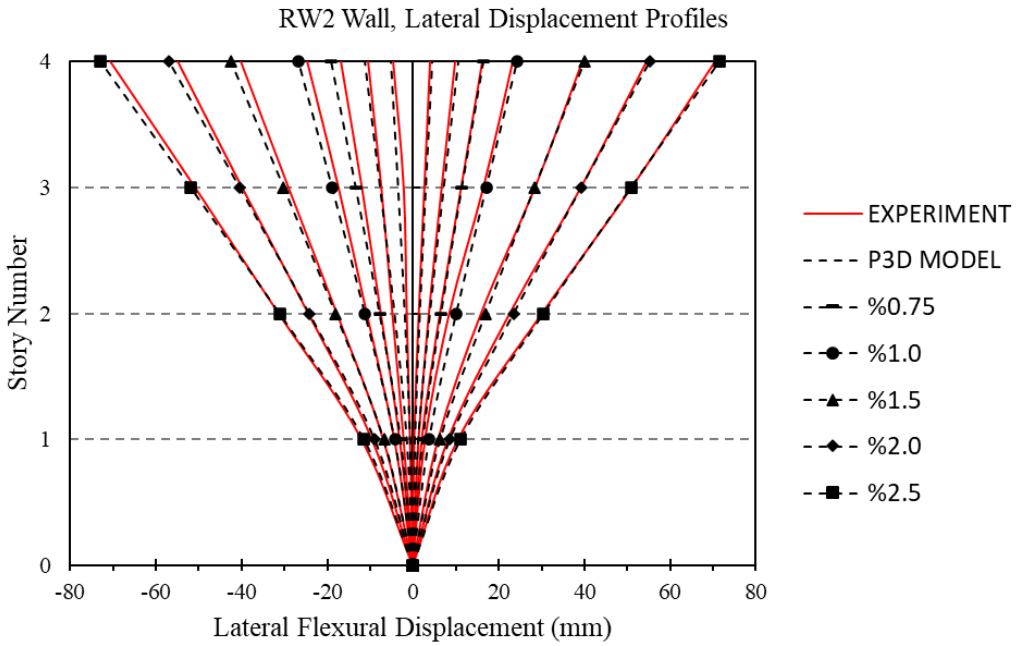

Figure 5.30 RW2 Lateral Displacement Profiles of Experiment and P3D Model (Model-31) for Different Drift Ratio

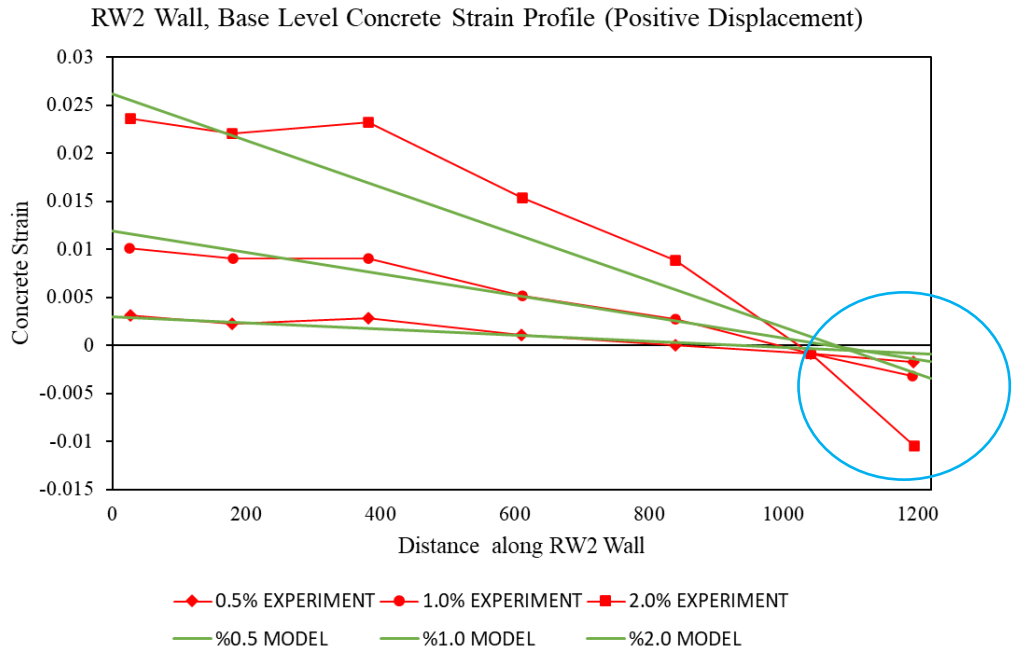

Figure 5.31 RW2 Wall, Base Level *Concrete* Strain Profiles of Experiment and P3D Model (Model-31) for Different Drift Ratios

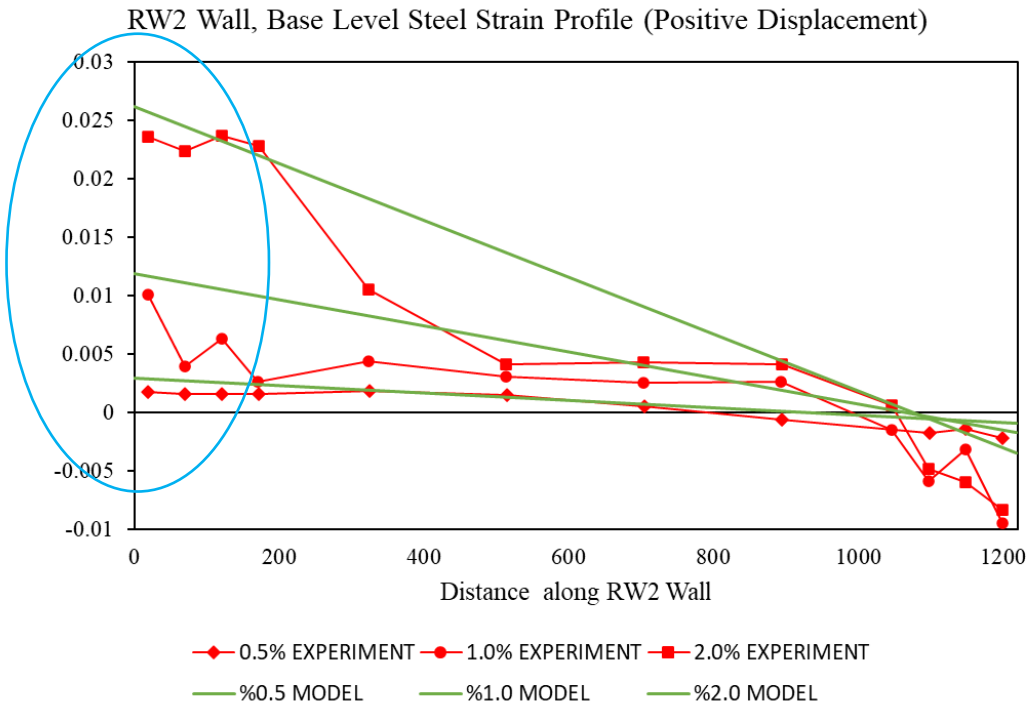

Figure 5.32 RW2 Wall, Base Level *Steel* Strain Profiles of Experiment and P3D Model (Model-31) for Different Drift Ratios

b) TW2

The ideal material parameters obtained as a result of the work on the RW2 sample work models are also used in TModel-1 for the T-shaped wall as a first trial. With various changes in material parameters, there is no need to change the ideal results obtained from RW2 model trials. Figure 5.33 shows a comparison of the test's cyclic response result with the P3D Model generated according to the ideal material parameter assignments for the TW2 wall. Although the overlap result in TW2 is not as good as like in RW2, it is reasonably acceptable. In positive displacement, the wall flange is under compression, while the wall flange is under tension in the negative displacement situation. In case of positive displacement, horizontal plastic displacement capacity is less than experimental value, while in case of negative displacement, experimental lateral load capacity and lateral load displacement capacity are less than P3D Model results (Figure 5.33). It may be said that acceptable

good results have been achieved in energy absorbing areas, stiffness degradation, and general hysteric shape.

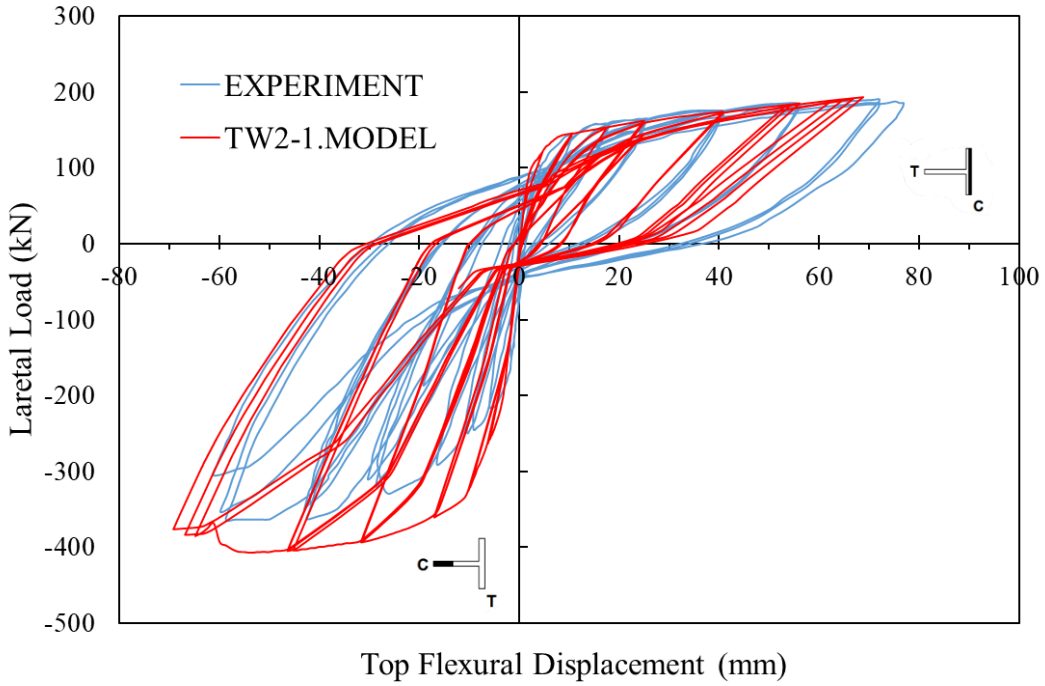

Figure 5.33 TW2, Ideal P3D Cyclic Response Result

As with RW2, for T-Shaped wall, TW2, experiment is compared with P3D Model having omitted parameters that are not very effective, simplified modeling conditions (Figure 5.34). Simplified model (TModel-13) achieves more pinching behavior, while the energy damping area is even smaller. For simpler and faster analysis, it is relatively acceptable to perform wall element modeling in accordance with the Table 5.10, TModel-13 definition.

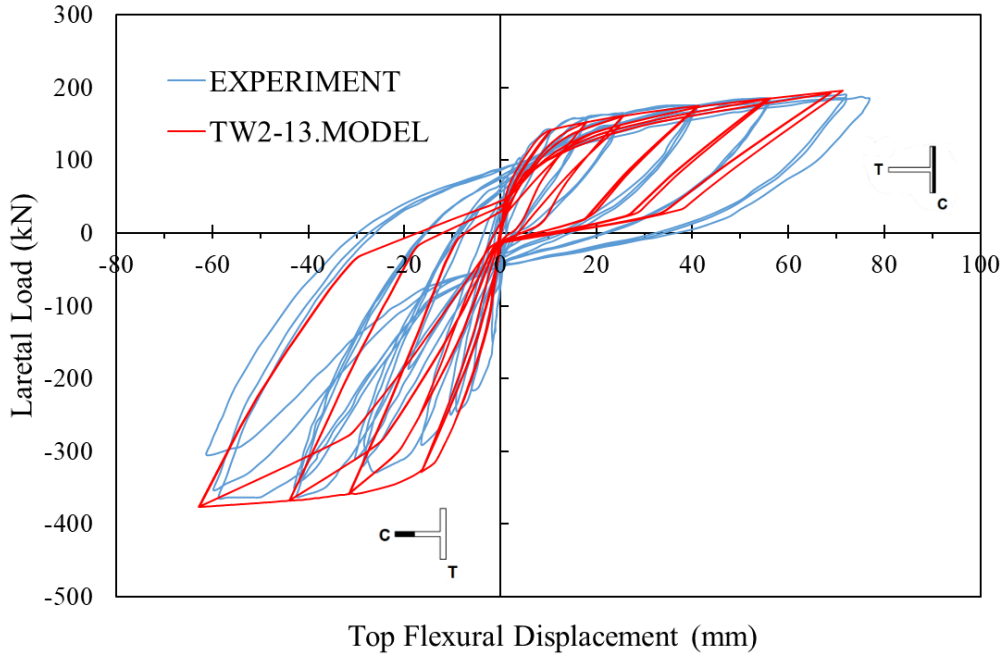

Figure 5.34 TW2, Close to Ideal P3D Cyclic Response Result for Rapid Analysis

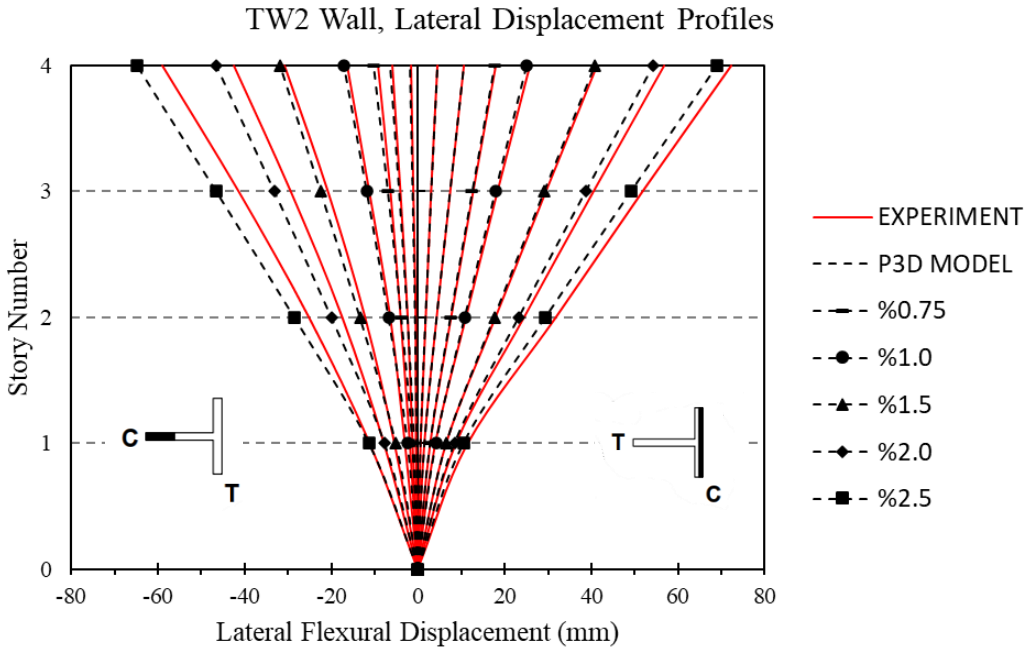

Figure 5.35 TW2 Lateral Displacement Profiles of Experiment and P3D Model for Different Drift Ratio

Model and test results comparisons are checked in terms of lateral displacement profile and reinforcement and concrete strain profile for TW2, T-Shaped wall. The displacement profile comparison is acceptable for both positive drift and negative drift ratios. This situation can be observed in Figure 5.35 through wall height and for different drift ratios.

TW2 wall simulation and experimental results for concrete and steel strain profile comparisons for different strain gage lengths 457 mm and 229 mm respectively are presented in Figure 5.36 and Figure 5.37. In both figures, concrete and reinforcement strain profiles are presented separately for positive and negative displacement. According to Figure 5.36, in case of positive and negative displacement or drifts, the concrete tensile strain values are in good condition, and overestimated as observed in the RW2 wall sample strain profile, while concrete compression strain values on P3D model are lower than the test results. In other word, for compression strain values, outcomes are underestimated. This situation applies to all drift ratios. On the other hand, the profiles may be generally successful in compatibility in terms of neutral axis location and general average line views.

Steel strain profiles of test and P3D model comparison results are presented in Figure 5.37 for both positive and negative displacements. In the case of positive displacement where the flange of T-wall is under compression, steel tension strain values of P3D model are above the test results for drift values of 0.5% and 1.0%, while partially below for the 2.0% drift ratio. On the other hand, in the case of negative displacement where the flange is under tension, steel tension strain values remain on the safe side and are higher than the test results for all drift values.

To sum up, for the TW2 wall sample, except perfectly agreement of strain profiles and concrete compression strain values, other global variables are successfully obtained by P3D modeling.

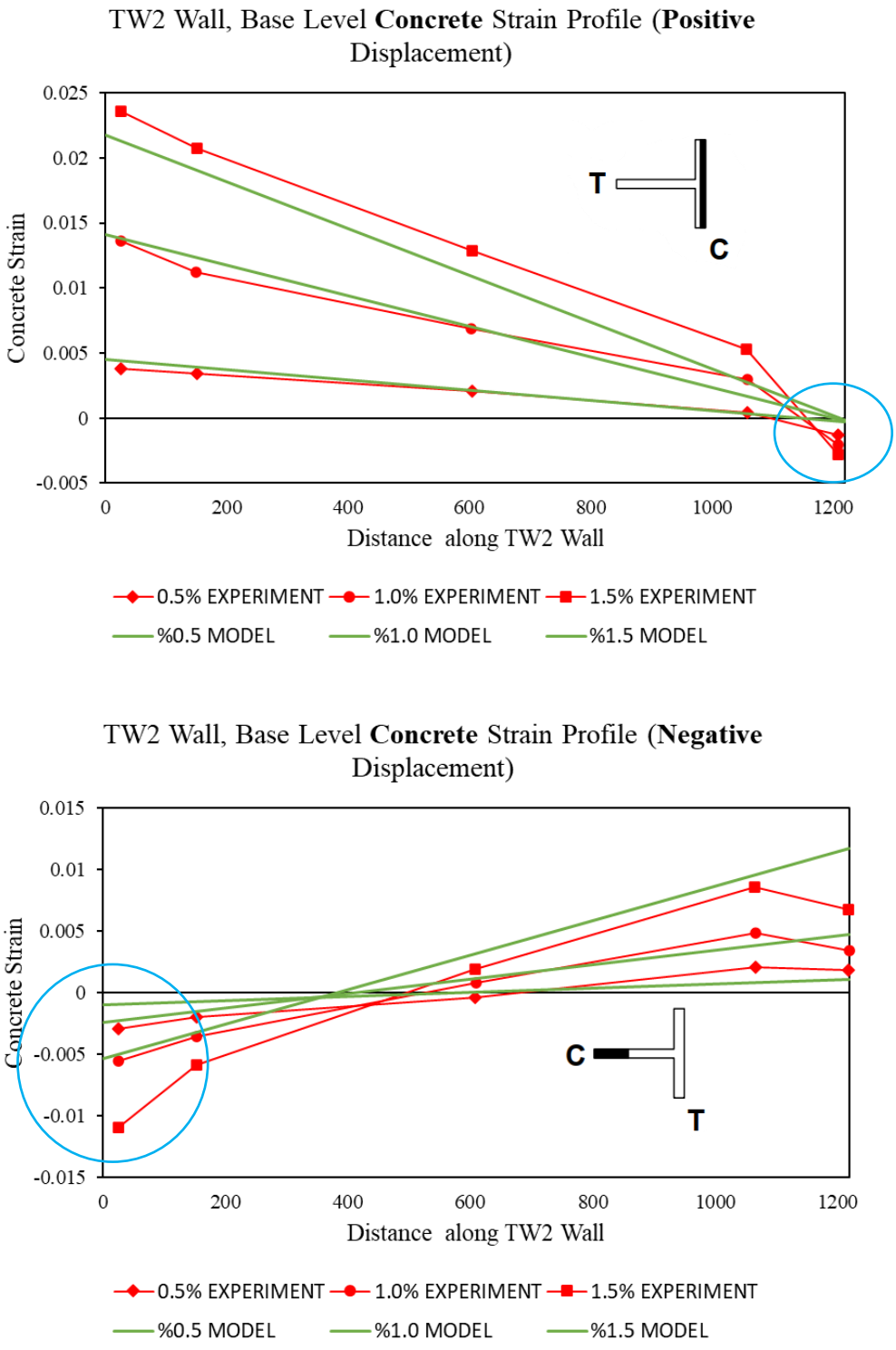

Figure 5.36 TW2 Wall, Base Level *Concrete* Strain Profiles of Experiment and P3D Model (TModel-1) for Different Drift Ratios

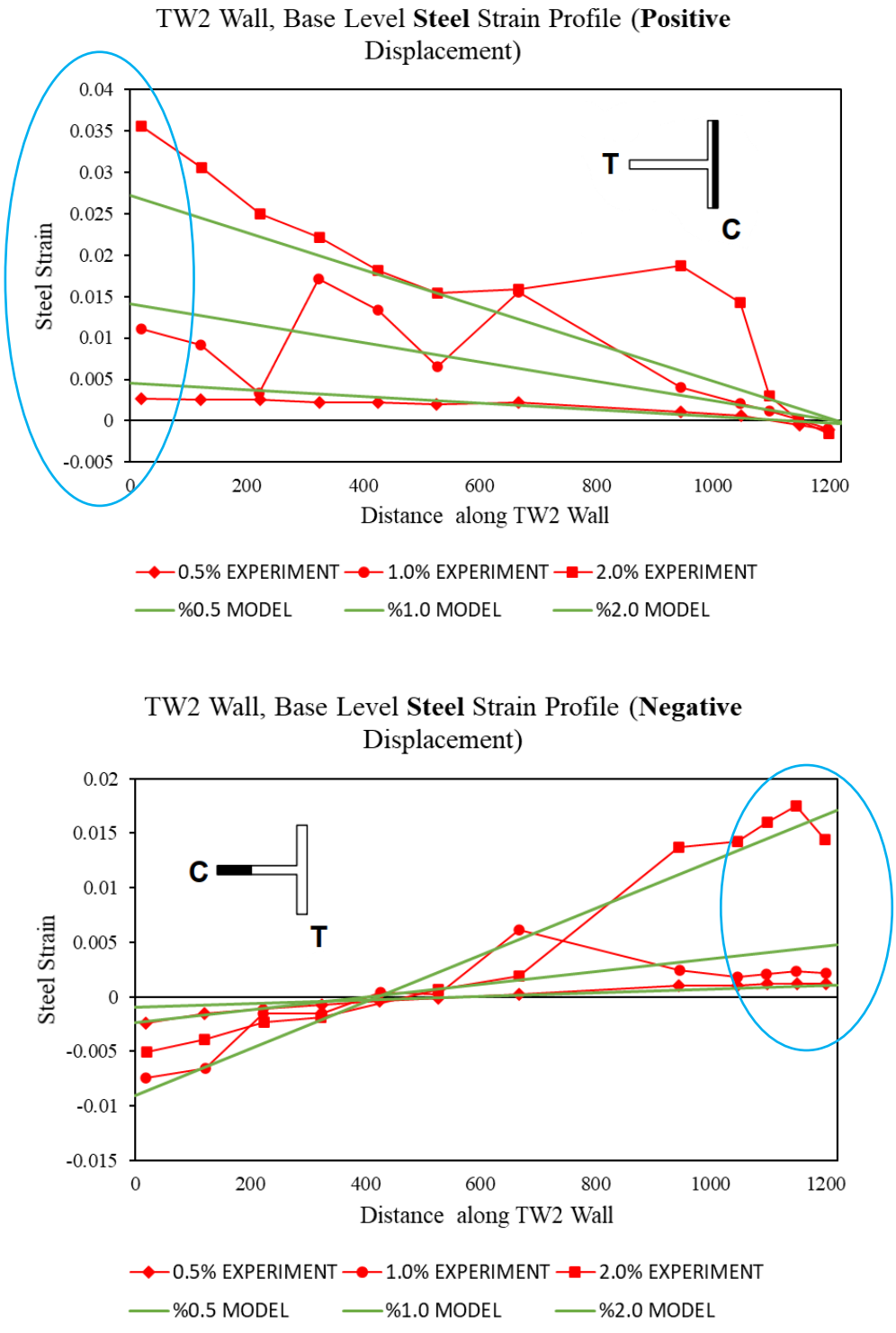

Figure 5.37 TW2 Wall, Base Level *Steel* Strain Profiles of Experiment and P3D Model (TModel-1) for Different Drift Ratios

c) U-Shaped Walls, Loaded Symmetric and Asymmetrically

Necessary comparisons have been made and evaluated for hysteric shape, lateral displacement profile and basement level strain profile results with the cyclic response modeling study on RW2 and TW2 wall samples. While very good results are obtained for the rectangular wall in the comparisons in the mentioned subjects, relatively better results are obtained for the T-shape wall than the rectangular wall results. The ideal modeling parameters of both sample walls are presented in Table 5.10. The conclusion of results that these material parameters are suitable and acceptable, is reached as a result of the model trial of different variations for both RW2 and TW2 walls. These ideal material parameters are used in the modeling for U-Shape wall. Displacement controlled force-drift ratio curves for both X and Y direction are obtained as a result of comparison with the test and P3D model results. X and Y direction force-drift ratio curves are shown in Figure 5.38.

As the most basic comparison, model and experimental results successfully agree in terms of hysteretic shape achieved in RW2 and TW2 but not to the degree sufficiently achieved for U-shape wall. Y-direction force-displacement curve compatibility is better than X-direction one. While wall behavior in the Y direction is more symmetrical and identifiable, the X-direction displacement profile of wall is more eccentric and complex. So, one of the reasons for increase in incompatibility can be interpreted in this way. From a simple structural wall shape such as a rectangle to a slightly more complex T-shape wall, and ultimately to the most complex U-shaped wall, after experiment and P3D model hysteric shape comparisons are explored, it may be concluded that there is a need for more investigation in terms of modeling of U-shaped wall force-displacement behavior. It seems that U-shaped wall work examined by Pegon et al. in Elsa Laboratory is not very detailed as the investigation done for rectangular and T-shaped wall by Orakcal K. The reasons for hysteric shape incompatibility in P3D model and experiment comparison for U-shaped wall may be inadequate modeling information on the material properties especially steel yield strength. For more complex wall shapes, such as the U and I curtains, it is clear that more experimental studies and more detailed ones are needed.

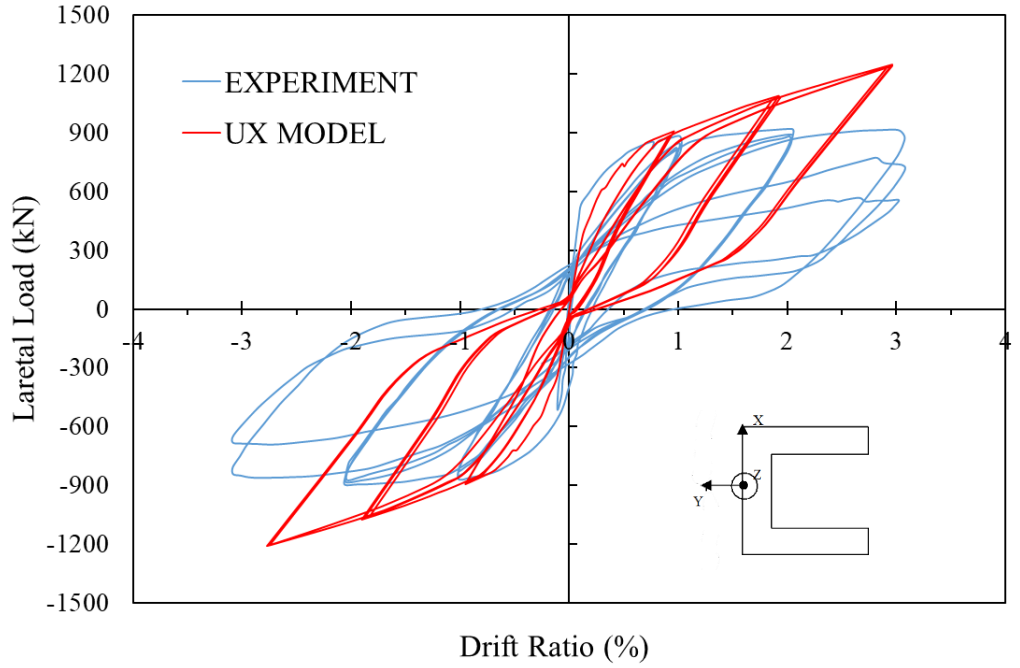

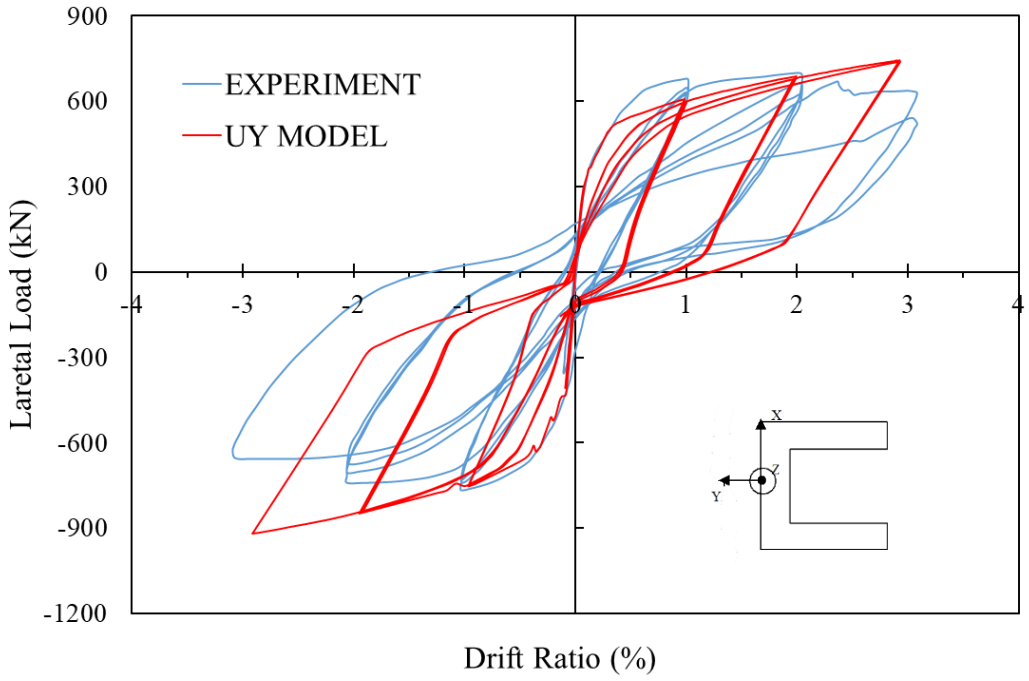

Figure 5.38 UX and UY, P3D Cyclic Response Result with Ideal Material Parameters

5.1.3.4 Mesh Sensitivity

In addition to accurately identifying material parameters in order to capture the correct behavior and results by modeling wall elements of structures with the Perform-3D program, it is important to make wall cross-section definitions and the number of wall element mesh correctly. The correct and efficient result will be obtained by getting an ideal modeling approach as a whole for accurate material parameters and together with optimum cross-section and mesh modeling. For this reason, necessary studies are carried out on wall cross-section modeling and mesh, and validation studies are fulfilled with the results of the experiment. Besides to working on optimum fiber numbers in cross-section definition, two different cross-section identification modes available in P3D, i.e., the "Fixed size" and "Auto size" modules, are compared. In addition to cross-section modeling, another work is also done on ideal wall mesh work and strain gage length.

a) Rectangular Wall, RW2

The optimum selection of the reinforcement and concrete fiber number in the cross-section of walls element is important for the rapid analysis of complex 3D structure. It is necessary to model the reinforcements, which usually settle at intervals of 15-20 cm through web portions of walls and more frequent in the wall boundary sections, and concrete fibers corresponding to them at ideal intervals. Modeling each reinforcement as fiber individually will greatly increase analysis time in complex high-rise structures. For this reason, different number of fiber modeling options is tried for the RW2 wall in order to look at the way to simplify the model so as not to affect the result too much (Figure 5.39). Accordingly, Model-31 of RW2, that is a very detailed model, is simplified and 7 new trial models is created from Model-31. With these trial models, differences and sensitivity between models are indicated in Table 5.12. In addition, hysteric shape comparisons of RW2 models having different fiber cross section modeling are presented in Figure 5.40.

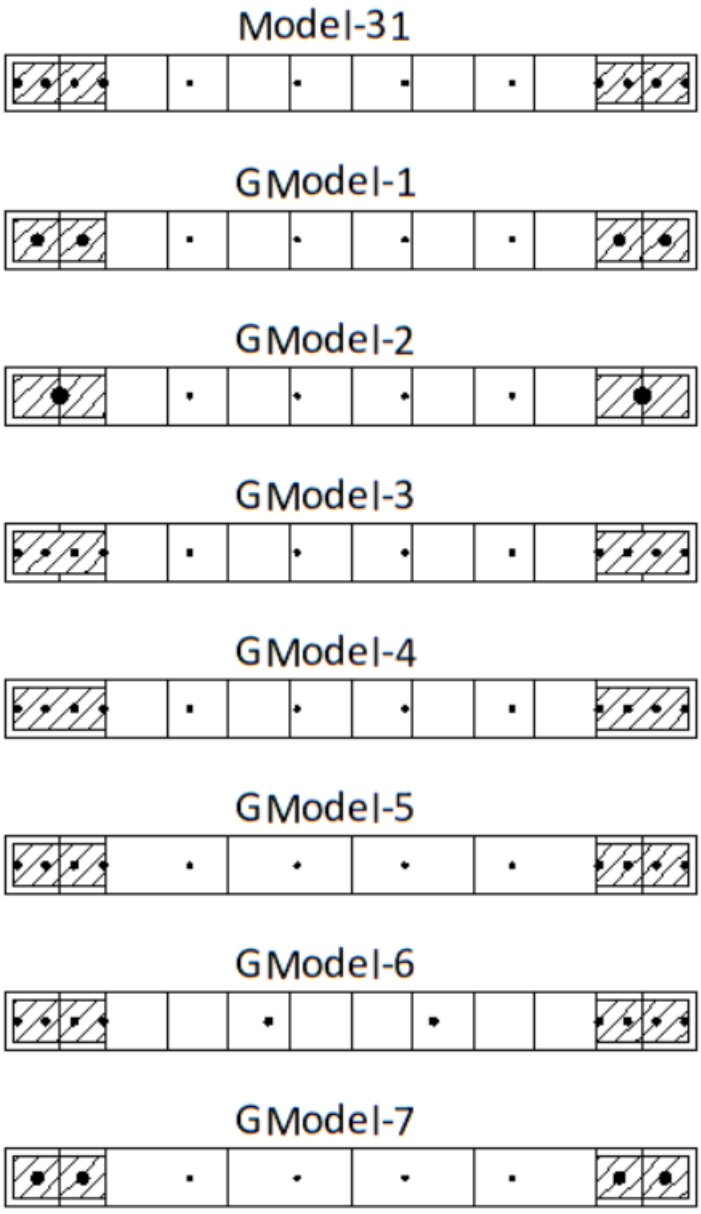

Figure 5.39 Different P3D Fiber Modeling Types for RW2

Table 5.12 Sensitivity Evaluation in Terms of Different Fiber Modelling for RW2 P3D Models

Model #	DIRFFERENCE FROM REFERENCE 31. MODEL IN TERMS OF FIBERS	SENSITIVITY
Model-31	Reference P3D Model (Model-31)	--
GModel-1	4 reinforcement fibers of boundary are decreased to 2 reinforcement fibers	Low
GModel-2	4 reinforcement fibers of boundary are decreased to 1 reinforcement fibers	High
GModel-3	2 concrete fibers of confined concrete of boundaries are decreased to 1 concrete fiber	Low
GModel-4	2 concrete fibers of confined and unconfined concrete of boundaries are decreased to 1 concrete fiber	Low
GModel-5	Web part of wall is modelled with 4 concrete fibers instead of 8 fibers	None
GModel-6	Web part of wall is modelled with 2 reinforcement fibers instead of 4 fibers	None
GModel-7	4 reinforcement fibers of boundary are decreased to 2 reinforcement fibers and web part of wall is modelled with 4 concrete and 4 reinforcement fibers.	Low

As a result of comparisons with different fiber modeling options, it can be concluded that, first of all, it is more important that the reinforcement should be modeled accurately compared to the concrete fibers. The fact that the number of concrete fibers has been reduced does not have much effect. In addition, it is observed that unconfined sections in boundary parts of wall do not need to be modeled additionally. Modeling reinforcement in boundary sections under high tension load according to the 1x1 aspect ratio is ideal, as seen with the GModel-7 (Figure 5.39) and GC7 (Figure 5.40). As can be observed in GModel-2 and GC2, inaccurate results are obtained with the insufficient number of tensile reinforcement fibers in boundary sections under high tension load.

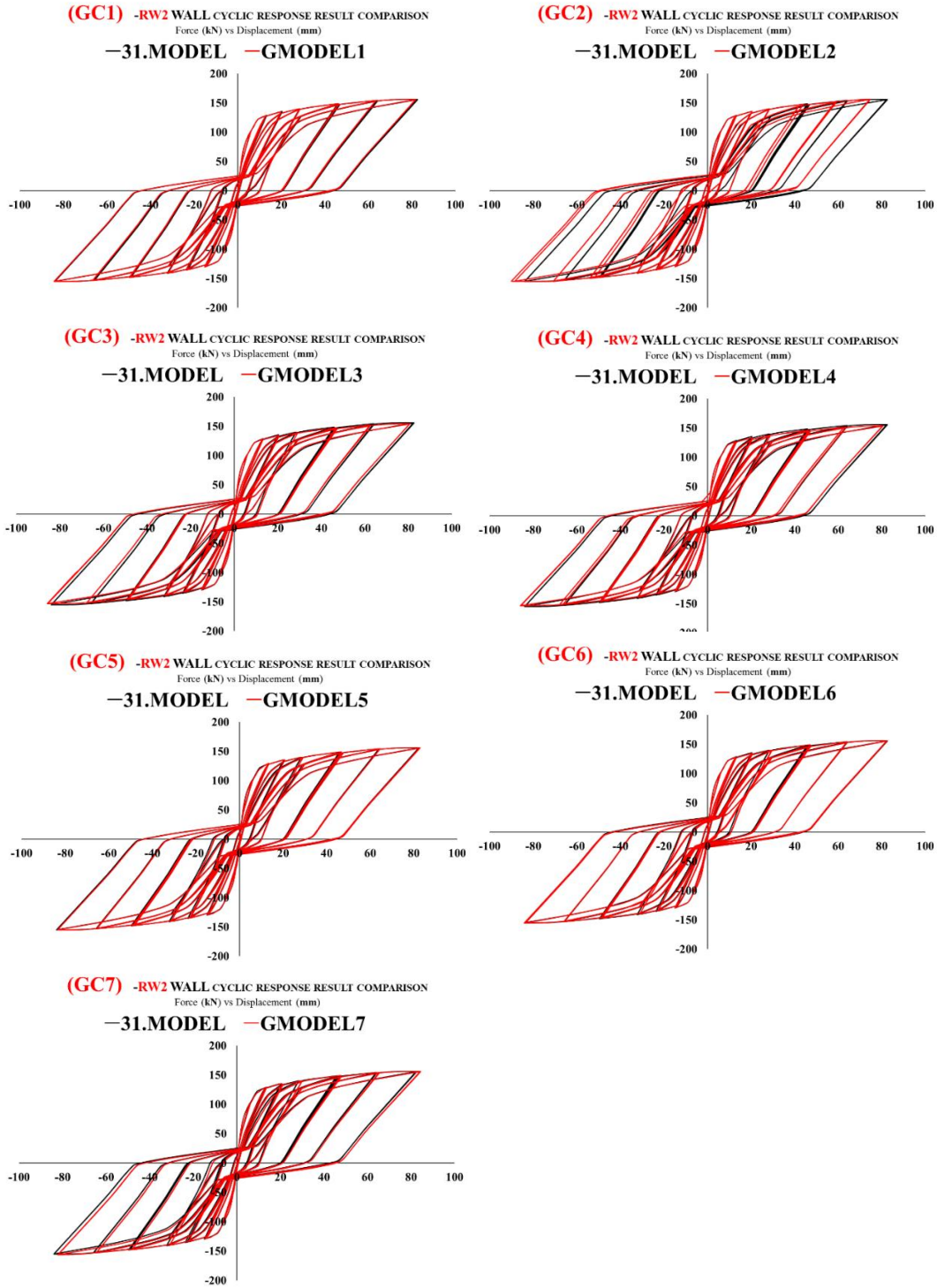

Figure 5.40 Cyclic Response Comparisons b/w GC1-GC7 in Terms of Different Fiber Modelling for RW2-P3D Models

b) P3D "Fixed Size" and "Auto Size" Modeling Option Comparison for RW2 and TW2

Perform 3D program offers 2 options for cross section fiber modeling of wall section, i.e., "Fixed size" and "Auto-size". “Fixed-size” module supplies a slower and less practical but more detailed modeling option, while “Auto-size” provides a more limited but faster modeling option (Figure 5.41). In the solution of large building systems, P3D users often prefer "Auto-size" option for fast and practical modeling. There was a need for more detailed modeling for work to compare RW2, TW2 and U-shaped sample walls with experiment results, so, "Fixed-size" model option was used for investigations before.

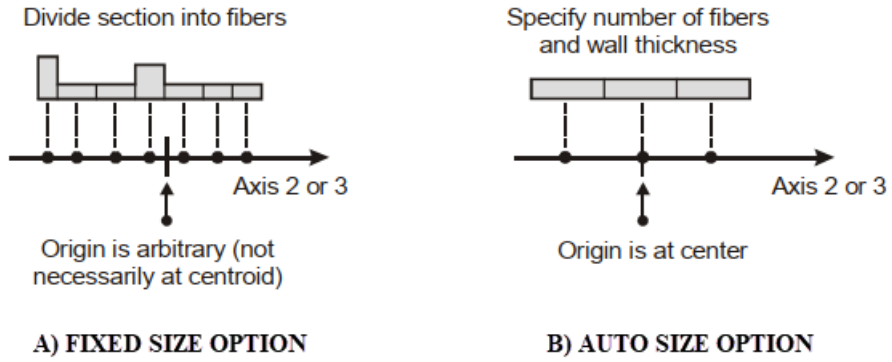

Figure 5.41 P3D Two Fiber Modeling Options, “Fixed Size” & “Auto Size” for Walls

It is questioned that how much difference in results occurred when RW2 and TW2 sample walls are modeled with the "auto-size" module, which engineers could commonly use in modeling. The cross-section fiber appearance of the RW2 and TW2 sample walls in the "Fixed size" and "Auto-size" modules is given in Figure 5.42.

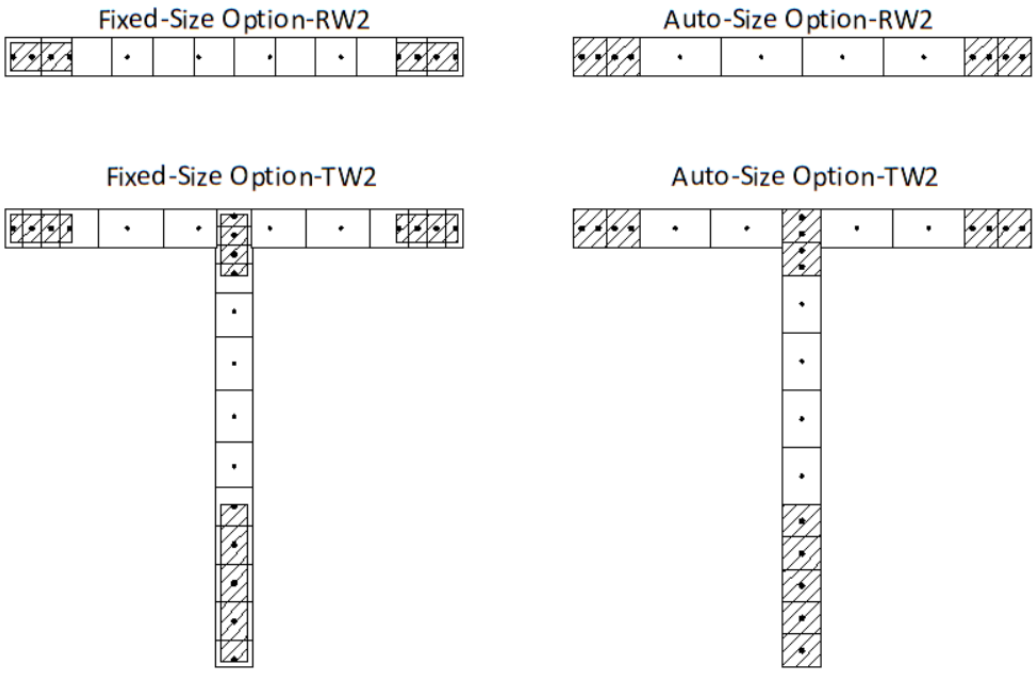

Figure 5.42 "Fixed Size" and "Auto-Size" P3D Modeling Options of RW2 and TW2

The results of the comparison of these two modules are examined on the basis of both hysteric shape and strain profile topics for RW2 wall sample solutions (Figure 5.43 and Figure 5.45). However, In TW2 wall sample solution, two fiber modeling shapes are compared only in terms of hysteric shape. In RW2 rectangular wall cross-section fiber modeling, the result of both modules in terms of hysteric shape is almost the same (Figure 5.43). In terms of strain profile match, modeling with the "Auto-size" fiber module causes a strain increase of 5-10% compared to modeling with the "Fixed-size" module, leaving the resulting evaluation on the safe side (Figure 5.45). While the effect of "Auto-size" module on TW2 wall sample makes no difference in the case of positive displacement, it causes an increase of up to 10% after a certain drift ratio in the lateral load capacity for negative displacement where the flange is under tension (Figure 5.44). Since usual building designs do not check capacity or strain control at high drift ratios, both modules can be seemed similar in T-shape for lower drift ratios.

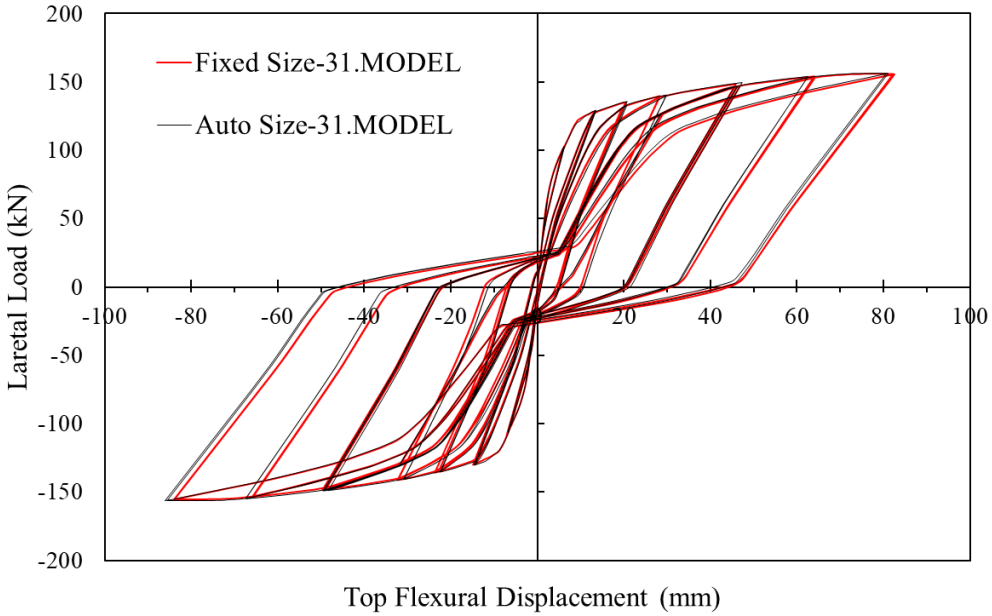

Figure 5.43 "Fixed Size" and "Auto Size" Modeling Option Cyclic Response Result of RW2

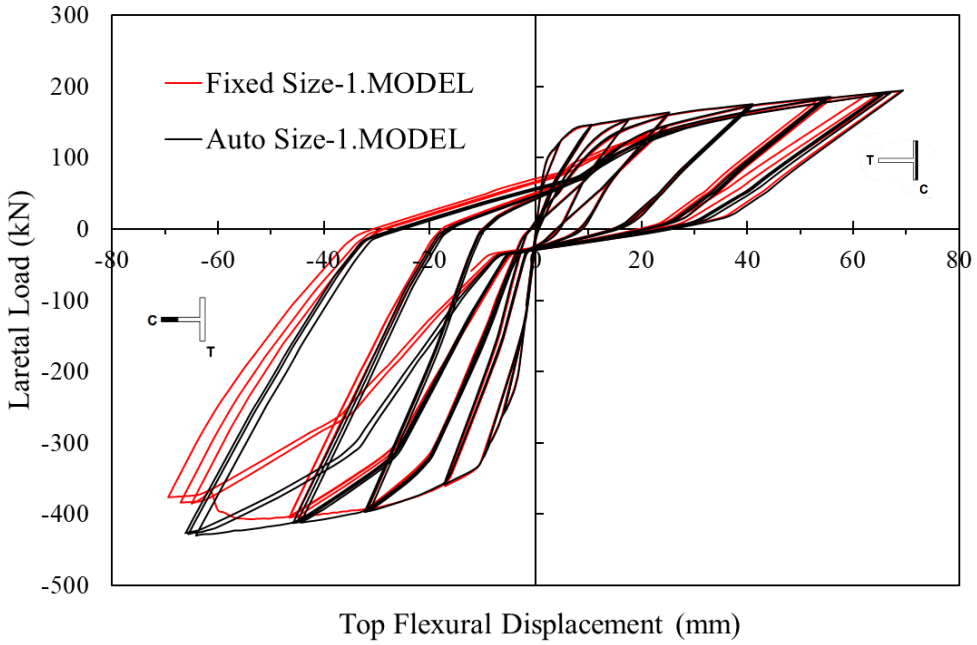

Figure 5.44 "Fixed Size" and "Auto Size" Modeling Option Cyclic Response Result of TW2

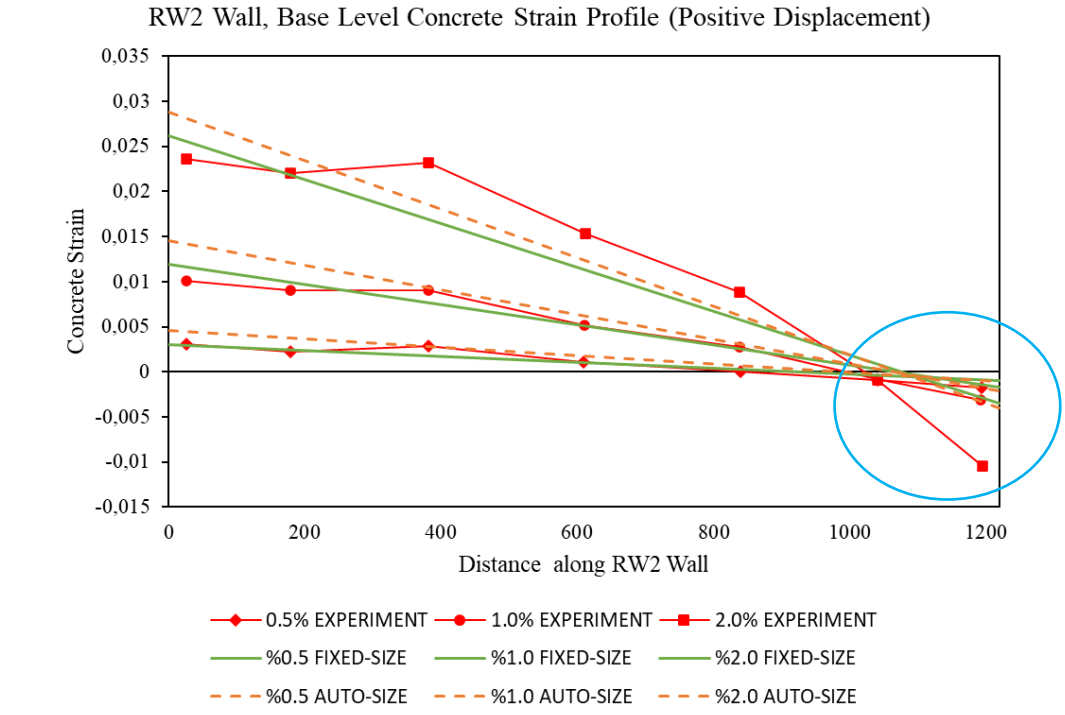

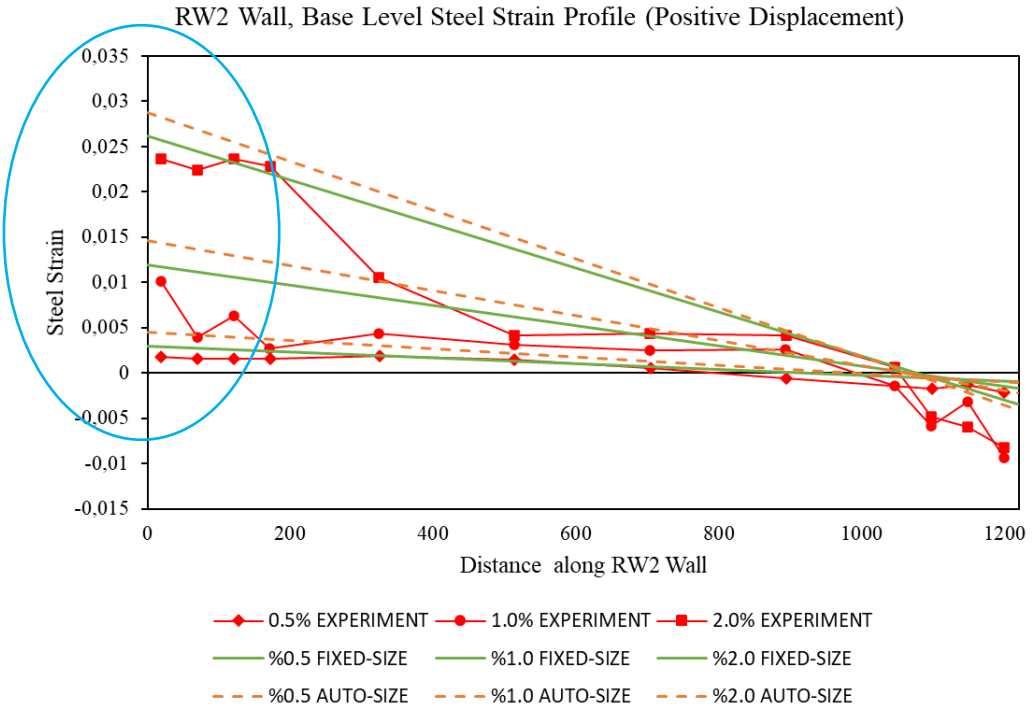

Figure 5.45 Concrete and Steel Strain Profiles of RW2, Wall for "Fixed Size" and "Auto Size" Option

c) Different Mesh and Gage Length Option for Cyclic Response Comparison

Using the minimum number of elements and fibers with providing real structural behavior in model will reduce analysis time and margin of error. Therefore, walls should be modeled as simple as possible.

The amount of mesh of the walls vertically and horizontally should be kept at the optimum level, so that both accurately reflecting the structure behavior and shortening the analysis time. In high-rise buildings, it may be enough to model one wall element on each floor in a vertical direction. Curvature, axial and shear strains are constant throughout each wall mesh element. For this reason, the number of elements can be increased or selected a reasonable height in the hinge section, which has plastic behavior for the walls.

Appropriate inelastic hinge section height is very important at modeling of walls because it affects the calculated strain and bending moment capacities. The correct height selection of elements representing hinge length is the very sensitive parameter that affects the accuracy of the calculated strain. According to ASCE 41, the hinge length of walls is minimum of one half of cross section depth and story height. In Turkish earthquake regulation, it is considered to use Equation 5.1.

$$L_g = maks\left(0.2\, l_w + 0.03 h_w; 0.08 h_w + 0.022 f_{ye} d_b\right) \qquad \textbf{(5.1)}$$

Here, l_w and h_w shows length and height of wall respectively. f_{ye} and d_b is taken as the average yielding resistance and the largest longitudinal reinforcement diameter.

In order to select hinge height correctly, investigation is done by P3D software on RW2 and TW2 walls with 5 different mesh and hinge height options with auto-size fiber module. Analyses are performed with 9x4, 8x4, 4x4 and 2x4 mesh options (Figure 5.46). 5 different types of mesh options automatically cause 5 different types of strain gage length options. Strain gage length-1 (SGL-1) is the experiment strain gage value, 229 mm. On the other hand, strain gage length-2 (SGL-2) is 271 mm calculated according to Equation 5.1 for RW2 and TW2. Also, strain gage length-3 (SGL-3) is half the height of the floor, while strain gage length-4 (SGL-4) refers to

floor height and strain gage length-5 (SGL-5) is 2 times the floor height (Figure 5.46). Strain gage lengths, SGL1, SGL2, SGL3, SGL4 and SGL5 are 229 mm, 271 mm, 457.2 mm, 914.4 mm and 1828.8 mm respectively.

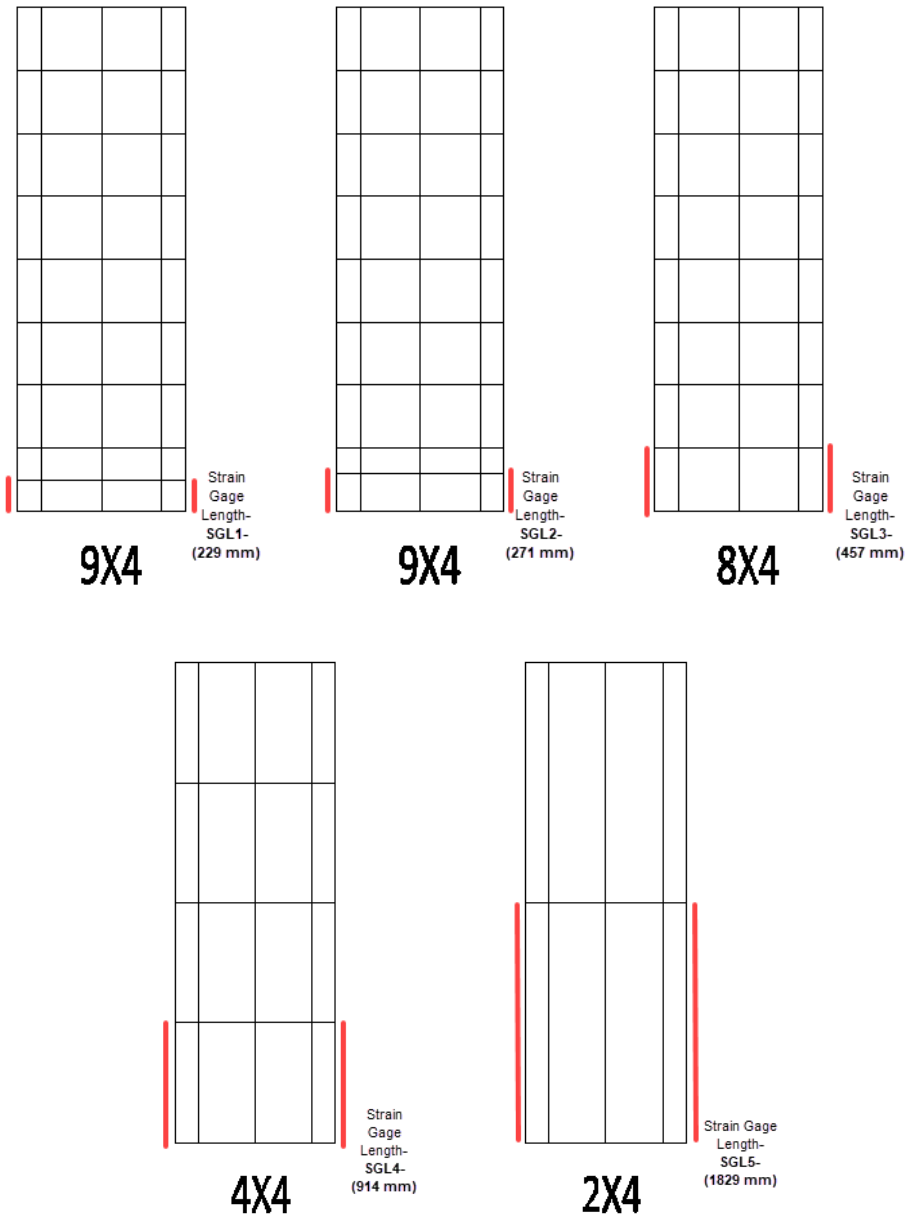

Figure 5.46 Vertical Mesh and Strain Gage Length Variations

Cyclic response results for 3 different P3D models with different mesh, that are matched with test results, are shown in Figure 5.47, Figure 5.48 and Figure 5.49 for

8x4, 4x4, 2x4 mesh respectively. These three models are generated with "Auto-size" cross-section module. In three different models, where the number of mesh decreases by simplifying from 8x4 mesh to 2x4 mesh, the agreement of the P3D model hysteric shape with the result of the experiment is gradually decreasing. Cyclic response resulted in the best model being the 8x4, while the 4x4 mesh model is acceptable but the model with 2x4 mesh is largely removed from results of the experiment.

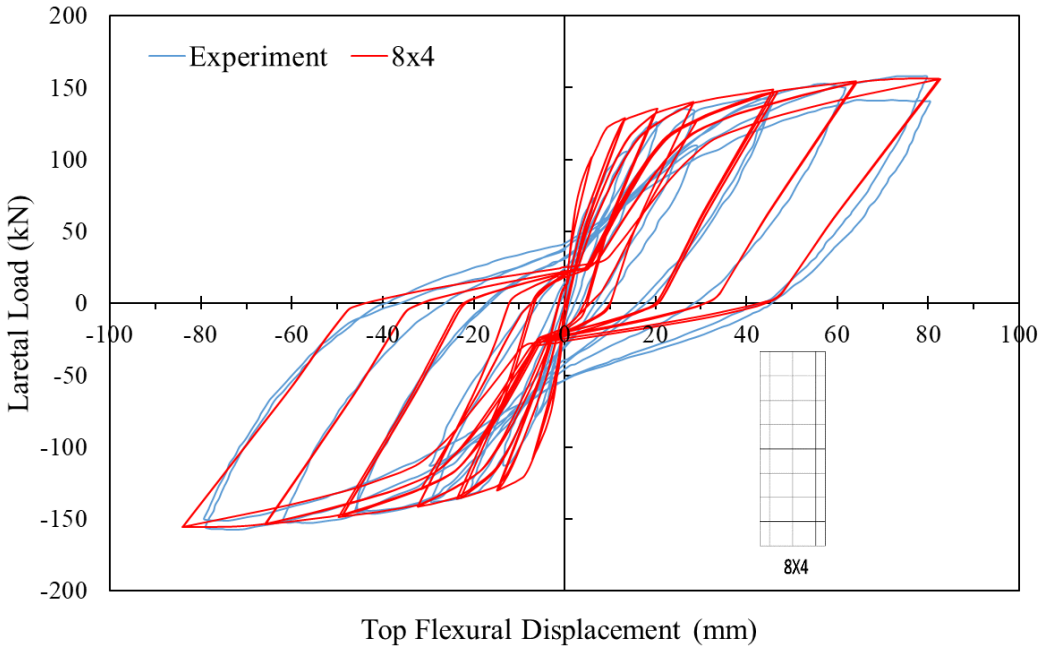

Figure 5.47 Cyclic Responses of Experiment and Model with 8x4 Mesh

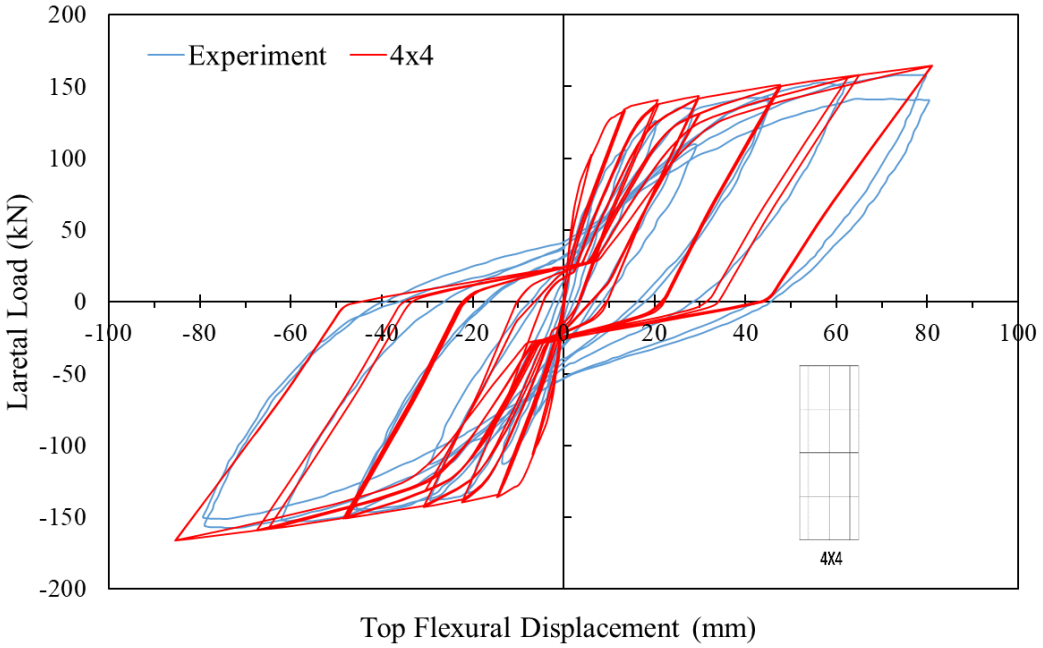

Figure 5.48 Cyclic Responses of Experiment and Model with 4x4 Mesh

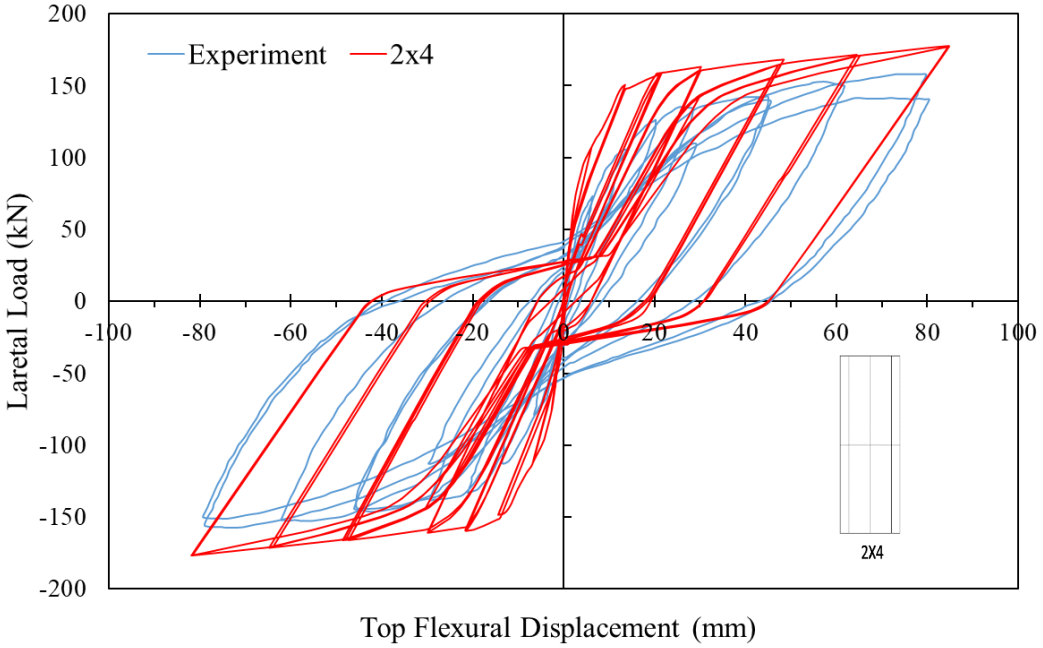

Figure 5.49 Cyclic Responses of Experiment and Model with 2x4 Mesh

It automatically consists of five different strain gage lengths with P3D model with five different mesh variations. At Perform 3D program, strain measurement is carried out between nodes closest to each other. When defining stain gage, a node cannot be skipped and tied to another desired node. For this reason, bottom mesh hinge height section of wall automatically determines the strain gage length. For five different strain gage lengths and mesh identifications, experiment strain profile is compared with P3D Models for concrete and reinforcement. Concrete and reinforcement strain profile result comparisons are presented in Figure 5.50 and Figure 5.51 respectively. Reinforcement tensile strain and concrete compressive strain checks are more important in terms of structural design. According to the strain checks of reinforcement under tension, the results of the 8x4 mesh model remain on the safe side, while the results of the 4x4 mesh model show a compatible match, on the other hand, the results with the 2x4 mesh model give incompatible and unacceptable results much lower than the test results. In terms of concrete compressive strain checks, model results with 8x4 mesh except 2% drift ratio give the most compatible results, while model results with 4x4 mesh are less accurate and model with 2x4 mesh are not accurate when compared with test results.

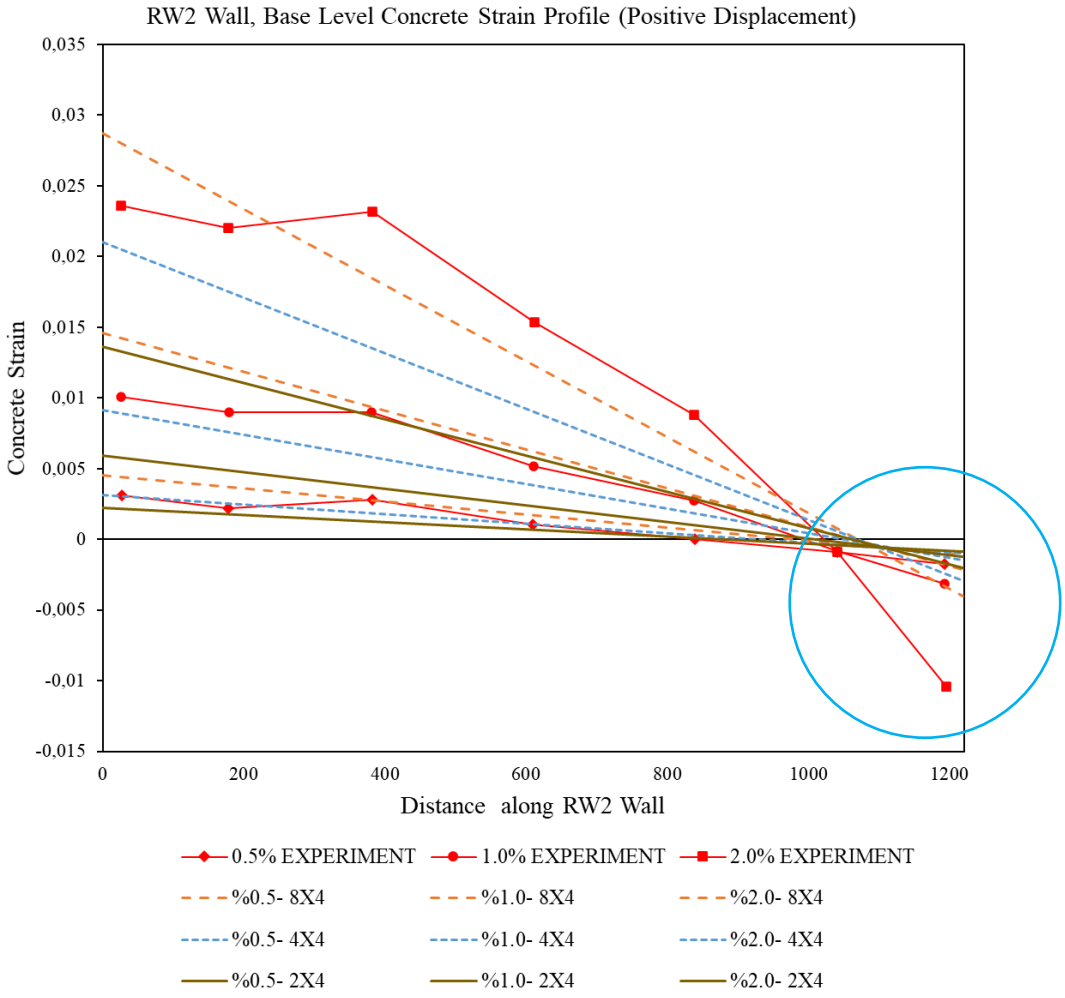

Figure 5.50 Concrete Strain Profiles of RW2 Wall for Different Mesh Variations

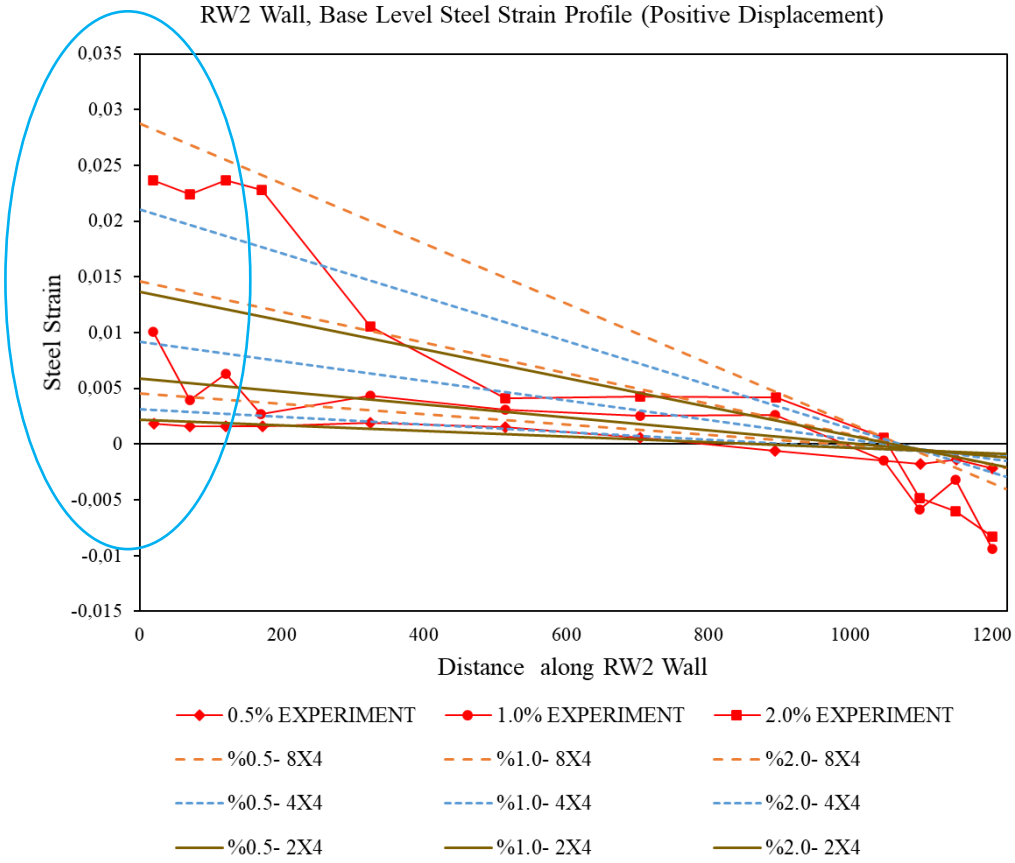

Figure 5.51 Steel Strain Profiles of RW2 Wall for Different Mesh Variations

Strain gage length value-SGL1 in experiment is 229 mm, and in order for comparison between model and experiment in terms of strain profile, strain gage length in P3D model must be 229 mm. For this reason, SGL-1 value is chosen as 229 mm. SGL2 is 271 mm, which is the strain gage length value that it is encountered as required by regulation calculated according to Equation 5.1. SGL3, SGL4 and SGL-5 are created to observe the extent to which mesh change affects total strain profile and cyclic response outcomes. Strain gage lengths, SGL3, SGL4 and SGL5 results are observed and presented them with figures between Figure 5.51 and Figure 5.57. Strain-based result evaluation is the basic approach in evaluation of wall structures in performance-based design. For this reason, it is of great importance to observe the extent of test and model compatibility in the evaluation of strain results according to strain gage length-1, SGL-1 measurement. For results of experiment strain gage

length, 229 mm, model and final strain profile evaluation are presented in Figure 5.52 to Figure 5.57 for both RW2 and TW2 wall test samples.

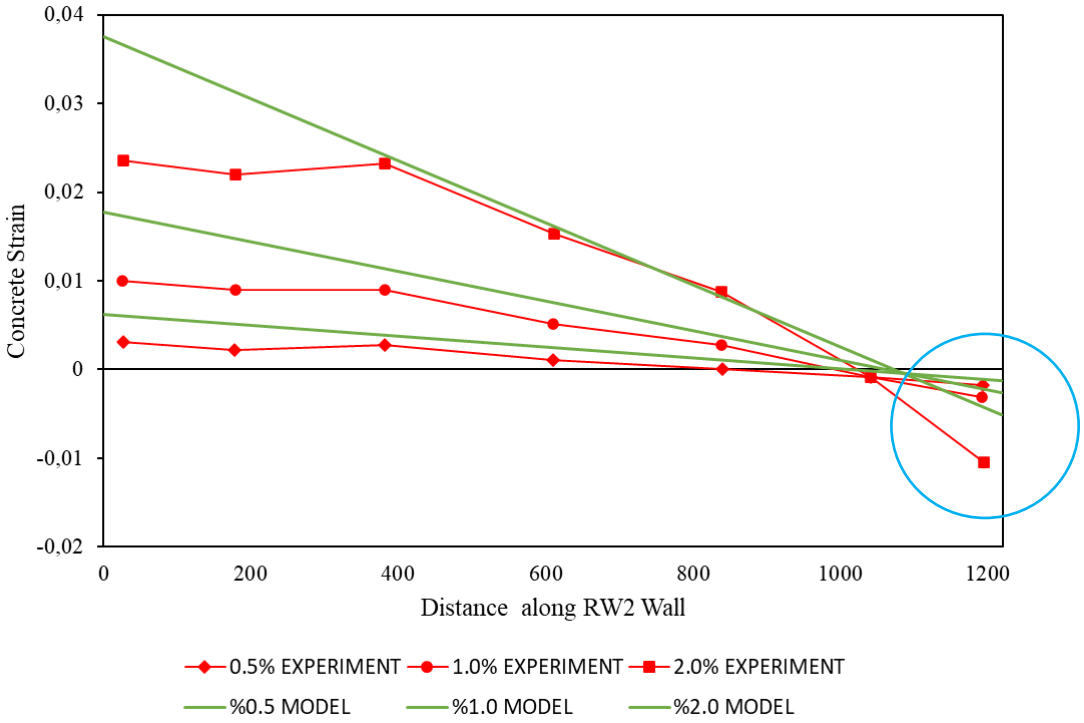

Figure 5.52 *RW2 Wall*, Base Level **Concrete** Strain Profile (Positive Displacement) for test strain gage length, SGL-1, 229 mm

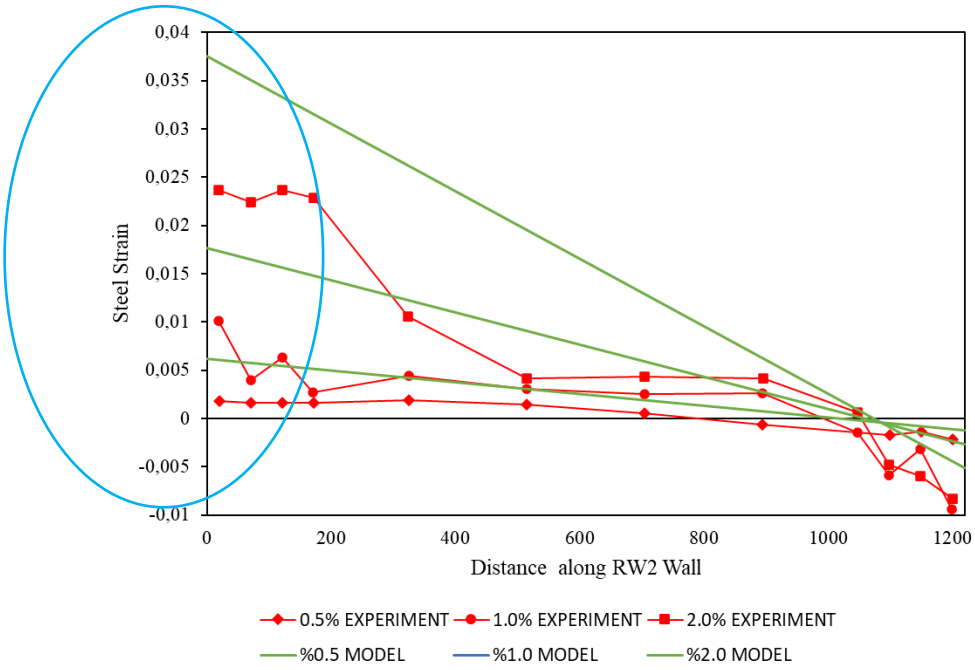

Figure 5.53 *RW2 Wall*, Base Level **Steel** Strain Profile (Positive Displacement) for test strain gage length, SGL-1, 229 mm

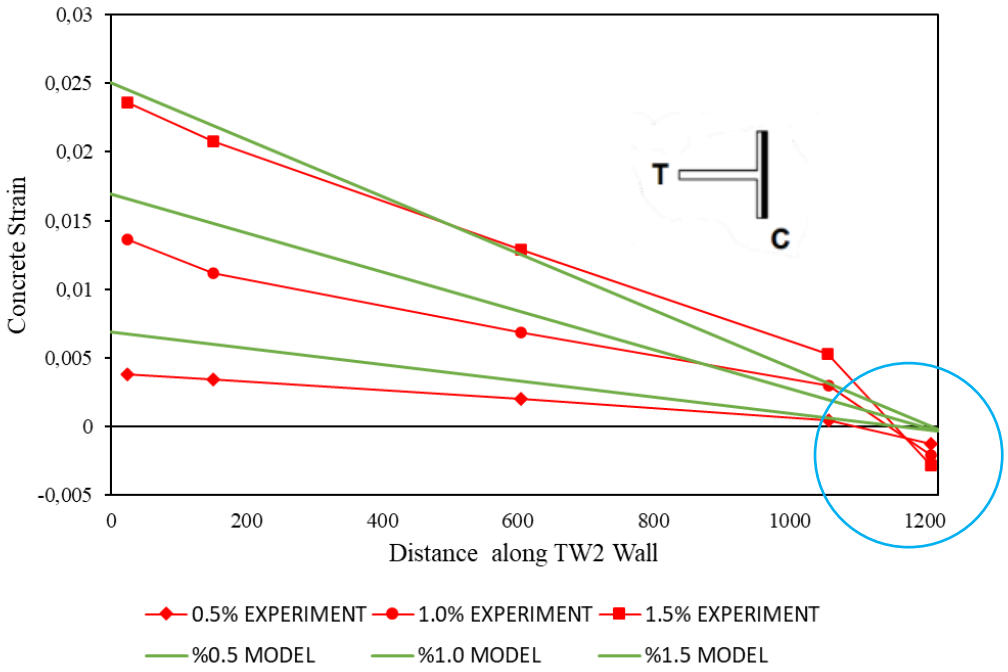

Figure 5.54 *TW2 Wall*, Base Level **Concrete** Strain Profile (Positive Displacement) for test strain gage length, SGL-1, 229 mm

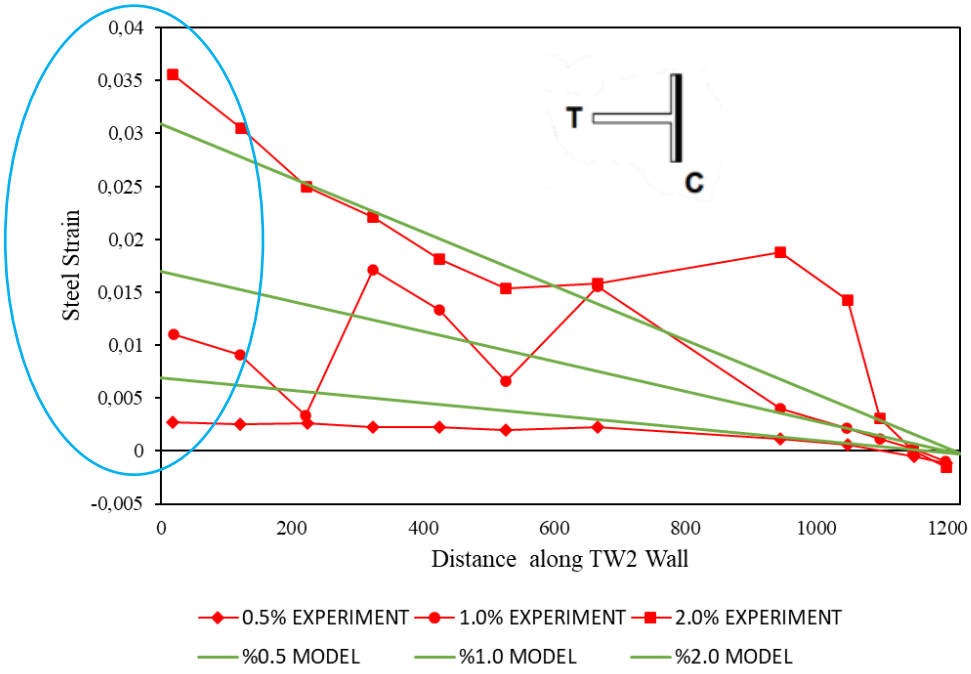

Figure 5.55 *TW2 Wall*, Base Level **Steel** Strain Profile (Positive Displacement) for test strain gage length, SGL-1, 229 mm

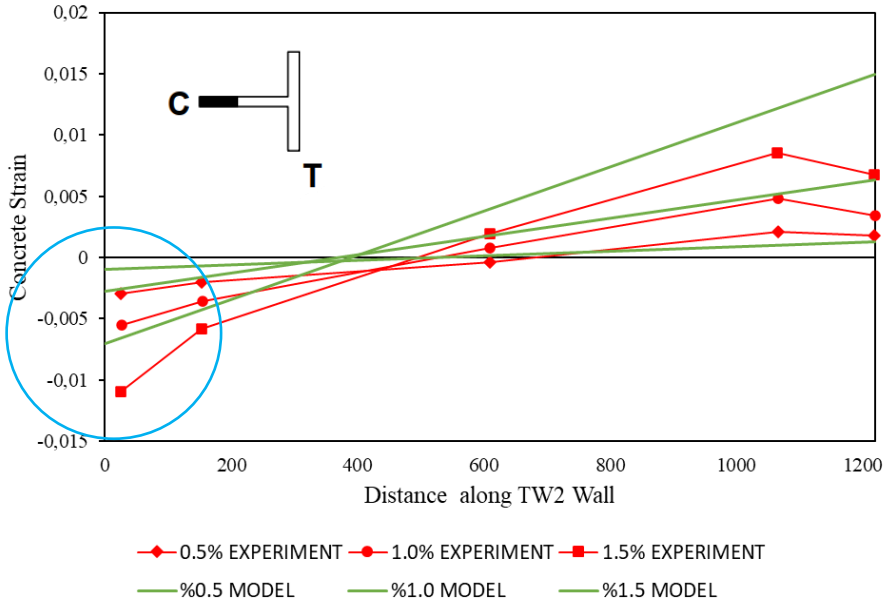

Figure 5.56 *TW2 Wall*, Base Level **Concrete** Strain Profile (**Negative** Displacement) for test strain gage length, SGL-1, 229 mm

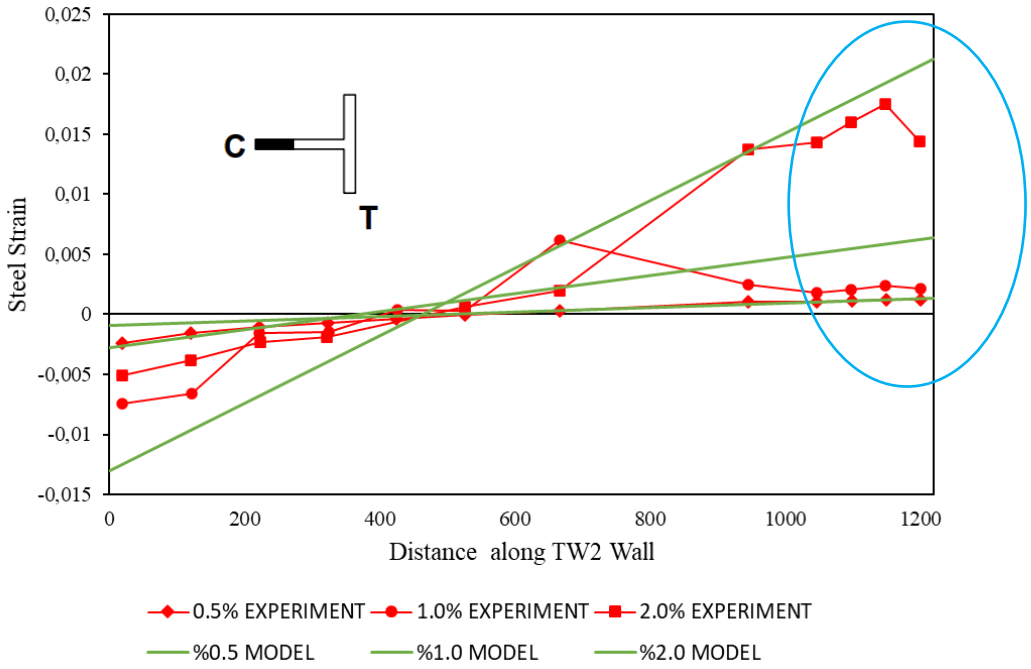

Figure 5.57 *TW2 Wall*, Base Level **Steel** Strain Profile (**Negative** Displacement) for test strain gage length, SGL-1, 229 mm

Test reinforcement tension strain values are lower than P3D model strain values according to strain profile on the base of RW2 and TW2 wall structural elements. In other words, a design is formed on the safe side in terms of reinforcement strain value evaluations. On the other hand, experiment concrete compression stain values are much higher than concrete strain values in P3D model. The fact that concrete strain in the model is low from the test values causes an inadequate and inappropriate evaluation in wall structural member design. Especially in the case of a positive drift for TW2 wall sample, i.e., under compression of wall flange section, concrete strain values are much lower from the model concrete strains. In terms of compatibility with the experimental results, negative drift behavior for TW2 wall sample reveals results more similar to that of RW2 wall.

A numerical study is conducted on Model-31 (RW2), TModel-1 (TW2) according to coefficient a created according to Equation 5.2 on how low concrete strain value is in the model according to the experiment. Coefficient “a” is the ratio of experimental

concrete strain, $\varepsilon_{c,experiment}$, to the model concrete strain, $\varepsilon_{c,P3D\ model}$. If coefficient "a" is greater than 1, this means that experimental result is larger from P3D model result. If coefficient "a" is 1, it means that both model and test result are the same, which is the ideal solution targeted. The coefficient "b" in Equation 5.3 shows the correlation between the experiment reinforcement strain,$\varepsilon_{s,experiment}$, and model reinforcement strain ,$\varepsilon_{s,P3D\ model}$, just like the coefficient "a".

$$a=\varepsilon_{c,experiment} / \varepsilon_{c,P3D\ model} \quad \textbf{(5.2)}$$

$$b=\varepsilon_{s,experiment} / \varepsilon_{s,P3D\ model} \quad \textbf{(5.3)}$$

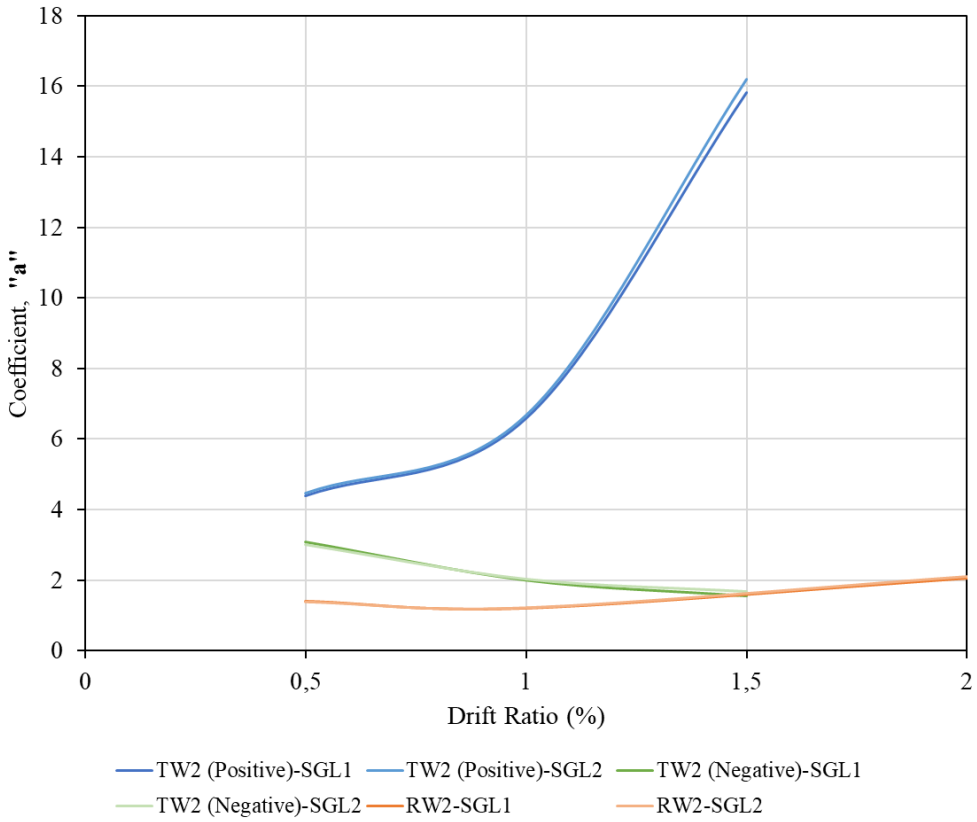

Figure 5.58 TW2 and RW2 Walls ***Concrete*** Strain Experiment-P3D Model Comparison Coefficient "a" vs Drift Ratio Graph

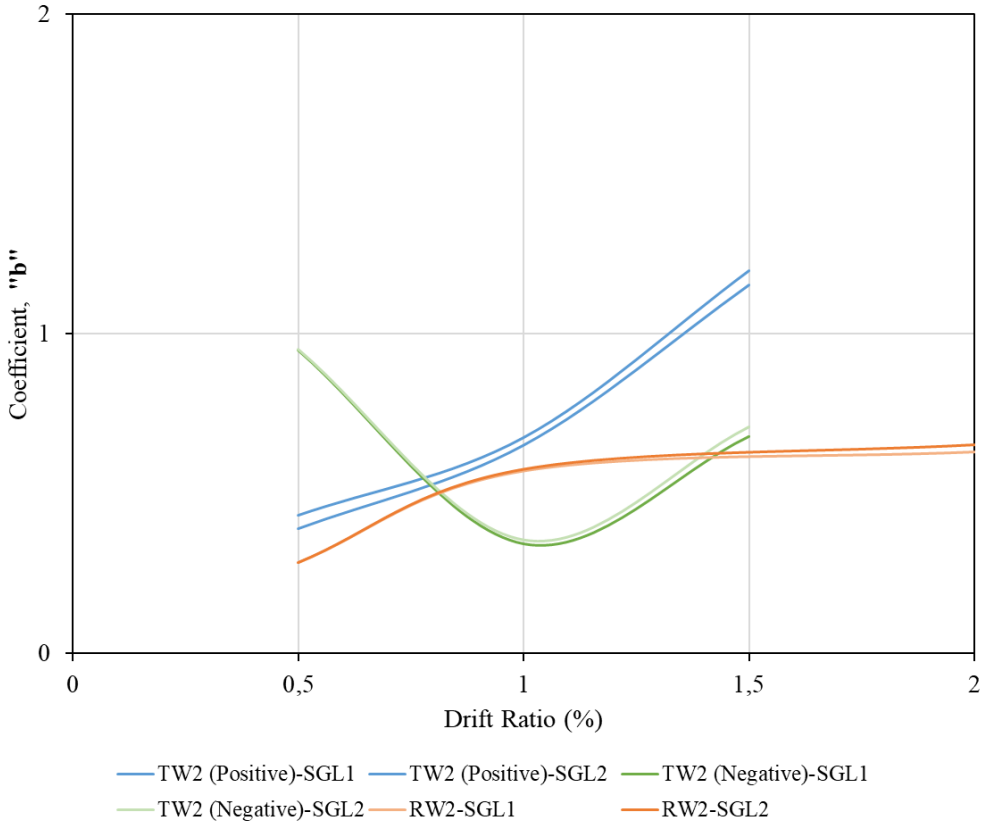

Figure 5.59 TW2 and RW2 Walls ***Steel*** Strain Experiment-P3D Model Comparison Coefficient "b" vs Drift Ratio Graph

According to Figure 5.58, the coefficient "a" is greater than 1 for RW2, TW2 negative and positive drifts, and this coefficient "a" is almost an average of 2 for RW2 and TW2 negative drift, on the other hand coefficient "a" is between 4 and 16 for TW2 positive drift, in which flange is under compression. This shows that P3D model concrete strain results are far and less from experiment results. While model concrete strain results for RW2 and TW2 under negative drift are about 2 times less than test strain results, however, it is between 4-16 times less than experiment concrete strains for TW2 under positive drift.

The coefficient b is less than 1 for all walls samples and drift directions according to Figure 5.59. In other words, the results of model reinforcement strains are higher

than experimental results under all these conditions. This is a safe-side situation to nonlinear design of structure and does not pose a problem.

Strain gage length-1 (SGL-1), 229 mm and strain gage length-2 (SGL-2), 271 mm are almost identical values, and as seen in Figure 5.57 and Figure 5.58, a and b values are almost identical to both strain gage lengths. For this reason, all interpretations and evaluations for a and b values are valid within strain gage length-2 (SGL-2) in Equation 5.1 required by the regulation.

To sum up, in the study for five different mesh types and strain gage lengths, the model containing 2x4 mesh and strain gage length-5 (SGL5) exceeds the multiple height in terms of both mesh and strain gage length. In 8x4 and 4x4 mesh models, the mesh and strain gage length dimensions are at the maximum floor height. Although P3D models having 8x4 and 4x4 mesh give sufficient results in terms of hysteric shape and strain profile matching, the 8x4 mesh model was more acceptable and give satisfactory results. Model results with 2x4 mesh are not acceptable results compatible with the test results. It is recommended not to exceed the floor height in mesh work and strain gage length, so design code restriction in terms of strain gage length, maximum strain gage length cannot be exceeded floor height, is also verified. On the other hand, with SGL-1 and SGL-2 study, P3D model and test compatibility of the strain profile is checked. Reinforcement strain in P3D model is higher than the results in experiment, it creates a result on the safe side in terms of nonlinear design, while concrete strain result is much lower than test results in the model. According to this study, in the design evaluations made with Perform 3D software, it is recommended to evaluate concrete strain results for the wall structural members by multiplying it by 2 and evaluating it with the limit value of the regulation.

5.2 CALIBRATION WORK FOR LINK BEAMS

One of the most important structural elements in meeting the seismic demands in high-rise buildings is the link beam. Earthquake force is effectively resisted together with the core wall group and the link beams. The clear span and heights of the link beams are generally available because of the fire escape, elevator usage and mechanical shaft areas that are architecturally necessary within core wall group. It is thought that accurate modeling of coupling beams, which are very effective in absorbing earthquake energy, will significantly affect the accuracy of the result in 3D structural performance analyses. For this reason, verification work should be carried out on experimental results for link beams similar to conducted for shear-walls.

Aspect ratio (clear span over beam height) is the important decisive parameter for a beam to be referred as a “frame beam" or a "coupling beam". Accordingly, reinforcement details and calculations will vary significantly. According to the Turkish Earthquake Regulation (2018), beams with an aspect ratio value of less than 2 and containing high shear force ($V_n > 0.35 \sqrt{f_{ck}}\ A_{cv}$) are classified as coupling beams, while those other than the specified limits are called frame beams. However, it is important to verify with accurate modeling and experimental results within the beams in the frame beam class, which have an aspect ratio value greater than 2 in high structures because they are similar in terms of behavior and the load they are exposed to. Because link beams with this type of high aspect ratio are widely used in high structures. The majority of the link beam beams in our case study building that we will analyze have high aspect ratio (Figure 5.60). LB1 type link beams have an aspect ratio of 6-7, while the aspect ratio is approximately 1 for LB2.

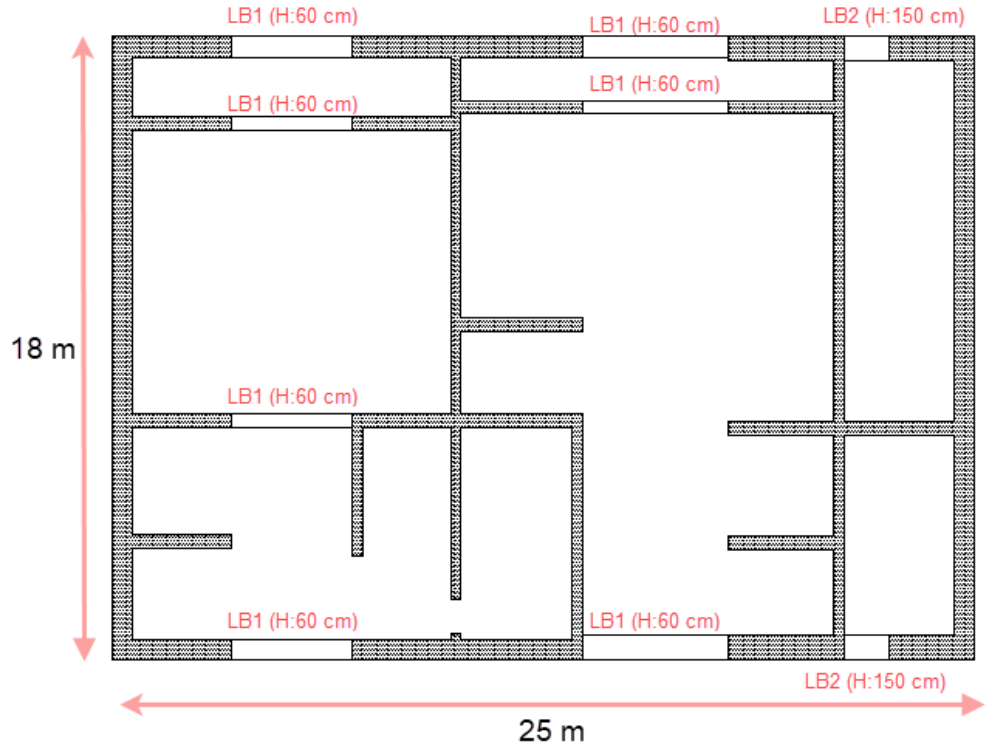

Figure 5.60 Link Beams of the Case Study Building

Experimental studies for commonly used link beams of case study building are selected for modelling with Perform-3D. Model and experiment lateral load-rotation response results are compared for link beam with 2 types of reinforcement details, flexural straight reinforcement (used in conventional link beam) and diagonal reinforcement (used in diagonal link beam). Firstly, necessary information about the experimental work is given for link beams separated as conventional and diagonal link beam.

5.2.1 Experimental Data for Link Beams

Link beam tested by Naish et al. is a reference for our calibration study (Naish et al., 2013a). This study was made on link beams having aspect ratio larger than 2 but less than 4. Modeling work was carried out on link beams labelled as CB33F and FB33

for diagonal and conventional link beams respectively (Figure 5.61 and Figure 5.62). Both sample link beams were studied on a 1/2 experimental scale.

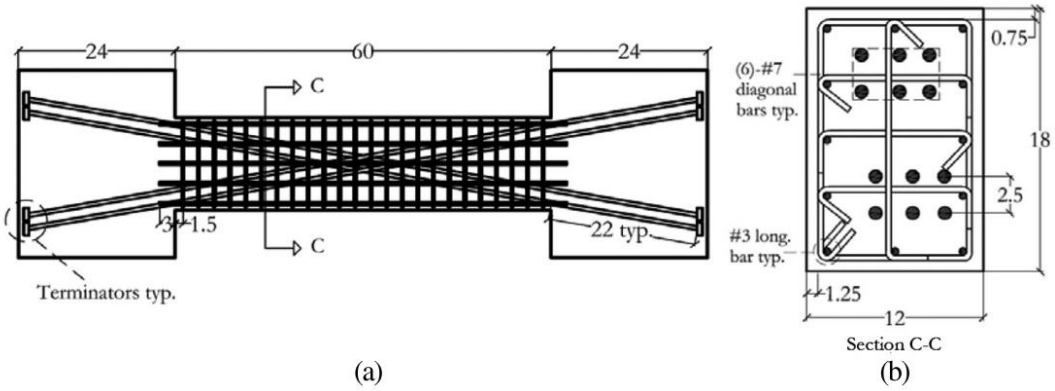

Figure 5.61 CB33F-Diagonal Sample Link Beam and Reinforcement Details (l_n/h=3.33 ; 1 in.=25.4 mm) (Naish et al., 2013a)

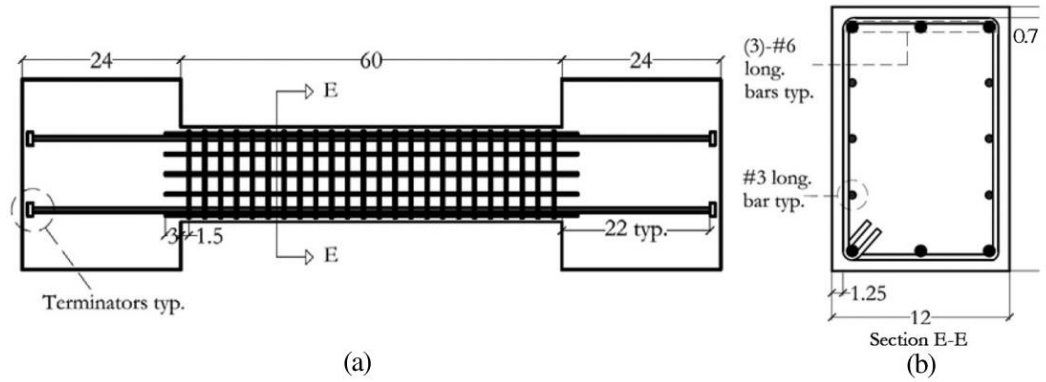

Figure 5.62 FB33-Conventional Sample Link Beam and Reinforcement Details (l_n/h=3.33; 1 in.=25.4 mm) (Naish et al., 2013a)

Diagonally reinforced link beam, CB33F, consists of ϕ9.5 straight flexural reinforcements and ϕ22 diagonal reinforcement bundle design as seen in Figure 5.61. While the diagonal reinforcement bundle is not confined with stirrups, stirrups and ties of beam is used 34% more than necessary. On the other hand, FB33, consists of conventionally reinforced link beam. There are ϕ19 reinforcements in the lower and upper sections of the beam, while ϕ9.5 reinforcements are available in the beam web

(Figure 5.62). It is only confined with stirrups (without any ties). Table 5.13 shows some geometric and material properties for these sample test link beams.

Table 5.13 Geometric and Material Properties of Test Sample Link Beams

	Aspect Ratio	Diagonal Bundles Angles	Clear Span	Beam Dimensions	Transverse Reinforcement (mm)
	l_n/h	α, degrees	l_n (mm)	b/h (mm)	Full Section
CB33F	3,33	12,3	1520	305/457	ϕ9.5 / 7.6
FB33	3,33	0	1520	305/457	ϕ9.5 / 7.6

	$(A_{sh,act} / A_{sh,req})_x$	$(A_{sh,act} / A_{sh,req})_y$	f_c' (MPa)	f_y' (MPa)	f_u' (MPa)
CB33F	1.34	1.26	47	483	620
FB33	--	--	41	483	620

A suitable experiment setup was established to provide both force and displacement control without creating axial force in link beams (Figure 5.63). Both vertical and horizontal actuators were used and necessary measures are taken to prevent negative factors such as slippage, rotation, etc. Linear variable differential transformers (LVDTs) were used for displacement measurements.

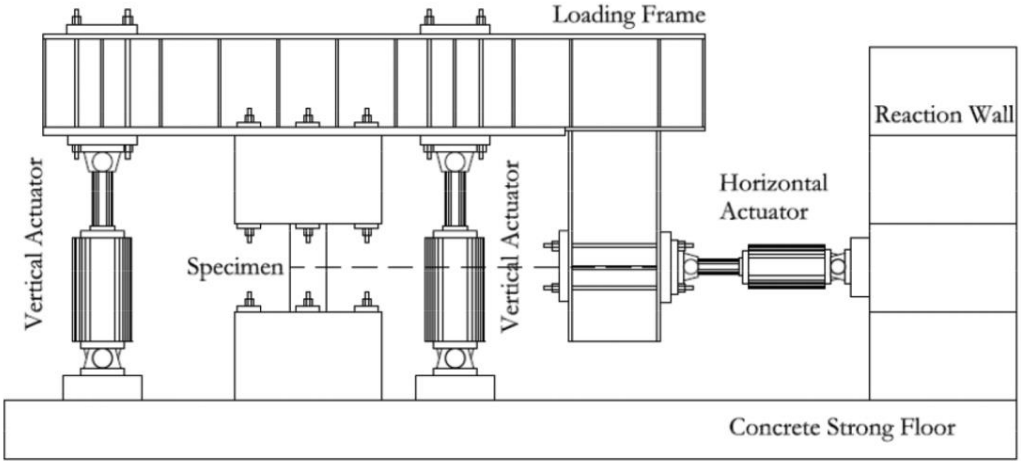

Figure 5.63 Link Beam Laboratory Test Setup

The link beam load protocol started with load-controlled approach and continues with displacement-controlled approach (Figure 5.64). Load controlled approach was thought according to yielding force through with 0.125, 0.25, 0.5, and 0.75 V_y where $V_y=2\ M_y/l_n$, respectively (Figure 5.64). The load-controlled protocol to capture yielding behavior continues with displacement-controlled protocol. In displacement controlled, percent chord rotation, where $\theta = \delta/l_n$ (δ: relative lateral displacement; l_n: beam clear span) was taken into account (Figure 5.64).

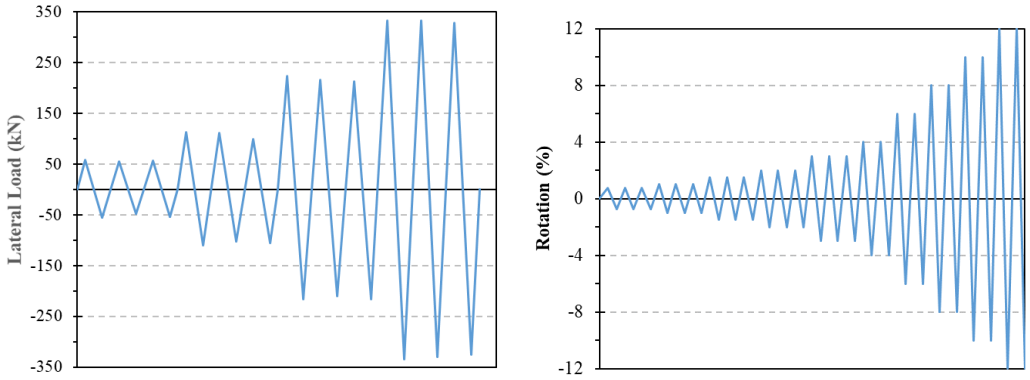

Figure 5.64 Loading protocol of link beam test, a) Load-controlled (kN) b) Displacement-controlled

Load-deformation response curves for diagonally-detailed, CB33F, and conventionally straight detailed, FB33, link beams are shown in Figure 5.65 and Figure 5.66, respectively. Firstly, it is seen that energy absorbing area of CB33F link beam is larger than FB33 and also FB33 exhibits more pinching behavior according to CB33F. Approximately both beams start to yield at a rotation of %1 chord rotation, while strength degradation starts at approximately 7-8% rotation for CB33F beam and 4-5% rotation for FB33 beam. Flexural, shear and slip-extension cracks at beam wall face contribute to the deformation failure mode in link beam. But the most effective is the slip-extension at beam face. In addition, as the beam rotation deformation increases, slip-extension deformation activity increases (Naish et al., 2013a).

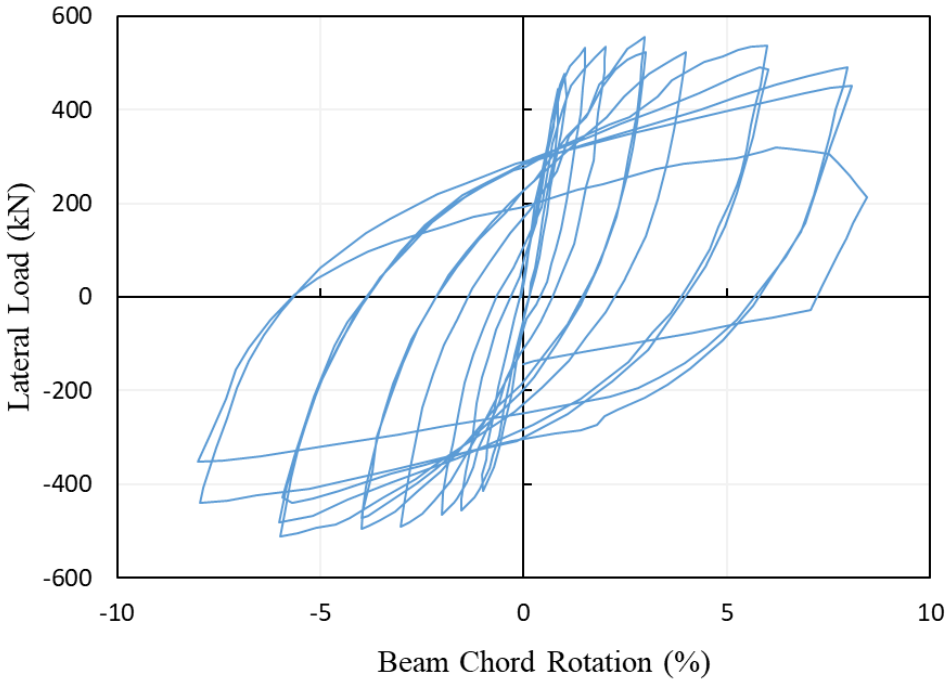

Figure 5.65 Link Beam, **CB33F**, Load Deformation Response

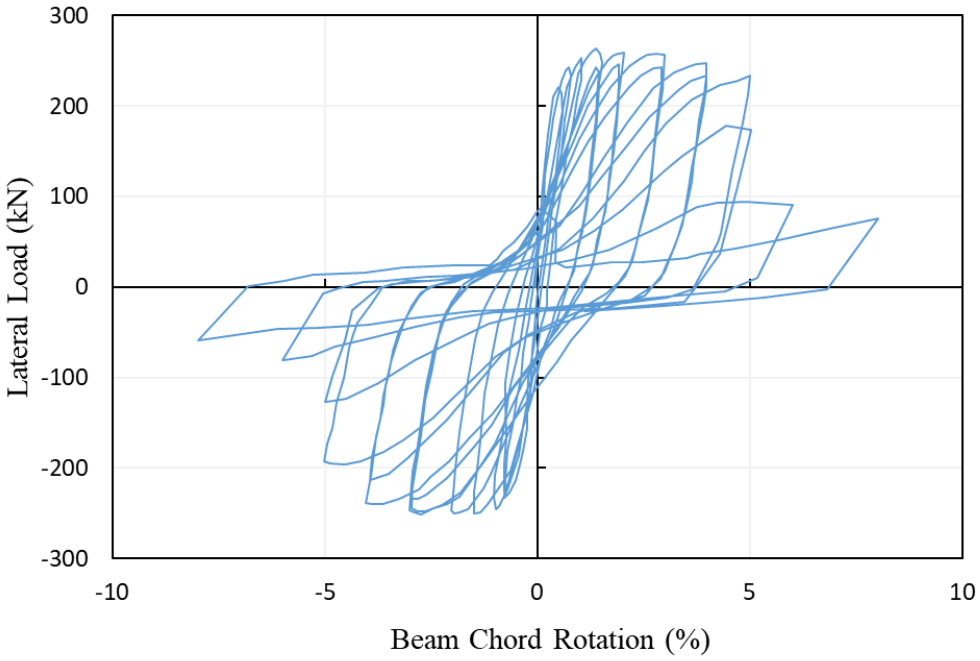

Figure 5.66 Link Beam, **FB33**, Load Deformation Response

5.2.2 Simulation of Link Beam Test Samples at Perform 3D V 7.0

5.2.2.1 General Views of Link Beam Perform 3D Models

Frame elements were used in the modeling of link beams with Perform 3D program. The link beam model was formed by combining the cross-section and inelastic component definitions in the component properties section in the "Frame member compound component" section at P3D. The P3D component joining approach can be done in 2 different ways. As the first approach, inelastic “moment rotation spring” can be assigned at the beam ends and cracked elastic beam section in the middle section. Secondly, inelastic “shear displacement hinge” component in the middle of the beam can be defined and remaining portions of beam will be cracked elastic portions (Figure 5.67).

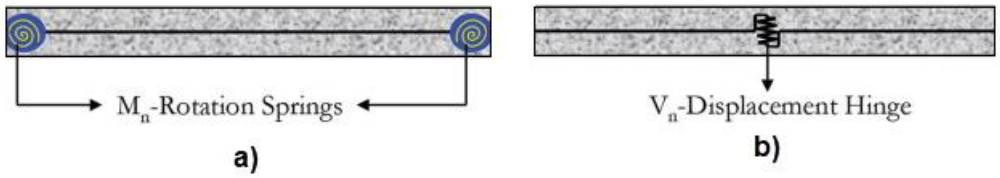

Figure 5.67 Two different Link beam Modeling Approaches: a) Moment Hinge Model b) Shear Hinge Model (Naish et al., 2013b)

It is appropriate to use a "Moment-hinge model" for conventionally reinforced link beams whose active behavior is flexure and is not under very high shear force. Modeling methods can be preferred for a link beam that is under high shear force detailed with diagonal reinforcements. So, for CB33F link beam from selected experimental samples, it is modeled in the P3D program with both modeling approaches, i.e., “Moment-hinge Model” and “Shear-hinge Model” and the relevant results were observed. On the other hand, for FB33 test sample beam detailed with conventional reinforcement, only the "Moment-hinge model" approach was used.

"Section Stiffness" and "Material Stiffness" properties were defined through the cross-section definition of beam sections. In addition, the effective stiffness ratio was

set to 0.15 E_cI_g. An effective stiffness ratio of 0.15 in link beams is the most appropriate choice (Naish et al., 2013b). According to this coefficient, the moment of inertia has been reduced.

Inelastic hinge behavior definitions in link beam can be created with the modules "Moment Hinge, Rotation Type" and "Shear Hinge, Displacement Type" at P3D. After cracked elastic beam section and inelastic hinge portions of link beam frame element were defined, these components were merged as a "compound component" at P3D according to two modeling methods mentioned earlier. After the appropriate combination of cross-section and inelastic components, modeling was completed with definition of link beam frame element before loading. Loading assignments were made according to specified loading protocol (Figure 5.64) and the results were evaluated.

5.2.2.2 P3D Model Parameters and Their Effects on Cyclic Response of Link Beams

It is important to correctly define inelastic hinge sections of link beams. CB33F diagonal link beam and FB33 conventional link beam were defined with the use of "Moment hinge, Rotation Type" and "Shear Hinge, Displacement Type" modules in the inelastic hinge sections.

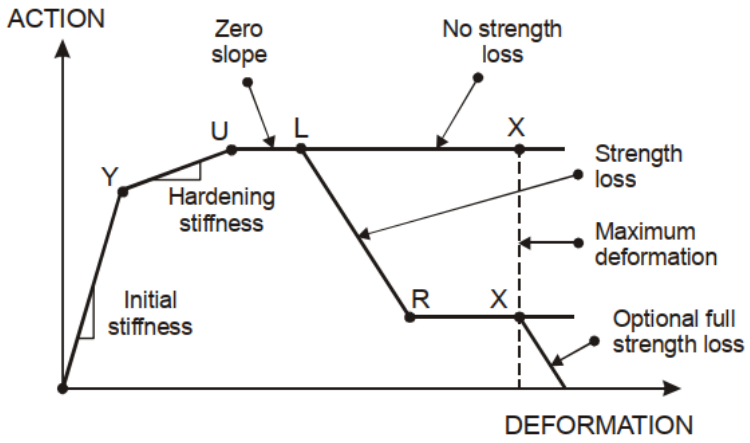

Figure 5.68 Perform 3D Hysteretic Loop Model(Computers and Structures, 2006)

As it can be remembered from the typical backbone curve definitions in Figure 5.68, the input values in the presented tables should be evaluated according to this figure. The action vs. deformation curves inputs for the module "Moment hinge, Rotation Type" and "Shear Hinge, Displacement Type" are in the form of moment (N.mm) vs. rotation (%) and shear Force (N) vs displacement (mm), respectively. However, all cyclic response comparison results of link beams are in the form of lateral load (kN) vs. beam chord rotation (%).

The most important parameters in the definition of link beam inelastic sections are yield and residual strength capacities, yielding (Y), ductile (L) and residual deformation limits. In addition to the correct definition of these parameters, assigning true cyclic degradation factor value correctly can have the most impact on cyclic response result. With the correct value of the cyclic degradation factor, the energy damping area and amount in the beam are adjusted. Although the effect of the stiffness degradation factor on the cyclic response result is not as much as the cyclic degradation factor, it is another parameter to be considered. According to the modeling approaches, the results of the cyclic response for diagonal and conventional link beam are presented with graphs in which the effect of each parameter is observed.

a) Calibration Work of "CB33F" (Diagonally Detailed Link Beam) with Shear Hinge Model Approach

Diagonal link beam "CB33F" was modeled with the shear hinge model approach in Perform-3D program. The reference model was created with appropriate, predicted input parameter values. Reference model and experimental cyclic response result comparison for the "CB33F" link beam is given in Figure 5.69. New model trials were created by changing the parameters over the reference model. With these new model trials, effect of the parameters was observed by comparing results of the cyclic response of the experiment. Descriptions of the new model trials were provided in Table 5.15.

In shear hinge model approach in diagonal link beams, yield shear force strength was theoretically calculated with Equation 5.4 according to the Turkish Earthquake Regulation-2018.

$$V_{\mathrm{d}} = (2f_{\mathrm{yd}}\sin\gamma)\, A_{\mathrm{sd}} \quad \textbf{(5.4)}$$

The value calculated by Equation 5.4 was compatible with the test value specified in Table 5.14. In addition, yielding (DY), strength degradation (DL) and residual strength (DR) deformation limits were proposed for this experimental sample as 1.0%, 6.0% and 9.0% respectively ((Naish et al., 2013b). For the CB33F test link beam sample with a clear span of 1524 mm, according to these specified chord rotation values, yielding (DY), strength degradation (DL) and residual strength (DR) deformation limits according to the "shear hinge, displacement model" approach were 15 mm, 90 mm and 130 mm respectively.

Table 5.14 CB33F and FB33 Link Beams Experimental Strength and Deformation Limits (Naish et al., 2013a)

	$M_n^{+/-}$, kN.m	V@ M_n, kN	Vn (ACI), kN	V_{ave}, kN	V_y, kN	V_{max}, kN	δ_y, mm	δ_u, mm
CB33F	408.5	536	479.7	526.4	479.3	551.8	15.2	137.2
FB33	163.9	215	-	250.5	213	258.5	7.8	76.2

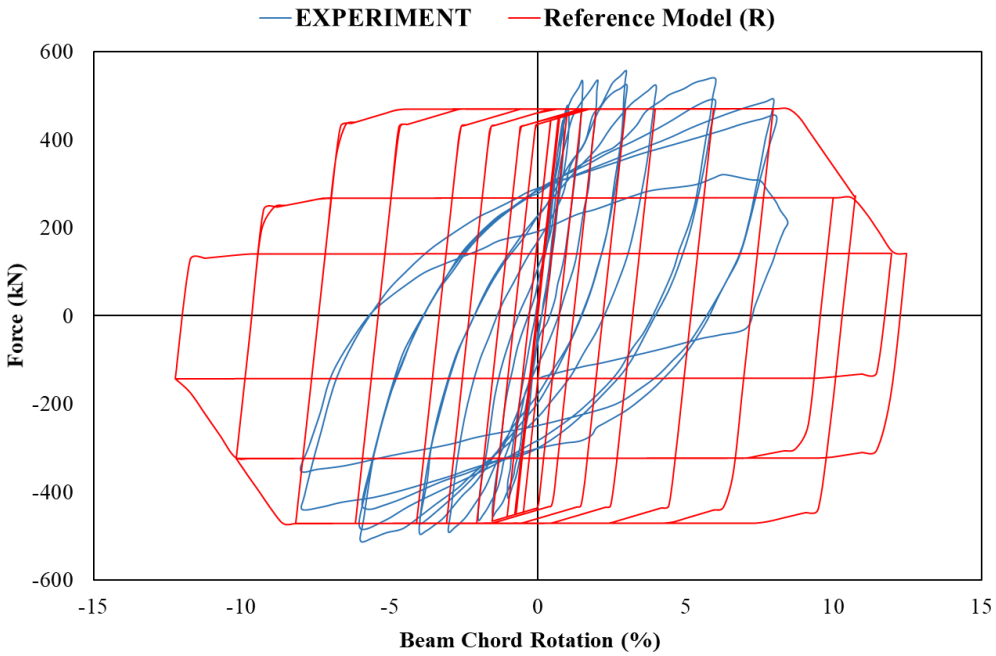

Figure 5.69 "CB33F Link Beam" Force-Deformation Response of Experiment and Reference P3D "Shear Hinge Model" (R)

Table 5.15 Model Trials Explanations Different from "CB33F" Reference Link Beam Shear Hinge Model

Model #	CHANGE FROM REFERENCE PD3 MODEL (R)	SENSITIVITY
R	Reference P3D Model	--
S-Model-1	Beam bending moment of inertia is taken as gross moment of inertia ($I=I_g$) instead of $I=0.15I_g$	High
S-Model-2	YULRX energy factors are used as Y:1 U:0.65 L:0.65 R:0.65 X:0.65	High
S-Model-3	Strength loss limits, DL and DR, are changed as 90 and 120 mm instead of 120 and 180 mm respectively.	High
S-Model-4	Strength loss limits, DL, DR and DX, are changed as 90, 120 and 130 mm instead of 120, 180 and 200 mm respectively.	High
S-Model-5	Strength loss limits, DL, DR and DX, are changed as 90, 120 and 130 mm instead of 120, 180 and 200 mm respectively. Also, YULRX energy factors are used as Y:1 U:0.65 L:0.65 R:0.65 X:0.65.	High

Each parameter change is indicated by the degree of impact in Table 5.15 together with a description. Each new model trial and reference model cyclic response result comparisons are given in Figure 5.70. According to these comparisons, strength and deformation assignments determine the limits for cyclic backbone curve. In addition, it can be easily determined from comparisons that the most important coefficient affecting the result is the energy degradation factor. If diagonal link beam is modeled with the shear hinge modeling approach, this value is determined to be 0.65. In addition, for the "CBF33" link beam, Table 5.16 provides that ideal model results are compared with reference model for each input parameter.

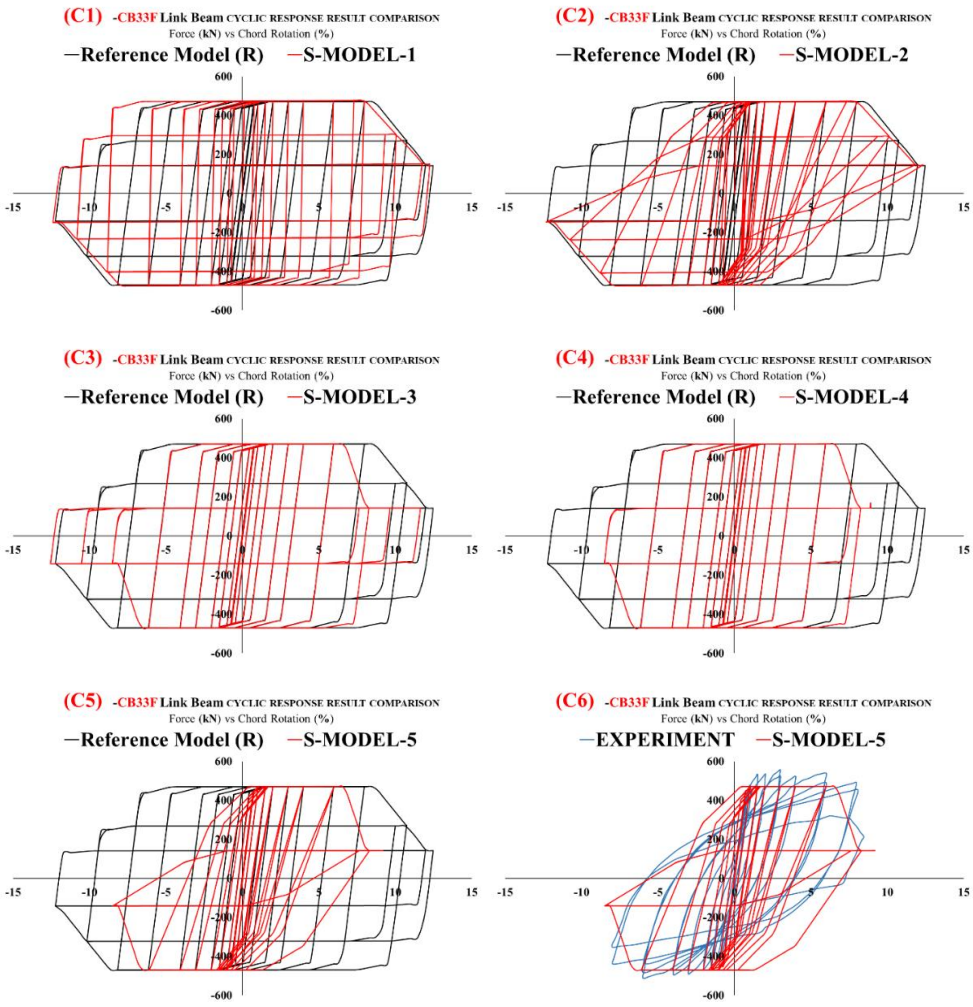

Figure 5.70 Cyclic Response Results Comparisons of P3D Model Trials for Diagonal Link Beam, **CB33F** with "**Shear Hinge, Displacement Type**" Module

Table 5.16 "CB33F" Link Beam "Shear Hinge Model" Input Parameters of Reference Model and Ideal Model

SHEAR HINGE, Displacement Type				Reference Model	Ideal Model
Material and Section Stiffness	**Mater.**	1	E (MPa)	3.26E+04	3.26E+04
		2	G (MPa)	1.36E+04	1.36E+04
	Section	3	Axial Area (mm^2)	139385	139385
		4	Shear Area (2)	0	0
		5	Shear Area (3)	0	0
		6	Bending Inertia-I_2 (mm^4)	1.62E+08	1.62E+08
		7	Bending Inertia-I_3 (mm^4)	3.64E+08	3.64E+08
		8	Torsional Inertia-J (mm^4)	2.73E+09	2.73E+09
Basic Relationship	**Pos.-Neg.**	9	FY (N)	450000	450000
		10	FU (N)	470000	470000
		11	DU (mm)	15	**15** (0.01 l_n)
		12	DX (mm)	200	**130** (0.09 l_n)
Strength Loss Deformations	**Pos.-Neg.**	13	DL (mm)	120	**90** (0.06 l_n)
		14	DR (mm)	180	**120** (0.08 l_n)
		15	FR/FU	0.3	0.3
	All	16	SLI	0	0
Cyclic Degradation	**Pos.-Neg.**	17	Y	-	**1**
		18	U	-	**0.65**
		19	L	-	**0.65**
		20	R	-	**0.65**
		21	X	-	**0.65**
		22	USF	0	0

SLI: Strength Loss Interaction; **USF:** Unloading Stiffness Factor; **Y:**Yielding; **U:**Ultimate; **L:**Ductile Limit; **R:**Residual Limit; **X:**Analysis Stop Limit

b) Calibration Work of “CB33F” (Diagonally Detailed Link Beam) with Moment Hinge Model Approach

CB33F diagonal link beam was also modelled with moment hinge assignment at both ends of link beam instead of modeling with the shear hinge model in the middle of the beam. According to this approach, firstly, reference model was generated with foreseen parameters. There were three different model trials that were changed separately from the reference model and the necessary definition explanations were made in Table 5.17. The calibration of the experimental sample cyclic response result with the "M-Model-3" trial results is ideal.

Table 5.17 Model Trials Explanations Different from “CB33F” Reference Link Beam Moment Hinge Model

Model #	CHANGE FROM REFERENCE (R)	SENSITIVITY
R	Reference P3D Model	--
M-Model-1	Rotation limits, DL, DR and DX, are changed as 0.06, 0.09 and 0.1 rad instead of 0.08, 0.12 and 0.15 rad respectively.	High
M-Model-2	Rotation limits, DL, DR and DX, are changed as 0.06, 0.09 and 0.1 rad instead of 0.08, 0.12 and 0.15 rad respectively. Also, YULRX energy factors are used as Y:1 U:0.65 L:0.65 R:0.65 X:0.65.	High
M-Model-3	Rotation limits, DL, DR and DX, are changed as 0.06, 0.09 and 0.1 rad instead of 0.08, 0.12 and 0.15 rad respectively. Also, YULRX energy factors are used as Y:1 U:0.5 L:0.5 R:0.5 X:0.5.	High

Figure 5.71 shows cyclic response comparisons of reference models and trial models of CB33F test sample link beam. Backbone curve limit definitions in the moment hinge model approach are equivalent to values used in the shear hinge model approach. However, it is more appropriate to use 0.5 for “moment hinge” model approach instead of 0.65 used in the cyclic energy degradation factor "shear hinge" model approach. According to Pacific Engineering Research Center, YULRX cyclic degradation factors are recommended as 0.5, 0.45, 0.4, 0.35, 0.35 respectively for

shear hinge" model approach (Moehle et al., 2011). This value is almost compatible with our calibrated value. The ideal definition parameters and reference model parameter values are presented in Table 5.18.

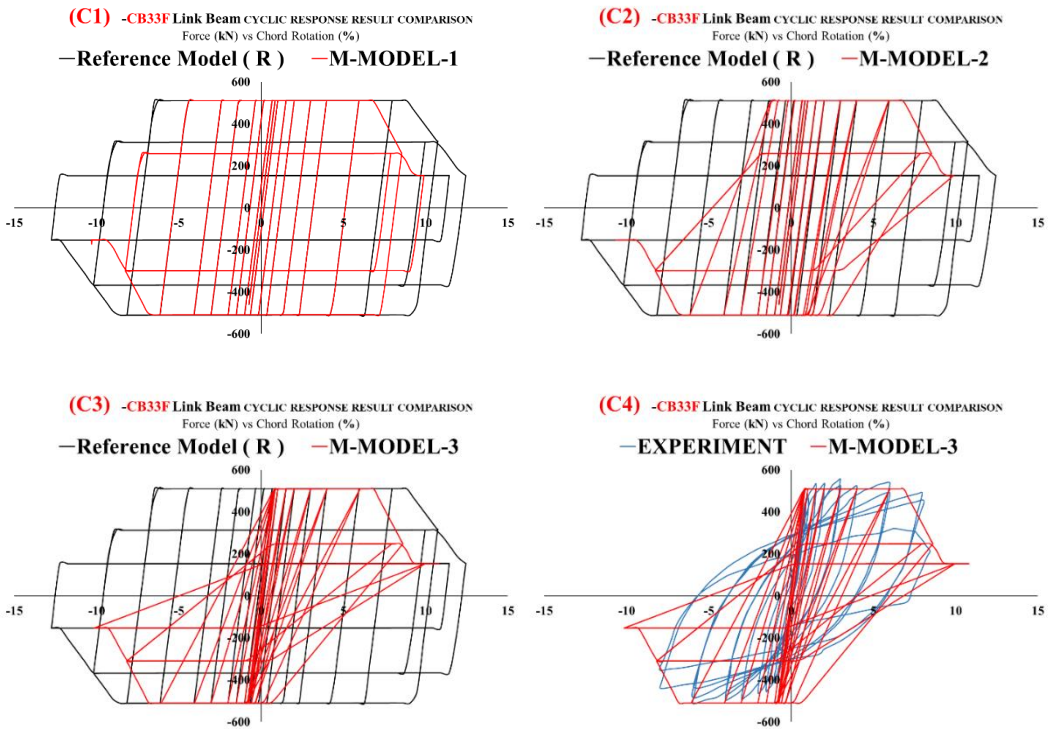

Figure 5.71 Cyclic Response Results Comparisons of P3D Model Trials for Diagonal Link Beam, **CB33F** with "**Moment Hinge, Rotation Type**" Module

Table 5.18 "CB33F" Link Beam "Moment Hinge Model" Input Parameters of Reference Model and Ideal Model

MOMENT HINGE, Displacement Type				Reference	Ideal
Material and Section Stiffness	**Mater.**	1	E (MPa)	3.26E+04	3.26E+04
		2	G (MPa)	1.36E+04	1.36E+04
	Section	3	Axial Area (mm^2)	139385	139385
		4	Shear Area (2)	0	0
		5	Shear Area (3)	0	0
		6	Bending Inertia-I_2 (mm^4)	1.62E+08	1.62E+08
		7	Bending Inertia-I_3 (mm^4)	3.64E+08	3.64E+08
		8	Torsional Inertia-J (mm^4)	2.73E+09	2.73E+09
Basic Relationship	**Pos.-Neg.**	9	FY (N.mm)	-	-
		10	FU (N.mm)	3.89E+08 *(1)*	3.89E+08 *(1)*
		11	DU (rad)	-	-
		12	DX (rad)	0.15	**0.1**
Strength Loss Deformations	**Pos.-Neg.**	13	DL (rad)	0.08	**0.06**
		14	DR (rad)	0.12	**0.09**
		15	FR/FU	0.3	0.3
	All	16	SLI	0	0
Cyclic Degradation	**Pos.-Neg.**	17	Y	-	**0.5**
		18	U	-	**0.5**
		19	L	-	**0.5**
		20	R	-	**0.5**
		21	X	-	**0.5**
		22	USF	0	0

SLI: Strength Loss Interaction; **USF:** Unloading Stiffness Factor; **Y:**Yielding; **U:**Ultimate; **L:**Ductile Limit; **R:**Residual Limit; **X:**Analysis Stop Limit; *(1)* $M_u = V_y * l_n / 2$; $V_y = 2 f_y \sin\gamma A_s$

c) Calibration Work of "FB33" (Conventionally Detailed Link Beam) with Moment Hinge Model Approach

The conventional link beam "FB33" test specimen, where the shear force does not have a very dominant effect and the bending behavior is more dominant, should only be modeled with the moment hinge model approach. In this direction, the necessary modeling is made with moment hinge model approach in the P3D program. The comparison of the experimental cyclic response result with the reference model having first trial parameter assignments, is shown in Figure 5.72.

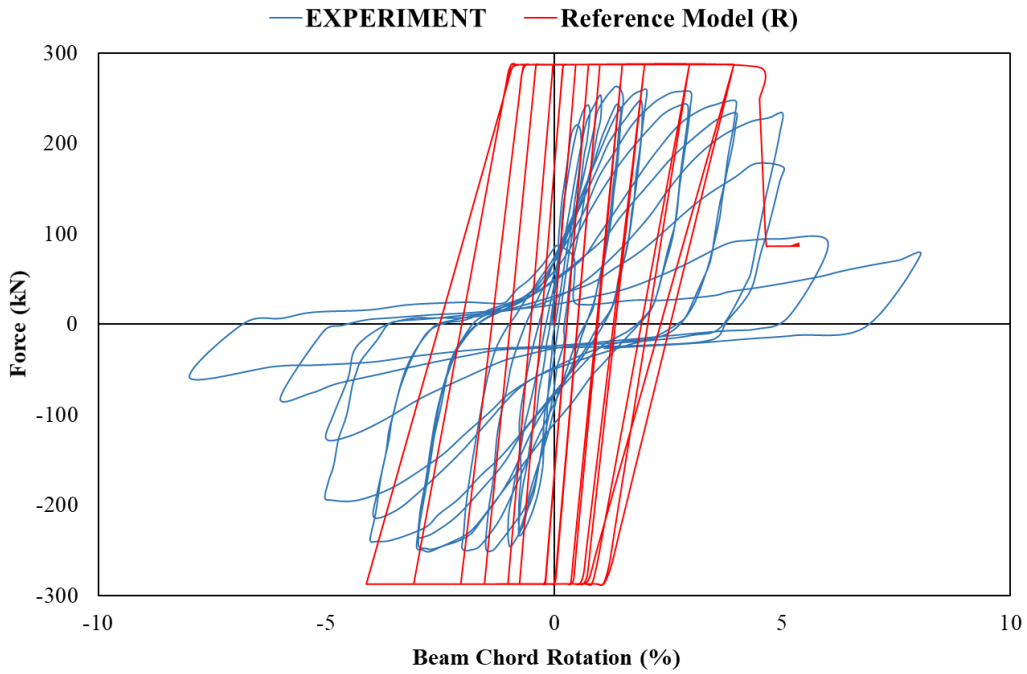

Figure 5.72 "FB33 Link Beam" Force-Deformation Response of Experiment and Reference P3D "Moment Hinge Model" (R)

Different P3D trial models have been created and descriptions related to trail models of which are given in Table 5.19. The cyclic response comparison results are given in Figure 5.73. The fitting between "F-Model-5" and "FB33" conventional link beam cyclic response result is obtained and thought as the most suitable calibrated work.

Table 5.19 Model Trials Explanations Different from "FB33" Reference Link Beam Moment Hinge Model

Model #	CHANGE FROM REFERENCE (R)	SENSITIVITY
R	Reference P3D Model	--
F-Model-1	Trilinear Shape of Force-rotation relationship is used instead of EPP (Elastic Perfectly Plastic) relationship. DU, DL, and FY are changed as 0.04 rad, 0.041 rad and 1.8E8 N.mm respectively.	High
F-Model-2	Trilinear Shape of Force-rotation relationship is used instead of EPP (Elastic Perfectly Plastic) relationship. DU, DL, DR, and DX are changed as 0.045, 0.047, 0.05 and 0.08 rad respectively. FY and FU are changed as 1.8E8 and 1.9E8 N.mm respectively. Also, YULRX energy factors are used as Y:0.3 U:0.25 L:0.23 R:0.22 X:0.2.	High
F-Model-3	All changed parameters are like F-Model-2. Only difference is that YULRX energy factors are used as Y:0.5 U:0.5 L:0.5 R:0.5 X:0.5.	High
F-Model-4	All changed parameters are like F-Model-2. Only difference is that Unloading Stiffness Factors (USF), "0.5" is used instead of "0".	High
F-Model-5	All changed parameters are like F-Model-2 Only difference is that Unloading Stiffness Factors (USF), "1.0" is used instead of "0".	High

DL and DR chord rotation definitions are to be between approximately 4.50-5.00%, when making conventional link beam backbone limit definitions (Naish et al., 2013b). These rotation values are suitable rotations obtained with a moment-curvature analysis with section properties in Table 5.20. Ultimate rotation limits can be easily obtained with the moment-curvature analysis, however to determine the correct value for energy degradation factor and unloading stiffness factor is the main subject for calibration work of conventionally detailed link beam with high aspect ratio. As a result, energy degradation factors should be recognized between 0.2-0.3, while unloading stiffness factor "USF" value is recommended to be "1.0". In terms of energy degradation factor, according to Pacific Engineering Research Center,

YULRX cyclic degradation factors are recommended as 0.24, 0.23, 0.22, 0.21, 0.2 respectively for frame beams (Moehle et al., 2011). These values are compatible with our calibrated value. In Figure 5.73, all model trial comparisons can be observed. In addition, in Table 5.20, the ideal model parameters compared with the reference model and the experimental results are presented.

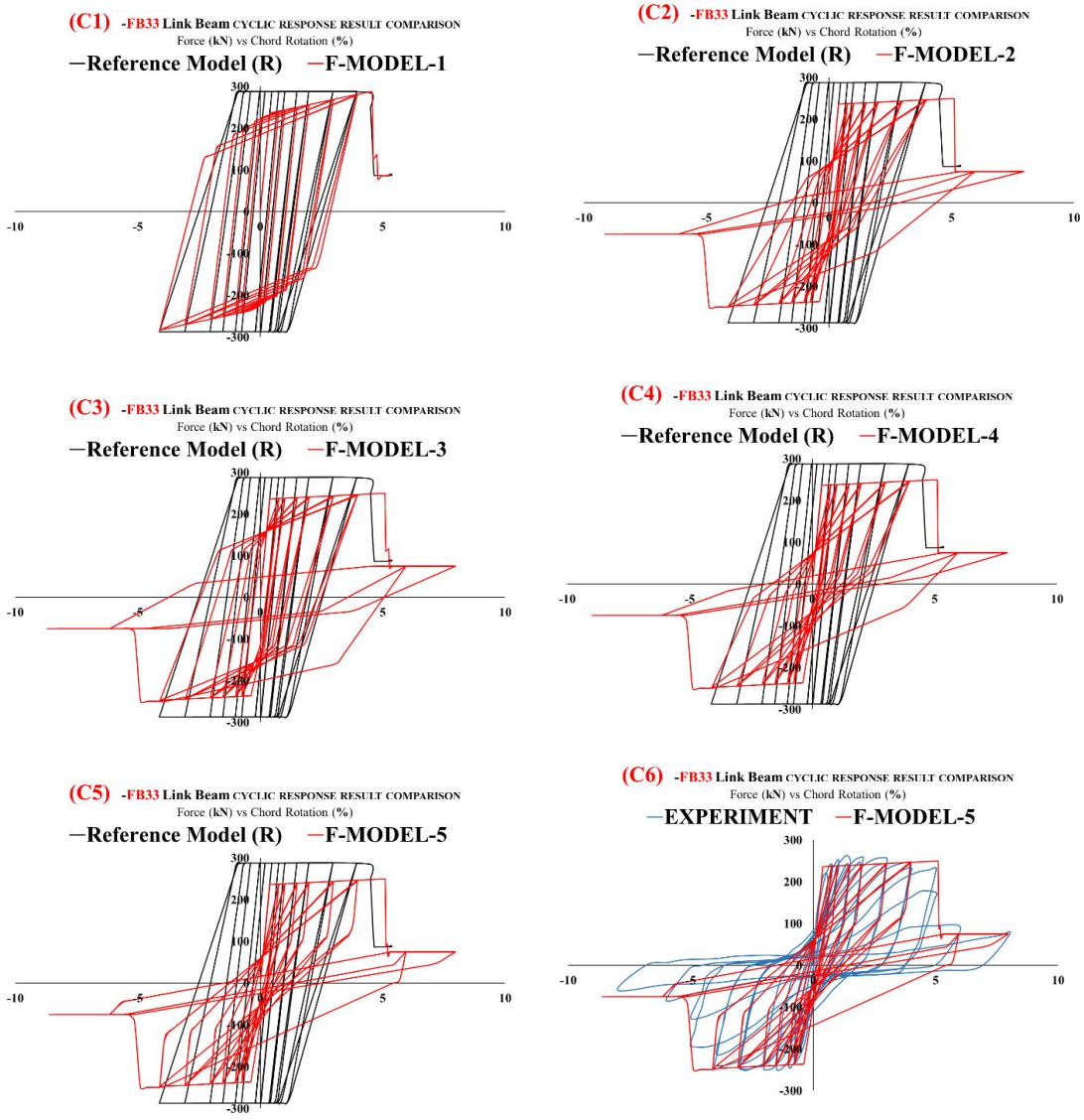

Figure 5.73 Cyclic Response Results Comparisons of P3D Model Trials for Conventional Link Beam, **FB33** with "**Moment Hinge, Rotation Type**" Module

Table 5.20 "FB33" Link Beam "Moment Hinge Model" Input Parameters of Reference Model and Ideal Model

MOMENT HINGE, Displacement Type				Reference	Ideal
Material and Section Stiffness	**Mater.**	1	E (MPa)	3.26E+04	3.26E+04
		2	G (MPa)	1.36E+04	1.36E+04
	Section	3	Axial Area (mm^2)	550	550
		4	Shear Area (2)	0	0
		5	Shear Area (3)	0	0
		6	Bending Inertia-I_2 (mm^4)	1.62E+08	1.62E+08
		7	Bending Inertia-I_3 (mm^4)	3.64E+08	3.64E+08
		8	Torsional Inertia-J (mm^4)	2.73E+09	2.73E+09
Basic Relationship	**Pos.-Neg.**	9	FY (N.mm)	-	**1.80E+08**
		10	FU (N.mm)	2.19E+08	**1.90E+08**
		11	DU (rad)	-	**0.045**
		12	DX (rad)	0.05	**0.08**
Strength Loss Deformations	**Pos.-Neg.**	13	DL (rad)	0.04	**0.047**
		14	DR (rad)	0.045	**0.05**
		15	FR/FU	0.3	0.3
	All	16	SLI	0	0
Cyclic Degradation	**Pos.-Neg.**	17	Y	1	**0.3**
		18	U	-	**0.25**
		19	L	0.65	**0.2**
		20	R	0.65	**0.22**
		21	X	0.65	**0.2**
		22	USF	0	**1**

SLI: Strength Loss Interaction; **USF:** Unloading Stiffness Factor; **Y:**Yielding; **U:**Ultimate; **L:**Ductile Limit; **R:**Residual Limit; **X:**Analysis Stop Limit

5.2.2.3 Summary of Calibration Work for Link Beams

Calibration work were completed with experimental force-beam chord rotation hysterical curve of CB33F diagonal link beam and FB33 conventional link beam by modeling with the Perform-3D program. The modeling method and parameter inputs that will obtain similar results with the experimental results are also presented separately in advance. Figure 5.74, Figure 5.75 and Figure 5.76 displays calibrated work results for CB33F and FB33 link beam test samples.

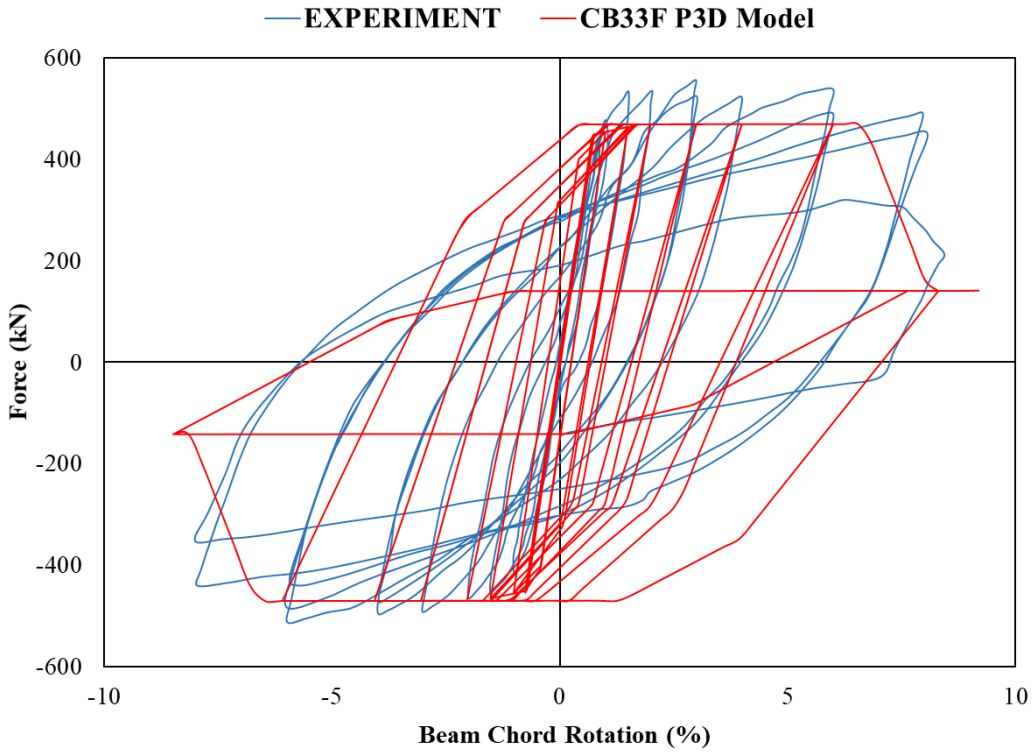

Figure 5.74 CB33F Link Beam Cyclic Response Calibration Work Result with Shear Hinge Approach

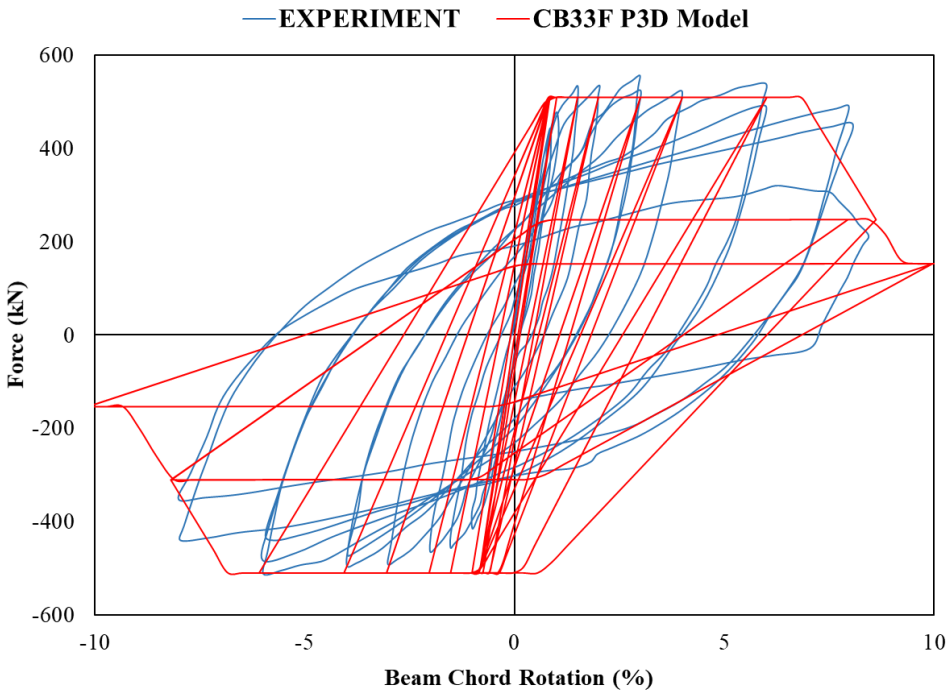

Figure 5.75 CB33F Link Beam Cyclic Response Calibration Work Result with Moment Hinge Approach

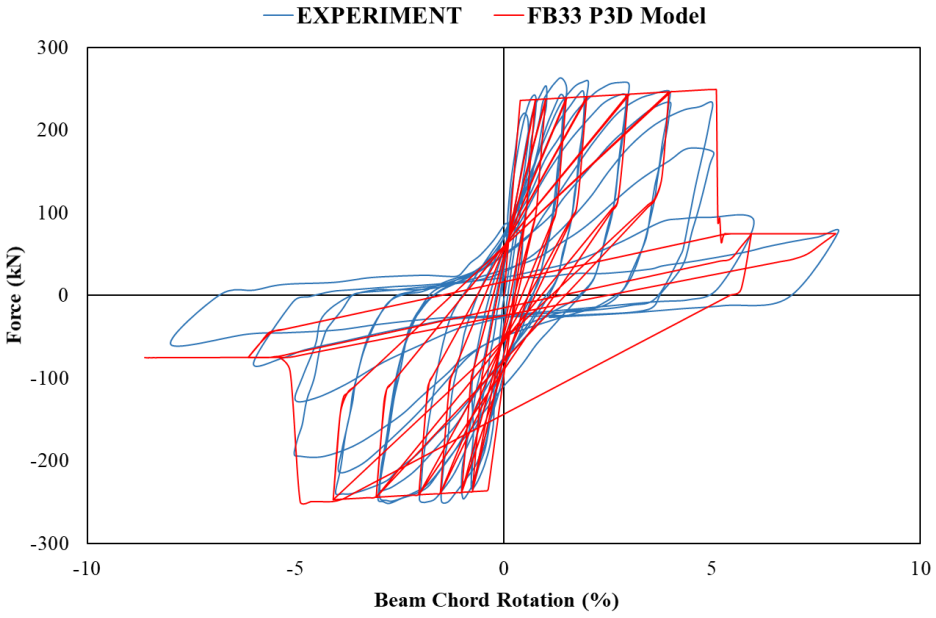

Figure 5.76 FB33 Link Beam Cyclic Response Calibration Work Result with Moment Hinge Approach

These calibration results are studies for experimental link beam samples reduced to 1/2 scale. Backbone deformation limits will vary for the exact beam scale. For this reason, a recommendation limits are established to be used in ACI 41-06 by editing deformation limits used as a result of the calibration study in the experimental samples (Naish et al., 2013b). According to the generalized force-deformation notation in Figure 5.77, recommendation limits for diagonally coupling beams are given in Table 5.21 according to shear force ratio and aspect ratio (l_n/h). However, the values of a, b and c for conventionally reinforced coupling should be calculated with moment-curvature analysis for section of link beam. For residual strength degradation ratio both diagonally reinforced and conventionally reinforced link beam, it is optimal to for a value of 0.3. As a result of the final evaluations, the proposal to define modeling in the Perform-3D program for coupling beams of 3D structures is given in Table 5.22.

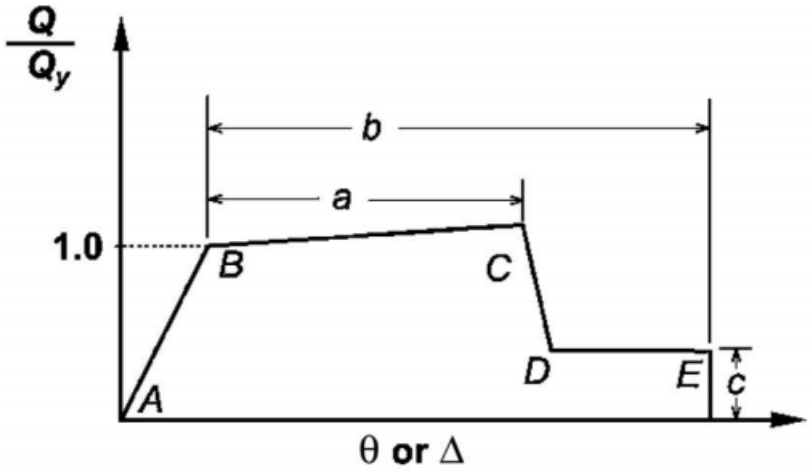

Figure 5.77 Generalized Force-Deformation Relation in ACI41-06 Code ("Seism. Eval. Retrofit Exist. Build.," 2017)

Table 5.21 Diagonally Reinforced Coupling Beam Proposed Deformation Limits in ACI41-06 Code ("Seism. Eval. Retrofit Exist. Build.," 2017)

Conditions		Plastic hinge rotation, rad		Residual strength ratio
l_n/h	$V/t_w l_w \sqrt{f_c'}$	a	b	c
≤2.0	≤6.0	0.045	0.065	0.30
≤2.0	≥8.0	0.035	0.055	0.30
≥3.0	≤6.0	0.050	0.070	0.30
≥3.0	≥8.0	0.045	0.065	0.30

Table 5.22 Summary P3D Input Parameters of Diagonally and Conventionally Reinforced Link Beam

				Diagonally Reinforced LB		Conventionally Reinforced LB
				SHA	**MHA**	**MHA**
Material and Section Stiffness	**Mater.**	1	E (Mpa)	E_c	E_c	E_c
		2	G (Mpa)	$0.4E_c$	$0.4E_c$	$0.4E_c$
		4	Shear Area (2)	0	0	0
		5	Shear Area (3)	0	0	0
		6	Bending Inertia-I_2	$0.15\ I_g$	$0.15\ I_g$	$0.15\ I_g$
		7	Bending Inertia-I_3	$0.15\ I_g$	$0.15\ I_g$	$0.15\ I_g$
Basic Relationship	**Pos.-Neg.**	9	FY	V_y	-	M_y
		10	FU	$1.05*V_y$	M_y[(1)]	$1.05*M_y$
		11	DU (rad)	$0.01^{(3)}\ l_n$	$0.01^{(3)}$	θ_U[(2)]
		12	DX (rad)	$0.09^{(3)}\ l_n$	$0.09^{(3)}$	θ_X[(2)]
Strength Loss	**Pos.-Neg.**	13	DL (rad)	$0.06^{(3)}\ l_n$	$0.06^{(3)}$	θ_L[(2)]
		14	DR (rad)	$0.08^{(3)}\ l_n$	$0.08^{(3)}$	θ_R[(2)]
		15	FR/FU	0,3	0,3	0,3
Cyclic Degradation	**Pos.-Neg.**	17	Y	1	0,5	0,3
		18	U	0,65	0,5	0,25
		19	L	0,65	0,5	0,22
		20	R	0,65	0,5	0,2
		21	X	0,65	0,5	0,2
		22	USF	0	0	1

USF: Unloading Stiffness Factor; **Y:**Yielding; **U:**Ultimate; **L:**Ductile Limit; **R:**Residual Limit; **X:**Analysis Stop Limit; **SHA:** Shear Hinge Approach; **MHA:** Moment Hinge Approach; **LB:** Link Beam; $\boldsymbol{V_y} = (2f_{yd}\sin\gamma)\ A_{sd}$**;**

(1) $\mathbf{M_y} = V_y * l_n / 2$; (2) θ: Calculated with Moment-Curvature Analysis; (3):It can be selected with Table 5.2

CHAPTER 6

PERFOMANCE BASED DESIGN OF THE CASE STUDY BUILDING

Performance based design of case study tall building that has been designed using linear elastic analysis method as described in Chapter 3. Reinforcement details and dimensions as a result of that design are preliminary requiring checks with PBD approach. In the nonlinear design check, CSI Perform 3D software is used. In Chapter 5, the structural walls and link beams models are calibrated using Perform 3D program to match the results of experimental cyclic response and strain profiles with model ones. Thus, how to model the structural walls and coupling beams by using Perform 3D software are studied in detail in Chapter 5. In this chapter, nonlinear performance analysis is performed for two different locations with low and high seismicity. Six different building models are created in this section. While the first and second of these model groups in each region have modeling requirements for wall and link beams created without model calibration, the third models are analyzed with calibrated parameters. In this way, it is possible to observe the extent to which the agreement with the results of calibration work affects the building response. In addition, it is observed to what extent the reinforcement and dimensions obtained by linear elastic design in low and high seismic areas, are affected with the performance-based design.

6.1 Performance Based Design Criteria

6.1.1 Design Earthquake Loads

The time history analysis method is used for case study building in terms of design earthquake load. According to the selected DD-2 level spectrum curves, preliminary design is conducted according to linear analysis requirements detailed in Chapter 3.

However, for the nonlinear performance analysis, time history earthquake data, matched with the DD-1 level spectrum curves as target spectrum curves, is used. DD2 level and DD-1 level spectrum curves are shown in Figure 6.1 for two different earthquake regions.

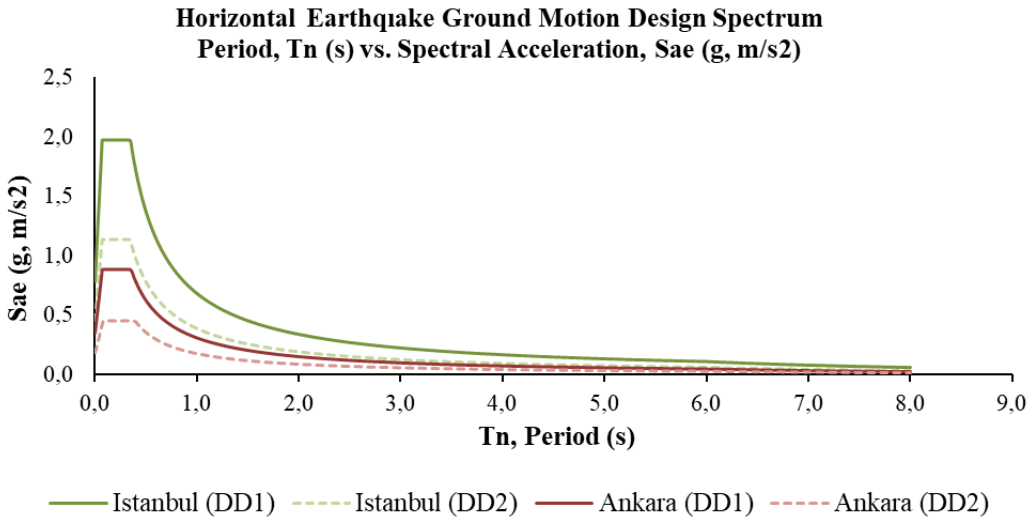

Figure 6.1 Design DD1 Level (Target Spectrum) and DD2 Level Response Spectrum Curves for Ankara and Istanbul

Seven earthquake records to be scaled are selected for the target spectrum curves (DD1 level) of both regions in Figure 6.1. Properties of selected scaled earthquake records for ZC soil class are shown in Table 6.1 & Table 6.2

Table 6.1 Selected Earthquake Records of Time History Analysis for Ankara

#	Earthquake Name	Year	Magnitude	Mechanism	V_{s30} (m/sec)	5-95% Duration (sec)	Arias Intensity (m/sec)
1	Loma Prieta	1989	6.93	Reverse Oblique	284.79	17.9	0.3
2	Landers	1992	7.28	strike slip	324.62	25.7	0.3
3	Duzce	1999	7.14	strike slip	481.0	15.5	0.2
4	Duzce	1999	7.14	strike slip	638.39	14.9	0.4
5	Landers	1992	7.28	strike slip	436.14	27.3	0.3
6	Darfield	2010	7.0	strike slip	204.0	20.0	1.1
7	Darfield	2010	7.0	strike slip	280.26	27.9	0.2

Table 6.2 Selected Earthquake Records of Time History Analysis for Istanbul

#	Earthquake Name	Year	Magnitude	Mechanism	V_{s30} (m/sec)	5-95% Duration (sec)	Arias Intensity (m/sec)
1	Kocaeli	1999	7.51	strike slip	386.75	34.3	1.0
2	Hector Mine	1999	7.13	strike slip	379.32	14.6	0.6
3	Landers	1992	7.28	strike slip	368.2	32.9	1.0
4	Tottori	2000	6.61	strike slip	616.55	9.9	0.4
5	Tottori	2000	6.61	strike slip	469.79	12.7	5.2
6	Tottori	2000	6.61	strike slip	420.2	11.1	2.9
7	Darfield	2010	7.0	strike slip	422.0	15.7	4.1

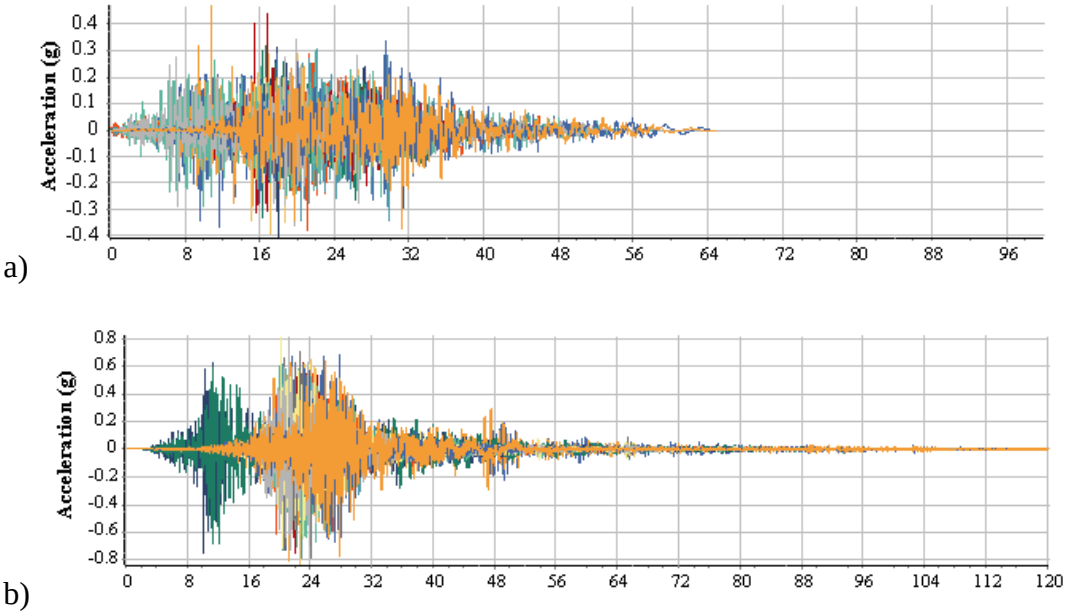

a)

b)

Figure 6.2 Scaled Time history Data Set a) for Ankara & b) for Istanbul

According to the target response spectra (DD1 level) in Figure 6.1, scaled time history records are obtained between 0.05-8 seconds (Figure 6.3). Scaled earthquake records for target spectrum curves for Ankara and Istanbul earthquake zones are shown in Figure 6.2.

a)

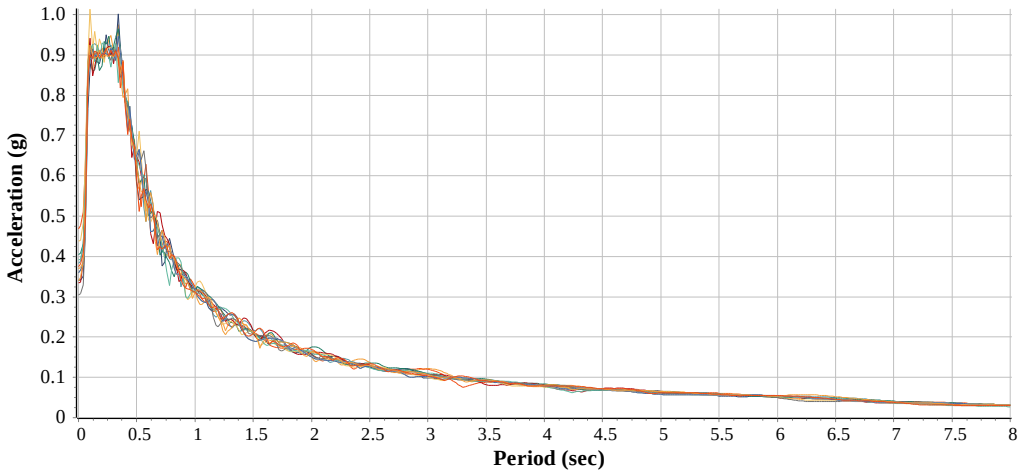

b)

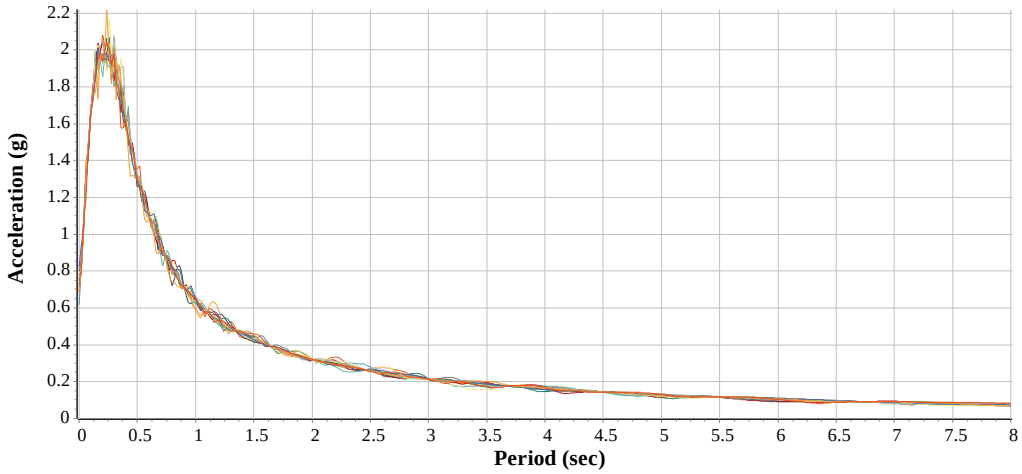

Figure 6.3 7 Matched EQ Spectrums for a) Ankara & for b) Istanbul

6.1.2 Some Design Criteria for the Case Study Building

- Earthquake design level for PBD is DD1 design level, i.e., peak ground acceleration (PGA) with an exceedance probability of %2 in 50 years and 2475 years return period.
- Structural performance level for case tall building for this earthquake design is collapse prevention (CP) in Ankara and in Istanbul respectively.

- Behaviors expected from structural elements in the performance-based design under DD1 level earthquake are shown in Table 6.3 for our case study tall building.

Table 6.3 Structural Members Actions and Behavior for Case Tall Building under DD1 Level Earthquake Design

	DEFORMATION CONTROLLED ACTION- Inelastic Behavior		
STRUCTURAL MEMBER	Under Moment	Under Shear Load	Under Axial Load
Shearwall	✓[1]	✗	✗
Frame Beam	✓[2]	✗	✗
Coupling Beam	✓	✓[3]	✗
	FORCED CONTROLLED ACTION- Elastic Behavior		
STRUCTURAL MEMBER	Under Moment	Under Shear Load	Under Axial Load
Shearwall	✗	✓	✓
Frame Beam	✗	✓	--
Coupling Beam	✗	✓[4]	--

[1] P-M-M yielding of wall base (on top of foundation or basement podiums), [2] Flexural yielding of beam ends, [3] Shear yielding of diagonally reinforced coupling beams, [4] Shear of conventionally reinforced coupling beams

- According to Turkish Earthquake Code-2018, damping ratio in high-rise buildings is taken as 2.5% for MCE_R (maximum considered earthquake), DD1 level.
- Used design characteristic and expected material properties are shown in Table 6.4.

Table 6.4 Design Expected Material Properties

Design Material	Characteristic Strength	Expected Strength
Concrete	f_{ck}=50 MPa	f_{ce}=65 MPa
Reinforcing Steel	f_{yk}=420 MPa	f_{ye}=504 MPa

6.2 Model of the Case Study Tall Building

Case study high-rise building was modeled with CSI Perform 3D program (Figure 6.4). In order to obtain the correct structural behavior, structure periods and mode shapes in linear analysis must be compatible with the model in nonlinear analysis. In this context, attention has been paid to mass definitions and modeling of building elements. Periods of case study building is shown in Figure 6.5. Case study building has core-wall connected by link beams in the middle and surrounded by perimeter columns. Tower has the first 4 floors of the basement and 28 floors above the basement, with flat slab system. Although all of the earthquake force is taken by core-wall and link beams in linear analysis, only the core-walls and link beams of the case study structure without slabs are not defined in nonlinear analysis. Tower perimeter columns and floors were included in the P3D model and a modeling close to the structure behavior in linear analysis was obtained. Flat slab was defined as effective beams on all floors (Figure 6.6 & Figure 6.8), while on the ground floor they were defined as shells only to observe the back stay effect (Figure 6.7). Effective frame beams for slabs and basement walls were modelled as elastic cracked members.

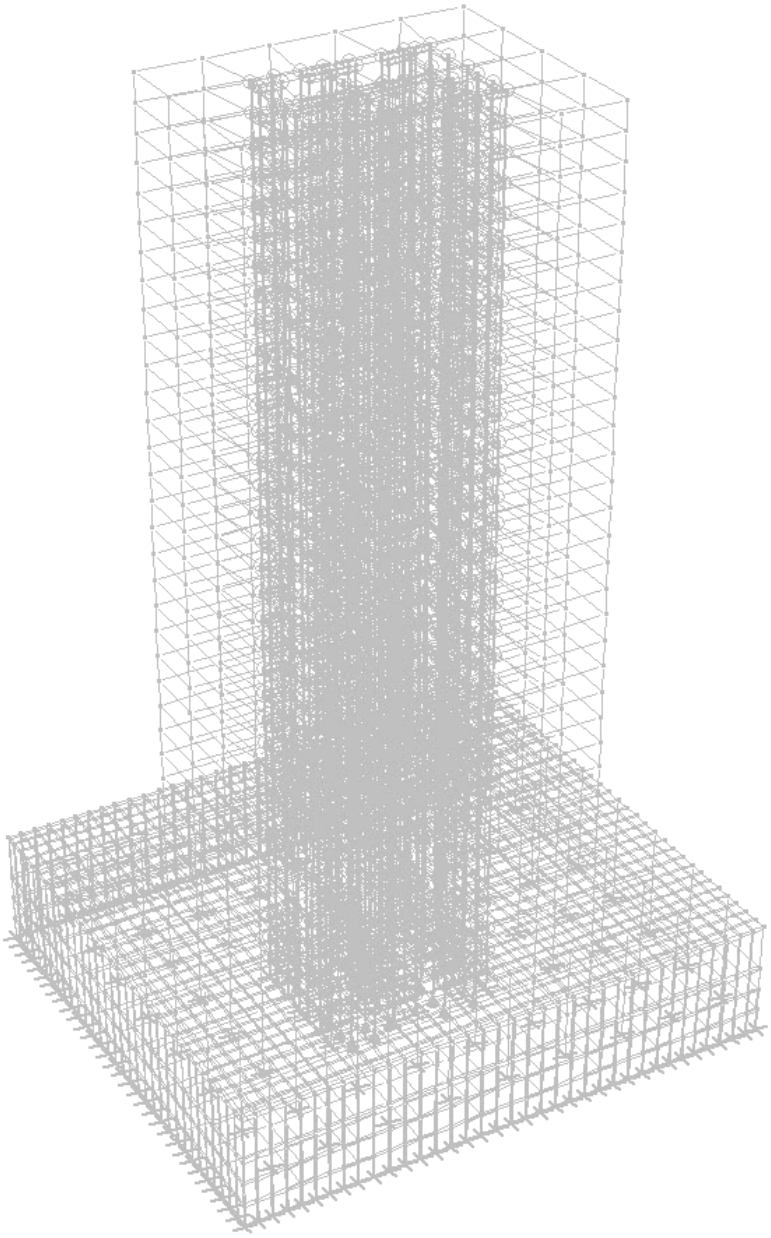

Figure 6.4 Nonlinear P3D Model of Case Study Tall Building

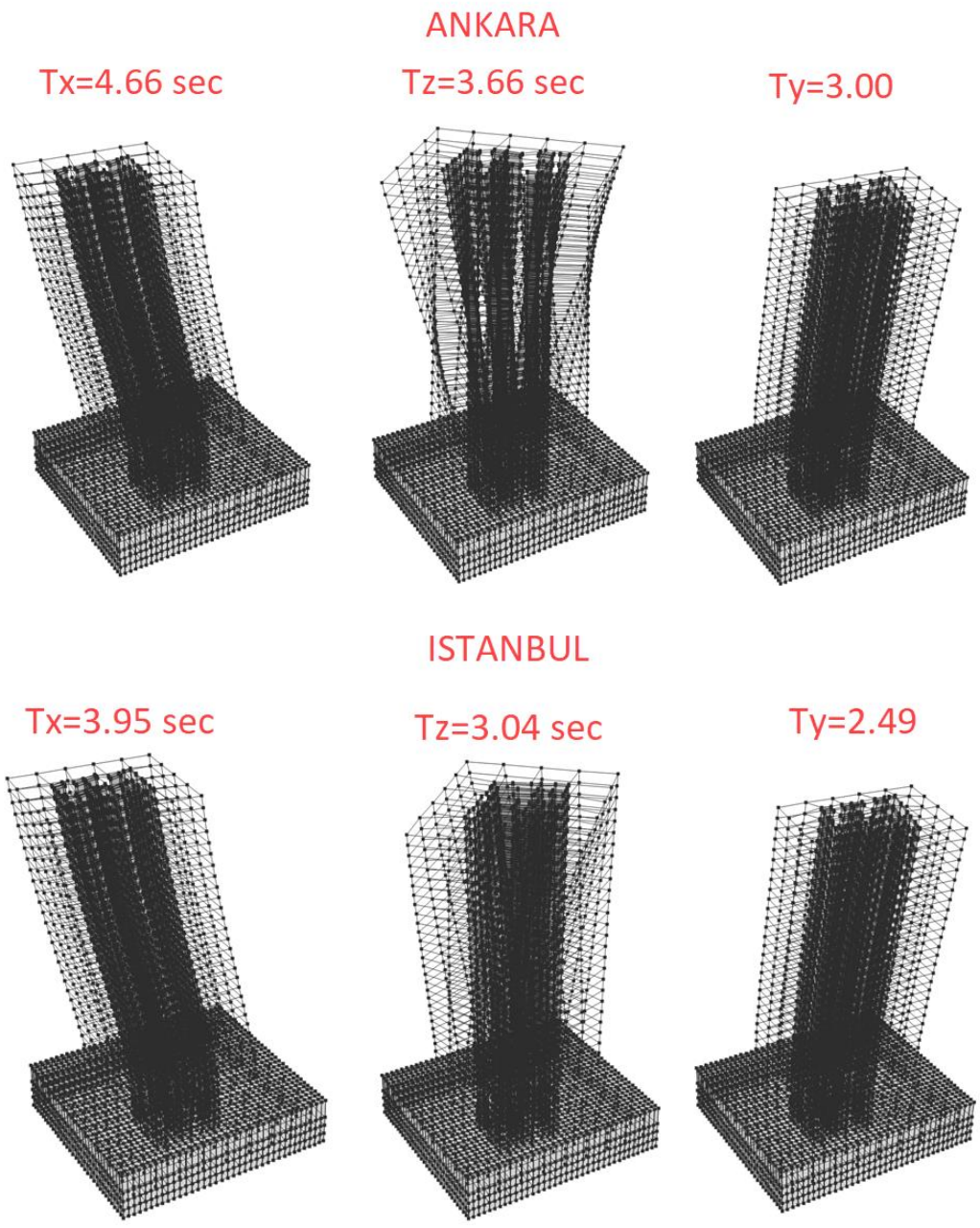

Figure 6.5 Periods of Case Study Building in Ankara & Istanbul at P3D

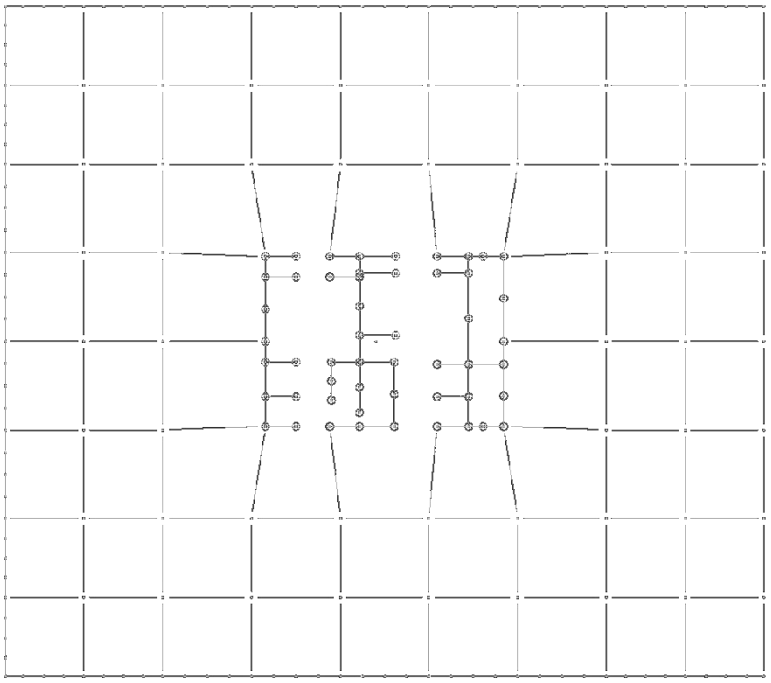

Figure 6.6 First Three Basement Floors Model with Effective Beams of Slab

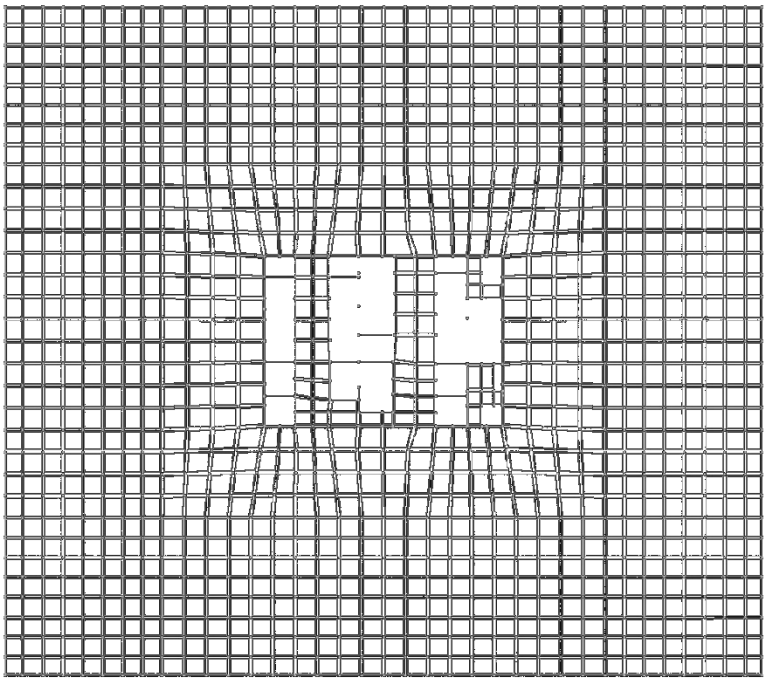

Figure 6.7 Ground Floor Plan Model with Shells of Slabs

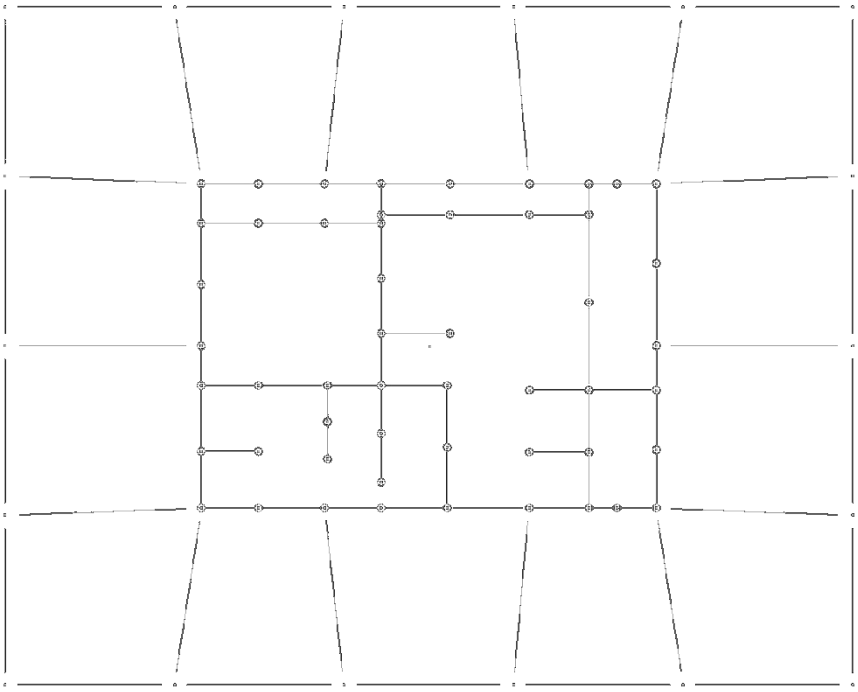

Figure 6.8 Typical Floor P3D Model Plan of the Case Study Tall Building

In the modeling of slabs, modeling was made according to rigid diaphragm acceptance with slaving module of P3D (Figure 6.9). The in-plane forces and displacements of transfer slab (4^{th} story) were taken into account by not being modeled as rigid diaphragm on the ground floor defined only in the shell. In addition, masses were defined in the mass center for all slabs (Figure 6.10).

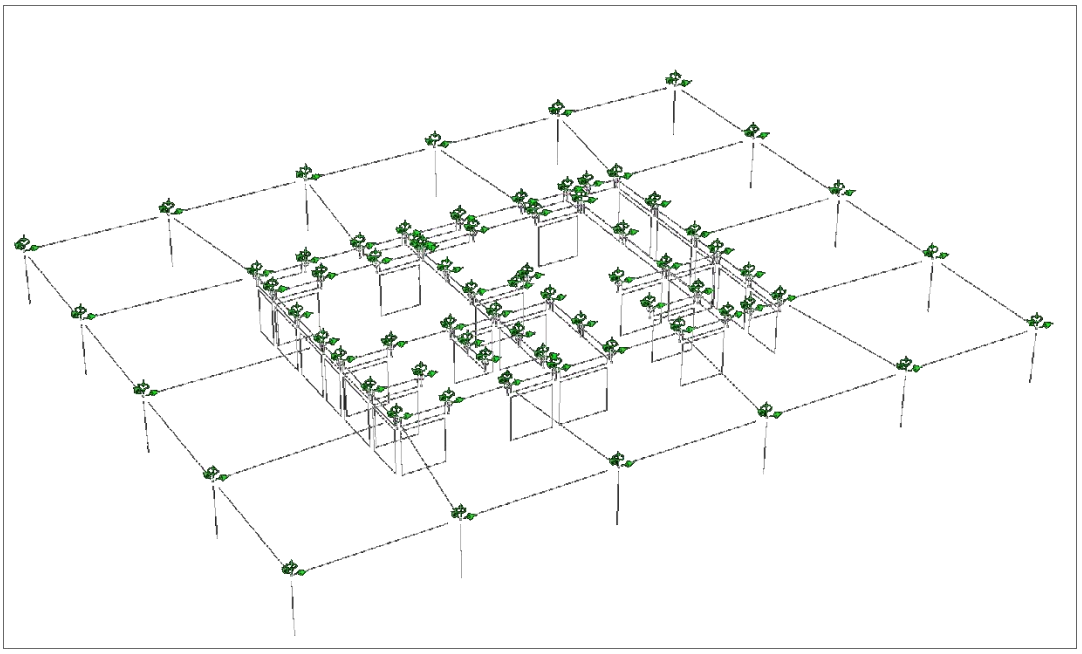

Figure 6.9 Rigid Diaphragms Assignment for Typical Floor of Case Building

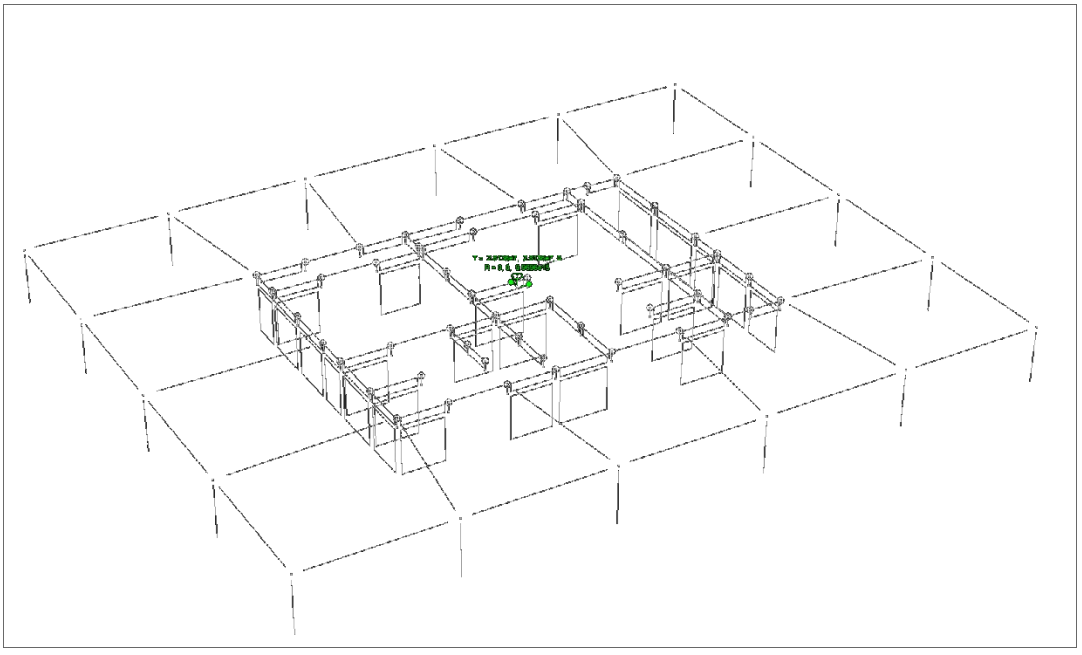

Figure 6.10 Mass Assignment at Mass Center for Typical Floor of Case Building

In the modeling of the case study building core-wall, the vertical fibers were defined according to the "fixed size" module approach of the P3D program. Accordingly,

concrete confined and unconfined areas and reinforcement areas were defined as fibers according to their coordinates. The wall boundary sections were modeled as reinforcement and concrete fiber partitions according to 0.5x1 or 1x1 mesh aspect ratio, while the wall web parts fibers were modeled as 2x1 aspect ratio (Figure 6.11). While the concrete and reinforcement fibers of the walls in the plan was modeled in the plan, the walls were divided at each story and the nodal points are created accordingly in the vertical direction (Figure 6.12). Taking into account the 60 cm depth of beams in the core-wall groups, horizontal and vertical embedded beams were defined to transfer the moments. For this reason, there has been an increase in vertical wall meshing. In the first basement floor (6.8 m height) under the ground floor, the first three floors (6.8 m and 3.8 m height) within the critical wall height, i.e., between basement-1 and 3th story in Figure 3.3, walls height were divided into two vertically. In the Perform 3D program, since the strain gages are defined only between the nodes, the vertical meshes also determine strain gage length automatically. Strain gage lengths were defined as full floor height except at the critical wall height and basement floors (excluding 1st basement floor, 6.8 m height), while within the critical wall height, strain gage lengths were defined as half of the floor height. These lengths are less than half of the length of the core-wall legs in the plan. Strain gages were laid out uniformly and properly in the plan to measure the strains in all boundaries and webs of core-walls. Strain gage positions are shown in Figure 6.13. Strain gage limits (Table 6.5) were defined according to TEC-2018 with expected concrete and steel strengths. In addition, according to TEC-2018, the limits created according to C50 and B420C characteristic material strength classes will be examined for the "Collapse Prevention (CP)" target design limit for the structures in Ankara and Istanbul respectively.

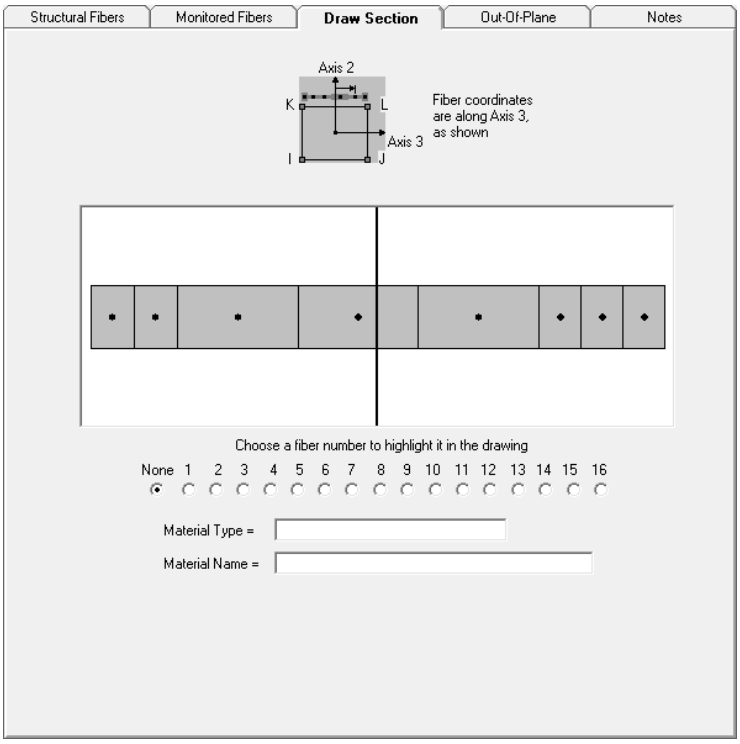

Figure 6.11 Core-wall Leg Fibers Aspect Ratio View

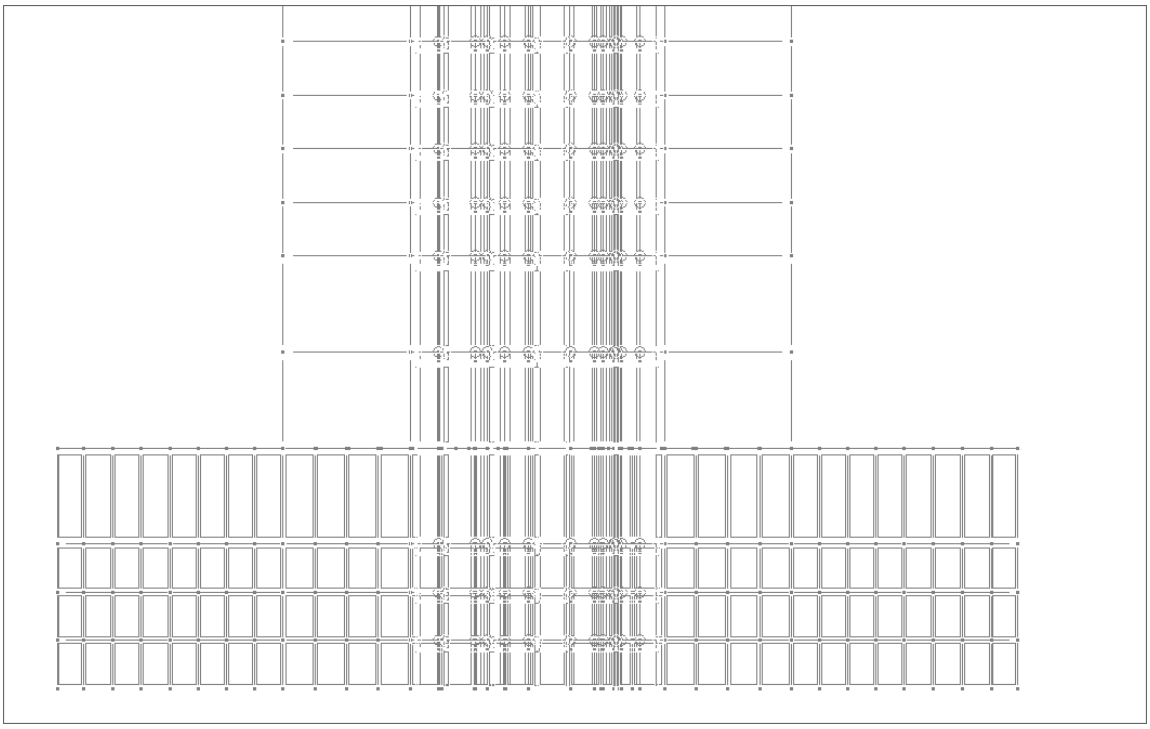

Figure 6.12 Wall Vertical Mesh View

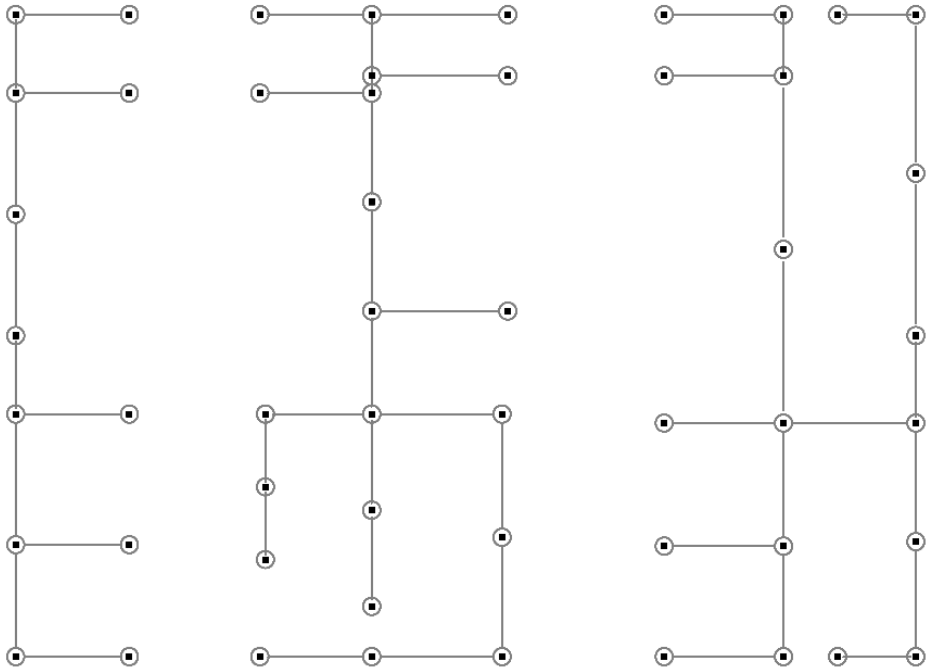

Figure 6.13 Core-wall Strain Gage Positions

Table 6.5 Defined Strain Gage Limits

		Compression Limits	
	Tension Limits	Unconfined Concrete Parts (for Web of Walls)	Confined Concrete Parts (for Boundary of Walls)
Operational (O)	0.005	0.00125	0.00125
Immediate Occupancy (IO)	0.0075	0.0025	0.0025
Life Safety (LS)	0.024	0.002625	0.0075
Collapse Prevention (CP)	0.032	0.0035	0.01

Wall reinforcement and concrete material definitions are conducted with the "Inelastic Steel Material, Non-Buckling" and "Inelastic 1D Concrete Material" modules, respectively (Figure 6.14 & Figure 6.15). In Chapter 5, it was observed that the reinforcement material parameters were very important in terms of the sensitivity

of response estimations. Accordingly, reinforcement yield strength, cyclic degradation factors and unloading stiffness factor parameters were determined as the most important sensitivity parameters. One of the main objectives of the case building study in this section is to observe the extent to which these highly sensitive parameters affect the nonlinear design results. For two locations with different seismicity, (i.e., Ankara and Istanbul), case study building nonlinear analysis was performed with the parameters obtained as a result of calibration (A3) and two different uncalibrated (A1-A2) alternatives and the performance analysis results were compared accordingly. The P3D parameter assignments of reinforcement and concrete material of wall for one calibrated and two non-calibrated alternatives are given in Table 6.6.

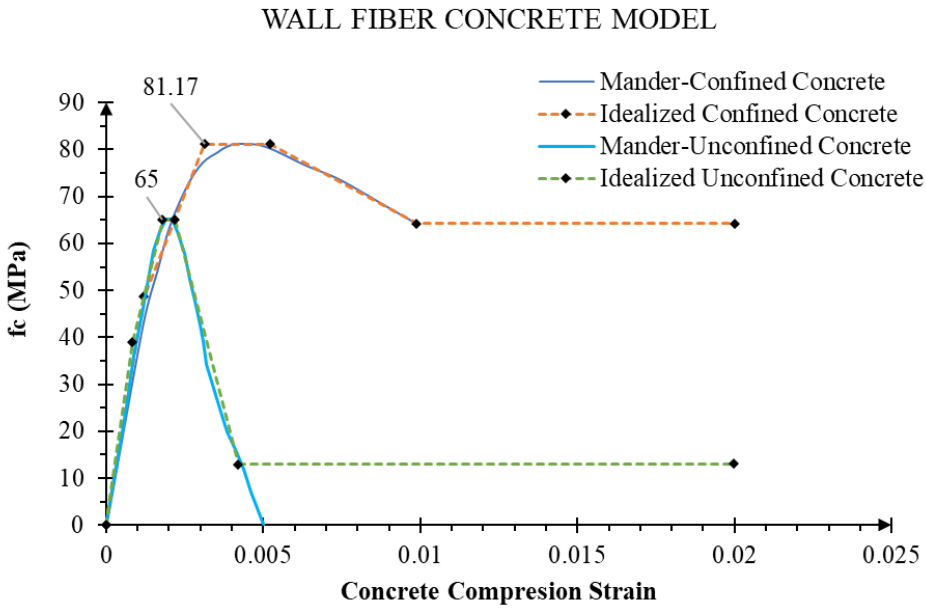

Figure 6.14 Concrete Material Model of Wall fibers

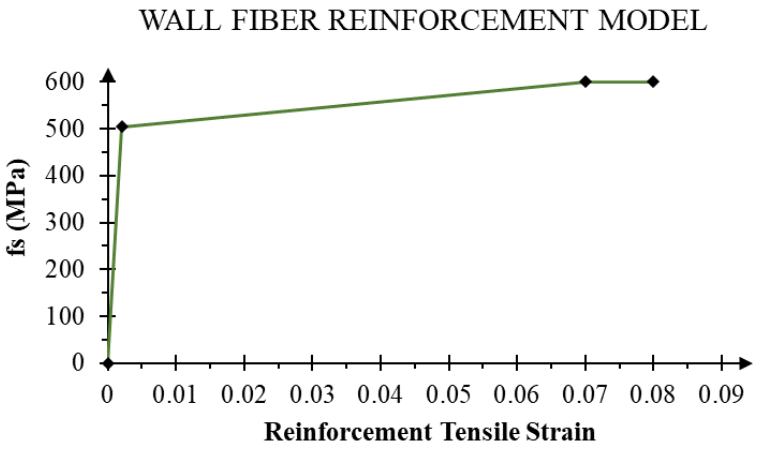

Figure 6.15 Reinforcement Material Model of Wall fibers

Table 6.6 Calibrated and Uncalibrated Concrete and Reinforcement Material Parameter Assignments of Core-walls

					MATERIALS						
					UNCALIBRATED				**CALIBRATED**		
					Rein. (A1)	**Rein. (A2)**	**Concrete**		**Rein. (A3)**	**CONCRETE**	
							Confined	**Unconfined**		**Confined**	**Unconfined**
Basic Relationship	All		1	E (Mpa)	2E+05	2E+05	40310	40310	2E+05	40310	40310
	Stresses	**Tens.**	2	FY (Mpa)	504	504	---	---	**440**	---	---
			3	FU (Mpa)	600	600	---	---	600	---	---
		Compr.	4	FY (Mpa)	504	504	45,4	39	504	45,4	39
			5	FU (Mpa)	600	600	75,7	65	600	75,7	65
	Strains	**Tens.**	6	DU	0,07	0,07	---	---	0,07	---	---
			7	DX	0,08	0,08	---	---	0,08	---	---
		Com	8	DU	0,07	0,07	0,003	0,0018	0,07	0,003	0,0018
			9	DX	0,08	0,08	0,02	0,02	0,08	0,02	0,02
Strength Loss	**Strains**	**Tension**	10	DL	---	---	---	---	---	---	---
			11	DR	---	---	---	---	---	---	---
			12	FR/FU	---	---	---	---	---	---	---
		Compr.	13	DL	---	---	0,0052	0,0022	---	0,0052	0,0022
			14	DR	---	---	0,01	0,0042	---	0,01	0,0042
			15	FR/FU	---	---	0,6	0,2	---	0,6	0,2
	All		16	TSLX	---	---	---	---	---	---	---
			17	SLI	---	---	---	---	---	---	---
Cyclic Degradation	Tension Strains **Energy**		18	Y	---	**0,35**	---	---	**0,65**	---	---
			19	U	---	**0,35**	---	---	**0,65**	---	---
			20	L	---	**0,35**	---	---	**0,65**	---	---
			21	R	---	**0,35**	---	---	**0,65**	---	---
			22	X	---	**0,35**	---	---	**0,65**	---	---
	Compr. Strains **Energy Factors**		23	Y	---	0,35	---	---	0,65	1	1
			24	U	---	0,35	---	---	0,65	0,4	0,4
			25	L	---	0,35	---	---	0,65	0,4	0,4
			26	R	---	0,35	---	---	0,65	0,1	0,1
			27	X	---	0,35	---	---	0,65	0,1	0,1
	All		28	USF	---	**1**	---	---	**-0,5**	---	---

TSLX: Total Strength Loss at Point X; **SLI:** Strength Loss Interaction; **USF:** Unloading Stiffness Factor; **Y:**Yielding; **U:**Ultimate; **L:**Ductile Limit; **R:**Residual Limit; **X:**Analysis Stop Limit

Three different reinforcement material parameters for walls are named as A1, A2 and A3 according to Table 6.5. A1 and A2 represent the uncalibrated material parameters. Cyclic degradation and unloading stiffness factors are not taken into

account in the A1 uncalibrated wall reinforcement material parameter assignment. According to the uncalibrated material parameter assignments A2, the cyclic degradation factors are approximately half of the values in calibrated parameters of A3.

The behavior under the out of plane and shear force was included as elastic in the modeling of walls. In the out of plane behavior, the rigidities of walls were reduced to one-fourth of the gross rigidity of the uncracked section according to TEC-2018.

Apart from the core-wall structural elements, the 60 cm deep beams between the core-wall groups and the 150 cm deep link beams were conveniently included in the models. For case study building in both Ankara and Istanbul, inelastic behavior modeling was carried out with the module "Moment Hinge, Rotation Type" at both ends of all frame beams with a height of 60 cm. For the 150 cm height conventional reinforced link beams, inelastic behavior modeling was performed with the "Moment Hinge, Rotation Type" module at both ends of the beam, while inelastic behavior modeling was performed at the middle of beam length with the "Shear Hinge, Displacement Type" module for the diagonally reinforced link beam at case study building in Istanbul. The remaining elastic sections, except for the moment and shear hinge sections of the beams, were reduced by calculating the effective cross-sectional rigidities according to Equation 6.1.

$$(EI)_e = \frac{M_y}{\theta_y}\frac{L_s}{3} \quad \textbf{(6.1)}$$

Calculated effective cross-sectional rigities after moment-curvature analysis according to beam sectional properties are given at Table 6.7 and Table 6.8 for case study building in Ankara and Istanbul respectively.

Table 6.7 Beam Effective Rigidity Properties of Case Study Building in Ankara

LABEL	L (mm)	M_y (kN.m)	d_b (mm)	φy (1/m)	L_s (mm)	θy	I (mm^4)	I_e (mm^4)	I_e/I
B40-60(1)	3500	485.4	22	0.00597	1750	0.00576	7.2E+09	1.22E+09	0.17
B40-60(2)	4200	485.4	22	0.00597	2100	0.00632	7.2E+09	1.33E+09	0.19
B40-150	1450	1969	25	0.00216	725	0.00668	1.13E+11	1.77E+09	0.02

Table 6.8 Beam Effective Rigidity Properties of Case Study Building in Istanbul

LABEL	L (mm)	M_y (kN.m)	d_b (mm)	ϕ_y (1/m)	L_s (mm)	θy	I (mm^4)	I_e (mm^4)	I_e/I
B40-60(1)	3500	874.9	30	0.00658	1750	0.00611	7.2E+09	2.07E+09	0.29
B40-60(2)	4200	874.9	30	0.00658	2100	0.00675	7.2E+09	2.25E+09	0.31
B60-60(1)	3500	1222	30	0.00655	1750	0.00609	1.08E+10	2.9E+09	0.27
B60-60(2)	4200	1222	30	0.00655	2100	0.00673	1.08E+10	3.15E+09	0.29
B60-150	1300	5083	30	0.00237	650	0.00721	1.69E+11	3.79E+09	0.02

Moment-curvature analysis were performed for all beams with the beam reinforcement details obtained according to the linear analysis design result. Accordingly, yielding, ultimate moment capacities and yielding and plastic rotation capacities of all beams were obtained (Figure 6.16 & Figure 6.27). The plastic rotational limits were determined according to Equation 6.2 at TEC-2018 (Table 6.9). Within all these information, the assigned values of the beam and link beam inelastic sections applicable to Ankara and Istanbul are shown in Table 6.10, Table 6.11 and Table 6.12. The rotational performance limits for the beams are shown in Table 6.9.

$$\theta_p{}^{CP} = \frac{2}{3}\left[(\phi_u - \phi_y)L_p\left(1 - \frac{0.5L_p}{L_s}\right) + 4.5\phi_u d_b\right] \quad \textbf{(6.2)}$$

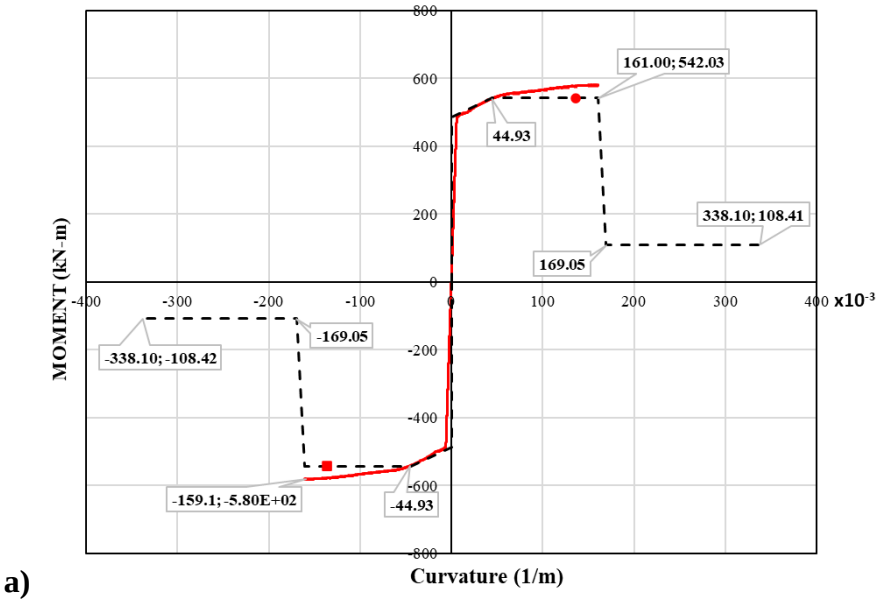

a)

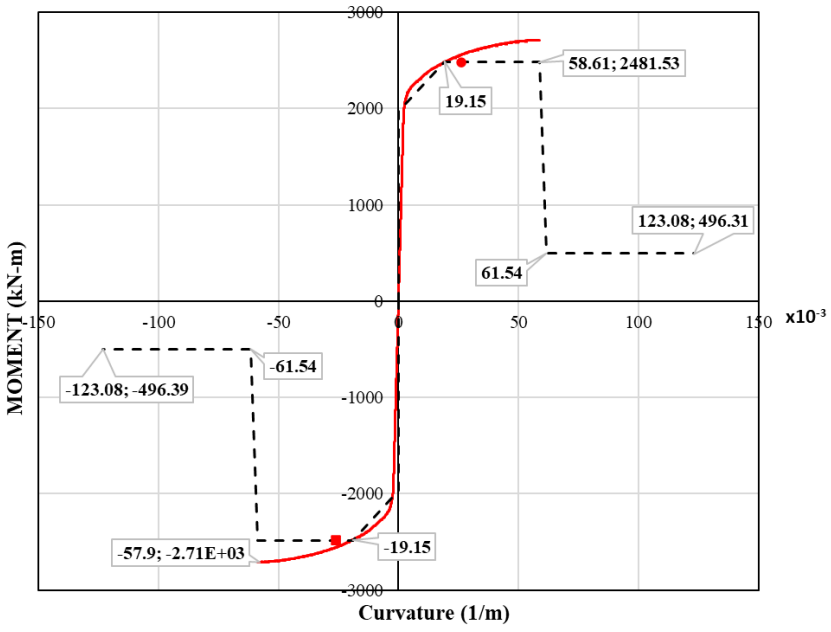

b)

Figure 6.16 Moment-Curvature Diagrams of Beams (**Ankara**) a) 40/60 Beams b) 40/150 Beams

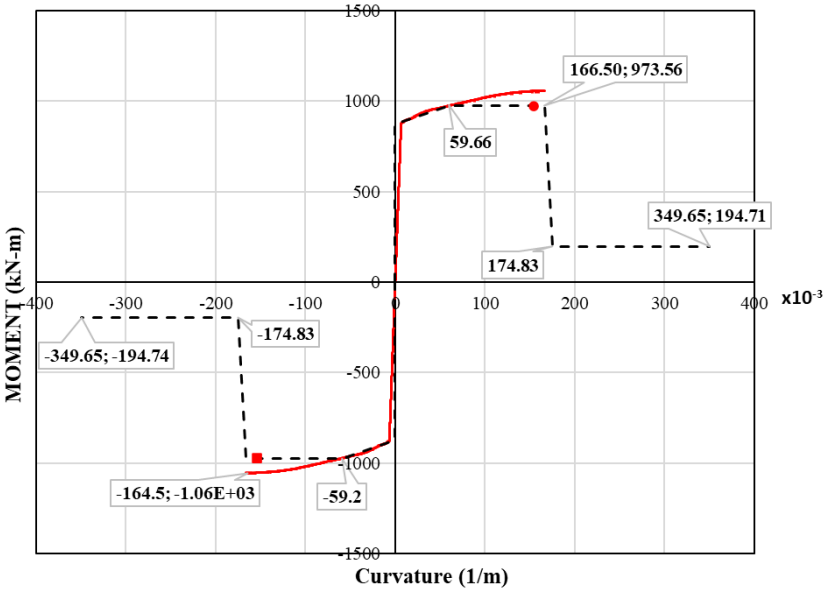

a)

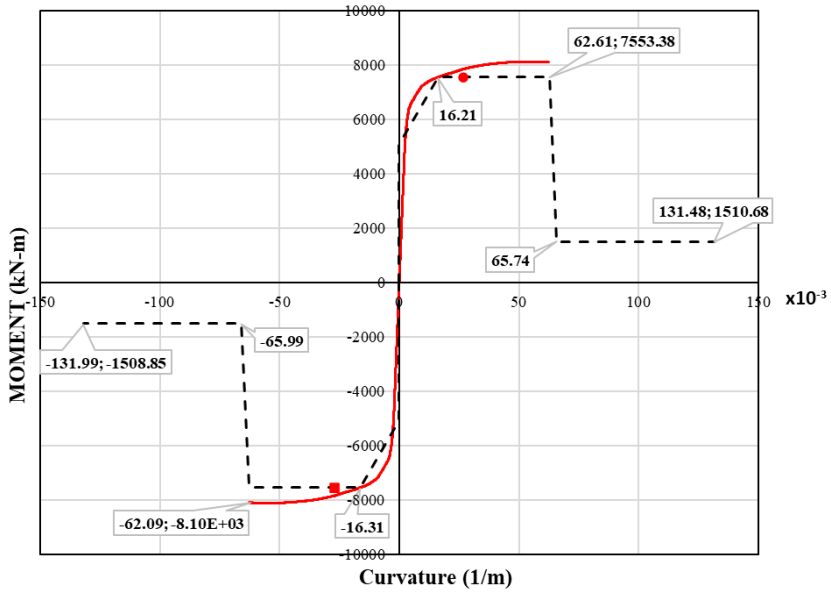

b)

Figure 6.17 Moment-Curvature Diagrams of Beams (**Istanbul**) a) 40/60 Beams b) 60/60 Beams

Table 6.9 Beam Rotation Limits

	BEAM	$\theta_{p,}^{CP}$
ANKARA	B40-60	0.041
	B40-150	0.020
ISTANBUL	B40-60	0.046
	B60-60	0.046
	B60-150	0.020

In the definitions in Table 6.10, Table 6.11 and Table 6.12, values for the beams are given for three different alternatives, i.e. A1, A2 and A3, in the calibrated and uncalibrated main headings as in the same wall modeling approach.

Table 6.10 Inelastic Component, "Moment Hinge, Rotation Type", Assigned Values of Beams for Building in Ankara for Calibrated and Uncalibrated Alternatives

MOMENT HINGE, Rotation Type				**IN ANKARA**					
				40/60 BEAM			**40/150 BEAM**		
(Trilinear Model)				**Uncalibrated**		**Calibrated**	**Uncalibrated**		**Calibrated**
				(A1)	**(A2)**	**(A3)**	**(A1)**	**(A2)**	**(A3)**
Basic Relationship	**Pos.-Neg.**	1	FY (kN.m)	485	485	485	1969	1969	1969
		2	FU (kN.m)	542	542	542	2482	2482	2482
		3	DU (rad)	0,0135	0,0135	0,0135	0,014	0,014	0,0144
		4	DX (rad)	0,1	0,1	0,1	0,1	0,1	0,1
Strength Loss Deformations	**Pos.-Neg.**	5	DL (rad)	0,048	0,048	0,048	0,044	0,044	0,044
		6	DR (rad)	0,051	0,051	0,051	0,046	0,046	0,046
		7	FR/FU	0,2	0,2	0,2	0,3	0,3	0,3
	All	8	SLI	0	0	0	0	0	0
Cyclic Degradation	**Pos.-Neg.**	9	Y	---	0,2	**0,3**	---	0,3	**0,5**
		10	U	---	0,2	**0,25**	---	0,25	**0,5**
		11	L	---	0,15	**0,22**	---	0,22	**0,5**
		12	R	---	0,15	**0,2**	---	0,2	**0,5**
		13	X	---	0,15	**0,2**	---	0,2	**0,5**
		14	USF	---	0,75	**1**	---	1	**0**

Table 6.11 Inelastic Component, "Moment Hinge, Rotation Type", Assigned Values of Beams for Building in Istanbul for Calibrated and Uncalibrated Alternatives

MOMENT HINGE, Rotation Type				**IN ISTANBUL**					
				40/60 BEAM			**60/60 BEAM**		
(Trilinear Model)				**Uncalibrated**		**Calibrated**	**Uncalibrated**		**Calibrated**
				(A1)	**(A2)**	**(A3)**	**(A1)**	**(A2)**	**(A3)**
Basic Relationship	**Pos.-Neg.**	1	FY (kN.m)	875	875	875	1358	1358	1358
		2	FU (kN.m)	974	974	974	1222	1222	1222
		3	DU (rad)	0,0178	0,0178	0,0178	0,017	0,017	0,0168
		4	DX (rad)	0,1	0,1	0,1	0,1	0,1	0,1
Strength Loss	**Pos.-Neg.**	5	DL (rad)	0,05	0,05	0,05	0,05	0,05	0,05
		6	DR (rad)	0,052	0,052	0,052	0,052	0,052	0,052
		7	FR/FU	0,2	0,2	0,2	0,2	0,2	0,2
	All	8	SLI	0	0	0	0	0	0
Cyclic Degradation	**Pos.-Neg.**	9	Y	---	0,2	**0,3**	---	0,3	**0,3**
		10	U	---	0,2	**0,25**	---	0,25	**0,25**
		11	L	---	0,15	**0,22**	---	0,22	**0,22**
		12	R	---	0,15	**0,2**	---	0,2	**0,2**
		13	X	---	0,15	**0,2**	---	0,2	**0,2**
		14	USF	---	0,75	**1**	---	1	**1**

Table 6.12 Inelastic Component, "Shear Hinge, Displacement Type", Assigned Values of Beams for Building in Istanbul for Calibrated and Uncalibrated Alternatives

Shear Hinge, Displacement Type				**IN ISTANBUL**		
				60/150 BEAM		
E-P-P (Elastic Perfectly Plastic)				**Uncalibrated**		**Calibrated**
				(A1)	**(A2)**	**(A3)**
Basic Relationship	**Pos.-Neg.**	1	FY (kN)	---	---	---
		2	FU (kN)	3844	3844	3844
		3	DU (mm)	---	---	---
		4	DX (mm)	180	180	180
Strength Loss	**Pos.-Neg.**	5	DL (mm)	78 *(0.06 l_n)*	78 *(0.06 l_n)*	78 *(0.06 l_n)*
		6	DR (mm)	130 *(0.1 l_n)*	130 *(0.1 l_n)*	130 *(0.1 l_n)*
		7	FR/FU	0,3	0,3	0,3
	All	8	SLI	0	0	0
Cyclic Degradation	**Pos.-Neg.**	9	Y	---	0,5	**1**
		10	U	---	0,3	**0,65**
		11	L	---	0,3	**0,65**
		12	R	---	0,3	**0,65**
		13	X	---	0,3	**0,65**

6.3 Performance Based Design Results of the Case Study Buildings

All performance-based design results for a total of 6 models are given with comparisons along with three alternatives, A1, A2 and A3, the parameters of which were given in the tables before in detail for the walls and beams for two different earthquake zones, i.e., Ankara and Istanbul.

Case study building has a flat plate system. In Figure 6.18 and Figure 6.19, the extent which structural members contribute to lateral resistance for Ankara and Istanbul buildings respectively. Accordingly, in all models, results are compatible with linear analysis and walls meet shear forces of 90% and columns share a level of 10%.

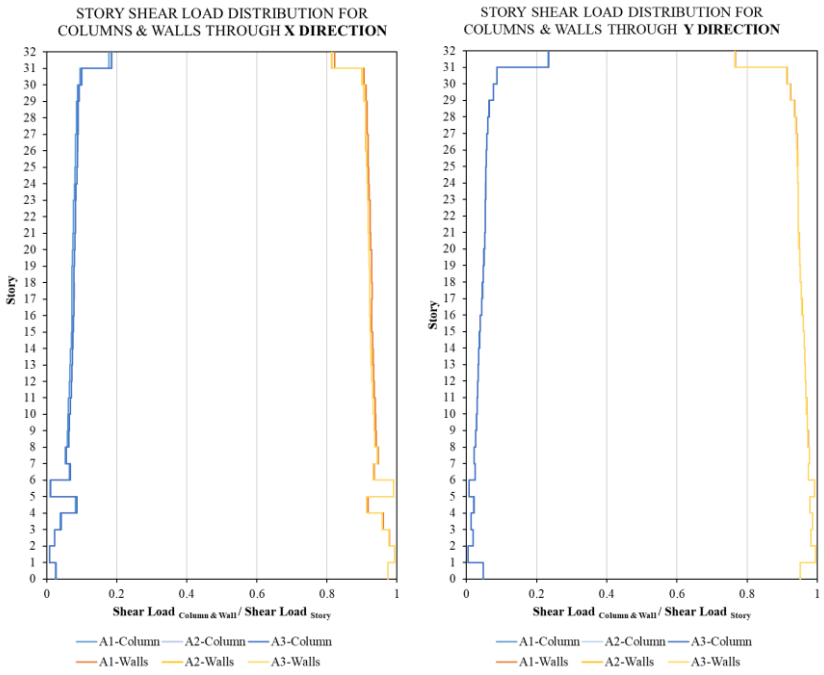

Figure 6.18 Story Shear Load Distribution for Columns & Walls through X and Y Direction (**Ankara**)

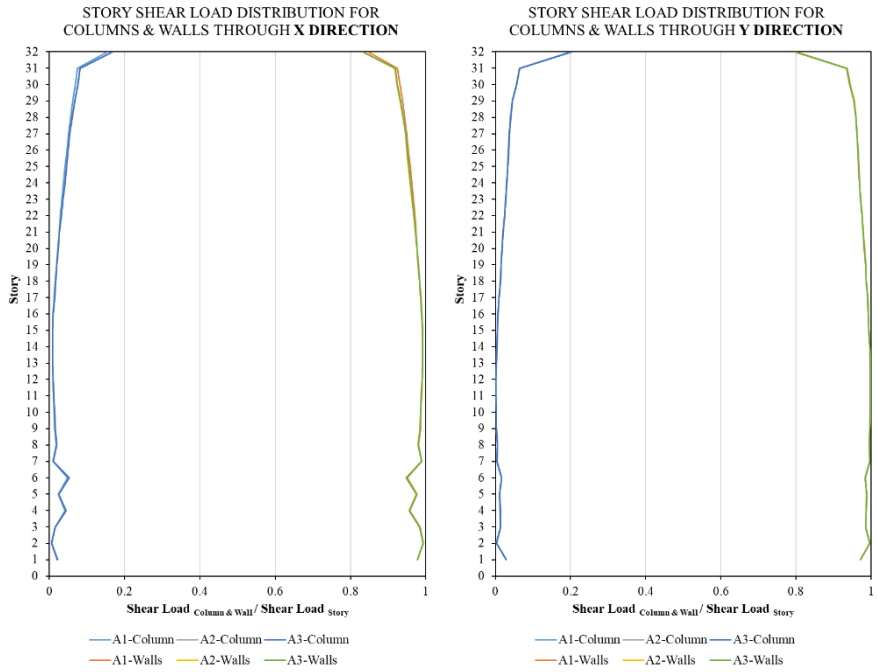

Figure 6.19 Story Shear Load Distribution for Columns & Walls through X and Y Direction (**Istanbul**)

6.3.1 Interstory Drift Ratios

Interstory drift ratios are presented in Figure 6.20 and Figure 6.21 for both regions. The drift ratios are approximately 0.005 and 0.01 for Ankara and Istabul, respectively. These values fall below the mean maximum value of 0.03 according to TEC-2018. Drift check of the calibrated model (A3) including 7 earthquake results is also presented in Figure 6.24 and Figure 6.25. Accordingly, the maximum drift limit applicable to any individual earthquake is not above 0.045. The result difference between the calibrated A3 and non-calibrated (A1-A2) models is seen by numerical comparison in Figure 6.22 and Figure 6.23. Accordingly, there seems to be more difference through X direction in which models show more ductile behavior. In the Y direction, the drift results between the models are almost the same. The uncalibrated model (A1), in which not taking into account energy reduction factors and unloading stiffness factor, and the other two models (A2; A3), A1 model has

less than 20 % difference in the drift ratios compared to the other models in the X direction where ductile behavior is active. The A2 model ,which has a lower energy degradation factor than the A3-calibrated model (half the order of the A3), and the A3 model, gave almost the same average drift results in both directions for both regions.

The approximate mean drift level of 0.005 and 0.01 through all stories respectively in Ankara and Istabul is important in determining the multiplication factor, “b” in Equation 5.2 at Chapter 5 proposed by us for the concrete strain evaluation of the wall structures.

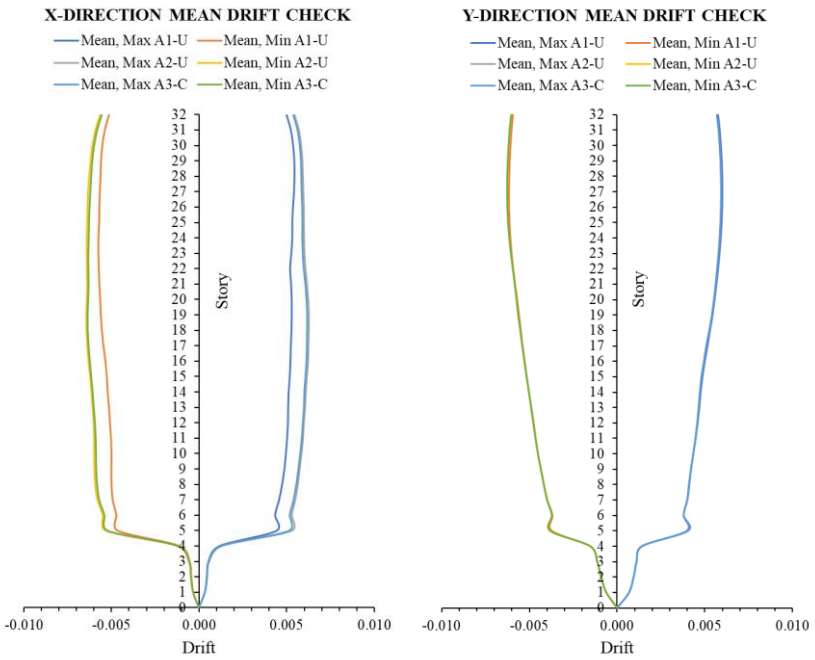

Figure 6.20 X and Y Direction Drift Check (<0.03) for Three Model Alternatives (A1, A2, A3) (**Ankara**)

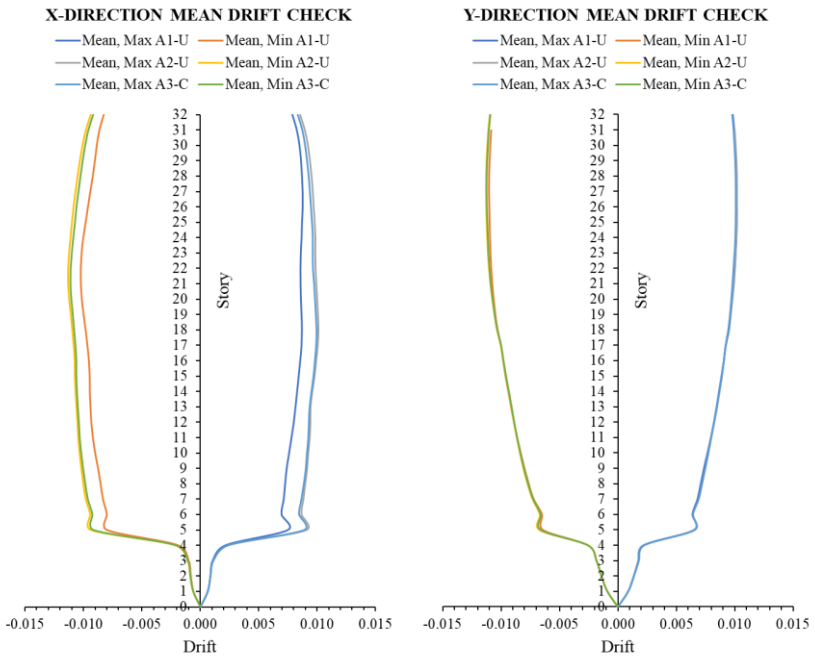

Figure 6.21 X and Y Direction Drift Check (<0.03) for Three Model Alternatives (A1, A2, A3) (**Istanbul**)

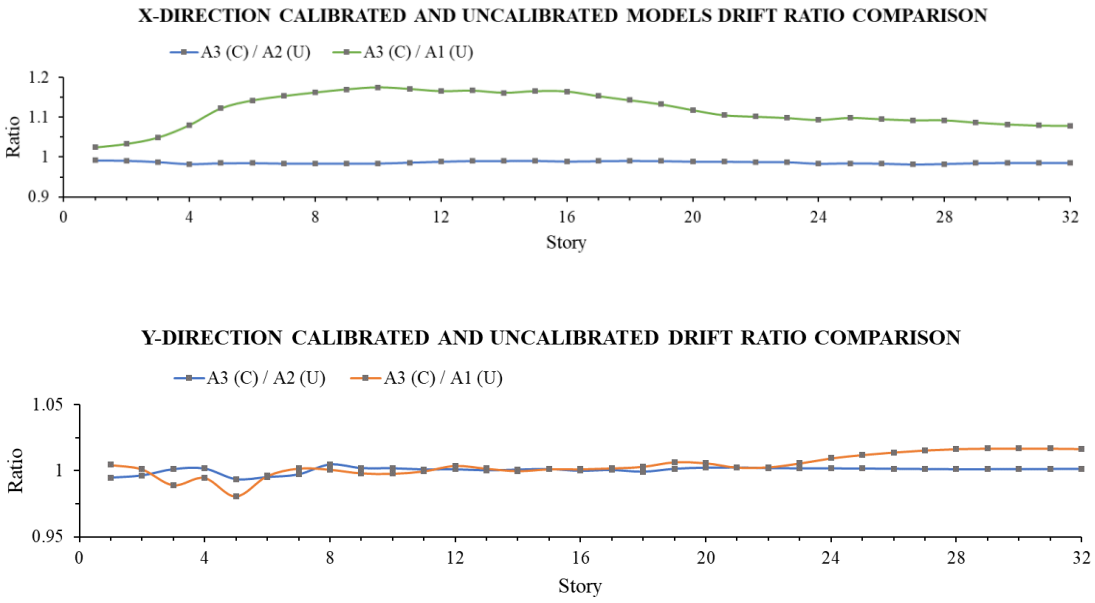

Figure 6.22 Calibrated (A3) and Uncalibrated Models (A1 & A2) Drift Ratio Comparisons for X & Y Direction (**Ankara**)

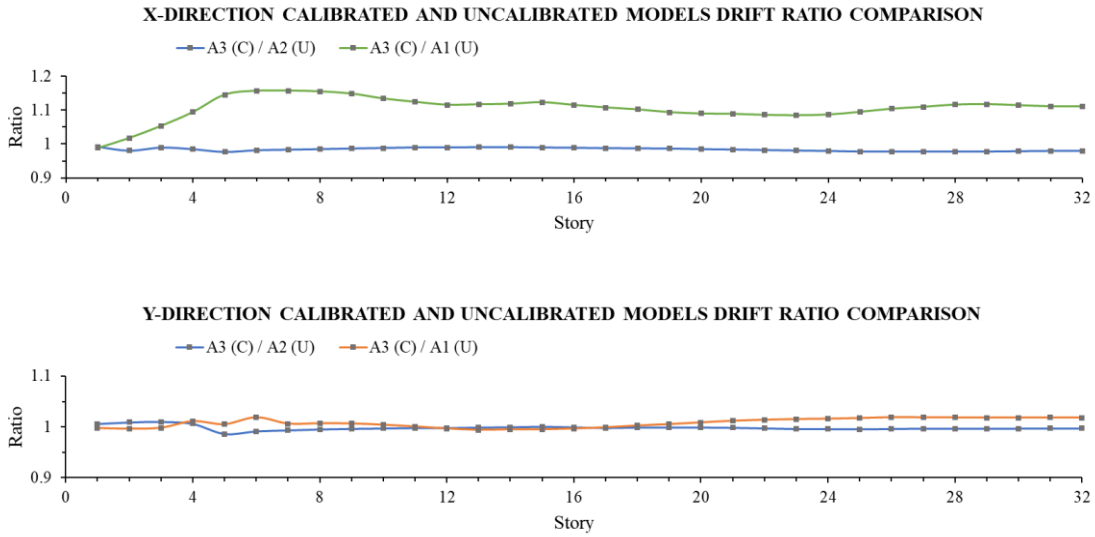

Figure 6.23 Calibrated (A3) and Uncalibrated Models (A1 & A2) Drift Ratio Comparisons for X & Y Direction (**Istanbul**)

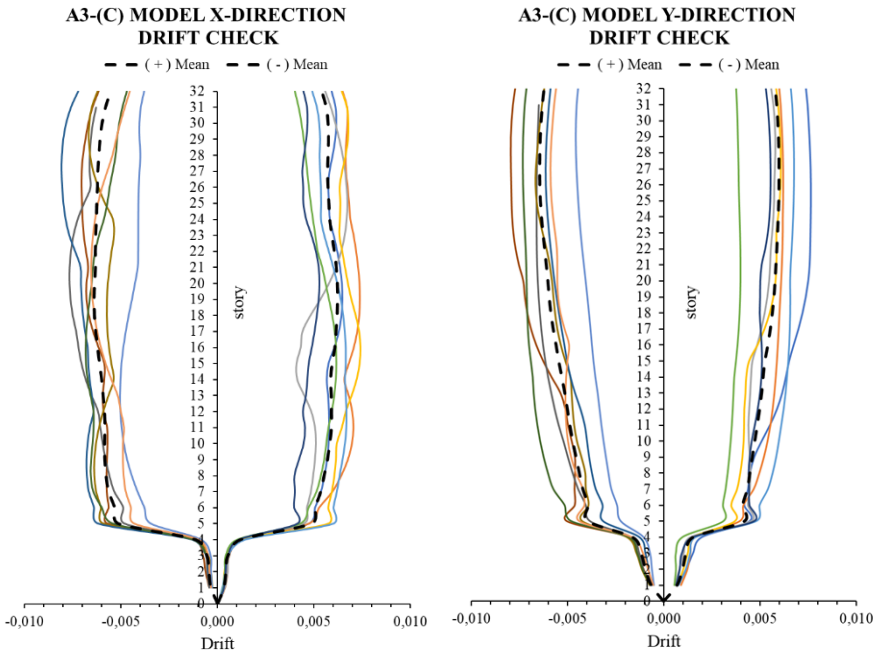

Figure 6.24 Calibrated Model (A3) Mean Drift Check (<0.03-mean; <0.045-max) with 7 Earthquakes for X and Y Direction (**Ankara**)

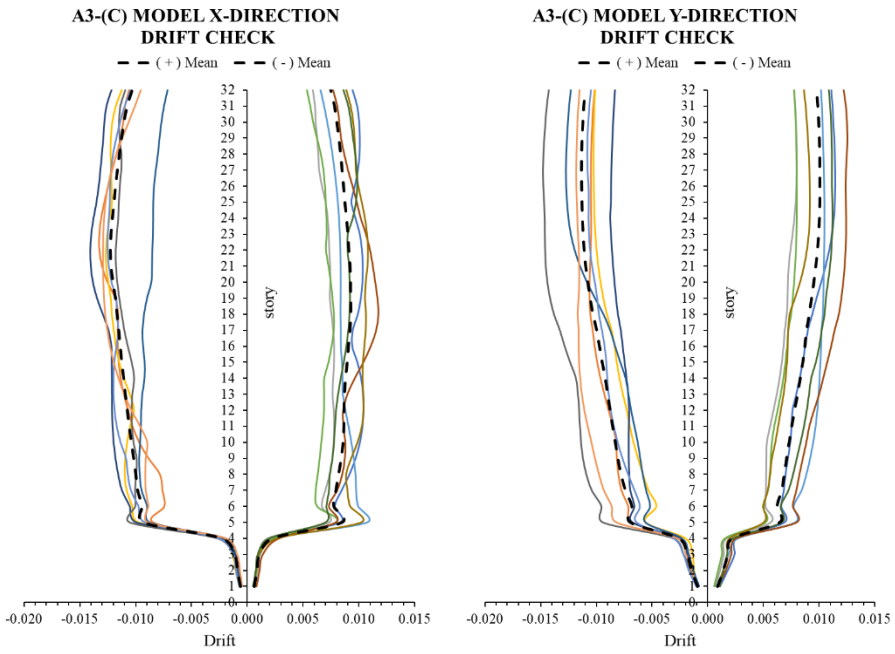

Figure 6.25 Calibrated Model (A3) Mean Drift Check (<0.03-mean; <0.045-max) with 7 Earthquakes for X and Y Direction (**Istanbul**)

6.3.2 Shear Force in the Walls

The shear force demand/capacity (D/C ratios) results of the walls are given in Figure 6.26 and Figure 6.27. Accordingly, as expected, the walls are forced under shear along the critical height from the basement. In addition, according to the wall labels in Figure 6.28, three different model alternatives for each wall and demand/capacity (D/C) ratios for each wall are given between Figure 6.29 and Figure 6.32 for each wall. Within both earthquake regions, there are some walls with D/C ratios exceeding 1. By about 5 % in Ankara building, while it was about 20 % with a maximum of 50 % in Istanbul. For the case study building in Ankara, W17, W20, W21 walls in the Y direction exceed the maximum shear stress ($0.85\sqrt{f_{ck}}$) at the order of 5%. For case study building in Istanbul, W10, W11, W15 and W16 walls in the X direction exceed the limit by up to 50 %, while the W19, W20, W21 and W22 walls in the Y direction exceed the limit up to 20 % (Figure 6.28).

The wall horizontal reinforcement designs carried out according to linear analysis in both earthquake zones were insufficient compared to nonlinear analysis. In Appendices A and B, the wall capacity and demand curves along all floors separately for Ankara and Istanbul are given in comparison with linear analysis capacity curves. Linear capacity curves are the calculations of the walls horizontal reinforcements obtained as a result of linear analysis according to the expected material values.

According to figures between Figure 6.29 and Figure 6.32, the D/C ratios of Model A1 are lower than those of A2 and A3. Avoiding the energy degradation factors in the nonlinear analysis tends to results in unsafe demand estimations for shear force design. The use of low values, as in the A2 model, gives safe results for the design of the walls under shear force. The D/C ratios of the calibrated A3 model and the non-calibrated A2 model are similar.

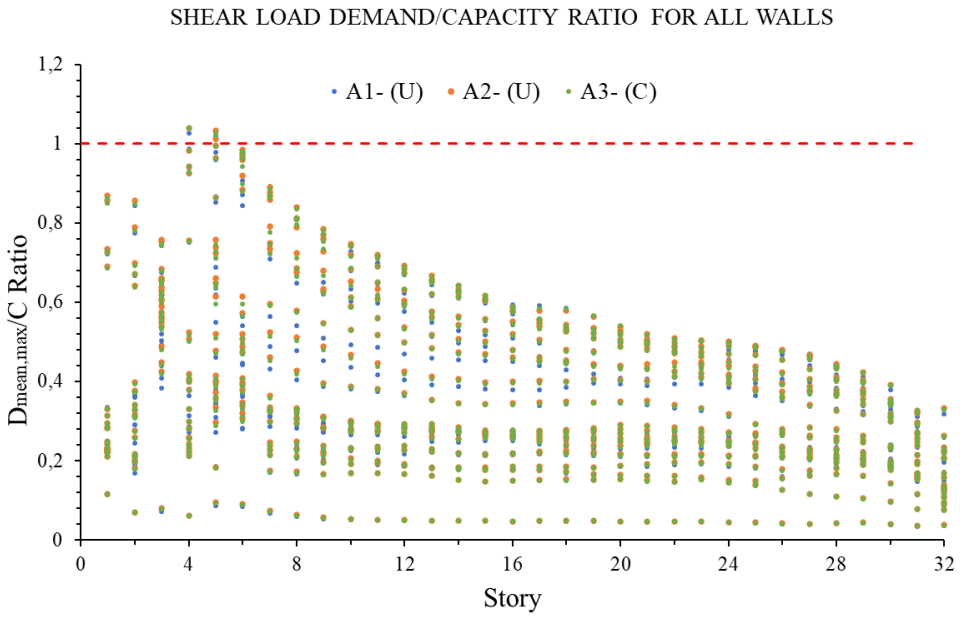

Figure 6.26 Shear Load Demand$_{mean,max}$/Capacity Ratio Check for Three Alternative Models for All Walls (Ankara)

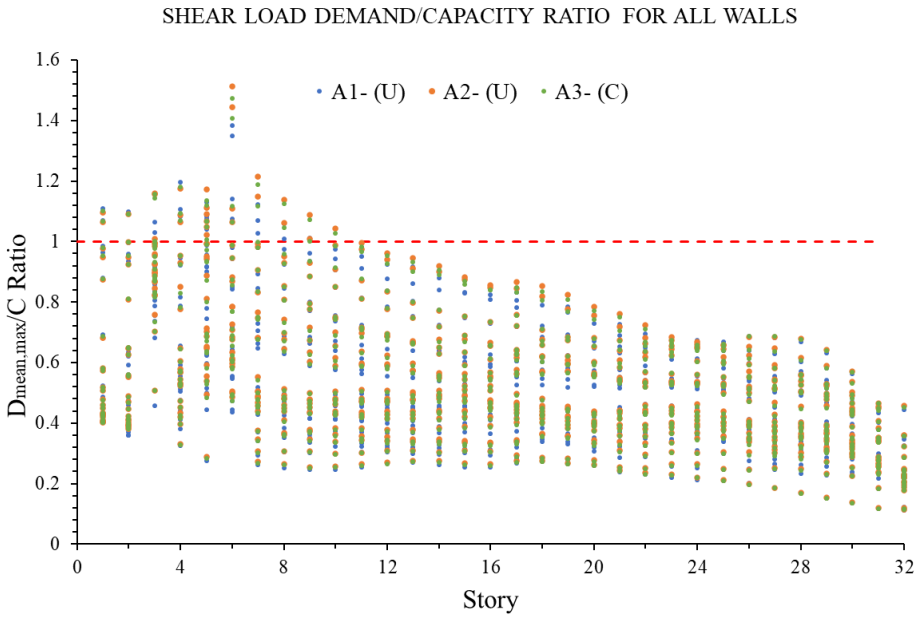

Figure 6.27 Shear Load Demand$_{mean,max}$/Capacity Ratio Check for Three Alternative Models for All Walls (**Istanbul**)

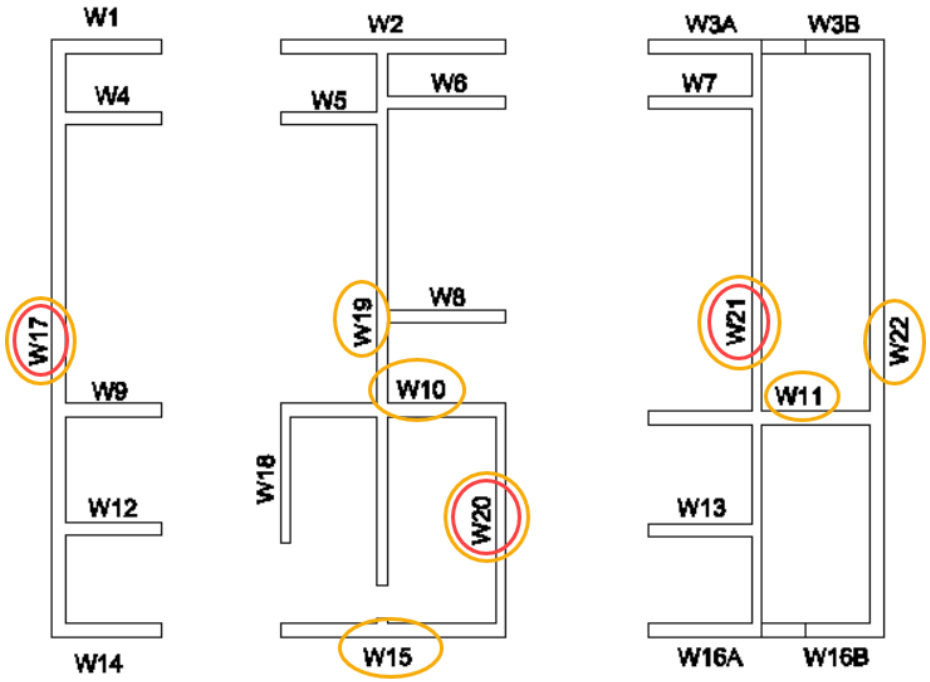

Figure 6.28 Wall Labels and Walls Shear Load Pass Max. Shear Capacity (Red Circle: in Ankara; Orange Circle: in Istanbul)

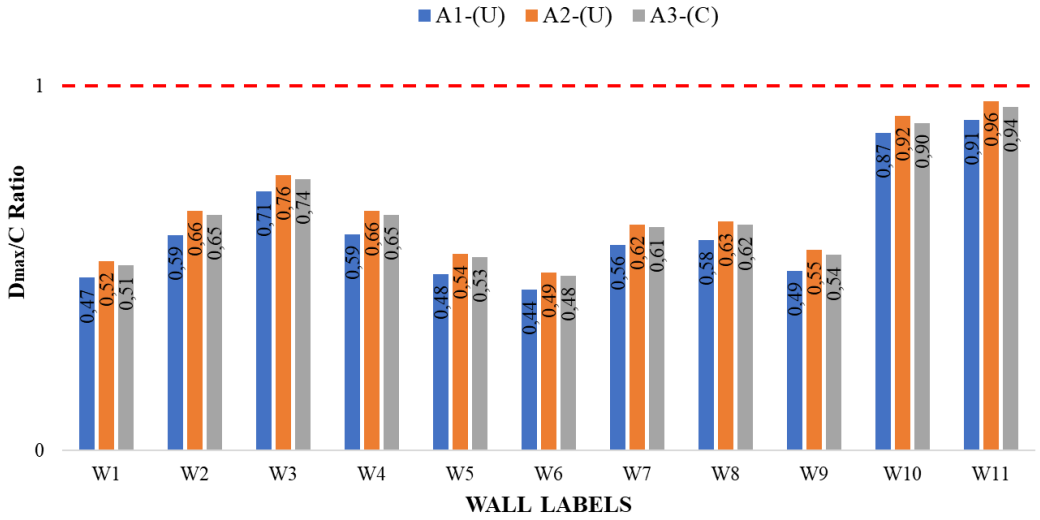

Figure 6.29 Shear Load Demand$_{mean,max}$/Capacity Ratio Check for Three Alternative Models for W1-W11 (**Ankara**)

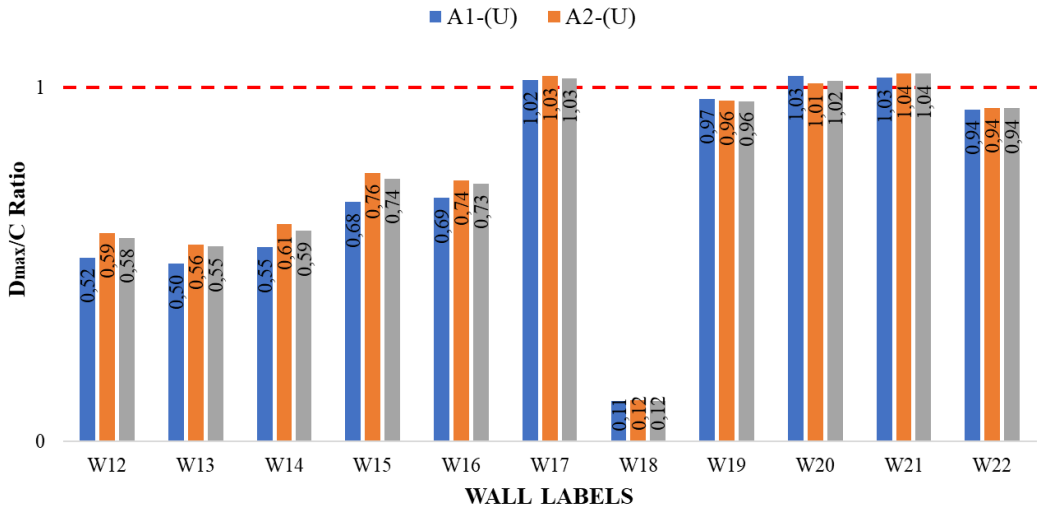

Figure 6.30 Shear Load Demand$_{mean,max}$/Capacity Ratio Check for Three Alternative Models for W12-W22 (**Ankara**)

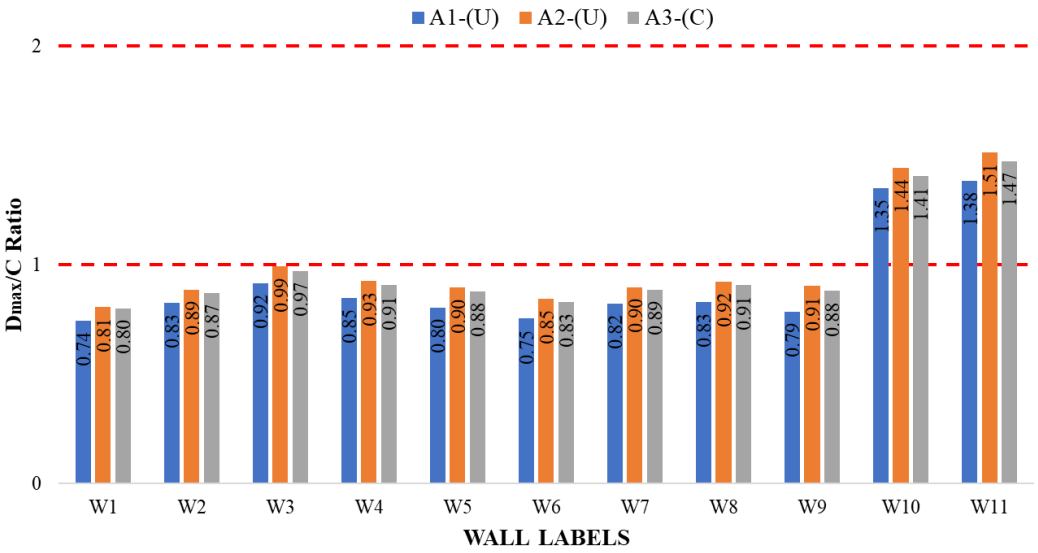

Figure 6.31 Shear Load Demand$_{mean,max}$/Capacity Ratio Check for Three Alternative Models for W1-W11 (**Istanbul**)

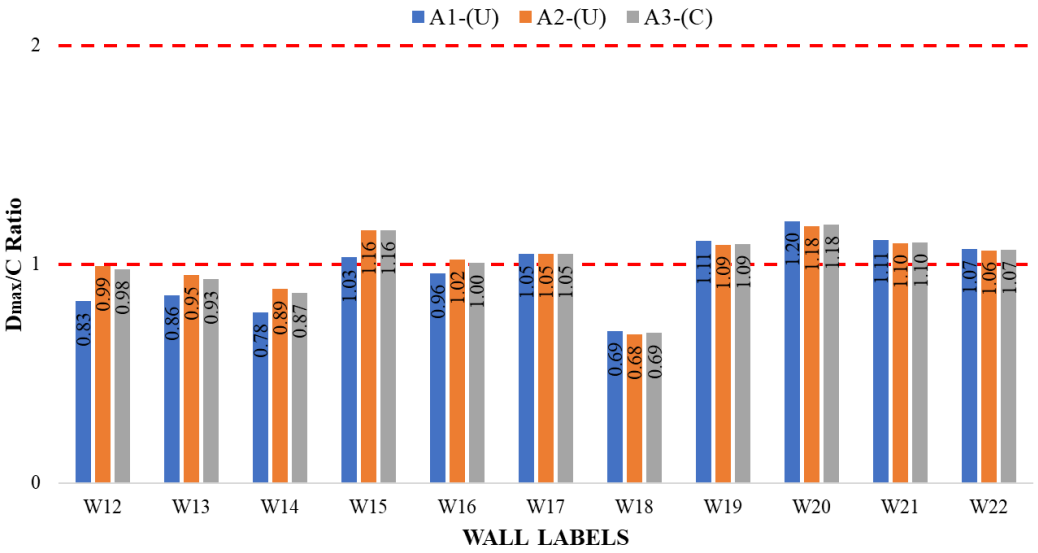

Figure 6.32 Shear Load Demand$_{mean,max}$/Capacity Ratio Check for Three Alternative Models for W12-W22 (**Istanbul**)

6.3.3 Strain Demands

The reinforcement tensile and concrete compression average strain values of the walls are measured and checked with 52 strain gages shown in Figure 6.33. In the concrete compression strain measurements from the strain gage in Figure 6.33, the "unconfined" concrete limit values are taken into consideration with strain gages in red circle, while the orange one's measure concrete compression strains of the "rectangular confined boundary" sections. The remaining strains gages of the red and orange circles are classified as strain gages of "flanged confined boundary" sections. In the figures between Figure 6.34 and Figure 6.39, $D_{mean,max}$/Capacity (D/C) values are given for all layers for strain gage values for concrete compressions in 3 different categories as "unconfined", "rectangular confined boundary" and "flanged confined boundary" for both earthquake zones and 3 model alternatives. "Unconfined", "rectangular confined boundary" and "flanged confined boundary" D/C ratios are maximum 0.3, 0.2, 0.2 respectively.

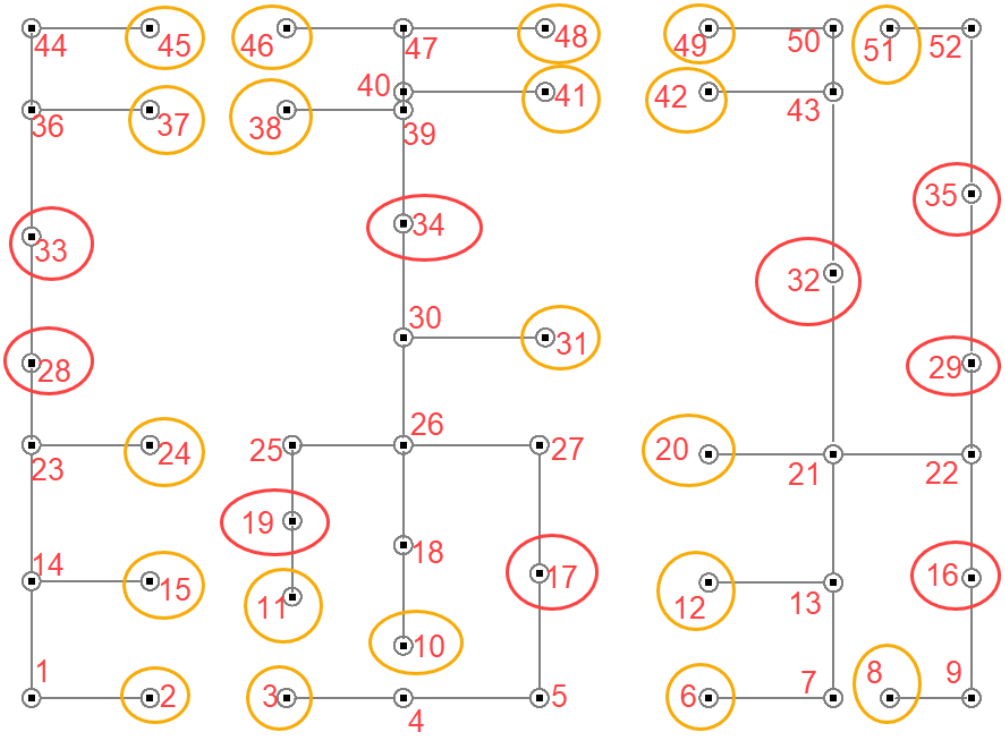

Figure 6.33 Strain Gage Labels of Core-Wall

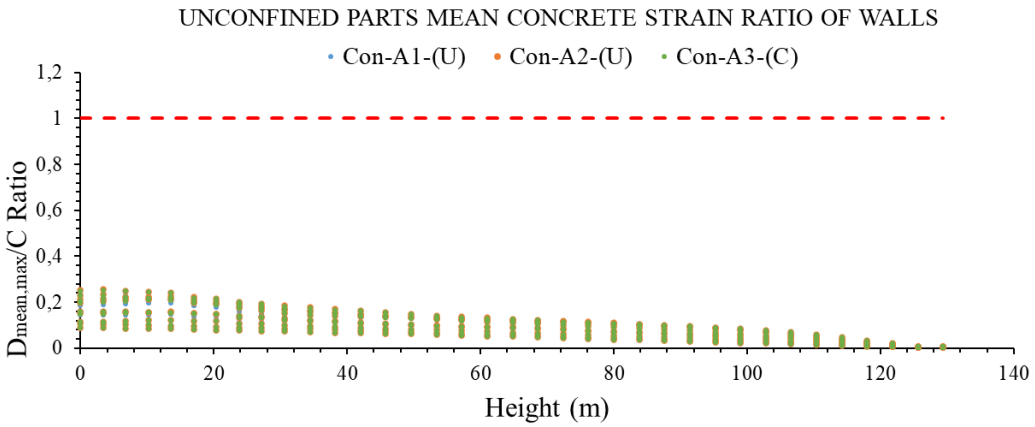

Figure 6.34 Unconfined Parts Mean Concrete Strain D/C Ratio of Walls for Three Model Alternatives (**Ankara**)

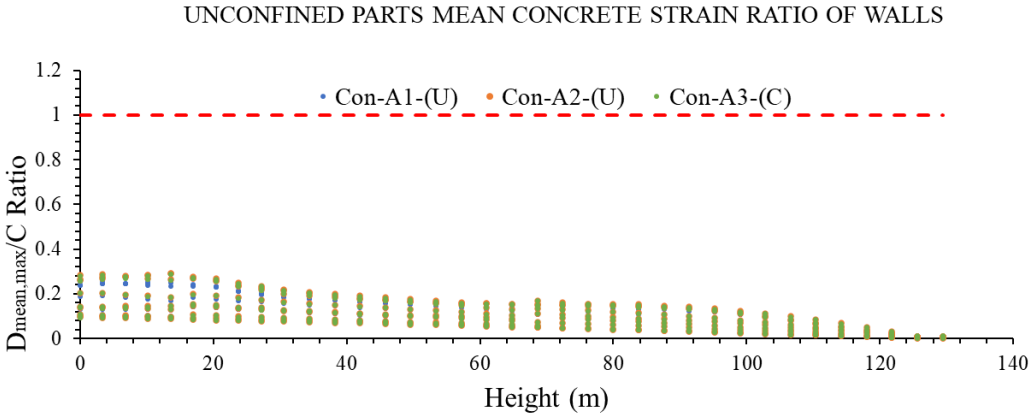

Figure 6.35 Unconfined Parts Mean Concrete Strain D/C Ratio of Walls for Three Model Alternatives (**Istanbul**)

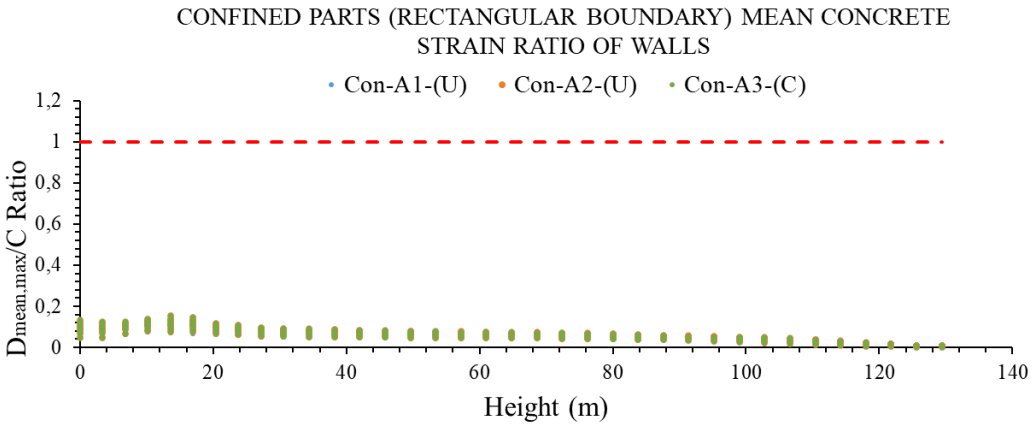

Figure 6.36 Confined Parts (Rectangular Boundary) Mean Concrete Strain D/C Ratio of Walls for Three Model Alternatives (**Ankara**)

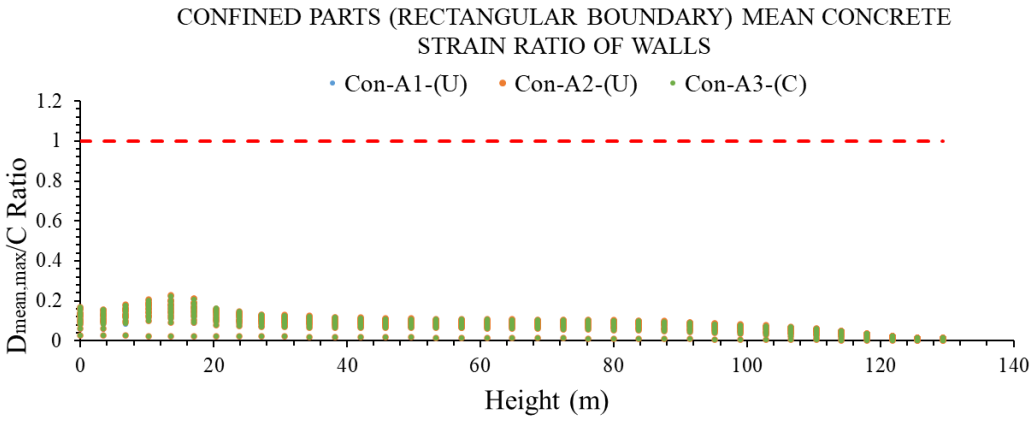

Figure 6.37 Confined Parts (Rectangular Boundary) Mean Concrete Strain D/C Ratio of Walls for Three Model Alternatives (**Istanbul**)

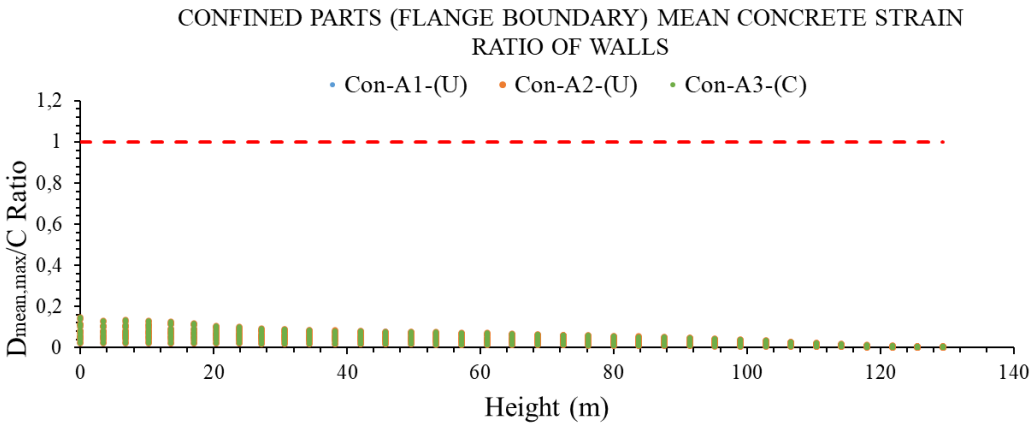

Figure 6.38 Confined Parts (Flange Boundary) Mean Concrete Strain D/C Ratio of Walls for Three Model Alternatives (**Ankara**)

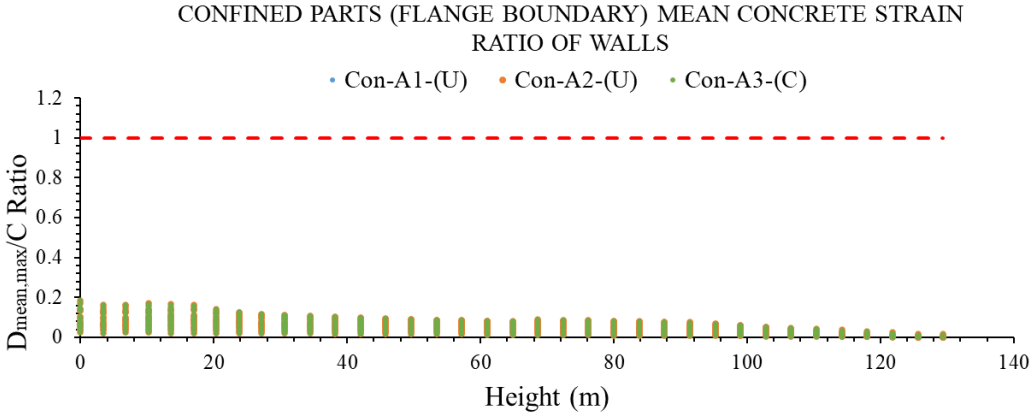

Figure 6.39 Confined Parts (Flange Boundary) Mean Concrete Strain D/C Ratio of Walls for Three Model Alternatives (**Istanbul**)

In the calibration study conducted in Chapter 5, modeling with Perform 3D showed that the concrete strain results are much lower than the experimental results. According to the value of "a" in Equation 6.3, Figure 5.59 shows the variability of the value "a" according to drift ratios.

$$a=\varepsilon_{c,experiment} / \varepsilon_{c,P3D\ model} \quad \textbf{(6.3)}$$

When evaluated according to this calibration results, it is proposed according to Figure 5.59 to multiply the P3D model concrete strain results by this coefficient “a” and "a" value should be taken "2" for the "rectangular confined" sections, as in the RW2 test sample, while in the case of a more distributed compression stress of the compression zone in the "flanged" form, such as TW2, it is recommended to use an increase coefficient between "4-16" with the value of "a" according to the structure drift ratio. While the dominant average drift rate in Ankara is 0.005, drift ratio demand for case study building in Istanbul is almost 0.01. Accordingly, the "unconfined" and "flanged confined" concrete sections concrete strains are magnified by multiplying the model strain gage values by the coefficient "a" as “4” and “6” in Ankara and in Istanbul respectively. Between Figure 6.40 and Figure 6.45, both earthquake zones and only calibrated A3 model concrete strain values are increased by the coefficient "a" and the demand/capacity (D/C) values along the stories are shown. Although the assumption that there is the same drift ratio on all floors in the magnification with the same coefficient "a" is not exactly valid for the basement floors, but it is accepted as such for convenience in terms of observation. However, what should happen is to determine and apply the correction coefficient "a" according to the story drift ratio determined according to Figure 5.59.

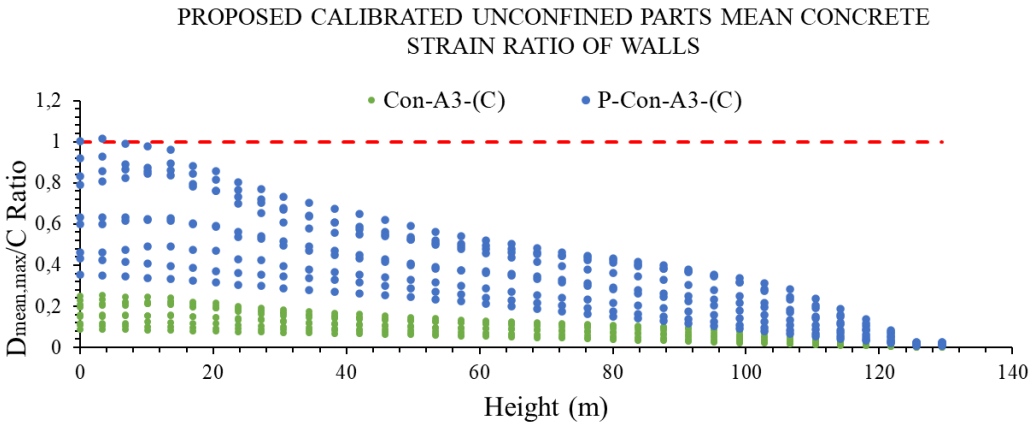

Figure 6.40 Proposed (Multiplied by “a=4”) & Available Calibrated Unconfined Parts Mean Concrete Strain D/C Ratio of Walls (**Ankara**)

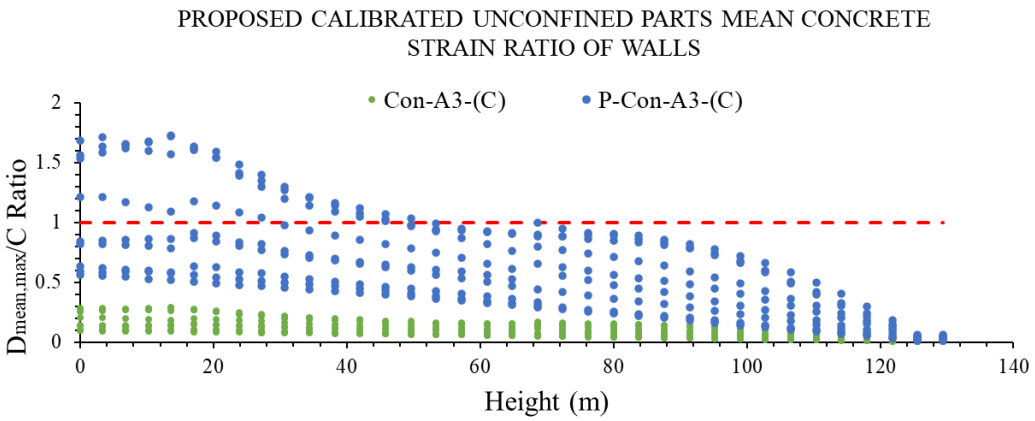

Figure 6.41 Proposed (Multiplied by "a=6") & Available Calibrated Unconfined Parts Mean Concrete Strain D/C Ratio of Walls (**Istanbul**)

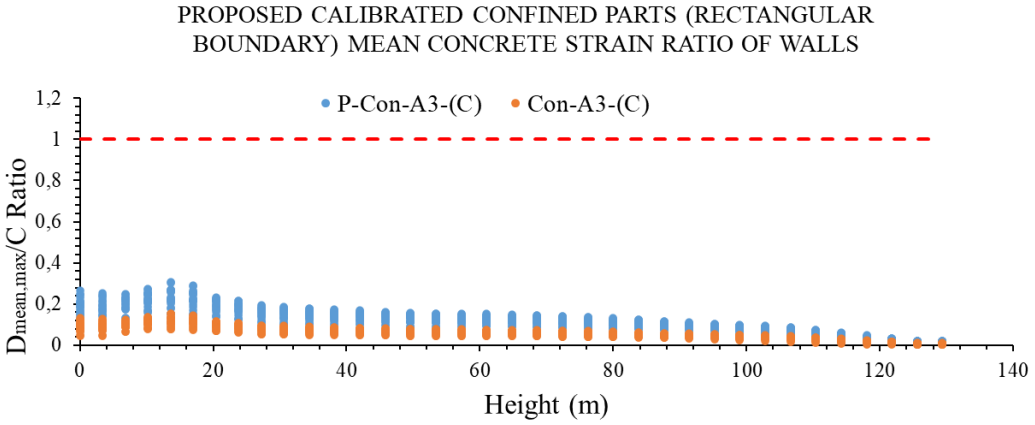

Figure 6.42 Proposed (Multiplied by "a=2") & Available Calibrated Confined Parts (Rectangular Boundary) Mean Concrete Strain D/C Ratio of Walls (**Ankara**)

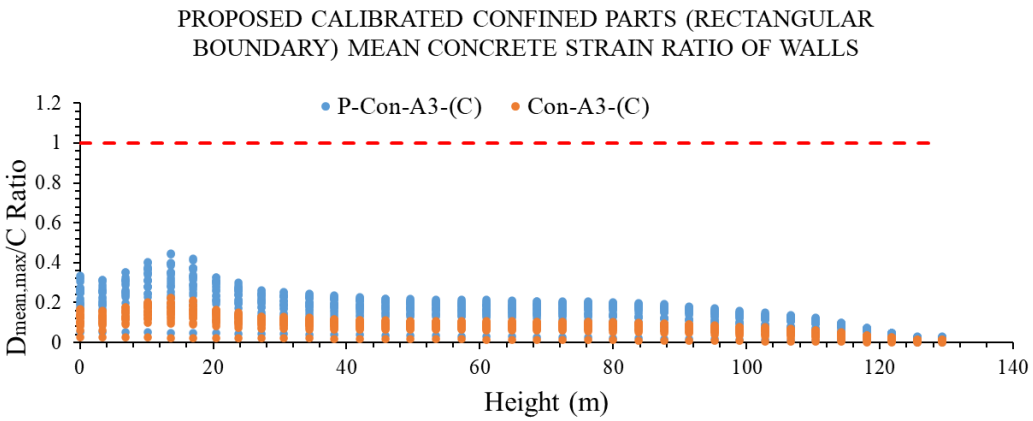

Figure 6.43 Proposed (Multiplied by "a=2") & Available Calibrated Confined Parts (Rectangular Boundary) Mean Concrete Strain D/C Ratio of Walls (**Istanbul**)

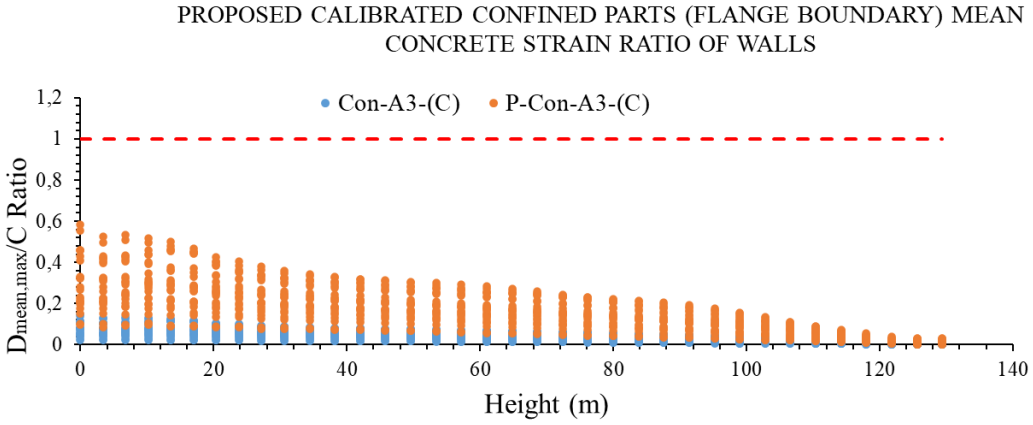

Figure 6.44 Proposed (Multiplied by "a=4") & Available Calibrated Confined Parts (Flange Boundary) Mean Concrete Strain D/C Ratio of Walls (**Ankara**)

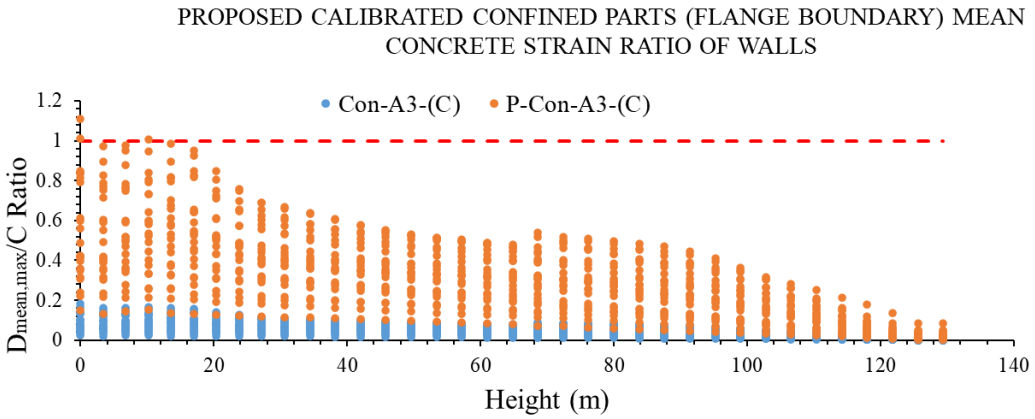

Figure 6.45 Proposed (Multiplied by "a=6") & Available Calibrated Confined Parts (Flange Boundary) Mean Concrete Strain D/C Ratio of Walls (**Istanbul**)

Both concrete and reinforcement strains for all strain gages are shown throughout all stories in Appendices C and D according to the proposed "a" coefficient correction for the case study building in Ankara and Istanbul respectively. As a result of the increases with the coefficient "a", concrete strain values of some strain gages exceeded the limit values in both Ankara and Istanbul. Since the limit value is lower in the "unconfined" sections than "confined" concrete parts, "unconfined" concrete fibers are more critical. So, in the building in Ankara, the concrete strain values multiplied with the "a" coefficient exceed the limit (Figure 6.46) while the concrete strain in other "unconfined" concrete sections approaches the limit strain values. Although the concrete strain is increased in the confined sections for the structure in Ankara, the D/C ratio is maximum 0.4 for "rectangular boundary" fibers and 0.6 for "flanged boundary" fibers.

The concrete strains at 16., 17., 19. and 35. strain gages of the "unconfined" concrete sections for the building in Istanbul pass the limit after the use of the coefficient "a". On the other hand, the concrete strains at 5. and 9. strain gages of the "flanged confined" concrete sections pass the limit after the use of the proposed "a" coefficient. Strain gages exceeding concrete strain limits after the use of coefficient "a" are shown in Figure 6.46.

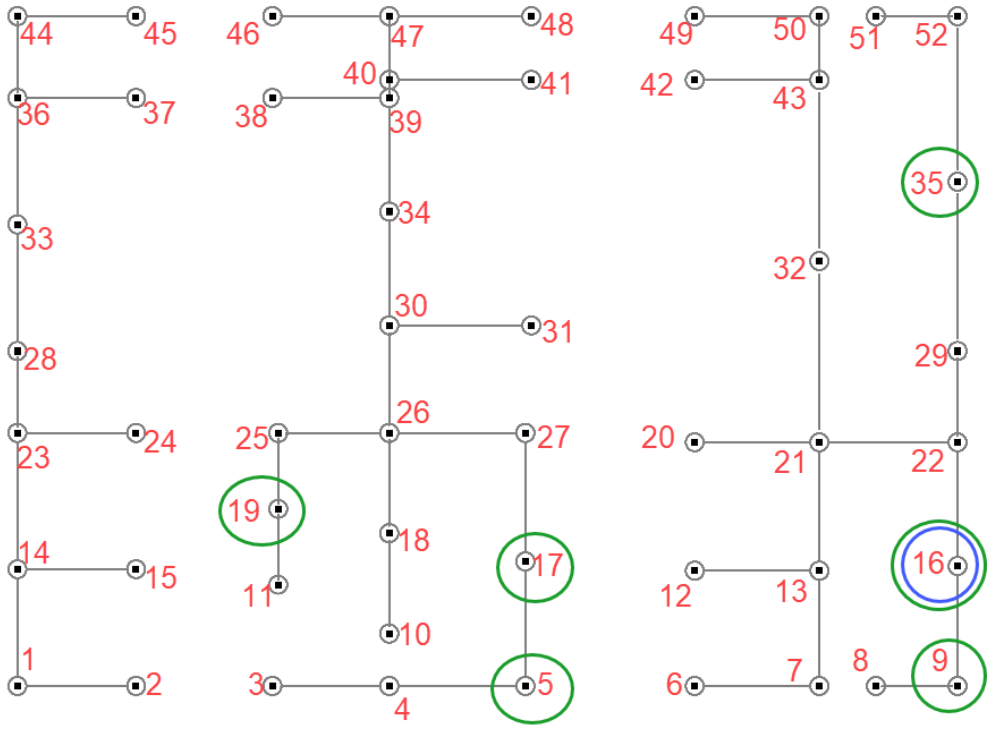

Figure 6.46 Strain Gages Exceed Concrete Strain Limits after Usage of "a" Proposed Multiplication (Green Circle: In Istanbul; Blue Circle: In Ankara)

Wall reinforcement strain D/C ratios are around 0.15 for the building in Ankara and 0.2-0.25 for the structure in Istanbul (Figure 6.47 & Fiure 6.48).

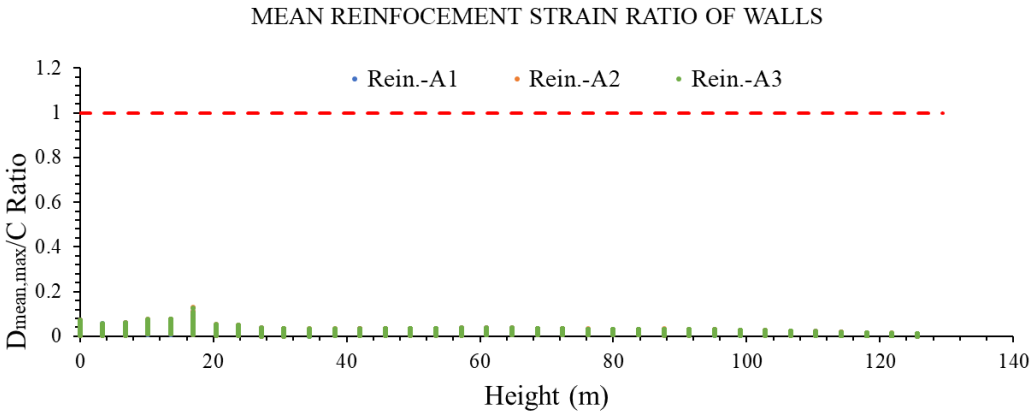

Figure 6.47 Mean Reinforcement Strain D/C Ratio for Three Alternative Models in **Ankara**

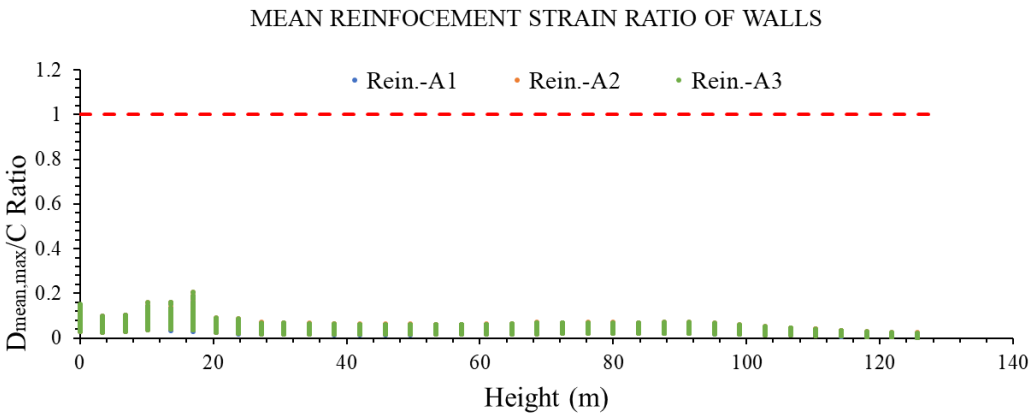

Figure 6.48 Mean Reinforcement Strain D/C Ratio for Three Alternative Models in **Istanbul**

Concrete and reinforcement strain value comparisons are made along the building height between 3 alternative models for wall structural member in the graphs between Figure 6.49 and Figure 6.56. Accordingly, in both concrete and reinforcement strains, the difference between the calibrated A3 model and the uncalibrated A1 model seems to be much greater than the difference between the calibrated A3 model and the uncalibrated A2 model. A2 model results are 5-10 % higher than A3 model values in both concrete and reinforcement strains. The much lower intake of energy degradation factors gives results that remain on the safe side of the design in terms of vertical strain results. On the other hand, in the A1 model, where energy degradation factors are not taken into consideration at all, it has given less results in the concrete strain, up to 40 % in the reinforcement strain and up to 15-20 % in concrete strain compared to the calibrated A3 model, and has given lesser results that are not on the safe side in terms of design.

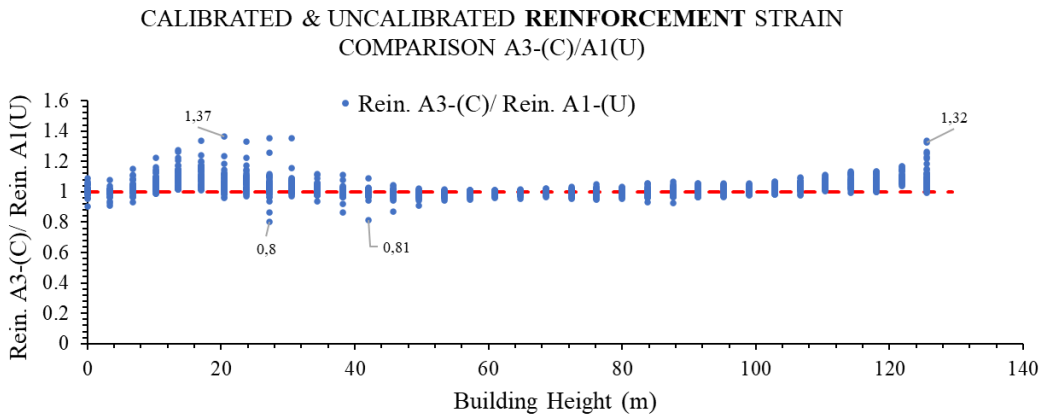

Figure 6.49 Reinforcement Strain Comparisons of Walls for Calibrated (A3-(C)) and Uncalibrated (A1-(U)) Models (**Ankara**)

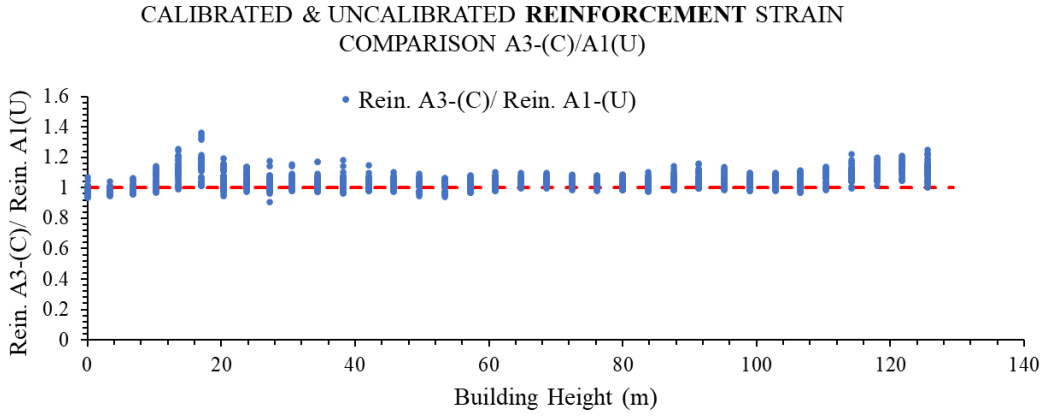

Figure 6.50 Reinforcement Strain Comparisons of Walls for Calibrated (A3-(C)) and Uncalibrated (A1-(U)) Models (**Istanbul**)

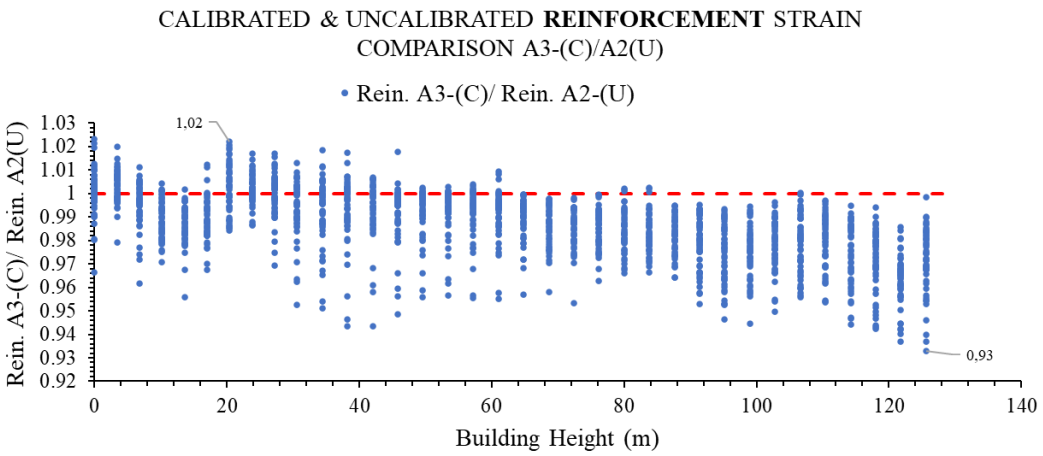

Figure 6.51 Reinforcement Strain Comparisons of Walls for Calibrated (A3-(C)) and Uncalibrated (A2-(U)) Models (**Ankara**)

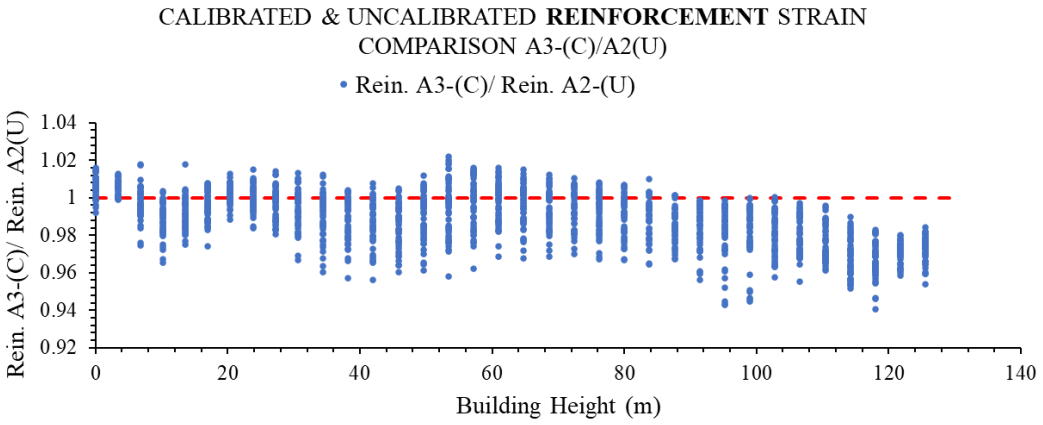

Figure 6.52 Reinforcement Strain Comparisons of Walls for Calibrated (A3-(C)) and Uncalibrated (A2-(U)) Models (**Istanbul**)

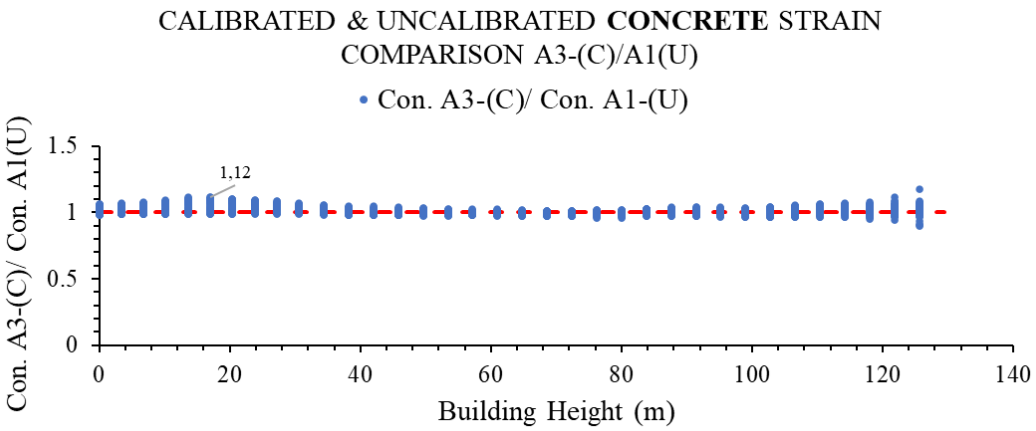

Figure 6.53 Concrete Strain Comparisons of Walls for Calibrated (A3-(C)) and Uncalibrated (A1-(U)) Models (**Ankara**)

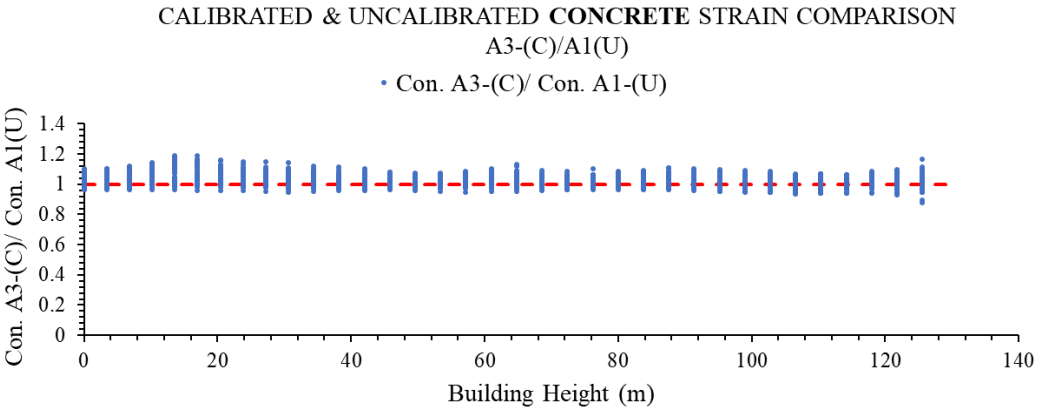

Figure 6.54 Concrete Strain Comparisons of Walls for Calibrated (A3-(C)) and Uncalibrated (A1-(U)) Models (**Istanbul**)

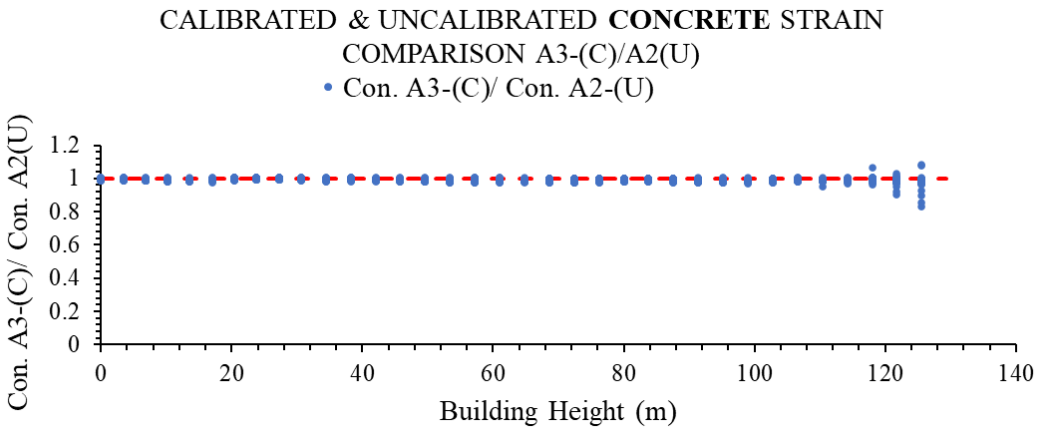

Figure 6.55 Concrete Strain Comparisons of Walls for Calibrated (A3-(C)) and Uncalibrated (A2-(U)) Models (**Ankara**)

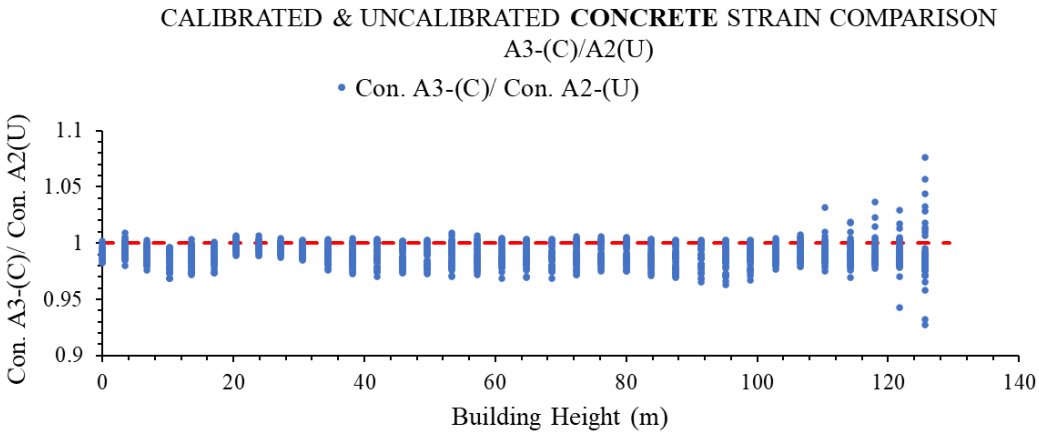

Figure 6.56 Concrete Strain Comparisons of Walls for Calibrated (A3-(C)) and Uncalibrated (A2-(U)) Models (**Istanbul**)

6.3.4 Rotation Demand in Beams

The beams named between B1 and B9 were shown in Figure 6.57. The B3 and B9 link beams have 150 cm depth, while the remaining beams are 60 cm deep. Instead of check of beam rotation limit for the diagonally detailled link beam in the building in Istanbul, the shear displacement inelastic behavior was checked. For both

earthquake zones between Figure 6.58 and Figure 6.61, the maximum average rotations of all beams over the building height except the diagonal reinforced link beams were given for thre calibrated and uncalibrated alternatives. Accordingly, there was no beam exceeding the collapse prevention (CP) rotation limits. In other words, the rotation of all beams was below the limits. It should be noted that the rotation of link beams (40/150) in Ankara were very small values on the upper floors.

Among the A1, A2 and A3 calibrated and uncalibrated models, the A2 uncalibrated model with the smallest energy degradation factor values gave the highest rotation values, while the A1 uncalibrated model gave the lowest rotation values, resulting in unsafe design results. The numerical comparison between the models was given between Figure 6.62 and Figure 6.69. The rotation result difference between the A1 non-calibrated model and the A3 calibrated model beams reached 30 %, while the beam rotation result difference between A2 and A3 models did not exceed 5 %.

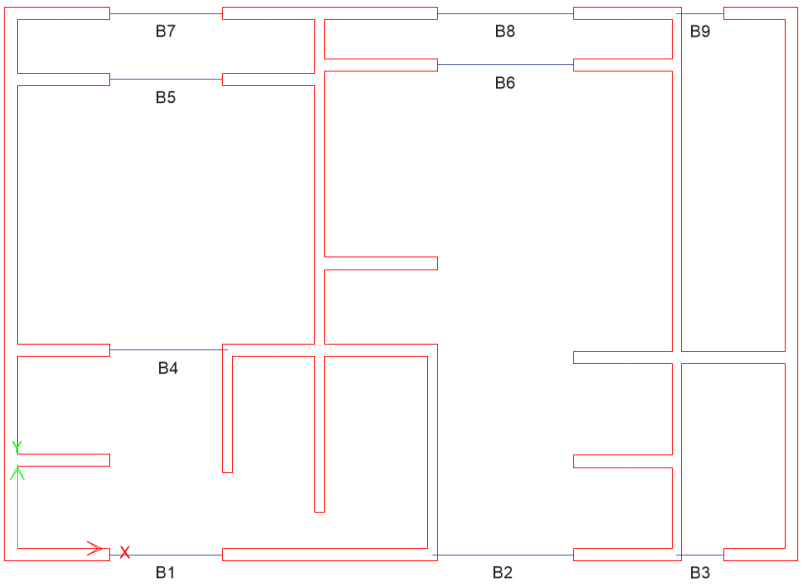

Figure 6.57 Label of Beams

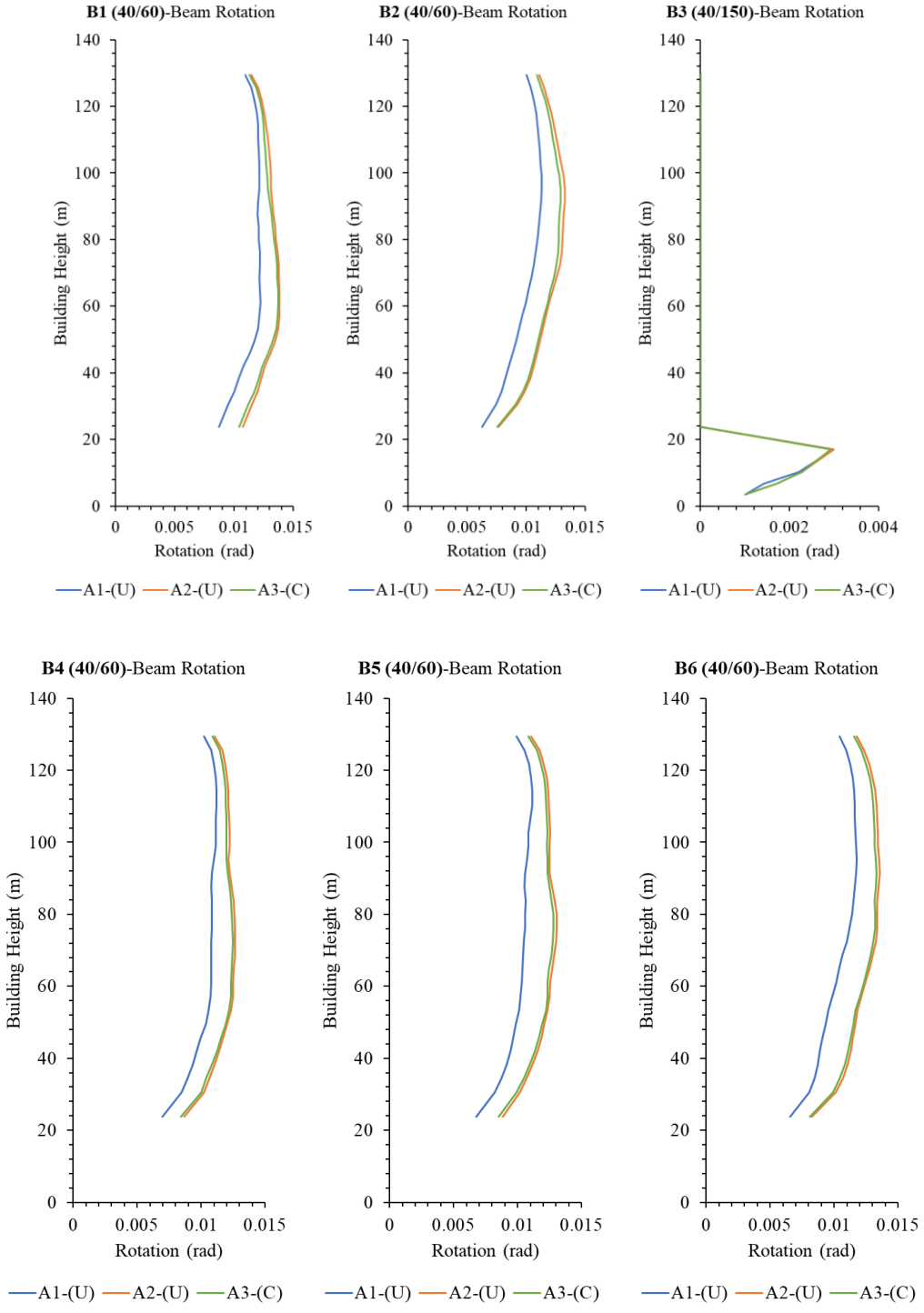

Figure 6.58 Beam Rotation Check (<0.041 (B40-60); <0,02 (B40-150)) for Three Model Alternatives between B1 & B6 (**Ankara**)

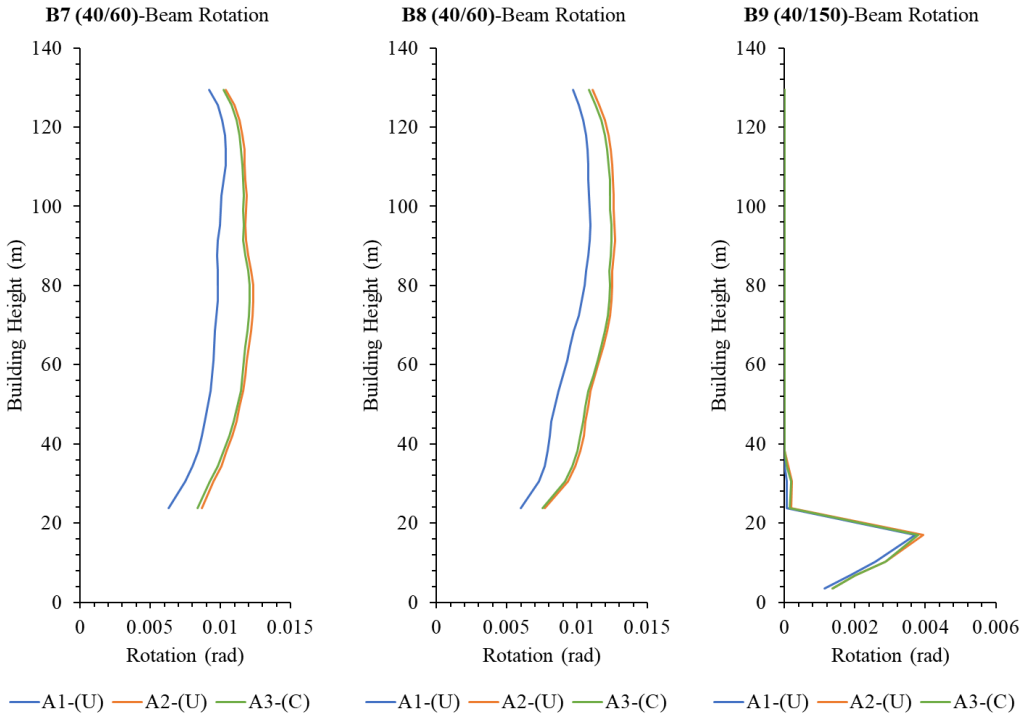

Figure 6.59 Beam Rotation Check (<0.041 (B40-60); <0,02 (B40-150)) for Three Model Alternatives between B7 & B9 (**Ankara**)

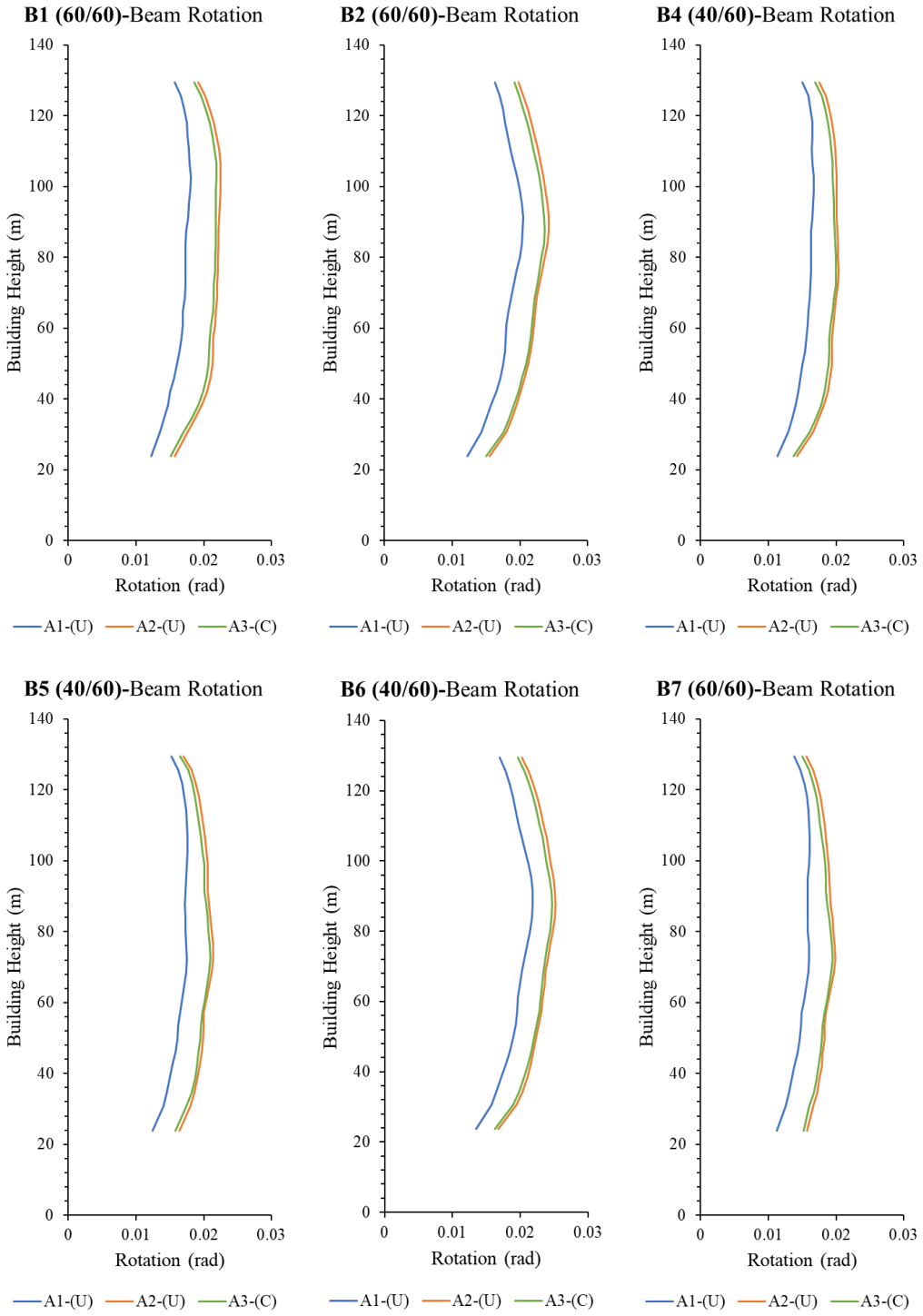

Figure 6.60 Beam Rotation Check (<0.046 (B40-60); <0.046 (B60-60); <0,02 (B40-150)) for Three Model Alternatives between B1 & B7 (**Istanbul**)

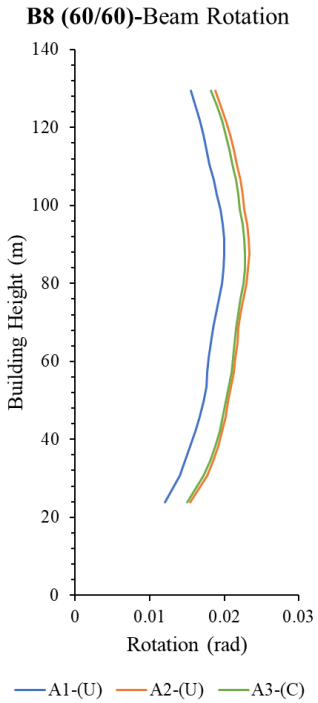

Figure 6.61 Beam Rotation Check (<0.046 (B60-60)) for Three Model Alternatives for B8 (**Istanbul**)

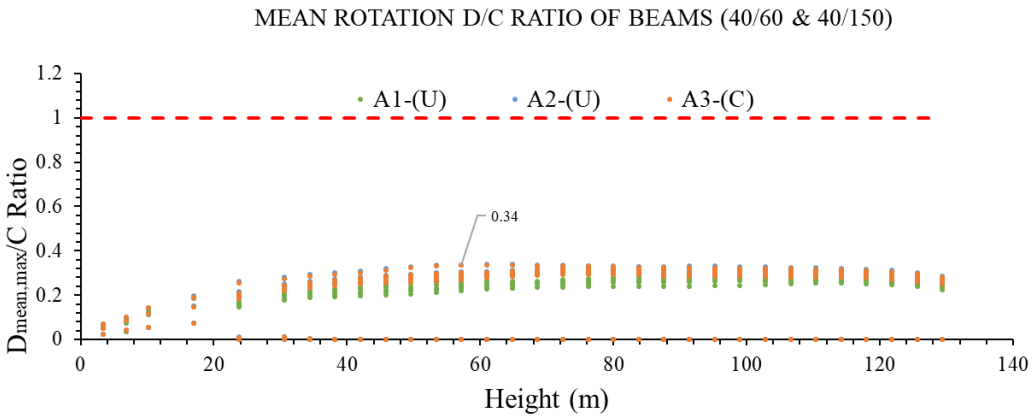

Figure 6.62 Mean Rotation D/C Ratio of Beams (**Ankara**)

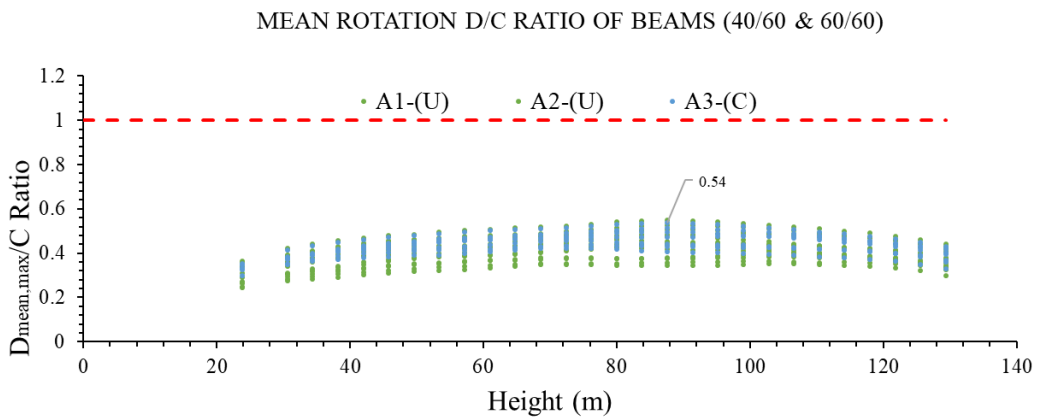

Figure 6.63 Mean Rotation D/C Ratio of Beams (**Istanbul**)

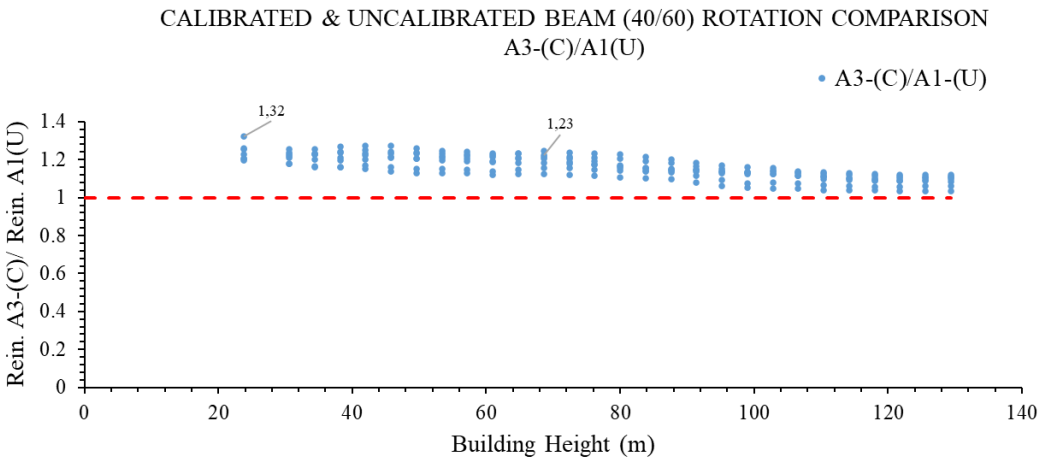

Figure 6.64 Calibrated (A3) and Uncalibrated (A1) Beam (40/60) Rotation Comparison Ratio, A3-(C)/A1(U) (**Ankara**)

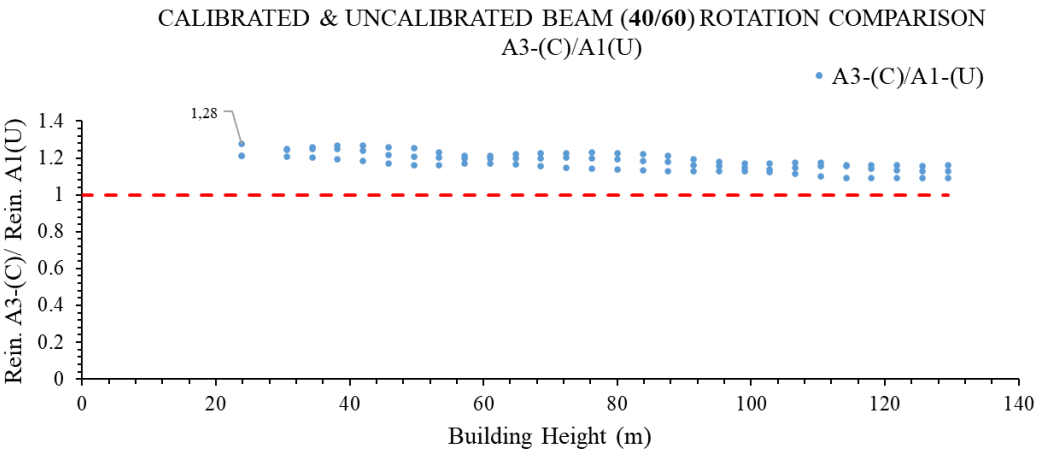

Figure 6.65 Calibrated (A3) and Uncalibrated (A1) Beam (40/60) Rotation Comparison Ratio, A3-(C)/A1(U) (**Istanbul**)

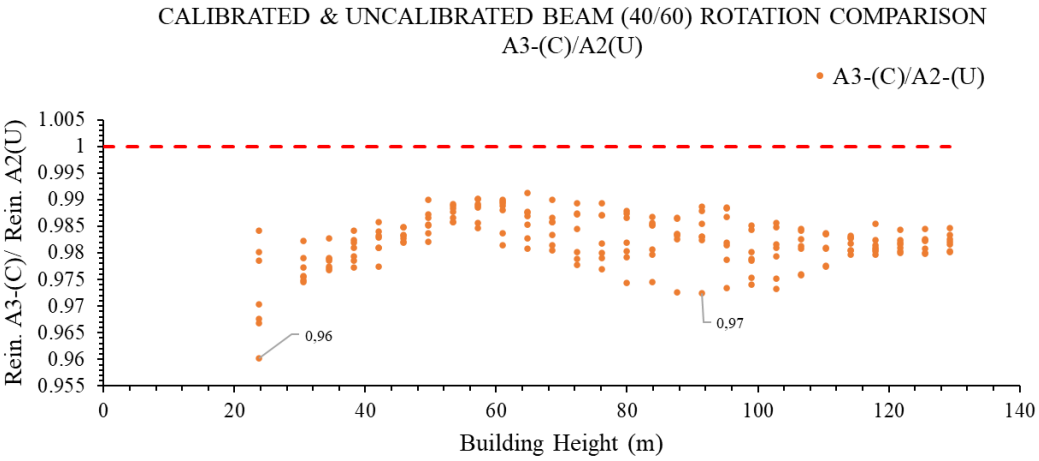

Figure 6.66 Calibrated (A3) and Uncalibrated (A2) Beam (40/60) Rotation Comparison Ratio, A3-(C)/A2(U) (**Ankara**)

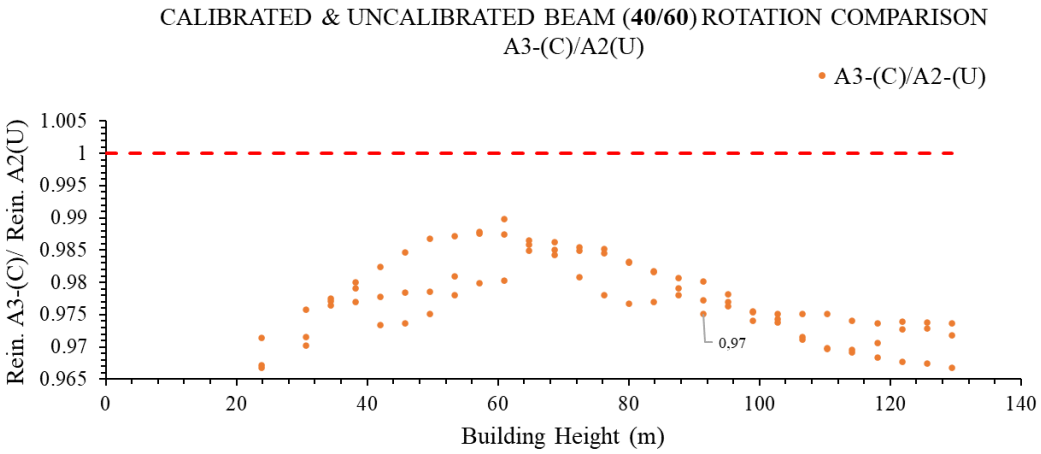

Figure 6.67 Calibrated (A3) and Uncalibrated (A2) Beam (40/60) Rotation Comparison Ratio, A3-(C)/A2(U) (**Istanbul**)

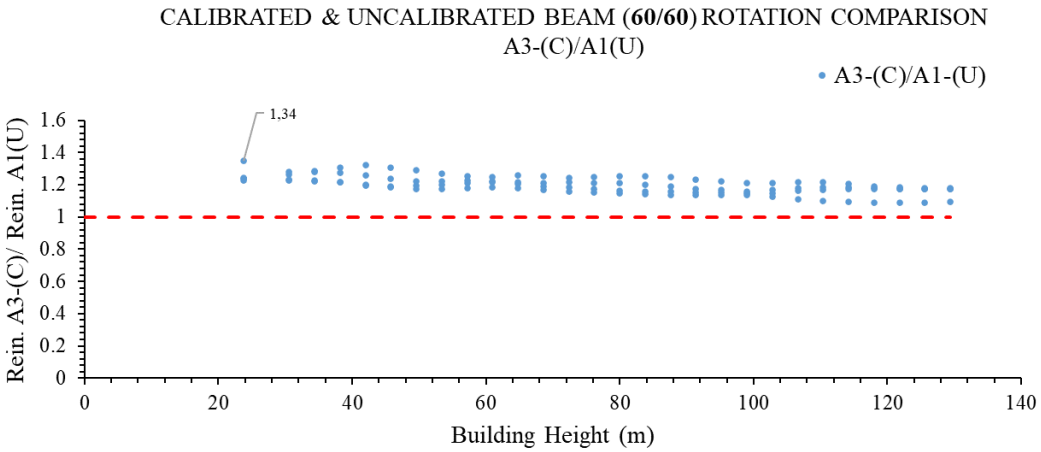

Figure 6.68 Calibrated (A3) and Uncalibrated (A1) Beam (60/60) Rotation Comparison Ratio, A3-(C)/A1(U) (**Istanbul**)

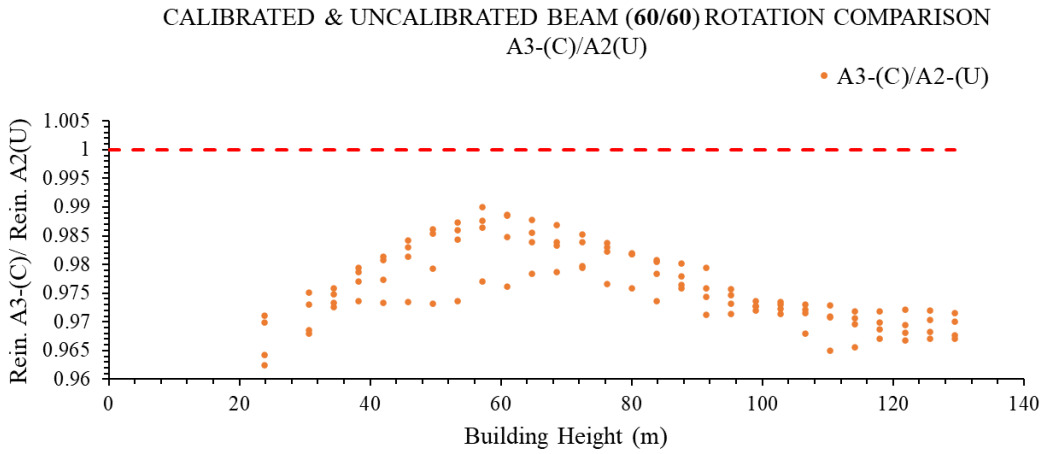

Figure 6.69 Calibrated (A3) and Uncalibrated (A2) Beam (60/60) Rotation Comparison Ratio, A3-(C)/A2 (U) (**Istanbul**)

6.3.5 Performance of Diagonally Reinforced Link Beams

Diagonally reinforced link beam shear force and shear displacement results are given in Figure 6.70 and Figure 6.71. According to these results, beam shear displacements are far from the maximum collapse prevention (CP) limit of 39 mm (0.03 l_n). According to this limit, the demand/capacity (D/C) ratios are 0.04, 0.1 and 0.08 for the A1, A2 and A3 models, respectively. The shear forces are almost at the inelastic limit. The A2 and A3 model shear displacements are almost the same, with a maximum difference of 8 % more than the A1 model displacements.

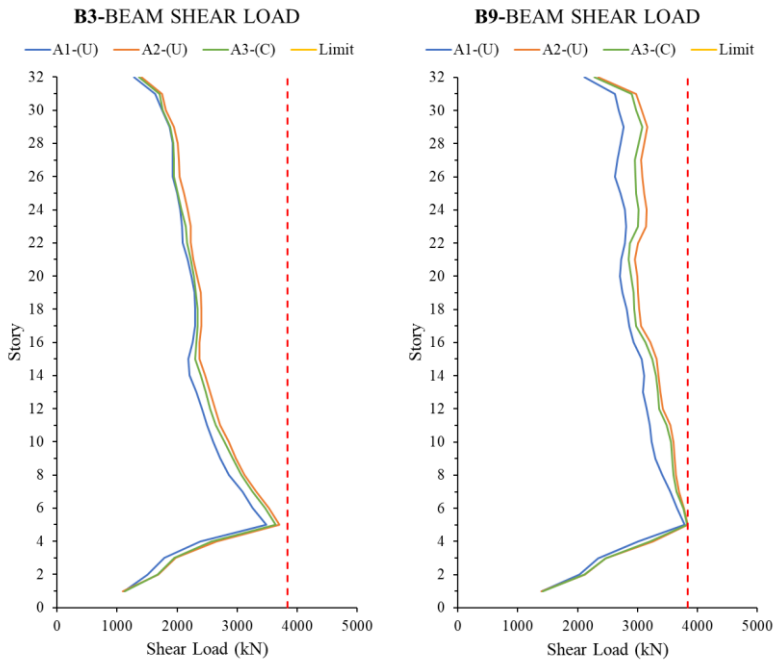

Figure 6.70 Shear Load Capacity Check (<3844 kN) of Diagonally Reinforced Link Beam (**Istanbul**)

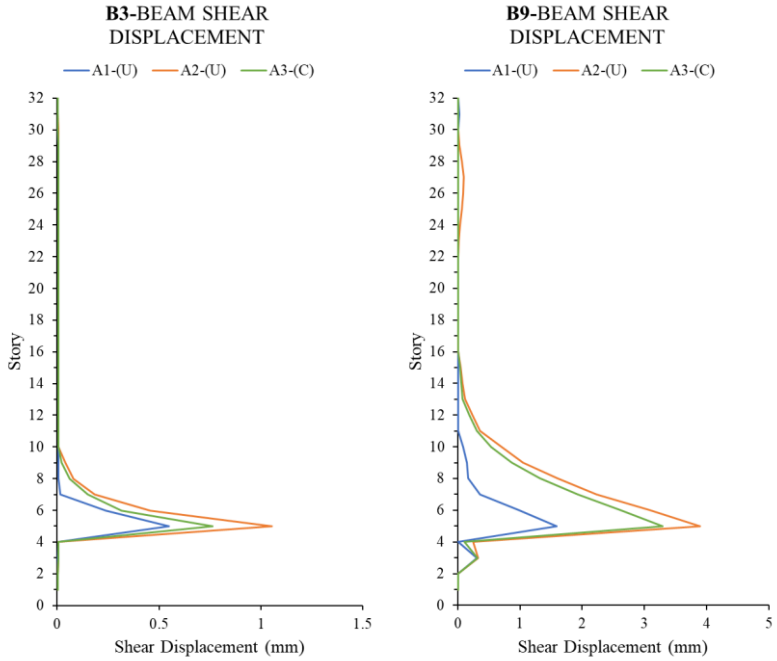

Figure 6.71 Shear Displacement Check (<39 mm (0.03 l_n)) of Diagonally Reinforced Link Beam (**Istanbul**)

6.3.6 Shear Load Capacity Check of Beams

In terms of the design of frame beam and link beams under the shear force, the $Demand_{mean,\ max}$/Capacity (D/C) ratios throughout stories are shown between Figure 6.72 and Figure 6.75. The D/C ratios of all the 60 cm deep beams in Ankara, except for conventionally reinforced link beams, are between 0.4-0.6. For the link beams (40/150) in Ankara, the shear laod D/C ratios exceeded limits and the preliminary design stirrups obtained as a result of linear analysis are insufficient.

Numerical comparisons were made between the three model alternatives,i.e., A1, A2 and A3, in terms of the beam shear load D/C ratios. The D/C ratio results were almost the same for all of beams with a height of 60 cm where shear force is not effective. However, for the conventionally reinforced link beam where shear force was active in the case study building in Ankara, the A1 uncalibrated model had 15-20 % less demand than results of the A3 calibrated model. The shear load D/C ratios of link beams (40/150) in the A2 non-calibration model and the A3 uncalibrated model were almost the same. Numerical comparisons between models can be observed in figures between Figure 6.76 and Figure 6.79.

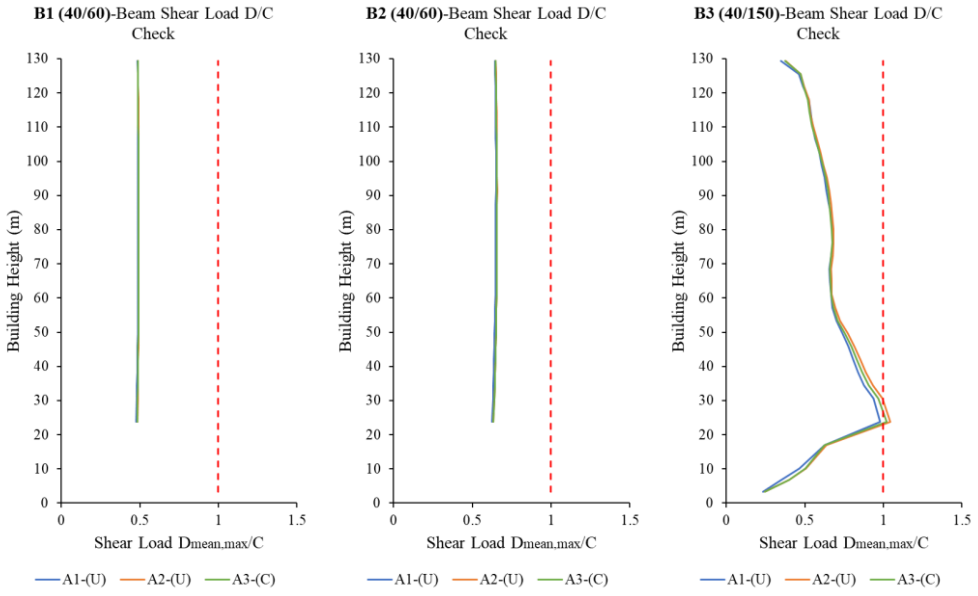

Figure 6.72 Beam Shear Load (D/C) Check between B1 & B3 (**Ankara**)

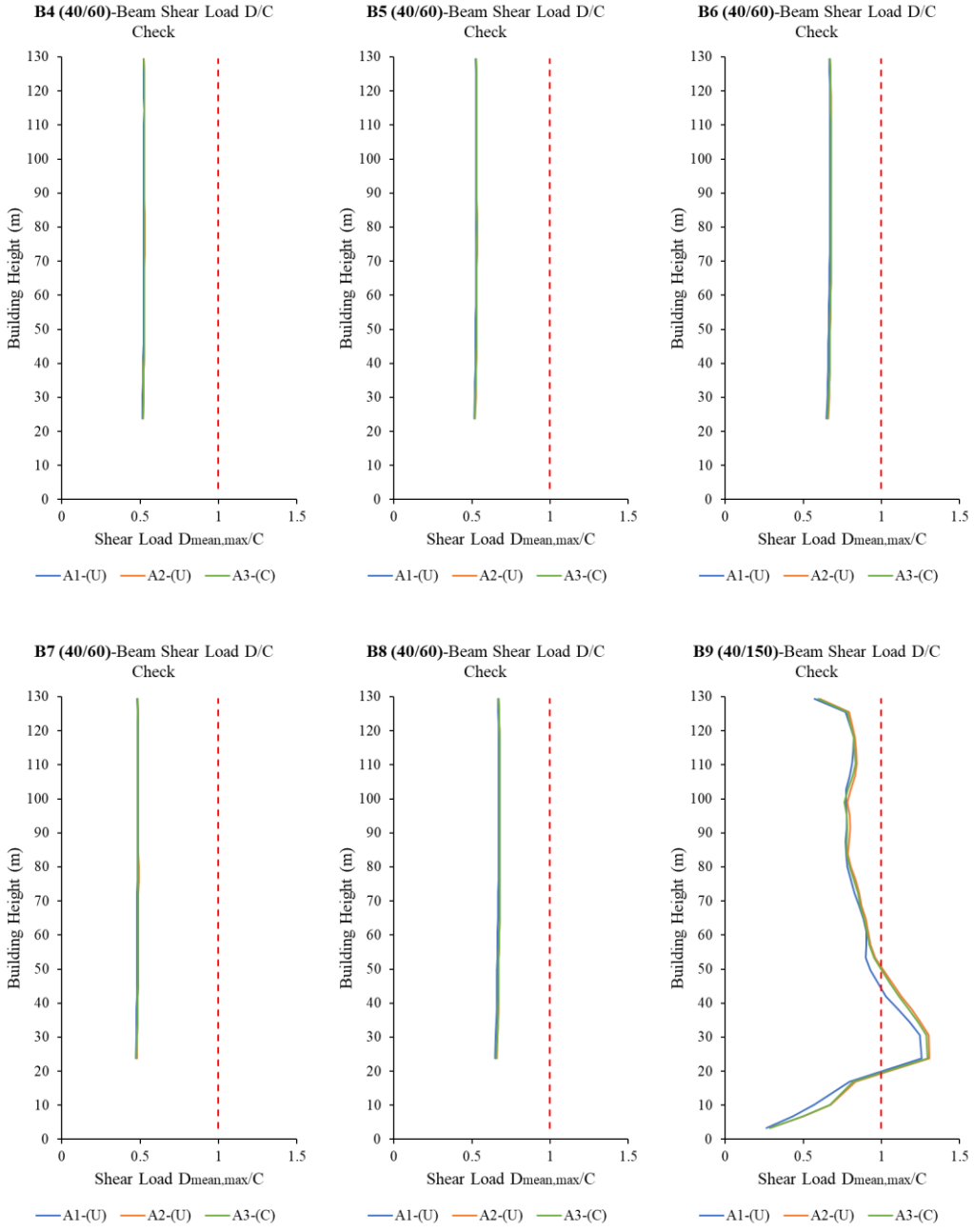

Figure 6.73 Beam Shear Load (D/C) Check between B1 & B6 (**Ankara**)

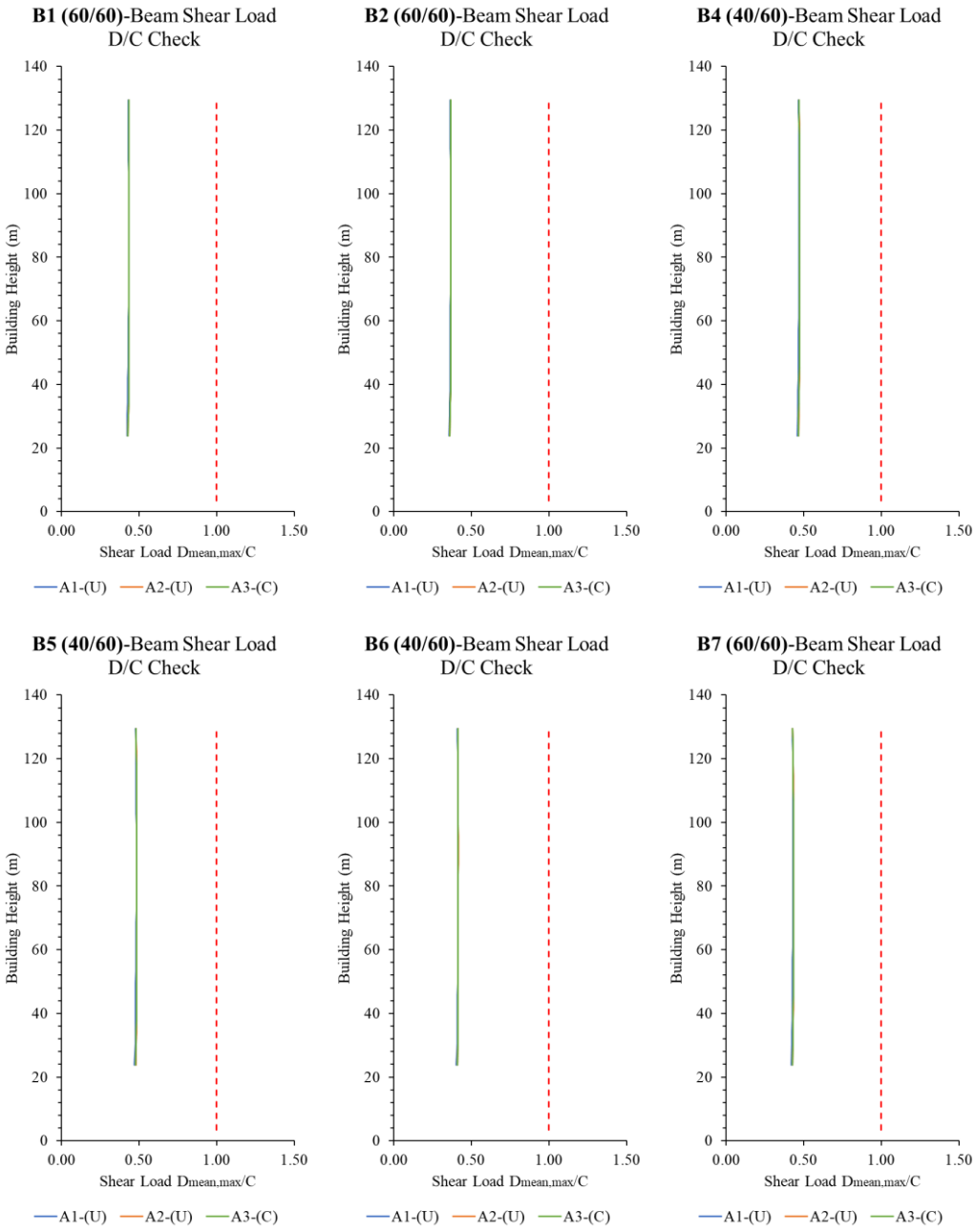

Figure 6.74 Beam Shear Load (D/C) Check between B1 & B7 (**Istanbul**)

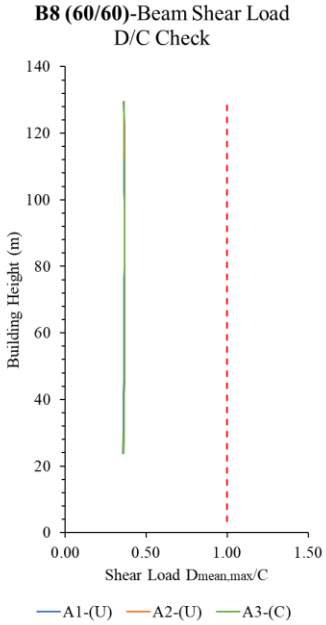

Figure 6.75 Beam Shear Load (D/C) Check for B8 (**Istanbul**)

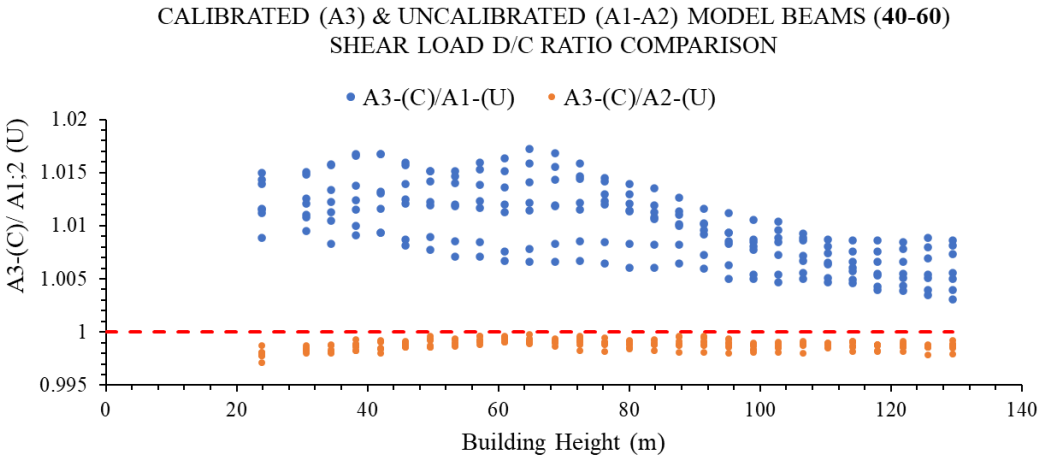

Figure 6.76 Calibrated (A3) & Uncalibrated (A1-A2) Model Beams (40/60) Shear load D/C Ratio Comparison (**Ankara**)

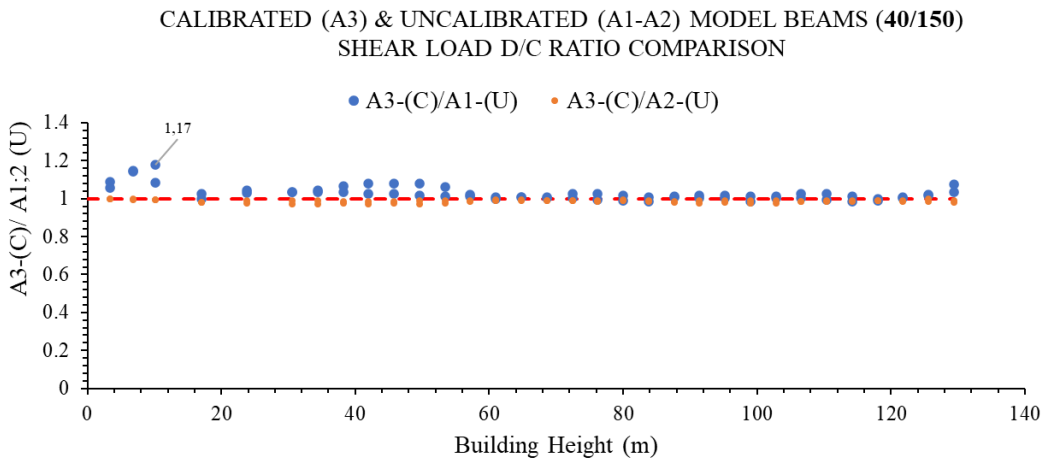

Figure 6.77 Calibrated (A3) & Uncalibrated (A1-A2) Model Beams (40/150) Shear load D/C Ratio Comparison (**Ankara**)

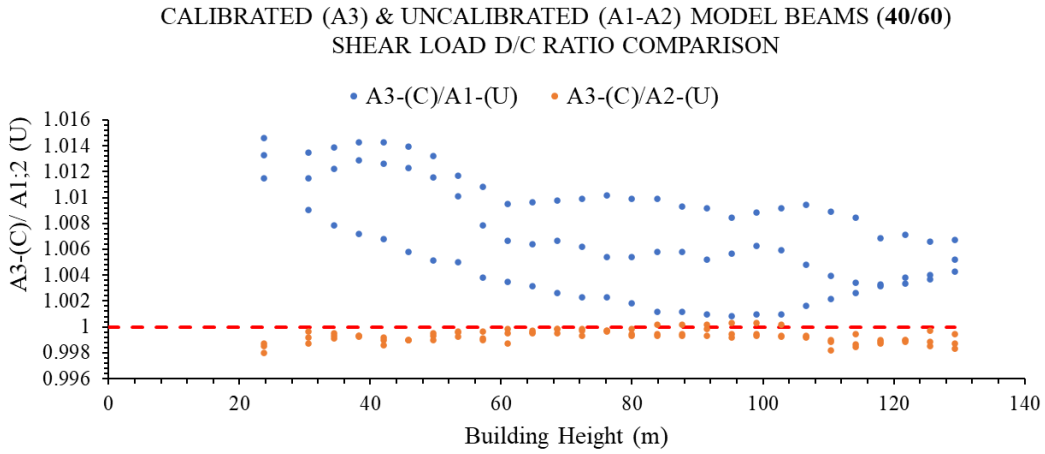

Figure 6.78 Calibrated (A3) & Uncalibrated (A1-A2) Model Beams (40/60) Shear load D/C Ratio Comparison (**Istanbul**)

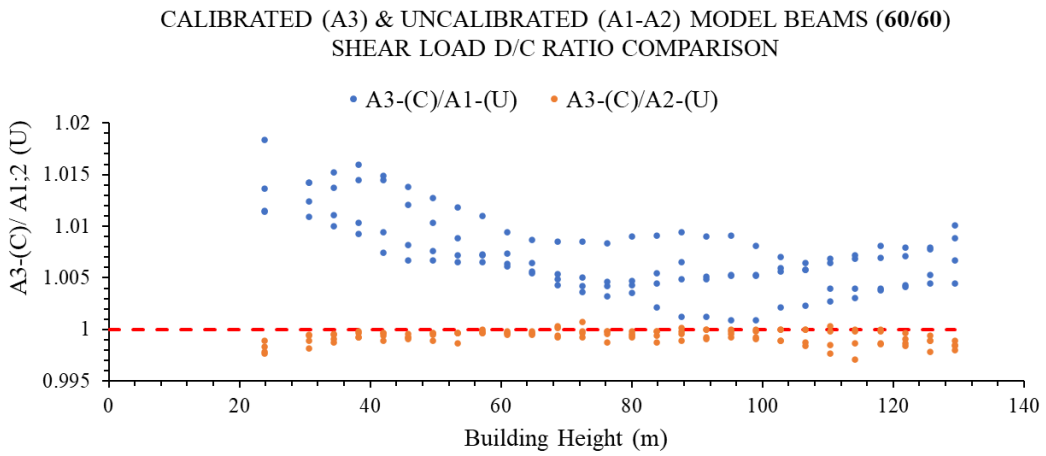

Figure 6.79 Calibrated (A3) & Uncalibrated (A1-A2) Model Beams (60/60) Shear load D/C Ratio Comparison (**Istanbul**)

6.3.7 Energy Dissipation Results

The dissipationf of earthquake energy provides engineers important information in terms of the building behavior. Building in both Ankara and Istanbul, 55-60 % of the total earthquake energy is dissipated through "damping", while 9-10 % is dissipated as “kinetic energy”. The "strain enegy" parts resulted from elastic displacement and "inelastic energy" dissipated by inelastic behavior differ as expected for buildings in Ankara and Istanbul. While dissipated inelastic energy is at the level of 8-10 % for the building in Ankara, this rate increases to about twice as high as 16-20 % in Istanbul. On the contrary, "strain energy" is around 12 % in the structure in Istanbul, while this value is around 24 % in the structure in Ankara. These expected results are shown in Figure 6.80 and Figure 6.81 for three different alternative models and two different earthquake zones. The energy ratio changes of the A3 (calibrated) model for 14 different earthquakes are also shown in Figure 6.82 and Figure 6.83.

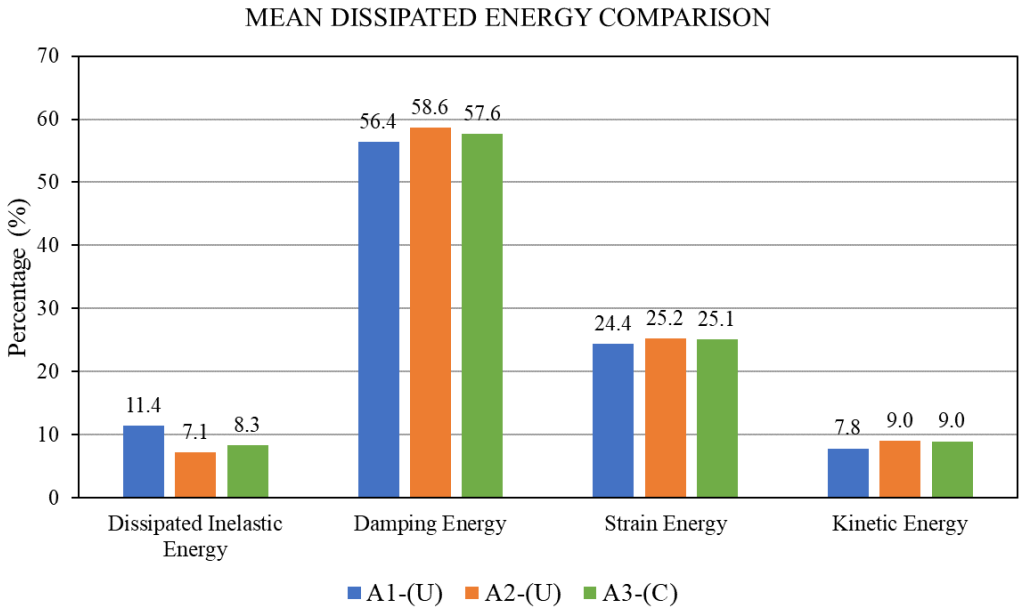

Figure 6.80 Energy Dissipation Comparisons of Calibrated (A3) & Uncalibrated (A1-A2) Models (**Ankara**)

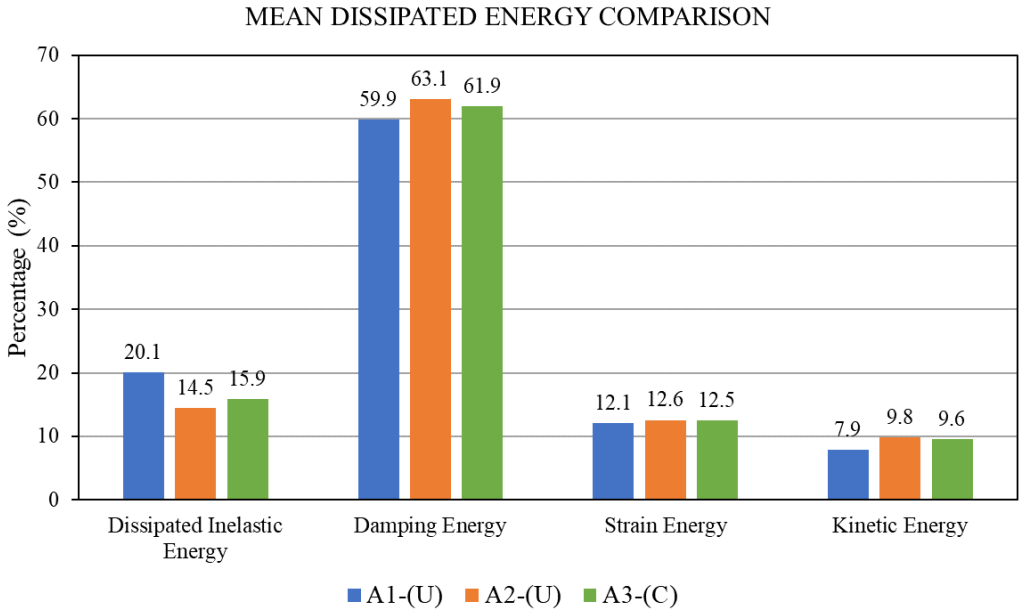

Figure 6.81 Energy Dissipation Comparisons of Calibrated (A3) & Uncalibrated (A1-A2) Models (**Istanbul**)

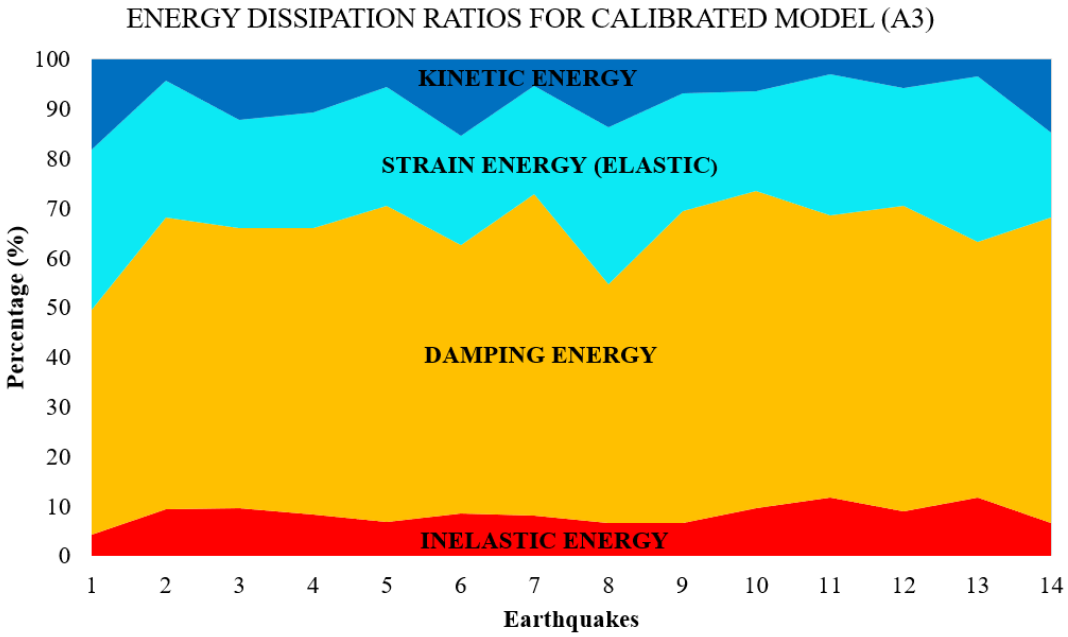

Figure 6.82 Energy Dissipation Distribution of 14 Earthquakes for Calibrated Model (A3) (**Ankara**)

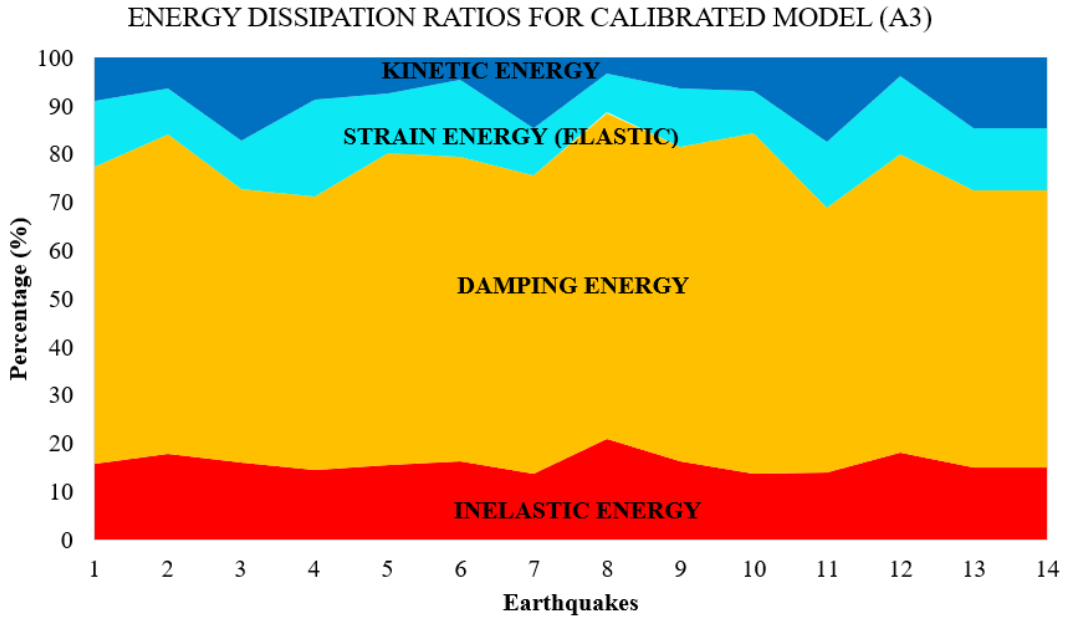

Figure 6.83 Energy Dissipation Distribution of 14 Earthquakes for Calibrated Model (A3) (**Istanbul**)

In the case study building examined, there are two basic types of structural member types that meet the earthquake force, which are wall and beams. The sharing of the dissipated inelastic energy between these two main structural member groups are given in Figure 6.84 and Figure 6.85 for three different model alternatives and two different earthquake zones. While 94 % and 6 % of the inelastic energy in the structure in Ankara is dissipated in the beams and the walls respectively, 80 % and 20 % of the inelastic energy in the building in Istanbul is shared in beams and core-wall, respectively.

While the A2 and A3 models give similar results in all energy sharing, the "inelastic dissipated energy" values in the A1 model are 33 % higher than in A2 and A3 models. In addition, in the A1 model, the “inelastic dissipated energy” is less in the walls and more in the beams than in the A2 and A3 models.

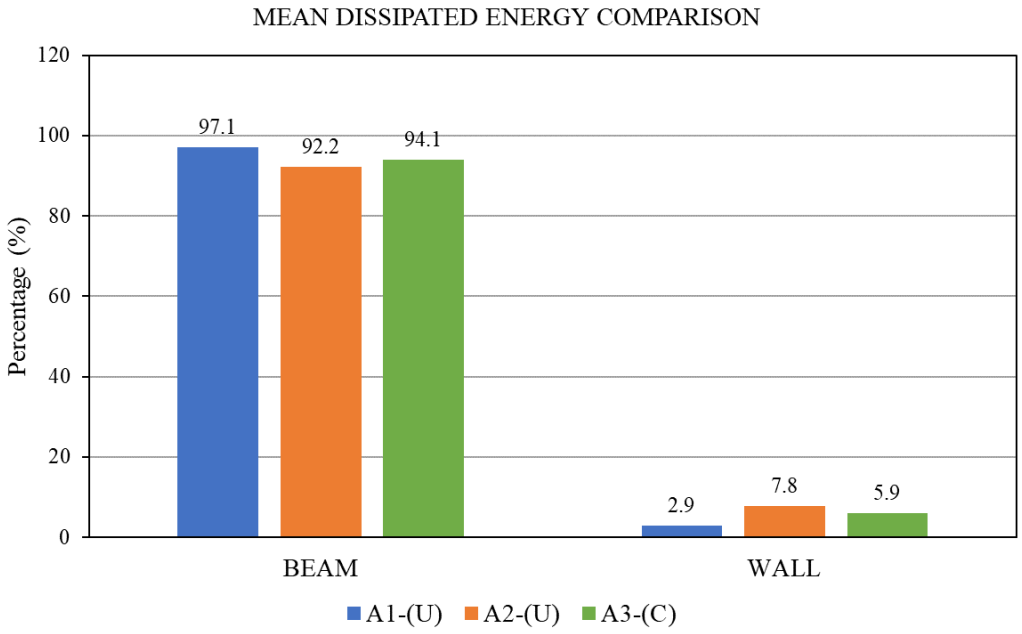

Figure 6.84 Mean Dissipated Inelastic Energy Distribution between Beams and Walls for Three Model Alternatives (**Ankara**)

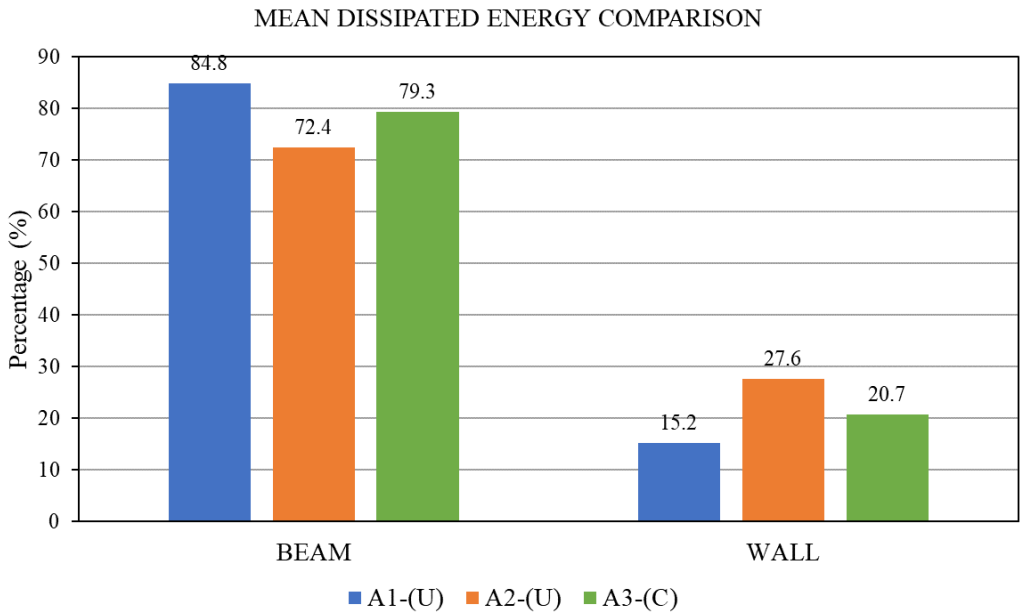

Figure 6.85 Mean Dissipated Inelastic Energy Distribution between Beams and Walls for Three Model Alternatives (**Istanbul**)

6.3.8 Summary of Performance Based Design of the Case Study Building

Case study building performance analysis results are given according to the topics and summary information for both earthquake zones in Table 6.14. More succinctly, Table 6.13 shows the insufficient design subjects. According to these, the wall horizontal reinforcements in both earthquake zones are insufficient according to the linear analysis. In both regions, there are walls exceeding maximum shear capacities and it is necessary to change the wall dimensions. According to the designs for the conventionally reinforced link beams in Ankara under shear force, the amount of stirrup should be increased. As for the concrete strain limit, when no increase is considered as a result of the P3D solution, all concrete strains are found sufficient for both regions. However, if the proposed "a" multiplication coefficient is used, fiber sections with insufficient concrete strain results are produced. Walls exceeding the maximum shear capacity, i.e. requiring a change in size, and fiber positions

exceeding the concrete strain limit as a result of the use of the "a" proposed coefficient are shown in Figure 6.86 on the same figure for both earthquake zones.

Table 6.15 provides numerical comparison results for the calibrated A3 model and uncalibrated A1 and A2 models. The table summarizes the ratios of the mean maximum D/C values between the models and summarizes the variations of the A1 and A2 uncalibrated values according to the calibrated A3 model. Accordingly, although the majority of all results are almost the same between the A2 model, which has very small energy degardation factors (0.2-0.3), and the calibrated A3 model, whose energy factors are medium (0.5-0.6), the A2 results give 5-10 % more results, pushing the limits more to give safe results in design. There is a difference of up to 10 % to 40 % between the results of the A1 uncalibrated model without the energy degardation factor (1.0) and the A3 calibrated model, giving results that are further smaller than the limits. Accordingly, it can be stated that energy degardation factor must be considered in performance based design.

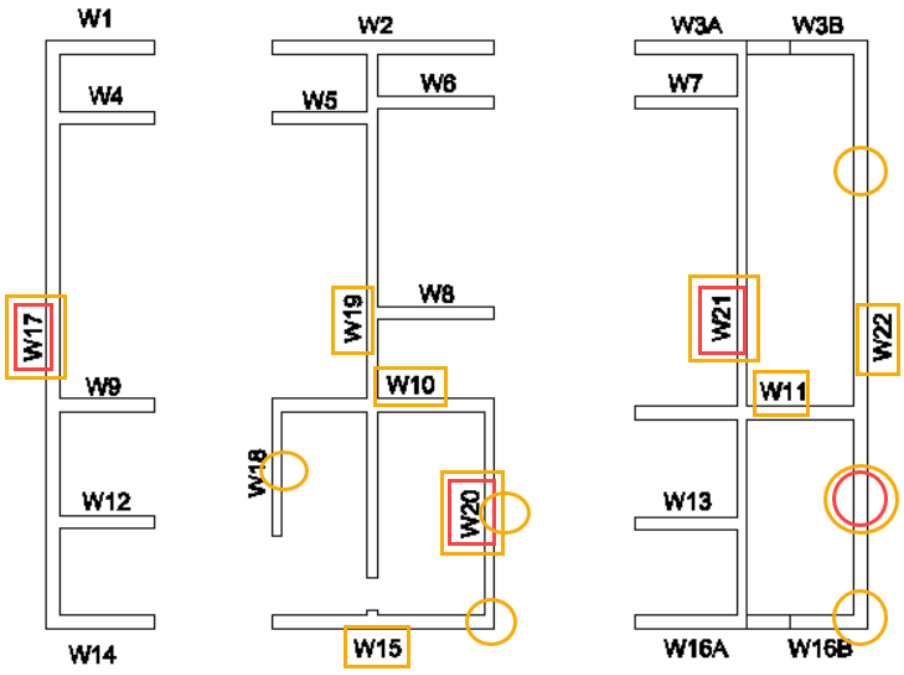

Figure 6.86 Walls Having Insufficient Shear Capacity (Orange Rectangle: in Istanbul; Red Rectangle: in Ankara) and Strain Fibers Passing the Limits after Using Proposed Multiplication factor "a" (Orange Circle: in Istanbul; Red Circle: in Ankara)

Table 6.13 PBD Summary Result Sufficiency Situation of Case Study Building

		PBD Result Sufficiency	
		Ankara	Istanbul
	Drift Check	✓	✓
Walls	Shear Check	✖	✖
	Concrete Strain	✓	✓
	Proposed Concrete Strain	✖	✖
	Reinforcement Strain	✓	✓
Beams	Rotation Check (40/60)	✓	✓
	Rotation Check (60/60)	--	✓
	Rotation Check (40/150)	✓	--
	Shear Displacement Check (60/150)	--	✓
	Shear Check (40/60)	✓	✓
	Shear Check (60/60)	--	✓
	Shear Check (40/150)	✖	--

Table 6.14 Summary of Performance Based Design of Case Study Building

SUBJECTS		ANKARA	ISTANBUL
Drift Check	General story mean nonlinear drift ratio	0.005	0.01
Walls Shear Design	# of walls whose linear analysis horizontal reinforcements revised after PBD	21/22	22/22
	# of walls pass max. shear capacity after PBD	3/22	8/22
	Max Shear D/C Ratio of Walls	1.04	1.2-1.5
Walls Strain Check	# of **reinforcement strain** gages passes the limit	none	none
	Max. mean **reinforcement strain** D/C ratio	0.15	0.2-0.25
	Max. mean **unconfined concrete strain** D/C ratio	0.3	0.3
	Max. mean confined **rectangular fibers concrete strain** D/C ratio	0.2	0.2
	Max. mean confined **flange fibers concrete strain** D/C ratio	0.2	0.2
	Max. mean **unconfined concrete strain** D/C ratio with usage of "a" proposed multiplication factor	1.03	1.17
	Max. mean **rectangular fibers concrete strain** D/C ratio with usage of "a" proposed multiplication factor	0.4	0.5
	Max. mean **flanged fibers concrete strain** D/C ratio with usage of "a" proposed multiplication factor	0.6	1.1
	# of **unconfined concrete strain gages** passes the limit with usage of "a" proposed multiplication factor	1	4
	# of **confined rectangular concrete strain gages** passes the limit with usage of "a" proposed multiplication factor	none	none
	# of **confined flanged concrete strain gages** passes the limit with usage of "a" proposed multiplication factor	none	2
Beam Rotation Check	# of beams pass max. rotation capacity after PBD	none	none
	Max Mean Rotation D/C Ratio of Beams	0.35	0.55
Beam Shear Check	# of beams with 60 cm height pass max. Shear capacity after PBD	none	none
	Max Mean Shear D/C Ratio of Beams with 60 cm Height	0.6	0.4
Link Beam Shear Check	# of link beams with 150 cm height pass max. shear capacity after PBD	2/2	none
	Max Mean Shear capacity or displacement D/C Ratio of Link Beams with 150 cm Height	1.3	0.1
Earthquake Energy Dissipation	Mean Inelastic Energy Sharing (%)	8%	16%
	Mean Strain Energy Sharing (%)	25%	12.5%
	Mean Damping Energy Sharing (%)	58%	62%
	Mean Kinetic Energy Sharing (%)	9%	9%
	Inelastic Energy Dissipation at Beams	94%	80%
	Inelastic Energy Dissipation at Walls	6%	20%

Table 6.15 Mean Maximum Results Comparison Ratios of Calibrated (A3) and Uncalibrated Models (A1 &A2) for Case Study Building in Ankara & Istanbul

		ANKARA						ISTANBUL					
		A3-(C) /A1-(U)			A3-(C) /A2-(U)			A3-(C) /A1-(U)			A3-(C) /A2-(U)		
		min.	max.	mean	min.	max.	mean	min.	max.	mean	min.	max.	mean
	Drift Check	1.02	**1.18**	1.10	0.98	0.99	0.99	0.99	**1.16**	1.08	0.98	0.99	0.99
Walls	Shear Check	0.95	**1.11**	1.03	0.97	1.00	0.99	0.93	**1.17**	1.05	0.96	1.00	0.98
	Concrete Strain	**0.90**	**1.18**	1.04	0.83	1.08	0.96	**0.88**	**1.19**	1.04	0.93	1.08	1.01
	Rein. Strain	**0.80**	**1.37**	1.09	0.93	1.02	0.98	0.91	**1.36**	1.14	0.94	1.02	0.98
Beams	Rotation Check (40/60)	0.98	**1.32**	1.15	0.96	1.00	0.98	1.09	**1.28**	1.19	0.97	0.99	0.98
	Rotation Check (60/60)	--	--	--	--	--	--	1.09	**1.35**	1.22	0.96	0.99	0.975
	Rotation Check (40/150)	0.98	**1.19**	1.09	0.96	1.03	1.00	--	--	--	--	--	--
	Shear Displa.t Check (60/150)	--	--	--	--	--	--	**0.70**	1.00	0.85	1.00	**1.39**	1.20
	Shear Check (40/60)	1.00	1.02	1.01	1.00	1.00	1.00	1.00	1.01	1.01	1.00	1.00	1.00
	Shear Check (60/60)	--	--	--	--	--	--	1.00	1.01	1.01	1.00	1.00	1.00
	Shear Check (40/150)	0.98	**1.18**	1.08	0.97	1.00	0.99	--	--	--	--	--	--
Energy Dissipation	Dissipated Inelastic Energy	--	--	**0.73**	--	--	**1.18**	--	--	**0.80**	--	--	**1.1**
	Strain Energy	--	--	1.02	--	--	1.00	--	--	1.04	--	--	1
	Damping Energy	--	--	1.02	--	--	0.98	--	--	1.03	--	--	0.98

CHAPTER 7

RESULTS AND INFERENCES OF THE THESIS WORK

Within the scope of this thesis work, both linear elastic design and performance-based designs of the case study tall building for two different seismic zones (in Ankara and Istanbul) were conducted according to TEC-2018 rules. With the linear elastic design, core-walls and beam dimensions were determined and all reinforcement details were calculated. Drift checks were made according to linear elastic analysis. The linear elastic analysis design results are detailed in Chapter 3. After linear elastic analysis of the case study tall building, selected load-deformation cyclic response experiments for wall and link beams were simulated in CSI Perform-3D program and calibration work was performed. With the calibration study, accurate modeling methods and appropriate P3D software parameter values were obtained. The sensitivity of the parameters is determined. Cyclic degradation factors, i.e., energy degradation factors, have been found to be the most effective parameters in the results. After the calibration study, performance-based designs of the case study buildings were carried out for two different earthquake zones. Strains were checked for walls and their designs were completed under shear force. Rotations were checked for the beams and their designs were also made under the shear force. Thus, differences between linear elastic design and performance-based nonlinear design results of the case study buildings in two different seismic regions (in Ankara and Istanbul) were observed. In addition, while performing performance-based designs of case study tall buildings, three different cyclic degradation factors including calibration values were selected and six different nonlinear models were created with two different earthquake zones. The results of the nonlinear design of models with three different cyclic degradation factors were compared. The PBD results of the A3 model with calibrated cyclic degradation factor and the models (A1, A2) with uncalibrated cyclic degradation factor were compared. In a performance-

based analysis in which calibration is not taken into account, the extent to which the results deviated was determined. The detailed conclusions of the thesis study are presented below in articles:

- Both linear and nonlinear performance analysis of the case study tall building was performed for two different seismic zones (Ankara and Istanbul) according to the Turkish Earthquake Code-2018 (TEC-2018). The preliminary design results of linear analysis in both regions were different and linear elastic design was found to be insufficient for both buildings. The nonlinear analysis of the case study building led to results requiring to change size of some of the walls in both earthquake zones because of insufficient shear capacity. Also, it was necessary to increase the horizontal reinforcements for the walls that did not require size changes for both earthquake zones. Performance based design of case study building in this thesis showed that nonlinear analysis is critical for the final design of walls.
- The design of the walls under shear force in the performance-based design in the case study building (CSB) has resulted in higher reinforcement amount than those obtained from linear analysis. Results are summarized in Table 7.1 and Table 7.2 respectively. Comparison of design base-shears for two different design approach can also be observed in Table 7.3 with base-shear demand ratios. While shear forces were increased with a dynamic magnification coefficient of "2.5" for linear analysis (Table 7.1), shear forces were increased with magnification coefficient "1.2-1.5" for the nonlinear analysis (Table 7.2) according to standard deviation. Design demand base-shear ratio of nonlinear analysis with respect to linear analysis was between "1.7" to "4.3" for case study tall building (Table 7.3). Although the spectral acceleration ratio of DD1 to DD2 was almost "2" for both seismic regions, base-shear force ratios without any correction or amplification were between "9" to"15". (Table 7.3). Shear forces from modal analysis with cracked member properties is lower than the mean base shear results of the nonlinear time history analysis of tall buildings. Period, stiffness, rigidity and behavior

of tall building continuously changes from initial to end time point of time history analysis. At nonlinear design approach, expected material strength of concrete and reinforcement was used. As an experience and trials, shear capacity increase for nonlinear design value was almost %50 percent compared to the shear force demand from linear analysis according to TEC-2018 clauses. However, the base-shear design demand increase was between "1.7" to "4.3". This shows that in high-rise buildings, if the demand/capacity (D/C) ratio is around to 1.0, it is likely that the horizontal reinforcements in the walls will change or walls sizes will be insufficient and require redesign based on the nonlinear design. Table 7.4 shows change and difference for both design stage in walls design under shear load for both seismic regions. Insufficient excessive shear capacity of walls at linear design stage led to the change of horizontal reinforcement or size of walls in both seismic regions after performance-based design of case study building. Based on this result, it can be recommended to design the walls of tall structures by limiting the demand/capacity (D/C) ratio not exceeding "0.5". In addition, the design of wall members with a constant shear rigidity reduction coefficient (0.5 G) in the plane behavior according to TEC-2018 seems questionable. The cracked rigidity values to compute shear demands should be further investigated in the nonlinear analysis stage to yield more consistent results with the linear elastic design stage. The choice of shear modulus rigidity reduction factor for walls between 0.1-0.5G, incline with the experimental observations may allow safer and suitable design.

Table 7.1 Linear Analysis Base-shear Values over Basement of CSB

		Ankara (ton)		Istanbul (ton)	
	Linear Analysis Base-shear over Basement	**X**	**Y**	**X**	**Y**
L-V1	Linear Modal Analysis Story Shear Force	461	791	1221	2277
L-V2	Minimum Limit Story Shear Force	1473	1473	3679	3679
L-V_d	Increased Design Shear Force (x **2.5**)	3683	3683	9198	9198

Table 7.2 Non-linear Analysis Base-shear Values over Basement of CSB

		Ankara (ton)		Istanbul (ton)	
	Nonlinear Analysis Base-shear over Basement (ton)	**X**	**Y**	**X**	**Y**
NL-V1	Mean Nonlinear Story Shear Force	5432	11735	11387	22464
NL-V_d	Mean Increased Design Story Shear Force (x **1.35**)	7333	15842	15373	30326

Table 7.3 Linear and Nonlinear Base-shear Demand Ratio of CSB

	Ankara		Istanbul	
	X	**Y**	**X**	**Y**
Design Base-shear Demand Ratio $_{Nonlinear}/_{Linear}$ **($NL\text{-}V_d$ / $L\text{-}V_d$)**	2.0	4.3	1.7	3.3
Base-shear Demand Ratio $_{Nonlinear}/_{Linear}$ **(NL-V1 / L-V1)**	11.8	14.8	9.3	9.9

Table 7.4 Nonlinear Shear Design Results of Walls after PBD for CSB

Walls Nonlinear Shear Design Results	**Ankara**	**Istanbul**
# of walls whose linear analysis horizontal reinforcements revised after PBD	21/22	22/22
# of walls pass max. shear capacity after PBD	3/22	8/22
Max Shear D/C Ratio of Walls	1.04	1.2-1.5

- Perform 3D Simulation calibration work was performed to compare with cyclic response test results for the most important building structural members, i.e, walls and link beams before the case study building 3D performance-based design. In this simulation study, the necessary work was done for the load-deformation cyclic response calibration work for rectangular, T-shaped and U-shaped walls. In the rectangular and T-shaped walls, the sensitivity degree of P3D material parameters on the result of cyclic response was investigated. Accordingly, the cyclic degradation factor

values (YULRX) of the reinforcement and the unloading stiffness factors (USF) are the sensitive parameters. Reinforcement yield and ultimate strength values are not very important, but they affect the result to a certain moderate extent. Incomplete or inadequate definitions in concrete material definitions have little effect on the cyclic response result. However, the most effective and dominant effect is the cyclic degradation factor (YULRX) values of the reinforcement under tension. Taking into account the embedded bar in concrete value proposed by Belarbi and Hsu (1994) for the reinforcement yield strength value (0.85-0.9 f_{sy}) is more compatible in terms of the test result yield strength. Although the effect of this small reduction in rebar models in 3D building performance-based design on the overall result is not considered much, a reduction of 10-15% can be achieved in terms of accurate modeling in the yield strength value in the reinforcement material model.

- While the ideal material parameters obtained after the sensitivity analysis of the material parameters and the cyclic response calibration results for the rectangular and T-shaped walls were satisfactory, however the same success could not be achieved for U-shaped. This may be because the selected U-shaped experimental data is not as solid as the rectangular and T-shaped wall experiment information. It is thought that experimental studies should further be conducted on non-rectangular walls to perform calibration studies.
- With the rectangular and T-shaped test walls simulation study, successful calibration results were obtained in cyclic response curves, lateral displacement and base level reinforcement strain profile results. However, the P3D base level concrete strain results are much lower than test results due to the plane section remains plane hypothesis where the other results are compatible with the test results. For estimating the concrete strain demands more accurately, the coefficient "a", which expresses the ratio of the test result to the model result, is proposed (Equation 7.1).

$$a=\varepsilon_{c,experiment} / \varepsilon_{c,P3D\ model} \quad \textbf{(7.1)}$$

The coefficient “a” is approximately "2" in the rectangular boundary section for drift rates of between 0.5% and 2.0% (Figure 7.1). When a wider "flanged boundary" condition occurs like the concrete compression section parts in the T-shaped walls, this coefficient ranges from "4-8" for drifts between 0.5% and 1.5%.

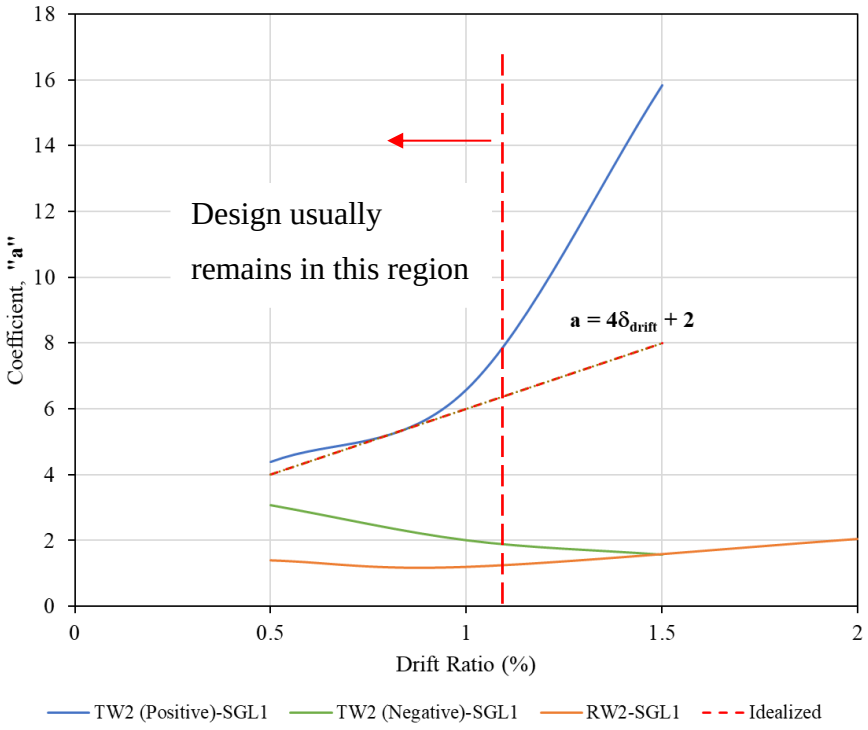

Figure 7.1 TW2 (T-Shaped) and RW2 (Rectangular) Walls Concrete Strain Experiment-P3D Model Comparison Coefficient “a” vs Drift Ratio Graph

Walls concrete strain results of the 3D case study tall building performance-based analysis can be multiplied by the proposed "a" coefficient to realistically estimate the seismic demands. According to the prevailing drift ratios of 0.5 % and 1.0 % in Ankara and Istanbul, "rectangular boundary" concrete fiber strains were increased by multiplying "2" and "flanged boundary" concrete fiber strains were increased by "4" and "6". In both earthquake zones, the concrete vertical strain values were found to be below the strain limits, however in the case of using an increase with the proposed

"a" coefficient, there were some concrete strain fibers that exceeded the limits. These limit violations were especially in unconfined concrete fiber sections with much lower limits than confined concrete. In the building model in Istanbul, there were a notable number of concrete strains that exceeded the limits. Since there has never been a situation that has exceeded the concrete strain limit among the engineers who are commonly involved in building design with Perform 3D, the issue of the accuracy of the model calculation results has always been questioned among them. With numerical data and calibration study, for drift levels below about 1.2%, a possible simple and practical value of coefficient “a” is given in Table 7.5.

Table 7.5 Proposed “a” Multiplication Factor for Concrete Fiber Strain

Concrete Fiber Condition	**a**
Confined rectangular boundary concrete fiber	2
Confined flanged boundary concrete fiber (in T-L shape region)	$4\ \delta_{drift}^{*}+2$
Unconfined concrete fiber	$4\delta_{drift}^{*}+2$

$^{*}\ \delta_{drift}$ in “%”

To demonstrate the appropriateness of the proposed coefficient "a", a strain profile examination just over basement level was performed on the core-wall group to observe the values at the strain gage points numbered in Figure 7.2 for case study tall building. Strain profile result check was made for the drift rate between 0.5-3.0% in the trial study for the structure in Ankara (Figure 7.3). Although there are meshed panel assignments in the wall vertically, resulting in nearly "plane section remains plane" observed in the group wall behavior. For the Perform 3D model results, concrete strain values remained very low away from the test limits in requiring some adjustment in future studies.

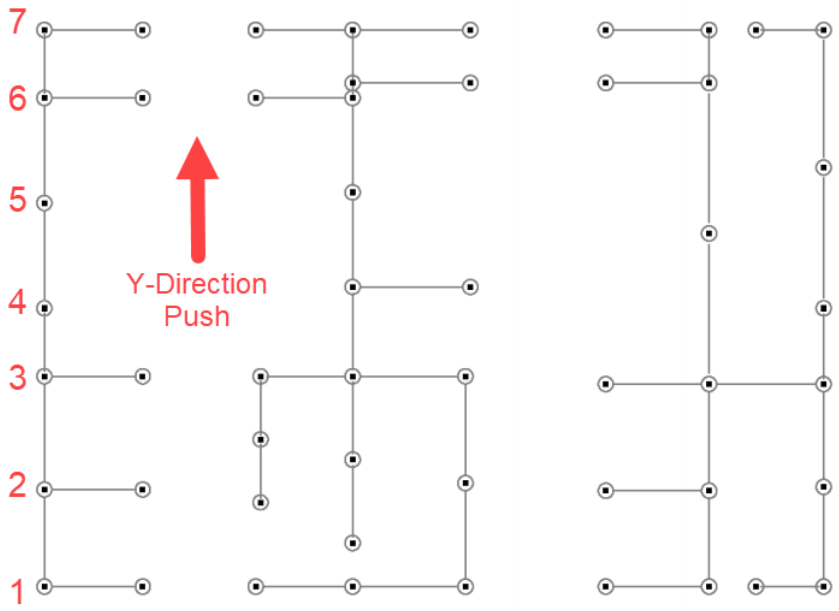

Figure 7.2 Check Strain Points of Selected Wall for Y- Direction Push

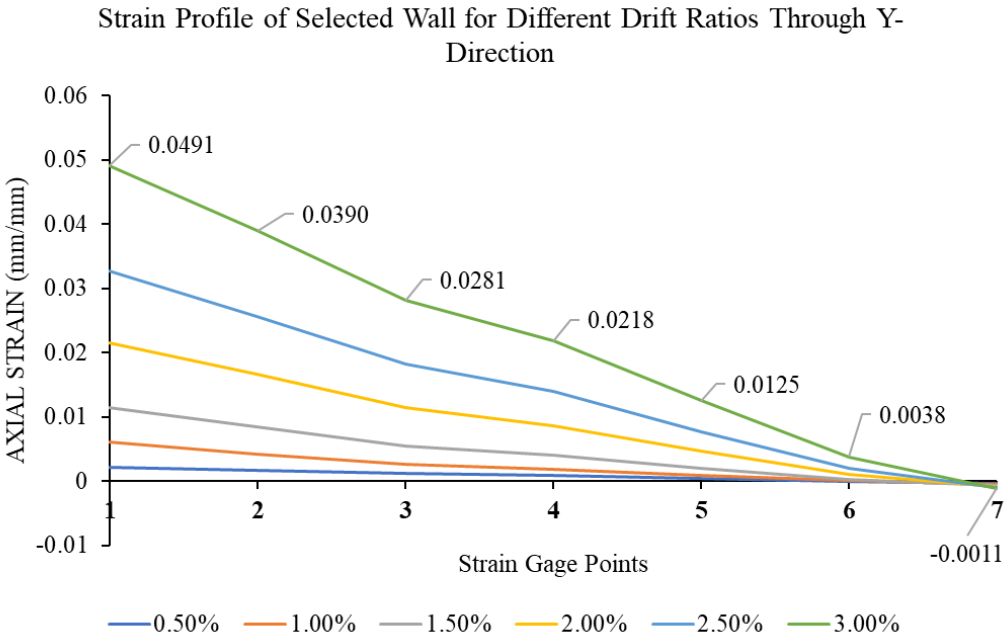

Figure 7.3 Strain Profile Observation for Selected Strain Points of Wall

This "a" increment coefficient proposed for concrete vertical compression strain was obtained for wall test samples under compression force "0.07-0.075 f_{ck} A_g". Conducting similar studies in wall test samples under different axial load stages will allow more accurate recommendations to be made in this regard.

- Mesh sensitivity work was done for walls. Both vertically and horizontally were modeled with different mesh options. For models with different concrete and reinforcement fiber arrangement alternatives made in the plan for rectangular walls, cyclic response results were compared with ideal model results. According to the thickness of the walls, the concrete fiber model with an aspect ratio of 1x1 is ideal for mesh work on the plan. In the wall boundary sections, reinforcement fibers can be meshed densely as 0.5x1 aspect ratio reinforcement fiber modeling will be appropriate according to the wall thickness.
- In the vertical mesh study, the fact that the mesh height is not more than the floor height is verified as a result of comparing both the base level strain and cyclic response results of different mesh options with the test results. It is also verified with test results that "hinge length of walls is minimum of one half of cross section depth and story height" according to ASCE-41 in the critical hinge sections of walls. In the case study building model, meshing of walls was done with the half of the floor heights on the 6.8 m story height at critical region of building, and so the strain gage length definition also was taken as the half of the floor heights at this critical region.
- In the Perform 3D model, the results of the fiber modeling options of walls, i.e., the "auto-size" and "fixed-size" modeling modules in the plan were compared in terms of both cyclic response and strain profile. The results of the "auto-size" module, which is easier to model, and the more laborious "fixed-size" module, have similar results in both cases. Strains results were a little more in the "auto-size" module, concluding in results that were on the safer side in terms of design. As a result, the easy-to-use "auto-size" module

of walls in the P3D program can be preferred for the fiber mesh option in the wall plan.

- Calibration work was also performed in accordance with the selected experiment for modeling in P3D software both for diagonally and conventionally reinforced link beam. In addition to the modeling method for both types of beams, cyclic degradation factor values compatible with the tests were obtained. Diagonally reinforced link beam was modeled with both "moment hinge approach" and "shear hinge approach" and calibrated. The cyclic degradation factors obtained as a result of calibration are given in summary in Table 7.6 for both beam and walls reinforcement material. In addition, the cyclic degradation factors recommended in the report of Pacific Earthquake Engineering Research Center, "Case Studies of the Seismic Performance of Tall Buildings Designed by Alternative Means" were added. Calibration study results and report recommendation seem to be compatible. In the wall structural member, the cyclic energy degradation factor under compression of concrete material and reinforcement are not very effective in the results and their sensitivities are low.

Table 7.6 Cyclic Degradation Factors after Calibration Work and Recommendation Values at PEER Center Report (Moehle et al., 2011)

	PROPOSED CYCLIC DEGRATION FACTORS						
	CALIBRATION WORK				PEER CENTER REPORT		
	Walls	Diagonally Reinforced Link Beam		Frame Beam	Walls	Diagonally Reinforced Link Beam	Frame Beam
	Reinfor.	Shear Hinge Approach	Moment Hinge Approach		Reinfor.	Shear Hinge Approach	
Y	0.65	1	0.5	0.3	0.7	0.5	0.24
U	0.65	0.65	0.5	0.25	0.68	0.45	0.23
L	0.65	0.65	0.5	0.22	0.64	0.4	0.22
R	0.65	0.65	0.5	0.2	0.62	0.35	0.21
X	0.65	0.65	0.5	0.2	0.6	0.35	0.2
USF	-0.5	0	0	1	0	0	0

- After obtaining the proper modeling methods and cyclic degradation factors as a result of calibration, in order to observe the extent to which these factors affect the 3D Case study building performance-based design results, A1, A2, A3 models with 3 different energy degradation values were analyzed in 2 different earthquake zones and the design results of six models were compared (Figure 7.4).

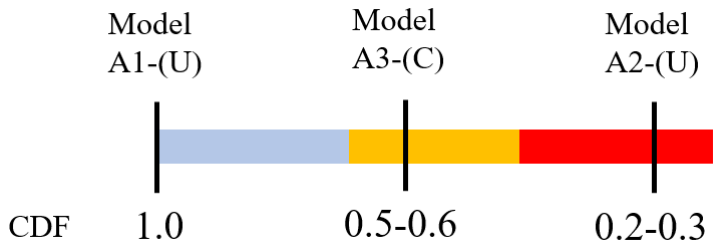

Figure 7.4 Cyclic Degradation Factor Alternatives for P3D Models

A1 and A2 are used with non-calibrated values in the case study building models, while calibrated values are used in A3. The summary values used are shown in Table 7.7. Table 7.8 shows the comparison of the performance-based design results of the models. Accordingly, cyclic energy degradation factors must be used in the models. The difference observed to be up to 30 % between the A1 model not include energy factors than the other models (A2, A3). A1 model results were less and unsafe side than the other models (A2, A3). The difference between the A3 model with medium cyclic energy degradation values, and the A2 uncalibrated model with low cyclic energy degradation values was between 0.25-0.35 in half order of the A3, which causes more energy reduction, is not very much. However, A2 model results remains on the safe side of the design by giving 5-10 % more D/C results than A3 model. As a results, in the performance analysis, it is more appropriate to use low cyclic degradation factor values to stay in the safe side of the design.

Table 7.7 A1, A2 ve A3 Model Cyclic Degradation Parameters

		A1-(U)	A2-(U)	A3-(C)
Walls Reinforcement	Y	1.0	0,35	0,65
	U	1.0	0,35	0,65
	L	1.0	0,35	0,65
	R	1.0	0,35	0,65
	X	1.0	0,35	0,65
	USF	---	1	-0,5
Beams with 60 cm Height	Y	1.0	0,2	0,3
	U	1.0	0,2	0,25
	L	1.0	0,15	0,22
	R	1.0	0,15	0,2
	X	1.0	0,15	0,2
	USF	---	0,75	1
Conventionally Reinforced Link Beams	Y	1.0	0,3	0,5
	U	1.0	0,25	0,5
	L	1.0	0,22	0,5
	R	1.0	0,2	0,5
	X	1.0	0,2	0,5
	USF	---	1	0
Diagonally Reinforced Link Beams	Y	1.0	0,5	1
	U	1.0	0,3	0,65
	L	1.0	0,3	0,65
	R	1.0	0,3	0,65
	X	1.0	0,3	0,65
	USF	---	1	-0,5

Table 7.8 Mean Maximum Results Comparison Ratios of Calibrated (A3) and Uncalibrated Models (A1 &A2) for Case Study Building in Ankara & Istanbul

		ANKARA						ISTANBUL					
		A3-(C) /A1-(U)			A3-(C) /A2-(U)			A3-(C) /A1-(U)			A3-(C) /A2-(U)		
		min.	max.	mean	min.	max.	mean	min.	max.	mean	min.	max.	mean
	Drift Check	1.02	**1.18**	1.10	0.98	0.99	0.99	0.99	**1.16**	1.08	0.98	0.99	0.99
Walls	Shear Check	0.95	**1.11**	1.03	0.97	1.00	0.99	0.93	**1.17**	1.05	0.96	1.00	0.98
	Concrete Strain	**0.90**	**1.18**	1.04	0.83	1.08	0.96	**0.88**	**1.19**	1.04	0.93	1.08	1.01
	Rein. Strain	**0.80**	**1.37**	1.09	0.93	1.02	0.98	0.91	**1.36**	1.14	0.94	1.02	0.98
Beams	Rotation Check (40/60)	0.98	**1.32**	1.15	0.96	1.00	0.98	1.09	**1.28**	1.19	0.97	0.99	0.98
	Rotation Check (60/60)	--	--	--	--	--	--	1.09	**1.35**	1.22	0.96	0.99	0.975
	Rotation Check (40/150)	0.98	**1.19**	1.09	0.96	1.03	1.00	--	--	--	--	--	--
	Shear Displa.t Check (60/150)	--	--	--	--	--	--	**0.70**	1.00	0.85	1.00	**1.39**	1.20
	Shear Check (40/60)	1.00	1.02	1.01	1.00	1.00	1.00	1.00	1.01	1.01	1.00	1.00	1.00
	Shear Check (60/60)	--	--	--	--	--	--	1.00	1.01	1.01	1.00	1.00	1.00
	Shear Check (40/150)	0.98	**1.18**	1.08	0.97	1.00	0.99	--	--	--	--	--	--
Energy Dissipation	Dissipated Inelastic Energy	--	--	**0.73**	--	--	**1.18**	--	--	**0.80**	--	--	**1.1**
	Strain Energy	--	--	1.02	--	--	1.00	--	--	1.04	--	--	1
	Damping Energy	--	--	1.02	--	--	0.98	--	--	1.03	--	--	0.98

- A2 uncalibrated model with very low cyclic reduction factors showed results at the safer side of the design than the other models (A1, A3). This showed us that if an engineer using the Perform 3D software conducted performance-based design according to the existing TEC-2018 rules without adjusting the calibration of structural members, it is seen that obtained results will be on the safe side with low cyclic degradation factor values and as if accurate modeling in line with the limits given by the regulation, as long as the cyclic degradation factor value is not taken as "none (1.0)".
- The beam rotation limit, θ_p^{CP} in TEC-2018 depends on the ultimate curvature calculation, ϕ_u. While conducting the ultimate curvature calculation, ϕ_u, code clause restricts the engineers to use reinforcement strain limit as only 40 % of the ultimate reinforcement strain (ε_s=0.4 ε_{su}) in TEC-2018 (5.8.1.2). This restriction causes the very low beam rotation limits, θ_p^{CP} that is very limited for seismic regions. According to ASCE 41-17, the beam rotation collapse prevention limits vary between 0.02-0.05, while according to TEC-2018, the ultimate curvature calculation, ϕ_u, is calculated for beam rotation limits, θ_p^{CP} as on the order of 0.01. This value order was also valid for the case study building beams. The experience of engineers performing nonlinear analysis is in line with this opinion. For this reason, it is recommended to take reinforcement strain, ε_s= ε_{su} in the calculation of beam rotation limit, θ_p^{CP}. Accordingly, the calculation values of beam rotation limits, θ_p^{CP} are compatible with ASCE 41-17. To determine the rotation limits (Table 6.9) of the beams of the case study building, reinforcement strain was taken as ε_s= ε_{su} instead of ε_s=0.4 ε_{su}.

REFERENCES

Computers and Structures, Inc., C. (2006). *Peform Components and Elements For Perform-3D and Perform-Collapse Version 4*. www.csiberkeley.com

Computers and Structures, I. . C. (2006). *PERFORM-3D Nonlinear Analysis and Performance Assessment for 3D Structures User Guide*. www.csiberkeley.com

Ile, N., & Reynouard, J. M. (2005). Behaviour of U-shaped walls subjected to uniaxial and biaxial cyclic lateral loading. *Journal of Earthquake Engineering*, *9*(1), 67–94. https://doi.org/10.1080/13632460509350534

Lowes, L. N., Lehman, D. E., & Baker, C. (2016). Recommendations for Modeling the Nonlinear Response of Slender Reinforced Concrete Walls Using PERFORM-3D. *SEAOC Convention*, *December*, 1–18.

Moehle, J., Bozorgnia, Y., Jayaram, N., Jones, P., Rahnama, M., & Shome, N. (2011). Case Studies of the Seismic Performance of Tall Buildings Designed by Alternative Means – Task 12 Report for the Tall Buildings Initiative: Final Report to California Seismic Safety Commission and California Emergency Management Agency. *Pacific Earthquake Engineering Research Center*, *July*.

Naish, D., Fry, A., Klemencic, R., & Wallace, J. (2013a). Reinforced Concrete Coupling Beams — Part I : Testing. *ACI Structural Journal*, *110*(6), 1057–1066. https://www.proquest.com/docview/1464009328?pq-origsite=gscholar&fromopenview=true

Naish, D., Fry, A., Klemencic, R., & Wallace, J. (2013b). Reinforced Concrete Coupling Beams — Part II : Modeling. *ACI Structural Journal*, *110*(6), 1067–1076. https://www.concrete.org/publications/internationalconcreteabstractsportal/m/details/id/51686161

NIST. (2014). (For Thesis) Guidelines for Nonlinear Structural Analysis for Design of Buildings Part I-General Applied Technology Council. *NIST GCR 17-917-46v1*.

Orakcal, K., Wallace, J. W., & Conte, J. P. (2004). Nonlinear modeling and analysis of slender reinforced concrete walls. *ACI Structural Journal*, *101*(5), 688–698. https://doi.org/10.14359/13391

Pacific Earthquake Engineering Center. (2017). Guidelines for Performance-Based Seismic Design of Tall Buildings. *PEER Report 2017/06, May*, 147.

PEER/ATC 72-1. (2010). Modeling and acceptance criteria for seismic design and analysis of tall buildings. *Applied Technology Council*, 1. http://peer.berkeley.edu/peer_ground_motion_database

Seismic Evaluation and Retrofit of Existing Buildings. (2017). In *Seismic Evaluation and Retrofit of Existing Buildings*. https://doi.org/10.1061/9780784414859

TBDY-2018. (2018). *Türkiye Bina Deprem Yönetmeliği*. 395. http://www.resmigazete.gov.tr/eskiler/2018/03/20180318M1.pdf

APPENDICES

A. Shear Load Capacity Diagrams of Walls for Three Alternative Models of the Case Study Building in Ankara (Performance Based Design)

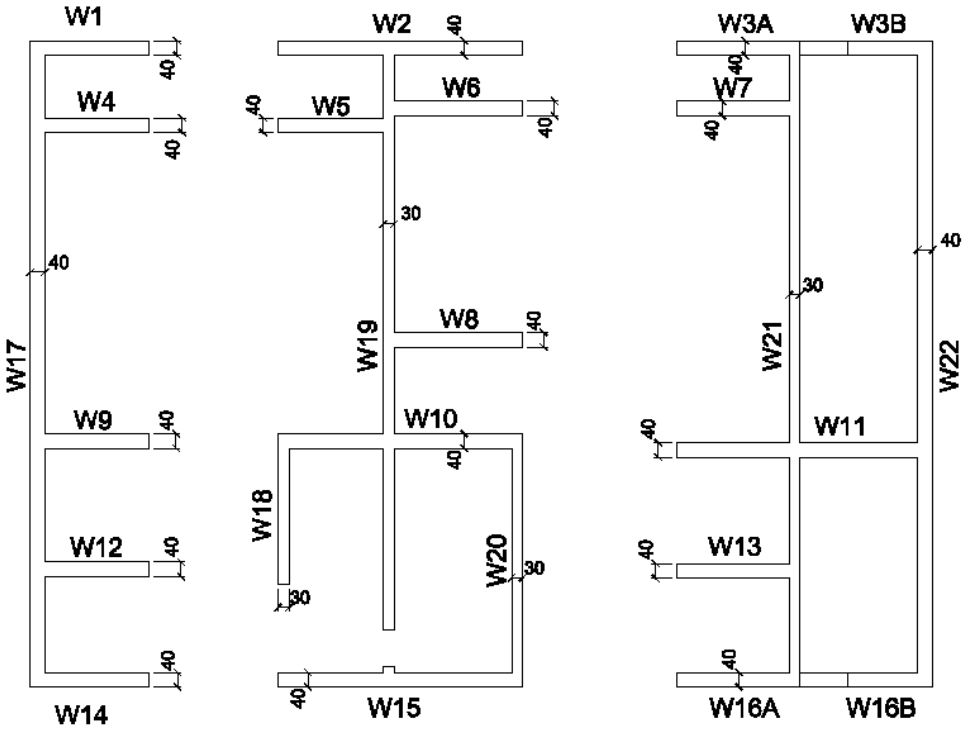

Figure A.1 Wall Labels

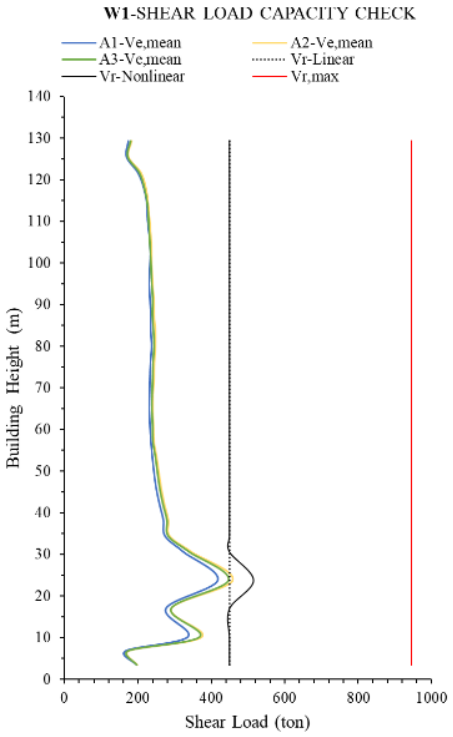
W1-SHEAR LOAD CAPACITY CHECK
A1-Ve,mean
A2-Ve,mean
A3-Ve,mean
Vr-Linear
Vr-Nonlinear
Vr,max
Building Height (m)
Shear Load (ton)

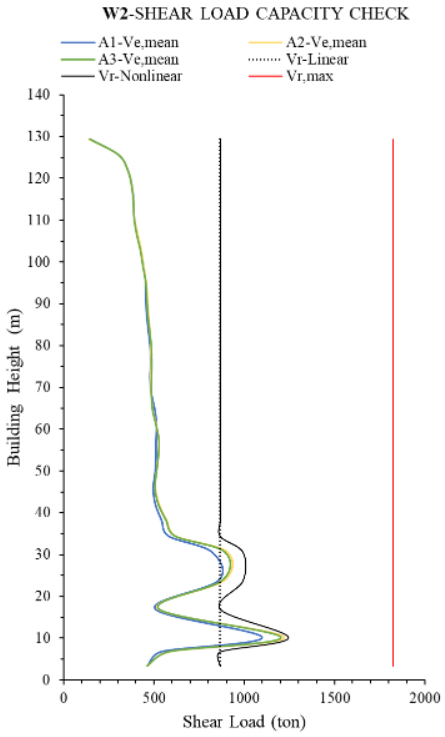
W2-SHEAR LOAD CAPACITY CHECK
A1-Ve,mean
A2-Ve,mean
A3-Ve,mean
Vr-Linear
Vr-Nonlinear
Vr,max
Building Height (m)
Shear Load (ton)

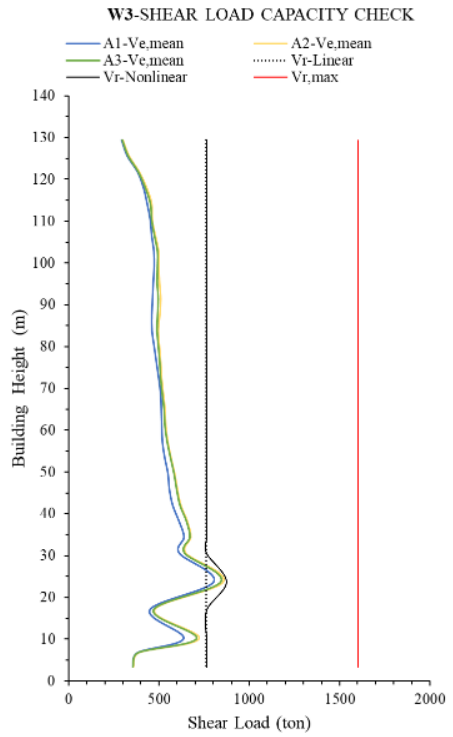
W3-SHEAR LOAD CAPACITY CHECK
A1-Ve,mean
A2-Ve,mean
A3-Ve,mean
Vr-Linear
Vr-Nonlinear
Vr,max
Building Height (m)
Shear Load (ton)

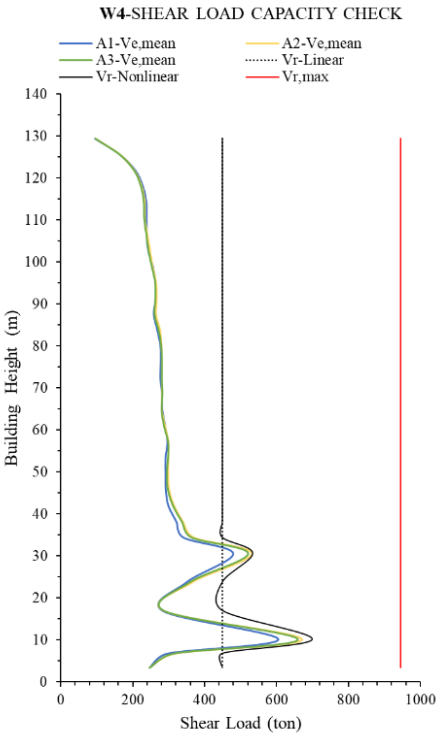
W4-SHEAR LOAD CAPACITY CHECK
A1-Ve,mean
A2-Ve,mean
A3-Ve,mean
Vr-Linear
Vr-Nonlinear
Vr,max
Building Height (m)
Shear Load (ton)

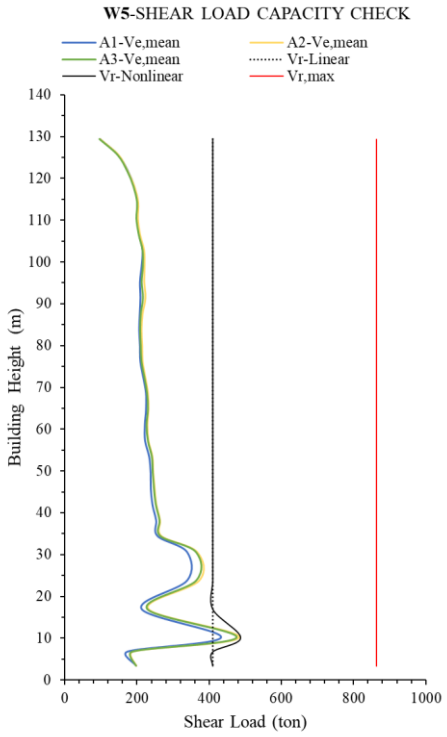
W5-SHEAR LOAD CAPACITY CHECK
A1-Ve,mean
A2-Ve,mean
A3-Ve,mean
Vr-Linear
Vr-Nonlinear
Vr,max
Building Height (m)
Shear Load (ton)

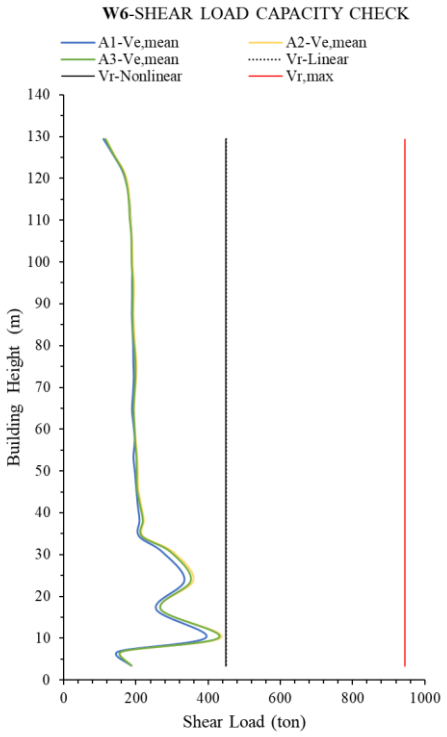
W6-SHEAR LOAD CAPACITY CHECK
A1-Ve,mean
A2-Ve,mean
A3-Ve,mean
Vr-Linear
Vr-Nonlinear
Vr,max
Building Height (m)
Shear Load (ton)

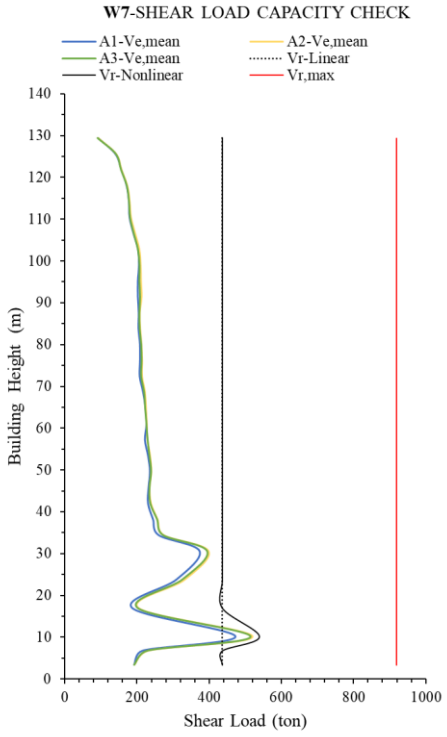
W7-SHEAR LOAD CAPACITY CHECK
A1-Ve,mean
A2-Ve,mean
A3-Ve,mean
Vr-Linear
Vr-Nonlinear
Vr,max
Building Height (m)
Shear Load (ton)

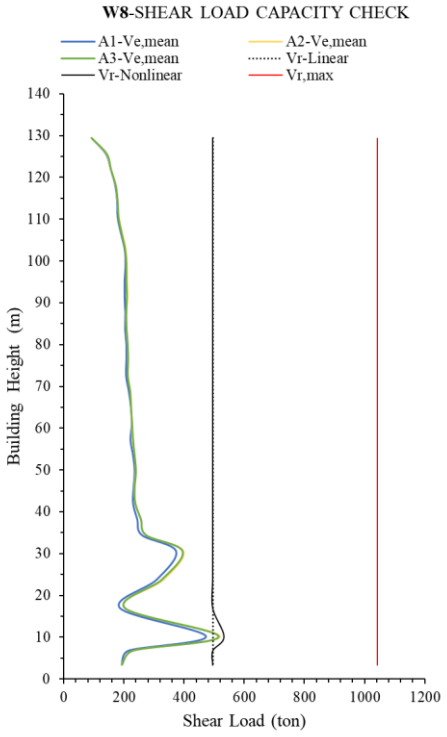
W8-SHEAR LOAD CAPACITY CHECK
A1-Ve,mean
A2-Ve,mean
A3-Ve,mean
Vr-Linear
Vr-Nonlinear
Vr,max
Building Height (m)
Shear Load (ton)

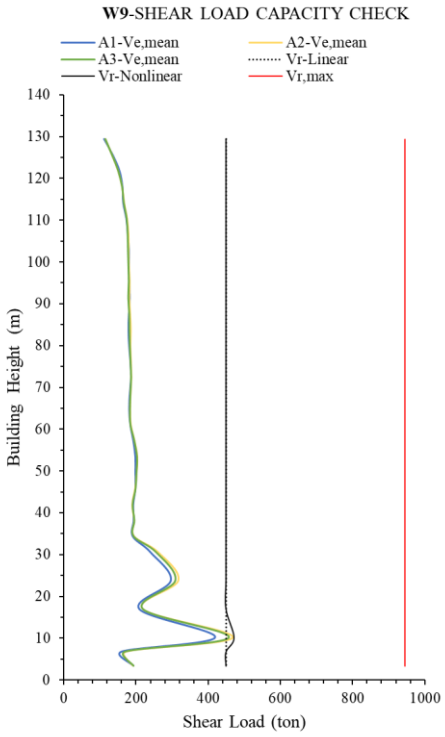
W9-SHEAR LOAD CAPACITY CHECK
A1-Ve,mean
A2-Ve,mean
A3-Ve,mean
Vr-Linear
Vr-Nonlinear
Vr,max
Building Height (m)
Shear Load (ton)

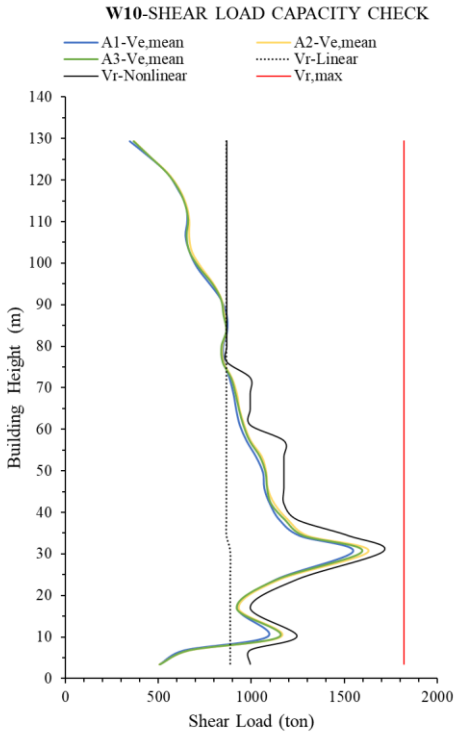
W10-SHEAR LOAD CAPACITY CHECK
A1-Ve,mean
A2-Ve,mean
A3-Ve,mean
Vr-Linear
Vr-Nonlinear
Vr,max
Building Height (m)
Shear Load (ton)

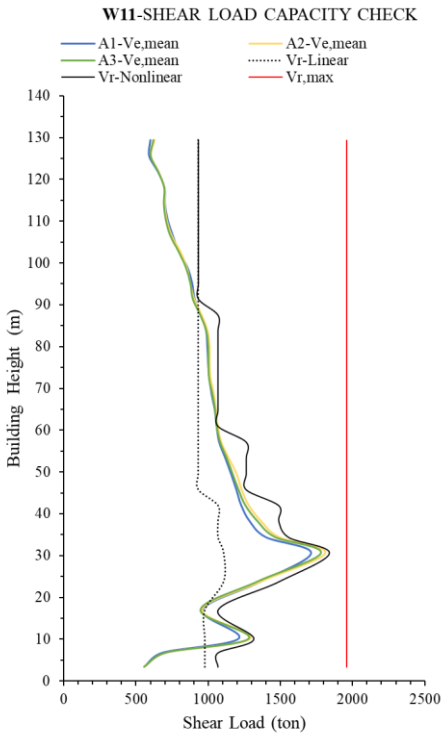
W11-SHEAR LOAD CAPACITY CHECK
A1-Ve,mean
A2-Ve,mean
A3-Ve,mean
Vr-Linear
Vr-Nonlinear
Vr,max
Building Height (m)
Shear Load (ton)

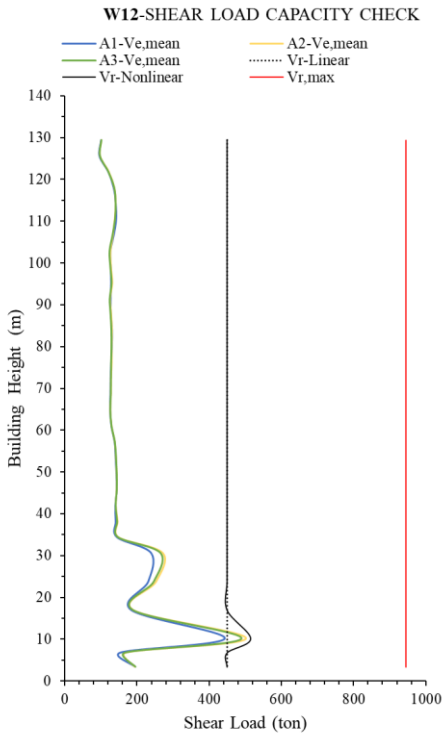
W12-SHEAR LOAD CAPACITY CHECK
A1-Ve,mean
A2-Ve,mean
A3-Ve,mean
Vr-Linear
Vr-Nonlinear
Vr,max
Building Height (m)
Shear Load (ton)

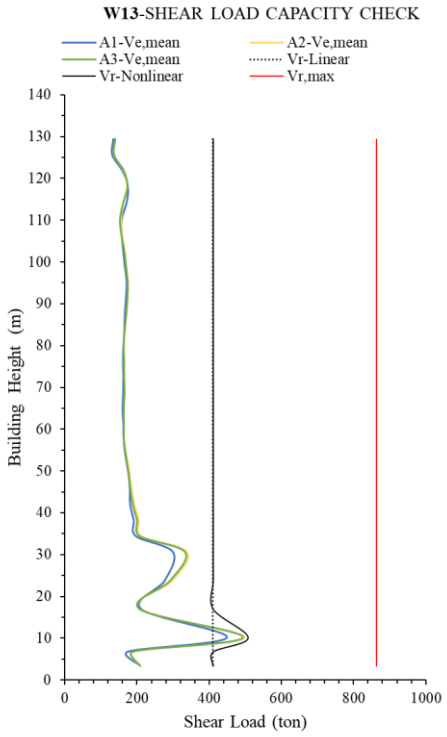
W13-SHEAR LOAD CAPACITY CHECK
A1-Ve,mean
A2-Ve,mean
A3-Ve,mean
Vr-Linear
Vr-Nonlinear
Vr,max
Building Height (m)
Shear Load (ton)

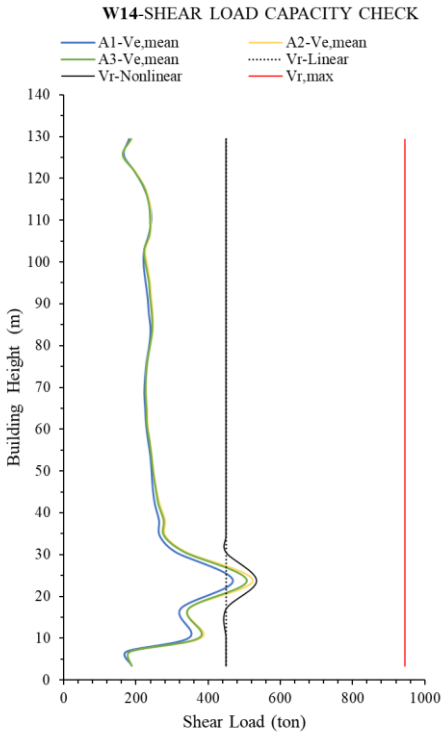
W14-SHEAR LOAD CAPACITY CHECK
A1-Ve,mean
A2-Ve,mean
A3-Ve,mean
Vr-Linear
Vr-Nonlinear
Vr,max
Building Height (m)
Shear Load (ton)

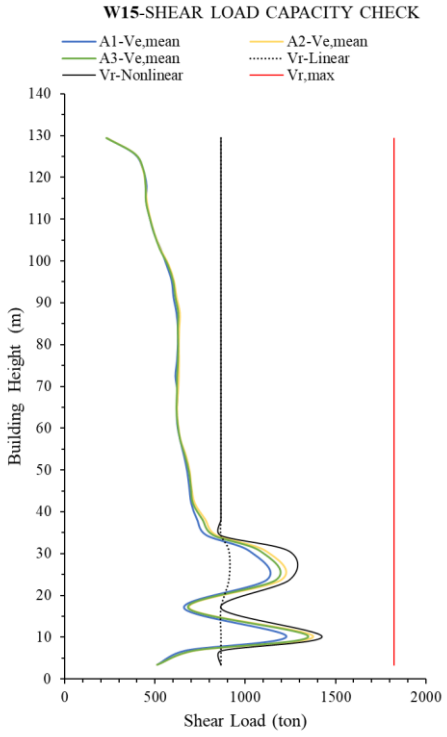
W15-SHEAR LOAD CAPACITY CHECK
A1-Ve,mean
A2-Ve,mean
A3-Ve,mean
Vr-Linear
Vr-Nonlinear
Vr,max
Building Height (m)
Shear Load (ton)

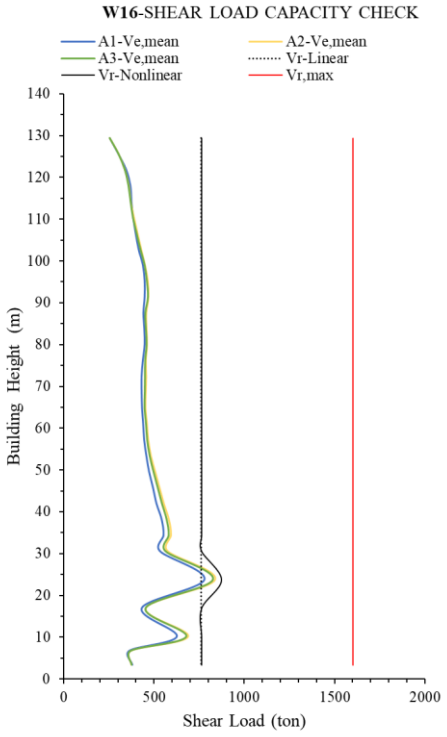
W16-SHEAR LOAD CAPACITY CHECK
A1-Ve,mean
A2-Ve,mean
A3-Ve,mean
Vr-Linear
Vr-Nonlinear
Vr,max
Building Height (m)
Shear Load (ton)

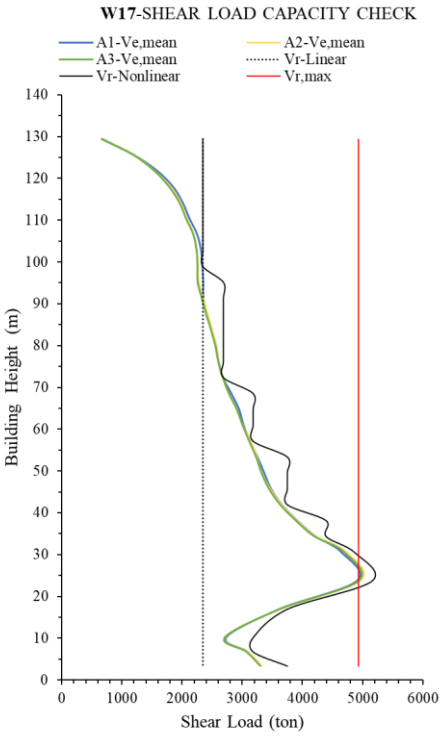
W17-SHEAR LOAD CAPACITY CHECK
A1-Ve,mean
A2-Ve,mean
A3-Ve,mean
Vr-Linear
Vr-Nonlinear
Vr,max
Building Height (m)
Shear Load (ton)

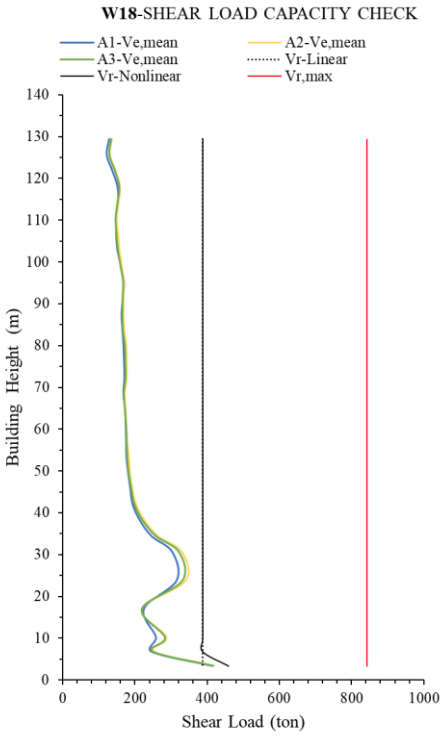
W18-SHEAR LOAD CAPACITY CHECK
A1-Ve,mean
A2-Ve,mean
A3-Ve,mean
Vr-Linear
Vr-Nonlinear
Vr,max
Building Height (m)
Shear Load (ton)

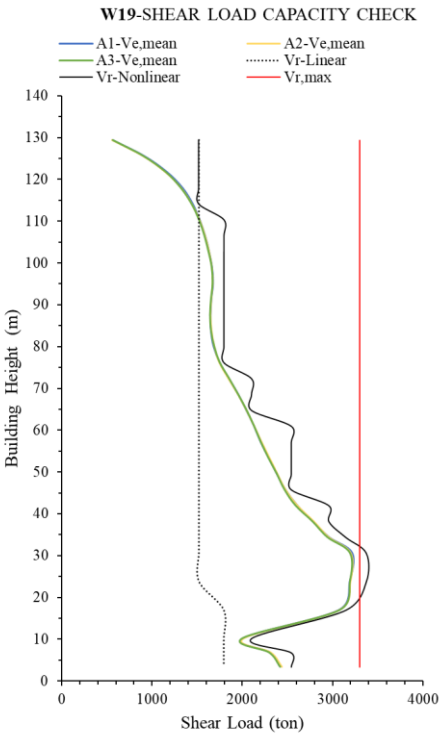
W19-SHEAR LOAD CAPACITY CHECK
A1-Ve,mean
A2-Ve,mean
A3-Ve,mean
Vr-Linear
Vr-Nonlinear
Vr,max
Building Height (m)
Shear Load (ton)

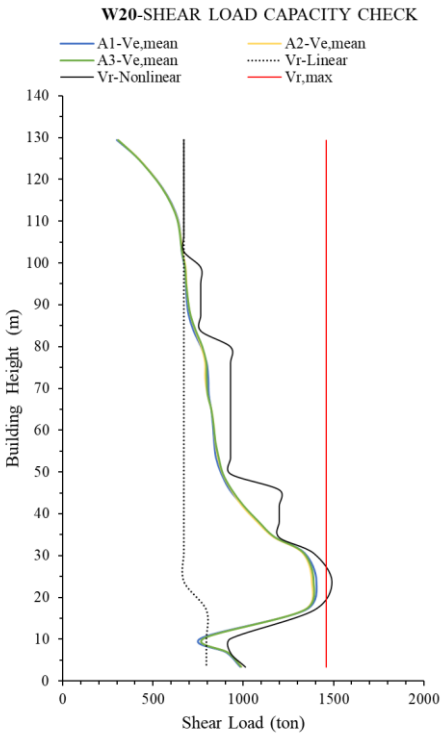
W20-SHEAR LOAD CAPACITY CHECK
A1-Ve,mean
A2-Ve,mean
A3-Ve,mean
Vr-Linear
Vr-Nonlinear
Vr,max
Building Height (m)
Shear Load (ton)

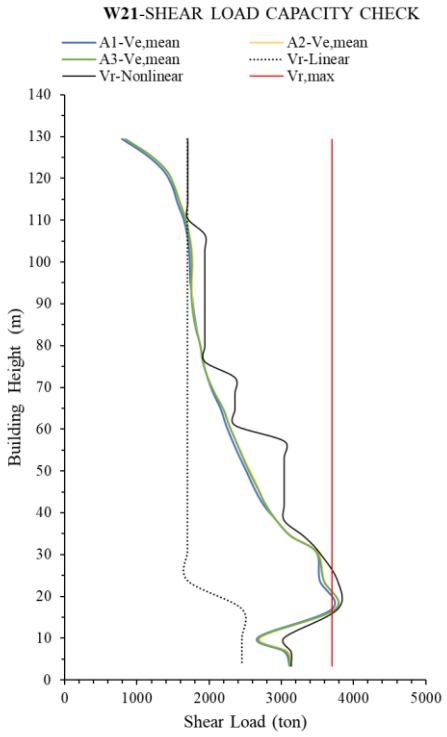
W21-SHEAR LOAD CAPACITY CHECK
A1-Ve,mean
A2-Ve,mean
A3-Ve,mean
Vr-Linear
Vr-Nonlinear
Vr,max
Building Height (m)
Shear Load (ton)
0
10
20
30
40
50
60
70
80
90
100
110
120
130
140
0
1000
2000
3000
4000
5000

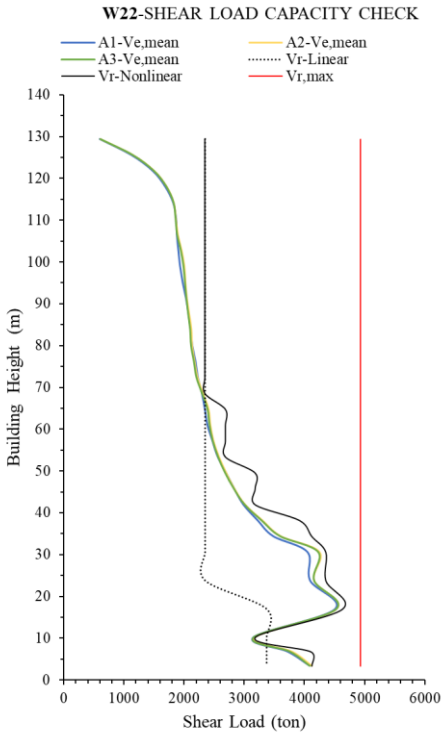
W22-SHEAR LOAD CAPACITY CHECK
A1-Ve,mean
A2-Ve,mean
A3-Ve,mean
Vr-Linear
Vr-Nonlinear
Vr,max
Building Height (m)
Shear Load (ton)
0
10
20
30
40
50
60
70
80
90
100
110
120
130
140
0
1000
2000
3000
4000
5000
6000

B. Shear Load Capacity Diagrams of Walls for Three Alternative Models of the Case Study Building in Istanbul (Performance Based Design)

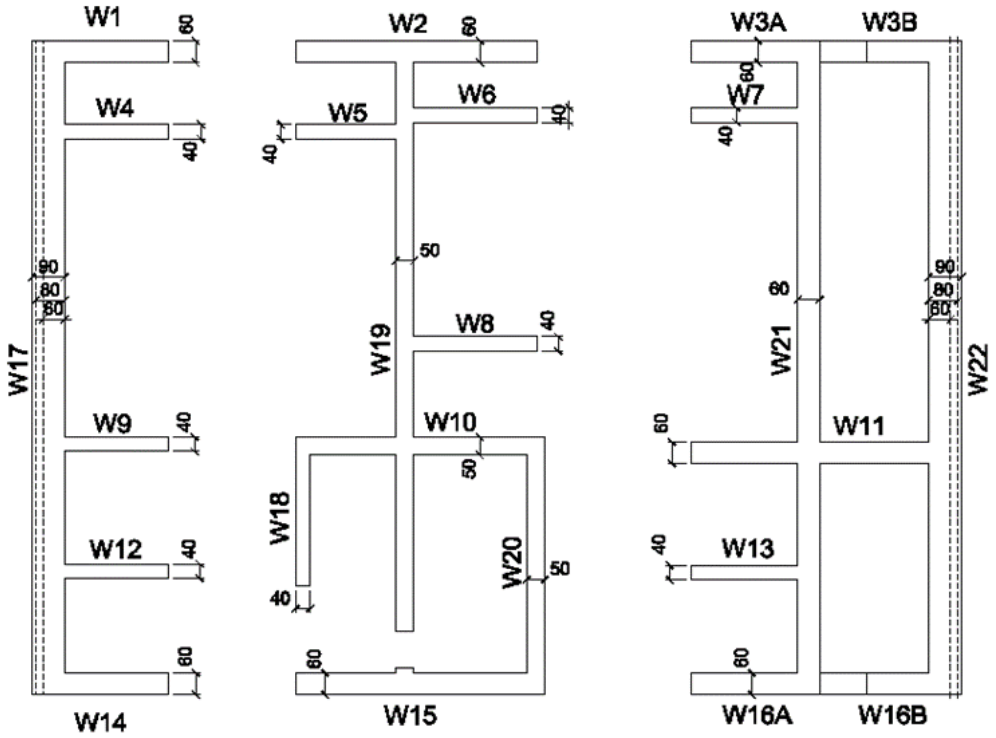

Figure B.1 Wall Labels

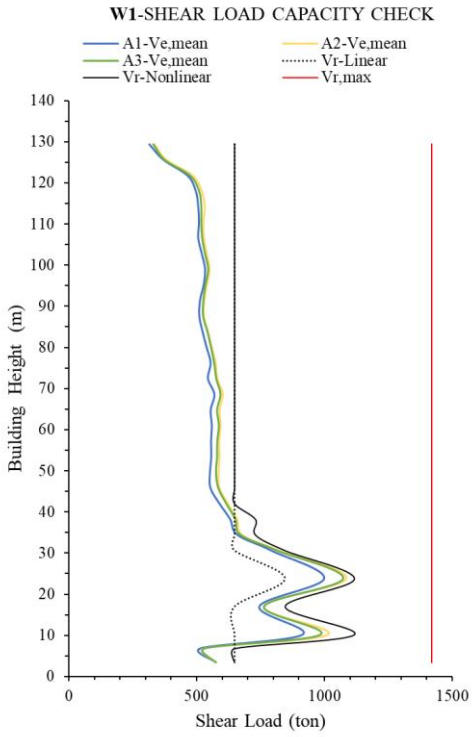
W1-SHEAR LOAD CAPACITY CHECK
A1-Ve,mean
A2-Ve,mean
A3-Ve,mean
Vr-Linear
Vr-Nonlinear
Vr,max
Building Height (m)
Shear Load (ton)

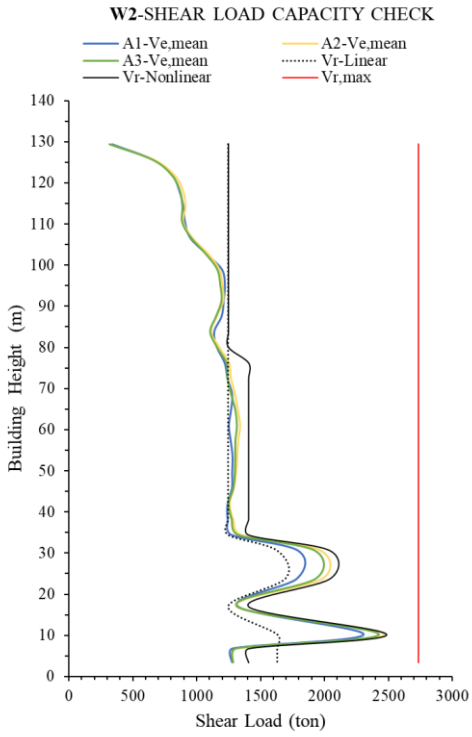
W2-SHEAR LOAD CAPACITY CHECK
A1-Ve,mean
A2-Ve,mean
A3-Ve,mean
Vr-Linear
Vr-Nonlinear
Vr,max
Building Height (m)
Shear Load (ton)

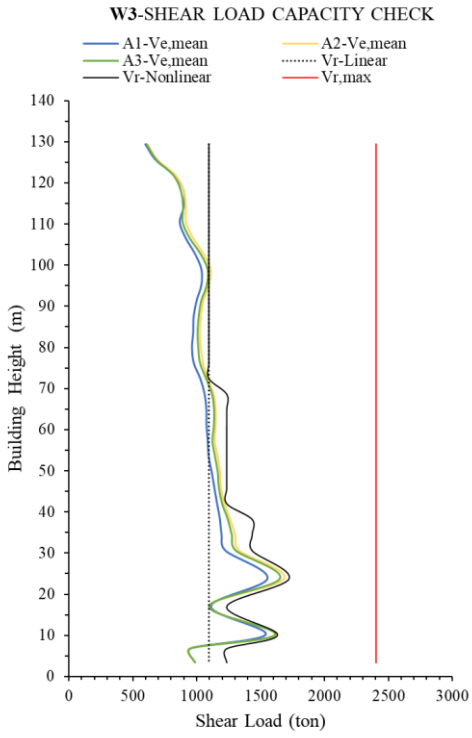
W3-SHEAR LOAD CAPACITY CHECK
A1-Ve,mean
A2-Ve,mean
A3-Ve,mean
Vr-Linear
Vr-Nonlinear
Vr,max
Building Height (m)
Shear Load (ton)

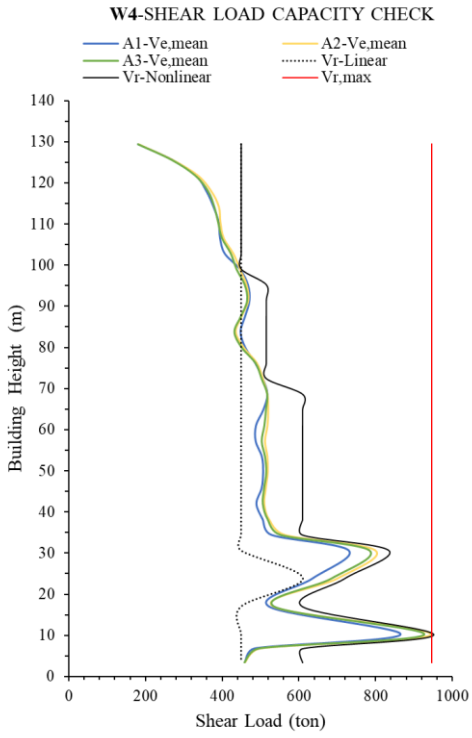
W4-SHEAR LOAD CAPACITY CHECK
A1-Ve,mean
A2-Ve,mean
A3-Ve,mean
Vr-Linear
Vr-Nonlinear
Vr,max
Building Height (m)
Shear Load (ton)

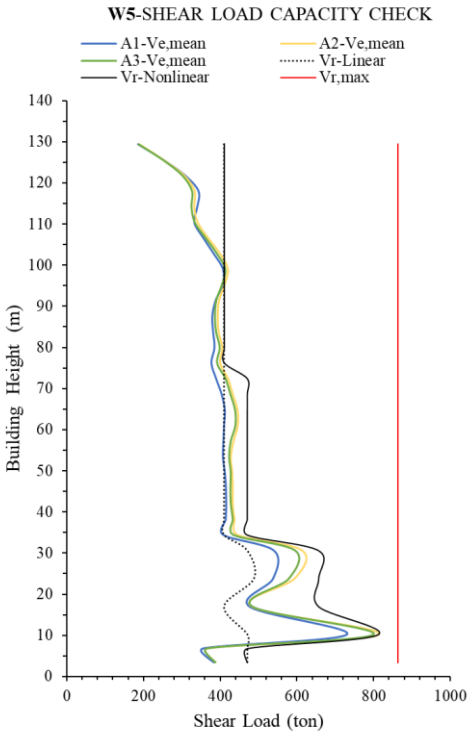
W5-SHEAR LOAD CAPACITY CHECK
A1-Ve,mean
A2-Ve,mean
A3-Ve,mean
Vr-Linear
Vr-Nonlinear
Vr,max
Building Height (m)
Shear Load (ton)

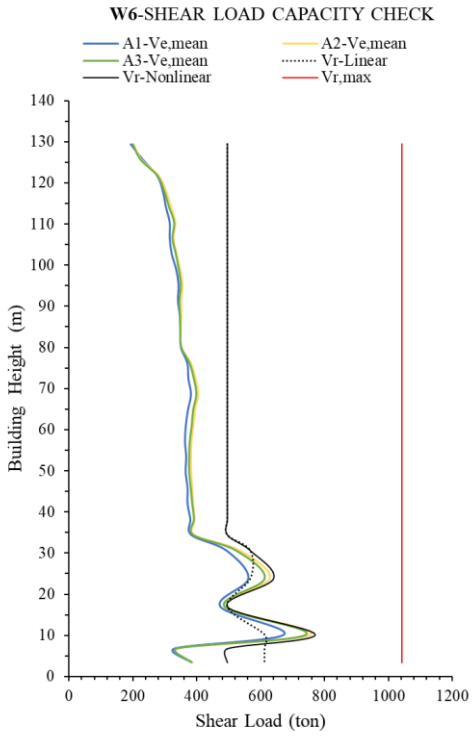
W6-SHEAR LOAD CAPACITY CHECK
A1-Ve,mean
A2-Ve,mean
A3-Ve,mean
Vr-Linear
Vr-Nonlinear
Vr,max
Building Height (m)
Shear Load (ton)

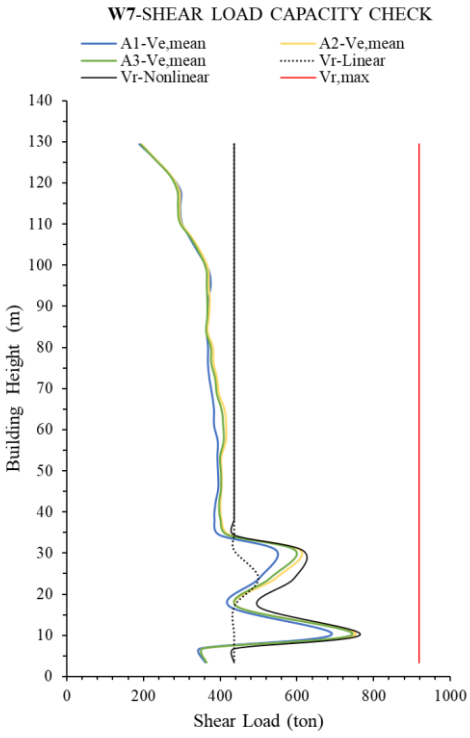
W7-SHEAR LOAD CAPACITY CHECK
A1-Ve,mean
A2-Ve,mean
A3-Ve,mean
Vr-Linear
Vr-Nonlinear
Vr,max
Building Height (m)
Shear Load (ton)

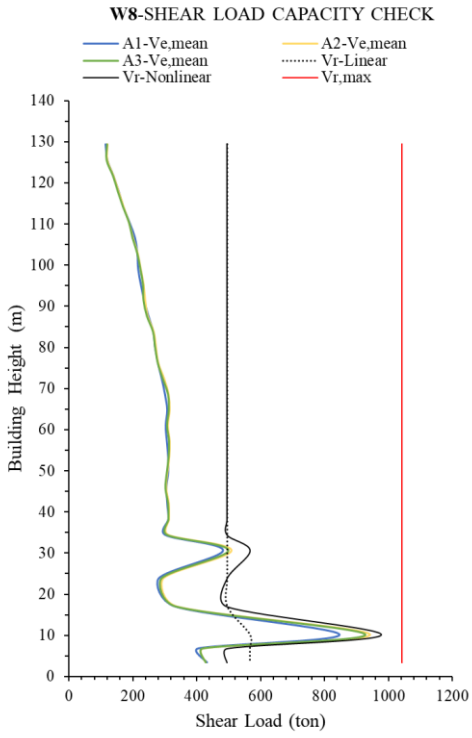
W8-SHEAR LOAD CAPACITY CHECK
A1-Ve,mean
A2-Ve,mean
A3-Ve,mean
Vr-Linear
Vr-Nonlinear
Vr,max
Building Height (m)
Shear Load (ton)

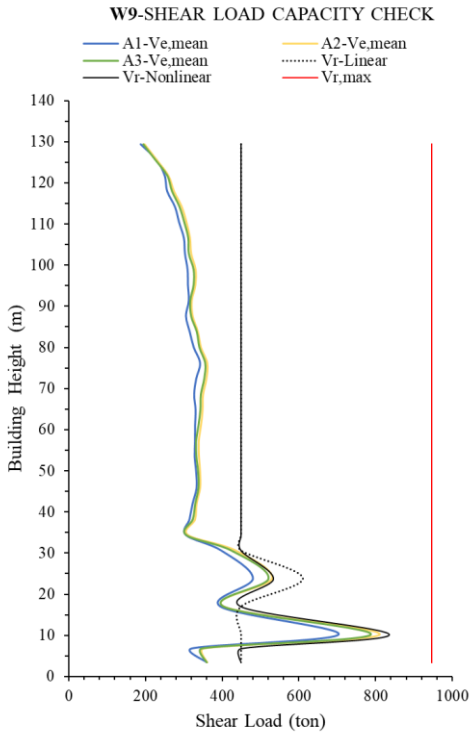
W9-SHEAR LOAD CAPACITY CHECK
A1-Ve,mean
A2-Ve,mean
A3-Ve,mean
Vr-Linear
Vr-Nonlinear
Vr,max
Building Height (m)
Shear Load (ton)

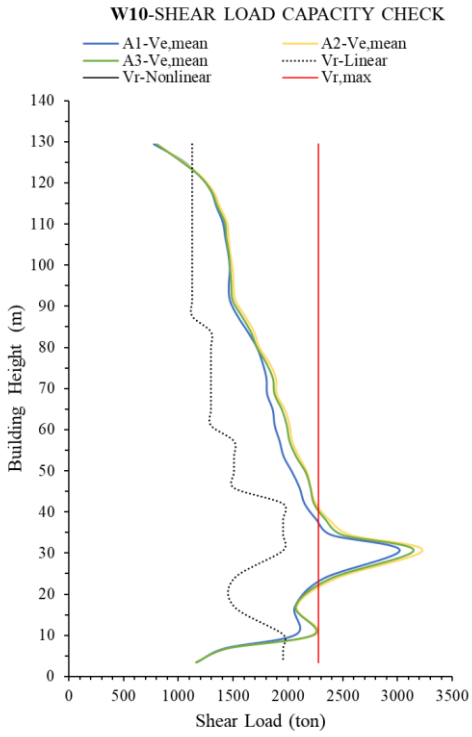
W10-SHEAR LOAD CAPACITY CHECK
A1-Ve,mean
A2-Ve,mean
A3-Ve,mean
Vr-Linear
Vr-Nonlinear
Vr,max
Building Height (m)
Shear Load (ton)

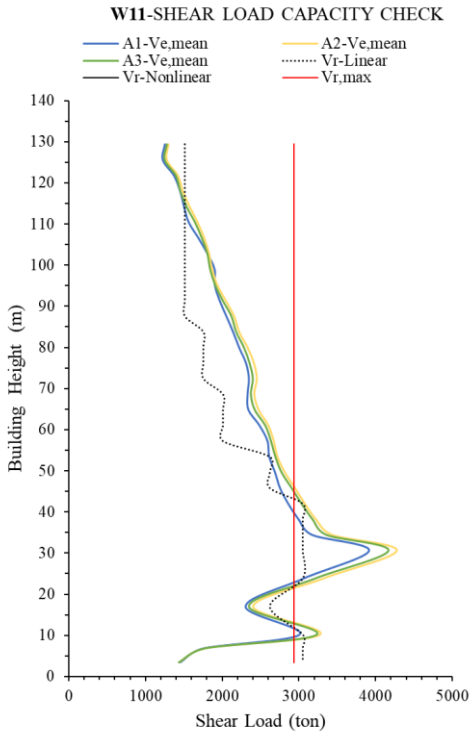
W11-SHEAR LOAD CAPACITY CHECK
A1-Ve,mean
A2-Ve,mean
A3-Ve,mean
Vr-Linear
Vr-Nonlinear
Vr,max
Building Height (m)
Shear Load (ton)

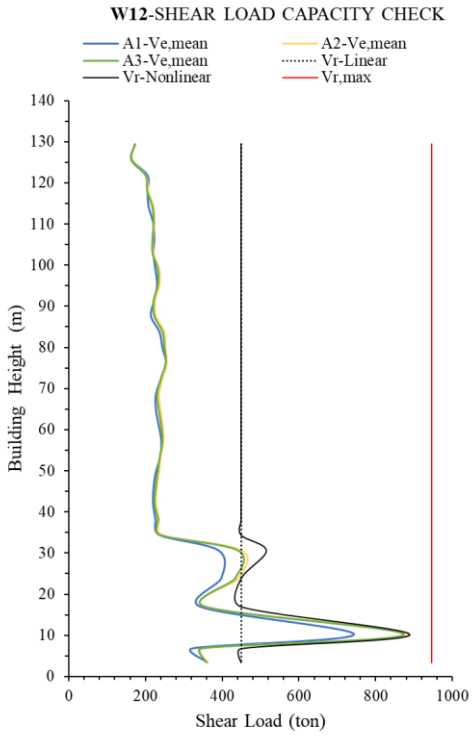
W12-SHEAR LOAD CAPACITY CHECK
A1-Ve,mean
A2-Ve,mean
A3-Ve,mean
Vr-Linear
Vr-Nonlinear
Vr,max
Building Height (m)
Shear Load (ton)

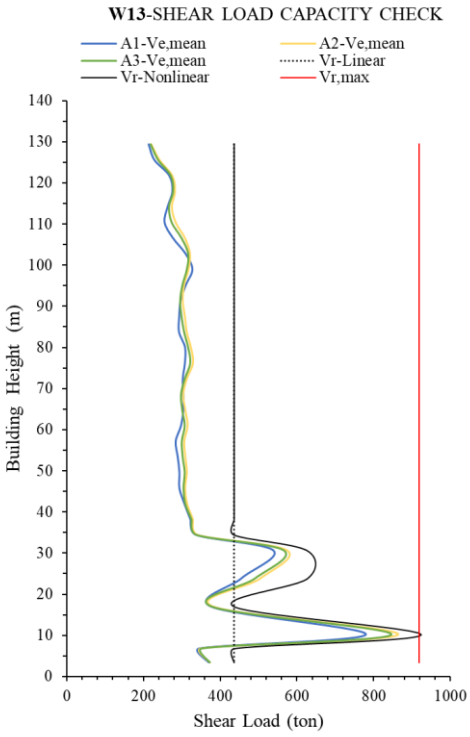
W13-SHEAR LOAD CAPACITY CHECK
A1-Ve,mean
A2-Ve,mean
A3-Ve,mean
Vr-Linear
Vr-Nonlinear
Vr,max
Building Height (m)
Shear Load (ton)

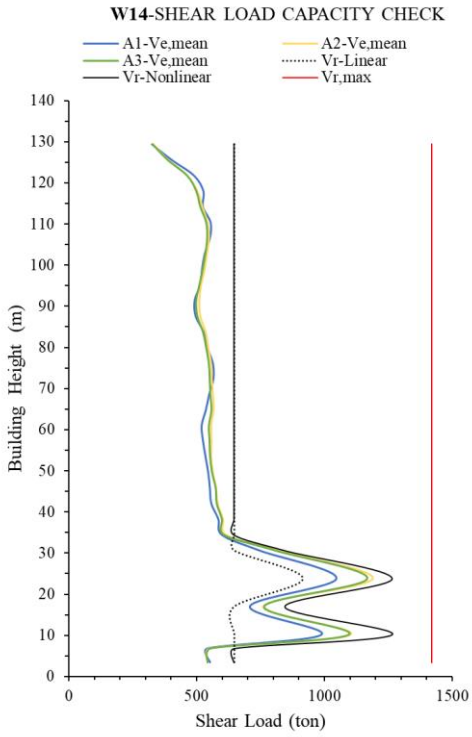
W14-SHEAR LOAD CAPACITY CHECK
A1-Ve,mean
A2-Ve,mean
A3-Ve,mean
Vr-Linear
Vr-Nonlinear
Vr,max
Building Height (m)
Shear Load (ton)

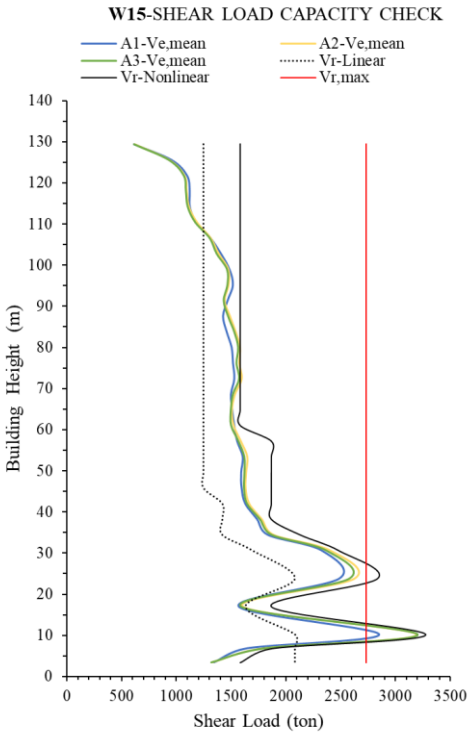
W15-SHEAR LOAD CAPACITY CHECK
A1-Ve,mean
A2-Ve,mean
A3-Ve,mean
Vr-Linear
Vr-Nonlinear
Vr,max
Building Height (m)
Shear Load (ton)

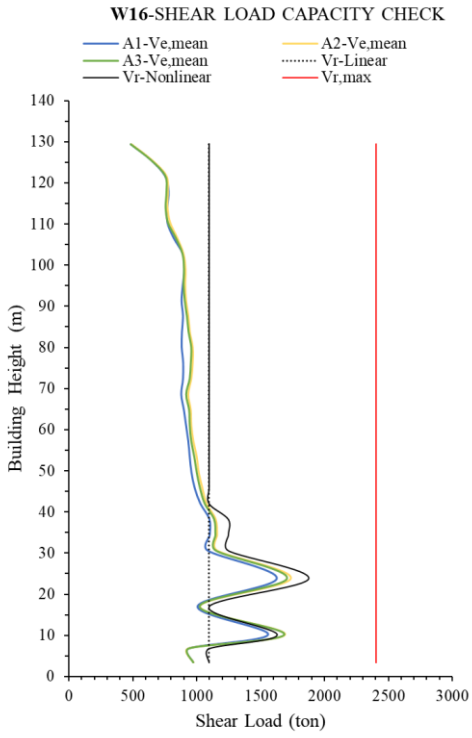
W16-SHEAR LOAD CAPACITY CHECK
A1-Ve,mean
A2-Ve,mean
A3-Ve,mean
Vr-Linear
Vr-Nonlinear
Vr,max
Building Height (m)
Shear Load (ton)

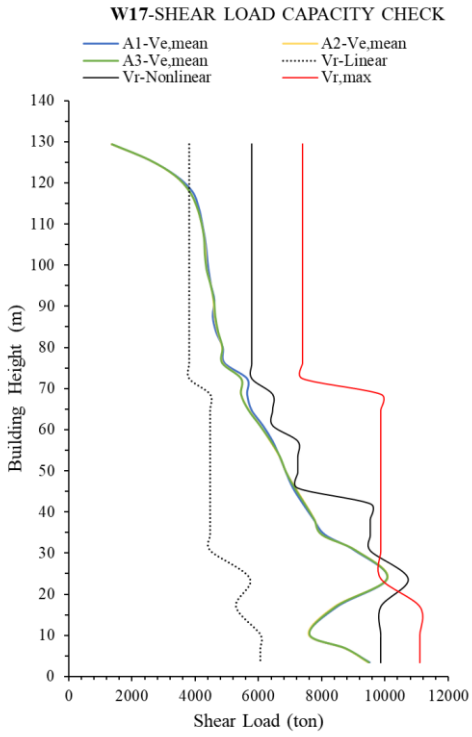
W17-SHEAR LOAD CAPACITY CHECK
A1-Ve,mean
A2-Ve,mean
A3-Ve,mean
Vr-Linear
Vr-Nonlinear
Vr,max
Building Height (m)
Shear Load (ton)

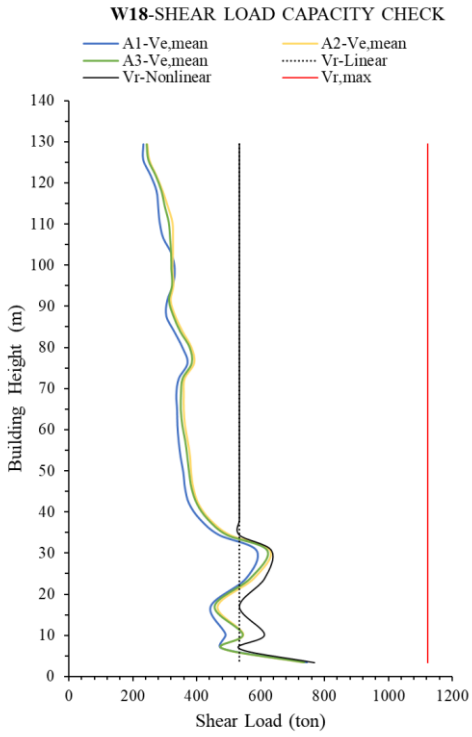
W18-SHEAR LOAD CAPACITY CHECK
A1-Ve,mean
A2-Ve,mean
A3-Ve,mean
Vr-Linear
Vr-Nonlinear
Vr,max
Building Height (m)
Shear Load (ton)

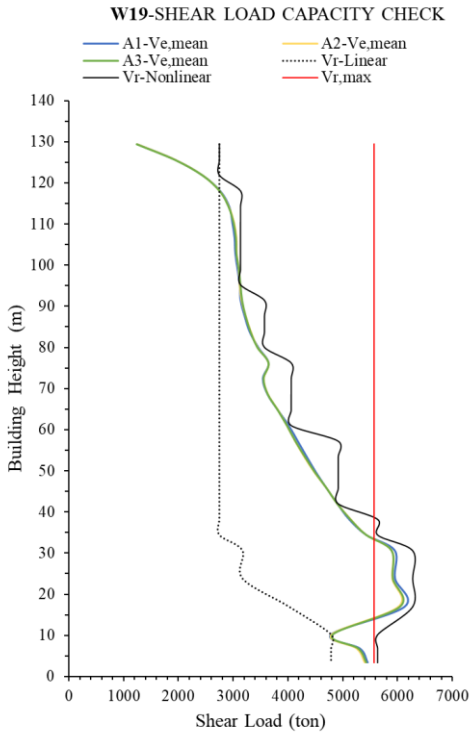
W19-SHEAR LOAD CAPACITY CHECK
A1-Ve,mean
A2-Ve,mean
A3-Ve,mean
Vr-Linear
Vr-Nonlinear
Vr,max
Building Height (m)
Shear Load (ton)

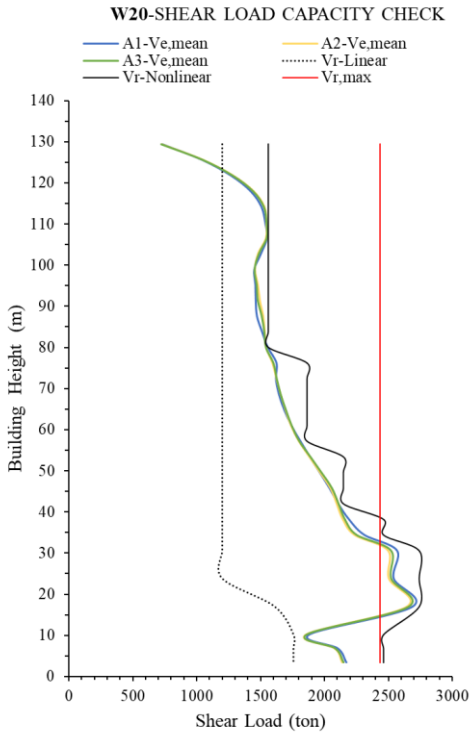
W20-SHEAR LOAD CAPACITY CHECK
A1-Ve,mean
A2-Ve,mean
A3-Ve,mean
Vr-Linear
Vr-Nonlinear
Vr,max
Building Height (m)
Shear Load (ton)

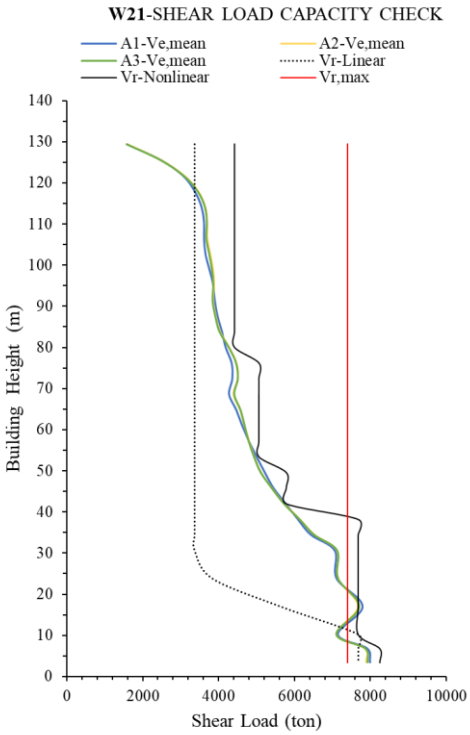
W21-SHEAR LOAD CAPACITY CHECK
A1-Ve,mean
A2-Ve,mean
A3-Ve,mean
Vr-Linear
Vr-Nonlinear
Vr,max
Building Height (m)
Shear Load (ton)
0
10
20
30
40
50
60
70
80
90
100
110
120
130
140
0
2000
4000
6000
8000
10000

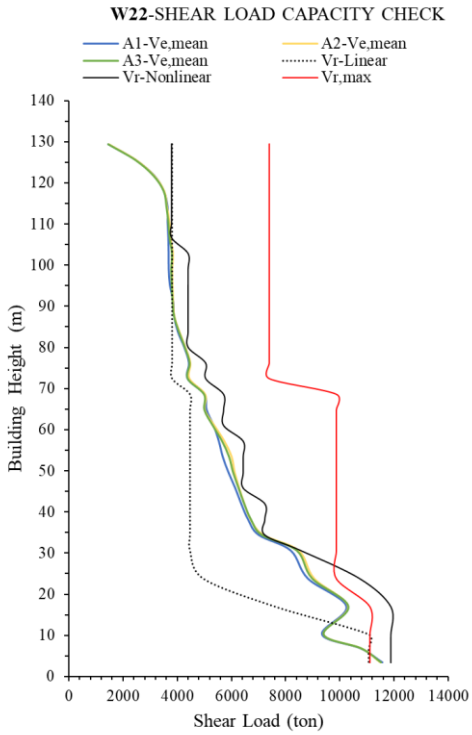
W22-SHEAR LOAD CAPACITY CHECK
A1-Ve,mean
A2-Ve,mean
A3-Ve,mean
Vr-Linear
Vr-Nonlinear
Vr,max
Building Height (m)
Shear Load (ton)
0
10
20
30
40
50
60
70
80
90
100
110
120
130
140
0
2000
4000
6000
8000
10000
12000
14000

C. Strain Check of Walls for Three Alternative Models of the Case Study Building in Ankara (Performance Based Design)

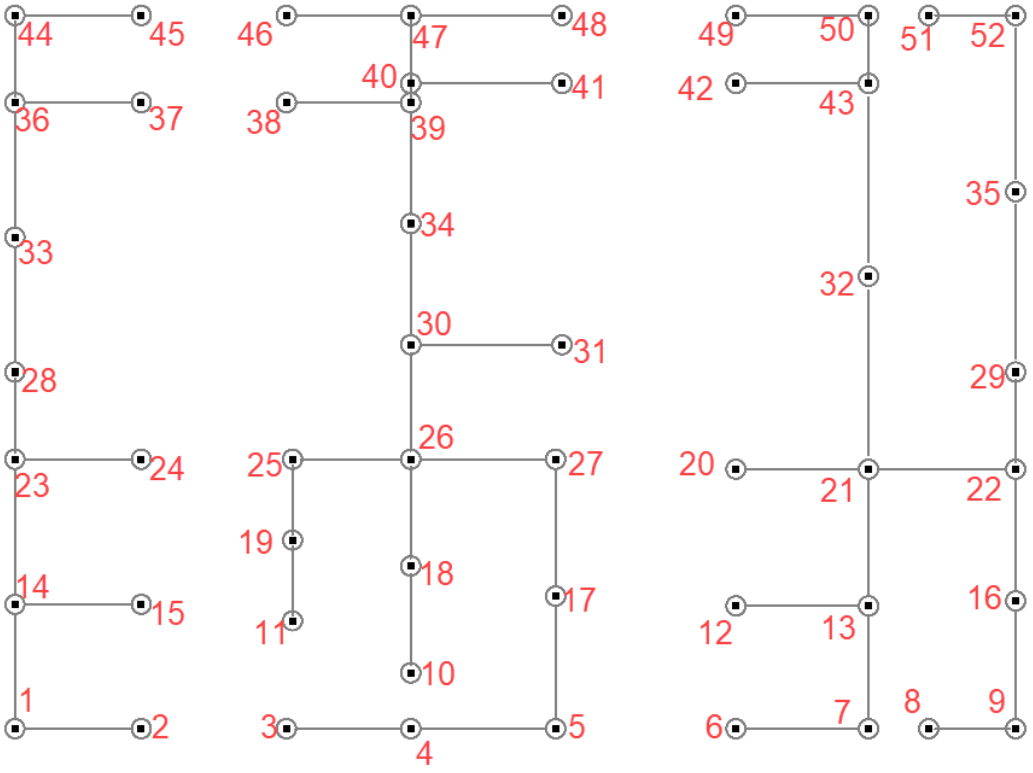

Figure C.1 Strain Gage Labels

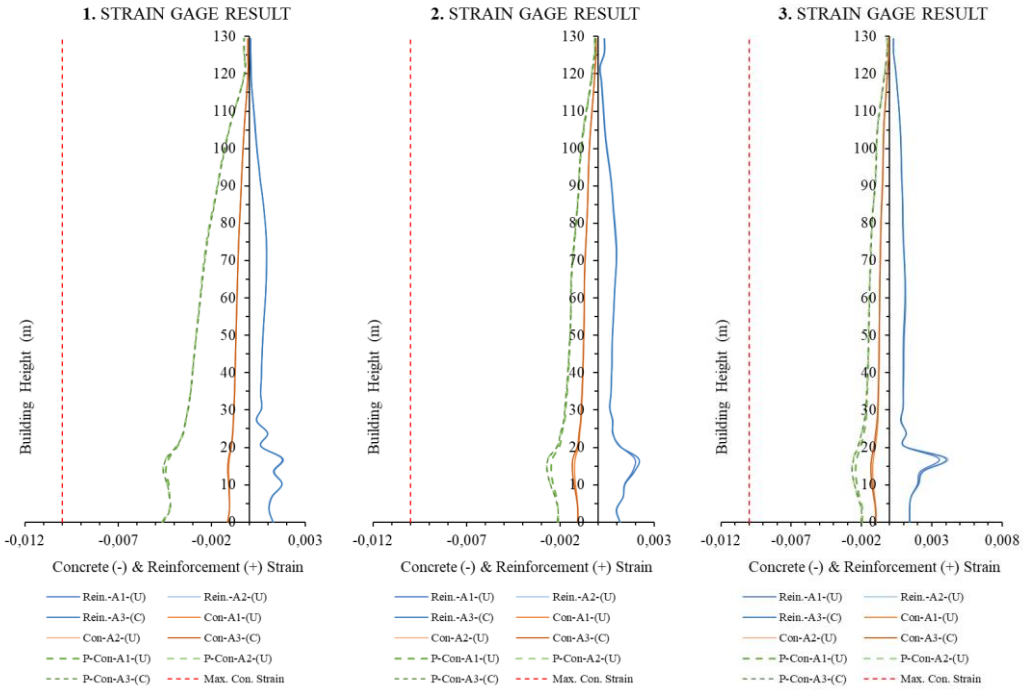
1. STRAIN GAGE RESULT
2. STRAIN GAGE RESULT
3. STRAIN GAGE RESULT
Building Height (m)
Concrete (-) & Reinforcement (+) Strain
Rein.-A1-(U)
Rein.-A2-(U)
Rein.-A3-(C)
Con-A1-(U)
Con-A2-(U)
Con-A3-(C)
P-Con-A1-(U)
P-Con-A2-(U)
P-Con-A3-(C)
Max. Con. Strain

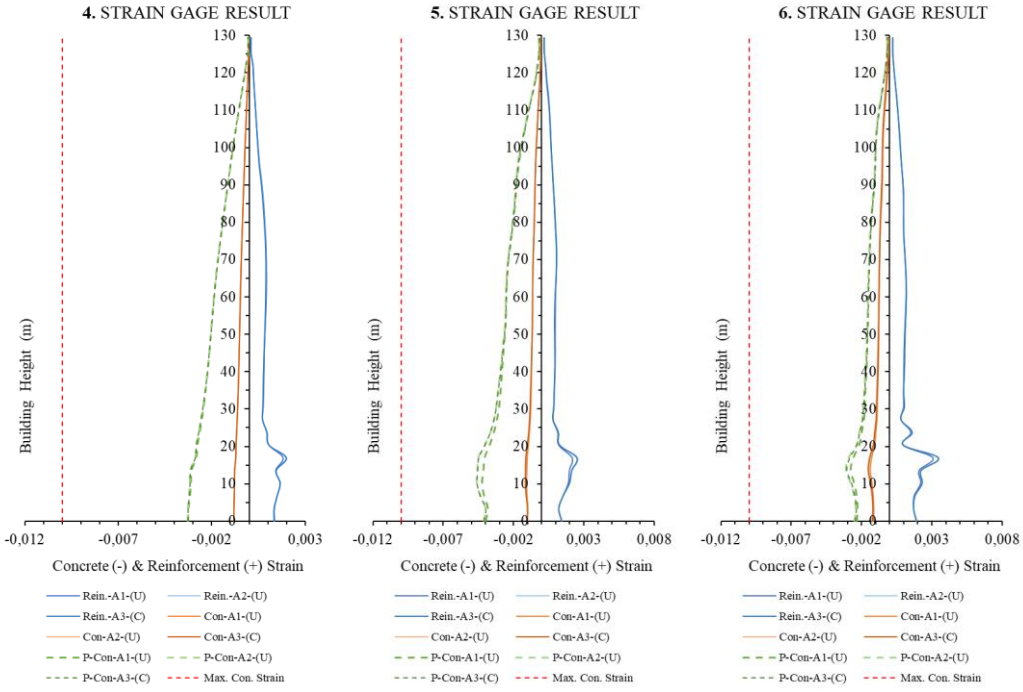
4. STRAIN GAGE RESULT
5. STRAIN GAGE RESULT
6. STRAIN GAGE RESULT
Building Height (m)
Concrete (-) & Reinforcement (+) Strain
Rein.-A1-(U)
Rein.-A2-(U)
Rein.-A3-(C)
Con-A1-(U)
Con-A2-(U)
Con-A3-(C)
P-Con-A1-(U)
P-Con-A2-(U)
P-Con-A3-(C)
Max. Con. Strain

7. STRAIN GAGE RESULT

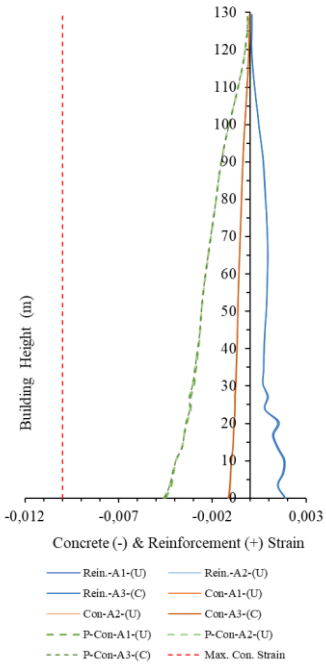

8. STRAIN GAGE RESULT

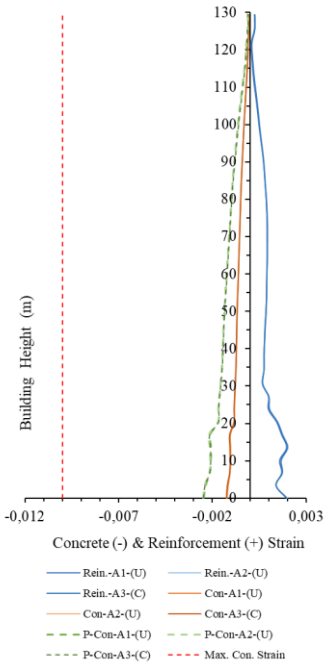

9. STRAIN GAGE RESULT

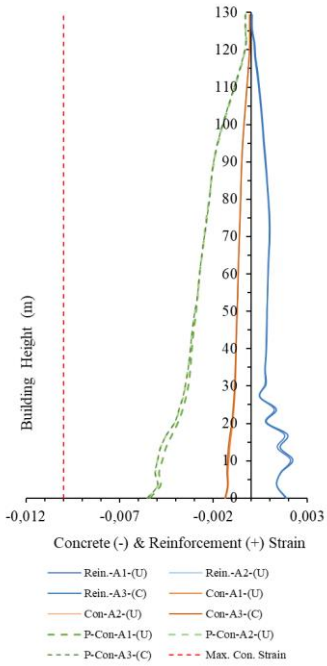

10. STRAIN GAGE RESULT

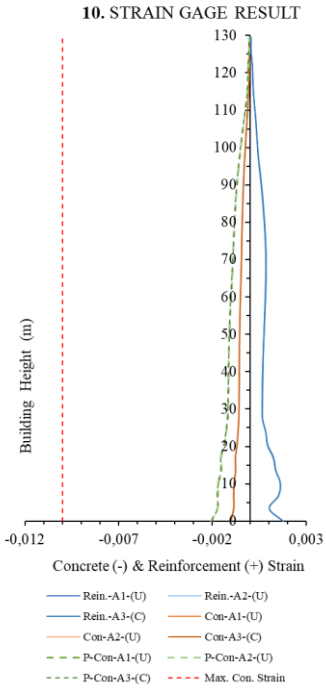

11. STRAIN GAGE RESULT

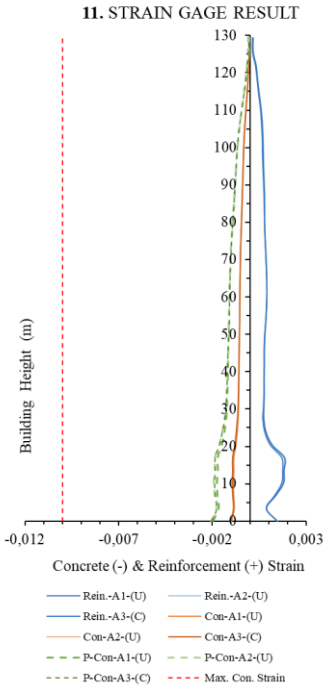

12. STRAIN GAGE RESULT

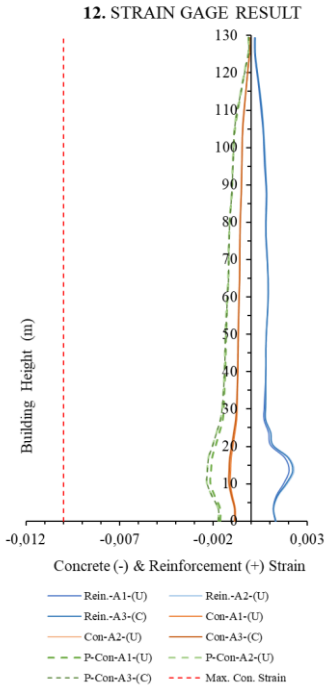

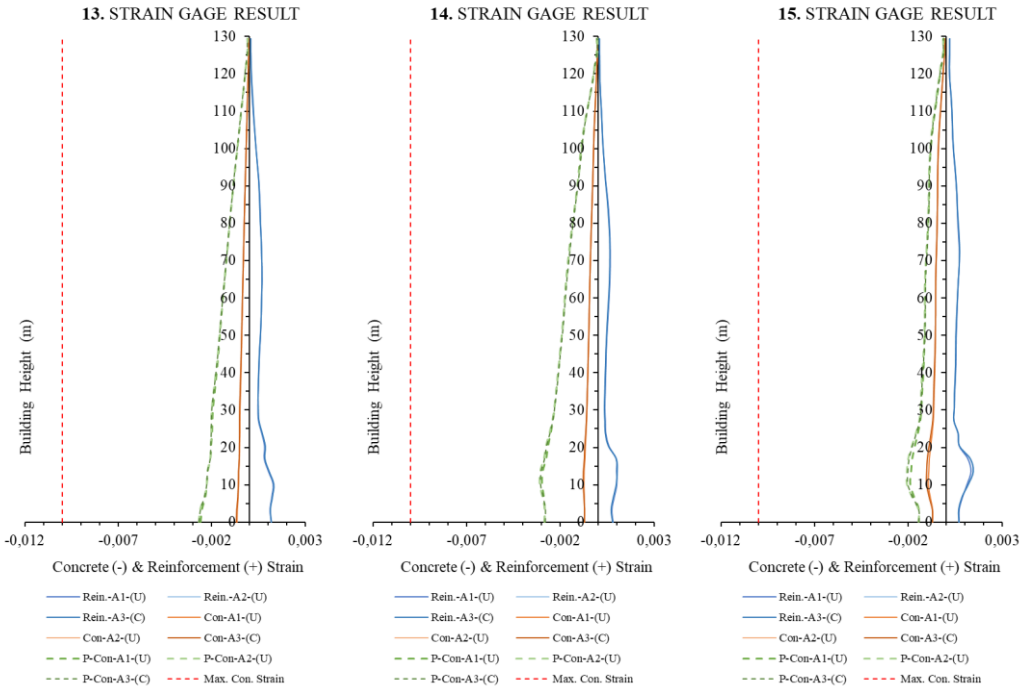
13. STRAIN GAGE RESULT
14. STRAIN GAGE RESULT
15. STRAIN GAGE RESULT
Building Height (m)
Concrete (-) & Reinforcement (+) Strain
Rein.-A1-(U)
Rein.-A2-(U)
Rein.-A3-(C)
Con-A1-(U)
Con-A2-(U)
Con-A3-(C)
P-Con-A1-(U)
P-Con-A2-(U)
P-Con-A3-(C)
Max. Con. Strain

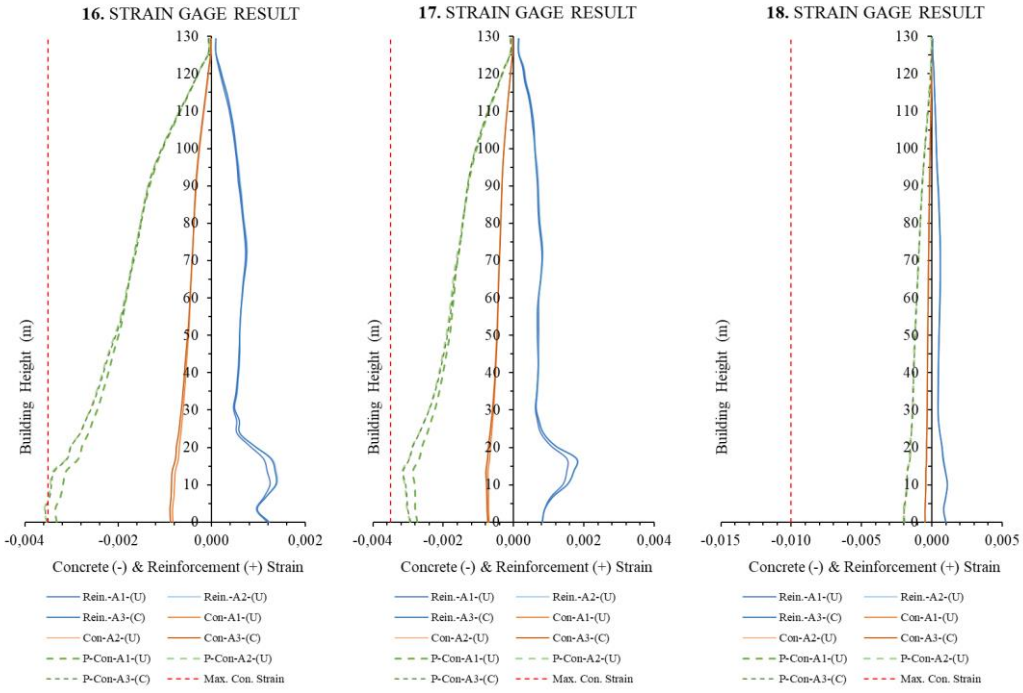
16. STRAIN GAGE RESULT
17. STRAIN GAGE RESULT
18. STRAIN GAGE RESULT
Building Height (m)
Concrete (-) & Reinforcement (+) Strain
Rein.-A1-(U)
Rein.-A2-(U)
Rein.-A3-(C)
Con-A1-(U)
Con-A2-(U)
Con-A3-(C)
P-Con-A1-(U)
P-Con-A2-(U)
P-Con-A3-(C)
Max. Con. Strain

19. STRAIN GAGE RESULT

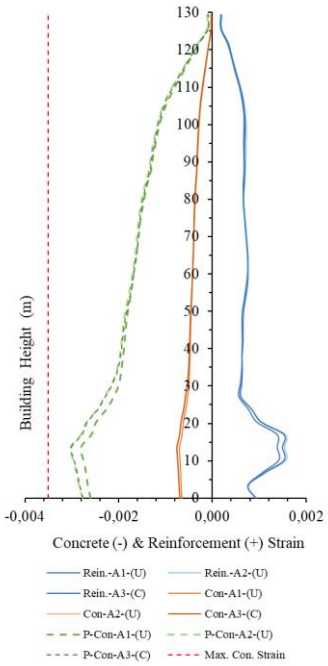

20. STRAIN GAGE RESULT

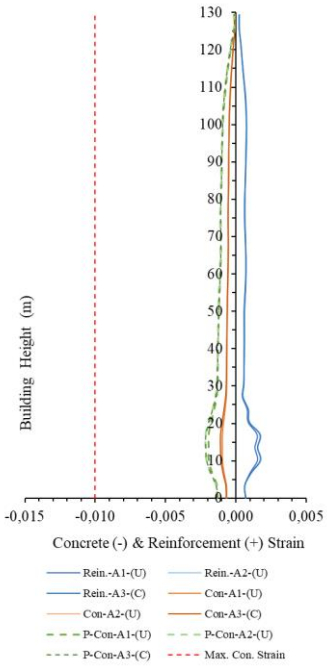

21. STRAIN GAGE RESULT

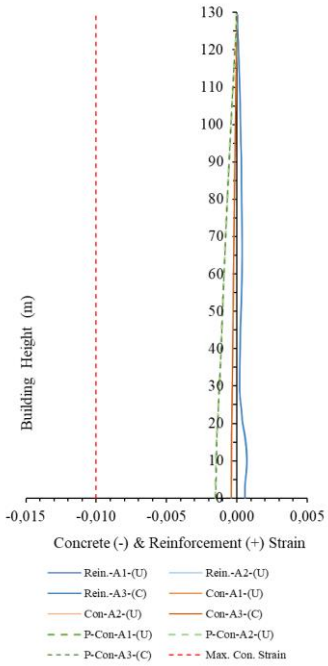

22. STRAIN GAGE RESULT

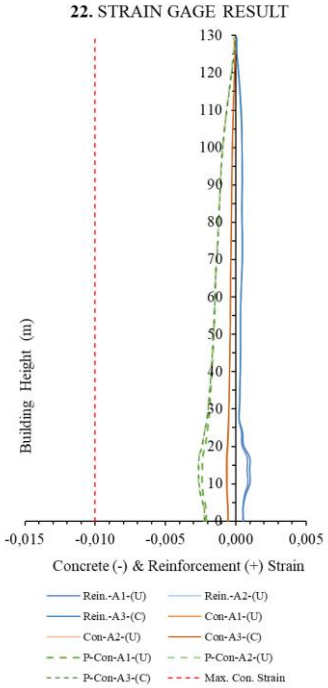

23. STRAIN GAGE RESULT

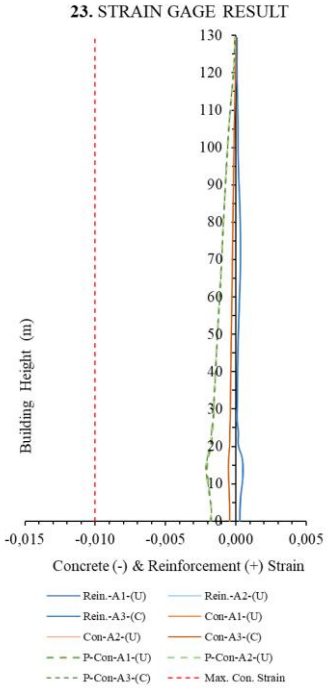

24. STRAIN GAGE RESULT

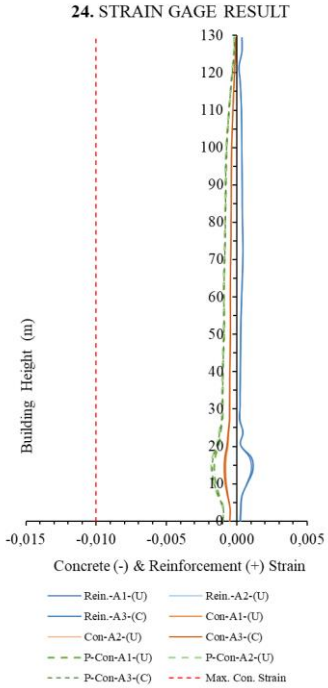

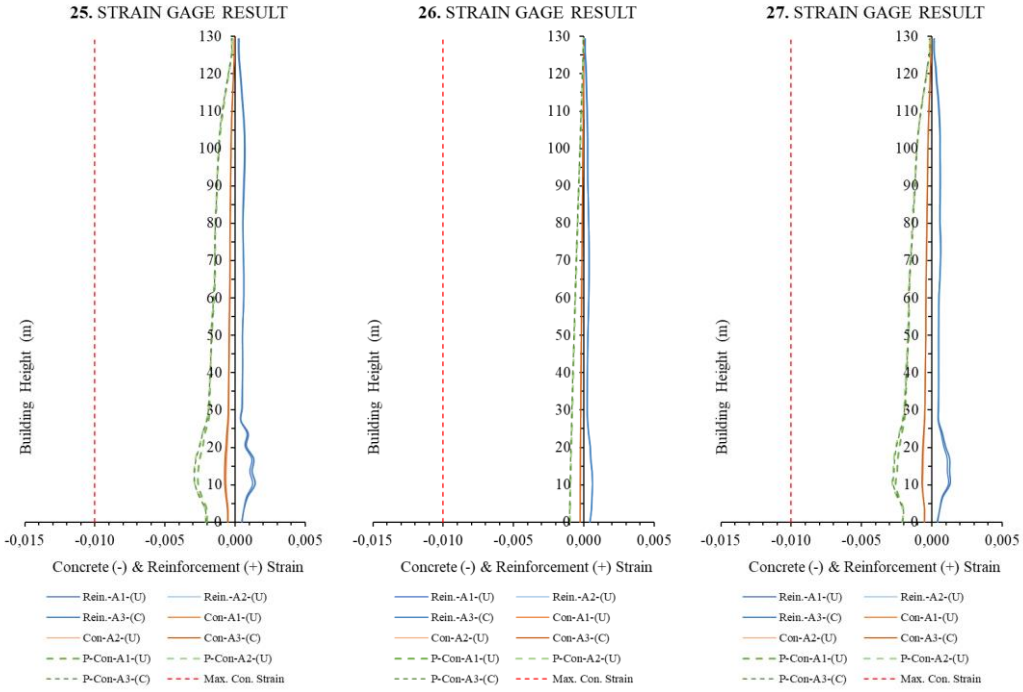
25. STRAIN GAGE RESULT
Building Height (m)
Concrete (-) & Reinforcement (+) Strain
Rein.-A1-(U)
Rein.-A2-(U)
Rein.-A3-(C)
Con-A1-(U)
Con-A2-(U)
Con-A3-(C)
P-Con-A1-(U)
P-Con-A2-(U)
P-Con-A3-(C)
Max. Con. Strain
26. STRAIN GAGE RESULT
Building Height (m)
Concrete (-) & Reinforcement (+) Strain
Rein.-A1-(U)
Rein.-A2-(U)
Rein.-A3-(C)
Con-A1-(U)
Con-A2-(U)
Con-A3-(C)
P-Con-A1-(U)
P-Con-A2-(U)
P-Con-A3-(C)
Max. Con. Strain
27. STRAIN GAGE RESULT
Building Height (m)
Concrete (-) & Reinforcement (+) Strain
Rein.-A1-(U)
Rein.-A2-(U)
Rein.-A3-(C)
Con-A1-(U)
Con-A2-(U)
Con-A3-(C)
P-Con-A1-(U)
P-Con-A2-(U)
P-Con-A3-(C)
Max. Con. Strain

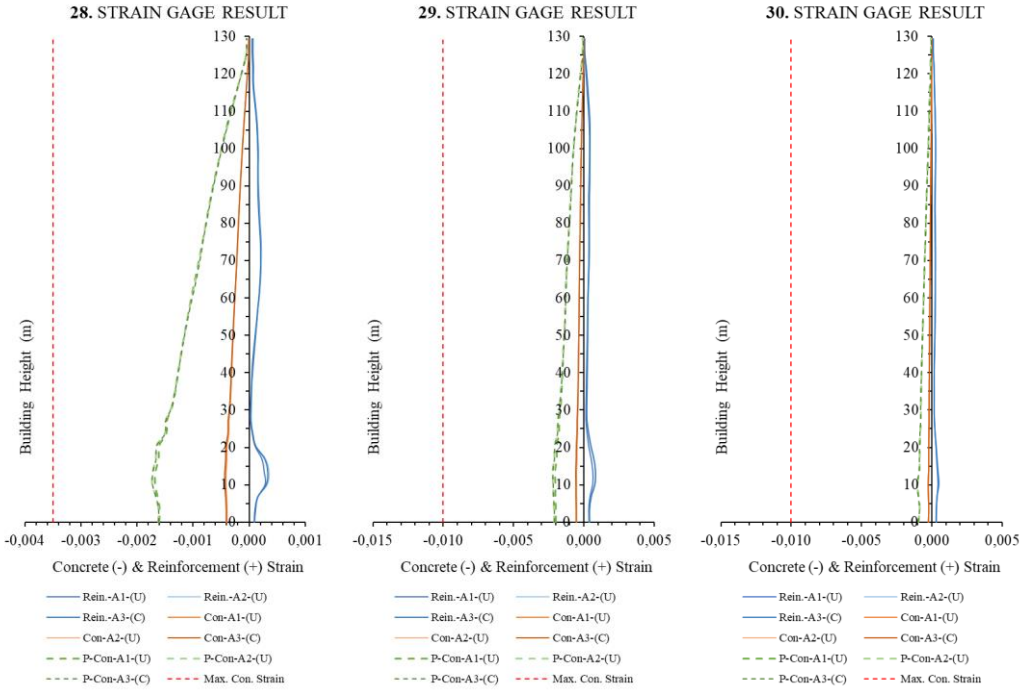
28. STRAIN GAGE RESULT
Building Height (m)
Concrete (-) & Reinforcement (+) Strain
Rein.-A1-(U)
Rein.-A2-(U)
Rein.-A3-(C)
Con-A1-(U)
Con-A2-(U)
Con-A3-(C)
P-Con-A1-(U)
P-Con-A2-(U)
P-Con-A3-(C)
Max. Con. Strain
29. STRAIN GAGE RESULT
Building Height (m)
Concrete (-) & Reinforcement (+) Strain
Rein.-A1-(U)
Rein.-A2-(U)
Rein.-A3-(C)
Con-A1-(U)
Con-A2-(U)
Con-A3-(C)
P-Con-A1-(U)
P-Con-A2-(U)
P-Con-A3-(C)
Max. Con. Strain
30. STRAIN GAGE RESULT
Building Height (m)
Concrete (-) & Reinforcement (+) Strain
Rein.-A1-(U)
Rein.-A2-(U)
Rein.-A3-(C)
Con-A1-(U)
Con-A2-(U)
Con-A3-(C)
P-Con-A1-(U)
P-Con-A2-(U)
P-Con-A3-(C)
Max. Con. Strain

31. STRAIN GAGE RESULT

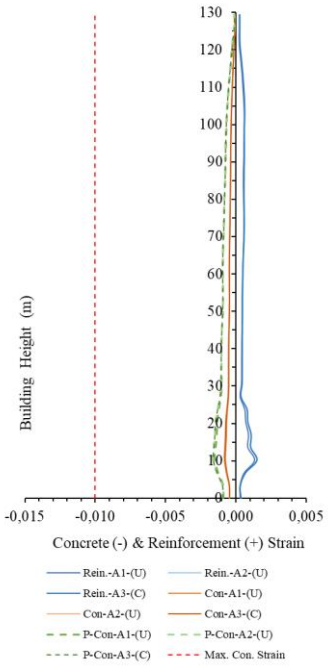

32. STRAIN GAGE RESULT

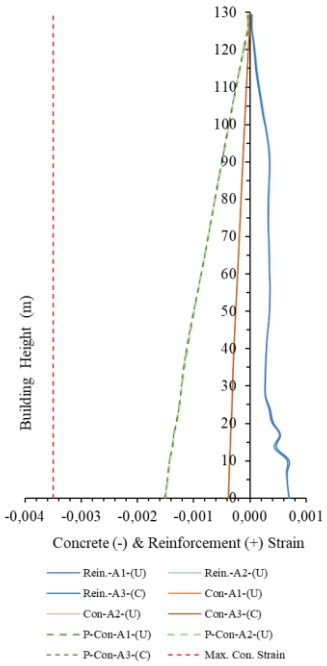

33. STRAIN GAGE RESULT

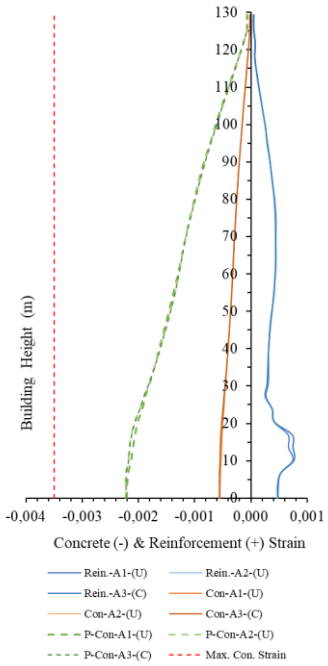

34. STRAIN GAGE RESULT

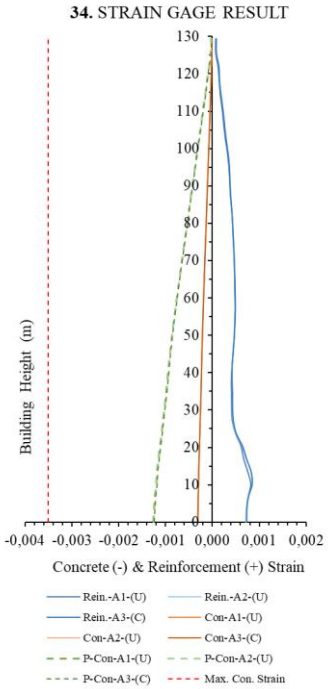

35. STRAIN GAGE RESULT

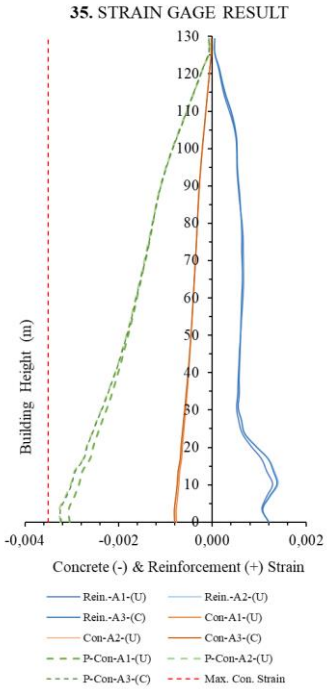

36. STRAIN GAGE RESULT

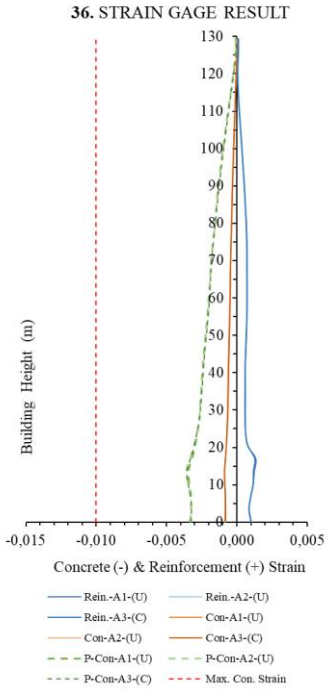

37. STRAIN GAGE RESULT

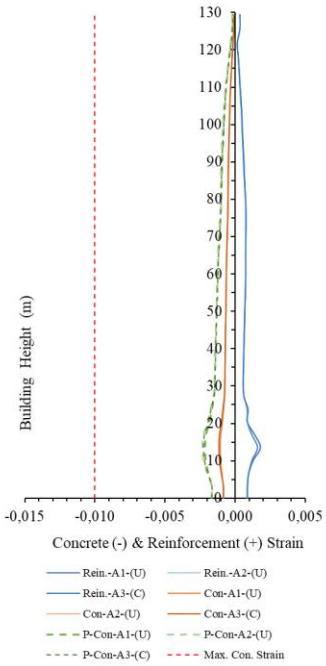

38. STRAIN GAGE RESULT

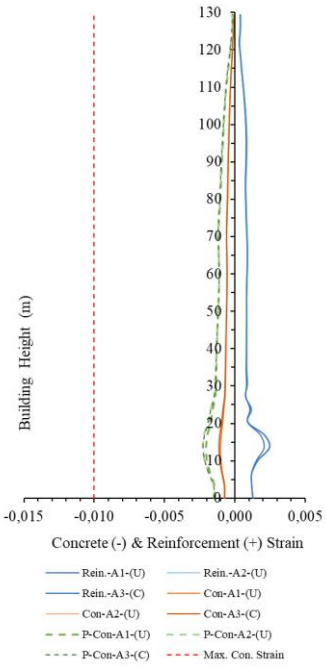

39. STRAIN GAGE RESULT

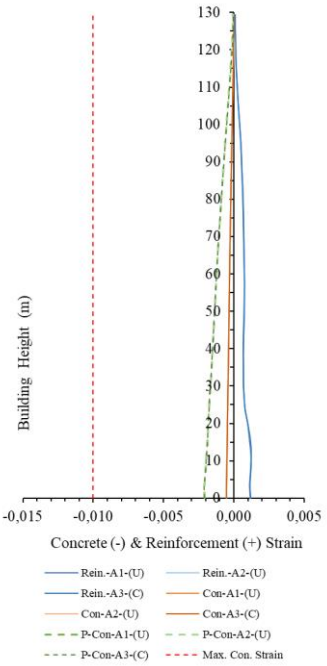

40. STRAIN GAGE RESULT

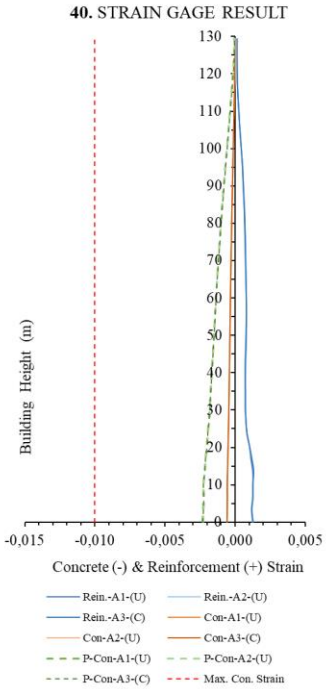

41. STRAIN GAGE RESULT

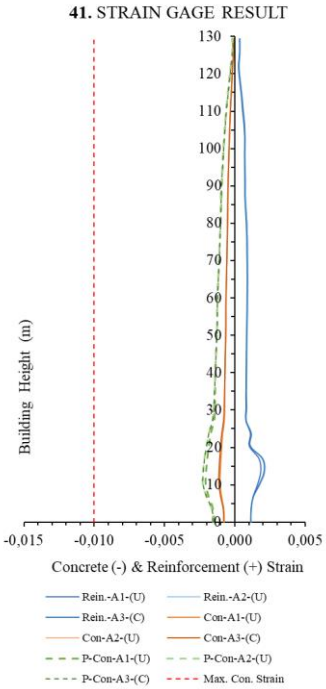

42. STRAIN GAGE RESULT

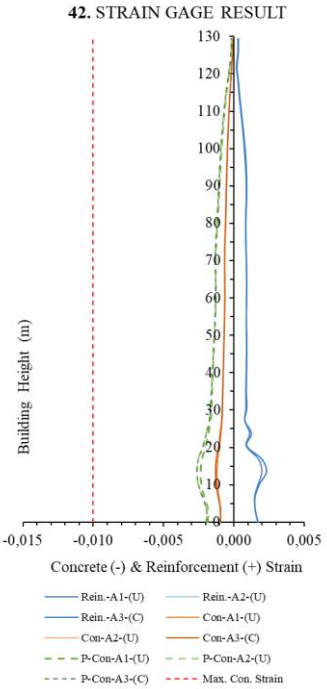

43. STRAIN GAGE RESULT

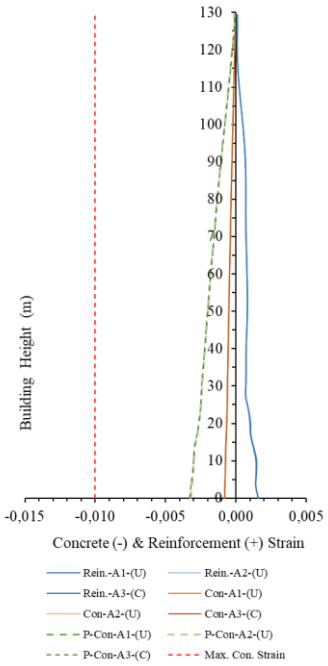

44. STRAIN GAGE RESULT

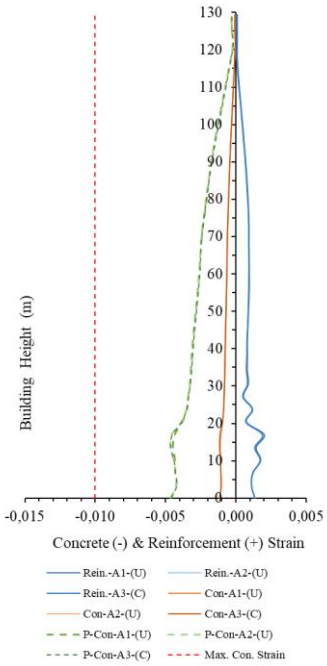

45. STRAIN GAGE RESULT

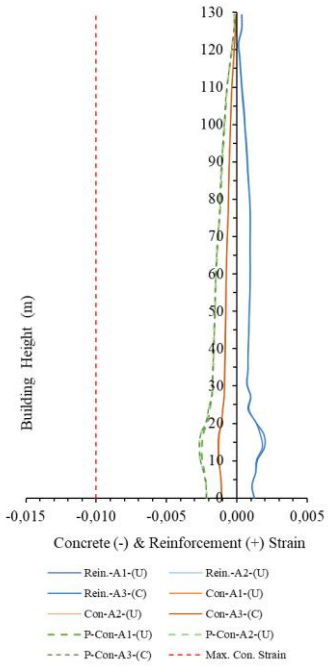

46. STRAIN GAGE RESULT

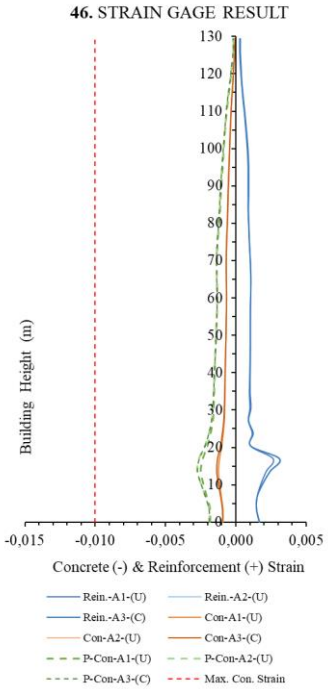

47. STRAIN GAGE RESULT

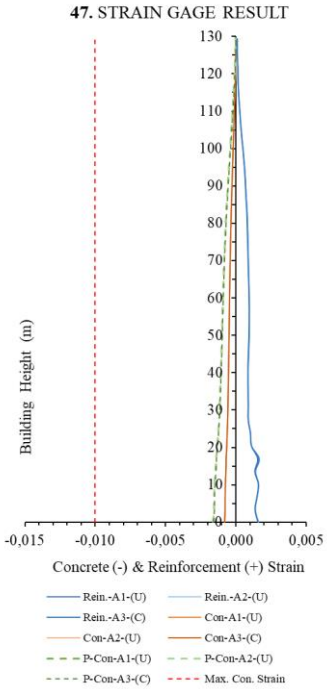

48. STRAIN GAGE RESULT

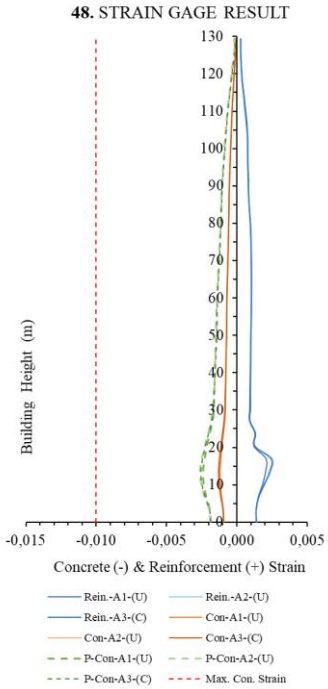

49. STRAIN GAGE RESULT

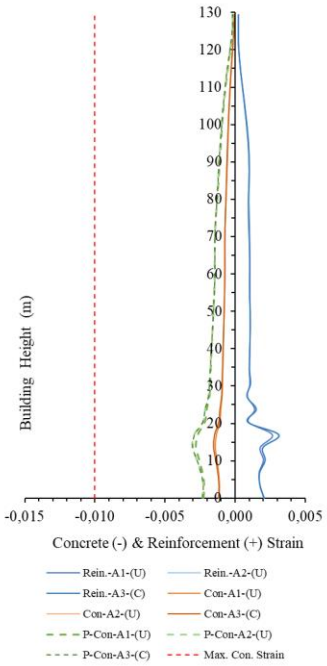

50. STRAIN GAGE RESULT

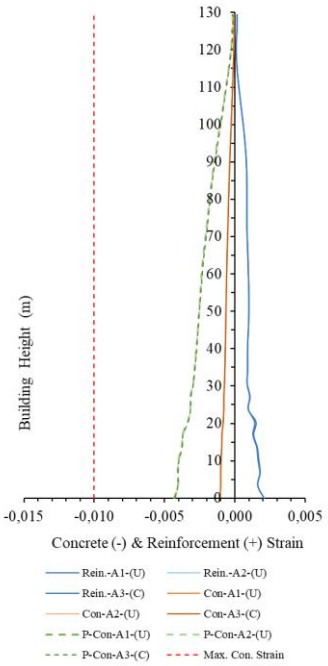

51. STRAIN GAGE RESULT

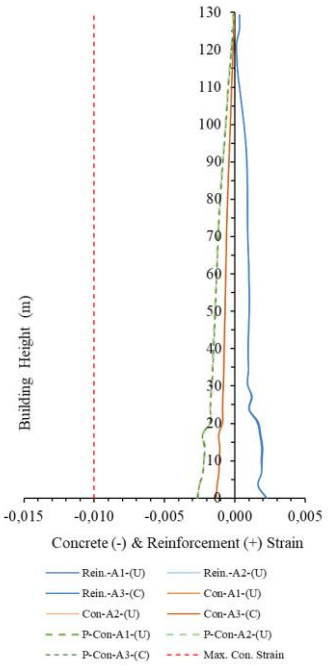

52. STRAIN GAGE RESULT

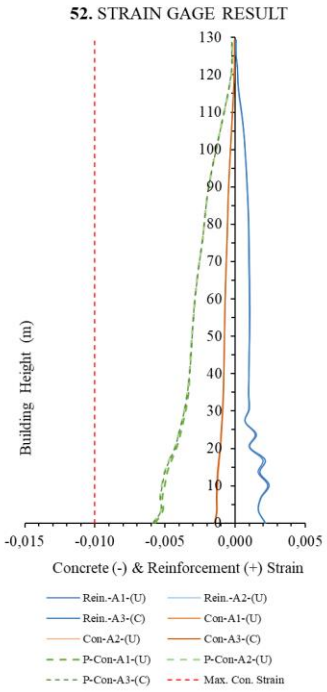

D. Strain Check of Walls for Three Alternative Models of the Case Study Building in Istanbul (Performance Based Design)

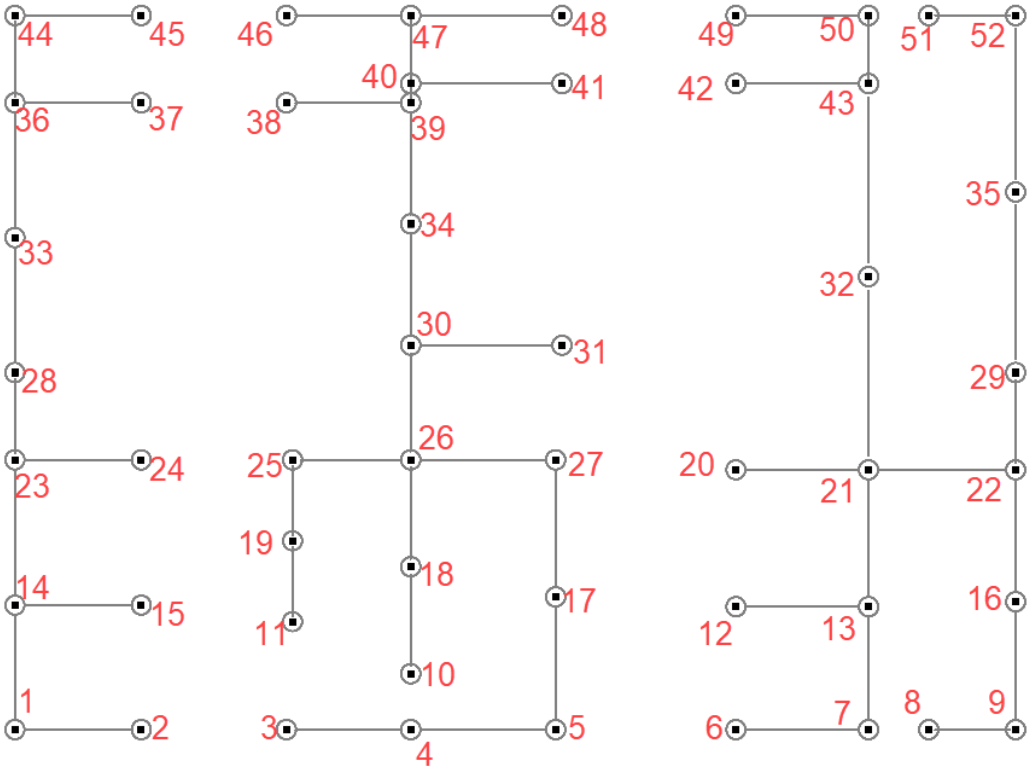

Figure D.1 Strain Gage Labels

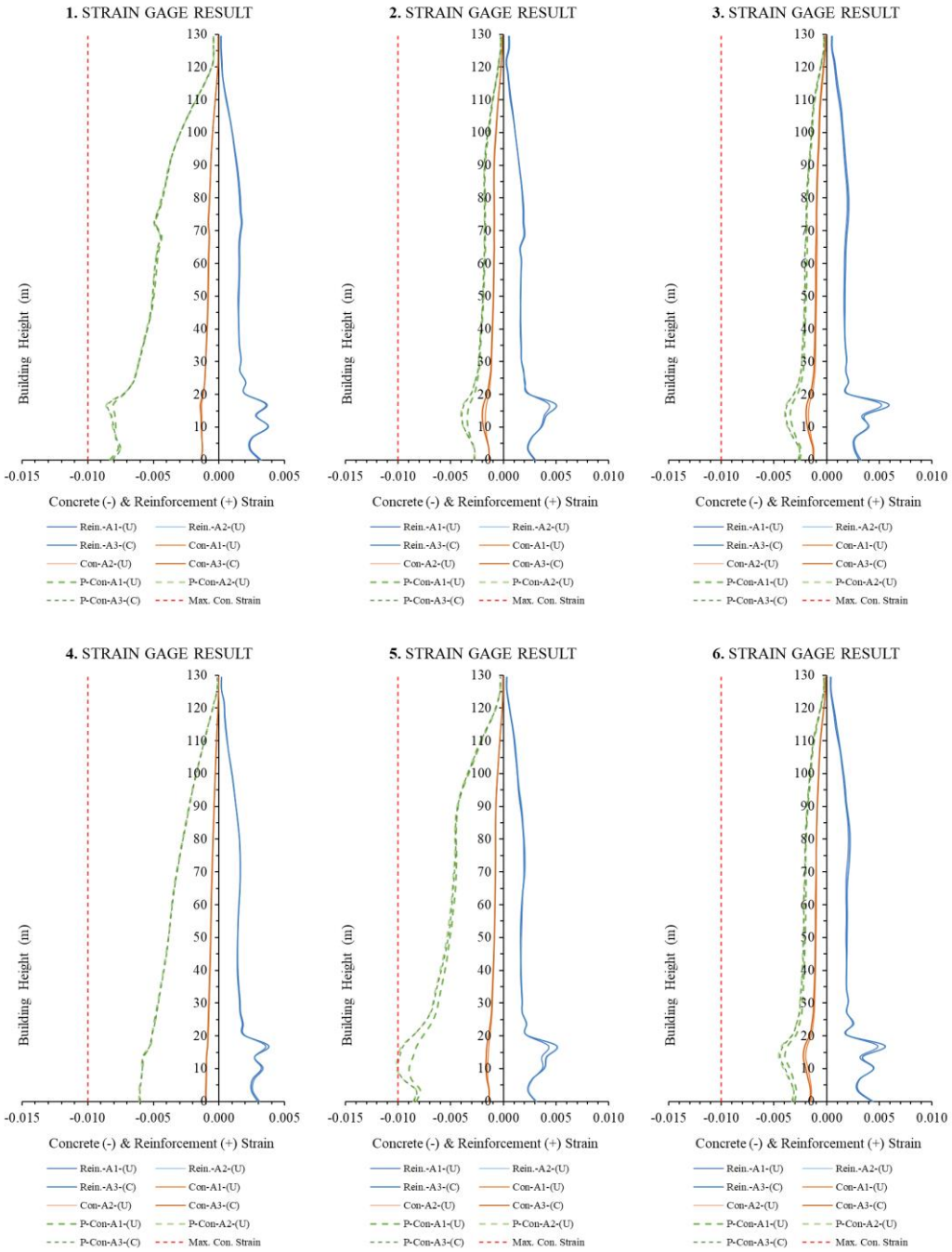
1. STRAIN GAGE RESULT
2. STRAIN GAGE RESULT
3. STRAIN GAGE RESULT
4. STRAIN GAGE RESULT
5. STRAIN GAGE RESULT
6. STRAIN GAGE RESULT
Building Height (m)
Concrete (-) & Reinforcement (+) Strain
Rein.-A1-(U)
Rein.-A2-(U)
Rein.-A3-(C)
Con-A1-(U)
Con-A2-(U)
Con-A3-(C)
P-Con-A1-(U)
P-Con-A2-(U)
P-Con-A3-(C)
Max. Con. Strain

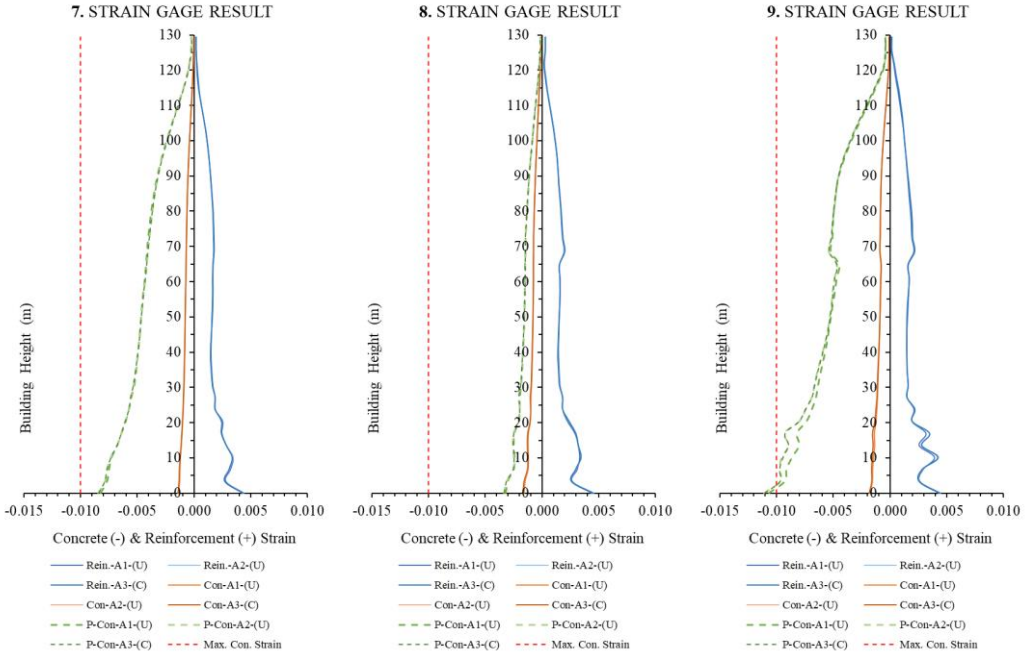
7. STRAIN GAGE RESULT
8. STRAIN GAGE RESULT
9. STRAIN GAGE RESULT
Building Height (m)
Concrete (-) & Reinforcement (+) Strain
Rein.-A1-(U)
Rein.-A2-(U)
Rein.-A3-(C)
Con-A1-(U)
Con-A2-(U)
Con-A3-(C)
P-Con-A1-(U)
P-Con-A2-(U)
P-Con-A3-(C)
Max. Con. Strain

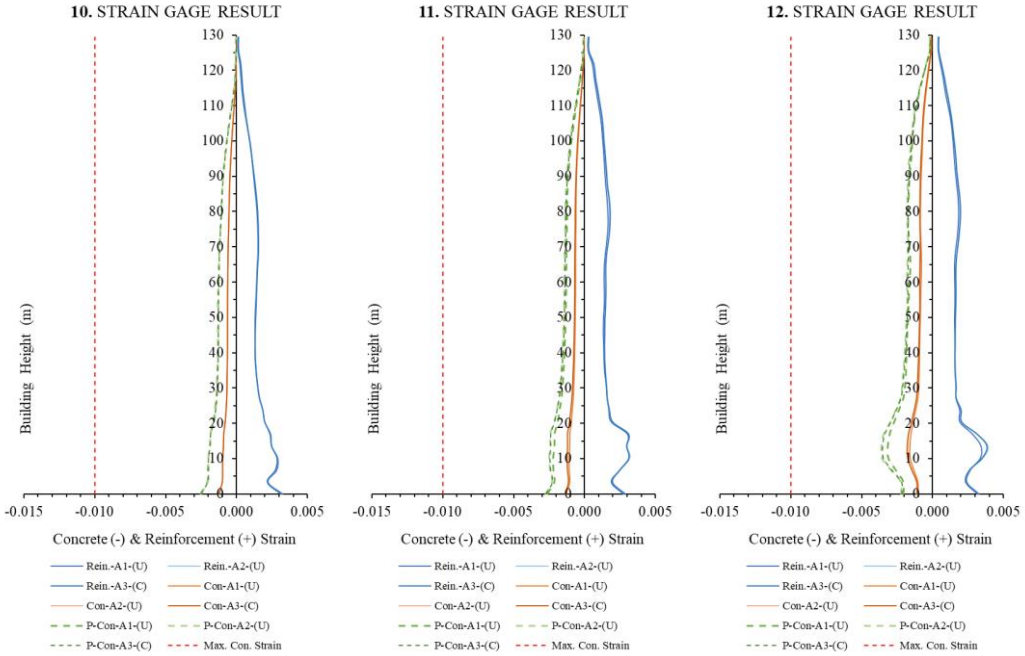
10. STRAIN GAGE RESULT
11. STRAIN GAGE RESULT
12. STRAIN GAGE RESULT
Building Height (m)
Concrete (-) & Reinforcement (+) Strain
Rein.-A1-(U)
Rein.-A2-(U)
Rein.-A3-(C)
Con-A1-(U)
Con-A2-(U)
Con-A3-(C)
P-Con-A1-(U)
P-Con-A2-(U)
P-Con-A3-(C)
Max. Con. Strain

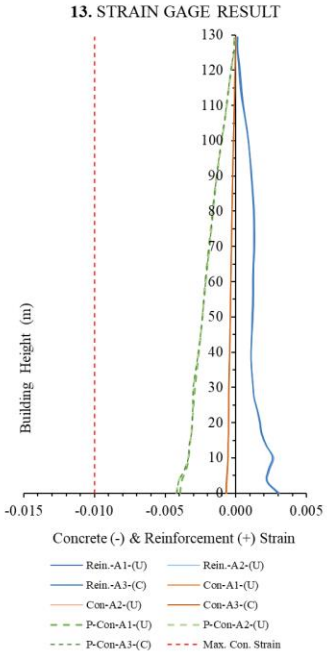
13. STRAIN GAGE RESULT
Building Height (m)
Concrete (-) & Reinforcement (+) Strain
Rein.-A1-(U)
Rein.-A2-(U)
Rein.-A3-(C)
Con-A1-(U)
Con-A2-(U)
Con-A3-(C)
P-Con-A1-(U)
P-Con-A2-(U)
P-Con-A3-(C)
Max. Con. Strain

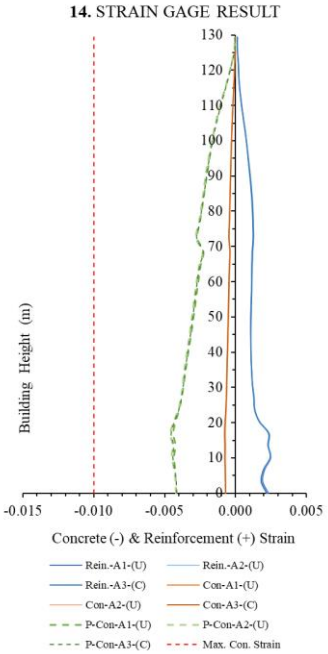
14. STRAIN GAGE RESULT
Building Height (m)
Concrete (-) & Reinforcement (+) Strain
Rein.-A1-(U)
Rein.-A2-(U)
Rein.-A3-(C)
Con-A1-(U)
Con-A2-(U)
Con-A3-(C)
P-Con-A1-(U)
P-Con-A2-(U)
P-Con-A3-(C)
Max. Con. Strain

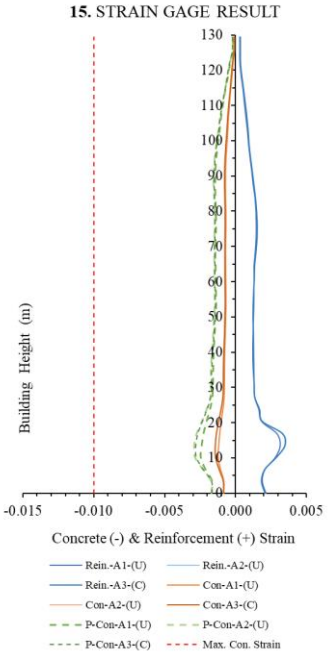
15. STRAIN GAGE RESULT
Building Height (m)
Concrete (-) & Reinforcement (+) Strain
Rein.-A1-(U)
Rein.-A2-(U)
Rein.-A3-(C)
Con-A1-(U)
Con-A2-(U)
Con-A3-(C)
P-Con-A1-(U)
P-Con-A2-(U)
P-Con-A3-(C)
Max. Con. Strain

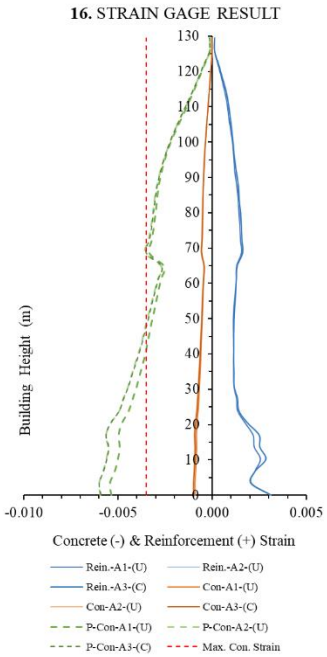
16. STRAIN GAGE RESULT
Building Height (m)
Concrete (-) & Reinforcement (+) Strain
Rein.-A1-(U)
Rein.-A2-(U)
Rein.-A3-(C)
Con-A1-(U)
Con-A2-(U)
Con-A3-(C)
P-Con-A1-(U)
P-Con-A2-(U)
P-Con-A3-(C)
Max. Con. Strain

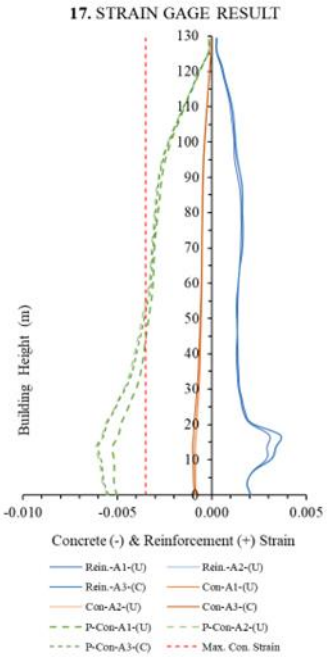
17. STRAIN GAGE RESULT
Building Height (m)
Concrete (-) & Reinforcement (+) Strain
Rein.-A1-(U)
Rein.-A2-(U)
Rein.-A3-(C)
Con-A1-(U)
Con-A2-(U)
Con-A3-(C)
P-Con-A1-(U)
P-Con-A2-(U)
P-Con-A3-(C)
Max. Con. Strain

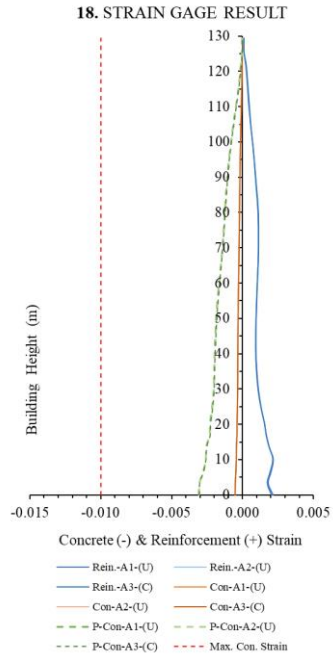
18. STRAIN GAGE RESULT
Building Height (m)
Concrete (-) & Reinforcement (+) Strain
Rein.-A1-(U)
Rein.-A2-(U)
Rein.-A3-(C)
Con-A1-(U)
Con-A2-(U)
Con-A3-(C)
P-Con-A1-(U)
P-Con-A2-(U)
P-Con-A3-(C)
Max. Con. Strain

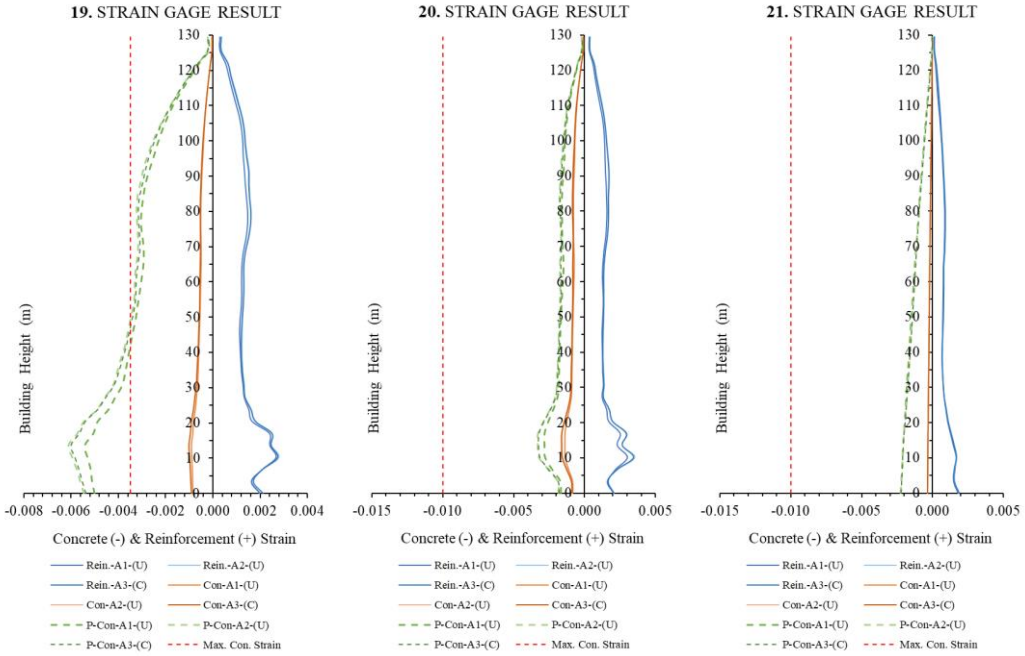
19. STRAIN GAGE RESULT
20. STRAIN GAGE RESULT
21. STRAIN GAGE RESULT
Building Height (m)
Concrete (-) & Reinforcement (+) Strain
Rein.-A1-(U)
Rein.-A2-(U)
Rein.-A3-(C)
Con-A1-(U)
Con-A2-(U)
Con-A3-(C)
P-Con-A1-(U)
P-Con-A2-(U)
P-Con-A3-(C)
Max. Con. Strain

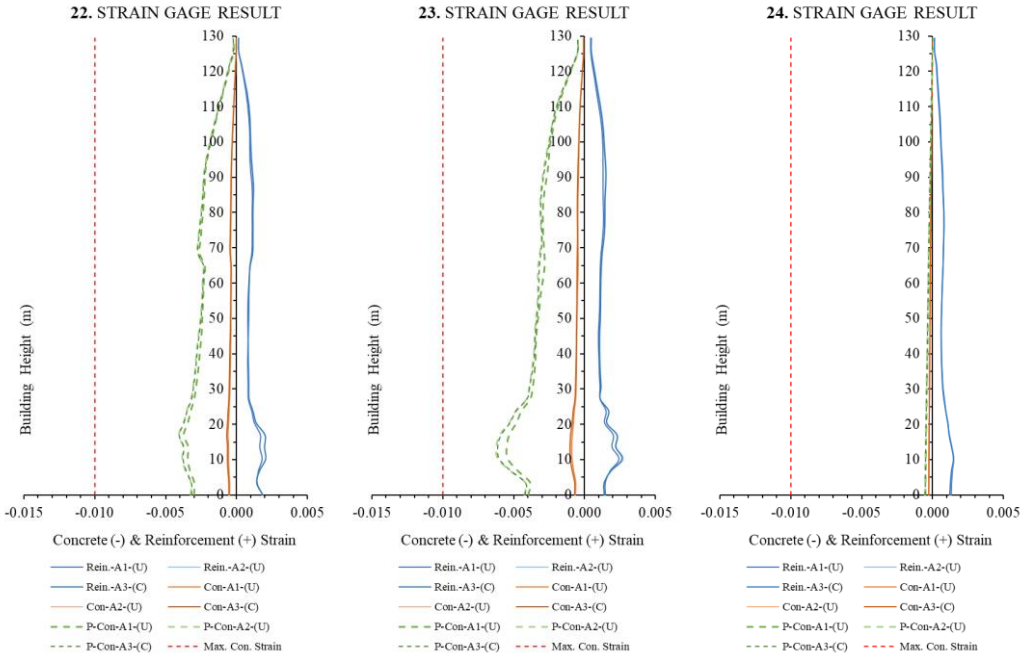
22. STRAIN GAGE RESULT
23. STRAIN GAGE RESULT
24. STRAIN GAGE RESULT
Building Height (m)
Concrete (-) & Reinforcement (+) Strain
Rein.-A1-(U)
Rein.-A2-(U)
Rein.-A3-(C)
Con-A1-(U)
Con-A2-(U)
Con-A3-(C)
P-Con-A1-(U)
P-Con-A2-(U)
P-Con-A3-(C)
Max. Con. Strain

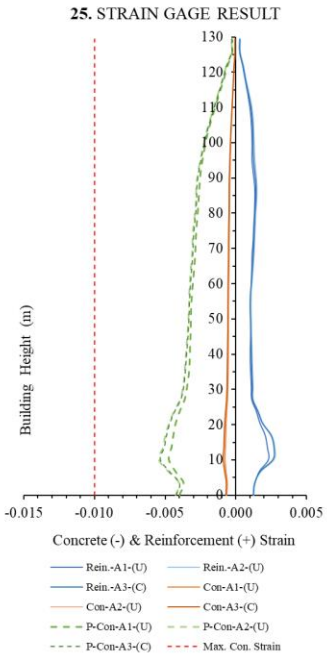
25. STRAIN GAGE RESULT
Building Height (m)
Concrete (-) & Reinforcement (+) Strain
Rein.-A1-(U)
Rein.-A2-(U)
Rein.-A3-(C)
Con-A1-(U)
Con-A2-(U)
Con-A3-(C)
P-Con-A1-(U)
P-Con-A2-(U)
P-Con-A3-(C)
Max. Con. Strain

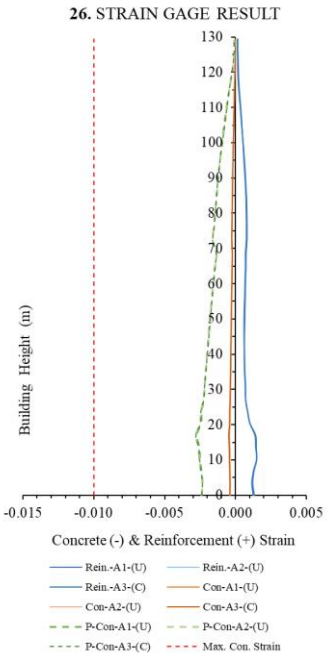
26. STRAIN GAGE RESULT
Building Height (m)
Concrete (-) & Reinforcement (+) Strain
Rein.-A1-(U)
Rein.-A2-(U)
Rein.-A3-(C)
Con-A1-(U)
Con-A2-(U)
Con-A3-(C)
P-Con-A1-(U)
P-Con-A2-(U)
P-Con-A3-(C)
Max. Con. Strain

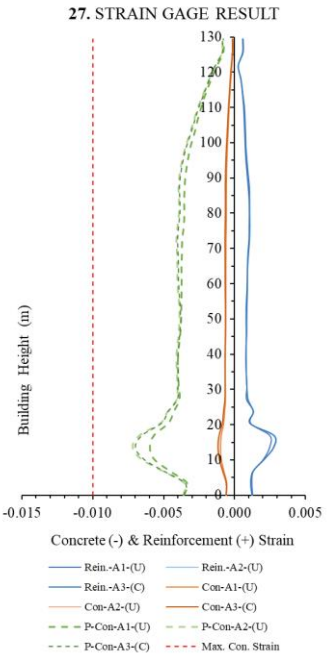
27. STRAIN GAGE RESULT
Building Height (m)
Concrete (-) & Reinforcement (+) Strain
Rein.-A1-(U)
Rein.-A2-(U)
Rein.-A3-(C)
Con-A1-(U)
Con-A2-(U)
Con-A3-(C)
P-Con-A1-(U)
P-Con-A2-(U)
P-Con-A3-(C)
Max. Con. Strain

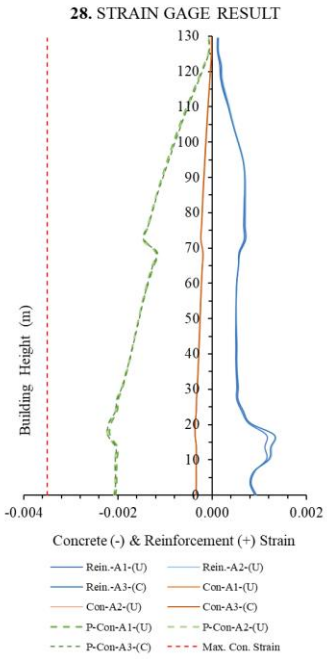
28. STRAIN GAGE RESULT
Building Height (m)
Concrete (-) & Reinforcement (+) Strain
Rein.-A1-(U)
Rein.-A2-(U)
Rein.-A3-(C)
Con-A1-(U)
Con-A2-(U)
Con-A3-(C)
P-Con-A1-(U)
P-Con-A2-(U)
P-Con-A3-(C)
Max. Con. Strain

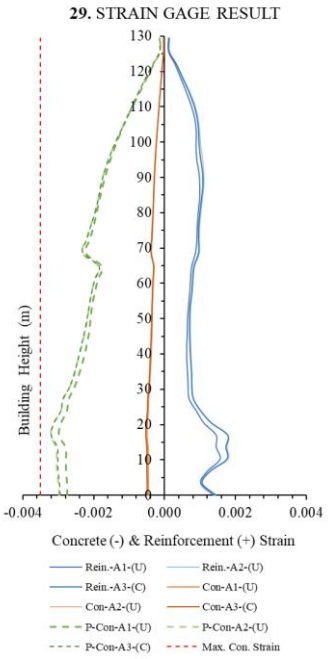
29. STRAIN GAGE RESULT
Building Height (m)
Concrete (-) & Reinforcement (+) Strain
Rein.-A1-(U)
Rein.-A2-(U)
Rein.-A3-(C)
Con-A1-(U)
Con-A2-(U)
Con-A3-(C)
P-Con-A1-(U)
P-Con-A2-(U)
P-Con-A3-(C)
Max. Con. Strain

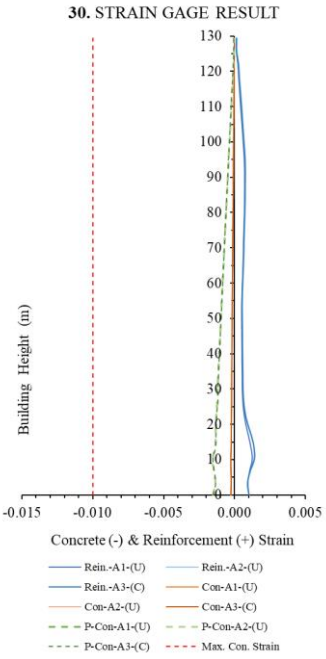
30. STRAIN GAGE RESULT
Building Height (m)
Concrete (-) & Reinforcement (+) Strain
Rein.-A1-(U)
Rein.-A2-(U)
Rein.-A3-(C)
Con-A1-(U)
Con-A2-(U)
Con-A3-(C)
P-Con-A1-(U)
P-Con-A2-(U)
P-Con-A3-(C)
Max. Con. Strain

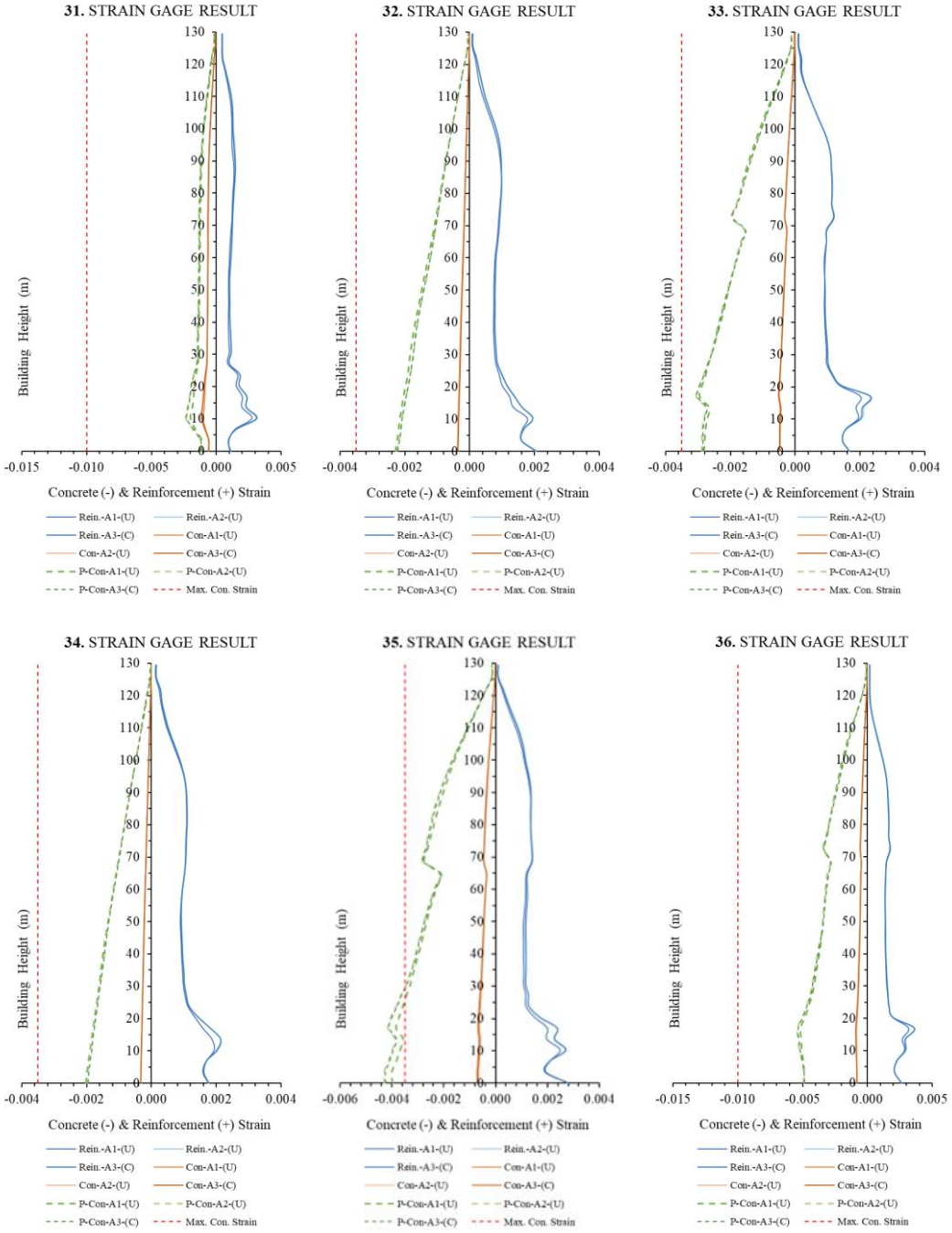
31. STRAIN GAGE RESULT
32. STRAIN GAGE RESULT
33. STRAIN GAGE RESULT
34. STRAIN GAGE RESULT
35. STRAIN GAGE RESULT
36. STRAIN GAGE RESULT
Building Height (m)
Concrete (-) & Reinforcement (+) Strain
Rein.-A1-(U)
Rein.-A2-(U)
Rein.-A3-(C)
Con-A1-(U)
Con-A2-(U)
Con-A3-(C)
P-Con-A1-(U)
P-Con-A2-(U)
P-Con-A3-(C)
Max. Con. Strain

37. STRAIN GAGE RESULT

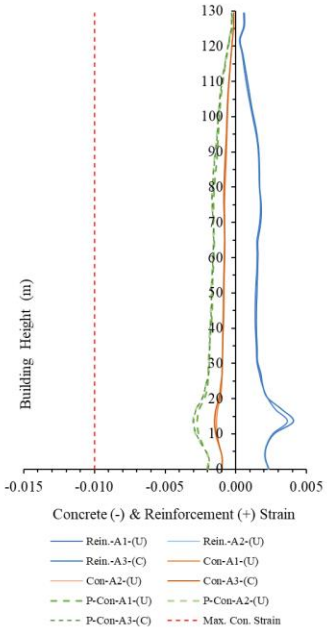

38. STRAIN GAGE RESULT

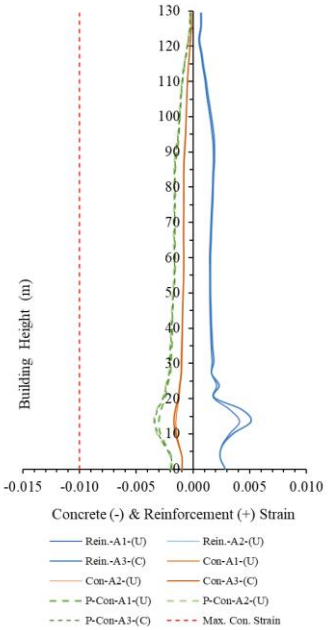

39. STRAIN GAGE RESULT

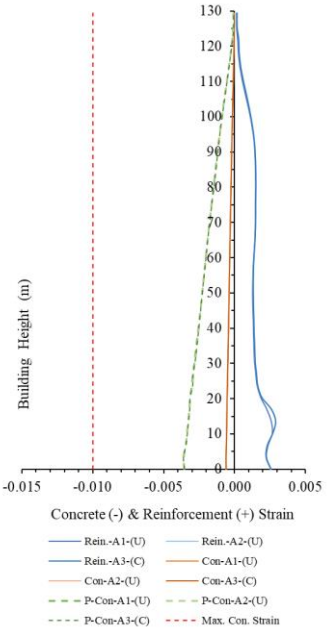

40. STRAIN GAGE RESULT

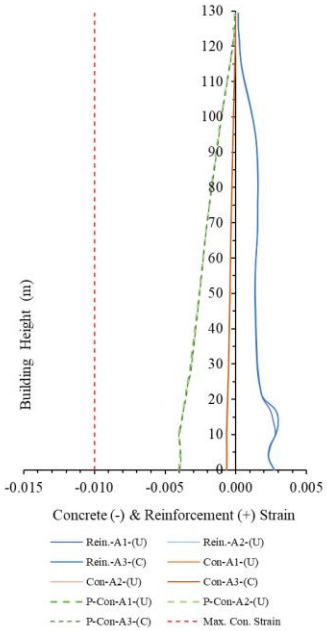

41. STRAIN GAGE RESULT

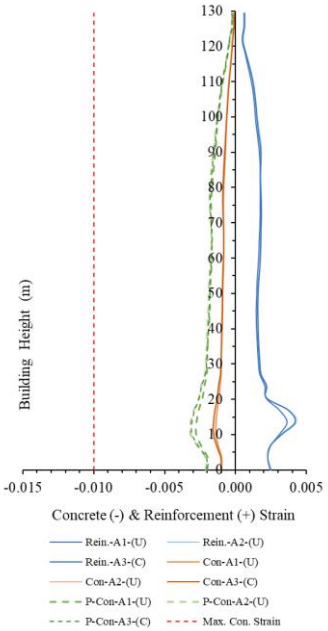

42. STRAIN GAGE RESULT

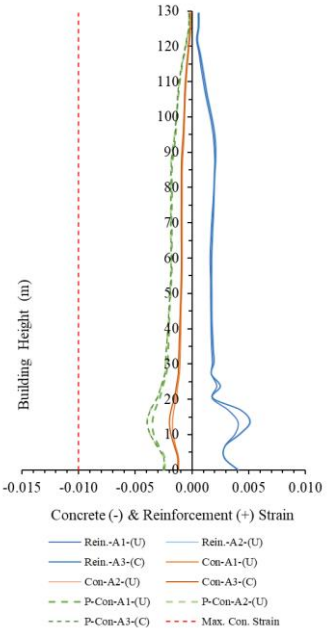

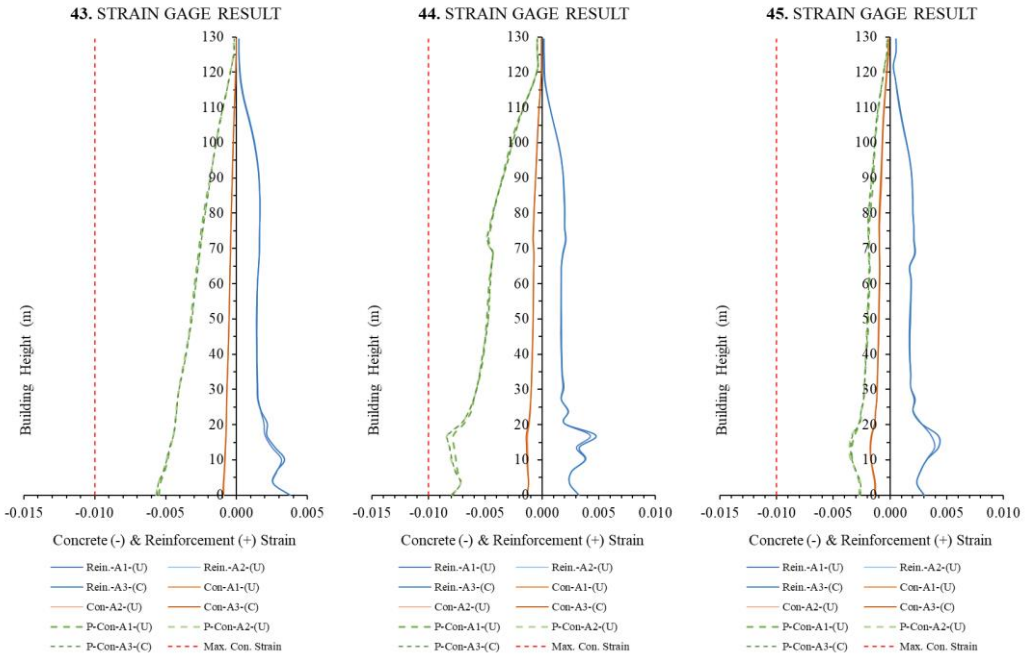
43. STRAIN GAGE RESULT
44. STRAIN GAGE RESULT
45. STRAIN GAGE RESULT
Building Height (m)
Concrete (-) & Reinforcement (+) Strain
Rein.-A1-(U)
Rein.-A2-(U)
Rein.-A3-(C)
Con-A1-(U)
Con-A2-(U)
Con-A3-(C)
P-Con-A1-(U)
P-Con-A2-(U)
P-Con-A3-(C)
Max. Con. Strain

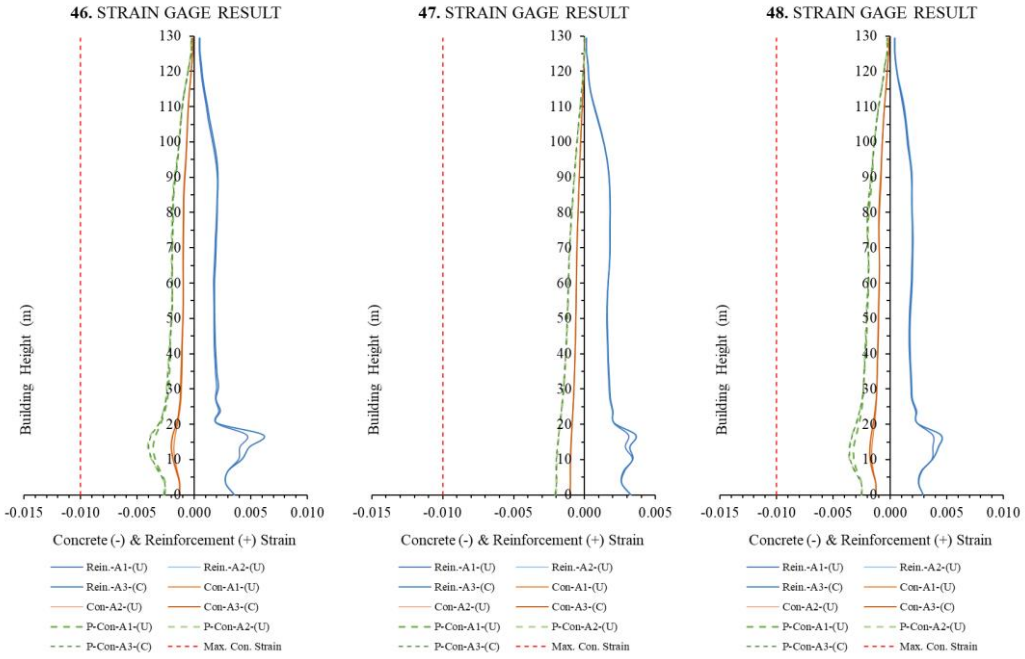
46. STRAIN GAGE RESULT
47. STRAIN GAGE RESULT
48. STRAIN GAGE RESULT
Building Height (m)
Concrete (-) & Reinforcement (+) Strain
Rein.-A1-(U)
Rein.-A2-(U)
Rein.-A3-(C)
Con-A1-(U)
Con-A2-(U)
Con-A3-(C)
P-Con-A1-(U)
P-Con-A2-(U)
P-Con-A3-(C)
Max. Con. Strain

49. STRAIN GAGE RESULT

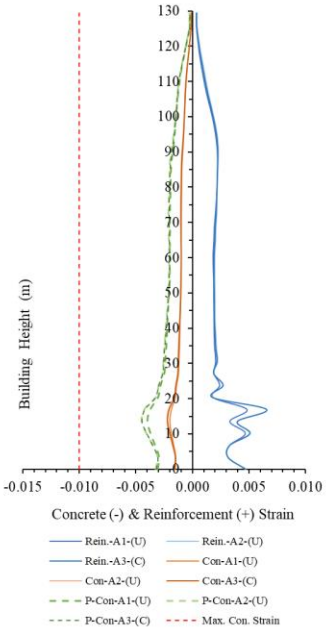

50. STRAIN GAGE RESULT

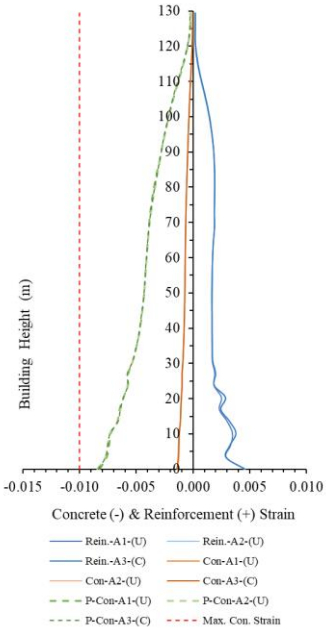

51. STRAIN GAGE RESULT

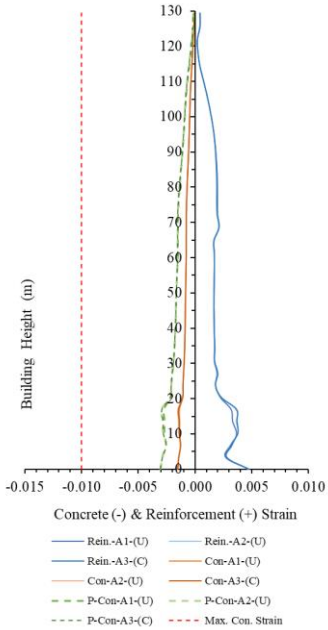

52. STRAIN GAGE RESULT